THE USE OF ELECTRON MICROSCOPY TO COMPARE WOOD DECAY MECHANISMS

A thesis submitted for the degree of

Doctor of Philosphy of the University of London

and for the Diploma of Membership of

the Imperial College of Science and Technology

by

Alan Crossley, B.Sc., A.R.C.S.

Department of Botany and Plant Technology
Imperial College of Science and Technology
London, S.W.7.

November 1979.

BIBL
LONDIN
UNIV

CONTAINS PULLOUTS

ABSTRACT

Scanning and transmission electron microscopy were used to examine the effect of Coniophora puteana (brown rot), Chaetomium globosum (soft rot) and Coriolus versicolor (white rot) on the ultrastructure of the wood cell walls of Betula sp. and Pinus sylvestris sapwoods.

A comparison of air drying and Critical Point drying preparation methods for scanning electron microscope examination resulted in use of the latter being recommended for studies of wood decay micromorphology. The scanning electron micrographs indicated that further study, by means of the transmission electron microscope, was required on the investments to the hyphae, which were believed to be mucilage. Satisfactory preservation of the extracellular mucilaginous sheaths of Rhinocladiella mansonii blastospores was achieved by combining a number of preparation procedures.

Detailed examination of the requirements and procedures in specimen preparation of decayed wood for transmission electron microscopy were made with subsequent development of new apparatus, techniques and methods to increase the reliability of the observed results.

The application of the mucilage preparation techniques in examinations of wood decay using the transmission electron microscope demonstrated the significant presence of mucilage in the micromorphological decay features produced by soft and white rot but not in the case of brown rot.

New observations on decay features associated with the test material, together with the generally agreed characteristics of each rot type have been utilised in the development of an explanation of the decay mechanisms for each of the three fungal types.

CONTENTS

	Page
TITLE PAGE	i
ABSTRACT	ii
CONTENTS	iii
INTRODUCTION	1
General	1
Brown rot	5
Soft rot	9
White rot	17
Aims of work	21
PART I SCANNING ELECTRON MICROSCOPY	23
1. Introduction	24
2. Materials	26
2.1 Wood	26
2.2 Fungi	26
3. Methods and their development	27
3.1 Test block format	27
3.2 Culturing mechanisms	28
3.3 Specimen preparation	31
3.3.1 Preparation of specimens from the decayed block	31
3.3.2 Dehydration methods	35
3.3.2.1 Air drying	35
3.3.2.2 Critical Point drying	35
3.3.3 Final S.E.M. preparations	38
3.3.4 Microscopy	41
4. Results	42
4.1 Comparisons of specimen preparations	44
4.1.1 General comments on preparation methods	44
4.1.2 Air dried material	46
4.1.3 Critical Point dried material	49
4.2 Comparisons of fungal types on each wood species	52
4.2.1 Brown rot, Coniophora puteana	52
4.2.1.1 On hardwood;- birch, (Betula sp.)	52
4.2.1.2 On softwood;- Scots pine, (Pinus sylvestris)	62
4.2.2 Soft rot, Chaetomium globosum	68
4.2.2.1 On hardwood;- birch, (Betula sp.)	68
4.2.2.2 On softwood;- Scots pine, (Pinus sylvestris)	76
4.2.3 White rot, Coriolus versicolor	79
4.2.3.1 On hardwood;- birch, (Betula sp.)	79
4.2.3.2 On softwood;- Scots pine, (Pinus sylvestris)	89
4.3 Mucilage	103
5. Discussion	110

PART II TRANSMISSION ELECTRON MICROSCOPY OF MUCILAGE 124

1. Introduction 125

2. Materials and methods 130

2.1 Culture growth and specimen selection 130
2.2 Fixation 130
2.3 Dehydration 132
2.4 Infiltration 132
2.5 Embedding 134
2.6 Mounting, trimming and sectioning 134

3. Results 135

4. Discussion 140

PART III TRANSMISSION ELECTRON MICROSCOPY OF WOOD DECAY 142

1. Introduction 143

1.1 Replicas 143
1.2 Sections with the embedding resin removed 144
1.3 Cryosectioning 144
1.4 Ultrathin sections 144
1.5 Problems and requirements of preparative techniques 145

2. Development and analysis of methods 147

2.1 Selection of specimen format 147
2.2 Specimen format - orientation and preparation 148
2.3 Resin selection 154
2.4 Resin matching 155
2.5 Compounding of the resin 156
2.6 Ease of infiltration of the embedding medium 159
2.7 Specimen handling 160
2.8 Vacuum infiltration and embedding 161

3. Materials and methods 163

3.1 Woods 163
3.2 Fungi 163
3.3 Preparation of decayed microspecimens 163
3.3.1 From blocks 163
3.3.2 Improved methods 164
3.4 Resin mixing 166
3.5 Preparation of orientation receiving blocks 167
3.6 Fixation 168
3.7 Dehydration 169
3.8 Infiltration 169
3.9 Use of specimen holder 170
3.10 Microspecimen insertion 170
3.11 Precautions and waste disposal 172
3.12 Trimming 172
3.13 Sectioning 174
3.14 Staining 177
3.15 Electron microscopy 177

4. Results 178

4.1 Brown rot, Coniophora puteana 180
4.1.1 On hardwood;- birch, (Betula sp.) 180
4.1.2 On softwood;- Scots pine, (Pinus sylvestris) 189
4.2 Soft rot, Chaetomium globosum 194
4.2.1 On hardwood;- birch, (Betula sp.) 194
4.2.2 On softwood;- Scots pine, (Pinus sylvestris) 205
4.3 White rot, Coriolus versicolor 212
4.3.1 On hardwood;- birch, (Betula sp.) 212
4.3.2 On softwood;- Scots pine, (Pinus sylvestris) 225

5. Discussion 229

PART IV PROPOSED DECAY MECHANISMS AND CONCLUSIONS 244

1. Proposed decay mechanisms 245
1.1 Brown rot 245
1.2 Soft rot 249
1.3 White rot 270

2. Conclusions 274

2.1 Conclusions from observations 274
2.2 Conclusions from techniques 275

ACKNOWLEDGEMENTS 277

APPENDICES

A :- Microspecimen preparation device 278

B :- The chemistry of the epoxy resin system used in this study 282

C :- Specimen preparation holder 290

D :- Computer program 295

PAPER 1 A versatile multi-specimen holder for processing and critical point drying of materials for examination in the scanning electron microscope (SEM) (1976) J. Microsc., 108 (3), pp. 349-352 296

PAPER 2 Proboscis hyphae in soft rot cavity formation (1977) J. Inst. Wood Sci., 7 (42), No. 6, pp.30-33 300

REFERENCES 304

INCLUSION Full drawing to build the specimen holder for T.E.M. preparation

INTRODUCTION

General introduction

For centuries man has used wood as a structural and decorative material and even with the introduction of synthetic products wood as a resource is still a heavily used commodity. Initially, heartwood of naturally durable timber species could be selected but as the demand increased and the raw material was depleted the less durable woods had to be used until we reach the situation of today where much of the timber used in the U.K. is of non-durable species and includes a high proportion of sapwood. This, therefore, evokes a need for wood preservation to extend the service life of timber structures and thus reduce the demands on the world's depleted forests.

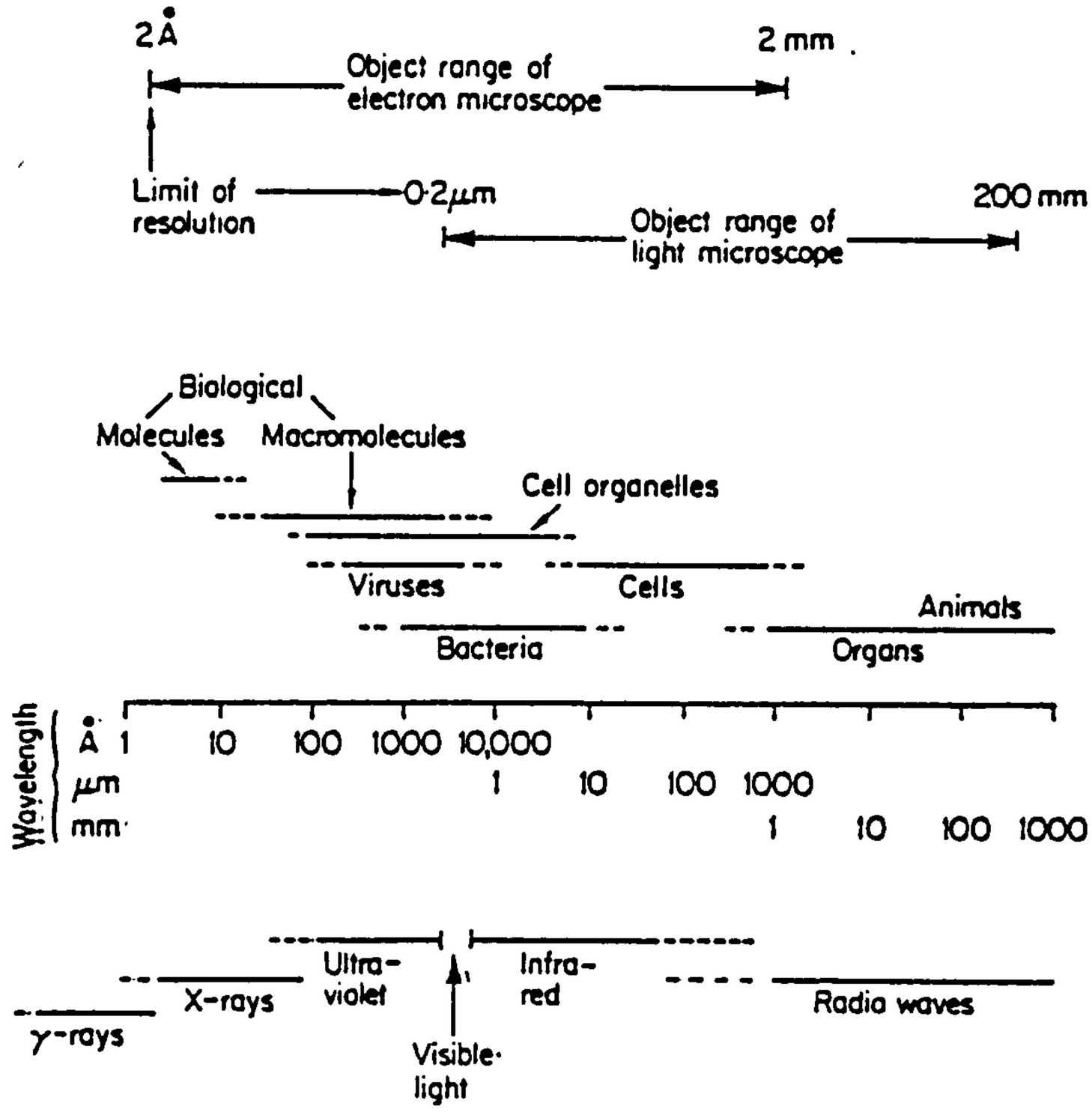
In nature, wood must ultimately yield to the natural recycling systems of the environment in which micro-organisms degrade the timber into simple compounds for reabsorption into the carbon cycle. Preservation aims at slowing down this rate of degrade or stalling the action of the micro-organisms long enough for the timber to have a useful period in service, but to know how and where to apply preservatives requires a detailed knowledge of the mechanisms by which fungal hyphae degrade wood cell walls.

In 1863 Schacht published light microscopical drawings of most of the micromorphological features of wood decay that we know today from scanning and transmission electron microscopy. However, he was unaware of the cause or significance of his observations and it was not until the experimental work of Hartig (1878) that wood decay was attributed to fungi. Initial studies were made using the light microscope with

excellent detailed results from Bailey and Vestal (1937) and Bailey (1954). Later work incorporated the technical developments of polarised light, fluorescence optics, histochemical staining and, to a limited extent, X-ray diffraction. The observations of structural changes were cross-correlated with studies determining the chemical composition and breakdown of wood to produce an overall picture of fungal attack patterns. However, the optical microscope reached its utilisable limit with the specialised techniques of Proctor (1941) and Wilcox (1968) examining the finer details of wood anatomy and its biodeterioration. More intensive studies were restricted by the resolution obtainable from the instrumentation. Resolution is the key word in the progressing technology of examining material at higher and higher magnifications.

The resolution of an optical system is dependant on the wavelength of the electromagnetic radiation being used. Radio waves may be from several kilometres long down to a few millimetres, infra-red wavelengths are measured in hundredths of a millimetre (microns) and visible light in thousandths of a millimetre (nanometres), see fig. A. Visible light waves can resolve objects as small as bacteria but cannot detect most viruses. The resolving power of a perfect optical system is approximately half the wavelength of the radiation employed. Thus the ultimate resolving power of a light microscope using visible light is approximately 0.25μm. The unaided human eye can only resolve about 0.25mm (this figure is only an approximation and will vary from person to person). Therefore, a light microscope can be used to magnify an image to a degree determined simply by the ratio of the resolving power of the eye to the resolving power of visible light,

FIG. A



Reproduced by kind permission of Dr. G.A. Meek (1976)

which would be approximately 1000 times. The development of the light microscope over the past 400 years has achieved this aim. There is no instrumental difficulty in obtaining sheer magnifications greater than this but no more spatial information can be gained from the image and, as such, magnifications in excess of 1000 times are often referred to as empty magnifications (Meek, 1976).

To increase the resolving power and thereby obtain more spatial information requires the use of shorter wavelength radiation. However, the eye is insensitive to such radiation and waves shorter than ultra-violet (see fig. A) cannot as yet be bent to form images. This

apparently unanswerable problem was overcome about forty years ago by employing electrons in an optical system. Unlike X-rays and other short wavelength radiations, electron beams can be easily refracted to form magnified images and the first developments were made by a team led by Max Knoll and included Ruska, von Borries, Knoblauch, Freundlich and Lubszynski. In 1931 a German patent was filed on behalf of the instrument division of Siemens for the principles of the electron microscope, from which the modern instruments have been developed.

The wavelength of the high voltage (30 - 100kV) electrons generally used in biological electron microscopy, which travel at about one third the velocity of light, is approximately 100,000 times smaller than that of visible light. From this, the theoretical resolving power of an electron microscope is approximately 0.02 Å but the best result achieved so far is about 2 Å. This difference is due to the technical problems involved in overcoming aberrations in the electron optic systems.

The introduction of the electron microscope and its application to biological problems initiated a new phase of information on ultra-structural aspects of wood and its biodeterioration. Since its first application to wood pathology (Liese and Hartmann-Fahnebrock, 1953; Meier, 1955) a large amount of information on the micromorphology and microchemistry of tissue and cell deterioration has been obtained. Preparation of material for examination in the electron microscope has developed along a number of lines, each with its applications and problems, and some of these are exampled in part III.

Early reviews on the light microscopical features of decay were

presented by Cartwright and Findlay (1943, 1958) and Wilhelmsen (1965). More recent classifications and characteristics of wood biodeterioration by micro-organisms, encompassing ultrastructural aspects revealed by the electron microscope, have been given by Liese (1970) and Wilcox (1970, 1973).

This study is confined to three decay groups, brown, soft and white rots, and their action on birch (a hardwood) and Scots pine (a softwood). It must be stressed, however, that the classifications brown, soft and white rot are in themselves generalisations and that there are variations within, and overlap between, these groups. The micromorphology of wood decay was referred to by Levy (1969) as a spectrum of interaction between fungi and wood.

The literature summaries that follow, therefore, detail the features of decay micromorphology that most workers are in agreement with and represent the average attack pattern of the fungal group. The information has been taken from studies using light, scanning electron and transmission electron microscopy together with chemical and biochemical evidence to present the features, prior to this study, of brown, soft and white rot decay patterns in wood.

Brown rot

In the advanced stages of decay the wood exhibits a cuboidal pattern of checking perpendicular to the grain, is extremely brittle and suffers a rapid loss of tensile strength (Kennedy, 1958). Brown rots preferentially attack softwoods with the hyphae penetrating through the rays and spreading into the tracheids (Liese, 1970). Schulze and Theden (1938) reported the earlywood of spruce and pine to be more resistant to brown rot than the latewood, whereas the reverse was

found by Meier (1955) for spruce and by Bravery (1972) for pine. Some of the cell types of hardwoods appear to be extremely resistant to decay, these being birch vessels (Meier, 1955)(Bravery, 1971) and sweetgum vessels and rays (Wilcox, 1968) although Greaves and Levy (1965) noted that in the advance stages of birch decay, cellulosic decomposition was detectable in all cells except latewood fibres.

Bore holes in the cell walls were the major evidence of attack using the light microscope (Cowling, 1965) with the hyphae usually found within cell lumina and seldom in the walls (Liese, 1970). The tori of bordered pits were easily destroyed though there was no observed preference for this pathway (Liese, 1970; Jutte and Sachs, 1976). The cell walls were penetrated as described by Proctor (1941) and bore holes could expand during fungal growth leading to larger openings (Courtois, 1965; Pechmann et al, 1967). Proctor (1941) concluded that wall penetration was enzymic, not mechanical.

Changes of the cell wall appearance along the line of the hyphae were rarely visible (Nečesaný, 1963). Yet with the progress of attack, cracks and fissures developed in the proximity of the hyphae pointing to a loss of material from the secondary wall below (Liese, 1970; Bravery, 1971,1972; Jutte and Zabel, 1974). Using the scanning electron microscope, Jutte and Zabel (1974) detected lysis zones along the hyphae together with an associated slime layer, especially in the early lysis development.

In addition to bore holes brown rot hyphae have been observed to produce axially orientated cavities, of variable size and shape, within the S_2 wall layer (Meier, 1955; Liese and Schmid, 1962; Wilcox, 1968).

The enzymes secreted by brown rot fungi have been shown to be only capable of degrading the carbohydrated fraction of the wood (Meier, 1955), although the molecular weight, methoxyl content and solubility of the remaining lignin may be substantially altered (Cowling, 1961). More detailed analyses (see Kirk, 1973) revealed that the modifications of lignin were only mild, with demethylation of the phenolic and non-phenolic units and minimal change of the aromatic rings. Nilsson (1974a) showed that in a study of 31 brown rot fungal species only 7 produced enzymes with the capability to attack pure cellulose with only limited cleavage of the chains. Nilsson, therefore, suggested that many brown rot fungi require lignin to digest cellulose and that its presence might stimulate cellulose degradation rather than reduce it as was previously thought.

Transmission electron microscopical studies of brown rot degrade of spruce wood cell walls together with microchemical analyses revealed the degraded S_2 as being a reticulate network of the residual lignin framework (see Bailey, 1954; Meier, 1955). This residue retained the overall integrity of the cell making decay difficult to detect in the light microscope. Only in the later stages when the matrix frequently collapsed could changes in the wall be noticed (Wilcox, 1968). Bravery (1972), George (1974) and Jutte and Sachs (1976) in S.E.M. studies noted the reticulate spongy appearance of severely lysed walls. Examinations of brown rotted tension wood revealed the S_2 to be completely degraded due to the absence of significant lignin in this type of reaction wood (Liese, 1970).

Meier (1955) observed the brown rot attack of birch and spruce walls to be similar, with the S_2 being degraded towards the middle lamella, the cellulose removal, where not uniform, led to cavities

in some areas while others remained essentially intact. Following the removal of the S_2 cellulose in spruce and the entire S_2 in birch the S_3 was degraded, and even at this advanced stage the S_1 and compound middle lamella were unattacked. The total removal of the birch S_2 was explained as being due to the low level of lignification compared with the softwood. Wilcox (1968) noted that with sweetgum (Liquidambar styraciflua) the S_1 was attacked before the S_3.

The pore size of the lignin framework in brown rotted spruce, shown by Meier (1955), could not be attributed to any known micro-structural feature of cellulose and the possibility of certain limited collapse was admitted as an explanation. Examinations of brown rot by Cowling (1961,1965) revealed that even after 66% weight loss there were no detectable pores within the residual wall. However, there was also a marked reduction in contrast between the S_2 and the compound middle lamella, with the entire wall pair appearing amorphous without any visible microfibrillar orientation visible in sound walls. This reduction in contrast was not expected and could not be satis-factorily explained.

The resistance of the S_3 to brown rot enzymes has been noted by a number of workers (Meier, 1955; Liese, 1963a; Wilcox, 1968) and also to the action of acids and alkalis (Wardrop and Dadswell, 1957; Liese, 1963a). Explanations of this resistance have been attributed to, a greater degree of microfibrillar order (Lange, 1954; Meier, 1955), heavier lignification (Jurášek, 1958; Liese, 1963a; Wilcox, 1968) and different chemical composition of the microfibrils (Meier, 1955). Prior delignification does not reduce the resistance of the S_3 (Meier, 1955).

The compound middle lamella was also resistant to brown rot action (Meier, 1955; Cowling, 1961; Wilcox, 1968) especially the thickened cell corners (Meier, 1955; Wilcox, 1968). The action of brown rot enzymes on cellulose occurred in a diffuse manner through the entire wall and differences in susceptibility to decay of various tissues, cell types and wall layers appears to be correlated with differences in chemical composition (Wilcox, 1968).

Soft rot

Macroscopically the affected wood is soft and becomes brittle on drying, often with surface checking, smaller but similar to brown rot. The soft rot fungi belong to the Ascomycetes and Deuteromycetes or fungi imperfecti groups and although first observed by Schacht (1850) they were characterised and termed by Savory (1954). Soft rot fungi tend to be found in high moisture content situations, cooling tower slats (Savory, 1954) and marine or freshwaters (Jones, 1963; Leightley and Eaton, 1977), and are more prevalent in hardwoods (Nilsson, 1973).

Corbett (1963) suggested that soft rots were intermediate between white/brown rot fungi and the stainers as they can display properties of both.

In hardwoods and softwoods the hyphae invade the tissues, preferentially through the vessels or rays, from where they grow into the lumina of the adjacent fibres or tracheids (Courtois, 1963; Liese, 1964; Corbett, 1965; Greaves and Levy, 1965; Levy and Stevens, 1966). Corbett (1965) found that the decay rate varied with the block face that was in contact with the hypha, with the order of decreasing decay being, transverse, tangential, radial. A higher lignin content of the

radial walls was reasoned for their slower destruction.

Penetration in the early stages of soft rot was reported to be via pits (Greaves and Levy, 1965; Levy, 1965; Levy and Stevens, 1966) and after destruction of the storage materials in the cell lumina, bore hole formation began (Greaves and Levy, 1965). Pits continued to be the primary passageways for tangential spread (Corbett, 1965) although bore holes were also found in tangential as well as radial growth (Liese, 1964).

The longitudinal hyphae in the cell lumina were relatively large, thick-walled and produced fine hyaline lateral branches, which penetrated the cell wall via bore holes of the same diameter and did not appear to increase in size (Corbett and Levy, 1963; Corbett, 1965; Levy, 1965; Levy and Stevens, 1966; Nilsson, 1974b; Unligil and Chafe, 1974). Although Liese (1970) suggested that the penetration was enzymic due to the lytic effect on the surrounding wall, which could lead to bore hole enlargement.

In hardwoods, the S_3 was often subject to direct enzymatic attack by overlying hyphae and degradation of the warts, if present, becomes apparent (Liese, 1970), though Nilsson (1973) reported the S_3 of hardwoods to be resistant. The lysis of the wall produced 'V' shaped notches which penetrated as far as the S_1 or even the compound middle lamella (Corbett, 1965; Levy and Stevens, 1966). This type of lysis being termed Type 2 by Corbett (1965). Vessels were generally less deteriorated than fibres (Liese, 1970).

In softwood species, however, the S_3 wall layer generally appeared to remain undegraded (Liese, 1970; Nilsson, 1973; Zainal, 1975). Apparently its chemical composition had a protective influence (Liese,

1970). This could be attributed to either a different type of polysaccharide, other forms of encrusting substances, or indications that there is a different lignin quality combined with the higher lignification than in hardwoods (Liese, 1970).

The classical form of deterioration attributed to soft rot fungi, Corbett Type 1 (1965), was the primary form of attack in softwoods. The decomposition consists of chains of conically tipped or diamond shaped cavities, localised around the hyphae growing in the S_2 wall layer and running helically around the cell axis, parallel to the microfibrils (Wilcox, 1973). Similar cavities have been observed in wood degraded by other cellulose destroying fungi but not with the frequency found in soft rot (Wilcox, 1973). Cavities have been reported to be more conspicuous in latewood of softwoods (Savory, 1954; Duncan, 1960) and earlywood in hardwoods (Levy and Stevens, 1966).

The pathway of the fine penetration hyphae into the S_2 can be variable. Changes of direction by hyphae passing through pits have been shown (Levi, 1965; Levi and Preston, 1965; Nilsson, 1974b) or the hyphae may 'T' branch within the S_2. The formation of a 'T' branch occurs when a hypha, penetrating the cell wall laterally, turns through 90° producing a side branch at the same time and the two hyphal tips align with the microfibrils as they grow in opposite directions (Corbett, 1965). This can occur, after passage through the S_3, from the lumen (Levy and Stevens, 1966; Leightley and Eaton, 1977), after further penetration across the middle lamella and branching in the S_2 of the adjacent cell wall (Corbett and Levy, 1963; Liese, 1964; Corbett, 1965; Levy and Stevens, 1966) or in more extreme cases after serial penetration of a number of cell wall pairs (Liese, 1964).

The two aligned hyphae of the 'T' branch grow, in length, at about the same rate and as they extend through the S_2 layer cavities form around them (Corbett, 1965). The rate of hyphal extension may be reduced while the cavities enlarge laterally and the cavity length appears to be inversely related to the hyphal diameter (Corbett, 1965).

The hyphae making the early penetrations along the microfibrils were extremely fine and Corbett(1965) referred to these as the "proboscis hyphae". Extensive studies on proboscis hyphal growth and cavity formation for marine and freshwater soft rots were made by Leightley (1977) using time lapse photography and the scanning electron microscope. Some of the details of this work showed the presence, and indicated the role, of proboscis hyphae in soft rot cavity formation (Leightley and Eaton, 1977). A clear demonstration of proboscis hyphae in birch degrade by Chaetomium globosum was made by Crossley and Levy (1977) using the S.E.M.

Levi (1965) and Levi and Preston (1965) put forward a number of suggestions to explain the abrupt change in direction of the penetration hypha forming a 'T' branch. First, certain properties of the S_3 layer, such as the degree of crystallinity, high degree of polymerisation, presence of inhibiting substances, etc., may act as a barrier. Second, the hypha may be penetrating through plasmodesmata or other capillaries that may be blind, although Liese (1970) indicates that no plasmodesmatic tube system, or any physical discontinuity, is known for the cell walls of tracheids. Third, there may be localised regions in the S_2 that readily support hyphal growth.

Levy (1965, 1967) suggests that the initiation of 'T' branching is stimulated by a biochemical factor of the cell wall, and Levy and

Stevens (1966) used the term haustoria to describe a foraging function of the 'T' branch hyphae.

In the formation of cavities there appears to be limited diffusion and action of the enzymes away from the hyphal surfaces (Meier, 1955; Liese, 1964; Levi, 1965). The shape and size of soft rot cavities varies greatly and the various forms were grouped by Courtois, (1963). With regard to this variation it must be remembered that every cavity represents a single phase in the successive morphological development of the hyphal system. Cavity size and shape are determined by the duration of attack, the fungal species, wood species, cell type and moisture content. In general the cavities originate from a small erosion canal around the proboscis hypha and with progressive decay they broaden to produce an oval shape in cross section. Their width in conifer, earlywood, tracheids is often 3 - 5µm and in latewood tracheids, 6 - 9µm, both with considerable variation in length between 5 - 100µm. Longer cavities develop in woods with higher moisture contents (Liese, 1970). The sequence of cavity formation can be altered by the physiological conditions of temperature and water content (Liese and Ammer, 1964). With progressive decay the S_2 becomes interlaced by confluent cavities and in the final stages only the heavily lignified middle lamella and S_3 are left, the latter often collapsing.

The characteristic, symmetrically pointed, cavities have inclusion angles varying between 47° and 54°, in softwoods, and 72° in beech (Courtois, 1963). Bailey and Vestal (1937) interpreted this shape as being due to two planes of enzymatic hydrolysis, one parallel with the microfibrils, and the second at an angle of 23° from that axis. They also noted that the inclusion angle of the conical points

varied with the moisture content, indicating that the hydrolysis planes responsible could be related to the unit cell dimensions of the cellulose crystallites in the secondary wall.

Frey-Wyssling (1938) supported this line of thought suggesting that the 454 plane of cellulose produced an angle of 23° and this was accepted by Meier (1955), Wardrop and Jutte (1968) and Jutte and Wardrop (1970), with other crystal planes, 434 and 414, being used to explain the angle variations previously observed by Courtois (1963). However, the use of the crystal lattice theory requires a high degree of tangential alignment for which there is no evidence (Preston, 1979).

Roelofsen (1956) suggested that the rate of decomposition of the wall was governed by the cellulose component, with the enzymes only capable of further diffusion after the removal of the substrate. This diffusion being at a greater rate along the microfibrils than across through the lignin regions. Thus it would not be possible to produce cavities in pure cellulose. Levi and Preston (1965) modified Roelofsen's theory by taking into account the need for enzymes other than cellulase and considered that the transfer of enzyme attack from one microfibril to the next must occur at a paracrystalline region of the recipient microfibril. In their oppinion the constrictions between cavities were due to restricted release of enzyme in the septal area of the hypha.

Liese (1970) suggested there was a fluctuation in the release of enzymes from the hyphal tip in conjunction with enzyme inhibition by metabolic products, such as toxic phenolic groups, resulting in active and inactive wall degrade producing the typical cavity shape.

Findlay (1970) showed by transmission electron microscopy that

the slopes of the conical cavities were extremely smooth and, with Fuller (1970), regarded lignin as a physical barrier interfering with free diffusion of the cellulase enzyme system resulting in localised degradation, producing cavities.

Nilsson (1974b and c) demonstrated that soft rot cavities could be produced in cellulose fibres, thus refuting Roelofsen's (1956) theory, and in a study of a wide range of soft rot fungi confirmed Levi and Preston's (1965) findings that cellulase, xylanase and mannanase are produced by the active hyphae.

Zainal (1976a and b) indicated that lignin might have an inhibitory effect to produce cavities and later put forward a theory that the cavity shape and proboscis hyphae development arise from sudden changes in the physiological activity of the hyphae brought about by unknown stimuli, resulting in periodic enzyme restriction, Zainal (1978). Fluctuations in the ectoenzymatic activity at the hyphal tip (Liese, 1970) accounted for the proboscis hyphae growth sequence and acceptance of Levi and Preston's (1965) diffusion rate model gave rise to the cavity shape. It was suggested that the inhibitory factor might be lignin or hemicellulose breakdown products and that the resistance factors of the S_3 might provide a clue to the identity of the inhibitory component.

Leightley and Eaton (1977) filmed the process of cavity formation by Halosphaeria mediosetigera in Pinus sylvestris clearly showing the phased growth of the proboscis hypha. After extension, the fine cavity around the proboscis hypha (0.2µm in diameter) enlarged laterally along its entire length, with associated hyphal expansion, and the cavity continued its lateral development without increase in length

even though the hypha had reached its maximum diameter of about 1.-1.5µm. Linear extension of a new proboscis hypha initiated the next phase of cavity development, and so on. They suggested that the enzymatic action on the cell wall may be further facilitated by the presence of a mucilaginous sheath around the hypha inside the cavity. Sheaths for some wood destroying fungi had already been demonstrated by Schmid and Liese (1965), Schmid (1966) and Maret (1972).

The most recent theory, proposed by Preston (1979) continued the ideas of Levi and Preston (1965) and put forward a testable mathematical model on the basis of diffusion rates and enzyme action on successive paracrystalline regions. The final shape of the cavity being determined by the surface area of the hypha involved in active enzyme release. This latter explanation, with the cavity increasing in length and width simultaneously but at different rates, appears to contradict the observations made by Leightley and Eaton (1977).

Further discussions on cavity formation and ideas on their conception will be made in part IV. Details of literature of soft rot fungi and their action on wood can also be found in Zainal (1975).

Studies on the chemical effects of soft rot fungi have been mainly limited to Chaetomium globosum on beech wood (Savory and Pinion, 1958; Levi and Preston, 1965; Seifert, 1966) though Nilsson (1974d) studied a range of organisms for their production of cellulases and hemicellulases.

Cellulose is removed faster than the hemicelluloses, measured as a percentage of the original amounts, with glucose and mannose removed at a constant rate and more rapidly than other wood sugars (xylose, arabinose and galactose) which are removed at an increasing rate, (Levi

and Preston, 1965). Soft rot fungi definitely deplete lignin although at a much slower rate than the carbohydrates (Savory and Pinion, 1958; Levi and Preston, 1965; Seifert, 1966).

Sinner et al (1976) developed the pre-cellulytic system theories of Bailey et al (1968) by showing that the hemicelluloses protect the cellulose from the cellulase enzyme systems that are not acting in conjunction with hemicellulases.

White rot

Severely white rotted wood has a bleached appearance and is extremely light, with strength loss being proportional to weight loss (Jutte and Zabel, 1974). White rot fungi belong to the Basidiomycetes and, in general, preferably attack hardwoods above ground and show equal preference for soft or hardwoods in ground contact situations with, perhaps, even a predominance for the former (Scheffer, 1973).

White rot hyphae have been reported to first extensively colonise the vessels or rays during the attack of hardwoods, entering the fibres only as decay progressed (Scheffer, 1936; Cowling, 1961; Greaves and Levy, 1965). Wilcox (1968), however, found hyphae in almost all the cells early in hardwood decay, although they were more numerous in rays and vessels. Jutte and Zabel (1974), using the S.E.M., observed numerous hyphae lying against the walls of vessels, with occasional pit penetration. Large and small hyphae were evenly dispersed, with extensive lysis regions being associated with the small hyphae. In softwoods the hyphae were present in all cells in the early stages but were more numerous in rays and resin canals (Wilcox, 1968).

In the early stages of decay some white rots penetrated pits instead of producing bore holes (Scheffer, 1936; Cowling, 1961;

Schmid and Liese, 1964; Greaves and Levy, 1965; Wilcox, 1968; Bravery, 1971, 1972; Jutte and Zabel, 1974) but eventually bore holes were produced as well (Wilcox, 1968; Jutte and Zabel, 1974). Bore holes were more numerous in the advanced stages of decay by white rot than brown rot (Wilcox, 1968) but the reverse situation was found by Cowling (1961). Kisser and Lohwog (1937) noted that the white rot fungus Fomes Hartigii preferentially degraded latewood tangential walls and, together with the results of differential swelling rate tests, attributed this to denser earlywood and radial latewood walls. Liese and Schmid (1966) found bore holes of Fomes pini more prevalent in tangential walls and attributed this to differences in lignification with the first signs of deterioration being shrinkage of the tangential walls of the first few rows of latewood tracheids.

Bore holes become enlarged with duration of attack and may lead to large openings between cells, Liese (1970). White rot fungi progressively degrade ray cells (Greaves and Levy, 1965) and greatly enlarge pit canals (Scheffer, 1936; Cowling, 1961; Jurášek, 1964; Wilcox, 1968; Bravery, 1971, 1972) resulting in bore holes and enlarged pit apertures becoming indistinguishable in the later stages of decay (Wilcox, 1968). The development of bore holes was by enzyme release from hyphal tips, as described by Proctor (1941). Hyphae are also capable of lateral enzyme release (Cartwright and Findlay, 1943; Cowling, 1961; Liese, 1965a; Liese and Schmid, 1966). Even in advanced decay the shape and outward appearance of the wood is still maintained (Scheffer, 1936; Cartwright and Findlay, 1943; Wilcox, 1968) though, Greaves and Levy (1965) found structural loss in advanced white rot of beech.

White rot ectoenzymes are capable of degrading all substances of the lignified cell wall (Liese, 1970) although the fungi have been subdivided into the following two groups based on their modes of wall dissolution by Meier (1955) and Liese (1970). The simultaneous rots degrade the lignin and carbohydrate fractions together, whereas, the white rots first remove the lignin before attacking the carbohydrates (Meier, 1955). This confusing terminology could be eliminated if the fungal grouping was based on the ultimate capacity for wall lysis.

Using light microscopy, a progressive thinning of the degraded walls can be observed in both hardwoods and softwoods (Scheffer, 1936; Cowling, 1961; Liese, 1970), but electron microscopical examinations (Meier, 1955; Cowling, 1961; Liese, 1970) reveal the process to be less uniform. Along the young hyphae lysis zones of restricted width occur in which the cell wall substances undergo alterations and one layer after another is affected, the initiation being indicated by the degraded warts of the warty layer, when present (Liese, 1970). Jutte and Zabel (1974) indicated that in the lysis of beech by Polyporus tulipiferus a copious slime envelope may be involved. The components of the various wall layers seemed to be almost totally absorbed by the hyphae, as no residues were evident in replicas, (Schmid and Liese, 1964). This supported Cowling (1961) who, on the basis of chemical analyses, stated that the wall substances were only depolymerised to such an extent that the products could be used by the fungal metabolism. Progressive decay of layers gave rise to channels in surface replicas and notches when viewed in section, Liese (1970). Channels were strikingly demonstrated by Bravery (1971, 1972), who called them erosion troughs, using the S.E.M. in a study

of Polystictus versicolor degrading Scots pine tracheids and beech vessels, with a prominent central ridge in the latter. During further lysis neighbouring zones unite so that larger regions became affected leading to the cell wall thinning so frequently observed in light microscopy. The width of the lysis zones remains nearly the same, therefore, new overgrowth of hyphae is required for progressive thinning (Liese, 1970; Bravery, 1971).

Rhomboid cavities similar to those of soft rot were observed in the S_2 (Liese and Schmid, 1962; Courtois, 1965; Liese and Schmid, 1966) and Liese (1963b) concluded that such cavities may be caused by all types of wood destroying fungi that hydrolyse cellulose. There was no evidence of hyphae in these cavities and it was presumed that the fungal cellulase had diffused through the S_3 (Liese and Schmid, 1966). Meier (1955) reported that the S_3 showed resistance even to the action of certain white rot fungi. The ability of the enzymes to diffuse away from the hypha was also postulated by Cowling (1961) based on his observations that thinning occurred at about the same rate in cells, with or without a hypha present.

Wilcox (1968), using sweetgum fibres and Bravery (1971), with beech vessels, have found evidence for the white rot degradation of lignin being slightly preferential to that of cellulose resulting in a cleaving of the microfibrils ahead of the cellulase activity.

The compound middle lamella appears to be the most resistant cell wall layer to white rot attack (Meier, 1955; Cowling, 1961; Wilcox, 1968) although the vessels and rays of sweetgum were also reported to be resistant (Wilcox, 1968). Attack on pit membranes was the only decomposition of the middle lamella observed in white

rot attack, producing a 79% weight loss (Cowling, 1961). Eventually the compound middle lamella is attacked in the more advanced stages of decay (Meier, 1955; Wilcox, 1968).

The rates of production and utilisation of degradation products are approximately equal and the polysaccharides and lignin remaining in white rotted wood, at various stages of decay, are not very different in property from these substances in sound wood (see Kirk, 1973).

Lewis (1976, 1977) concluded that the occurrence of white rots in hardwoods and softwoods is dependant on their natural enzyme activity. Those with greater mannanase production being dominant on softwoods and those with more xylanase on hardwoods.

Aims of the present work

The latest comparative studies on wood decay micromorphology of brown, soft and white rots were made by Bravery (1971, 1972) using light and scanning electron microscopy. Developments in transmission electron microscopy of soft rots (Findlay,1970; Zainal, 1975) have indicated that detailed analyses of wood decay mechanisms requires high resolution, high magnification studies employing the electron microscopes.

This project, therefore, aimed at making a comparative study, using S.E.M. and T.E.M., of brown, soft and white rot decay in birch (Betula sp.) and Scots pine (Pinus sylvestris), especially the early stages, and applying more recent techniques and procedures. The selected representatives of each decay type were:-

Brown rot - Coniophora puteana (Schum ex Fr.) Karst.

Soft rot - Chaetomium globosum Kunze ex Fr.

White rot - Coriolus versicolor (L. ex Fr.) Quel.

Emphasis was placed on preparative procedures, as it was soon apparent that these had not been adequately documented (with the possible exception of Zainal, 1975) in previous work on decayed wood. Attempts at reducing specimen artefacts in S.E.M. preparations were made by introducing the Critical Point Drying technique, in comparison with the more frequently used air drying methods, to the study of fungi in wood. Methods and apparatus were selected, developed and analysed in an attempt to achieve S.E.M. and especially T.E.M. preparation procedures from which consistent and reproducible results could be obtained.

The possible role of mucilage in wood decay has already been tentatively indicated (Liese, 1970; Leightley and Eaton, 1977) and a method was therefore developed to preserve and examine such a delicate material in the T.E.M.. By applying this preparation procedure to the decay studies the significant presence of mucilage in certain decay type micromorphologies could be demonstrated.

PART I

SCANNING ELECTRON MICROSCOPY

1. INTRODUCTION

Since 1965 the Scanning Reflection Electron Microscope (S.E.M.) has been available for the examination of surfaces. Within the field of wood science the S.E.M. was first used by Wagenfuhr and Zimmer (1968) in a study of wood cell walls. However, Findlay (1970) expanded the use of the S.E.M. in wood science research, after Findlay and Levy (1969) had indicated the potential of this instrument, not only for wood anatomy but also for wood decay studies.

The S.E.M. has subsequently been extensively used by many workers to increase our knowledge of wood anatomy, Scurfield and Silva (1970), Banks (1971), Meylan and Butterfield (1972), Greaves (1973), and of wood decay, Bravery (1971), Jutte and Levy (1971 a & b), Jutte (1973), George (1974), Jutte and Zabel (1974), Levy (1974), Sach et al (1974), Zainal (1975), Leightley and Eaton (1977) and Crossley and Levy (1977).

The basic application of the instrument, a Cambridge Stereoscan II A, to the study of decayed wood in this work was very much the same as described by Findlay (1970) with the exception that new preparation techniques have been examined to try to improve the specimen quality together with optimising the microscope performance specifically for the individual specimens under observation.

The introduction of Critical Point Drying into the specimen preparation was to reduce the effects of surface tension damage to fungal hyphae, during dehydration, as occurs in normal air drying methods. The Critical Point was defined in 1880 by Ramsay as "that point at which the liquid, owing to expansion, and the gas, owing to compression, acquire the same specific gravity and consequently mix with each other." Every liquid has a characteristic critical temperature

above which it can exist in only one fluid phase whose surface tension is zero, Anderson (1951).

This Critical Point Drying technique was first applied to biological tissues by Anderson (1951) with a rather crude but effective 'bomb' type apparatus. Since then it has been regularly applied to research, Cohen et al (1968), Boyde and Wood (1969) for both S.E.M. and T.E.M. applications. Unfortunately the Critical Point of water is 374.0°C which precludes the use of the technique directly on untreated biological tissues. Other liquids such as carbon dioxide, nitrous oxide and Freon 13 have more convenient critical temperatures of 31.1°C, 36.5°C and 28.8°C respectively. It is these liquids which are employed in the preparation of biological tissue.

The tissue water is removed by solvent extraction with either ethanol or acetone which is replaced by one of the above transition fluids which will exhibit the desired effect of changing from the liquid to the vapour state, instantaneously, without surface tension, at the Critical Point.

By using a sealed vessel to contain the specimens and liquid during warming from room temperature to the critical temperature the combined expansion and compression effects are achieved in one operation. This simple design has resulted in a number of commercial instruments being available and in this work the Polaron E3000 critical point drier was used with carbon dioxide as the transition fluid.

For most work on wood anatomy this technique is a considerable advance in specimen preparation. There could, however, be instances where the solvents used might have an effect on the specimen to be examined and this should not be forgotten when using this technique.

2. MATERIALS

2.1 Wood

The wood species were selected as having been extensively investigated previously and included Scots pine, specified in British Standard 838 (1961) for test work on evaluation of wood preservatives against fungal attack.

Scots pine:- Pinus sylvestris L.

Birch :- Betula sp.

Only the sapwood was utilised as it was readily degradable by the fungi under laboratory conditions. The material was carefully selected so as to represent sound, clear wood of medium rate of growth.

2.2 Fungi

Three test fungi were selected as being representative of the three rot types under examination.

Coniophora puteana	F.P.R.L. 11E	Brown rot
Chaetomium globosum	F.P.R.L. S70L	Soft rot
Coriolus versicolor	F.P.R.L. 28A	White rot

These fungi were sub-cultured continuously on 2% malt agar in an effort to maintain vigorous and active growth. No attempt was made to induce high degrade rates by selecting out strains grown on a wood nutrient base or other such method.

3. METHODS AND THEIR DEVELOPMENT

3.1 Test block format

Zainal (1975) recommended the use of 3mm. orientated cubes of the test wood as a suitable block for innoculation. However, such a block created preparation problems, due to its extremely small dimensions, especially with the introduction of new safety regulations for the use of circular saws.

It was decided that the format should be changed to a more easily prepared block. To be acceptable as a test block it had to satisfy the following requirements:

1. The block had to be of a convenient size to prepare by the normal methods of planing and sawing.

2. The block had to be small enough to be economic on the test wood species, as this might be limited, and yet satisfy the requirements laid down in 1.

3. The block had to be such that it would decay within reasonable test periods to prevent time consuming long term incubation periods.

4. The block had to be of a size such that microtomy of its external faces was possible without any further trimming in the sledge microtomes available in the laboratory.

The blocks used by previous workers usually presented cuboidal or rectangular formats, where either the faces were TS = RLS = TLS, as in the former, or RLS > TLS > TS, as in the latter. (See fig. A). It has been established that during colonisation of a block of wood the rate of penetration is variable with the exposed face and that the penetration rates for the three face types are TS > TLS > RLS. This really is representative of the proportion of open ended cell elements, ie. TS = tracheids, vessels, fibres and parenchyma, TLS = rays and RLS little except the natural crossfield and bordered pits.

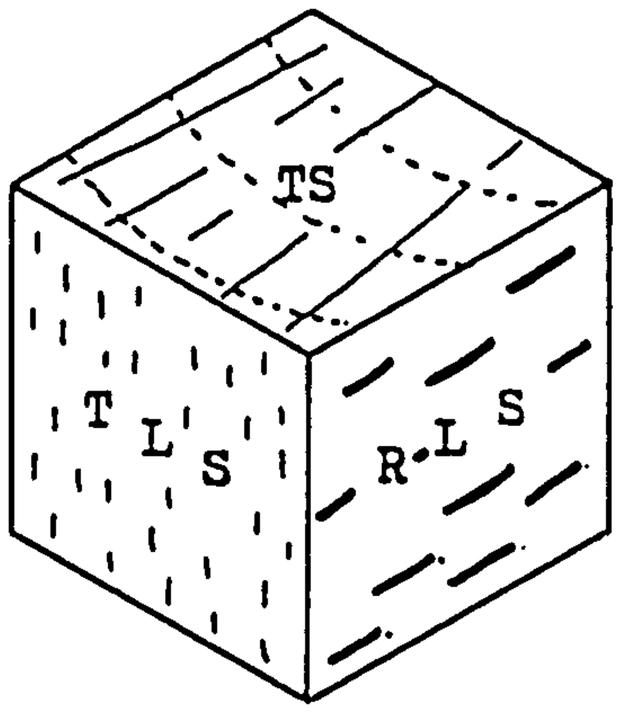
From this the most easily penetrated block would have face areas of TS > TLS > RLS but the final block format selected was that of fig. B. This resulted in a test block with a transverse face representing 65% of the total surface area. These were prepared from selected half-rounds or two inch through and through sawn timber by the process detailed in fig. C. This method reduced the differences between the replicate blocks used in the test to a minimum.

3.2 Culturing mechanisms

Previous workers, including Zainal (1975), have found a 2% malt, 2% agar medium satisfactory for culturing these fungal species for decay tests on wood. Plastic meshes, Bravery (1972), to prevent waterlogging, were placed onto the culture medium surface to support the blocks clear of the agar but still accessible to the fungi. The fungi were cultured on the 2% malt, 2% agar in a constant temperature room at 22°C for one week. After this period the hyphal growth front was usually close to the side of the petri dish. Plastic rings ($\frac{1}{8}$ inch diamond mesh, 8 cm outer diameter and 2 cm inner diameter) were cut and autoclaved between aluminium foil before placing onto sterile 2% malt-agar plates. 6 mm core innoculi from the hyphal fronts were cut and positioned in the centre of the ring and the dishes incubated at 22°C for two days.

Because small dimension timbers were used in the cutting of the two inch planks the annual rings present within the blocks showed a slight curve. Thus it was possible to distinguish between the two tangential faces of the block. The younger growth rings were selected as being the front with which the fungal hyphae made contact first and this was called the leading face of the block.

FIG. A



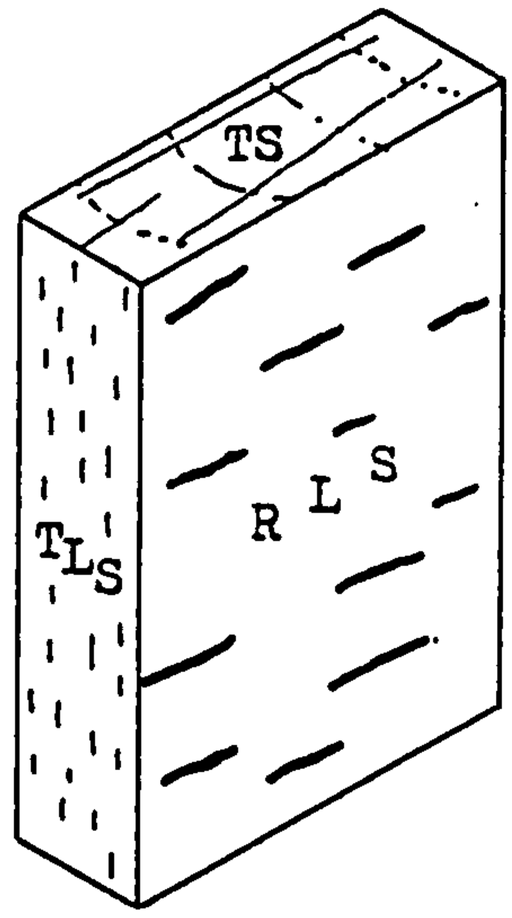


FIG. B

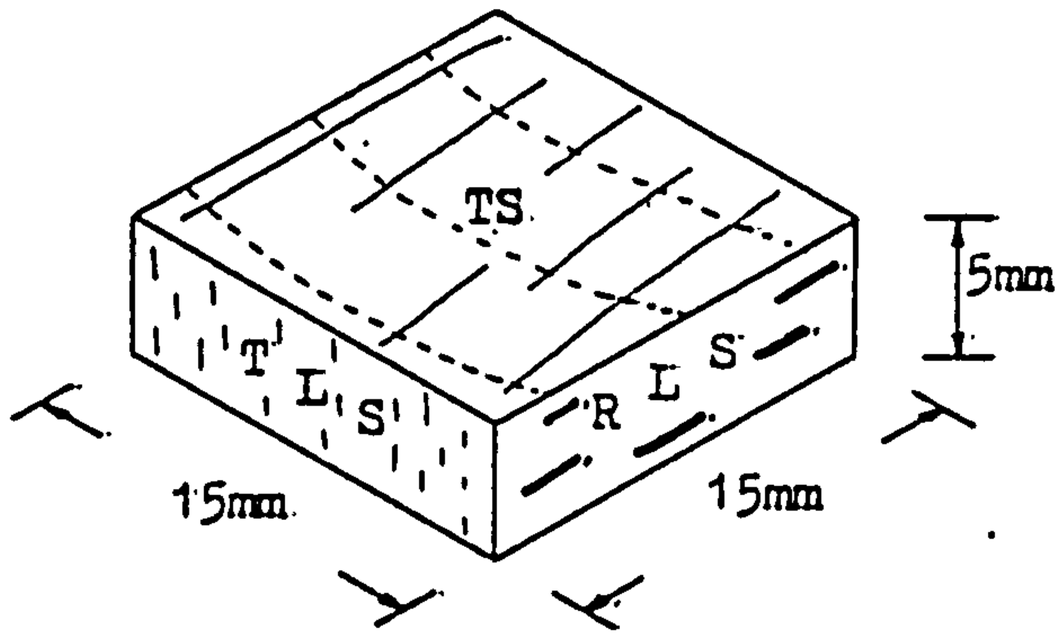
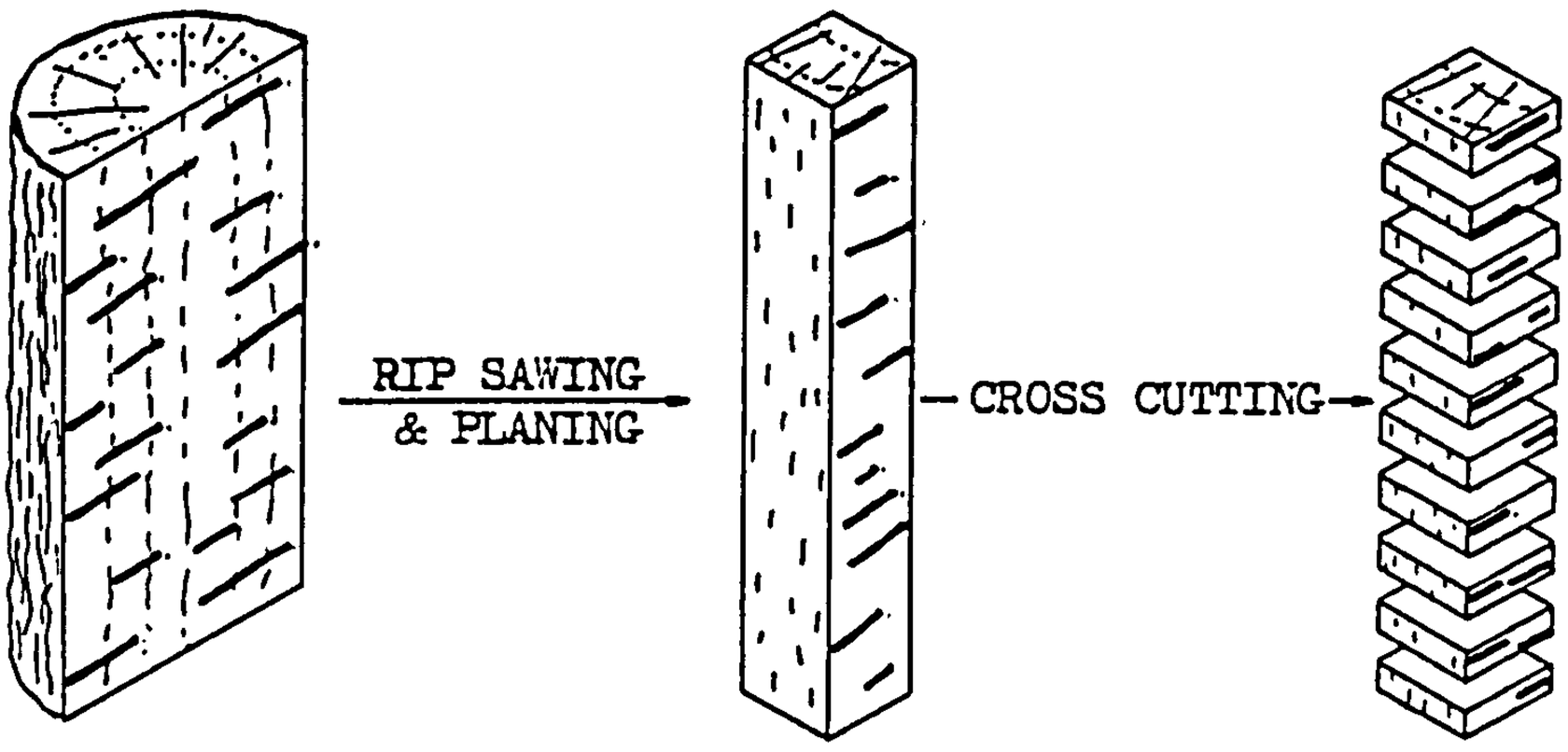


FIG. C



HALF ROUND OR 2"
THROUGH & THROUGH

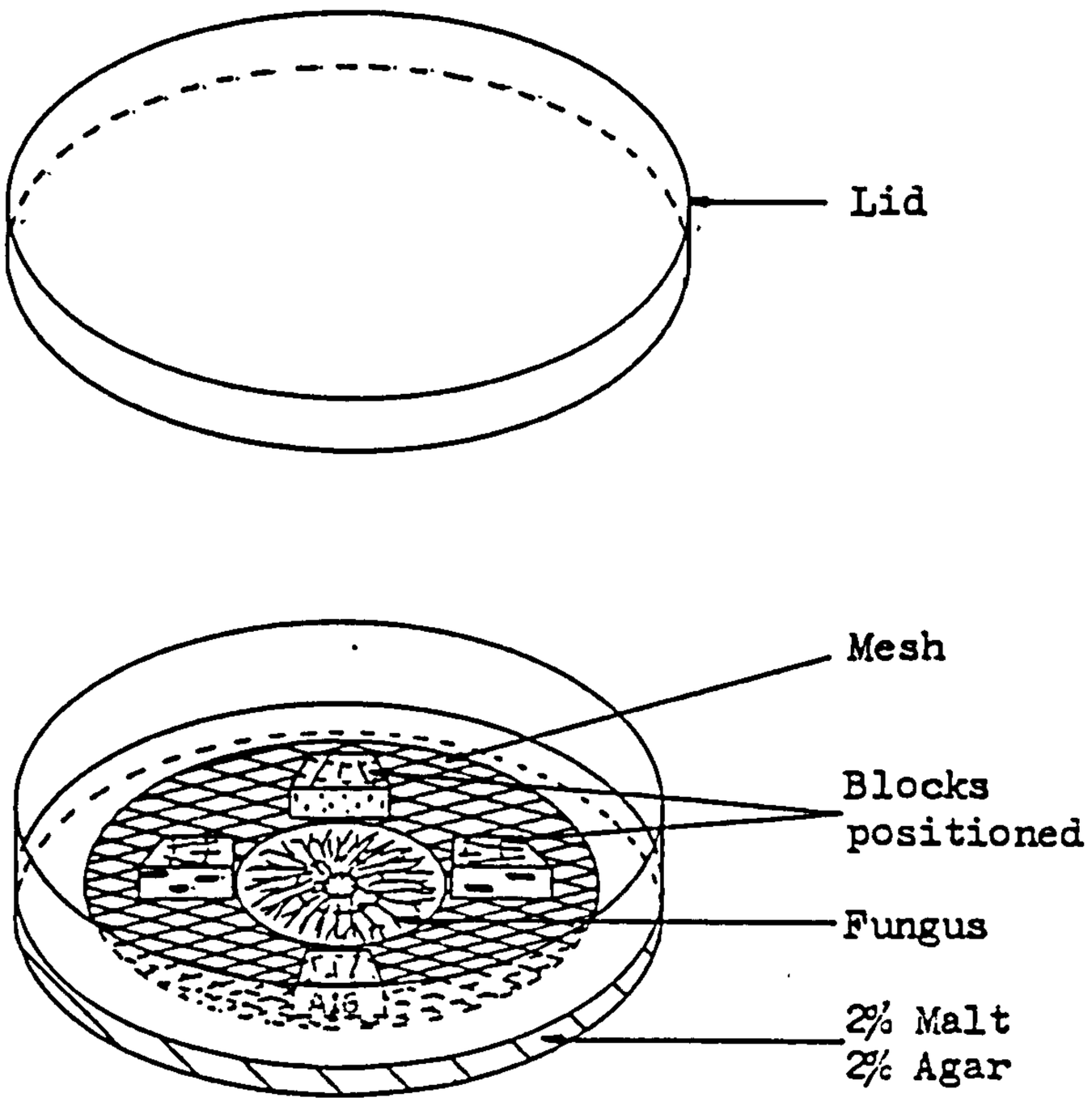
STICKS
VARIOUS LENGTHS
x 15mm x 15mm

SLICES
15mm x 15mm x 5mm

The trailing face was labelled with a code number, for example A. 16, identifying the block as being slice 16 from stick A, see fig. C. All the blocks were labelled in this way and sterilised by autoclaving at 120°C for 1 hour. After the two day culture incubation the blocks were positioned on the mesh with the leading face just touching the actively growing hyphal front. See fig. D. A block positioned in such a way exposed a large transverse face to the hyphae colonising from below and the second most rapid colonisation pathway, the tangential face, was presented to the surface hyphal front.

By preculturing in this way, then at time zero when the blocks were placed it was certain they were in direct contact with the hyphae. This was very important when short incubation periods were being studied.

FIG. D



It was proposed that a study of the decay process should be carried out at different incubation periods. These times were 2 days, 5 days, 1 week, 2 weeks, 3 weeks, 4 weeks, 6 weeks and 8 weeks. Two replicate blocks, ie. adjacent slices of each wood species per fungal type, were used; thus for two test woods with three test fungi twelve blocks were required, six of Scots pine and six of birch. With the eight time periods this resulted in 96 blocks which were arranged within the culture dishes such that the least amount of disturbance to the system occured when sampling. Four blocks, 2 replicates of birch, 2 of Scots pine, were placed in each dish. In this way only three plates had to be removed from the incubation room at each sampling.

3.3 Specimen preparation

3.3.1 Preparation of the specimens from the decayed block

After their relevant incubation periods the blocks were removed from the dishes and fixed by being plunged into a 2.5% aqueous glutaraldehyde solution (practical grade). The specimens were kept under fixative until required for sectioning.

To cut the specimens accurately from the blocks required the use of a sledge microtome and a modified stereo binocular microscope, fig. E. The microscope was set up to view the microtome in a horizontal plane and a cross-wire graticule in one eyepiece was aligned with the plane of the knife edge secured in the sledge. See fig. F. The decayed block was clamped in the microtome holder with either a TLS or RLS face uppermost but such that the leading face of the block was cut first by the knife. See fig. G. Using the holder adjustments and viewing through the microscope, with

FIG. E

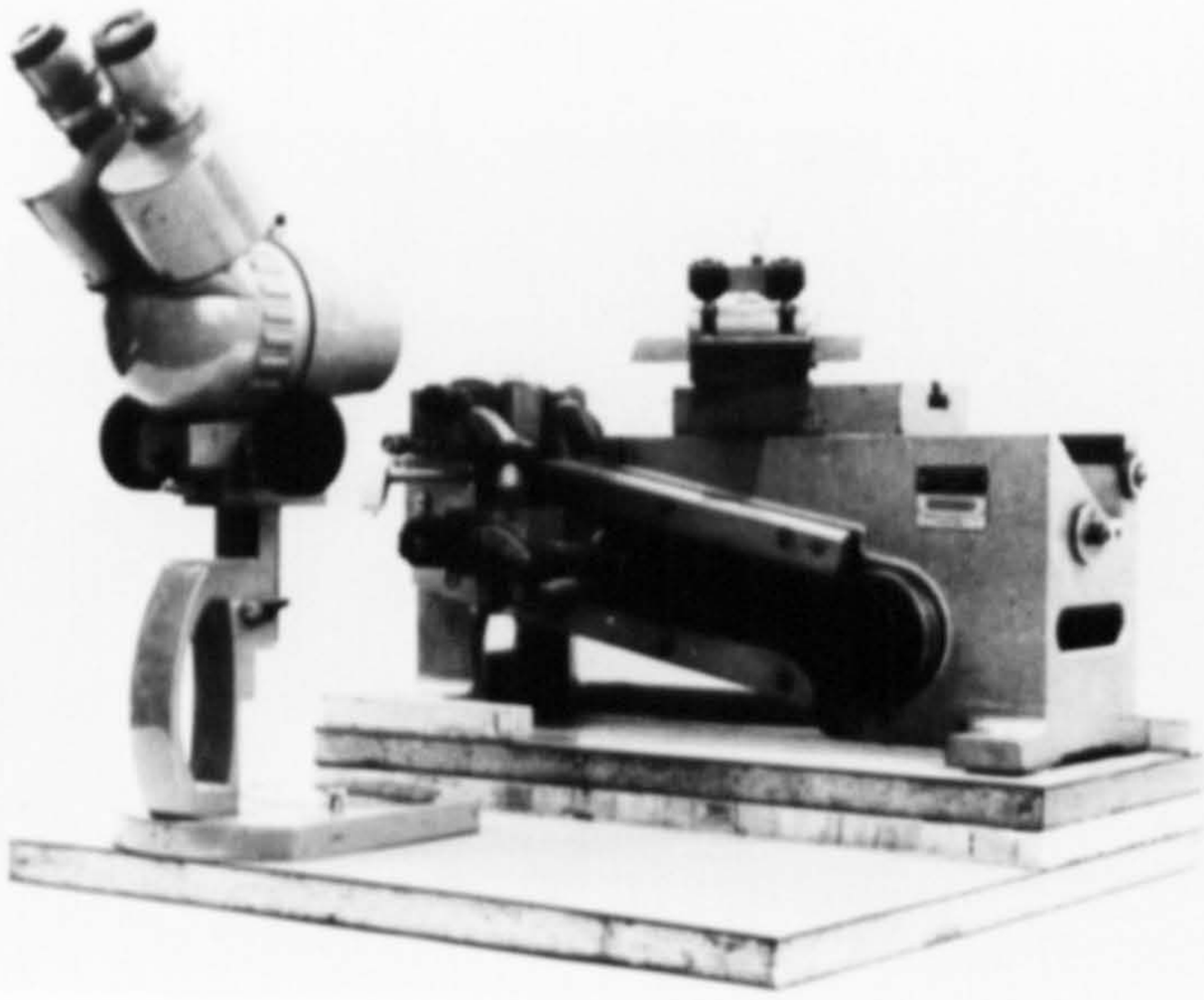


FIG. F

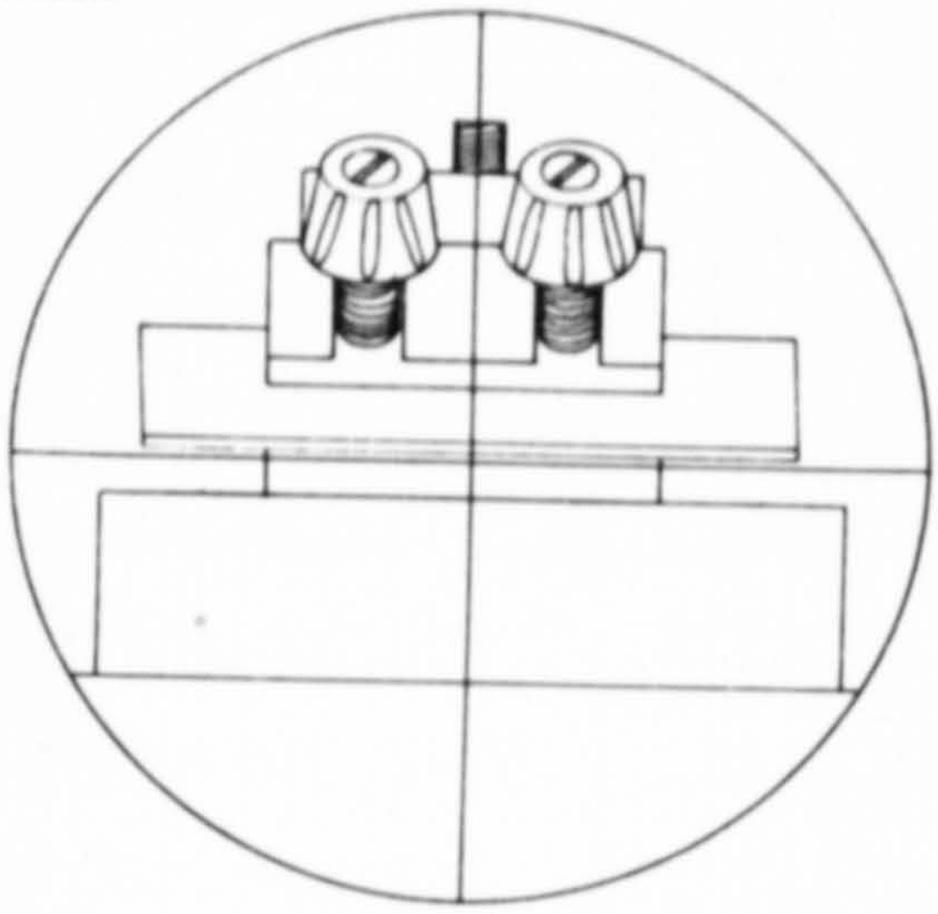


FIG. G First orientation step

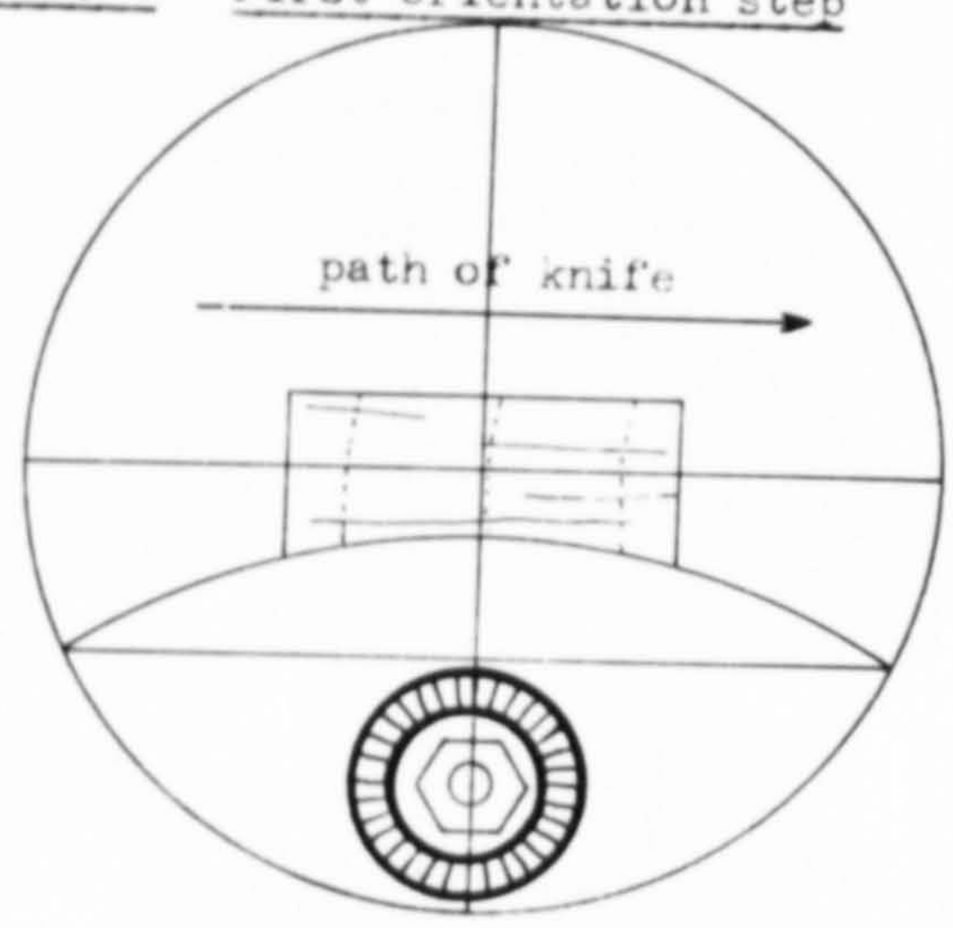


FIG. H Second orientation step

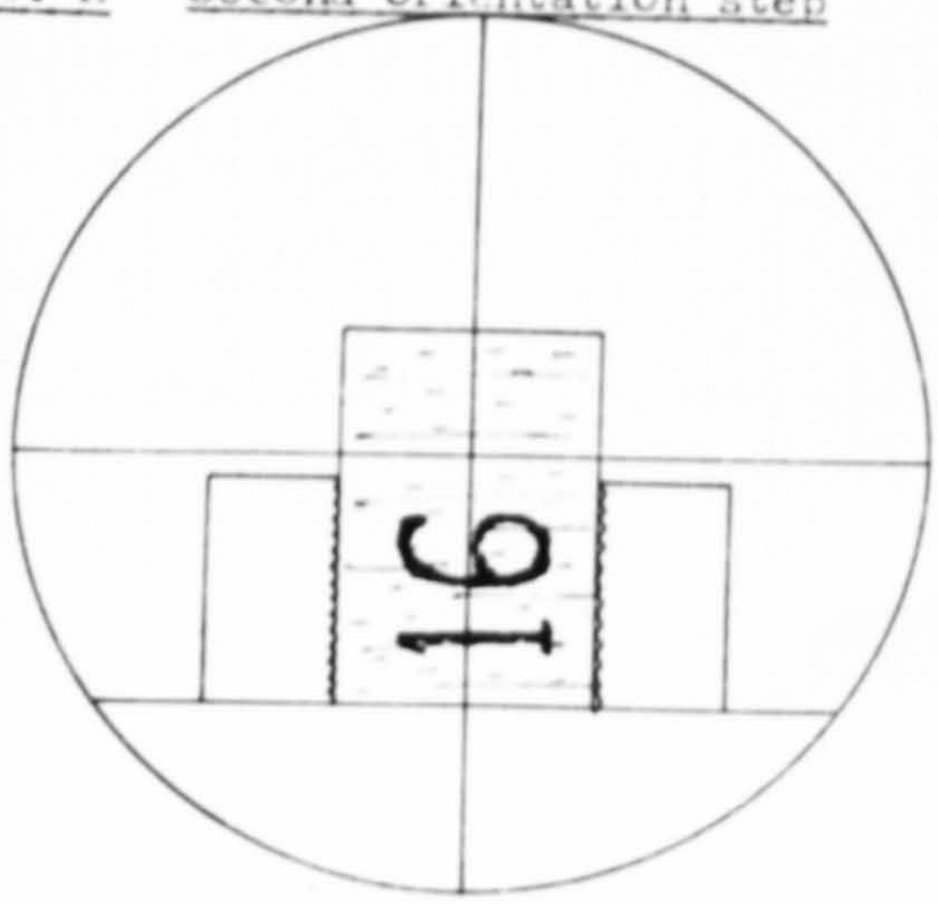
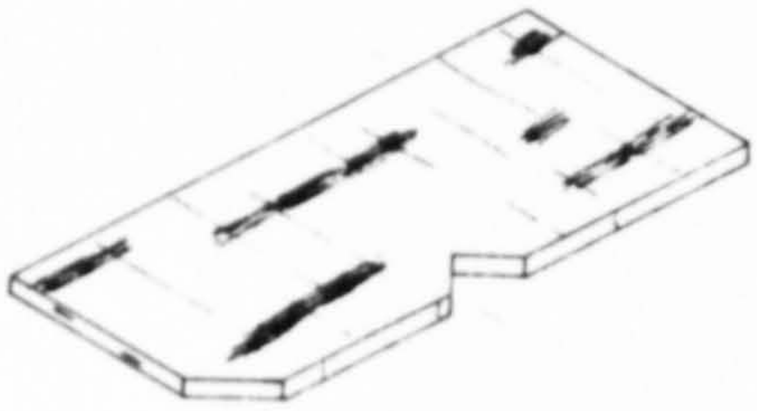


FIG. I

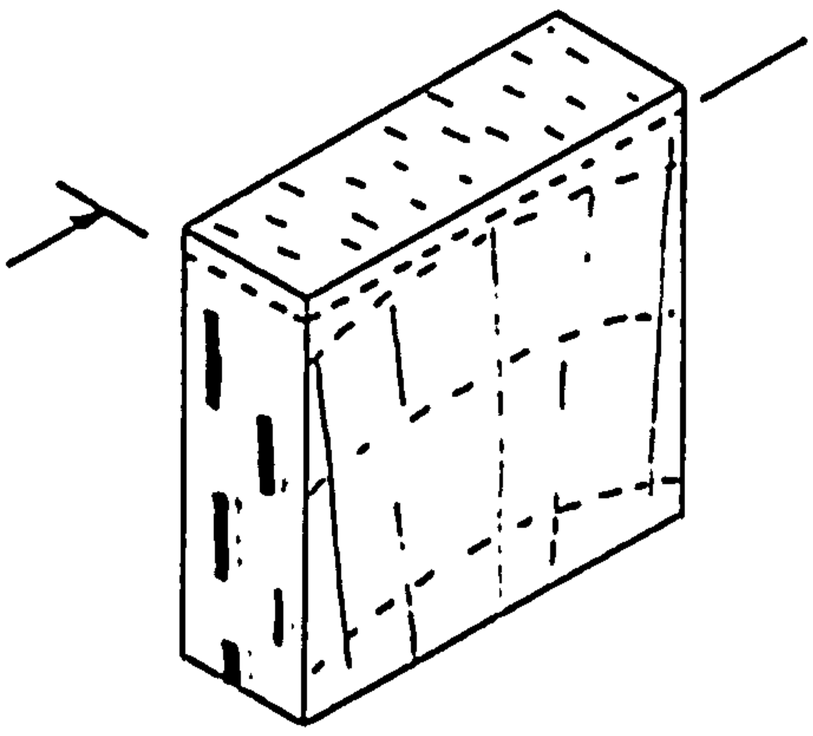


good illumination the block was orientated.

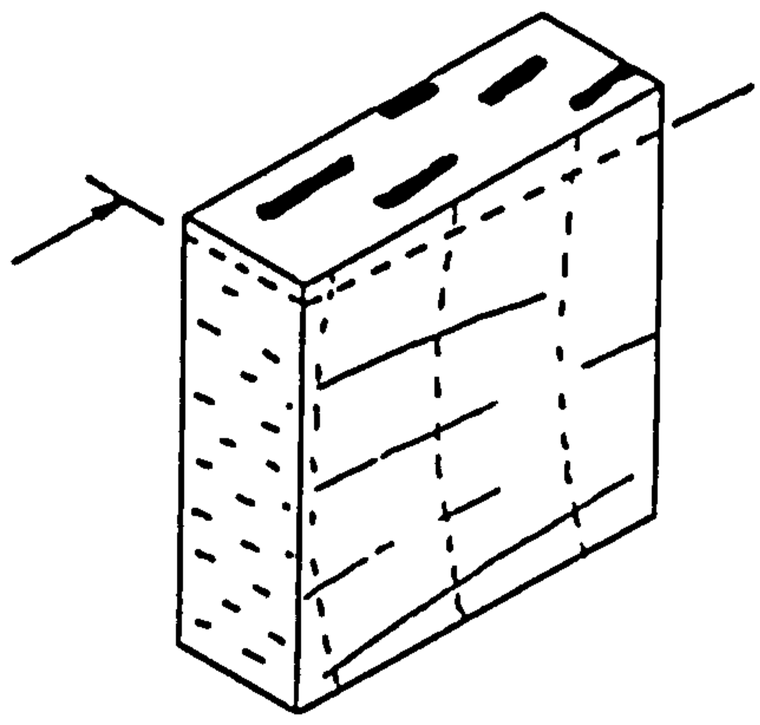
The initial setting up of the cross-wire with the knife edge must not be altered during the alignment procedure. Firstly, the block was tilted about an axis at right-angles to the sledge path to bring the required plane of section, for example RLS, as viewed on the TS face, into line with the cross-wire, see fig. G. This correctly aligned the block along one axis. The second alignment was carried out by rotating the stage through 90°, to view the side of the block, in this example the tangential face. Then with the second set of adjusters the axial plane of the wood elements was aligned with the cross-wire, see fig. H. This completed the orientation procedure ensuring that the cutting plane of the knife was along the line of the desired section. The block was then cut until complete sections were produced at which point a few (30 micron) sections were cut to "clean up" the block face before a thick 100 micron cut was made. Sections produced in this way were then notched in one edge and an adjacent corner with a single edged razor blade so as to identify the clean face (see fig. I.) before placing into a compartmentalised petri dish (Sterilin), clean face uppermost, under the fixative solution for storage. Throughout the sectioning sequence the block was kept moist with fixative solution applied with a pasteur pipette.

By reorientating the block then both radial and tangential sections could be produced from one decayed block and the resulting clean corner could be utilised as a three dimensional specimen, if so desired. See fig. J.

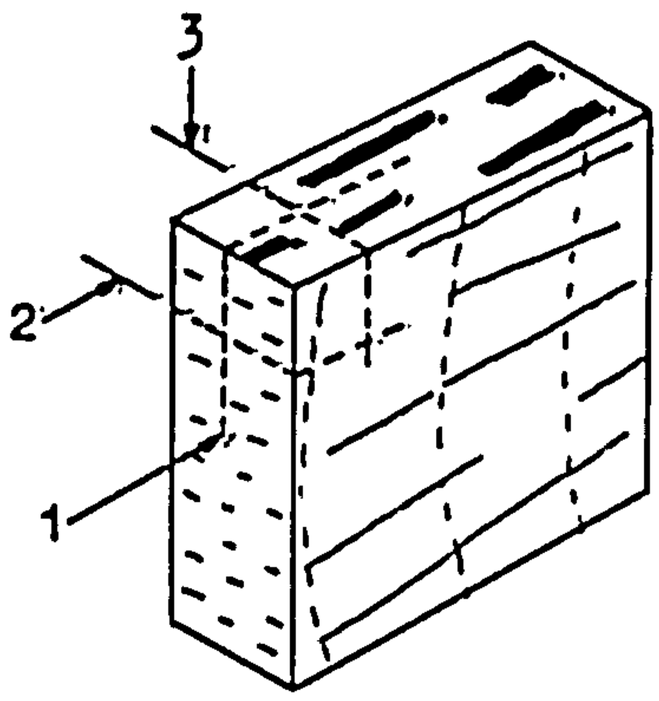
FIG. J



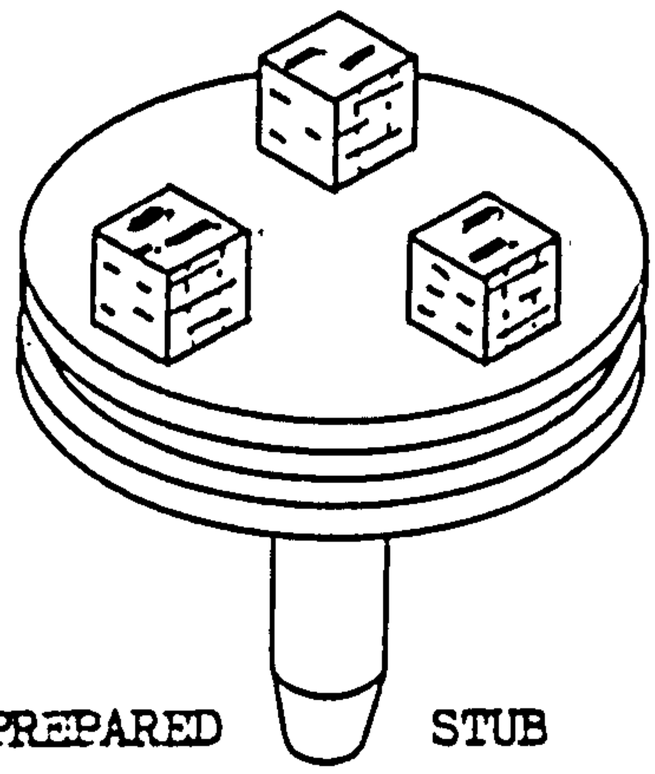
T.L.S. SECTIONS



R.L.S. SECTIONS



SAW CUTS: 1,. 2,. & 3



PREPARED STUB

The standard specimen support stubs for the Cambridge IIA S.E.M. are 12 mm in diameter and together with a normal working distance of 12 mm limits the maximum dimensions of any specimen to approximately 1 cm^3.

Because of the time lost in letting the microscope down to air during specimen changes then the more specimens there are on a stub the less operating time is lost. Therefore, a compromise must be reached between the maximum area of the specimen to be viewed ard the number of specimens per stub. A specimen dimension of 2.5 mm x 2.5 mm x 100 µm was chosen as being suitable in this study, allowing up to five specimens per stub.

By a combination of light miscroscope and dissecting microscope

observations the large sections were surveyed to select out the decayed areas which were cut out to the above format using a single edged razor blade and notched as before to indicate the clean surface. These S.E.M. size pieces were again stored under fixative ready for the subsequent preparation stages. For each variable two replicates were used such that a stub carried two TLS and two RLS pieces. Therefore, one stub represented one of the decay fungi on one of the test woods for one incubation period.

3.3.2. Dehydration methods

3.3.2.1. Air drying

This was achieved using the method of Findlay (1970). The small pieces of wood were laid, clean face uppermost, on filter paper in a closed petri dish at room temperature for several days. The filter paper was labelled to identify the pieces drying. Once dry the specimens were stored in a dessicator ready for the preparation of the stubs. Air dried material was prepared for only one incubation period, 6 weeks, as a comparison to the Critical Point Drying method which was used for all other preparations.

3.3.2.2 Critical Point Drying

Preparation of material by this method was more involved and as already outlined in the introduction first required solvent dehydration. However, it was clear from the number of variables in the preparation of the decayed specimens that even with mixing of wood types (which could be separated later by direct observation) the minimum number of variables during processing was 24, each being of two woods with two variables of two planes of section. It was impossible to separate out the decay types or the incubation times.

One operator could only process accurately to a timing schedule six dishes of material, thus only a quarter of the total material was prepared for Critical Point Drying at any one time.

The dehydration was carried out in glass stain blocks using ethanol in the following series:

Fixative solution (2.5% Glutaraldehyde)

25%	ethanol / distilled water	for 2 hrs
50%	ethanol / distilled water	for 2 hrs
75%	ethanol / distilled water	for 2 hrs.
100%	ethanol	overnight
100%	ethanol	for 2 hrs

The fluids were changed by the careful use of a fine pasteur pipette ensuring that the specimens were kept under liquid at all times. Unfortunately ethanol is immiscible with liquid CO_2 and therefore had to be substituted with acetone or Freon 113. If the specimens were such that dehydration in acetone was possible this would have reduced the work involved. However, it was the author's belief that ethanol dehydration was less aggressive and therefore less likely to cause cellular distortions and so was used in this work. Therefore a second substitution series from ethanol to acetone was needed.

100%	ethanol	
25%	acetone / ethanol (100%)	for 2 hrs
50%	acetone / ethanol (100%)	for 2 hrs
75%	acetone / ethanol (100%)	for 2 hrs
100%	acetone	overnight
100%	acetone	for 2 hrs

The apparently excessive infusion times were necessary to ensure that all traces of the previous fluid had been removed. Although Freon 113 could have been used, the scale of preparation involved here precluded this costly chemical. Once the specimens were in absolute acetone they were transferred to a dessicator and glass lids placed over the stain blocks to reduce evaporation. This was

necessary due to the limited number of specimens that could be dried down at any one time.

Three tissue baskets were available with the Critical Point Drier and these were positioned in the transfer boat. The boat was then filled with acetone and, with a soft camel hair brush, the contents of three of the stain blocks were transferred into the baskets and a note made of the contents of each. This transfer was carried out as quickly as possible to avoid air drying of the specimens.

Because of the limited capacity of the specimen boat a large number of drying runs were required to complete the preparation of all the specimens. This was not only tedious but also meant that cross comparison between specimens of different drying runs could be questioned due to their different treatments. What was required was a specimen holder which could process large numbers of the specimens at any one time so that interpretation of the results would be more accurate. To achieve this a specimen holder was designed capable of processing up to eighty different specimens, and the details of this device are contained in a paper included with the thesis.

The holder was made out of brass and contained twenty specimen chambers. Each chamber was 5 mm in diameter and 5 mm high with T.E.M. grids housed by plates acting as a "sieve" mechanism to contain the specimens but allow free flow of the various substitution fluids used in the preparation stages of the method. The relatively large volume of each chamber meant that four specimens could be accomodated with ease and where mixing of these specimens was not desirable then simple devices for partitioning the chambers could be constructed. With this piece of apparatus the equivalent of ten stubs could be processed in one operation, simply and effectively, with each

chamber holding two replicate samples. The specimens were loaded into the apparatus for dehydration and substitution, which was achieved by simply transferring the whole block through the various solutions. This design was used for the rest of the specimen preparations carried out for the S.E.M.

3.3.3. Final S.E.M. preparations

Before the specimens could be examined in the microscope they had to be secured to the stereoscan stub. The specimen details were written on small self-adhesive labels which were fixed to the underside of the stub. To assist in positioning the specimen on to the stub a drill chuck was set up below a dissecting microscope to enable the operator to view clearly and precisely the positioning of each specimen. By positioning the specimens with their longitudinal axes parallel to the radii of the stub, as recommended by Findlay (1970), the degree of specimen manipulation within the microscope was greatly reduced.

Standard methods of securing specimens were, double-sided Sellotape, Durofix and Silver Dag. These were rejected for this work because it was found that it was very easy to dislodge specimens from the double-sided Sellotape and Silver Dag unless they had been firmly pressed into the adhesive, which resulted in severe damage to the specimen surface. Durofix and Silver Dag to some extent had the tendency to rapidly form a skin which resulted in poor bonding. For good bonding this skin had to be broken, which invariably caused the adhesive to flood around and over the specimens. Durofix also had the serious drawback of producing very long thin strands of dry adhesive when applying the glue and positioning specimens, due to the withdrawal of tube and forceps from wet adhesive regions.

These strands projecting from the stub surface often made contact with the final lens of the microscope triggering a sensitive alarm devised to protect this lens from physical damage.

The adhesive selected was Rapid Araldite (Ciba Geigy) on the following counts:

1. The adhesive had a convenient setting time of about 10 minutes allowing the operator plenty of time for specimen orientation.

2. It did not form a skin until final polymerization was proceeding, whereupon the adhesive was rubbery and ineffective. Therefore, the specimens had to be positioned before the adhesive reached this condition.

3. The stub was smeared with adhesive using a cocktail stick and the specimens gently placed in the desired orientation. The nature of the adhesive was such that the specimens tended to sink into it providing excellent bonding without pressure.

4. Any fine strands produced during positioning of the specimens always disappeared on polymerization.

This resulted in well bonded, uncontaminated specimens capable of withstanding a certain amount of rough handling.

To provide storage boxes for the prepared stubs, $\frac{3}{8}$ inch slabs of polystyrene were cut to fit square petri dishes and a series of holes drilled into them which were coded for ease of specimen identification. The stubs were placed in these boxes and kept in a dessicator for coating.

Specimens which were natural conductors, for example metal surfaces, could now be examined in the microscope. However, wood is not such a material and if examined at this stage would lead to severe specimen charging, Findlay (1970). To overcome this problem the stubs should be coated with a conductive layer of carbon, gold-

palladium or other metals. This was usually achieved in a shadow coating unit, standard in most electron microscope units and was the method used by Findlay (1970), Bravery (1972) and Zainal (1975) in their work. However, this type of coating depends entirely on the full manipulation of the specimen during the coating process to ensure that all the fine recesses and holes within the specimen surface area have been coated with the metal, which is issuing from the evaporating point source. Failure to do this resulted in localised specimen charging and specimen damage by the beam. It was also very difficult to determine precisely the thickness of the layer of deposited metal on the specimen.

A new coating process called "sputter coating" has been developed in recent years and works on the principle of ion discharge. A number of designs are available on the market and the model used in this work was the Polaron E5000 coater. The principles of operation are briefly outlined below.

The instrument operates under a vacuum of about 1×10^{-3} torr, achieved by a good rotary pump. The specimen chamber of the instrument consists of three components.

(i) An anode plate of thin gold, approximately 8 cms in diameter.

(ii) The specimen securing stage in which six stubs are clamped and which represents the 'target' cathode.

(iii) A pipe leading to the space between anode and cathode for the introduction of Argon gas.

Once loaded with six stubs the chamber was closed and pumped out. The control of the gold deposition was determined by,

(i) The high tension (HT) between anode and cathode.

(ii) The duration of this potential.

(iii) The current between anode and cathode which is governed by the inflow of Argon into the discharge field.

With a HT setting of 1200 V and current rating of 40 mA, gold was deposited on the target at a rate of 240 Å/min. The eveness of the coating is due to the charge attraction of the gold ions due to the target possessing a high negative charge which is uniformly distributed over all areas of the specimen surface. The use of a very good insulator as the specimen adhesive has resulted in no adverse effects whatsoever on the quality of the specimen surface with this coating method.

The specimens were coated for two minutes leaving a 475 Å layer of gold on the material which was sufficient to eliminate specimen charging but not so thick as to reduce surface detail. Once coated the stubs were returned to the dessicator in readiness for observation..

3.3.4 Microscopy

The specimen examinations were made in a Cambridge Stereoscan Mk IIA. operating at 20 KV accelerating voltage. The final aperture was 100 µm in diameter and the specimens were tilted to approximately 45°.. Precision tilting was aimed at achieving the optimum signal to noise ratio.. Gamma function was used extensively to improve the final image where there was high specimen contrast, for example in cross-field and bordered pits and fungal bore holes. The nominal working distance was 12 mm (this was dependant on the specimen thickness) and the scan rotation facility was employed to give continuous variablility of the magnification between the coarse settings. Photographs were taken on Ilford pan F film which was developed in Promicrol for nine minutes at 24°C, stopped in Indical 1:40 (Acustop) and fixed in Ilford Hypam 1:4 for five minutes before thorough washing in filtered water, followed by deionised water, before drying.

4. RESULTS

In this type of study where the results are visual observations recorded as photographs it is impractical to attempt to include every observation made in the presentation of the work. From extensive examination of the specimens, selected areas were chosen as being representative and photographed together with unusual but prominent features. The total results available are a subjective representation of each characteristic observation made by the author. From these a number are presented as typical examples of the types of feature observed and as such represent only a fraction of the total recordings made on each feature.

The general pattern of colonisation for both birch and Scots pine was similar to that reported by previous workers, (Bravery 1972, George 1974), where primary colonisation via the vessels or tracheids, and to a lesser extent the rays, spread laterally into ray or fibre tissue. The results, in general, confirm the observations made by these earlier workers, although the interpretation, in the light of later work, is different in a number of instances. This study is concerned with the use of the techniques of electron microscopy to compare wood decay mechanisms and so high magnifications, giving greater detail of wall degrade, have been extensively used. This section deals only with the Scanning Electron Microscope (S.E.M.) but clearly the results given here must be used and discussed in conjunction with the results in parts II and III (p. 124 et seq.) before arriving at realistic conclusions.

The results are presented in the following way:-

4.1 Comparison of specimen preparations

4.1.1 General comments on preparation methods

4.1.2 Air dried material

4.1.3 Critical Point Dried material

4.2 Comparison of fungal types on each wood species

4.2.1 Brown rot, Coniophora puteana

4.2.1.1 on hardwood:- birch (Betula sp.)

4.2.1.2 on softwood:- Scots pine (Pinus sylvestris)

4.2.2 Soft rot, Chaetomium globosum

4.2.2.1 on hardwood:- birch (Betula sp.)

4.2.2.2 on softwood:- Scots pine (Pinus sylvestris)

4.2.3 White rot, Coriolus versicolor

4.2.3.1 on hardwood, birch (Betula sp.)

4.2.3.2 on softwood, Scots pine (Pinus sylvestris)

4.3 Mucilage

Specific details and points of interest in the micrographs have been indicated in the figure captions opposite each plate.

4.1 Comparison of specimen preparations

4.1.1 General comments on preparation methods

As described in the method section samples were prepared, with a range of incubation times, but from initial observations of this range it was evident that the degree of decay seen was dependant on the area of the specimen being viewed. Within any one block there was a range of fungal effect on the wood from early colonisation to, later, heavy wall degrade. The long term incubation periods were predominantly of the latter type (with the exception of Chaetomium globosum on Scots pine where little decay was observed) and short term periods gave rise mainly to the former pattern. However, intermediate time periods showed the whole spectrum of interaction within each block and, because of the time required to examine every specimen in detail, the study was restricted mainly to the four and six week material where the whole decay range could be examined in one specimen, especially the early lysis of the wall.

The usefulness of radial and tangential longitudinal sections was very apparent. Radial longitudinal surface views were more difficult to cut without damaging the specimen surface as the rays tended to act as planes of weakness causing shearing of the cell elements. Tangential longitudinal surfaces, on the other hand, were much easier to prepare 'clean' because sectioning the rays (in TS) stabilised the cutting plane. Sections in the radial plane, however, yielded more information on the interrelationships of the fungus and the different cell elements. This type of surface produced lumen views of bordered and cross-field pitting together with longitudinal sections of the rays and vessels. Tangential

views were more limited in the information obtainable for ray degrade but yielded more on the anatomical construction of the cross-field and bordered pits and the effect of the fungus, if present, on these regions.

On the basis of the above considerations, most observational work concentrated on radial longitudinal surface views although cross-reference to the tangential view was frequently employed. The ability of the system, described in the methods section, to produce planes of section of the desired orientation has been satisfactorily demonstrated, as can be seen in figure 51.

The micrographs presented in the results were taken at two gamma settings on the instrument and this has been indicated in the captions by the number in brackets after the figure magnification. The effective use of gamma can be seen by comparison of figures 12 and 13. By amplification of low signal (dark) areas otherwise lost information is revealed. The higher the gamma setting the greater the signal amplification but this is accompanied by a reduction in image contrast. In some of the micrographs a distortion of the image was apparent, especially where negatives had been enlarged above screen size, and this was due to an instability in the microscope scan generator. The control of the horizontal scan was subject to periodic fluctuation causing the scan to jump back to the previous line, resulting in blank zones in the image.

4.1.2 Air dried material (figures 1 - 3)

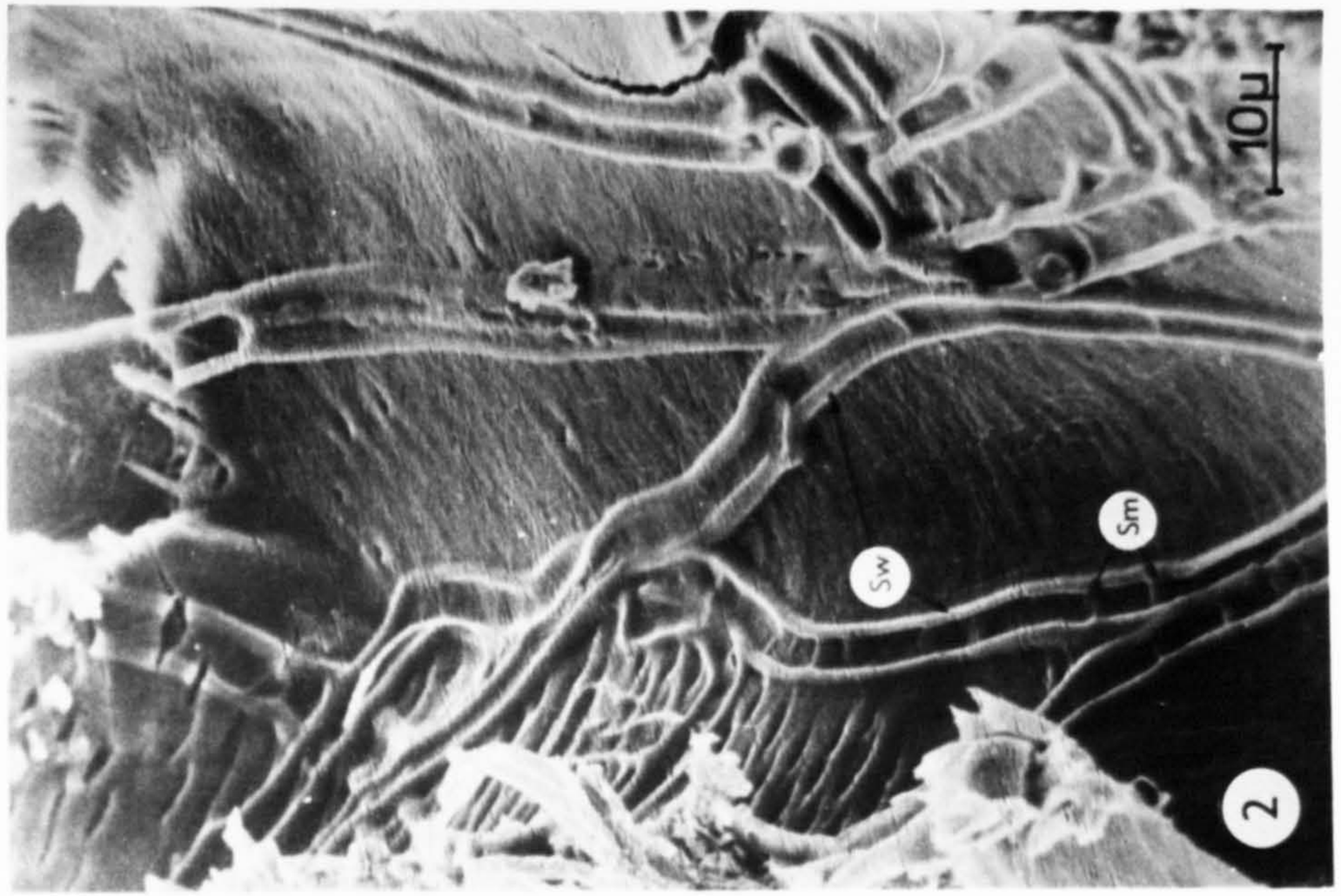
By this method of slow air drying the wood elements appeared to be well preserved with little evidence of the checking and splitting encountered in uncontrolled air dried specimens. All three examples given were of birch (Betula sp.), radial longitudinal surfaces, of six week incubations and concentrated on the vessels where fungal hyphae were present in abundance. Although the wood seemed to be unaffected by air drying the hyphae exhibited severe collapse, appearing as flattened ribbon-like structures, see figures 1 - 3. The three fungal types, however, showed characteristic differences from one another when air dried. The hypae of Coniophora puteana apparently lacked any defined structure, figure 1, whereas Chaetomium globosum, figure 2, showed strongly pronounced side walls and septa, whilst the hyphae of Coriolus versicolor had less pronounced side walls and fewer septa, figure 3. Due to the hyphal collapse, interpretation of certain decay features was made difficult, for example, bore holes and the comparitive relationships between the dimensions of hole and hypha.

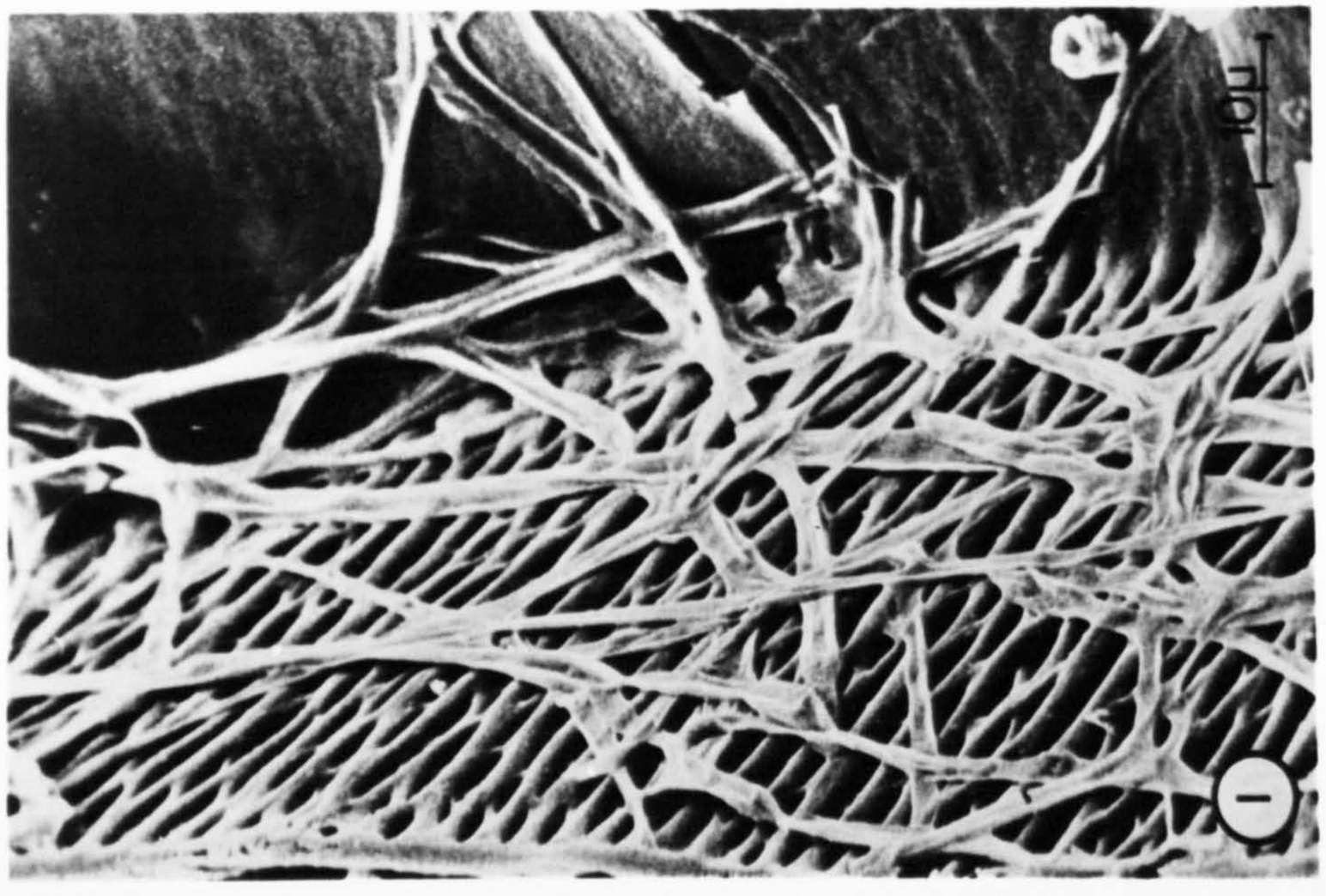
4.1.2 Air dried material, birch (Betula sp.), 6 weeks

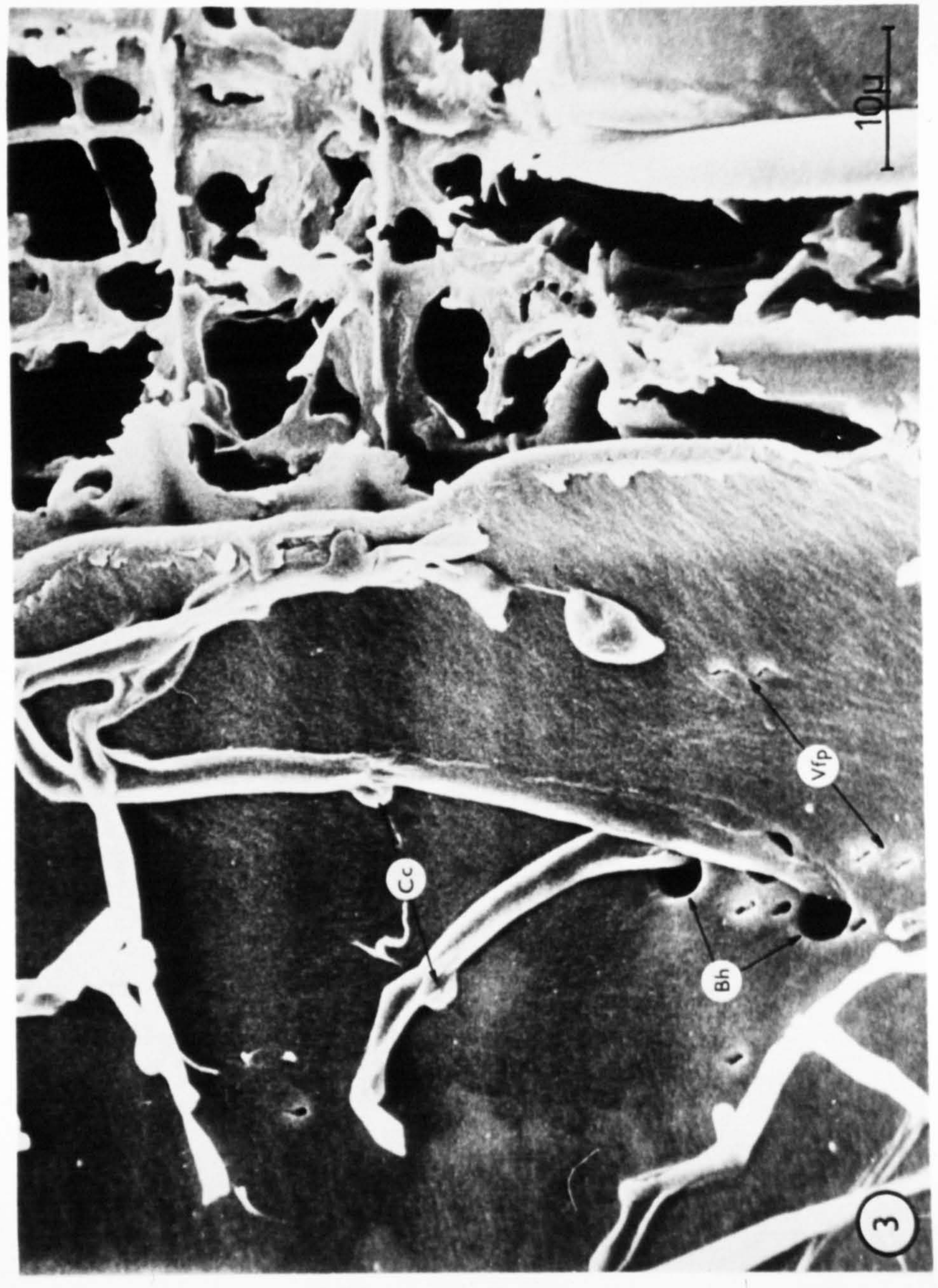
Fig. 1 (x 1360(1)) shows extensive colonisation of a vessel by Coniophora puteana. The hyphae have collapsed and very little of their surface detail is discernible. Note the characteristic reticulate-minute intervascular pitting on the tangential wall of the vessel. The importance of the pitting in the wood will be discussed later.

Fig. 2 (x 1320(2)) illustrates complete collapse of the hyphae of Chaetomium globosum colonising a vessel. Clearly evident are the side walls (Sw) and septa (Sm) of this Ascomycete.

Fig. 3 (x 1750(1)). This specimen features both vessel and ray degrade. Bore holes (Bh), distinct from the normal vessel - fibre pitting (Vfp), have been produced in the vessel wall by hyphae of Coriolus versicolor which are now dehydrated and partially collapsed. Possibly the hyphae also exhibit clamp connections (Cc) but these are not very clear. There is extensive degrade of the connecting ray tissue on the right.


10µ
Sw
Sm
2


10µ
1


10µ
Vfp
Cc
Bh
3

4.1.3 Critical Point Dried material (figures 4 - 6)

Critical Point Drying produced similar results to air drying for the wood elements but completely different appearances for the fungal hyphae. The examples illustrated are of six week material and in general the hyphae were tubular, showing little evidence of collapse, figures 4 - 6. Details of surface structures were now apparent, figure 6, and the overall impression was that this represented a closer to life situation than with air dried material. Whether the information generated by Critical Point Drying can be regarded as being fact or artefact can only be established by the frequency with which such a feature is observed and by cross-reference to other preparative methods and observations. Light microscopy of living fungi and freeze dried preparations reveal hyphae to be tubular structures and, therefore, it would seem reasonable to assume that the gross structure revealed by Critical Point Drying was closer to life than that of air drying.

Although Critical Point Drying does not reveal information about the internal structure of the hyphae, as in air drying, figure 2, the more realistic appearance of the hyphae has made it possible to observe more clearly the wall lysis patterns relative to hyphal dimensions. It was therefore decided to use Critical Point Dried material and the remaining results illustrated were all taken from Critical Point Dried specimens. In their interpretation, however, one must be constantly aware of the effects that the solvent exchange preparation process might have had on the finer details of the specimens.

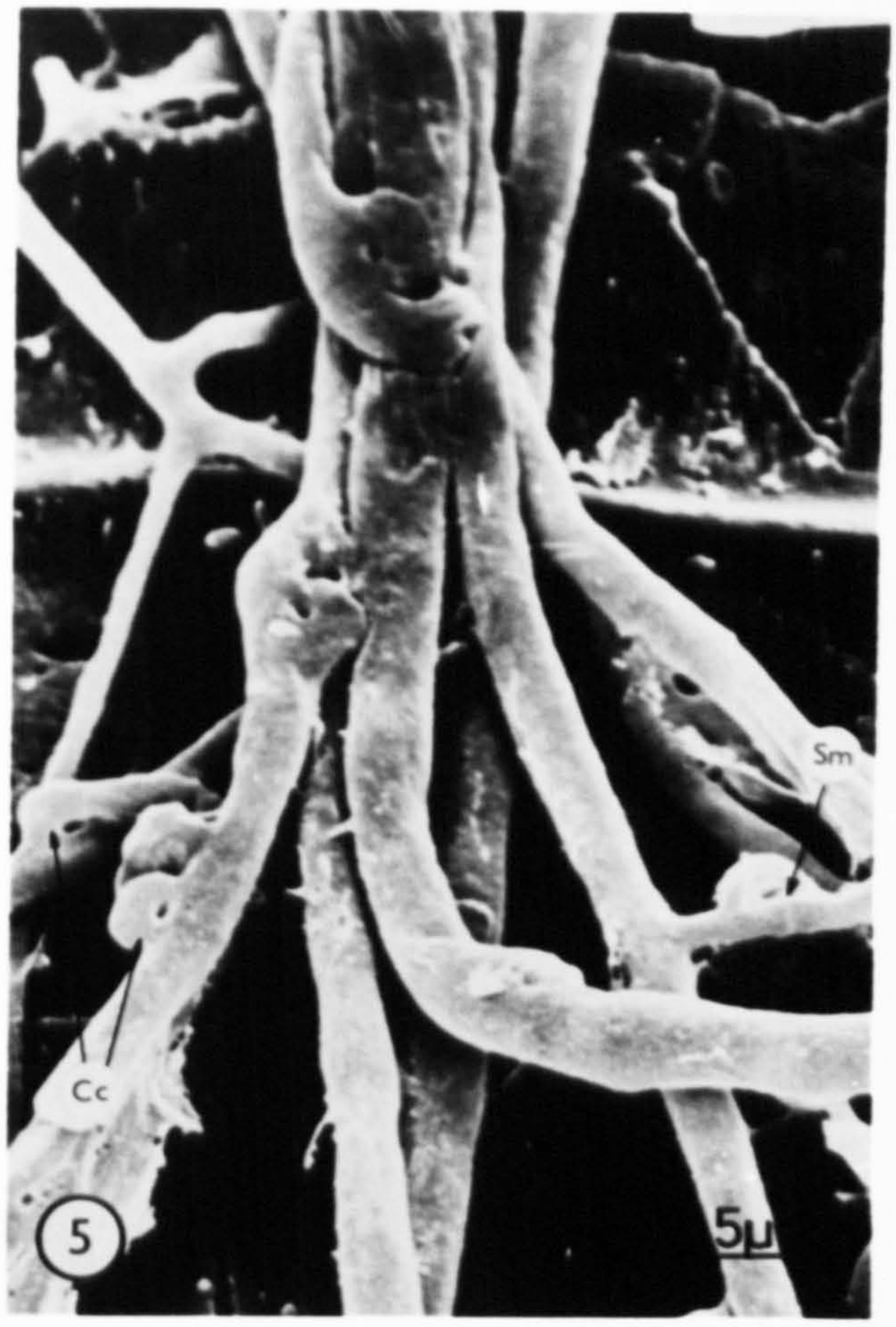
4.1.3 Critical Point Dried material, birch (Betula sp.), 6 weeks

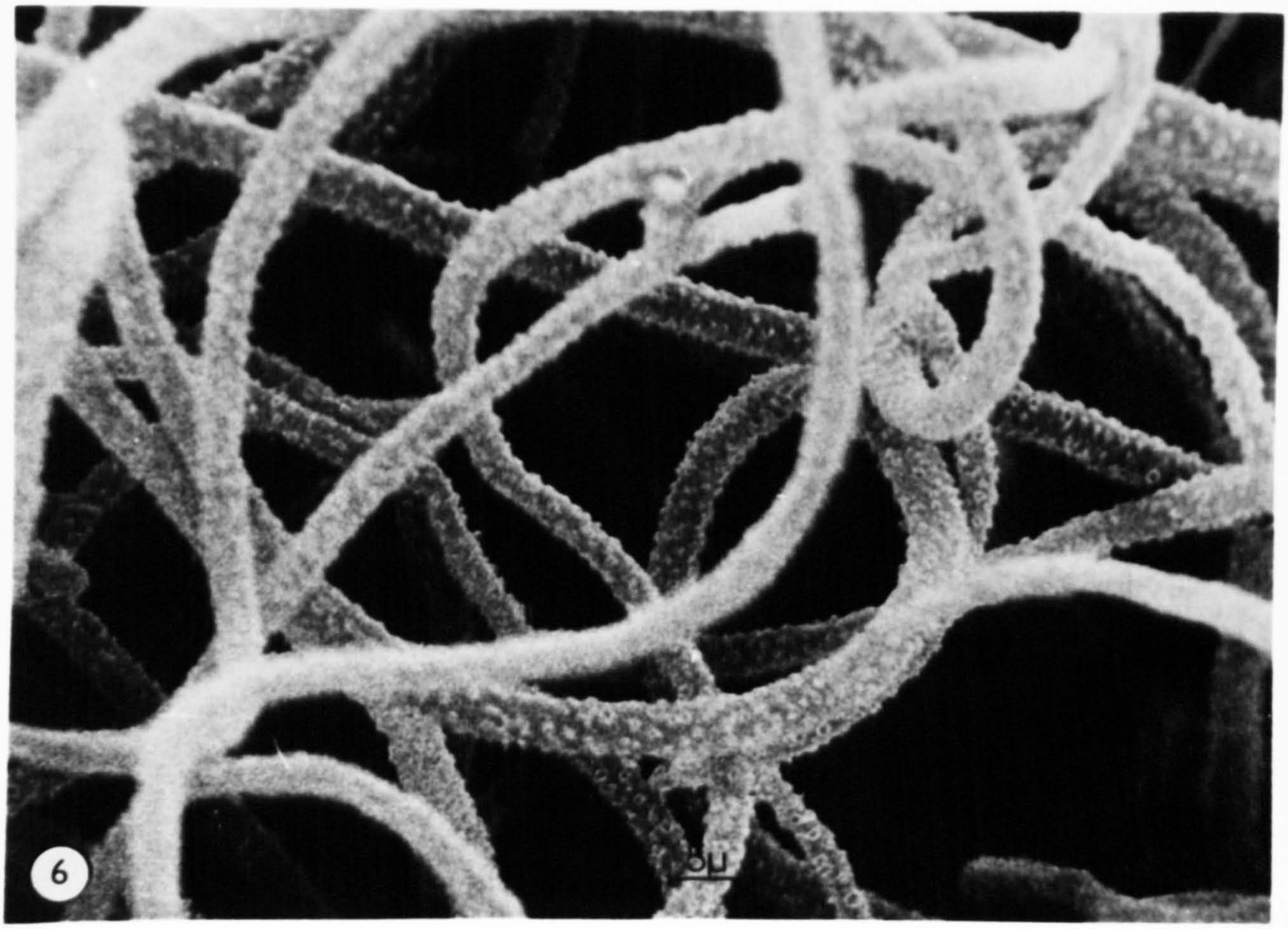
Fig. 4 (x 830(1)) is a tangential longitudinal section revealing colonisation of a vessel by the hyphae of Coniophora puteana. The hyphae have grown through the scalariform perforation plate and are variable in diameter but with smooth surfaces.

Fig. 5 (x 2570(1)) is a radial longitudinal face of the birch block colonised by Coriolus versicolor. The hyphal details are clear with several clamp connections (Cc) present. The underlying ray cells show damage probably incurred during block preparation. Note the septum (Sm) that the clamp connection bypasses.

Fig. 6 (x 2260(1)) shows hyphae of Chaetomium globosum which were colonising the surface of a decayed block. The hyphae show numerous surface structures which do not occur on hyphae which develop inside the wood specimens. These surface structures appear similar to those shown by George (1974) in freeze dried material, but throughout this investigation were only seen in Critical Point Dried specimens.


4
25µ


Cc
Sm
5
5µ


6
5µ

4.2 Comparison of fungal types on each wood species

4.2.1 Brown rot, Coniophora puteana

4.2.1.1 C. puteana on hardwood:- Birch(Betula sp.)

The colonization of vessels and lateral spread are indicated in figures 7 and 8 together with the type of information revealed by the two planes of section as mentioned earlier. More attention was paid to the details of the fungal attack on the wood than its colonization and figure 9 illustrates the destructive effect of this fungus on birch fibres after only 4 weeks incubation. The hyphae apparently overlying cut walls have been displaced during specimen preparation. This figure shows most of the decay features observed with a general progression from light to heavy wall degrade from left to right in the micrograph. This does not necessarily imply that there was a sequence through adjacent cells but merely was an example where the range could be observed. The spongy appearance of the S_3 increases to the right of the figure due to the coalescence of the regions of wall lysis. The S_3 wall layer appeared more resistant than the S_2 and this was confirmed by close examination of the broken walls between the adjacent fibres. Such a wall, figure 10, indicates the comparitive resistance of the S_3 and the middle lamella and primary wall complex over the extremely heavily degraded S_2. This degradation resulted in a fibrous-spongy appearance.

The cross-field pits exhibited extremely high resistance to lysis, figures 10 and 11, even when the entire surrounding wall had been degraded, figures 12 and 13. Despite this resistance the pits were a frequent pathway for the fungus into an adjacent cell achieved via a very neat small hole in the membrane, the details of which are

clearly revealed by the use of gamma in figures 12 and 13. The possible significance of the fine strands between the hypha and the pit side walls, figure 13, together with the 'woolly' appearance of some of the hyphae, figure 24, will be discussed later.

Complete coalescence of the lytic zones in the S_3 resulted in an extremely fibrous randomly orientated residue of the wall layers, figures 14 and 15. However, the dissolution of the S_3 layer was by no means uniform with the frequent appearance of 'sinuous trails' of relatively intact S_3 material overlying the heavily degraded S_2, figures 16 and 17. In the severe cases, figure 17, only the 'trail' S_3 region was left.

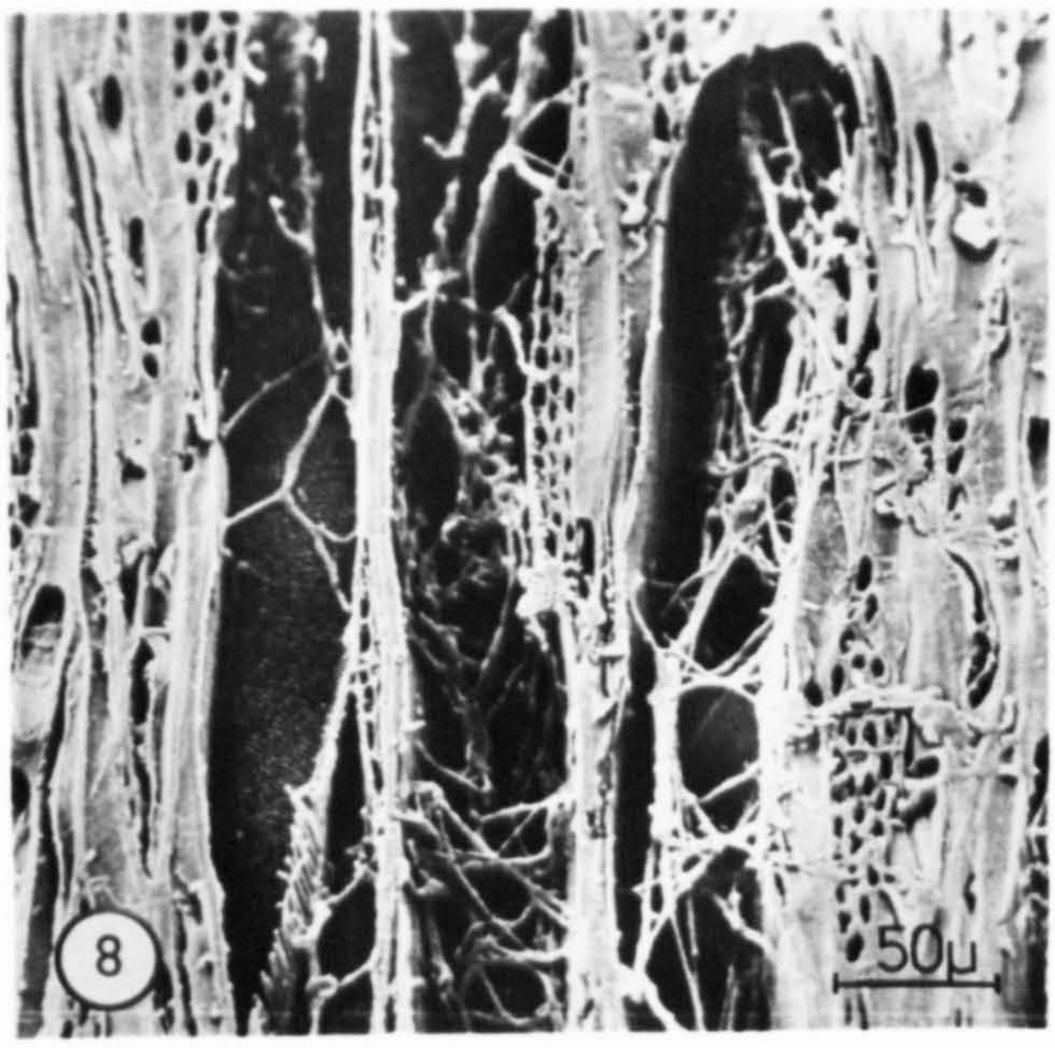
A possible clue to explain these features was the often adjacent fungal hypha, figures 18, 20, 21, and 22, which in many cases followed the line of the trail so precisely that they might in fact have been displaced from the intact S_3 during preparation. Whether the resistance was permanent might be indicated by figure 19 where the remaining S_3 shows signs of being degraded from the S_2 side, this would then result in fibres with the total wall degrade appearance of figures 14 and 15. Higher magnification could not reveal any particular structural reason why the S_3 should be more resistant in certain areas, figure 23.

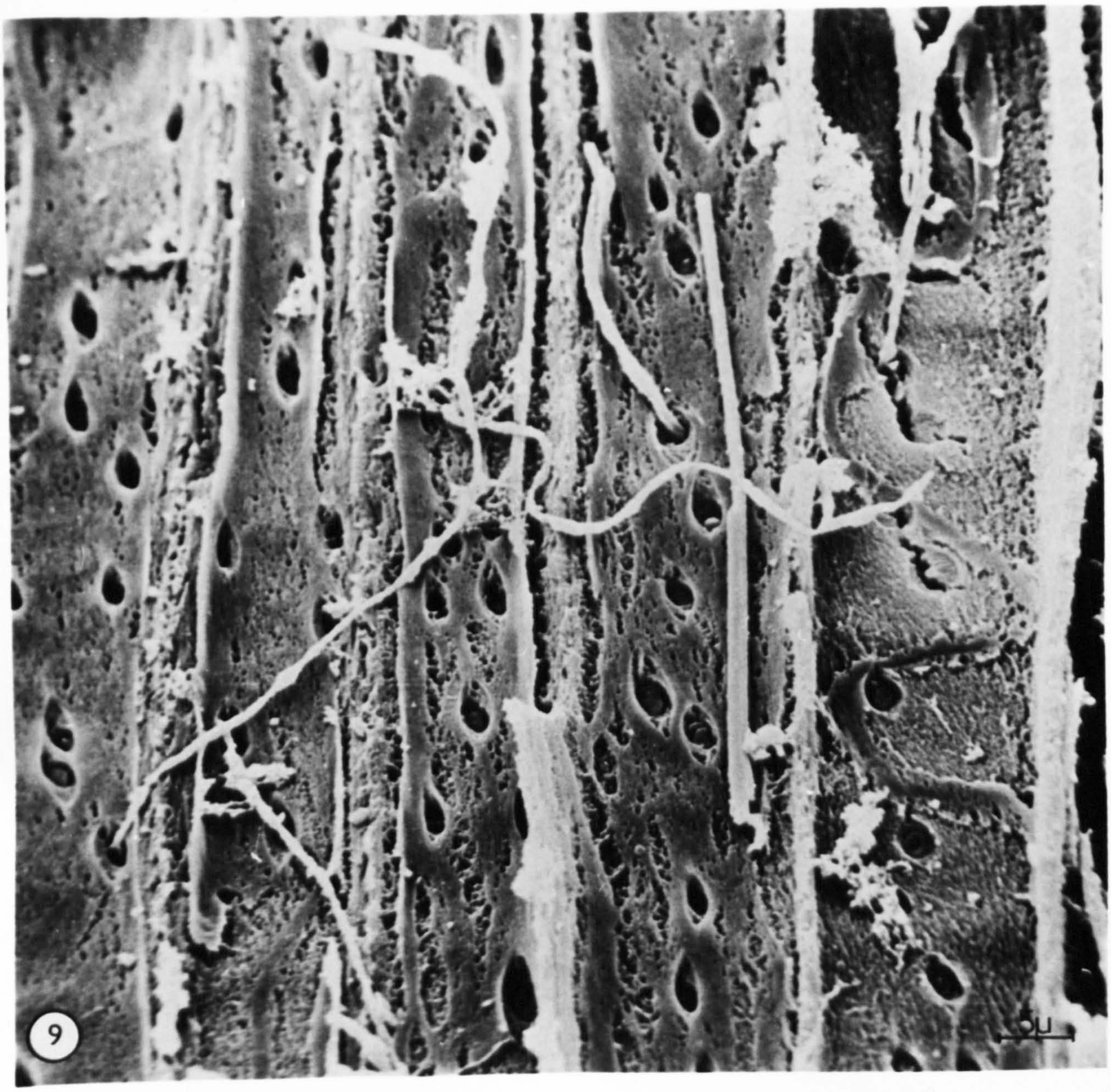
4.2.1.1 Coniophora puteana on birch (Betula sp.), 4 weeks

Figs. 7 (x 110(1)) and 8 (x 230(1)) are low magnifications showing, in both figures, extensive colonisation of the vessels with lateral spread of the hyphae into adjacent fibres and rays. Fig. 7, being a radial longitudinal view, shows the interrelation of vessels, fibres and rays. The tangential longitudingal view of fig. 8 indicates the distribution and size of the rays together with the intervascular pitting which is predominantly confined to the tangential walls.

Fig. 9 (x 2140(1)) is a general radial longitudinal view of the decay of five fibres in a cross-field region. Note the colonisation via existing pits and the extremely spongy appearance of the walls. Some displacement of hyphae has occured during preparation, these can be seen overlying cut or broken walls. Details of this wall lysis are covered later in this section.


7
100μ


8
50μ


9
5μ

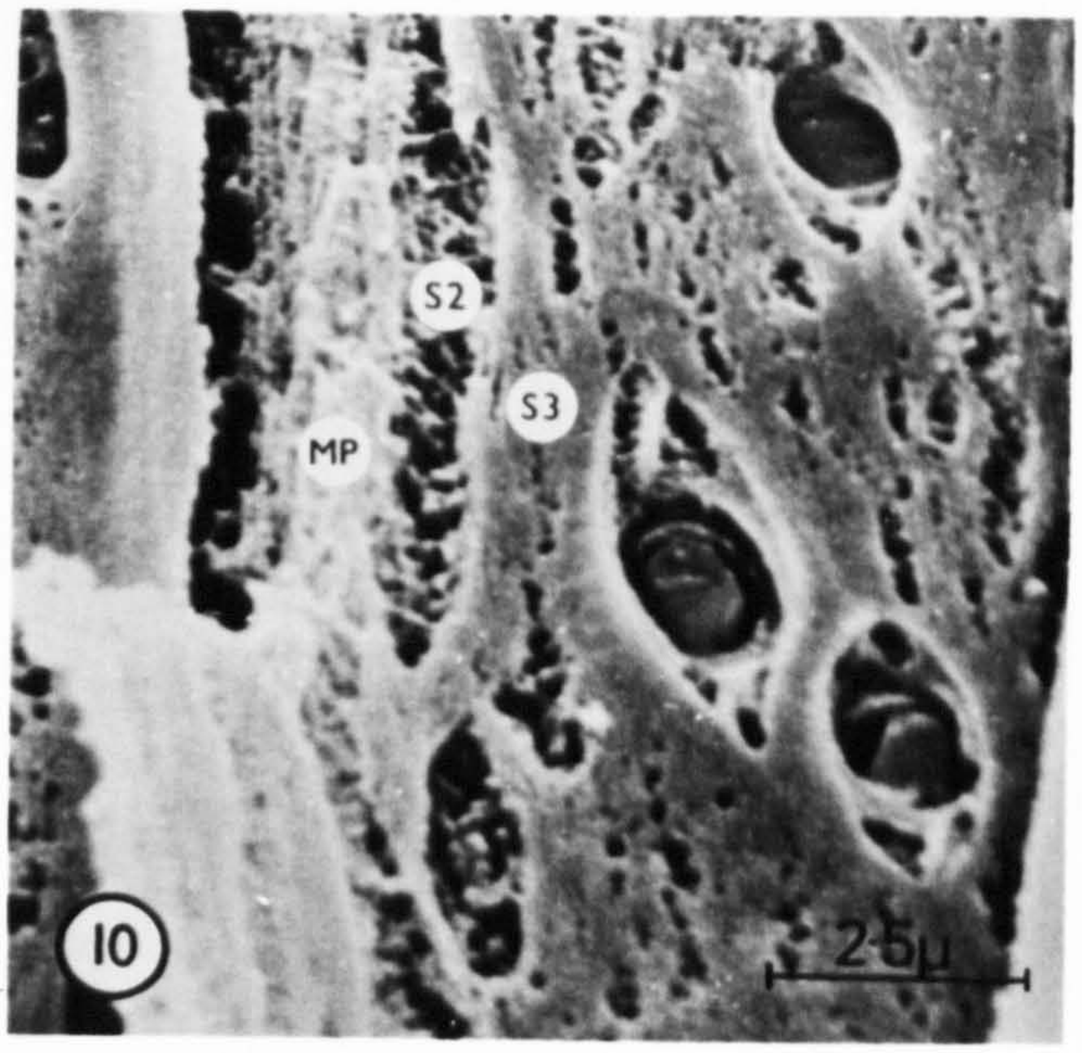
4.2.1.1 Coniophora puteana on birch (Betula sp.), 4 weeks

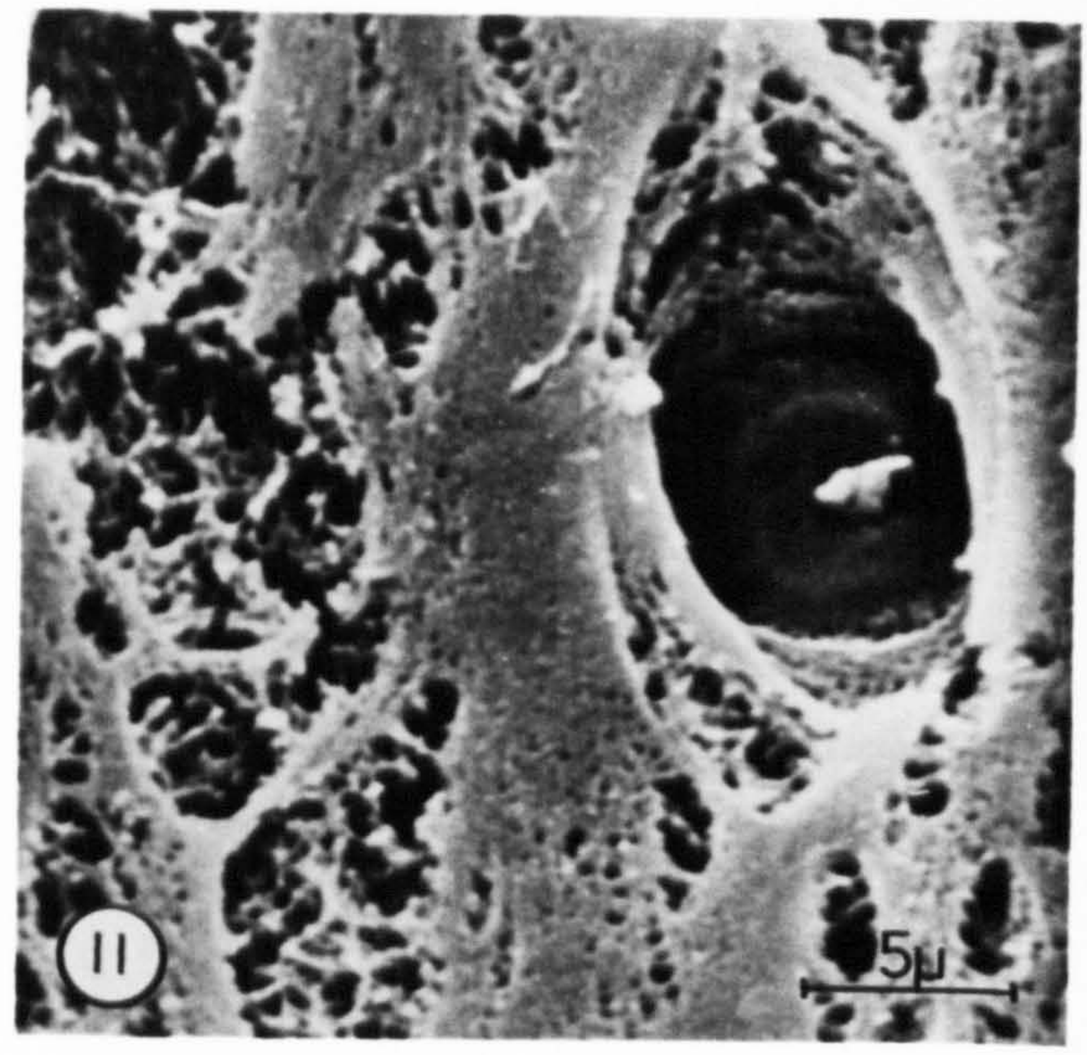
Fig. 10 (x 3090(1)) is a high power view of the fibre - ray pits to show their resistance to decay in comparison with the adjacent wall layers. Note the fractured wall on the left with heavily decayed S_2 in comparison with the S_3 and the middle lamella - primary wall complex (MP).

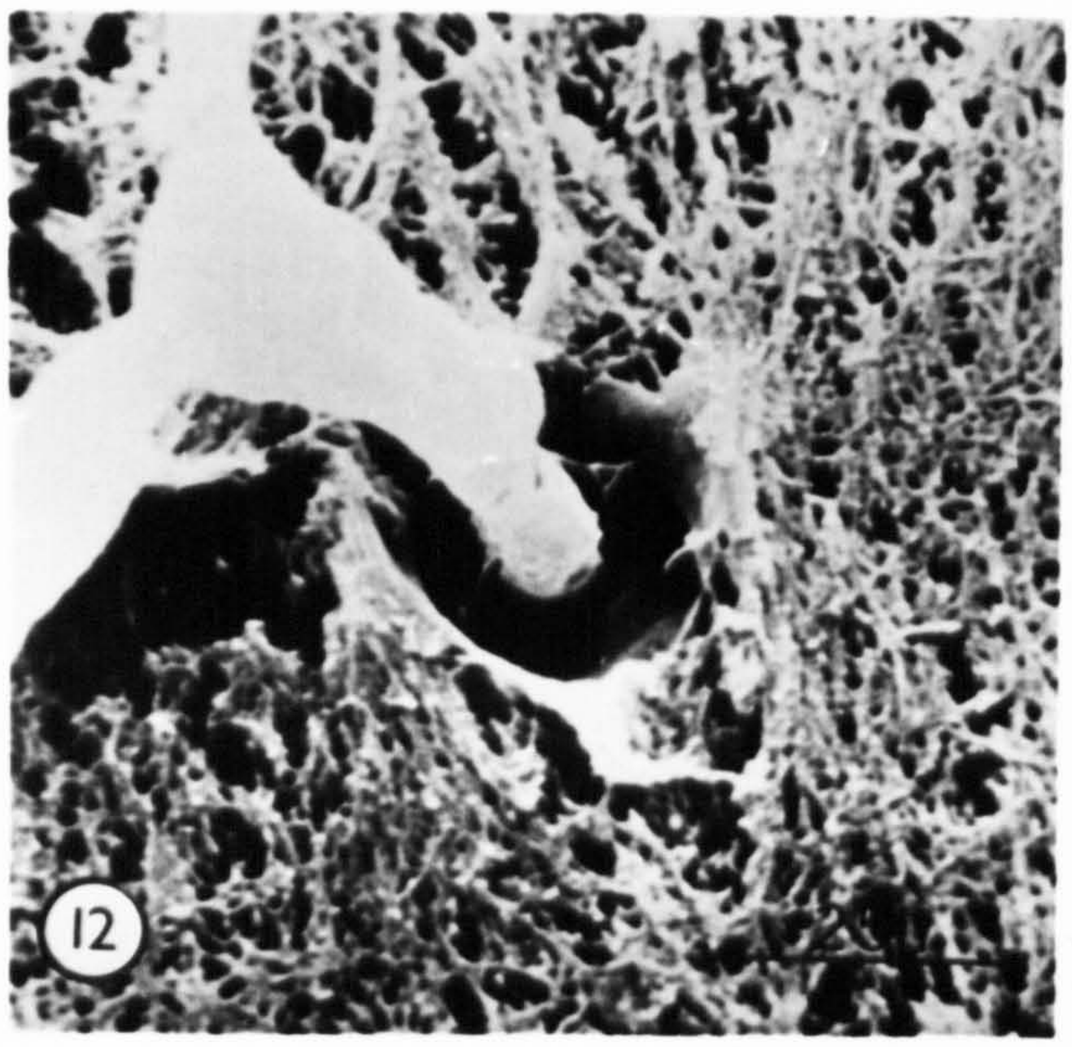
Fig. 11 (x 7860(1)) is a very high magnification of a typical fibre pit, with its intact membrane resisting the lysis occuring in the wall to the left. The S_3 layer appears to be more resistant than the S_2 which shows heavier decay.

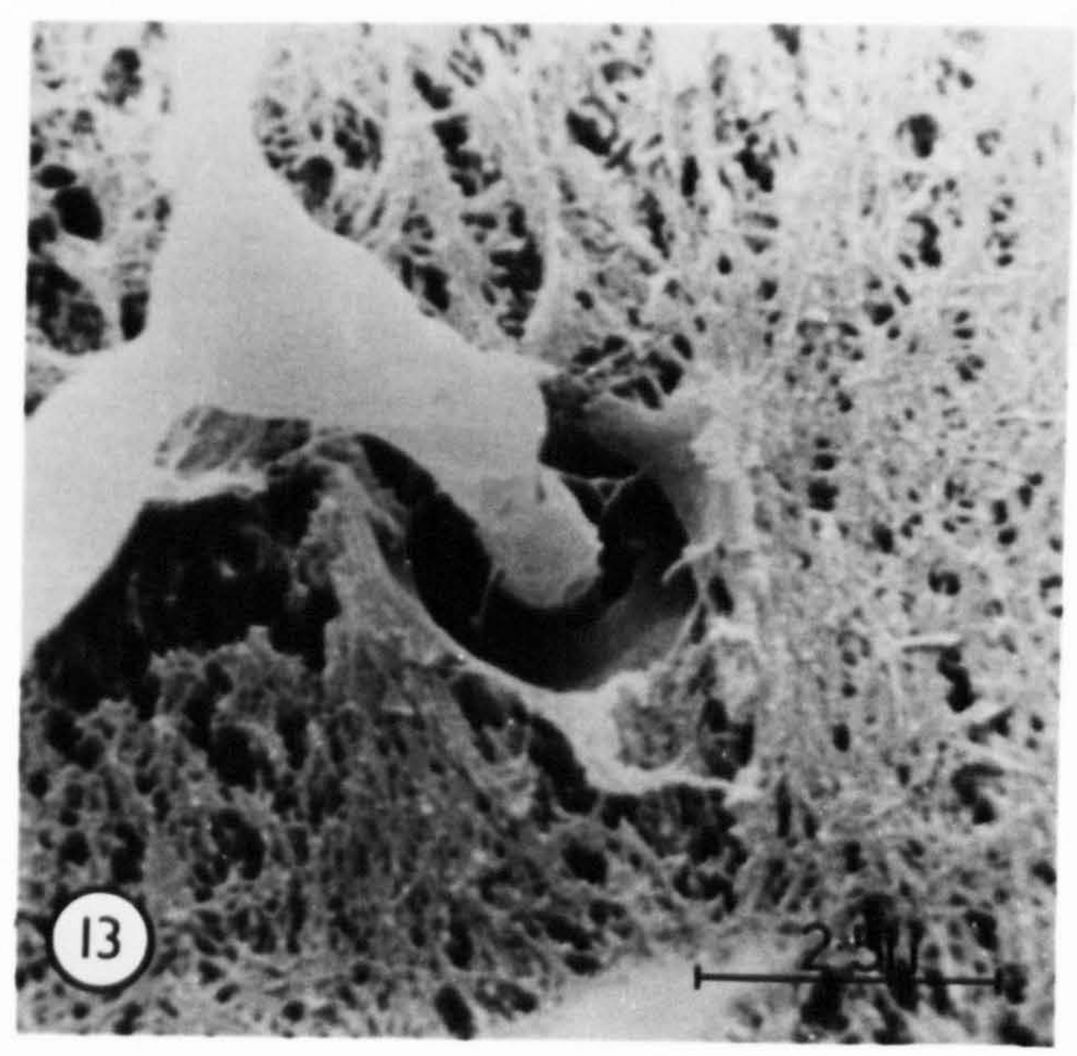
Figs. 12 (x 9150(1)) and 13 (x 9100(2)) are used to demonstrate the application of the gamma control. In fig. 13 the image is softer but reveals more detail within the dark areas of fig. 12. The hypha has penetrated the pit membrane via a very fine hole not much larger than the hyphal diameter. The fine strands could have originated from the hypha. Note the sides of the pit aperture show less degrade than the surrounding wall.

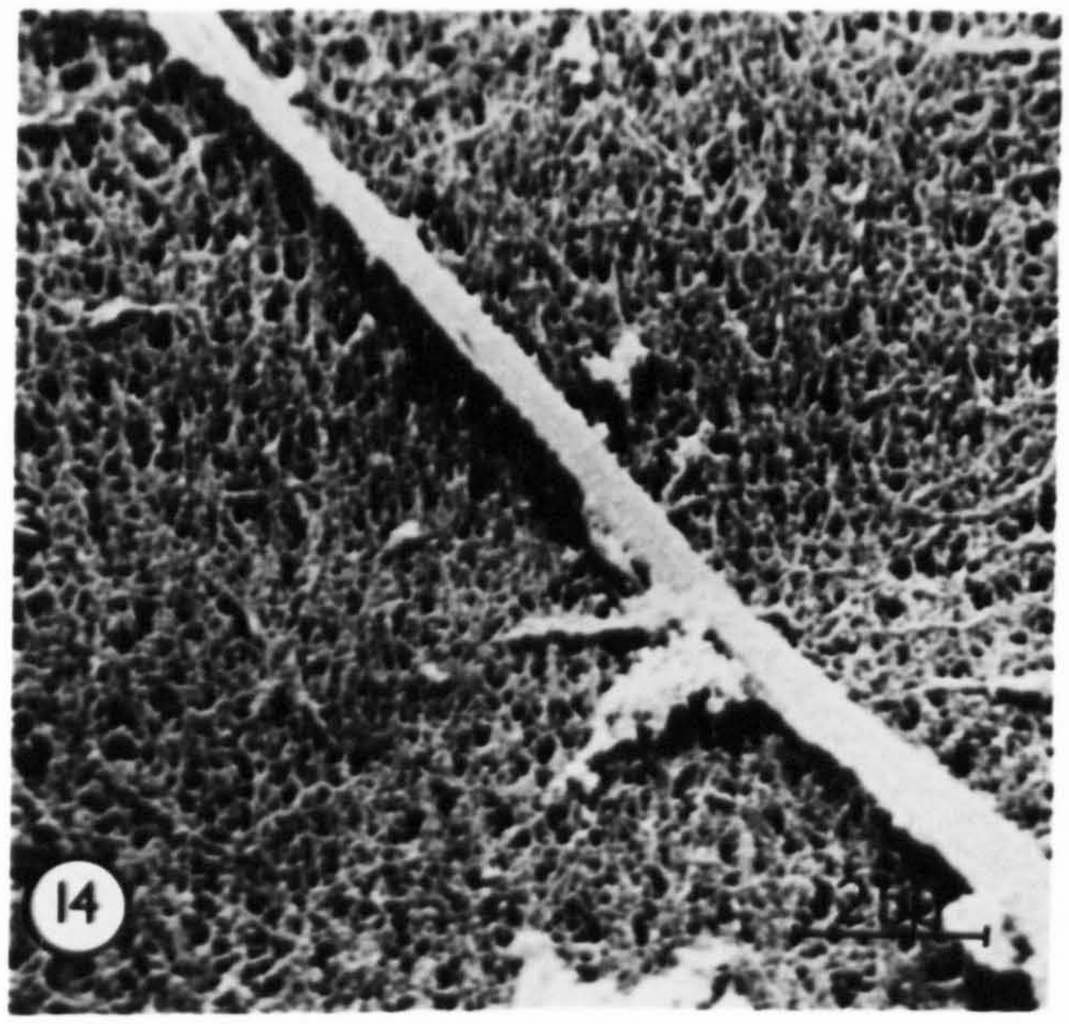
Figs. 14 (x 5800(1)) and 15 (x 8400(1)) show the detailed structure of the degraded fibre walls where the S_3 has been completely removed. Note the smooth hyphal tip in fig. 15 and the extremely fibrous, spongy appearance of the residual wall material.

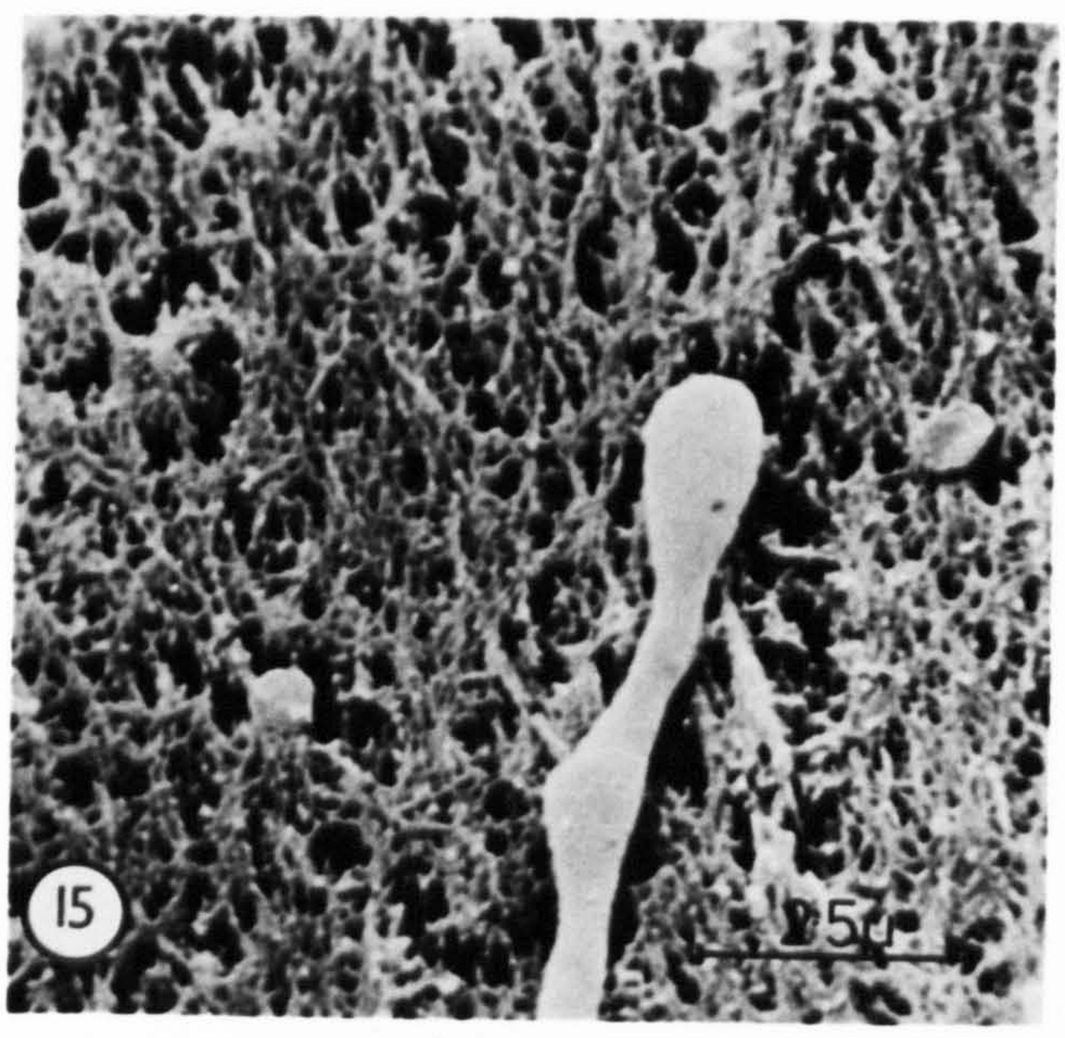

S2
S3
MP
10
2·5μ


11
5μ


12


13


14


15

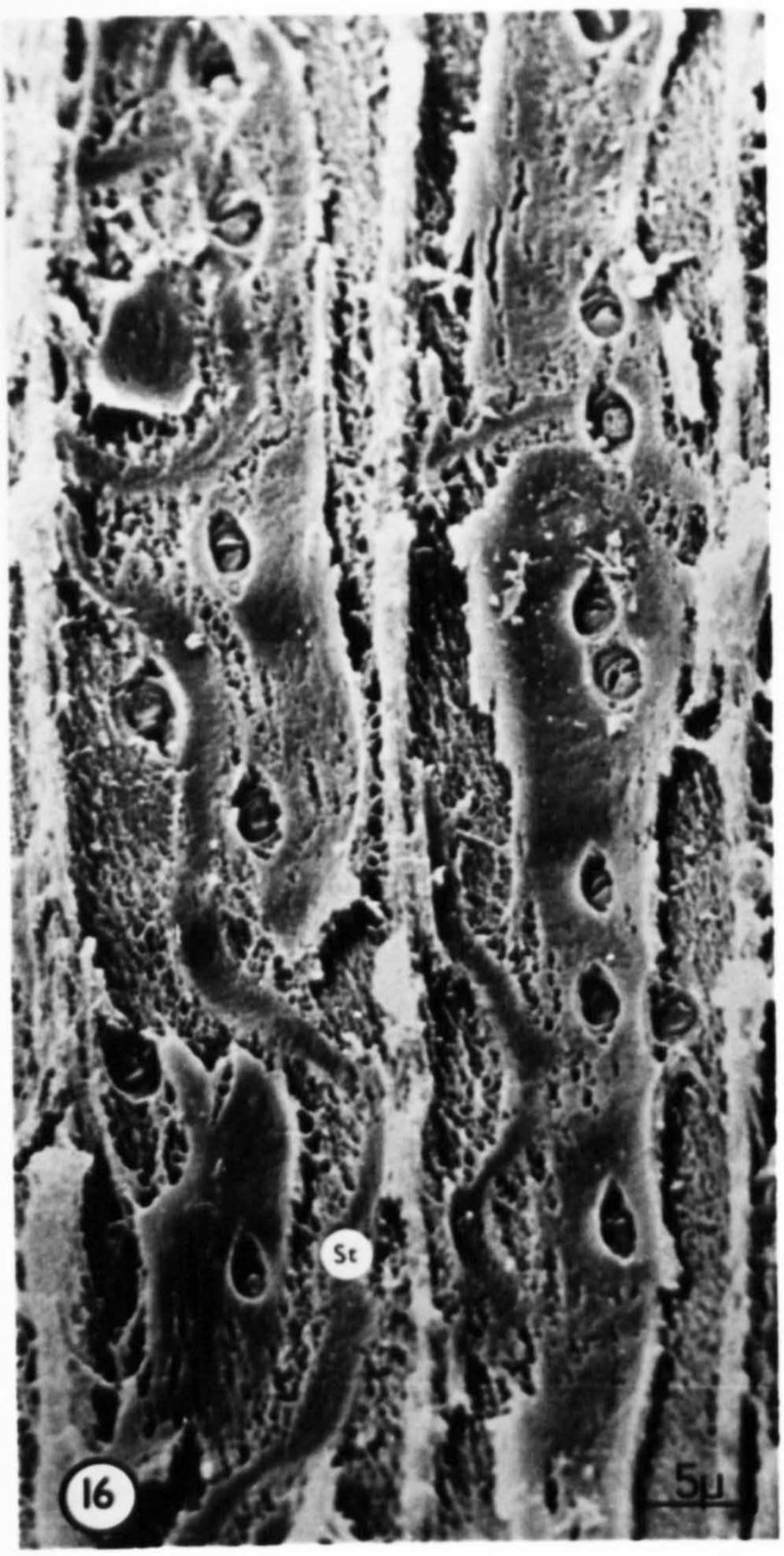
4.2.1.1 Coniophora puteana on birch (Betula sp.), 4 weeks

Fig. 16 (x 2380(1)) shows two fibres in the cross-field region where again the pits and the S_3 exhibited some degree of resistance to decay together with 'sinuous trails' (St) on the S_3.

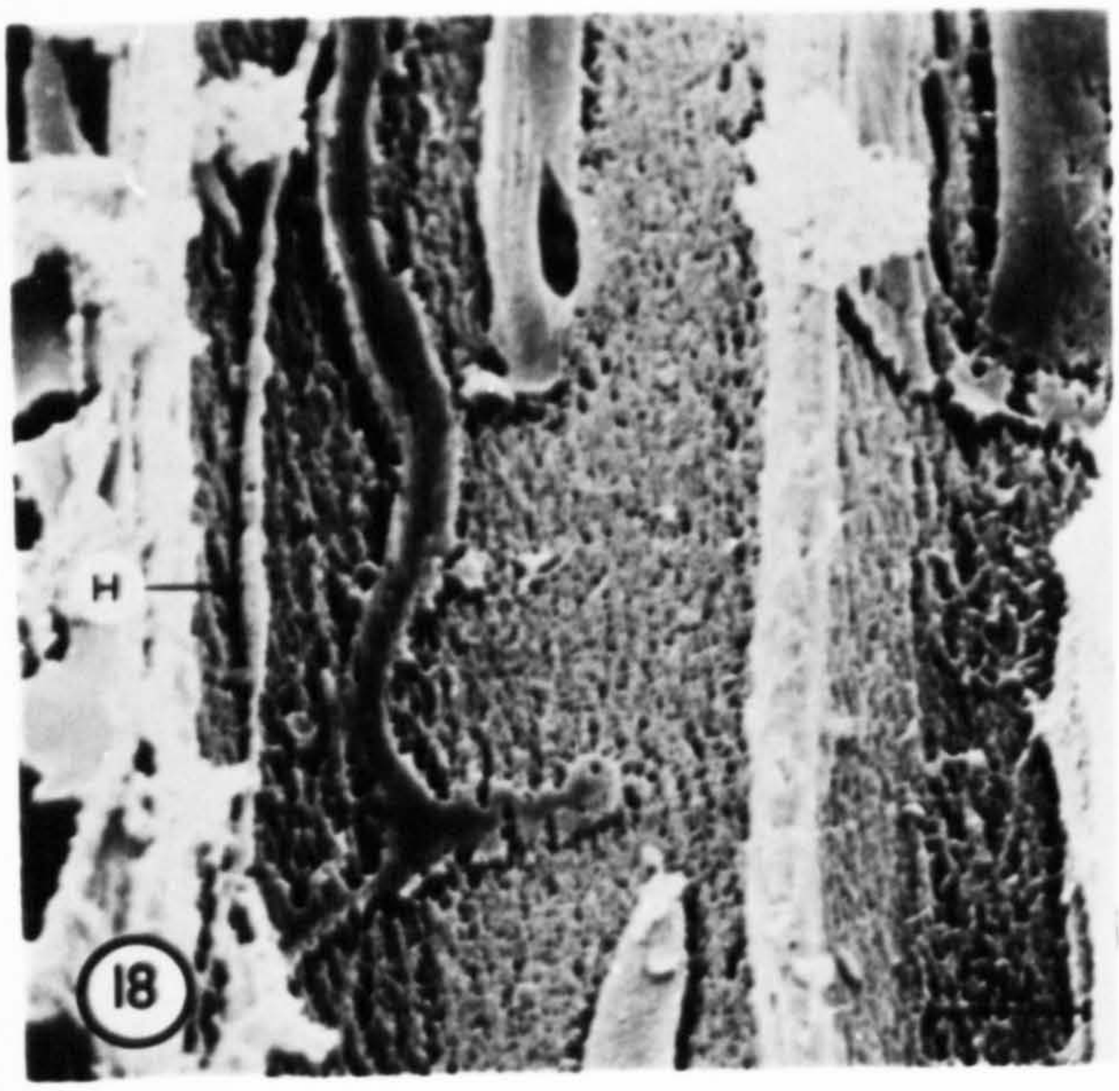
Fig. 17 (x 3180(1)) shows detail of a 'sinuous trail' (St) in another fibre. The remaining S_3 has been degraded to the spongy structure. Note the fungal penetration of the pit in the upper half of the figure and severe wall cracking around these pits.

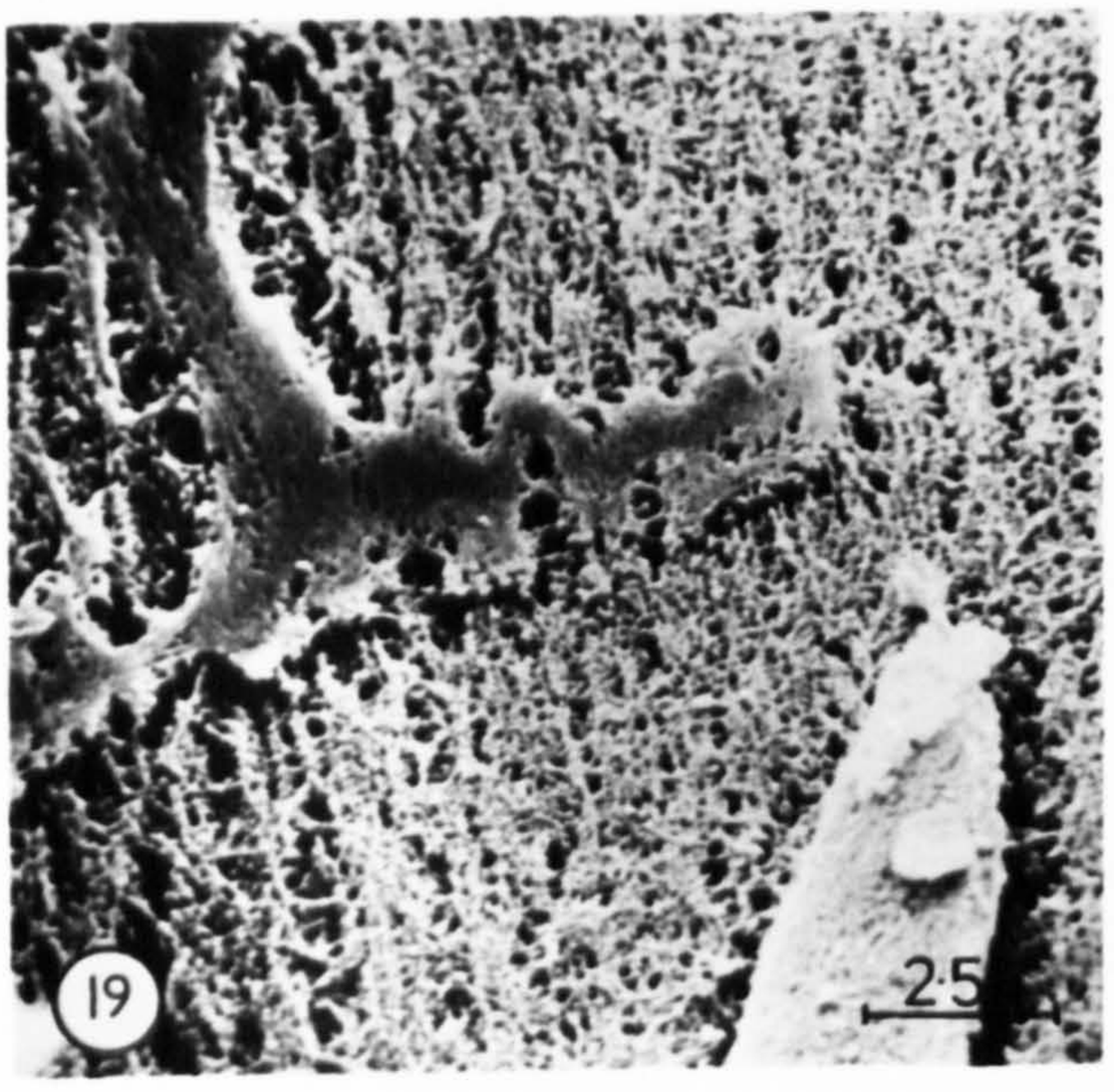
Fig. 18 (x 2170(1)). Another 'trail', this time with an adjacent hypha (H) which was probably dislodged from the line of the trail.

Fig. 19 (x 5600(1)) is a high magnification detail of fig. 18 to show the gradation between virtually sound and degraded S_3 as exemplified by the possible dissolution of the 'trail', apparently from below.


St
16
5μ


St
17
5μ


H
18


19
2·5

4.2.1.1 Coniophora puteana on birch (Betula sp.), 4 weeks

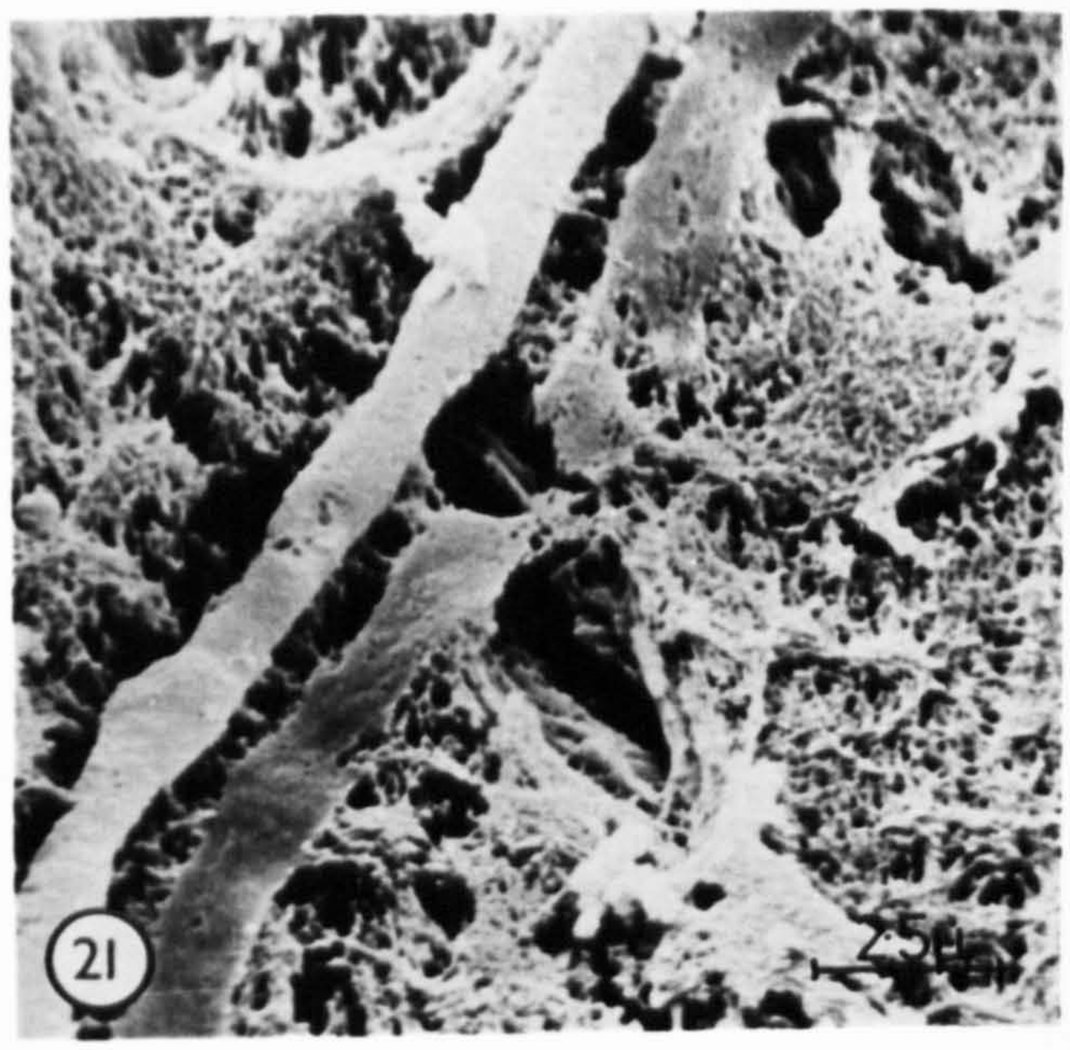
Fig. 20 (x 5040(1)) shows a hypha dislodged from the trail during specimen preparation. The remainder of the fibre cell wall being completely degraded.

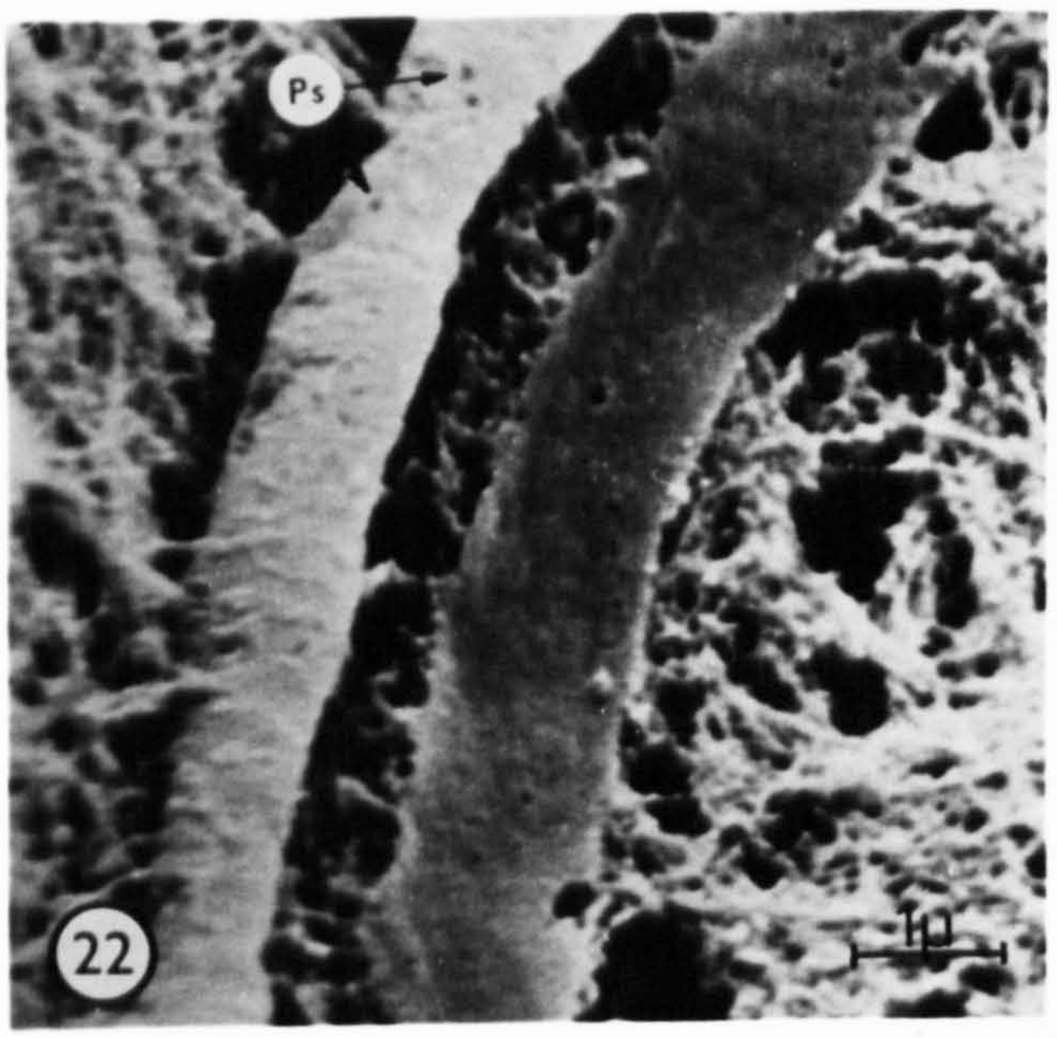
Fig. 21 (x 5700(1)). Extensive wall degrade but still a trail persists close to the dislodged hypha. Fig. 22 (x 11300(1)) is a high magnification detail of fig. 21 clearly showing the trail to be well preserved wall. In this and previous figures, 20 and 21, there appear to be pores (Ps) in the hyphal wall, the significance of which is uncertain.

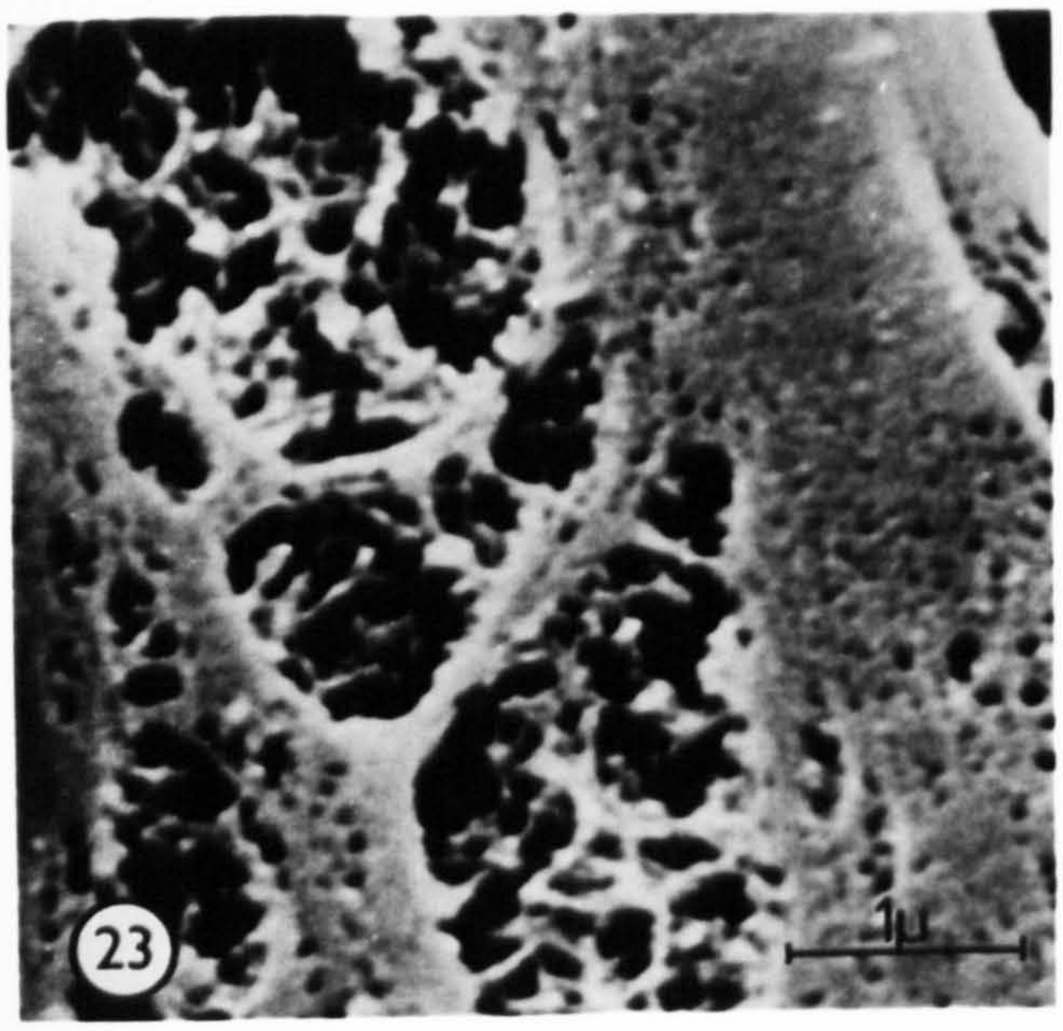
Fig. 23 (x 18130(1)) is an extremely high powered detail of an area of fig. 11 close to a pit to illustrate the details of the decayed regions of the wall compared with the less decayed regions closer to the pit. The honeycombed spongy residue of the wall is clearly evident but there appears to be no significant factor causing this resistance.

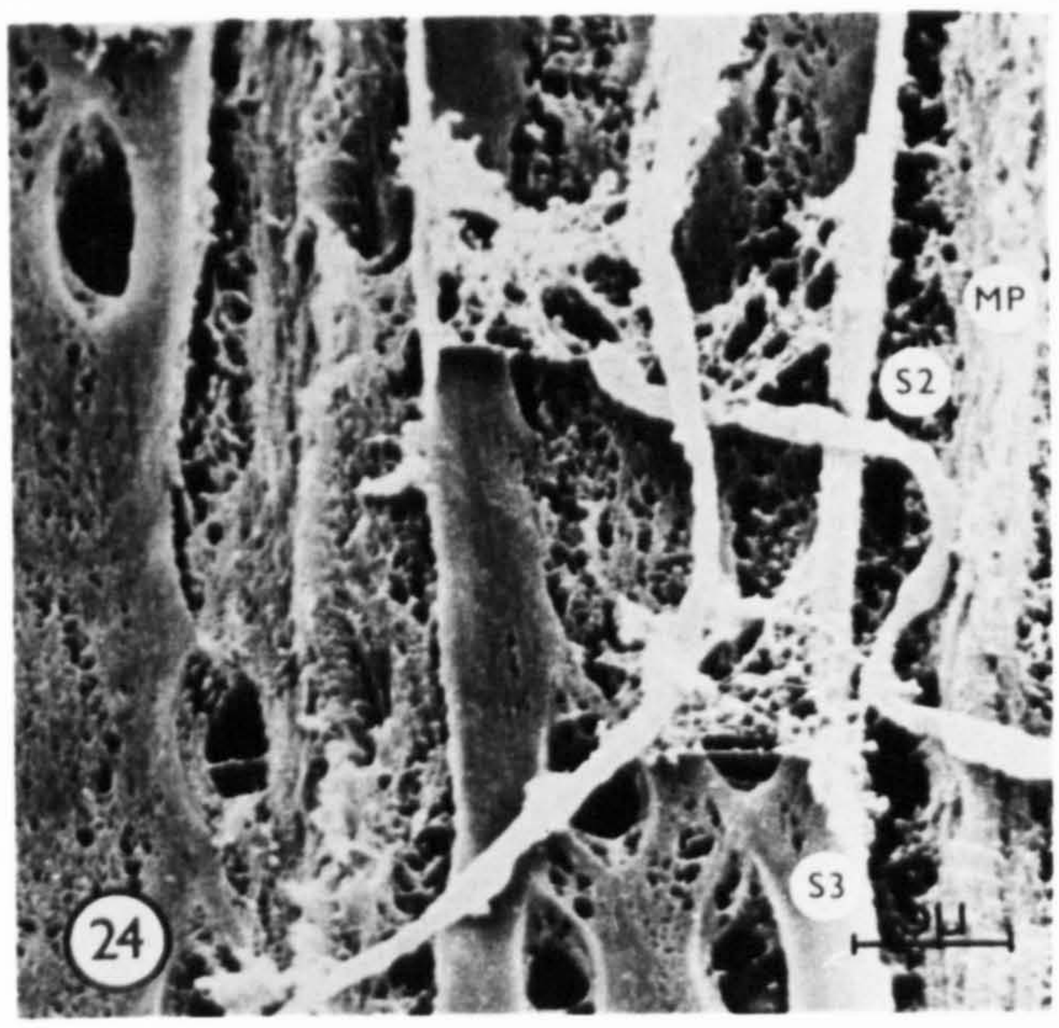
Fig. 24 (x 2410(1)) is a detail of fig. 9 to illustrate two features, firstly the presence of fine strands connected to the hyphae, and secondly to emphasise the susceptibility of the S_2 to attack, as revealed by the broken wall on the right. Both the S_3 and the middle lamella - primary wall - S_1 complex (MP) regions are more structurally sound than the S_2. The hyphae crossing over broken and cut walls are due to displacement during preparation.


20
1μ


21


Ps
22
1μ


23
1μ


MP
S2
S3
24
1μ

4.2.1.2 C. puteana on softwood:- Scots pine (Pinus sylvestris)

The appearance of the hyphae in most of these results was extremely poor and this could be due to low activity of the fungus with poor growth and degrade capacity or possibly to a certain degree of air drying during the preparation. With this low degrade capacity the most obvious effect on the wood was the splitting of the pit borders, figure 25. The borders appeared extremely thin and it was difficult to determine whether this effect was due to the fungus but it was significant that sound bordered pits were found only where the hyphae were scarce.

The splits showed a prefered orientation with the S_2 microfibrillar angle, bearing in mind the geometry of wall construction around bordered pits. This splitting had occured during drying as indicated by the hypha in the lower right of figure 25 and was probably due to stresses set up in the wall by the removal of the water. The splits may be interpreted as artefacts but the significance of the hyphal presence could indicate a weakening effect by the fungus.

The limited degree of wall lysis occurred initially with the stripping of the S_3 wall layer revealing the steep S_2 microfibrillar angle, figures 26, 27 and 28. The warts apparently resisted this early stage of attack. Further degrade was exemplified by deeper cracks appearing in the S_2 together with the development of a more spongy appearance to the attacked wall, figures 29 and 30.

As in the birch examples the fungus made use of natural pitting to pass from one cell to another, again with a very neat bore hole, through the torus of the bordered pits, figures 29 and 31. Only one

example of direct bore hole formation in the wall was encountered, this was in an early wood tracheid, figure 32, where possibly the wall was thin enough to warrant this approach.

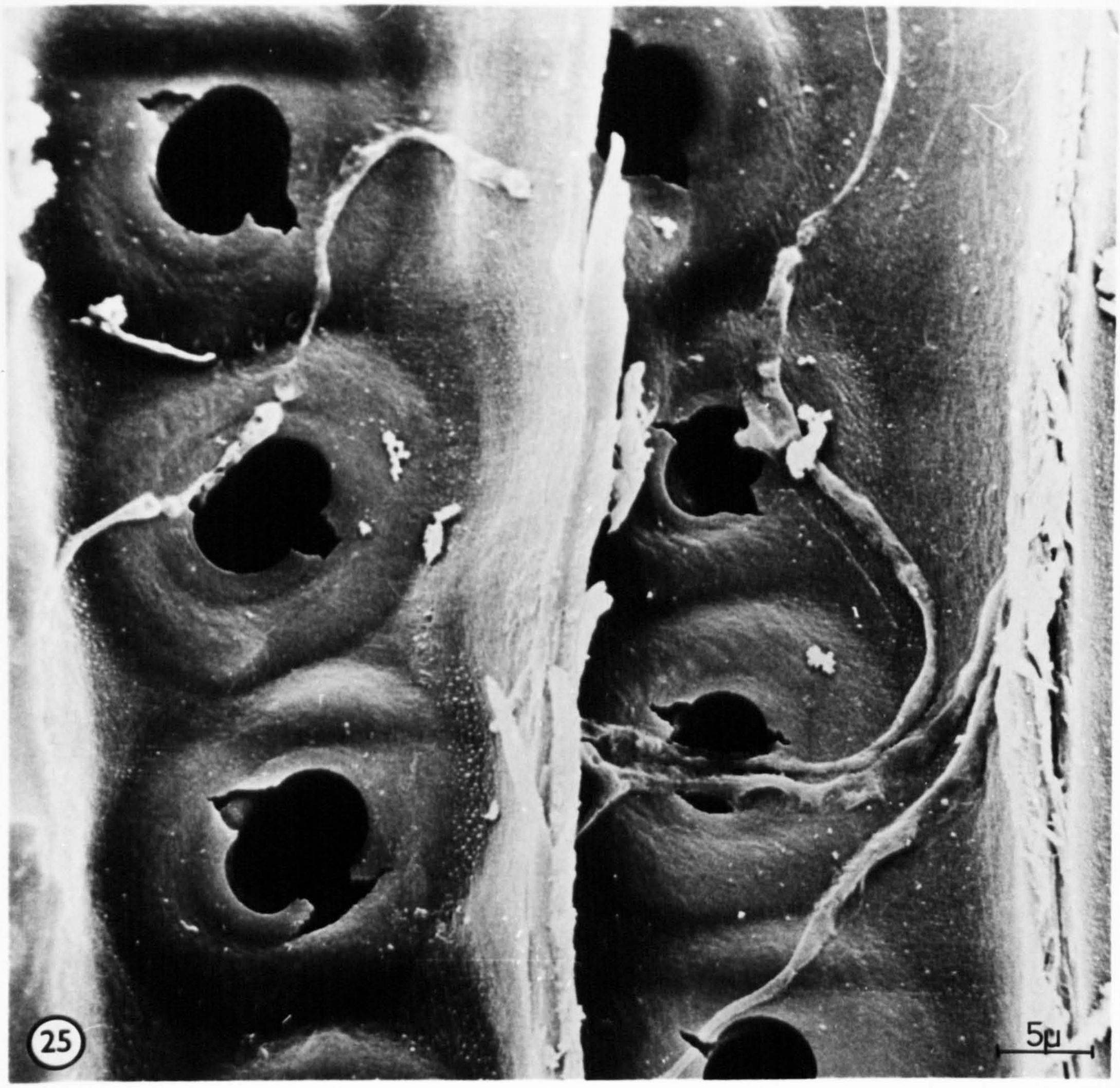
4.2.1.2 Coniophora puteana on Scots pine (Pinus sylvestris), 4 weeks

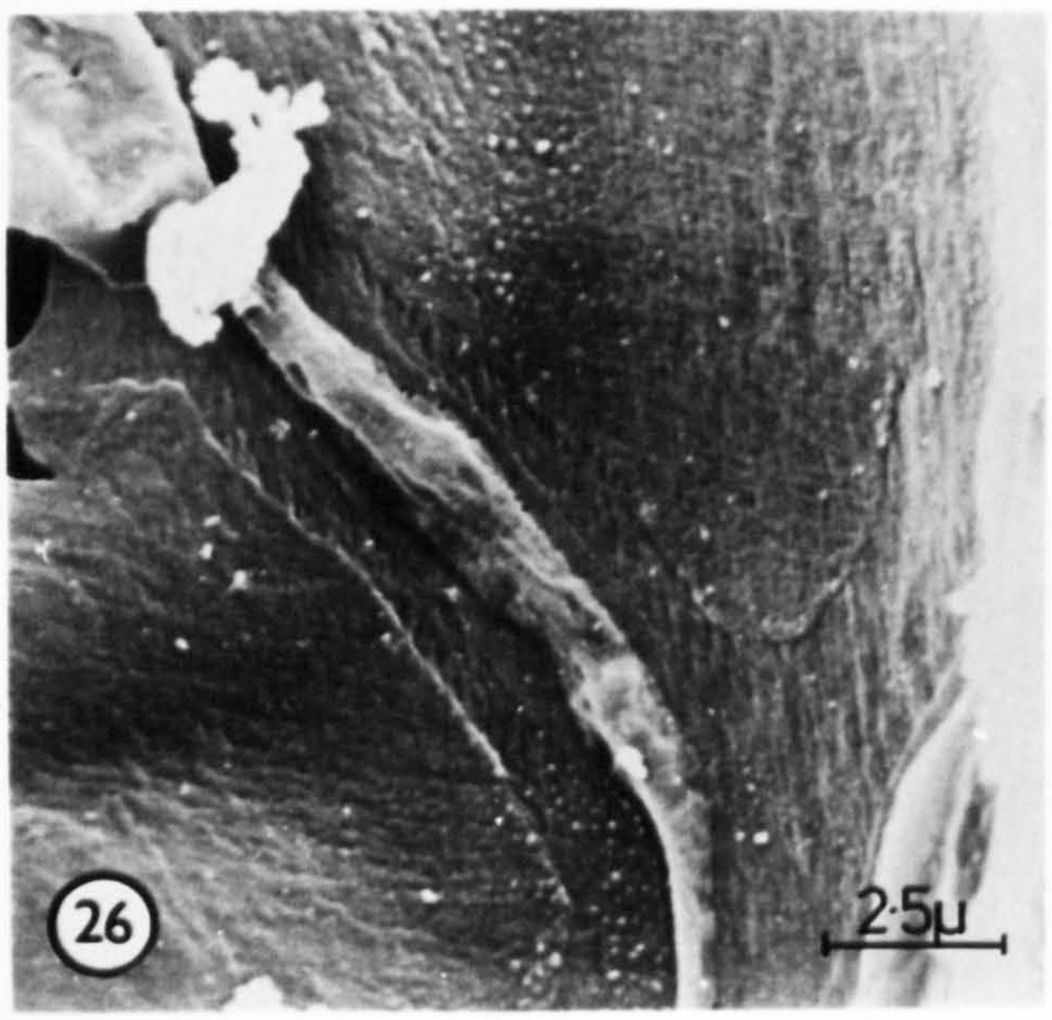
Fig. 25 (x 2690(1)) is a general view of tracheid colonisation to illustrate a common feature observed for this fungus. The presence of the hyphae has resulted in the pit borders being weakened and subsequently splitting on drying. The orientation of the splits being along the general line of the S_2 microfibrils. The borders appear thinner than normal and the hyphal preservation was not as good as with other material.

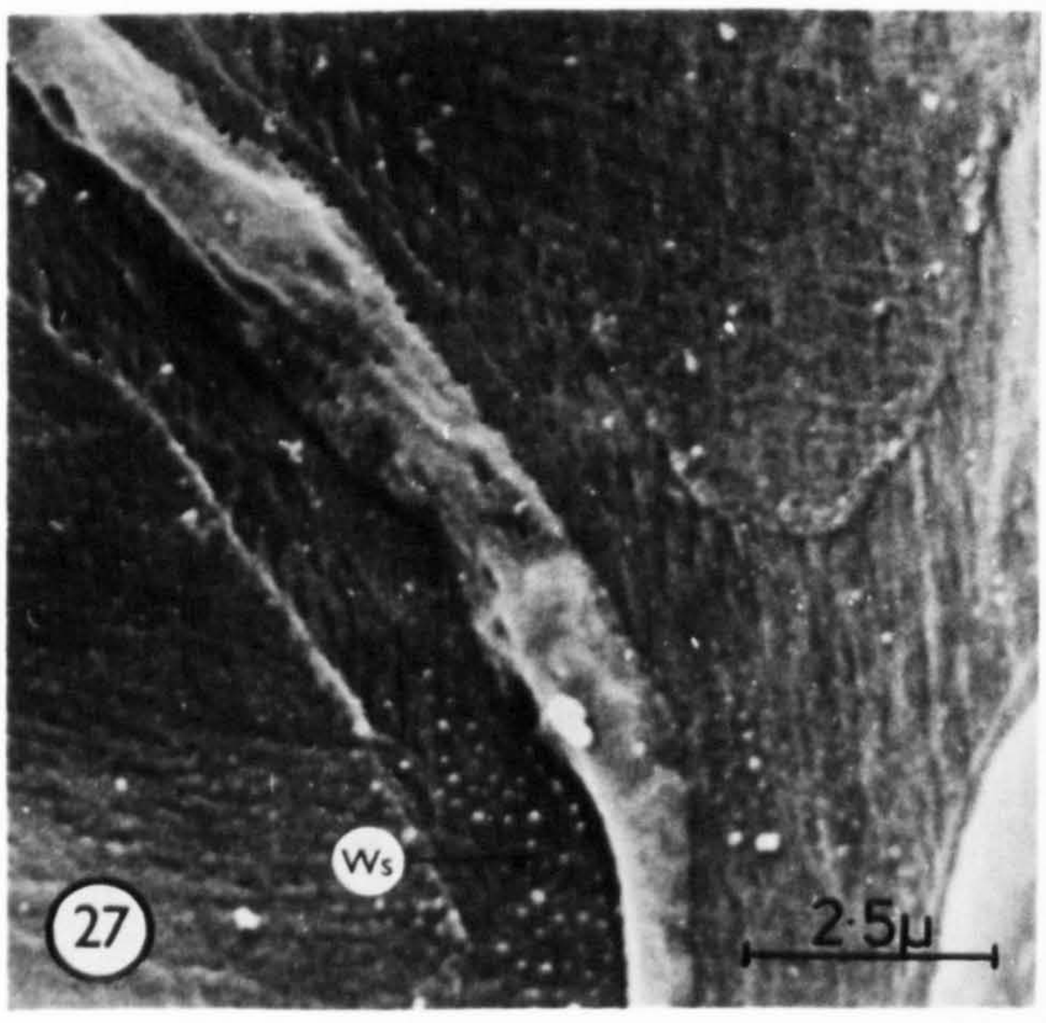
Figs. 26 (x 5520(1)) and 27 (x 7730(1)) show the effect of the colonising hyphae on the tracheid wall. The S_3 layer has been removed in the wall region close to the hypha revealing the steeper S_2 microfibrillar orientation.

The apparent inconsistency between the angle of the splits and the observed S_2 microfibrillar angle, due to wall lysis, can be explained by the way the microfibrils are laid down around a bordered pit such that they are almost parallel with the cell axis to the top left and bottom right of a pit. See also figs. 77 and 78.

It would appear that the warts (Ws) show a certain degree of resistance to dissolution by the hypha, see fig. 27.


25
5μ


26
2·5μ


Ws
27
2·5μ

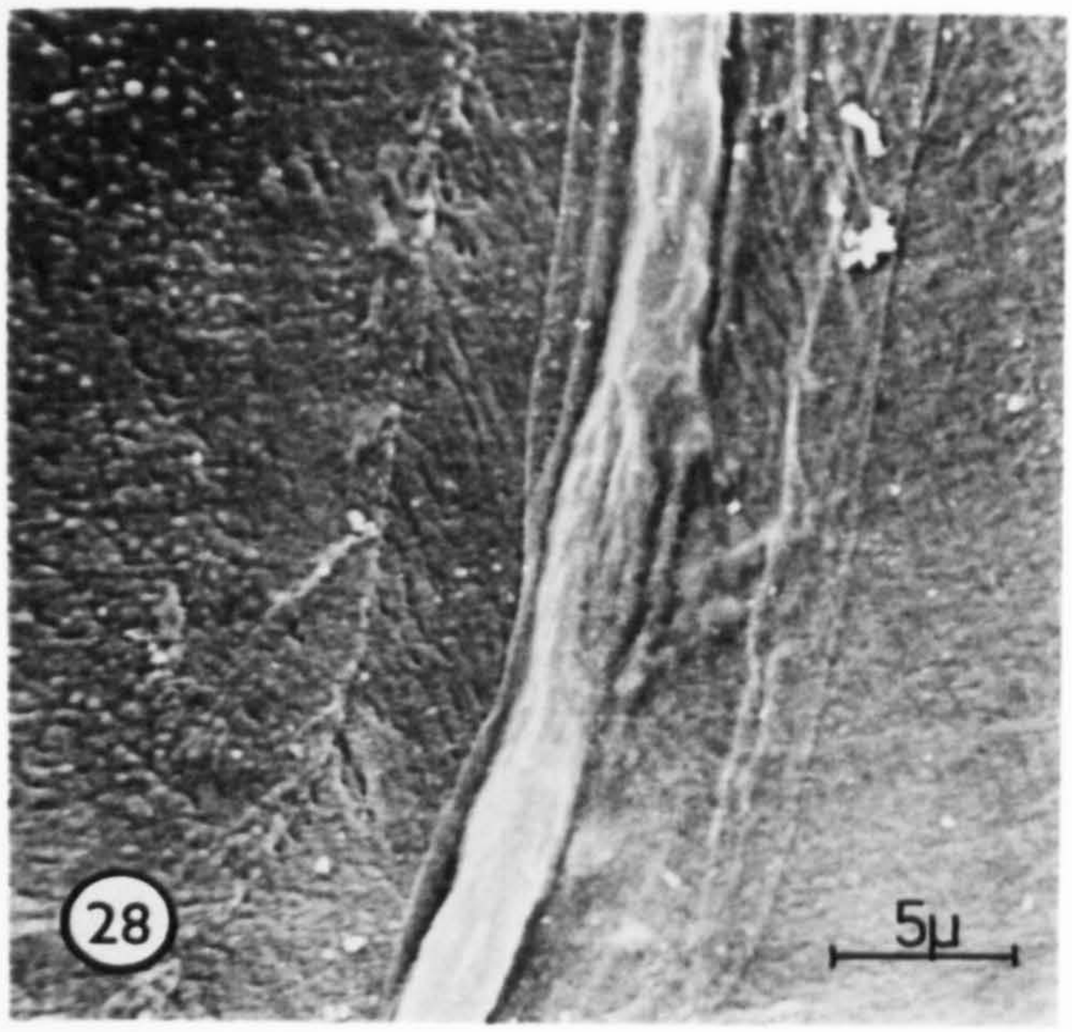
4.2.1.2 Coniophora puteana on Scots pine (Pinus sylvestris), 4 weeks

Fig. 28 (x 5600(1)). Another example of the very slight wall lysis, comparable with fig. 26, indicating how thin the S_3 layer is.

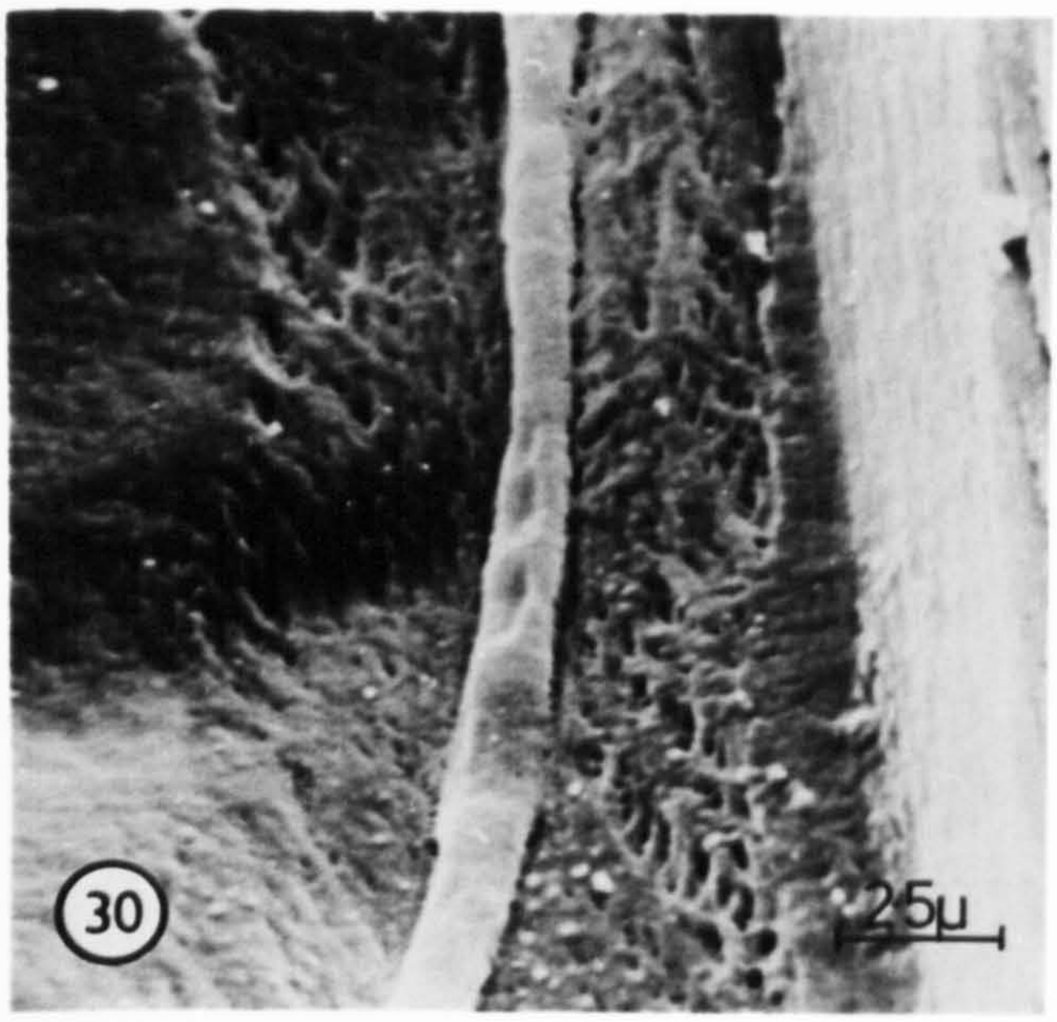
Figs. 29 (x4340(1)) and 30 (x 8140(1)) are of more advanced decay of the wall showing extensive cracking. The decayed regions are beginning to take on a spongy appearance but still the warts (Ws) appear to be resistant. penetration of the bordered pit was via a neat hole in the torus, see also fig. 31.

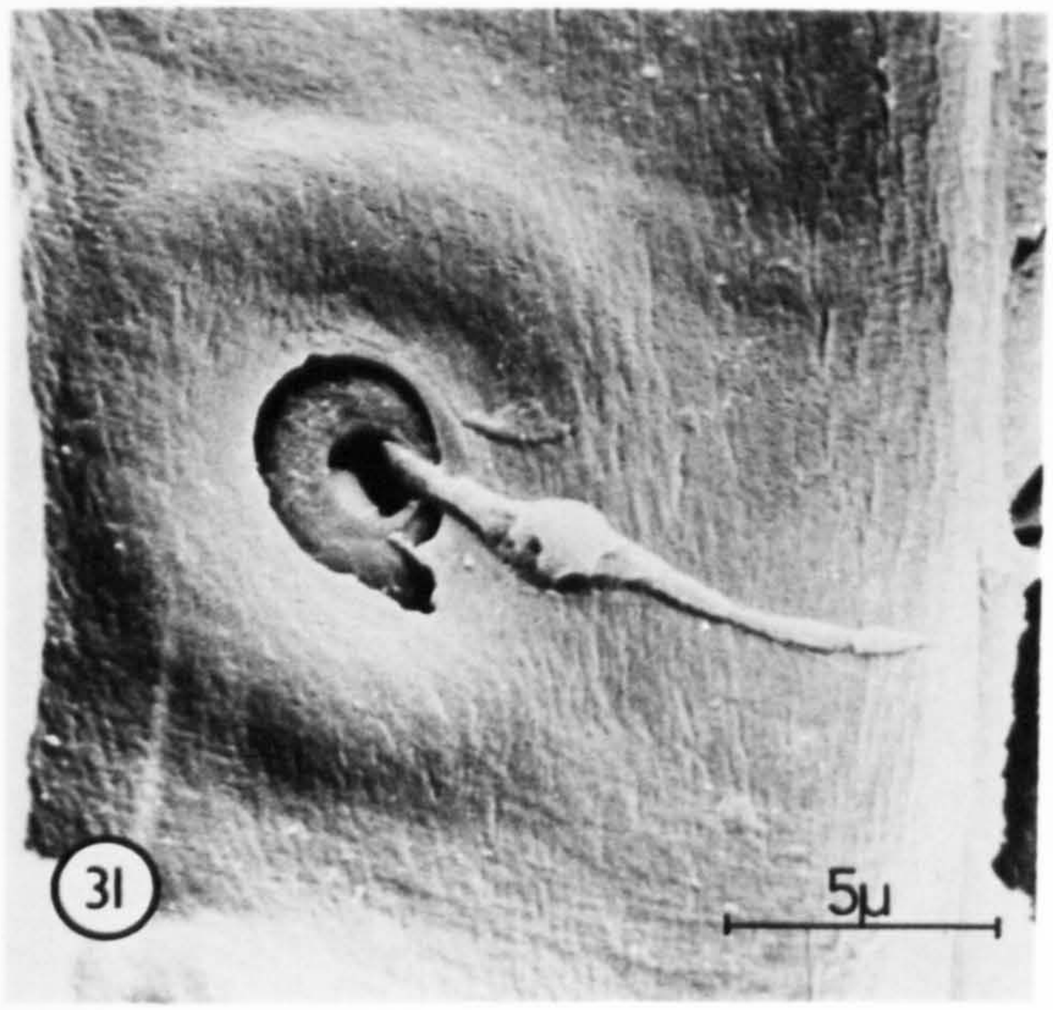
Fig. 31 (x 4110(1)) shows a hypha penetrating through the centre of the bordered pit torus again via a neat small hole. Note there is no significant degradation of the wall.

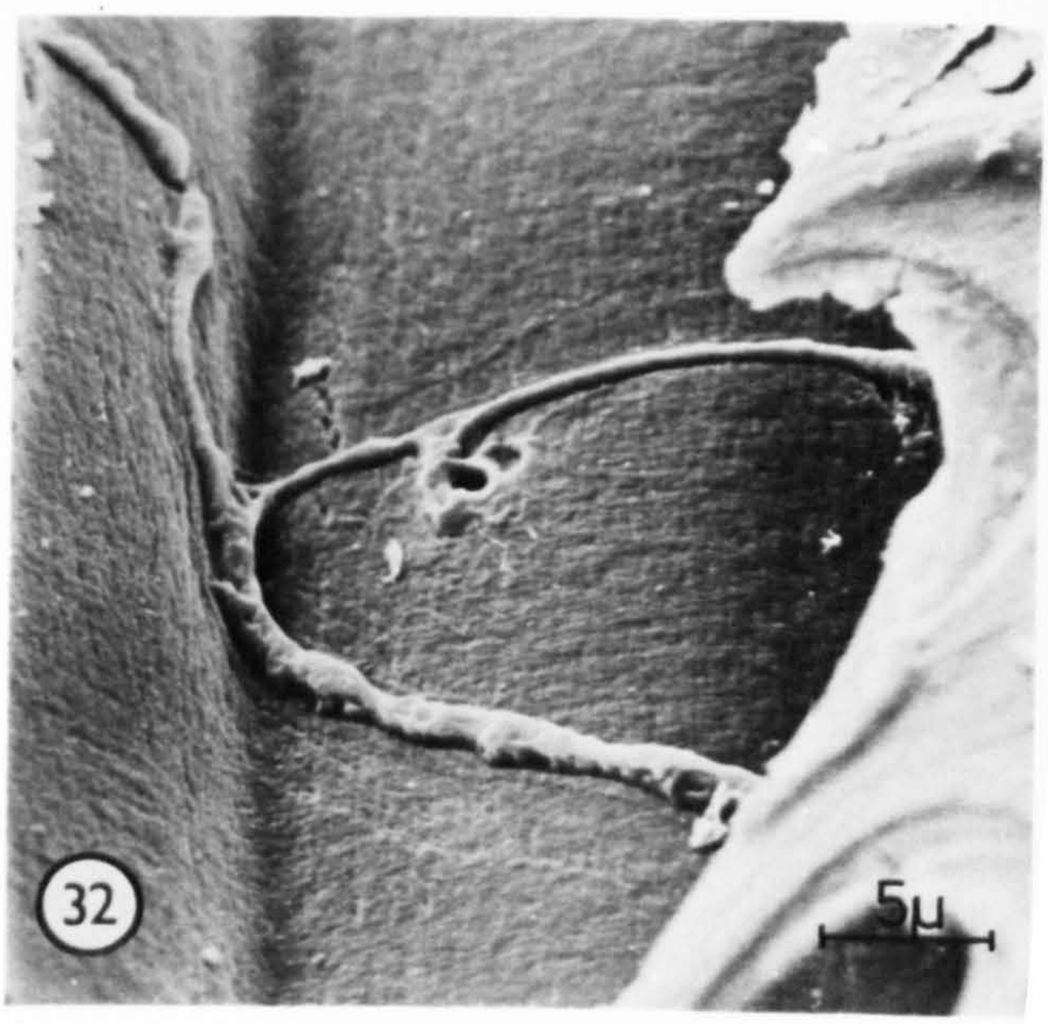
Fig. 32 (x 2630(1)) illustrates bore hole formation in an early wood tracheid. A certain degree of shallow wall lysis is evident.


28
5μ


Ws
29
2·5μ


30
2·5μ


31
5μ


32
5μ

4.2.2 Soft rot, Chaetomium globosum

4.2.2.1 C. globosum on hardwwod:- Birch (Betula sp.)

The material for these results came from two incubation times, 8 weeks (figures 33 - 42) and 6 weeks (figures 43 - 47). Only in one small region in one of the 8 week specimens was soft rot decay observed to any appreciable extent. Blocks were otherwise extensively colonized but there was very little active degrade of the walls. The specimen examined was an external tangential, longitudinal, surface of the decayed block and numerous cavities were observed on this surface. The cavities were only formed in the region closest to the culture medium surface and although there was a great deal of general debris on the specimen details of the cavities could be picked out, figures 33 - 34. The cavities had broken through the S_3 layer of the fibres revealing the extremely nodular appearance of the hyphae, which tapered at the ends of the cavity, figures 34 and 38. The cavities were all inclined to the fibre axis indicating the line of the S_2 microfibrils which the hyphae follow during cavity formation.

Close to this extensively degraded region a long thin cavity was found, figure 39, which contained a very clear example of a cavity hypha and indicated a number of features involved in cavity formation; the adjacent cavity was empty. The hypha bore a nodular investment and tapered at both ends to fine smooth hyphae which could be seen projecting along the line of the macrofibrils for some distance beyond the cavity, figure 40. These were the proboscis hyphae, detailed in figures 41 and 42, frequently seen in light microscopy but never this clearly in Scanning Electron Microscopy.

Since two long proboscis hyphae were present this must have been the first cavity formed by the 'T' branch, the possible site of which could be the slight bulge in the cavity hypha.

The 6 week material showed no signs of cavity formation although numerous bore holes were encountered, figures 43 - 45, in which the hole diameter far exceeded that of the hypha. A peculiar investment was frequently observed on these otherwise smooth hyphae colonizing the block interior, figure 6.

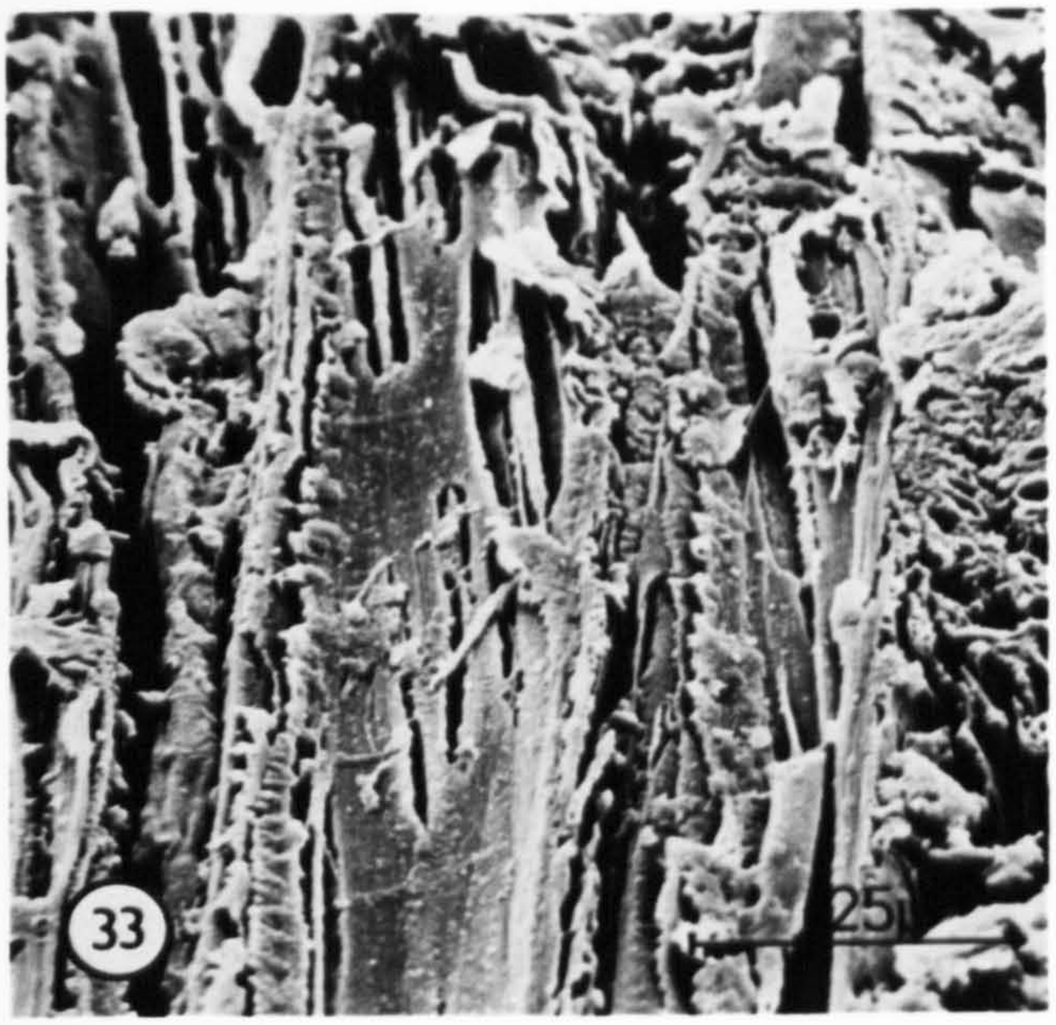
Normal cross-field pitting between birch fibres could be easily confused with cavities, figures 46 and 47, especially when fungal hyphae penetrating the pits are present.

4.2.2.1 Chaetomium globosum on birch (Betula sp.), figures 33 - 42 are 8 week material and figures 43 - 47, 6 week material.

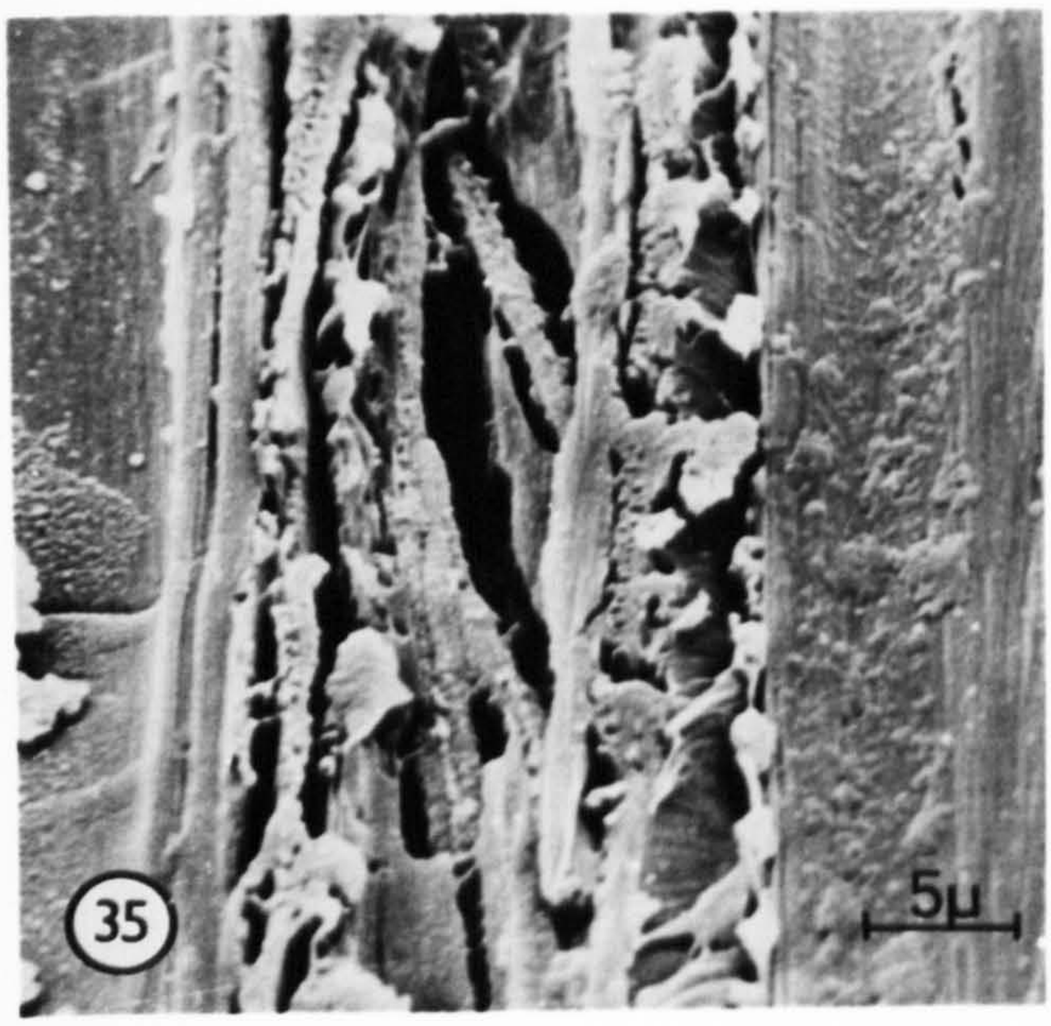
Figs. 33 (x 1000(1)) and 34 (x 2280(1)) illustrate the general condition of the decayed block surface. Heavy cavity formation within the S_2 has occured, breaking through the S_3 layer of the fibres, enabling the cavities to be seen from the lumen. The detail in fig. 34 reveals hyphae within the cavities bearing a nodular investment and tapering at the ends of the cavities.

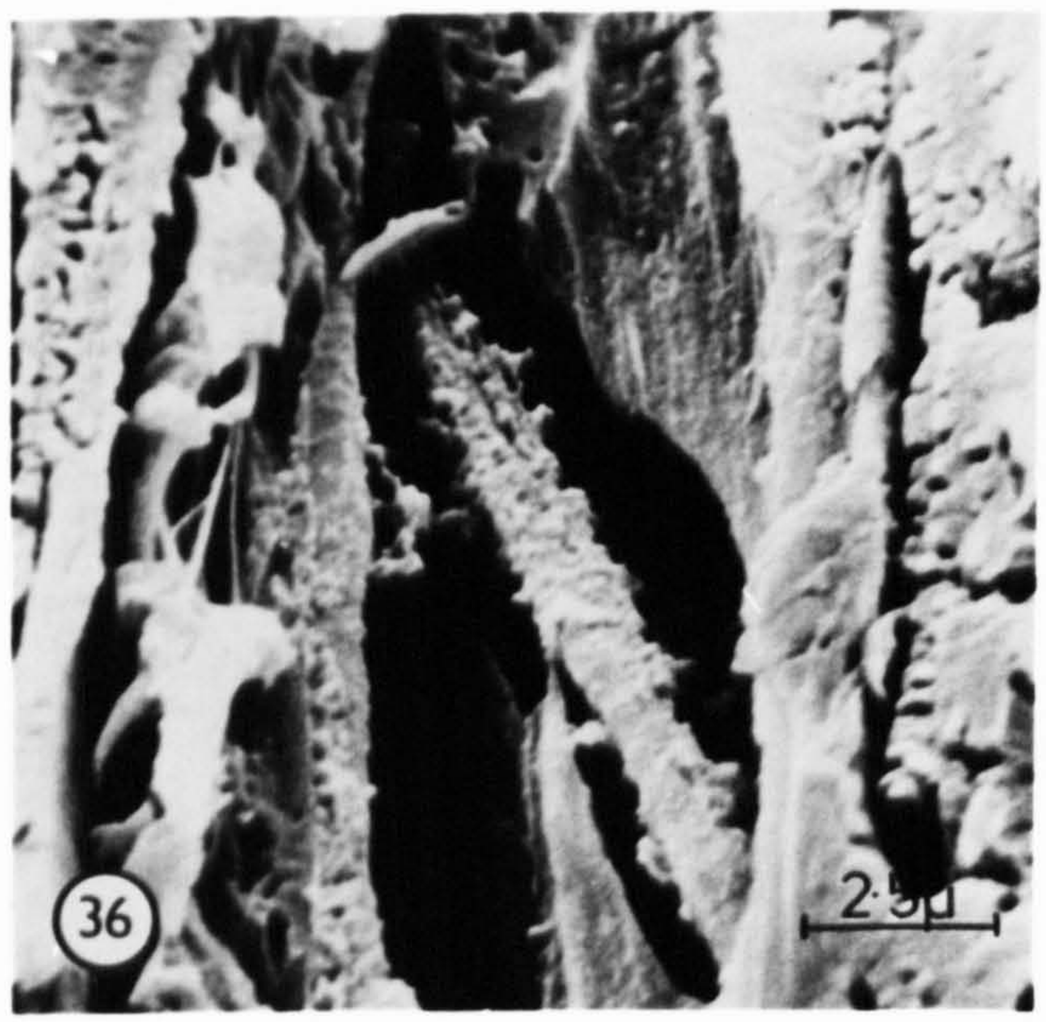
Figs. 35 (x 2140(1)) and 36 (x 5910(1)) give details of another fibre wall cavity again containing a hypha with some form of extracellular material on its surface.

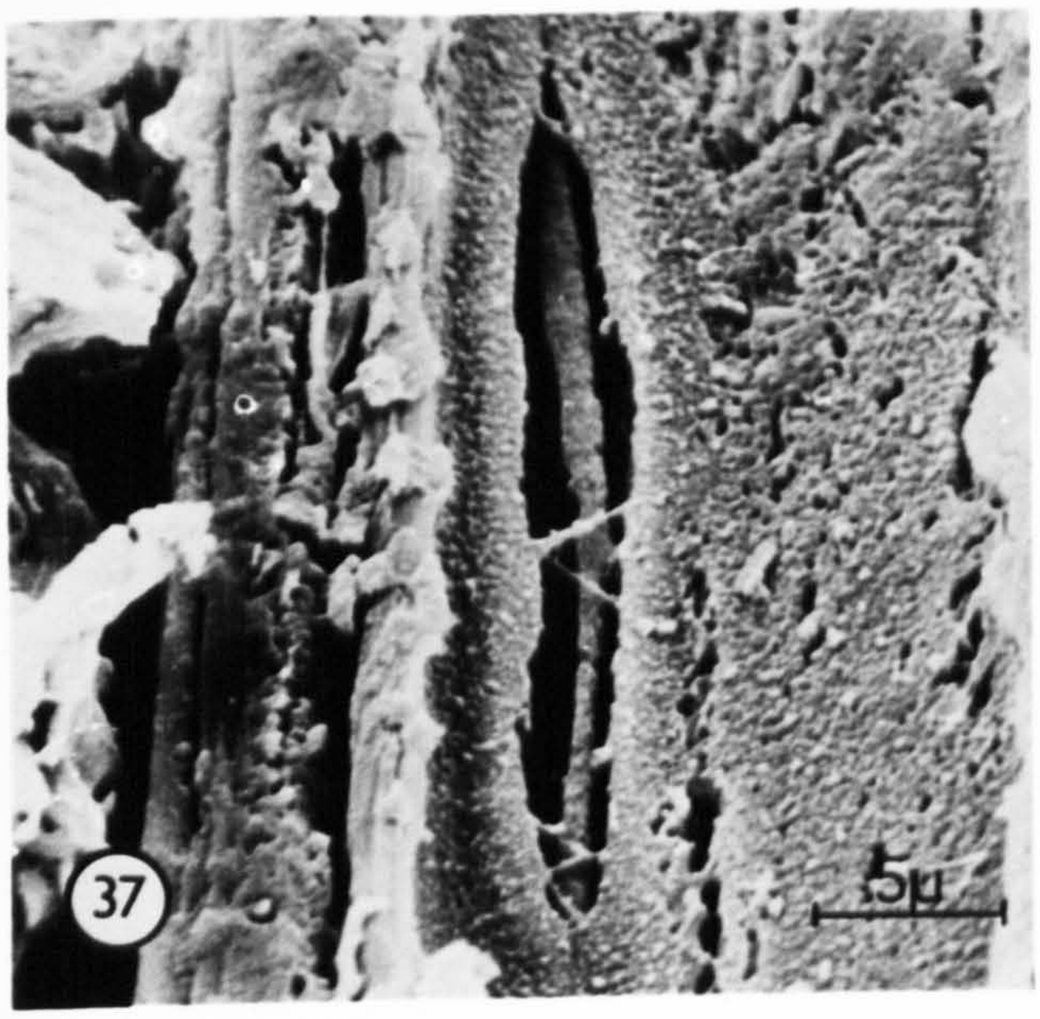
Fig. 37 (x 2930(1)) shows a single fibre cavity and a chain of two cavities can be seen in fig. 38 (x 2410(1)). Only the upper one bears the hypha which tapers at one end and is broken at the other.

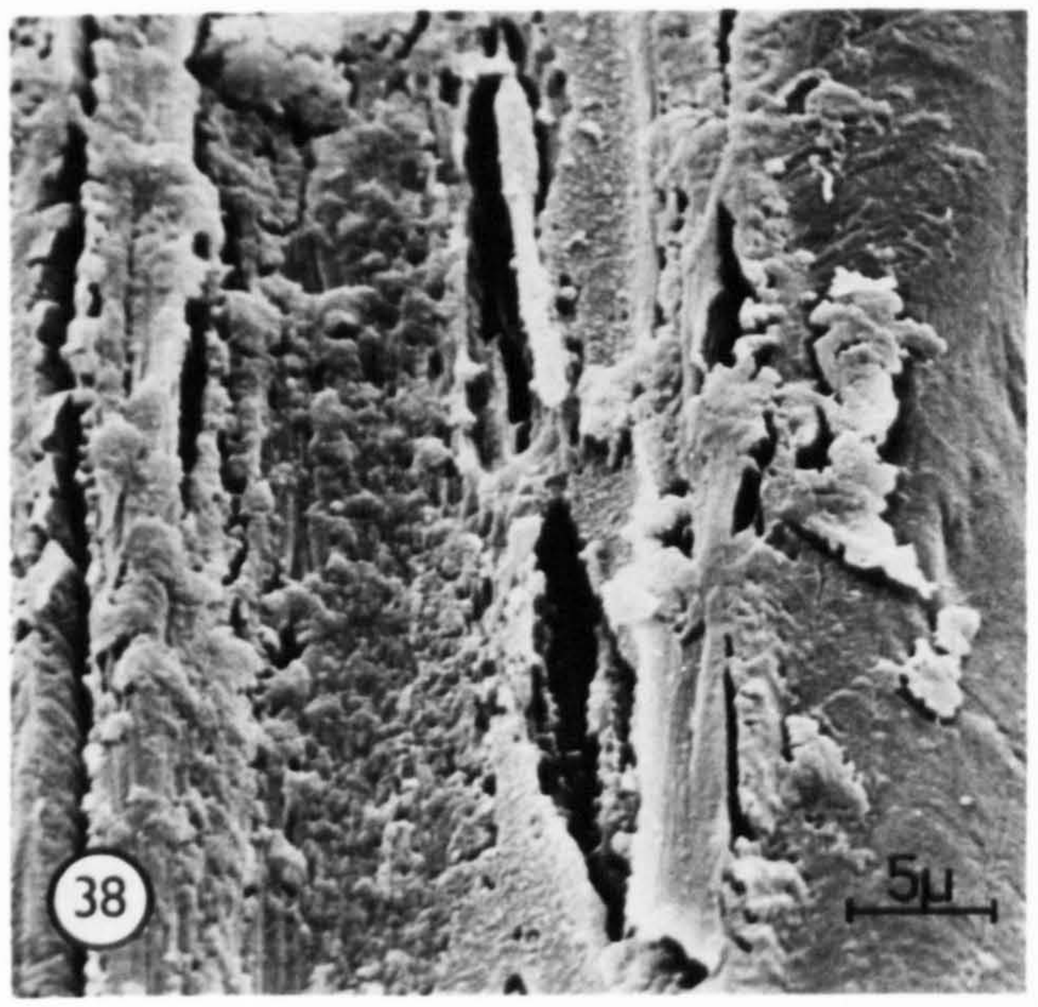

33
25


34
5μ


35
5μ


36
2·5μ

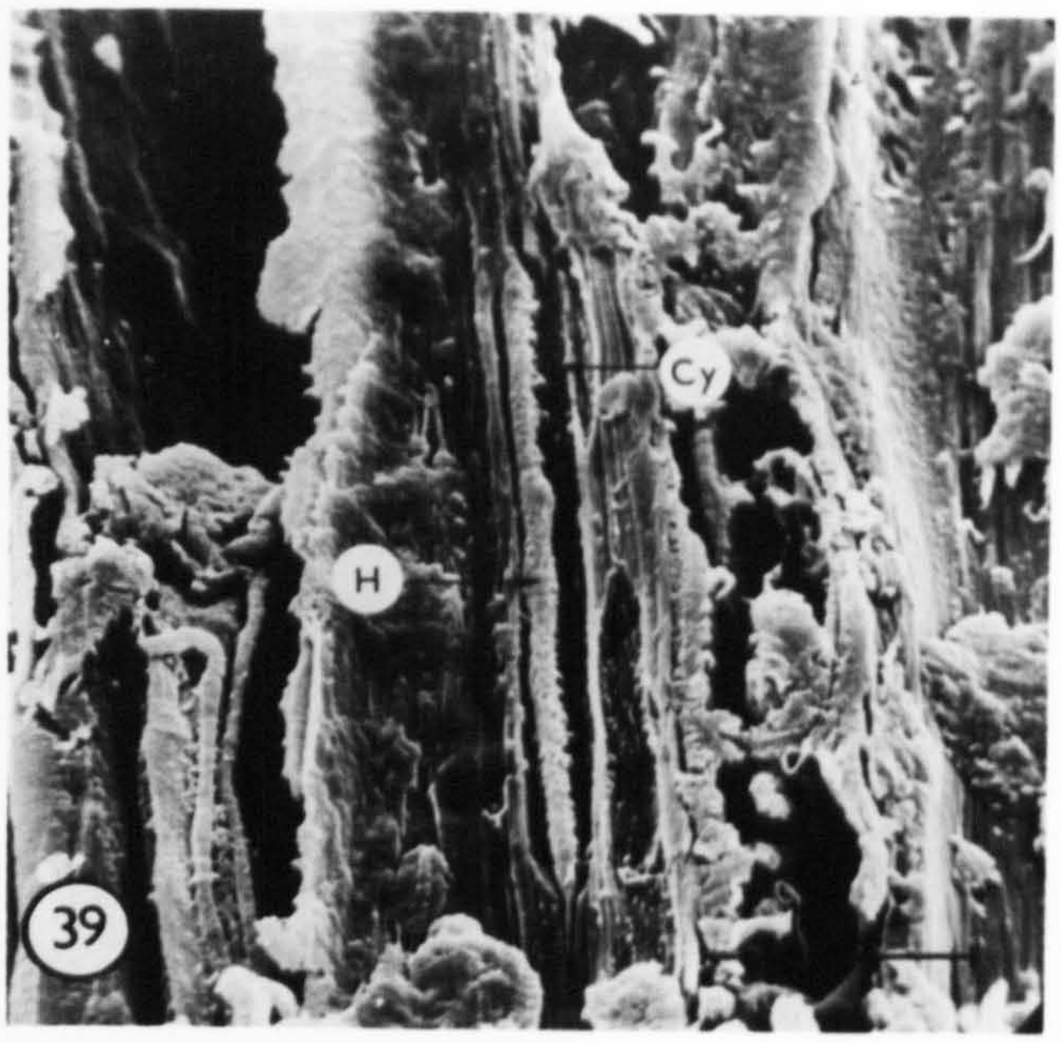

37
5μ


38
5μ

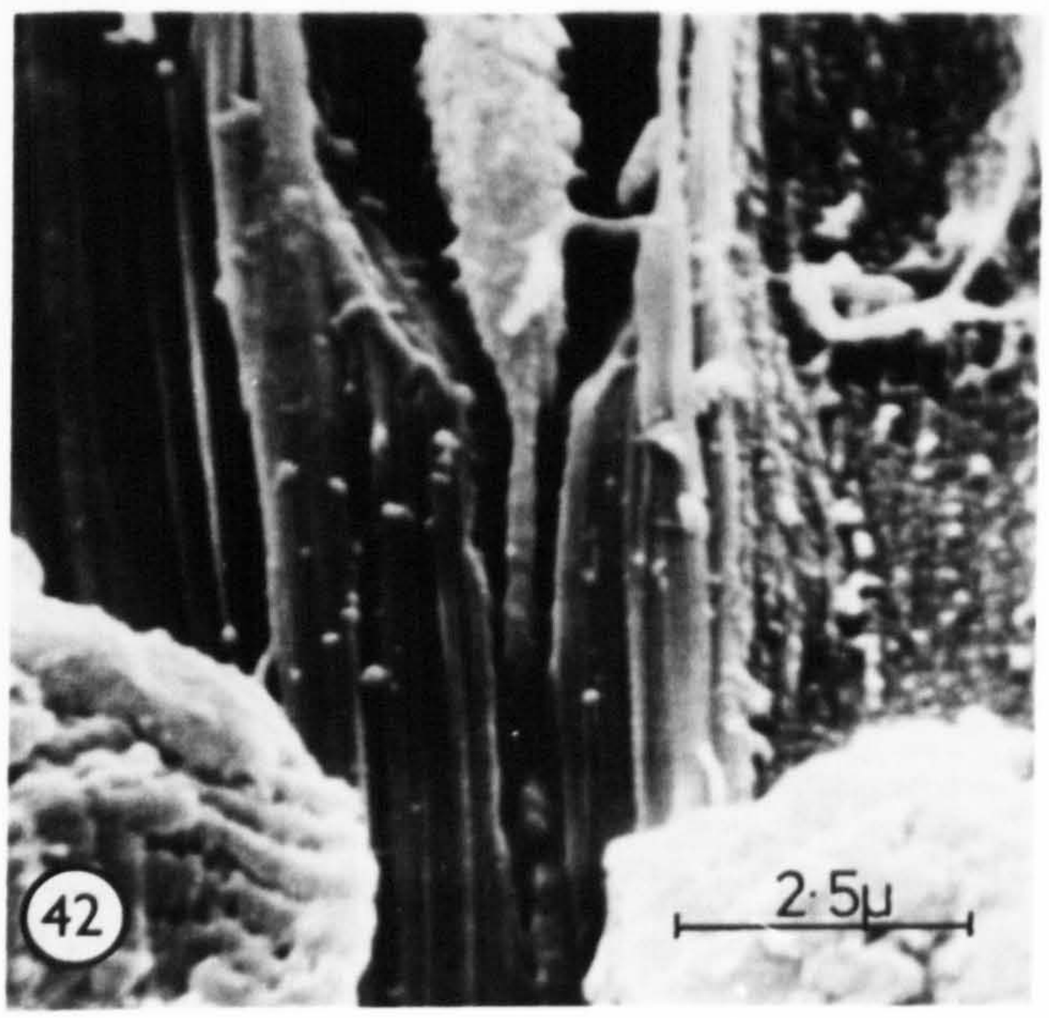
4.2.2.1 Chaetomium globosum on birch (Betula sp.)

Fig. 39 (x 1950(1)). This tangential longitudinal surface features a cavity containing a hypha in a damaged fibre wall with an adjacent empty cavity. The details of the hypha can be clearly seen in fig. 40 (x 4540(1)) and this reveals that the hypha is constricted at both ends to produce fine proboscis hyphae (Ph), the top one extending out of the field of view. The probable connection of the 'T' branch penetration hypha is indicated (Tb). Note the regular smooth pattern to the inner surface of the empty cavity (Cy). Also present is the extremely nodular investment to the cavity hypha, as already mentioned for fig. 34, but note the proboscis hyphae appear very smooth.

Figs. 41 (x 9090(1)) and 42 (x 9090(1)) are high magnifications of the two proboscis hyphae detailing the change from rough nodular cavity hyphae to smooth finer proboscis hyphae.


H
Cy
39


41
5μ

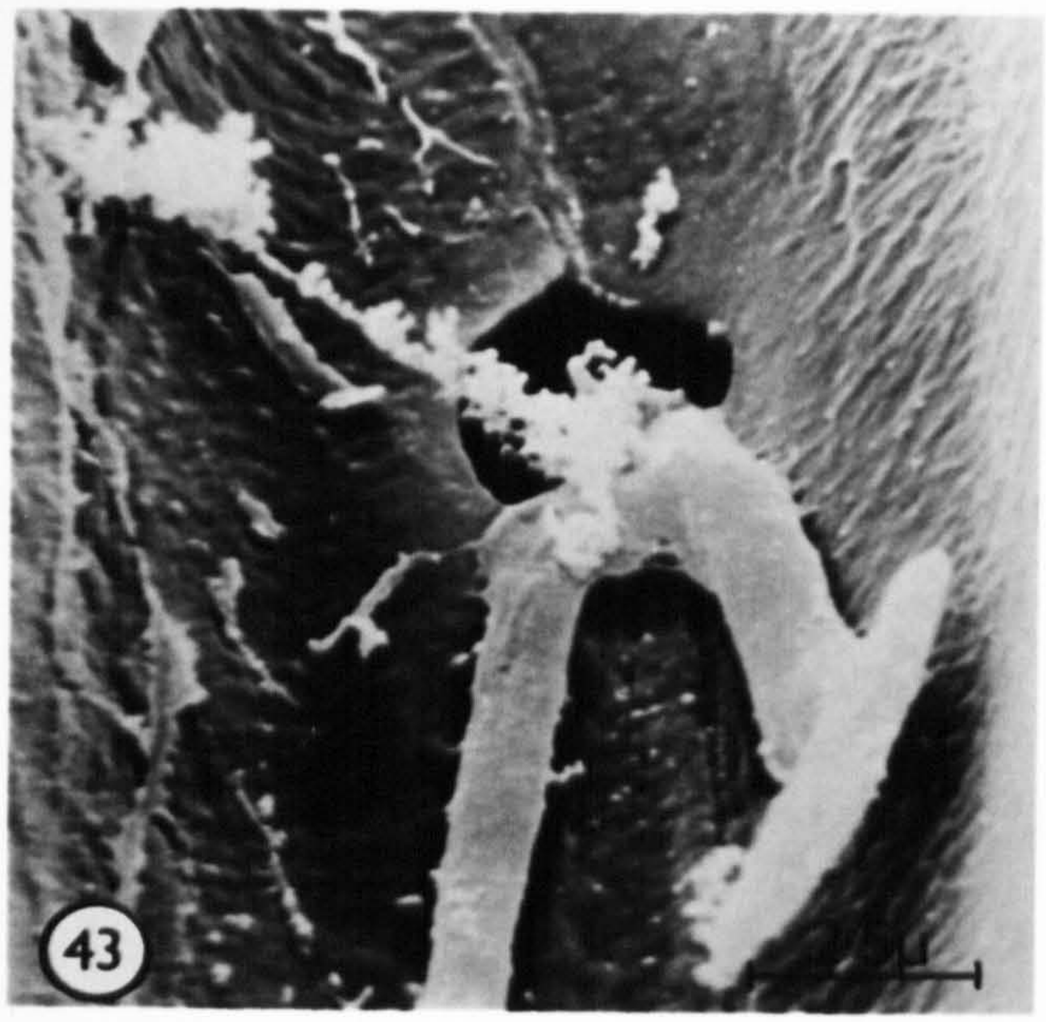

42
2·5μ

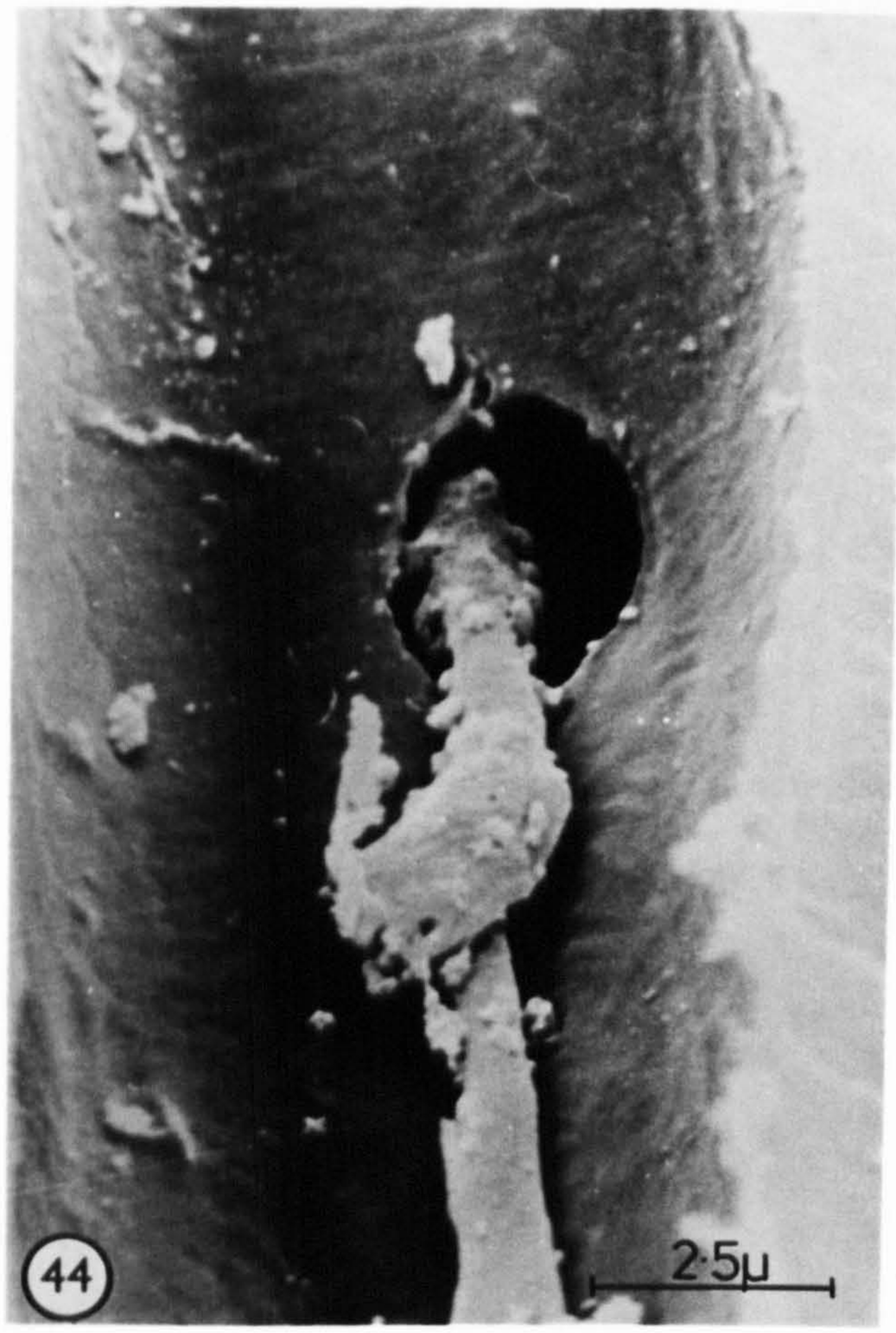

Ph
Tb
Cy
Ph
40
5μ

4.2.2.1 Chaetomium globosum on birch (Betula sp.)

Figs. 43 (x 7010(1)), 44 (x 8720(1)) and 45 (x 5020(1)) are all of bore hole formation in the fibres and all illustrate that the bore hole is much wider than the hypha. Figs. 43 and 45 also reveal the presence of a fine 'woolly' material on the hyphae, the significance of which will be discussed later.

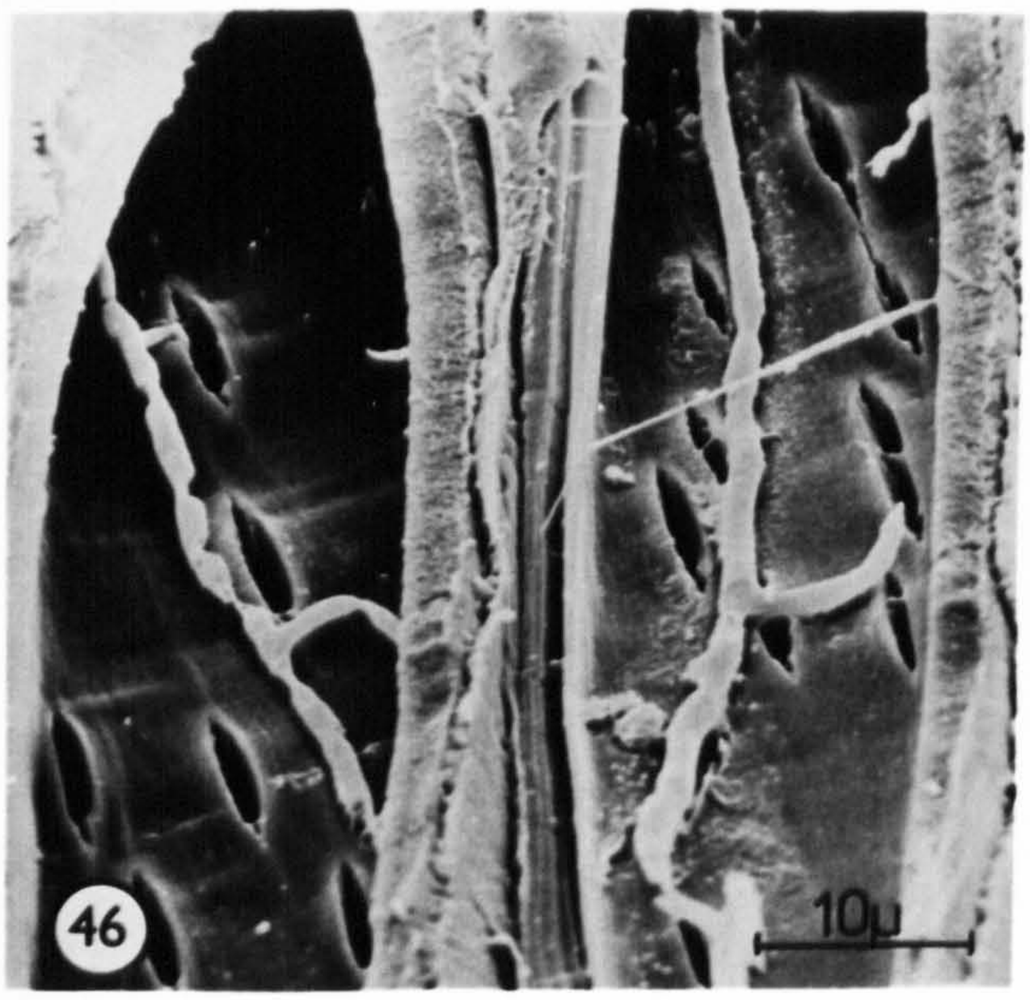
Figs. 46 (x 1670(1)) and 47 (x 3400(2)) have been included to demonstrate how normal fibre pitting can sometimes be confused with cavities. In the left hand fibre of fig. 46 the hypha can be seen penetrating the pit but there appears to be more hyphal activity in the right hand fibre. The geometry of the pits has been revealed in fig. 47 by the stripping of the S_3 and S_2 wall layers in the left hand fibre. The splits to each end of the pits, parallel with the microfibrillar orientation, have probably resulted from stresses set up in the wall by the removal of the water during drying.


43


44
2·5μ


45


47
5μ

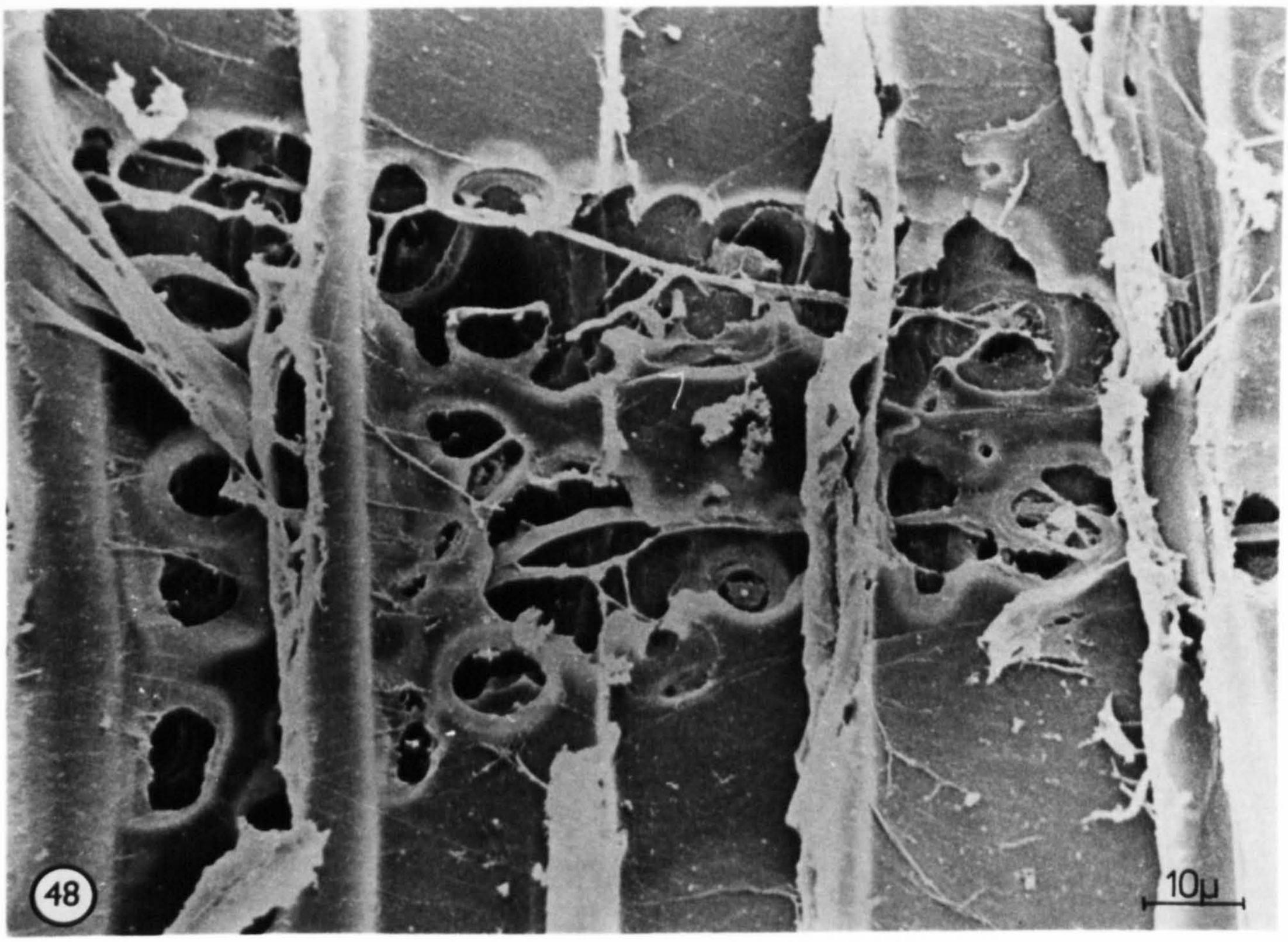

46
10μ

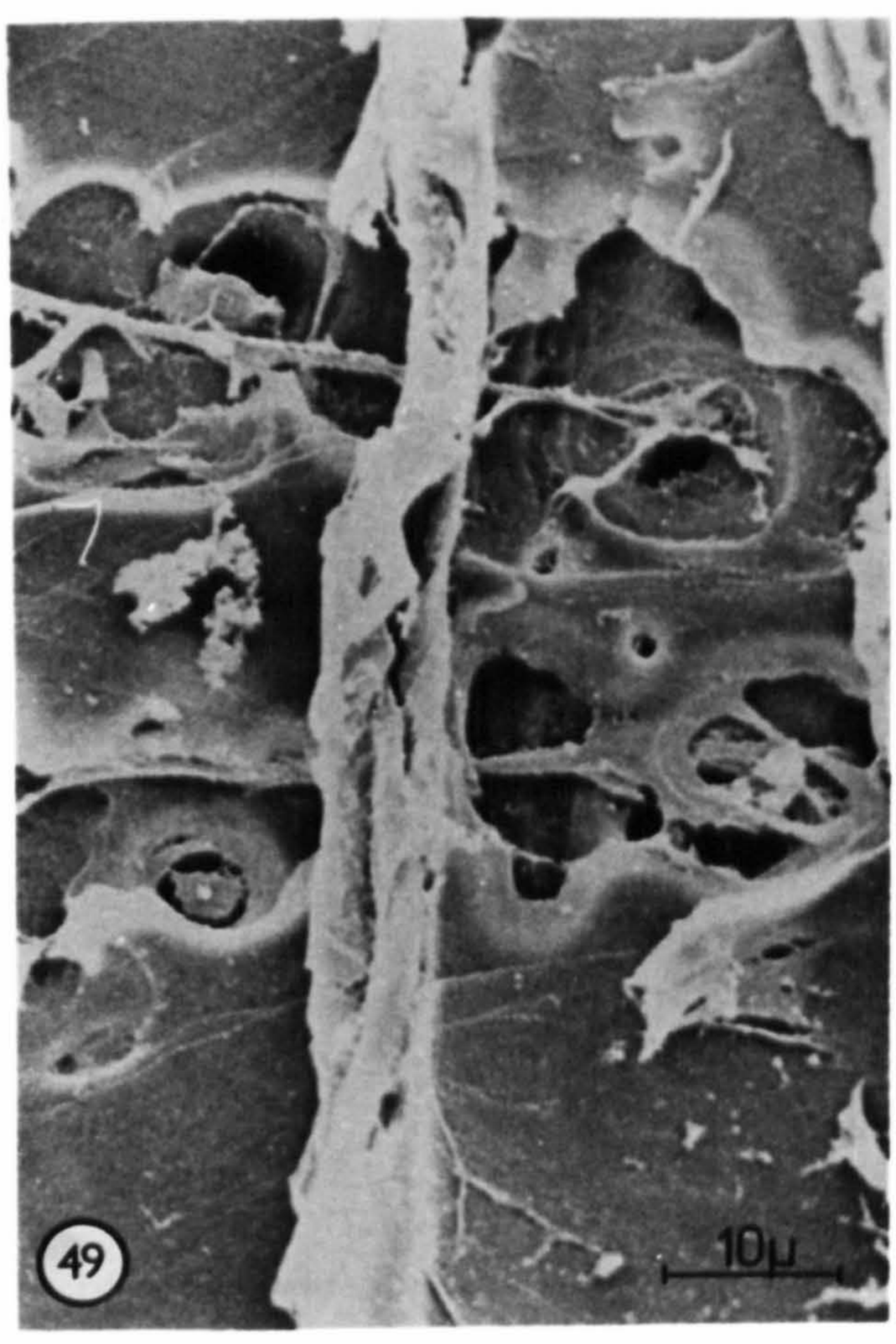
4.2.2.2 C. globosum on softwood:- Scots pine (Pinus sylvestris)

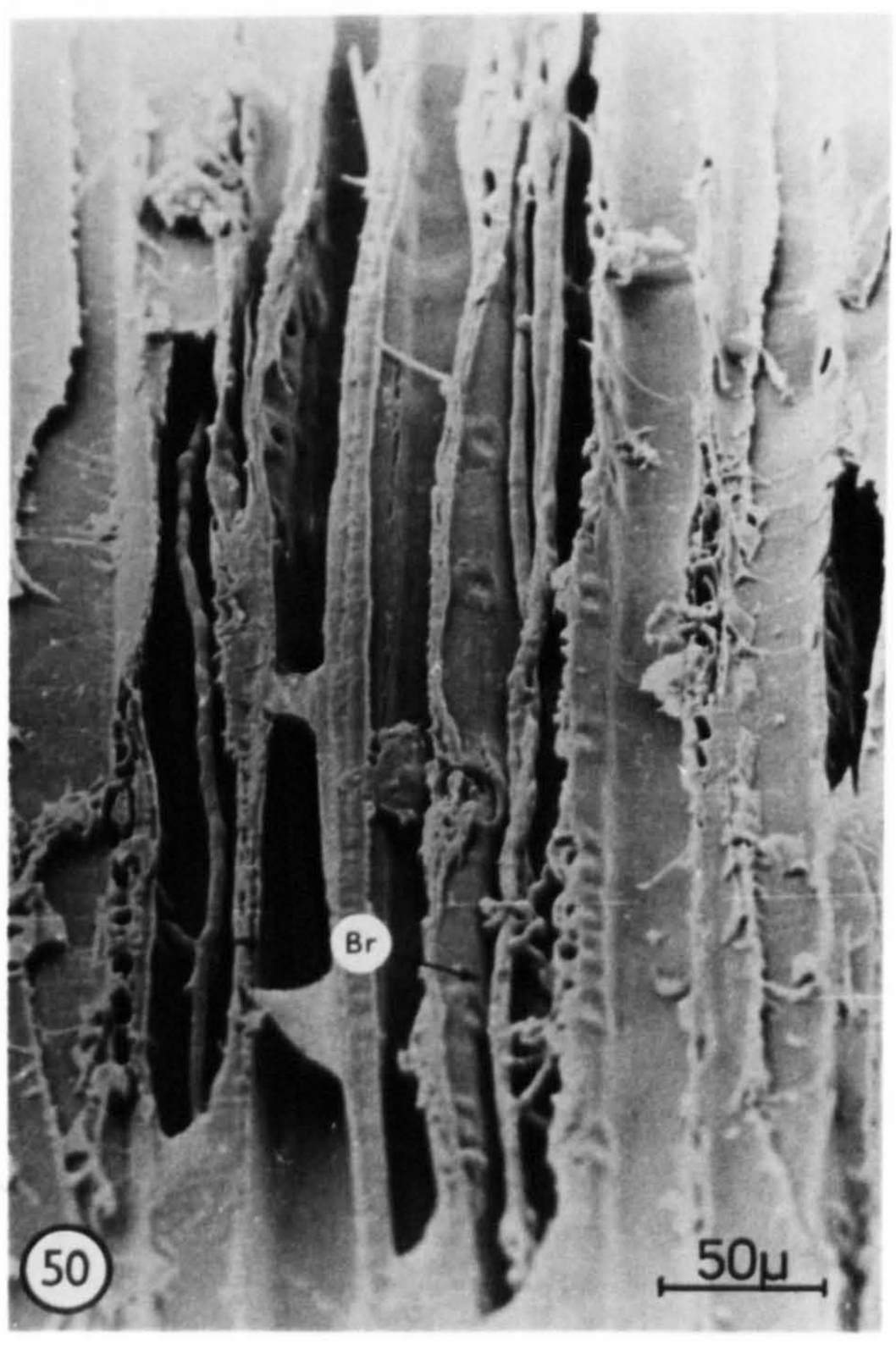
Soft rot develops characteristically more slowly in softwoods than in hardwoods and as mentioned earlier very little decay was observed for this fungus - wood combination, even in the 8 week incubated material. It is also likely that the blocks did not wet up to a high enough moisture content for active decay to take place within 8 weeks. Longer incubation periods or wetter blocks might have produced more significant results. Instead the activity of the fungus on the wood was restricted to poor colonization with a certain amount of ray degrade by very fine hyphae, figures 48 and 49. The main colonizing hyphae were extremely thick by comparison, figure 50, and were deeply pigmented making them readily visible under the light microscope. These hyphae exhibited profuse lateral branching in the vicinity of ray tissue but these branch hyphae were much larger than those seen in the destruction of the ray tissue in figures 48 and 49. Other than this behaviour, typically exhibited by stainers, there was little effect on the bulk of the wood elements.

4.2.2.2 Chaetomium globosum on Scots pine (Pinus sylvestris), 6 weeks

Fig. 48 (x 1280(2)) reveals fairly extensive colonisation of the ray tissue, with large numbers of cross-field pit membranes being destroyed. The detail in fig. 49 (x 1590(2)) shows the hyphae to be very fine and delicate, totally dissimilar to those in fig. 50 (x 300(2)) which were frequently encountered. These extremely thick hyphae can be seen colonising the tracheids, some producing lateral branches (Br) near the rays. These thick hyphae could easily be seen in the light microscope.


48
10µ


49
10µ


Br
50
50µ

4.2.3 White rot, Coriolus versicolor

4.2.3.1 C. versicolor on hardwood:- birch (Betula sp.)

Extensive colonization of the vessels spread into the ray and fibre tissue resulting in severe degrade of the ray tissue and to a lesser extent the fibres. Figures 50 to 54 illustrate the general appearance of this type of degrade. Hyphae can be seen within the vessels yet not in the ray tissue where there has been heavy degrade. Numerous bore holes or pit enlargements have occured in this tissue with a number of cases where large areas of wall have been totally degraded. Although the rays showed the severest attack, adjacent fibres and vessels were also penetrated. The ability of this fungus to utilise all the wall material is clearly demonstrated in figures 55 and 56 where the vessel - ray walls and interconnecting pits have undergone heavy degrade. It is possible that there was a slight preference, (or greater capacity), to degrade the proportionately less cellulosic wall material of the cross-field pit membranes than that of the secondary cell wall layers.

Extensive degrade, especially in rays and cross-field zones, was observed with the presence of hyphae, figures 57 and 58, and fibre degrade was also evident. Lysis appeared to be initiated with bore holes which may or may not coincide with existing pitting. The subsequent development of the bore hole frequently resulted in extremely large areas of wall being lysed.

Details of ray colonization, lateral and vertical spread, can be seen in figures 59 and 60. The role of side branching in the development of new lysis regions was indicated in figure 59 and figure 60 where a range of lysis types are demonstrated.

The occurrence of fine strands in association with the normal colonizing hyphae was noted, figures 60, 66 and 67. Whether the strands are fine hyphal branches or a peculiar dehydration of an extracellular hyphal component is not known. Bore holes and lysis regions around lateral branches were frequently associated with a definite thinning of lysis margins, figure 61, or an apparent 'halo' of less dense wall material, figures 62 and 59, which could also indicate thinning. As with other fungal types the utilisation of natural pitting was observed, especially in ray tissue, and figures 64 and 65 detail this feature in the axial parenchyma.

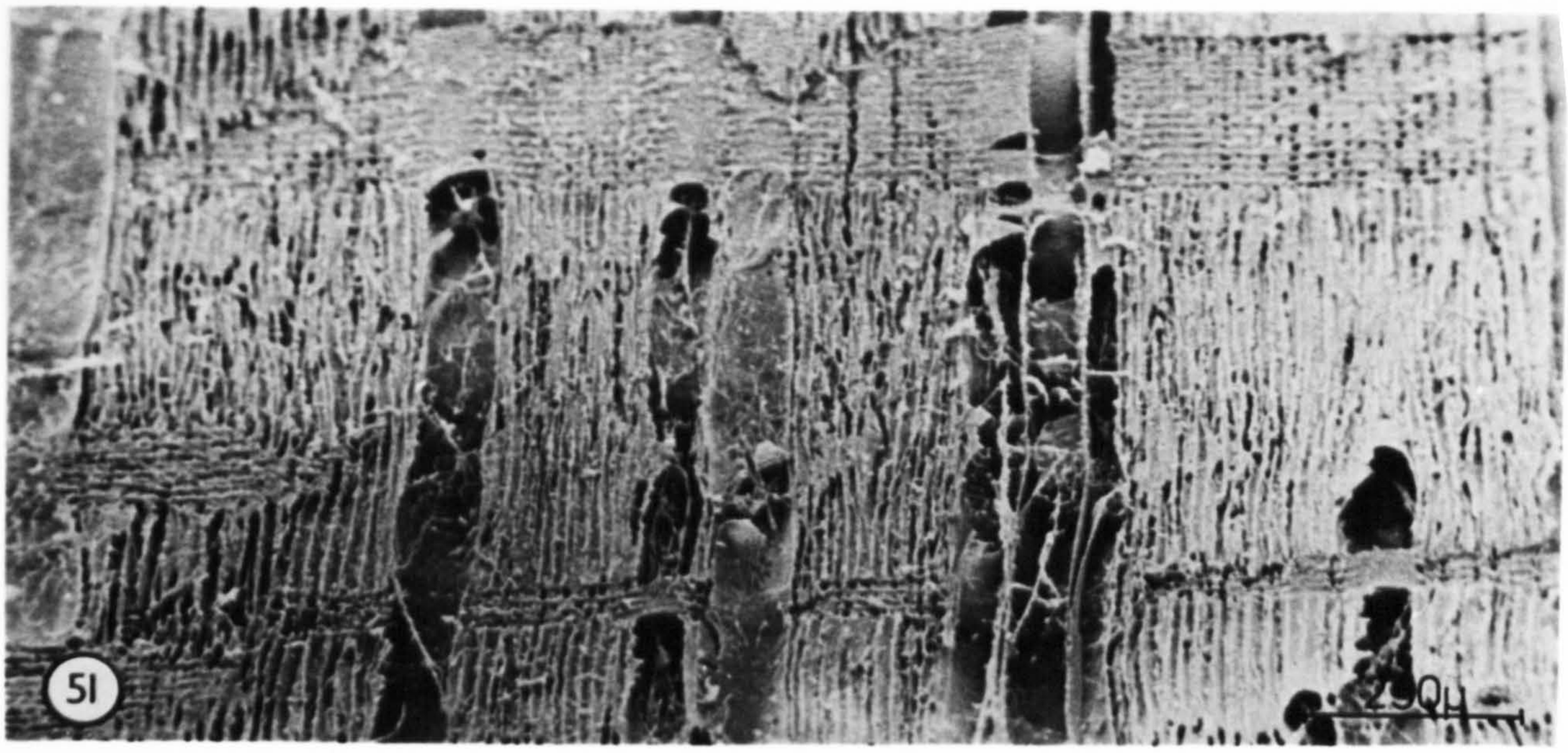
The predominant lysis forms were pit enlargement, bore holes and spreading lysis zones, (probably late stages of the previous two). The only occurence of white rot channelling, as reported by previous workers, was in a few fibres, figures 68 to 71. Regions of intact wall could be seen with surrounding lytic zones. The lysis appeared to show a preference for the matrix material resulting in the microfibrils being more pronounced. Their steep angle indicated that the exposed fibrils were probably part of the S_2 but there was no evidence in this fibre of the presence of a normal S_3, even in the unattacked regions. The details of these shallow troughs or channels, figures 69 to 71, show deeply indented margins when the trough crosses the microfibrillar line and very sharp margins when parallel.

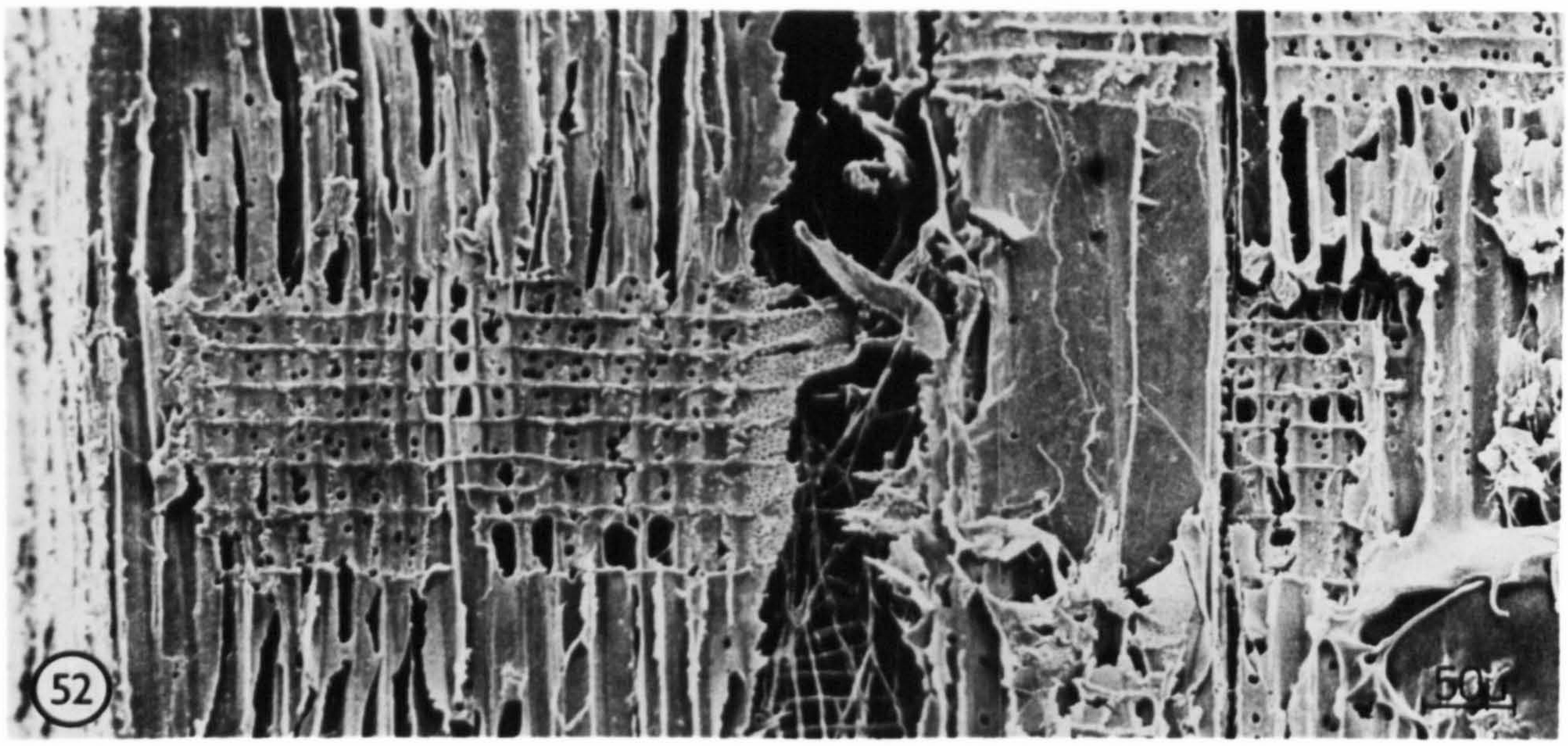
4.2.3.1 C. versicolor on birch (Betula sp.), 4 weeks

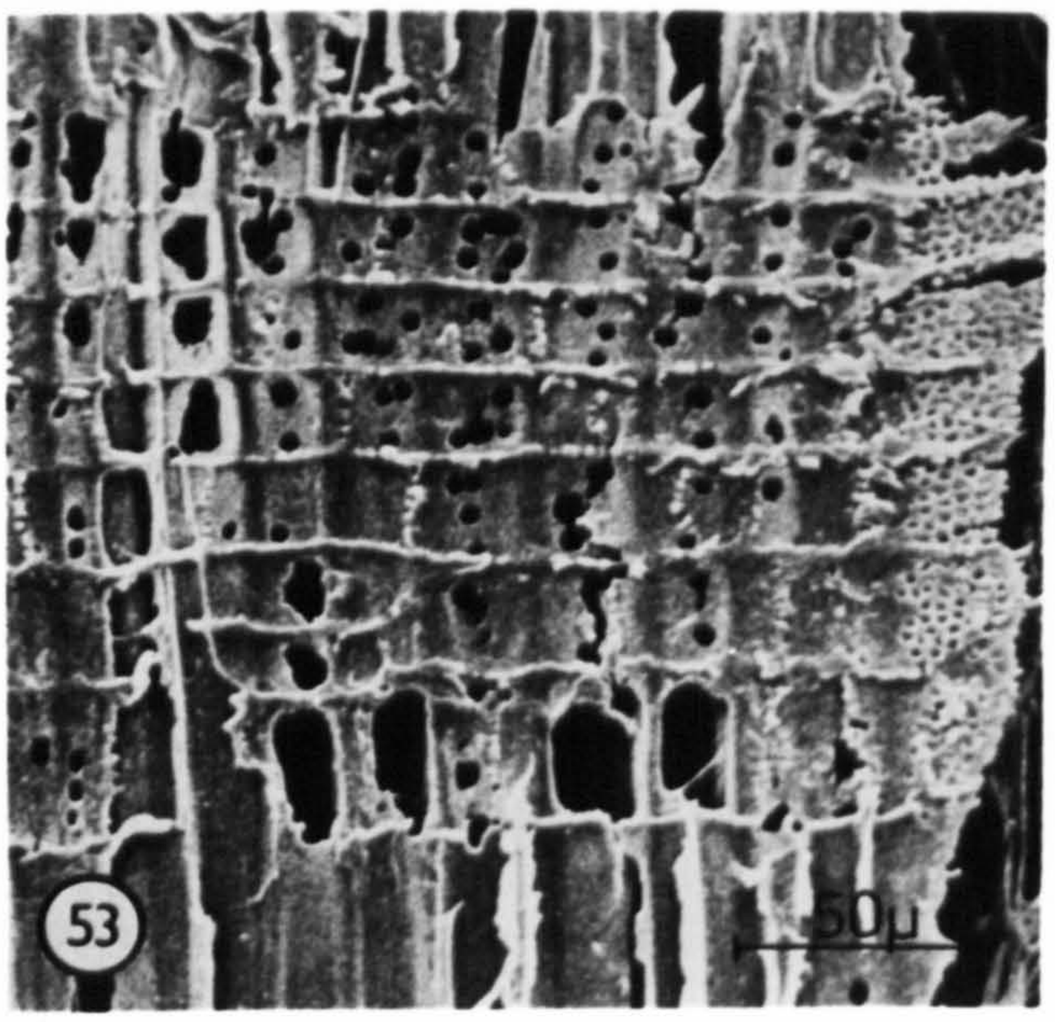
Fig. 51 (x 90(2)) is included to demonstrate the ability of the preparation system to produce accurately orientated sections as mentioned in 4.1.1. This radial longitudinal section shows heavy colonisation of the vessel elements and indicates the height that some rays can achieve,(top of figure).

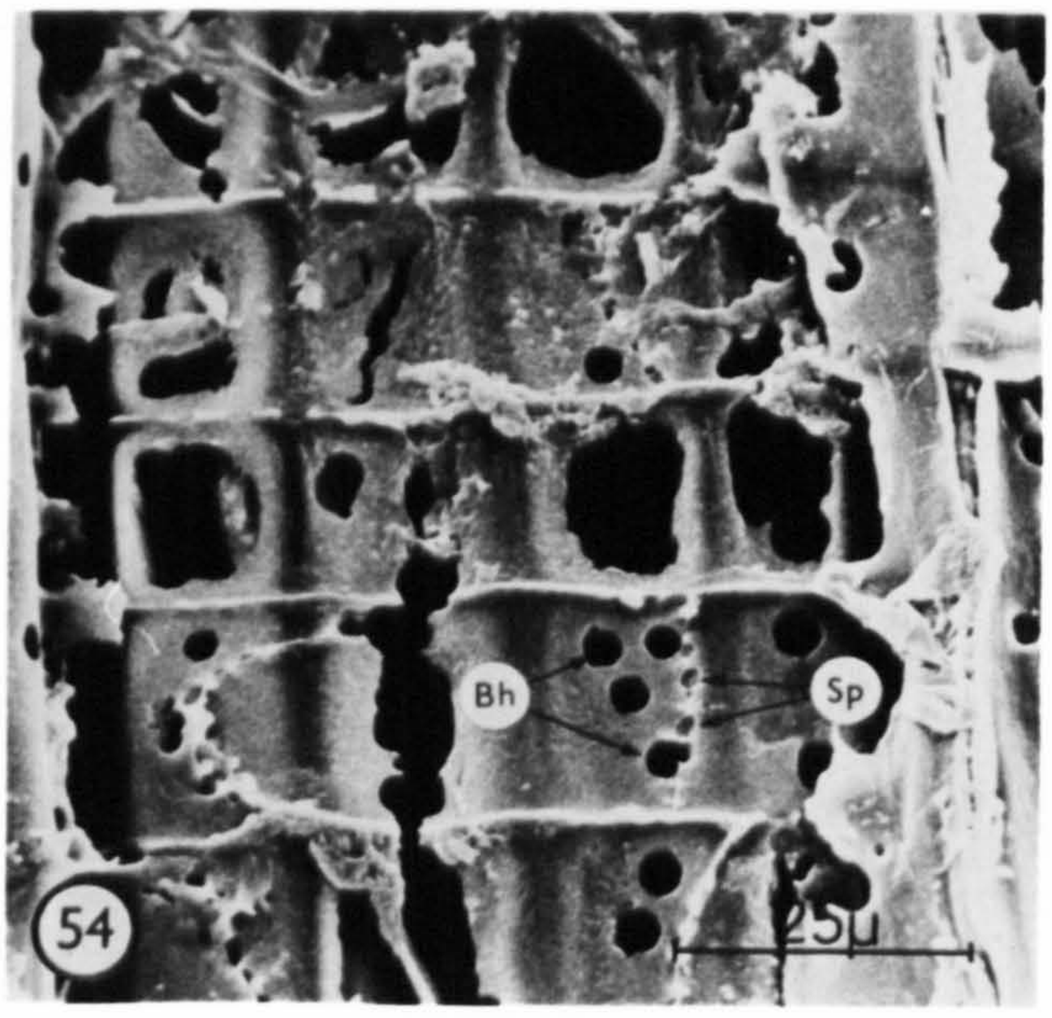
Figs. 52 (x 200(1)), 53 (x 380(1)) and 54 (x 900(1)) illustrate the destructive effect of this fungus especially on ray tissue. Numerous bore holes are evident yet,with the exception of the vessels, the hyphae are absent. Note the change in pitting type where the ray is adjacent to a vessel, right hand side, rather than the fibres in fig. 53.

Frequently the bore holes are said to be enlargements of simple pits which are certainly numerous in ray tissue, especially between ray cells. Ray - fibre pitting is not as prolific and as such the random bore holes (Bh) of fig. 54 could be regarded as being distinct from enlargement of the simple pits (Sp) which cen be seen to occur in ordered rows.


51
29QH


52
50L

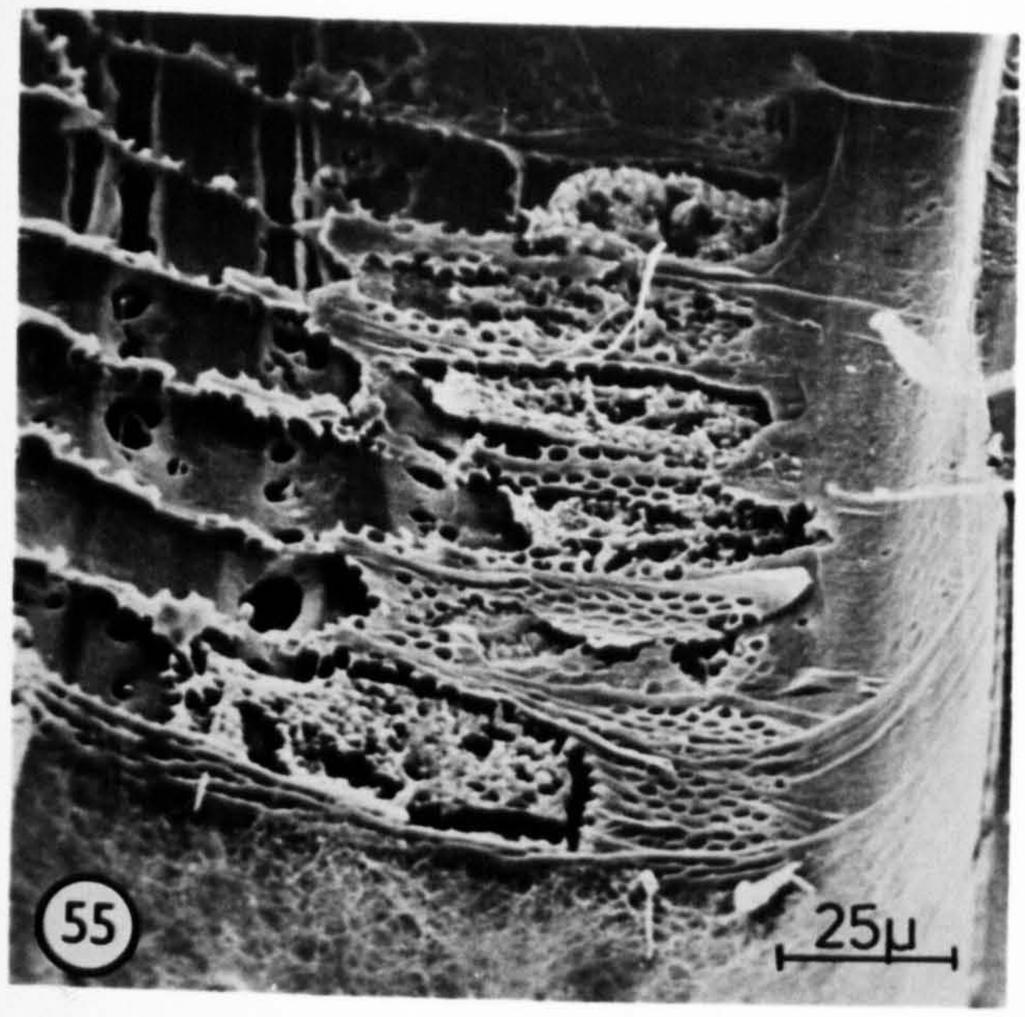

53
50µ

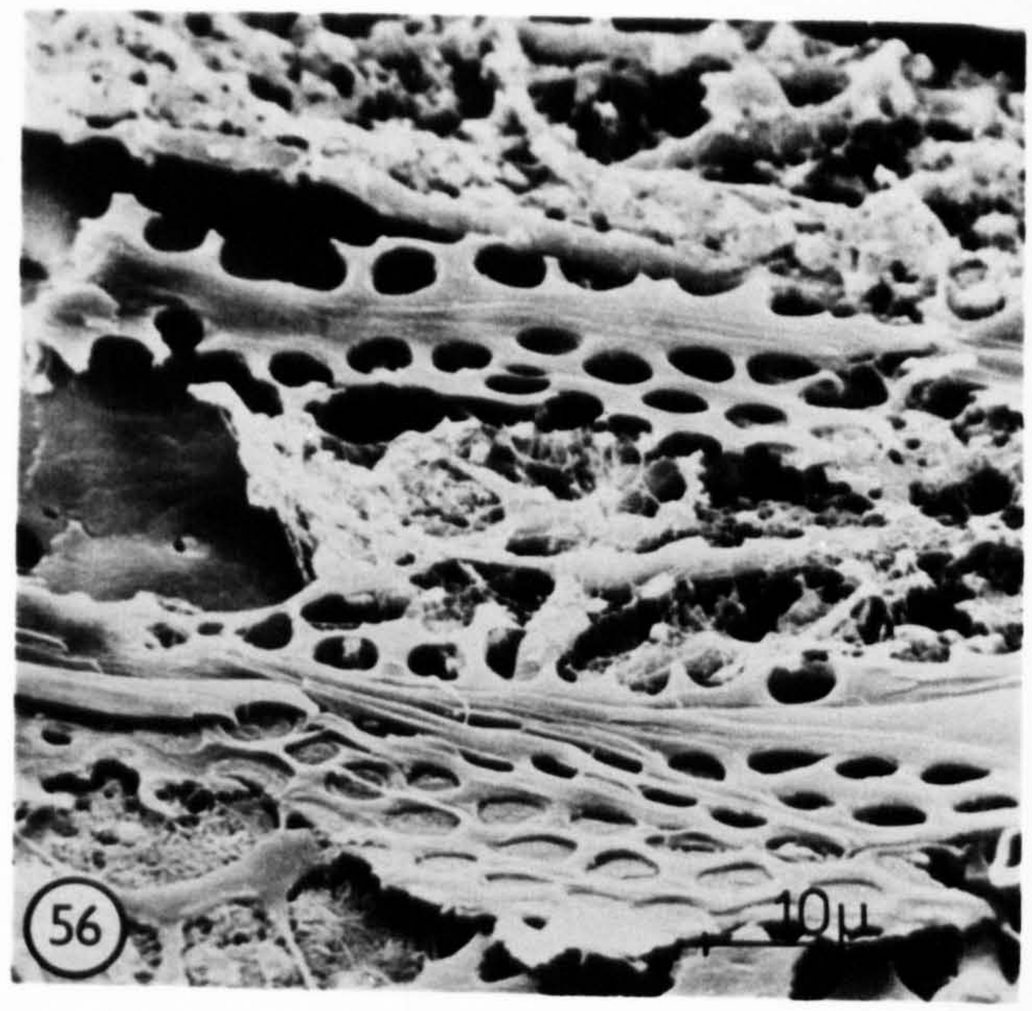

Bh
Sp
54
25µ

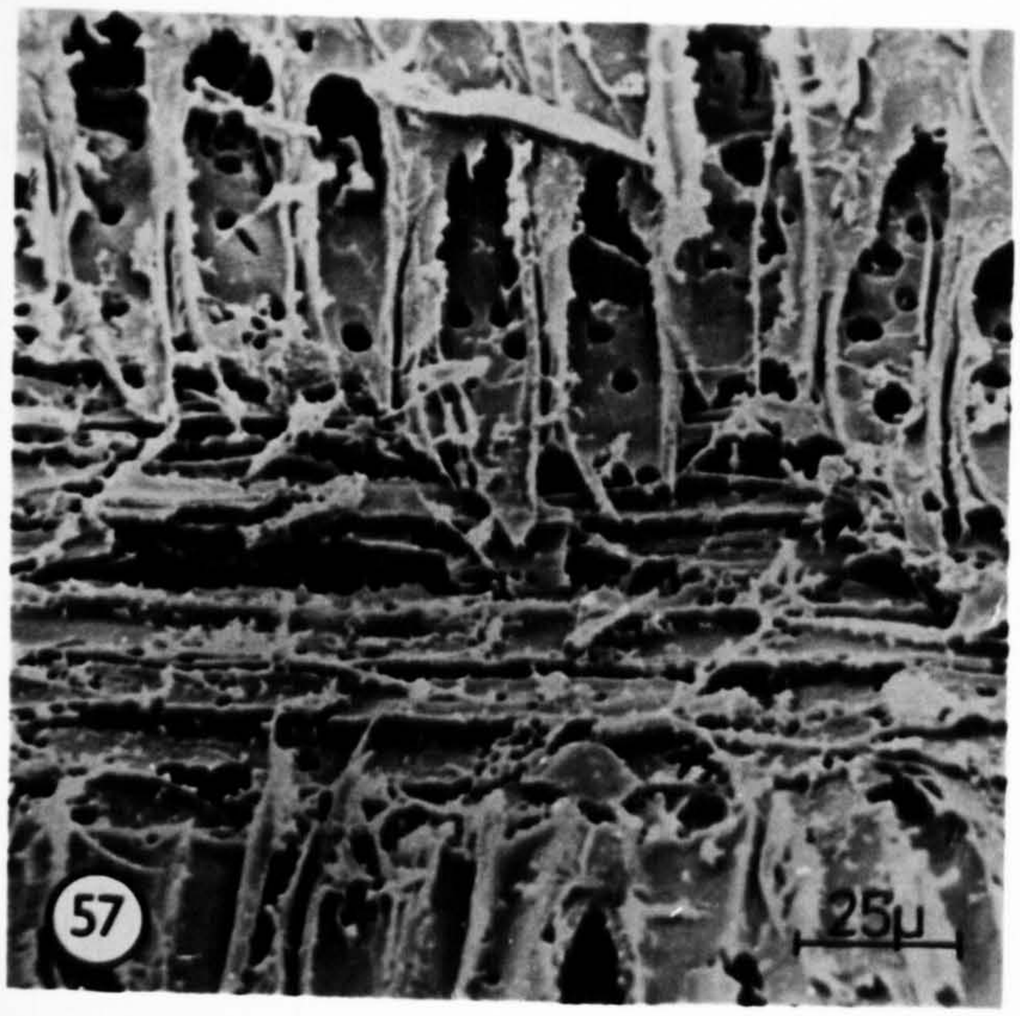
4.2.3.1 Coriolus versicolor on birch (Betula sp.), 4 weeks

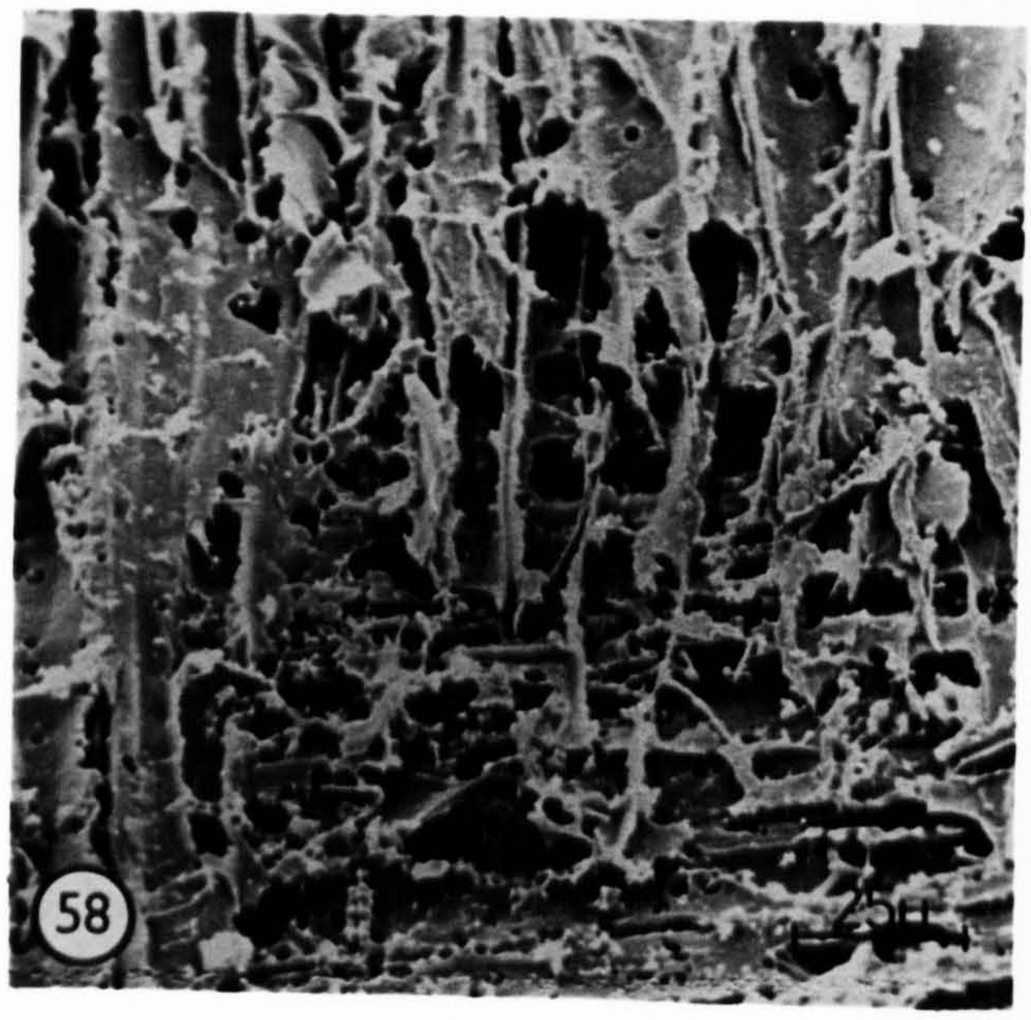
Figs. 55 (x 540(1)) and 56 (x 2160(1)) reveal the lysis of ray tissue adjacent to a vessel. The detail of fig. 56 shows the hyphae surrounded by a fibrillar and granular matrix dissolving the cross-field pit membranes and secondary walls of both ray and vessel origin. Figs. 57 (x 530(2)) and 58 (x 500(2)) also show lysis of ray and fibre tissue but with the hyphae present. Pits again have been enlarged together with extensive degrade of the rays.

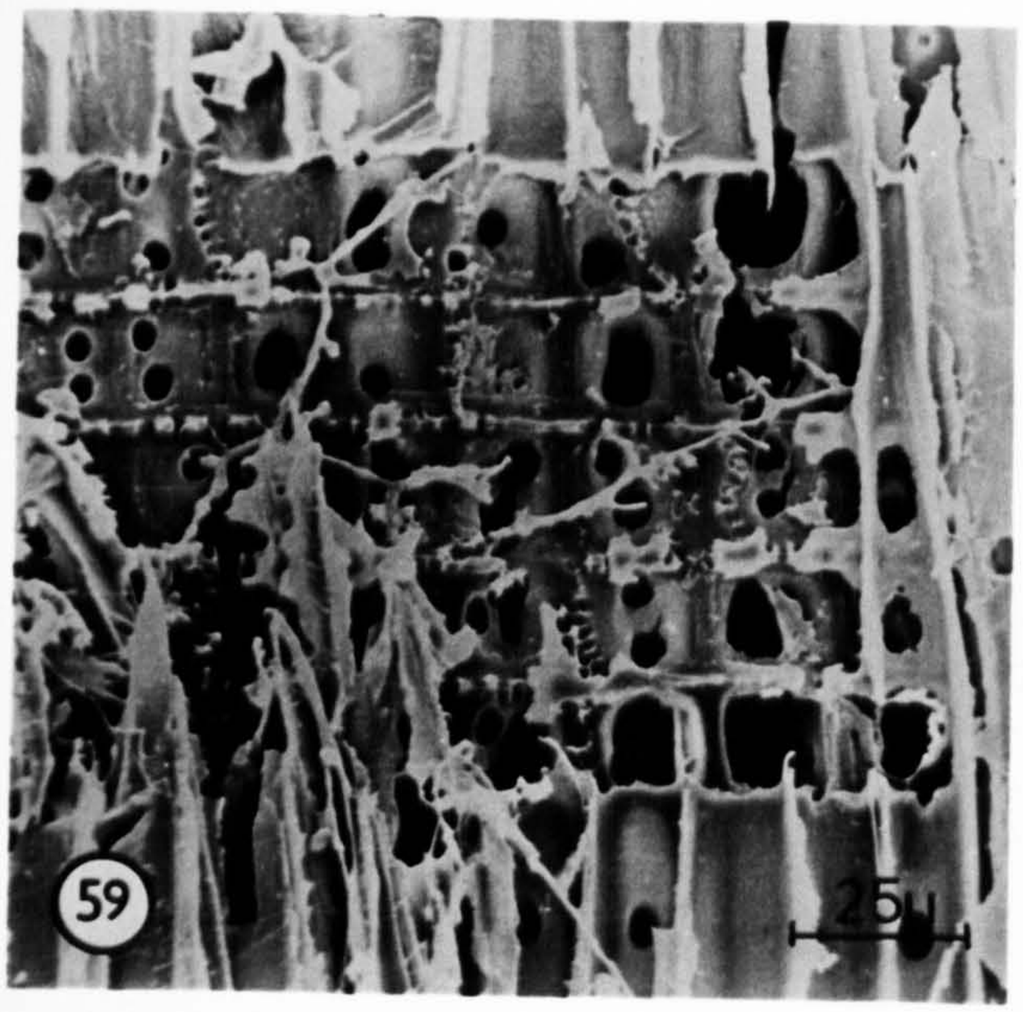
Fig. 59 (x 540(2)). Colonisation of the ray tissue with pit enlargement, wall lysis and spread into the adjacent fibres, fig. 60 (x 990(1)), are clearly shown. Note also the 'halo' effect to some of the lysis regions in fig. 59. In fig. 60 the right hand ray tissue was connecting to a vessel, see also fig. 55.

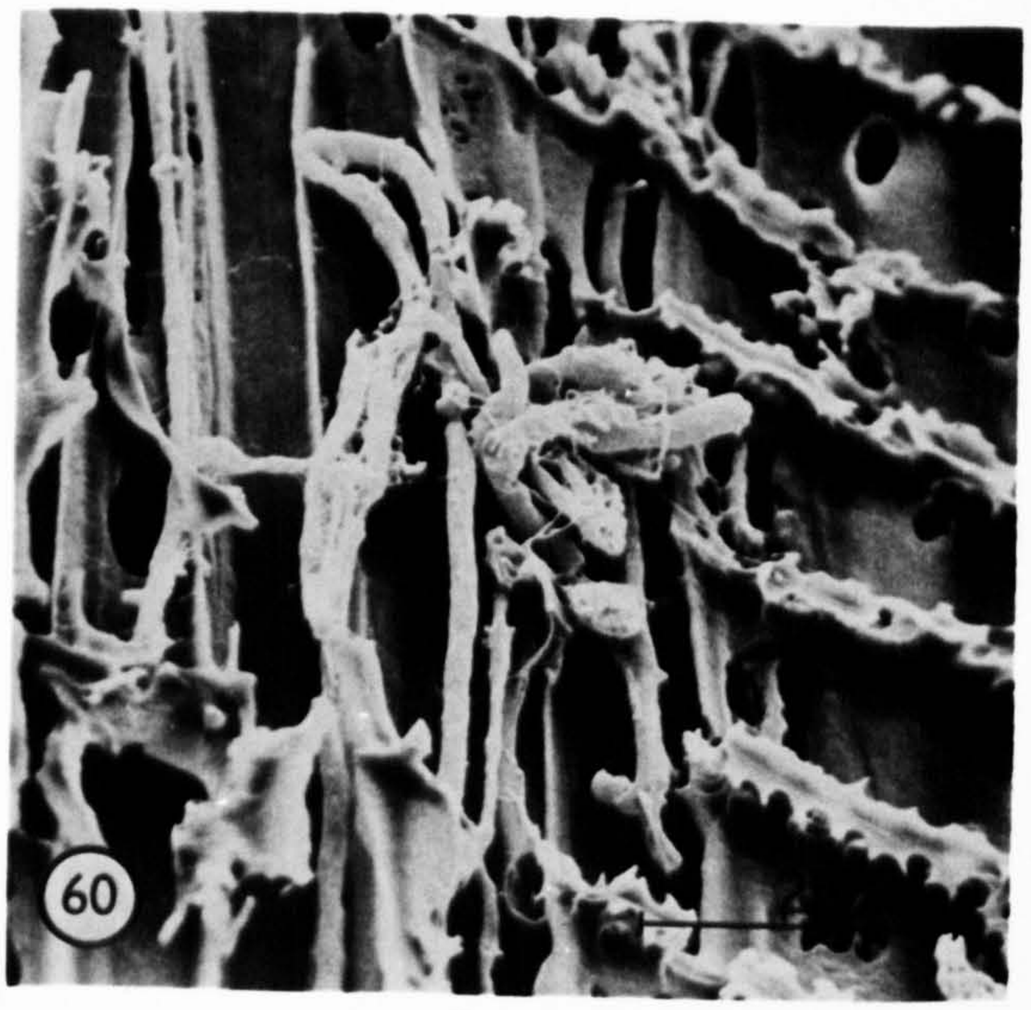

55
25μ


56
10μ


57
25μ


58
25μ


59
25μ


60

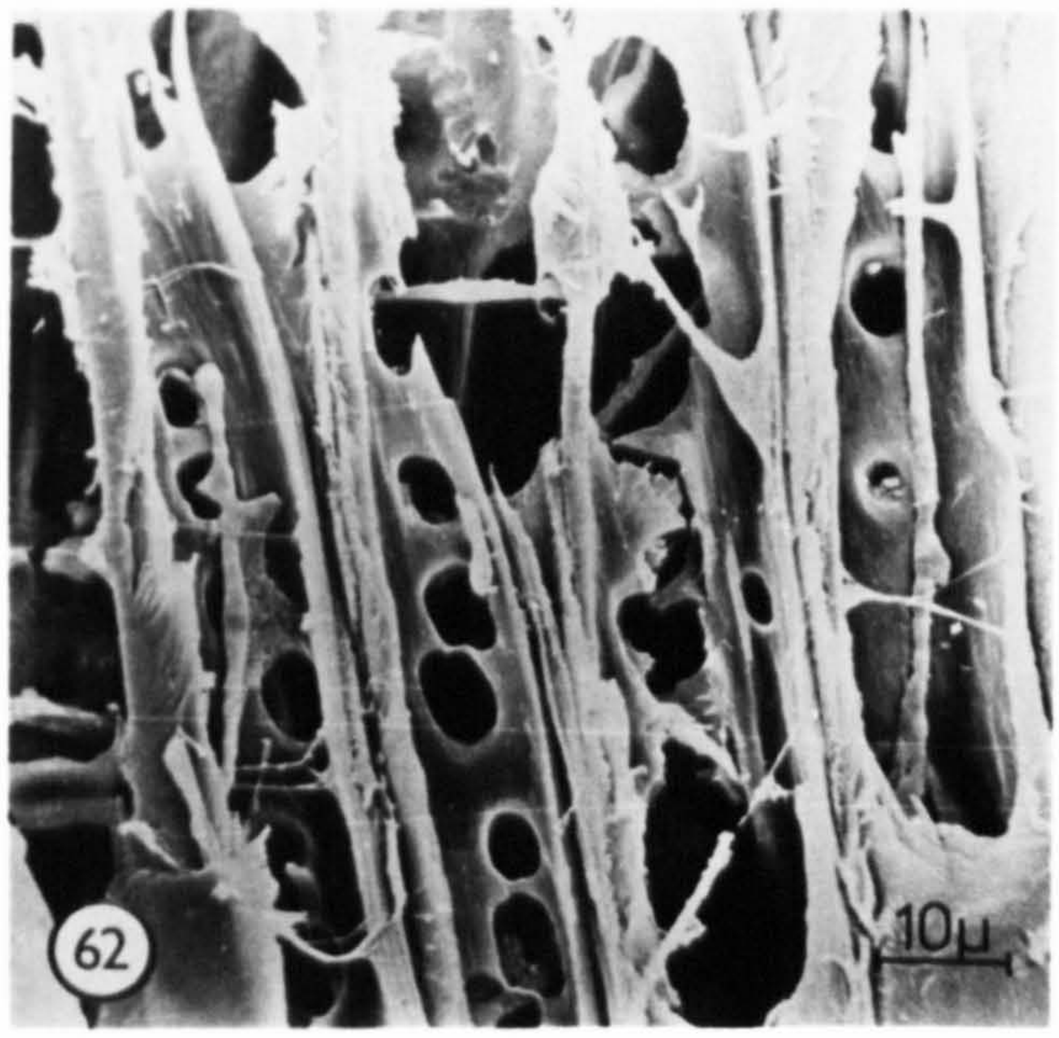
4.2.3.1 Coriolus versicolor on birch (Betula sp.), 4 weeks

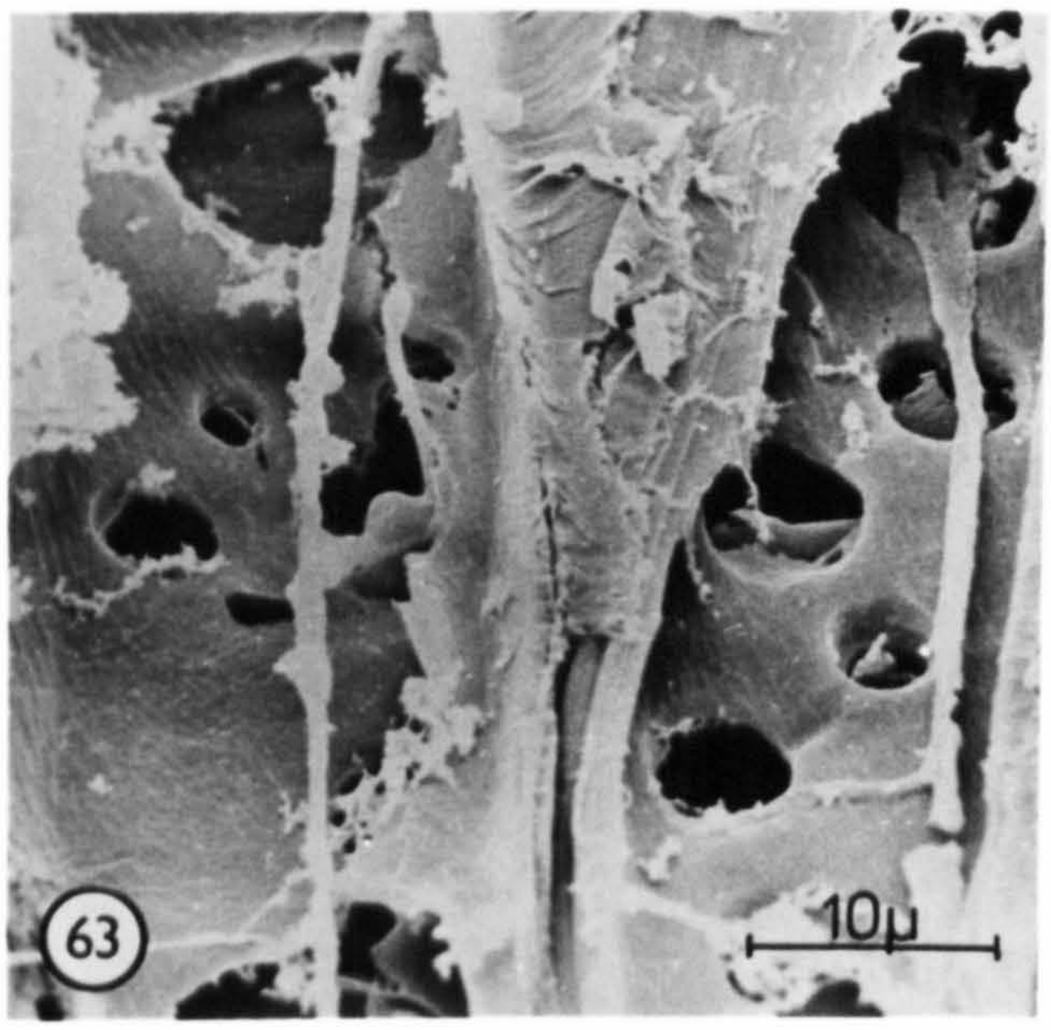
Fig. 61 (x 3890(1)) shows bore hole formation in a fibre with the bore holes being much wider than the hypha. The margins (Tm) of the bore holes appear much thinner than the surrounding wall. The predominantly steep orientation of the S_2 appears to be confused with shallow S_3 type lines which are in fact wrinkles in the weakened wall, produced during specimen preparation.

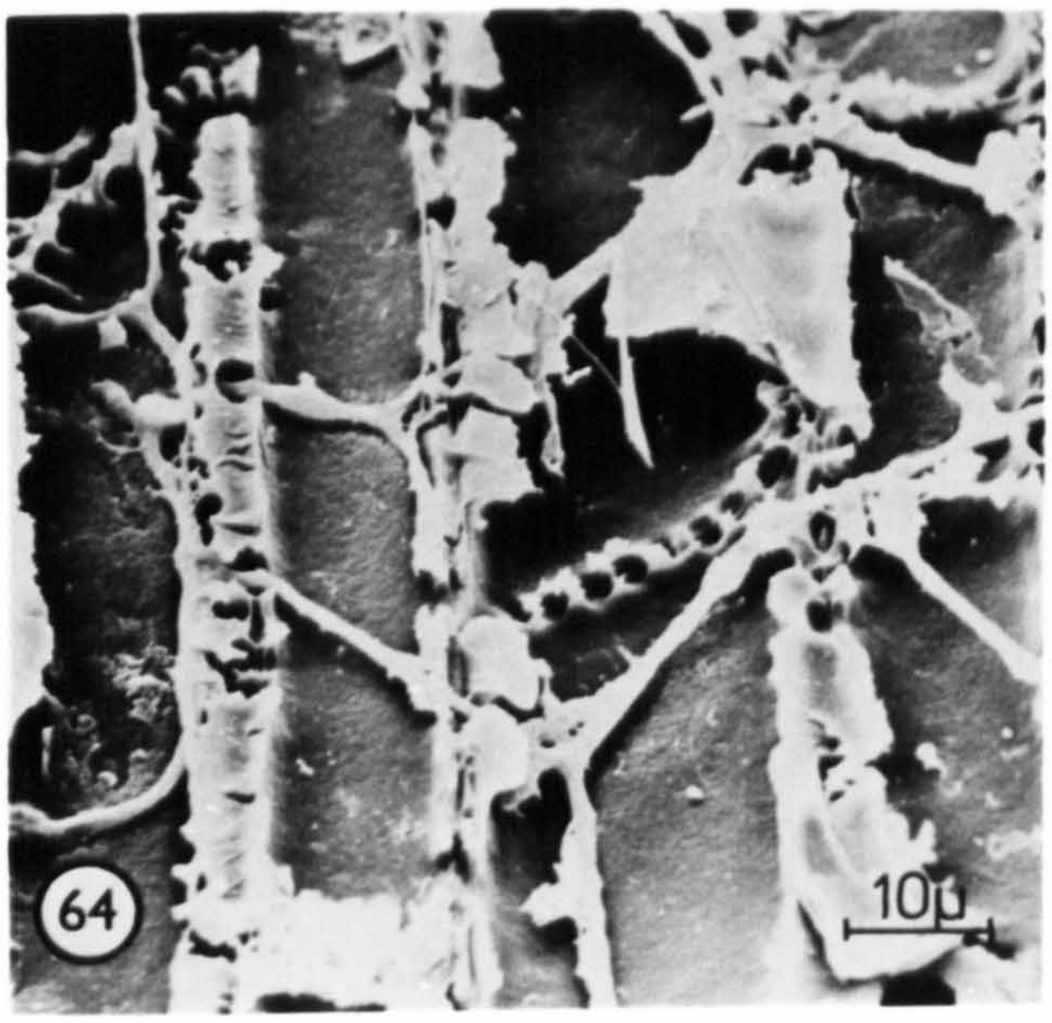
Later stages of fibre degrade can be seen in figs. 62 (x 1030(2)) and 63 (x 1900(2)).

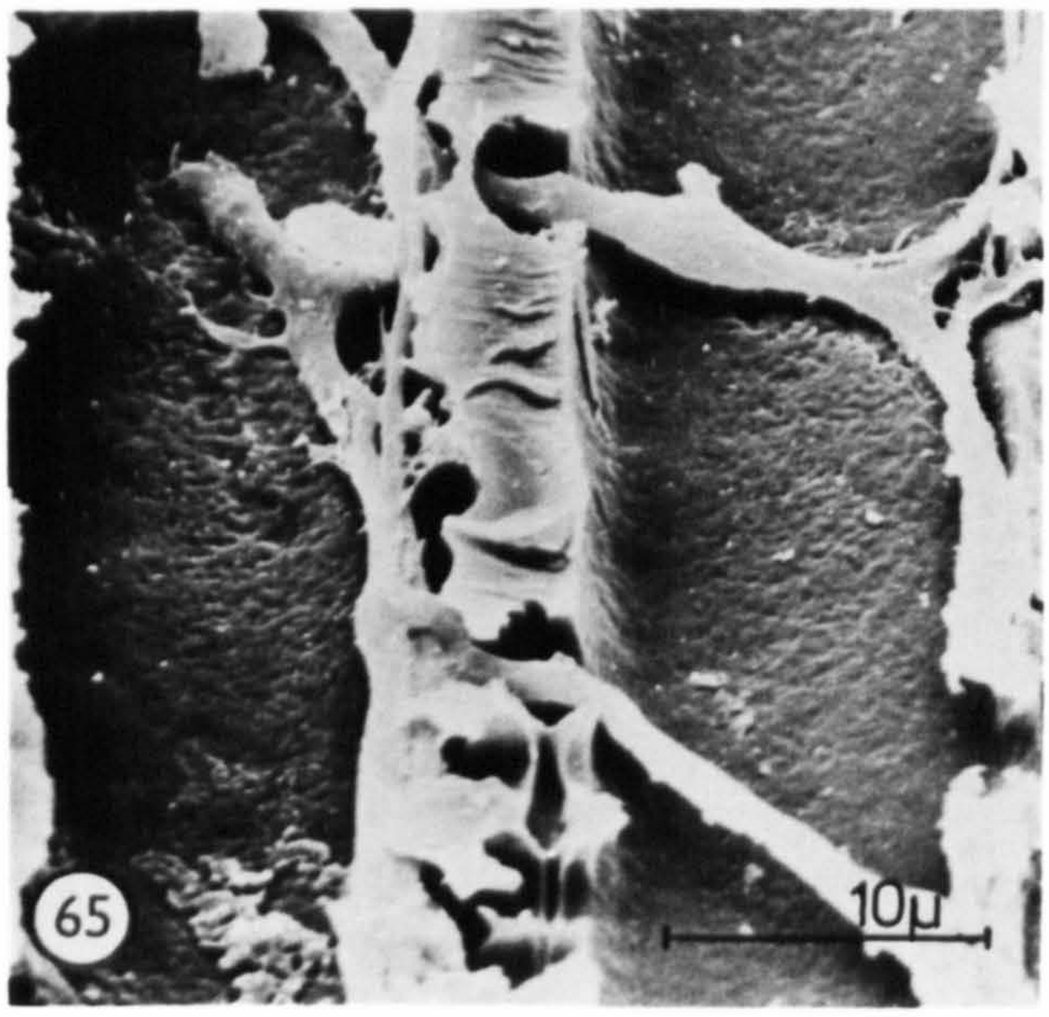
Figs. 64 (x 1090(1)) and 65 (x 2540(1)) demonstrate the utilisation of natural pitting in axial parenchyma as a colonisation pathway. The simple pits can be clearly seen in the centre of fig. 64 as regularly spaced and precise cell connections. The growth of hyphae through such pits can be seen in the adjacent cell to the left, and this is detailed in fig. 65.


Tm
61
5μ


62
10μ


63
10μ


64
10μ


65
10μ

4.2.3.2 C. versicolor on softwood:- Scots pine (Pinus sylvestris)

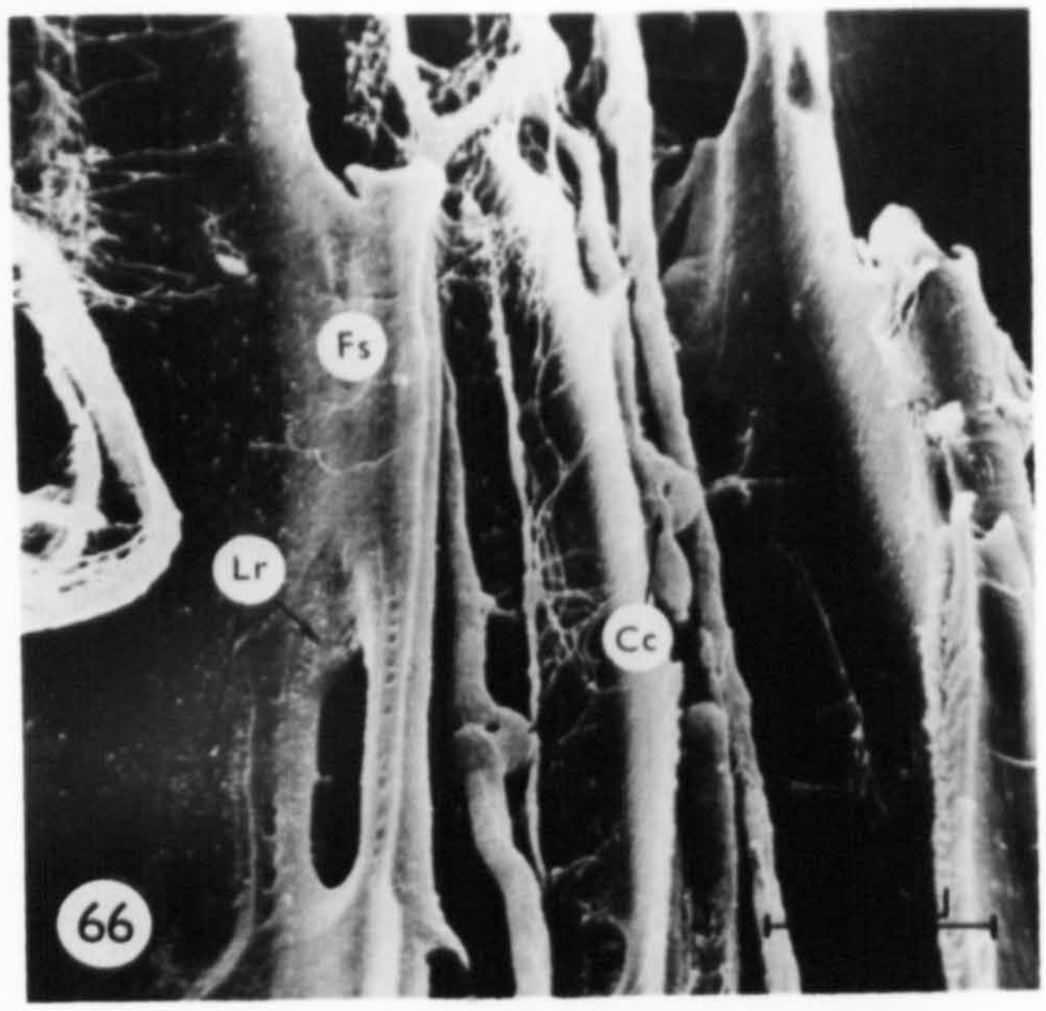
Bordered pits and cross-field pitting were common pathways of colonization, figures 72 - 75. The effect of this fungus on Scots pine ranged from the shallowest of lysis troughs to deep splits and severe pit enlargement with accompanying wall lysis, all of which can be seen at low magnification in the first four figures. The initial effect on the wall was the removal of the S_3 wall layer, figure 76. The significance of the material on and around the hypha will be discussed later. Further wall degradation cuts through the S_3, accompanied by a broadening of the channel, to reveal the steeper angle of the S_2 microfibrils, figure 77 and detailed in figure 78. There was more dissolution of the material around the microfibrils producing fine splits in the S_2 layering. The proliferation of these channels can be seen in figure 79, where a hypha emerging from the now enlarged bordered pit aperture has branched several times and this is reflected by the wall lysis pattern observed, detailed in figure 80.

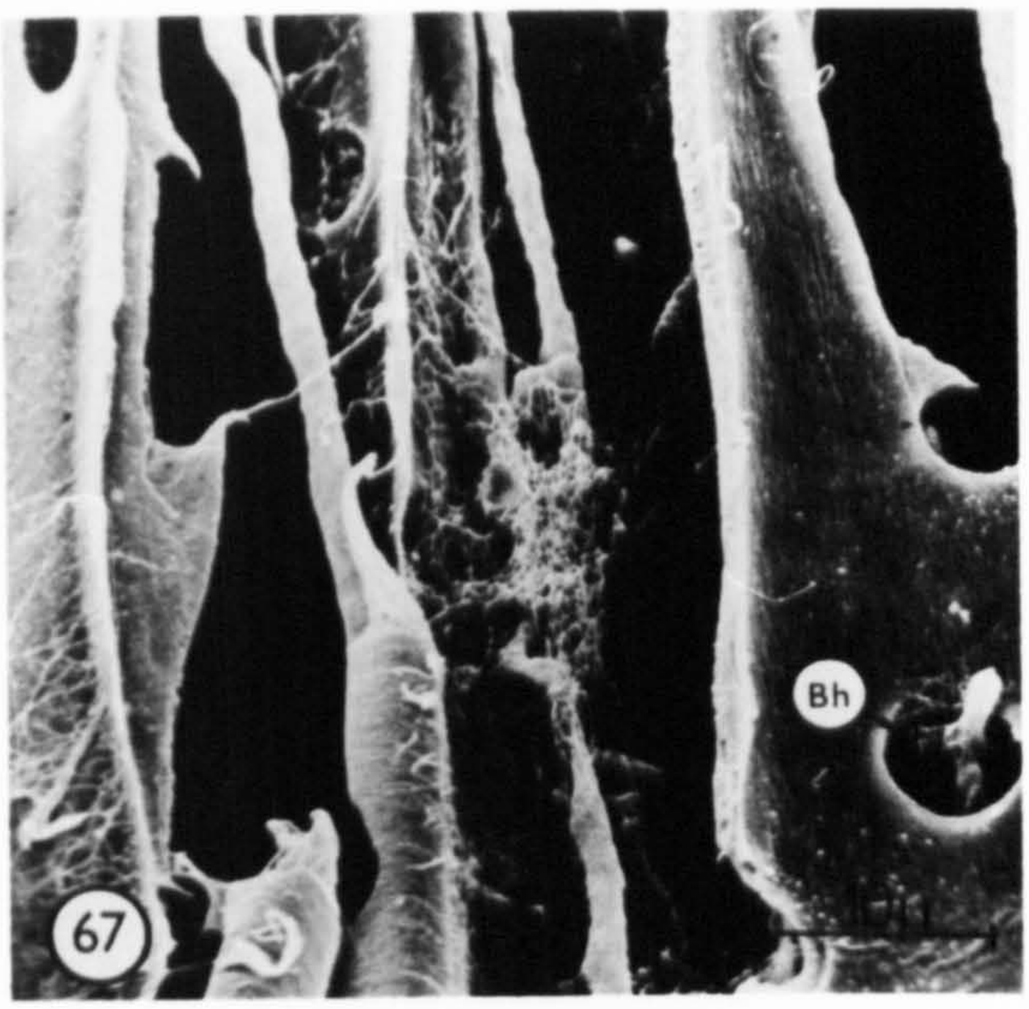
The destruction of bordered pits was very evident and an attempt to produce the sequence of events is given by figures 81 - 86. It must be noted, however, that a number of different tracheids were used in the compilation. The hyphae involved progressively increased the size of the pit aperture, initially leaving it smooth as in figure 81, but when the S_2 layering of the border was encountered the margins appeared more fibrillar, figures 82 and 83, with a marked dissolution of the matrix material prior to the microfibrils, figure 84. Continued aperture enlargement reduced the pit borders to insignificance, figure 85, creating extremely wide openings in

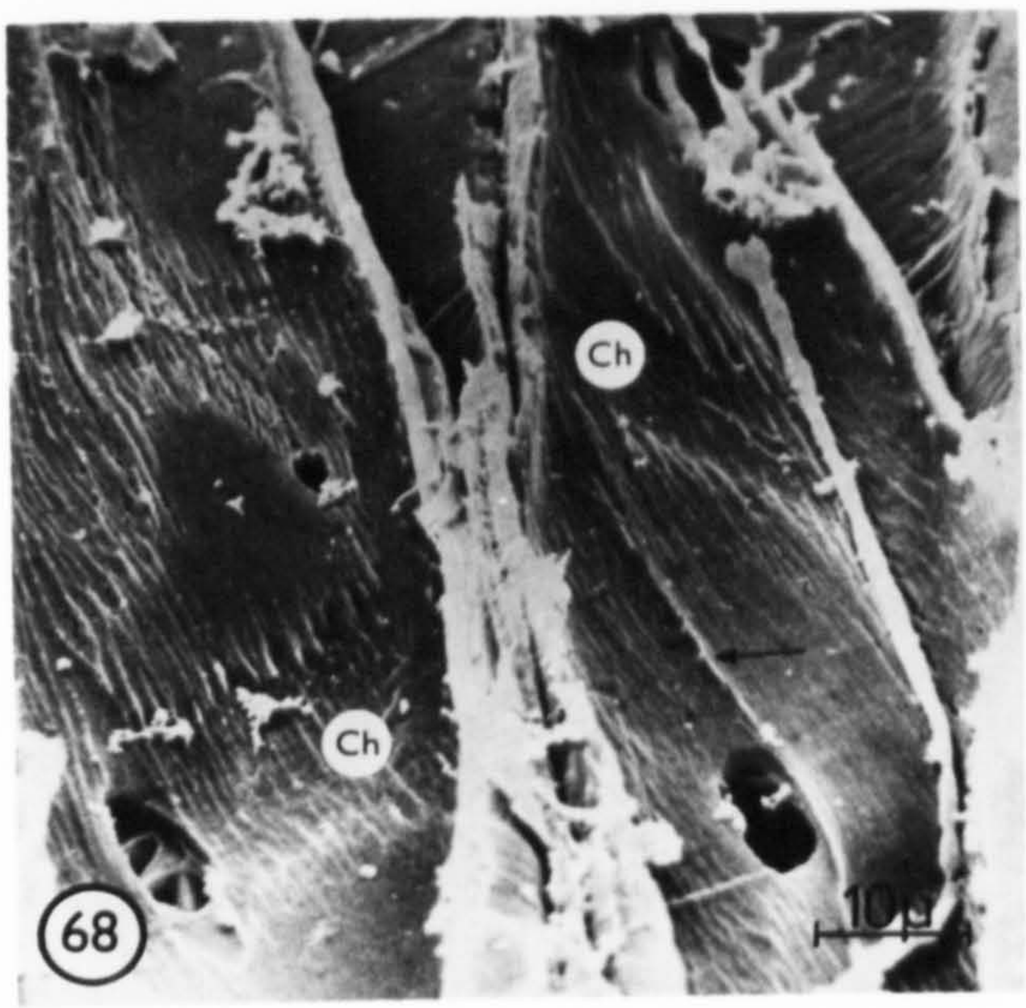
4.2.3.1 Coriolus versicolor on birch (Betula sp.), 4 weeks

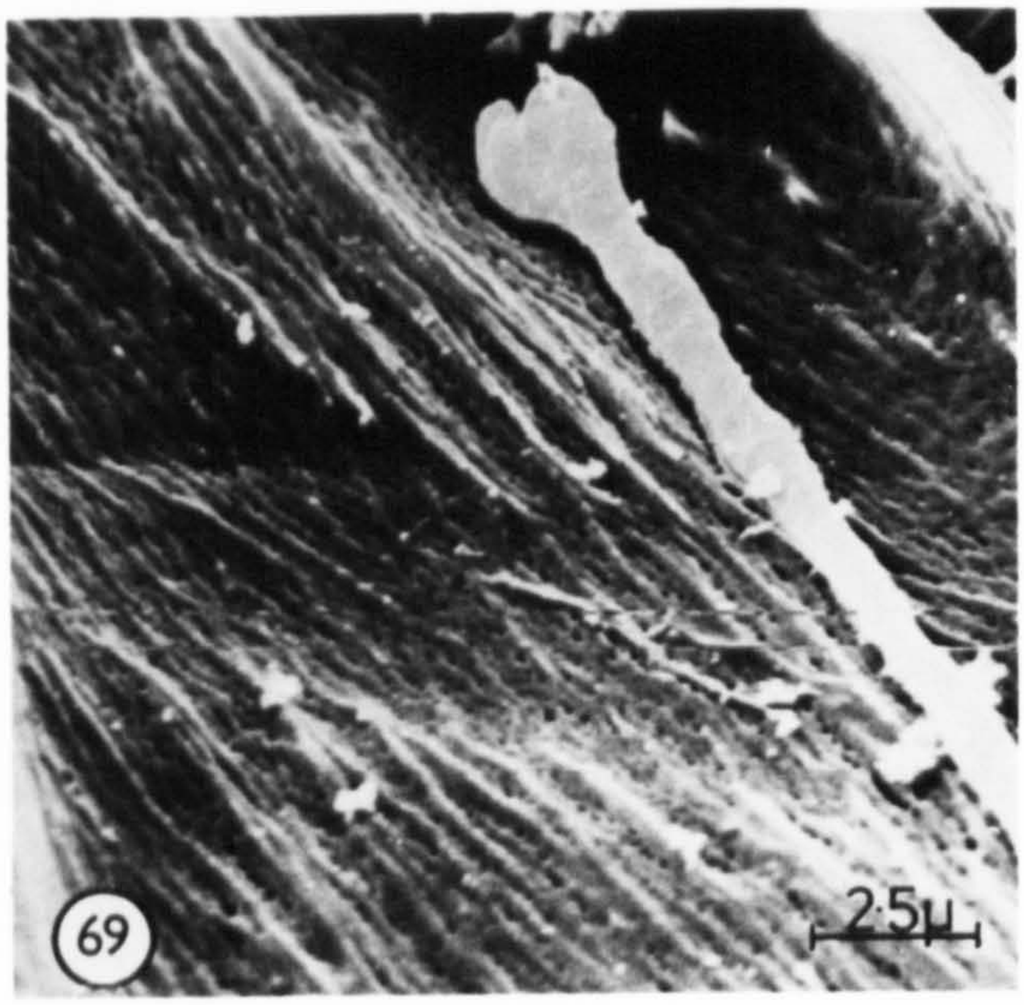
Figs. 66 (x 1900(1)) and 67 (x 1900(1)) clearly demonstrate the presence of fine strands (Fs) in association with the hyphae. Fig. 66 shows that the normal hyphae, with their clamp connections, (Cc) are many times the diameter of the fine strands which may be fine hyphae or a peculiar dehydration artefact of a mucilaginous sheath. Note also the large window-like lysis region in the fibre wall. The network seen in fig. 67 is very similar to that around the hyphae in the ray tissue of fig. 56. A large bore hole (Bh), with causal hypha, can be seen in the lower right of the micrograph.

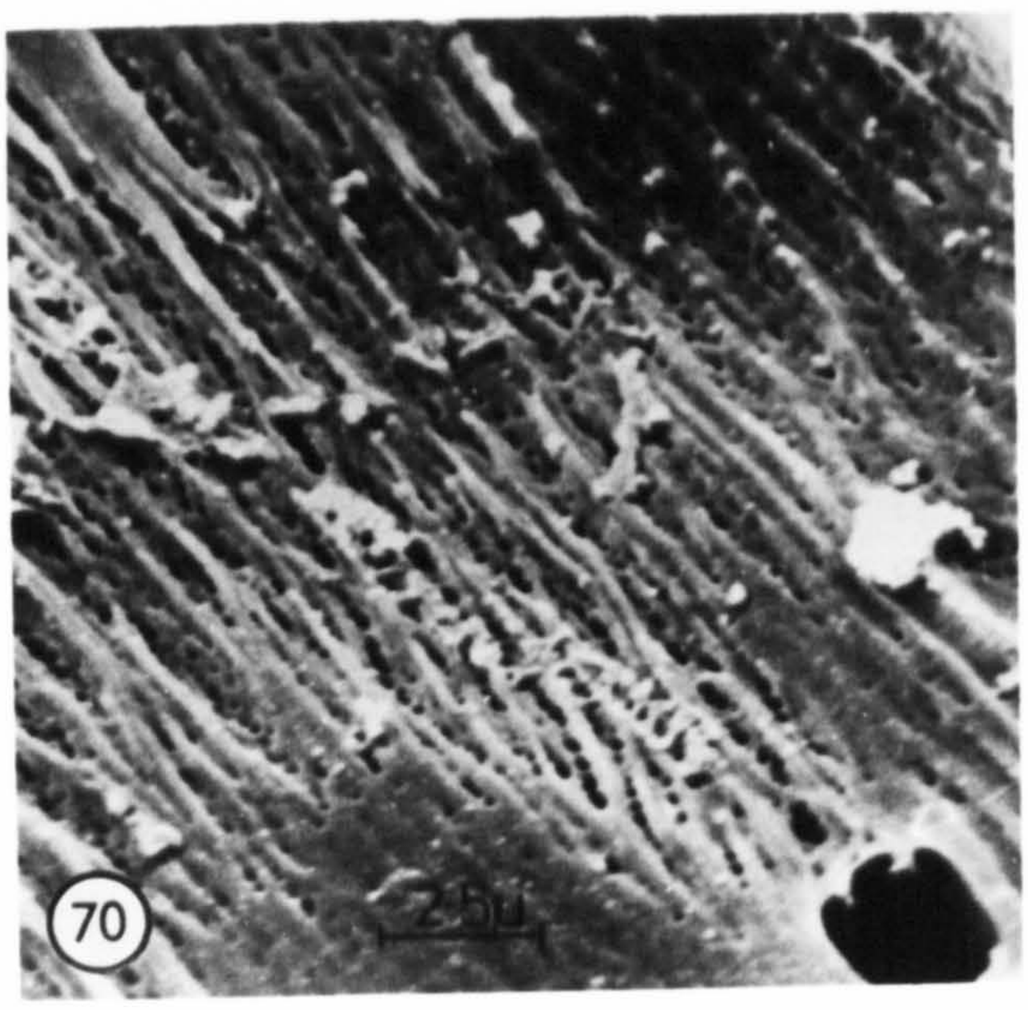
Degrade of fibres with the development of channels (Ch) can be seen in fig. 68 (x 1150(2)), detailed in figs. 69 (x 5280(1)), 70 (x 5280(1)) and 71 (x 2360(2)). A steep S_2 type microfibrillar orientation is clearly defined and the detail of the unattacked wall in fig. 71 does not indicate the presence of an S_3 layer on the basis of microfibrillar orientation. The formation of the channels with a preferential dissolution of the matrix material between the microfibrils can be seen in figs. 70 and 71. Note the well defined limit (arrowed) of the channel when parallel with the microfibrillar angle in contrast to when at right angles, fig. 68. The presence of the bore hole (Bh) indicated in fig. 71 appears to have resulted in a slightly increased wall lysis alongthe microfibrillar line, fig. 70.

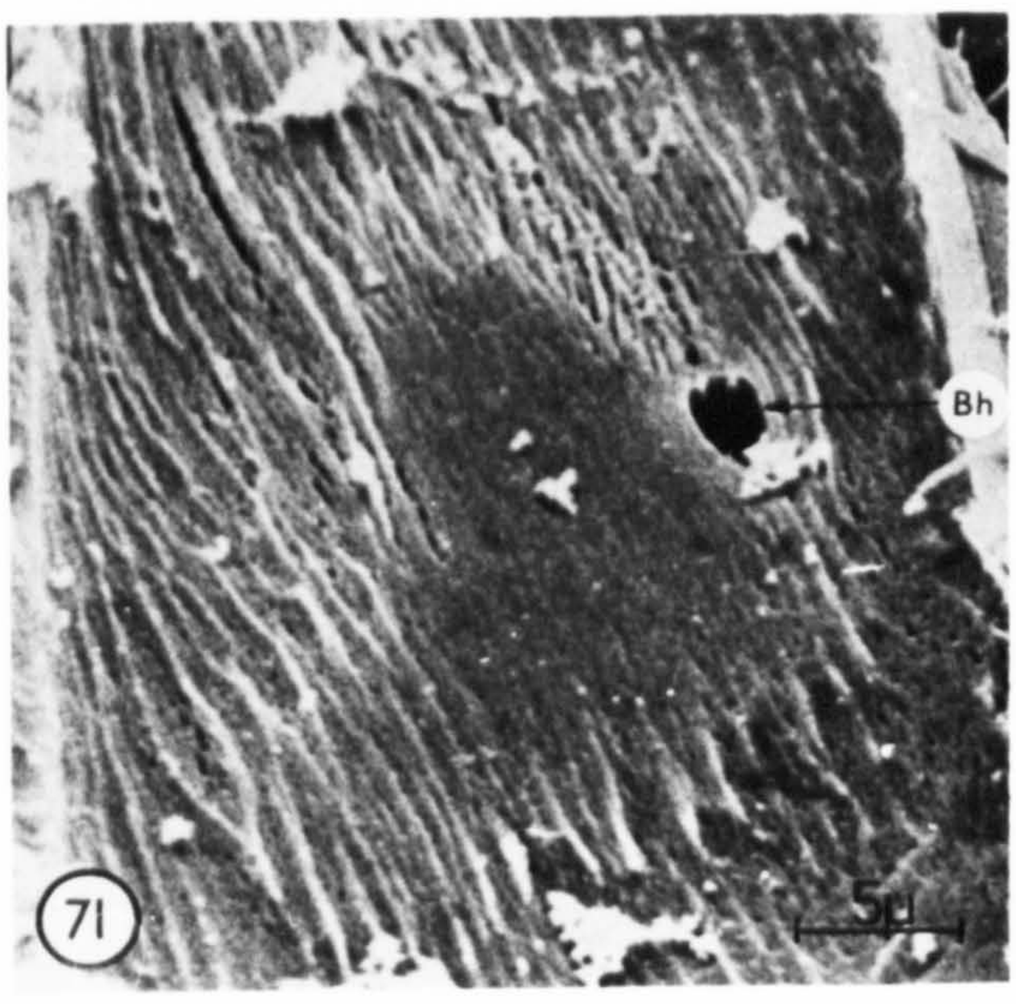

Fs
Lr
Cc
66


Bh
67


Ch
Ch
68
10μ


69
2.5μ


70
2.5μ


Bh
71
5μ

4.2.3.2 C. versicolor on softwood:- Scots pine (Pinus sylvestris)

Bordered pits and cross-field pitting were common pathways of colonization, figures 72 - 75. The effect of this fungus on Scots pine ranged from the shallowest of lysis troughs to deep splits and severe pit enlargement with accompanying wall lysis, all of which can be seen at low magnification in the first four figures. The initial effect on the wall was the removal of the S_3 wall layer, figure 76. The significance of the material on and around the hypha will be discussed later. Further wall degradation cuts through the S_3, accompanied by a broadening of the channel, to reveal the steeper angle of the S_2 microfibrils, figure 77 and detailed in figure 78. There was more dissolution of the material around the microfibrils producing fine splits in the S_2 layering. The proliferation of these channels can be seen in figure 79, where a hypha emerging from the now enlarged bordered pit aperture has branched several times and this is reflected by the wall lysis pattern observed, detailed in figure 80.

The destruction of bordered pits was very evident and an attempt to produce the sequence of events is given by figures 81 - 86. It must be noted, however, that a number of different tracheids were used in the compilation. The hyphae involved progressively increased the size of the pit aperture, initially leaving it smooth as in figure 81, but when the S_2 layering of the border was encountered the margins appeared more fibrillar, figures 82 and 83, with a marked dissolution of the matrix material prior to the microfibrils, figure 84. Continued aperture enlargement reduced the pit borders to insignificance, figure 85, creating extremely wide openings in

the tracheid wall. Occasionally the destruction resulted in the microfibrillar orientation within the border being revealed, figure 86.

Bore holes were frequently observed and although they were usually very neat, smooth sided, penetrations, figures 82 and 91, occasionally fibrillar apertures were formed, figures 89 and 90. It may be significant that the left hand tracheid of figure 72 was the first earlywood tracheid of a growth ring and exhibited the fibrillar features illustrated in the micrographs of 83, 84, 89 and 90.

In the majority of the decayed material some degree of wall erosion, in the form of channels, could be seen and the early stages of channelling are to be seen in figures 93 to 95. The hyphae are absent but definite removal or smoothing of the S_3 has occured. As lysis continued the channels became deeper and broader cutting into the steeper S_2 and there was penetration between the micro-fibrils, figures 96 and 97.

On many channels a central line of debris could be seen with or without the hypha being present, figures 98 and 99, and the details given in figures 100 to 103 may provide clues for the interpretation of channel formation and the significance of the observed residues.

4.2.3.2 C. versicolor on Scots pine (Pinus sylvestris), 4 weeks

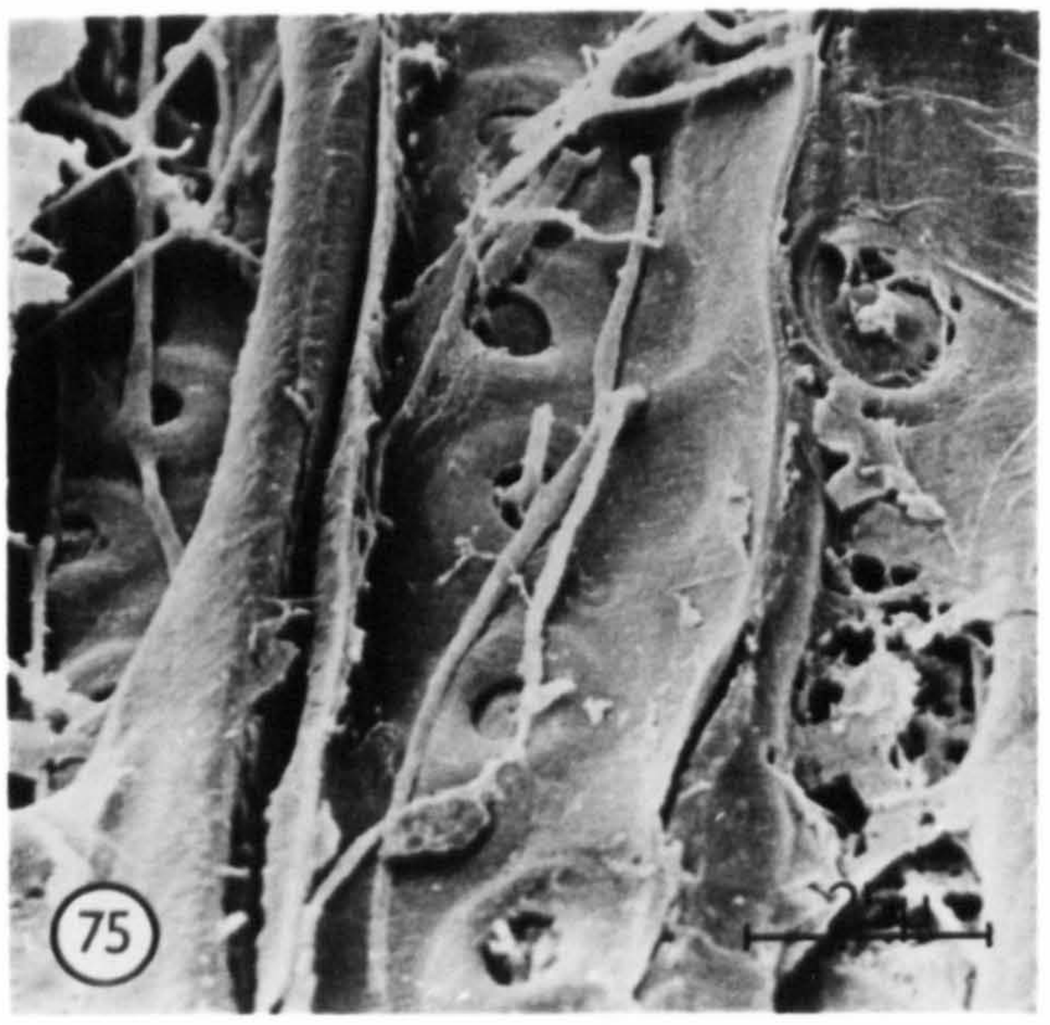
Figs. 72 (x 910(1)), 73 (x 1020(2)), 74 (x 720(1)) and 75 (x 740(2)) are all radial longitudinal views showing the general features of tracheid colonisation.

In fig. 72 the left hand tracheid shows heavy wall lysis of the fibrillar type, the right hand tracheid reveals only colonising hyphae. In fig. 73 the heavy attack can be seen on the right with a broad channel, pit degradation and deep splitting of the S_2. Figs. 74 and 75 are general views of the early stages of channelling. Lysis troughs can clearly be seen in fig. 74 with the centre line being marked by hyphae or residue in many of them. The S_3 has just been degraded on the bordered pit in fig. 75.


72
25μ


73
10μ


74
25μ

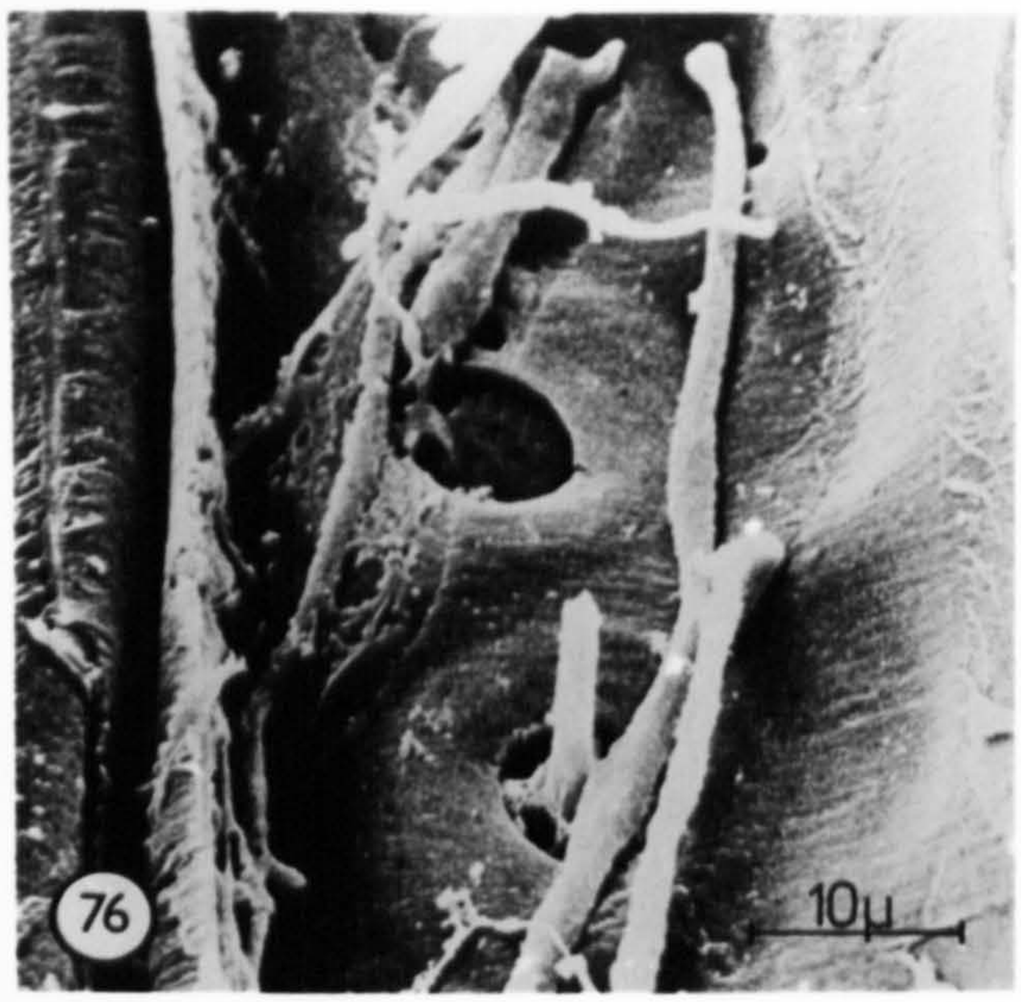

75

4.2.3.2 C. versicolor on Scots pine (Pinus sylvestris), 4 weeks

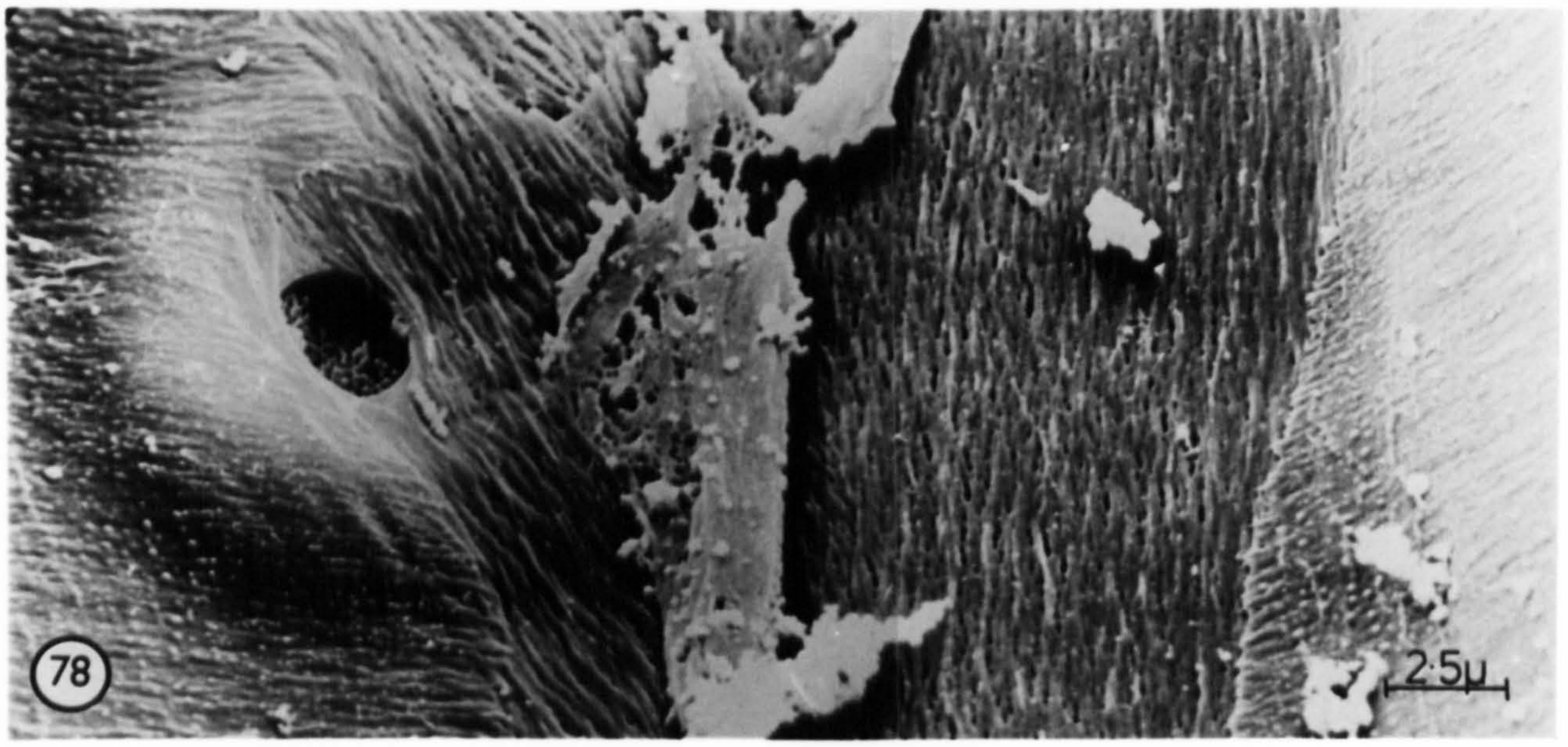
Fig. 76 (x 1650(1)) is a high magnification of fig. 75 detailing the features of the shallow channel formed by the hypha as it grew over the pit border. Note the presence of extensive surface material on the hypha and the adjacent wall where erosion has occured.

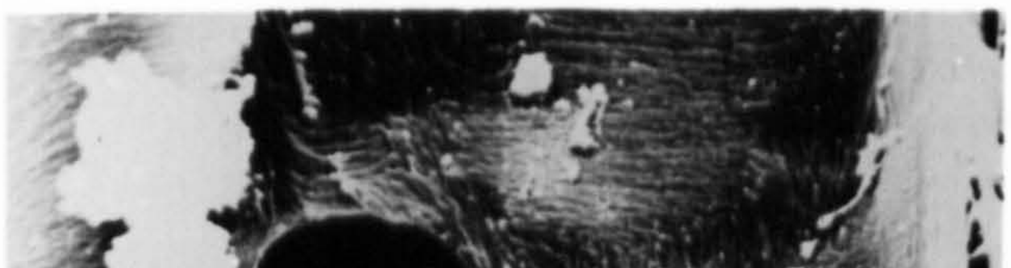
Figs. 77 (x 2140(1)) and 78 (x 5250(1)) clearly show the stripping of the wall layers from the warty layer through the shallow helices of the S_3 into the almost vertically orientated microfibrils of the S_2 in which small cracks are appearing. The apparent difference in S_2 orientation to left and right of the residue covered hypha is due to the microfibrillar orientation generated by the large cross-field pit above.

Figs. 79 (x 2200(1)) and 80 (x 4980(1)) reveal shallower channels which were produced by a hypha dividing as it emerged from the enlarged bordered pit. The detail shows the warts to be removed first, then the S_3 leading to cracks appearing in the S_2. Note also the presence of a residue along the centre line of the top channel in fig. 80.


76
10μ


77
5μ


78
2·5μ


79
5μ


80
5μ

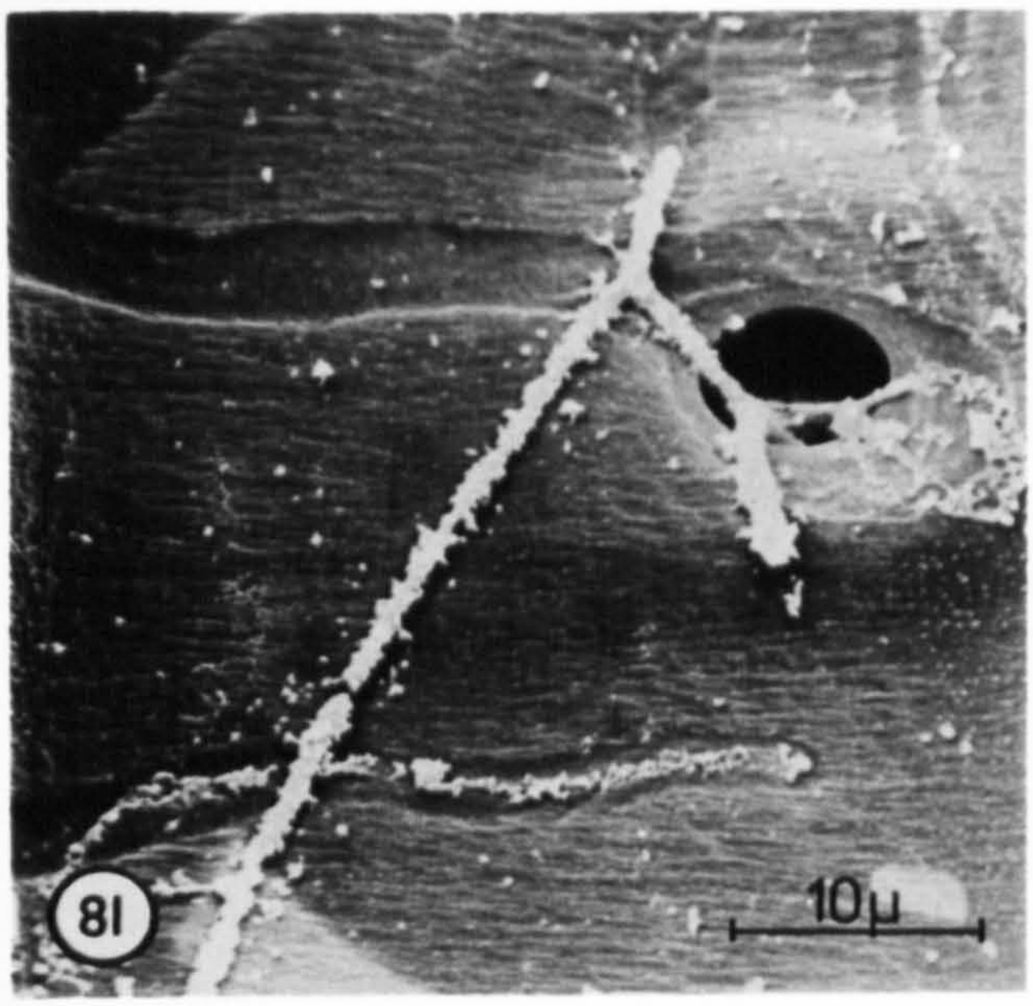
4.2.3.2 C. versicolor on Scots pine (Pinus sylvestris), 4 weeks

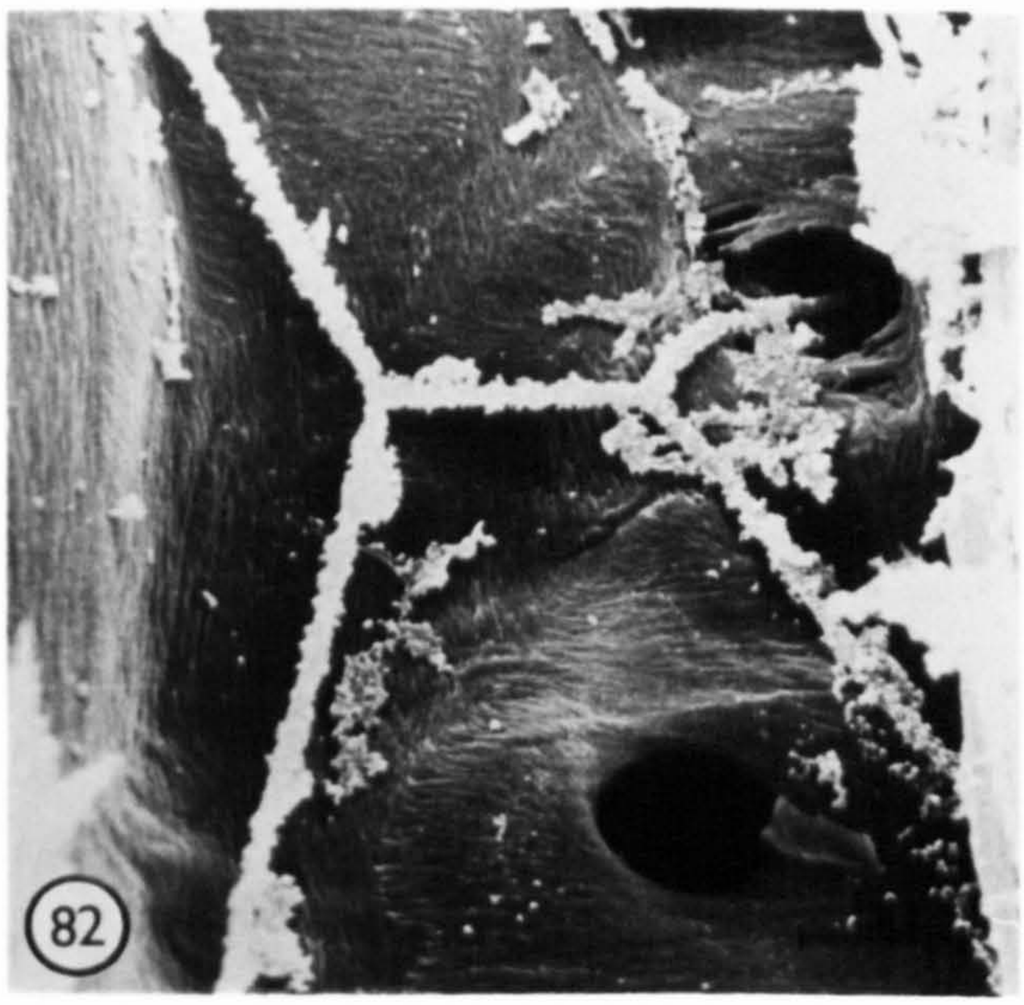
Figs. 81 to 86 show the progressive enlargement and lysis of bordered pits.

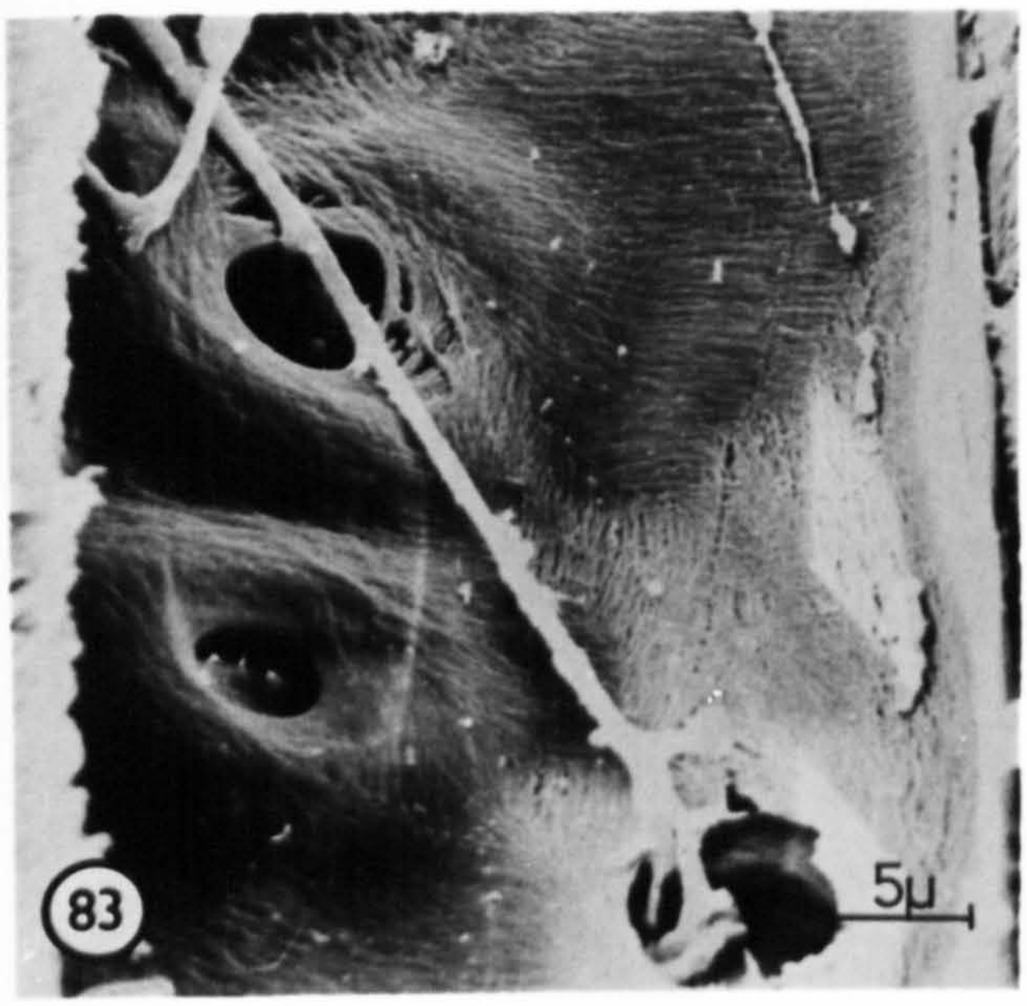
Fig. 81 (x 1970(1)) is of an earlywood tracheid with hyphal enlargement of the pit aperture leaving a smooth margin and smooth channel to the pit. The hypha seen penetrating the pit was probably dislodged from the channel. Note the residue present along the centre line of the other channels present.

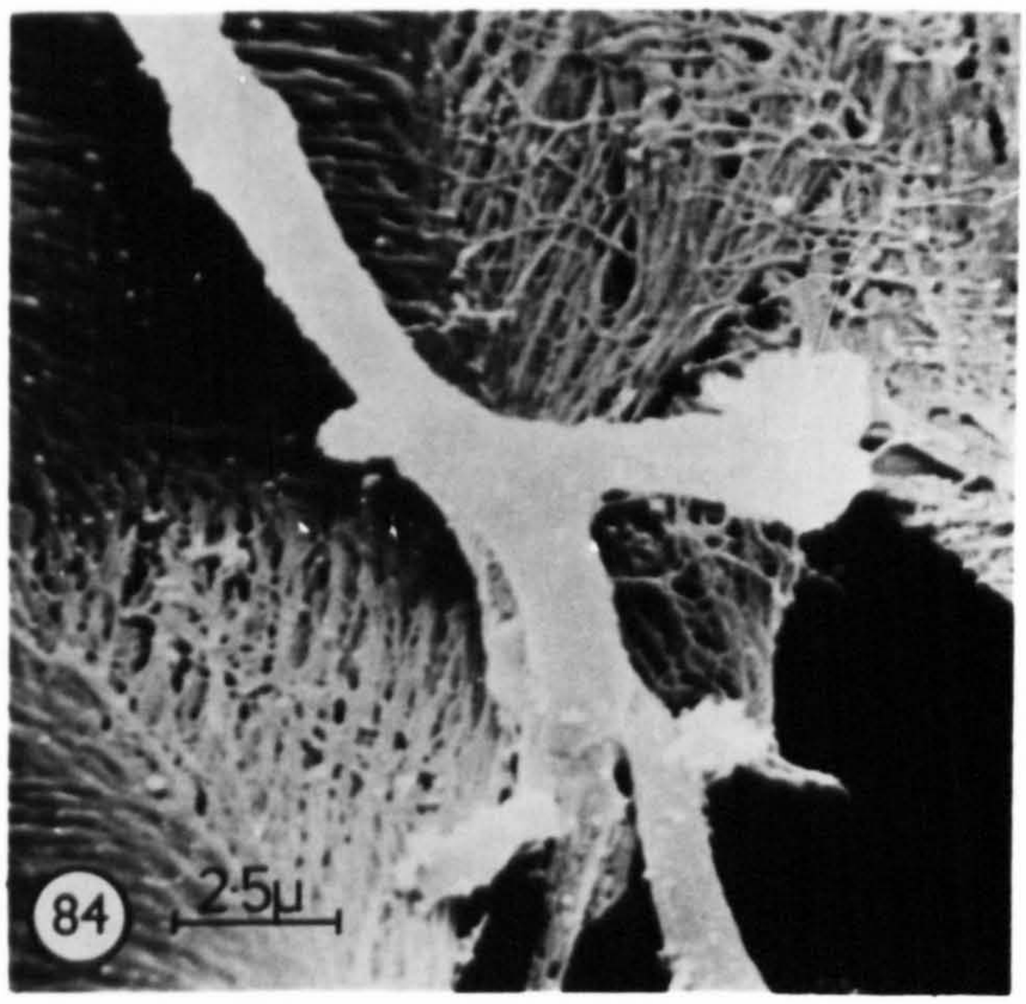
Further wall lysis and pit enlargement, figs. 82 (x 2300(1)) and 83 (x 2190(1)) is accompanied by a more distinct appearance of the macrofibrils. The high magnification detail of fig. 84 (x 5250(1)) clearly shows the dissolution of the matrix material in preference to the microfibrils.

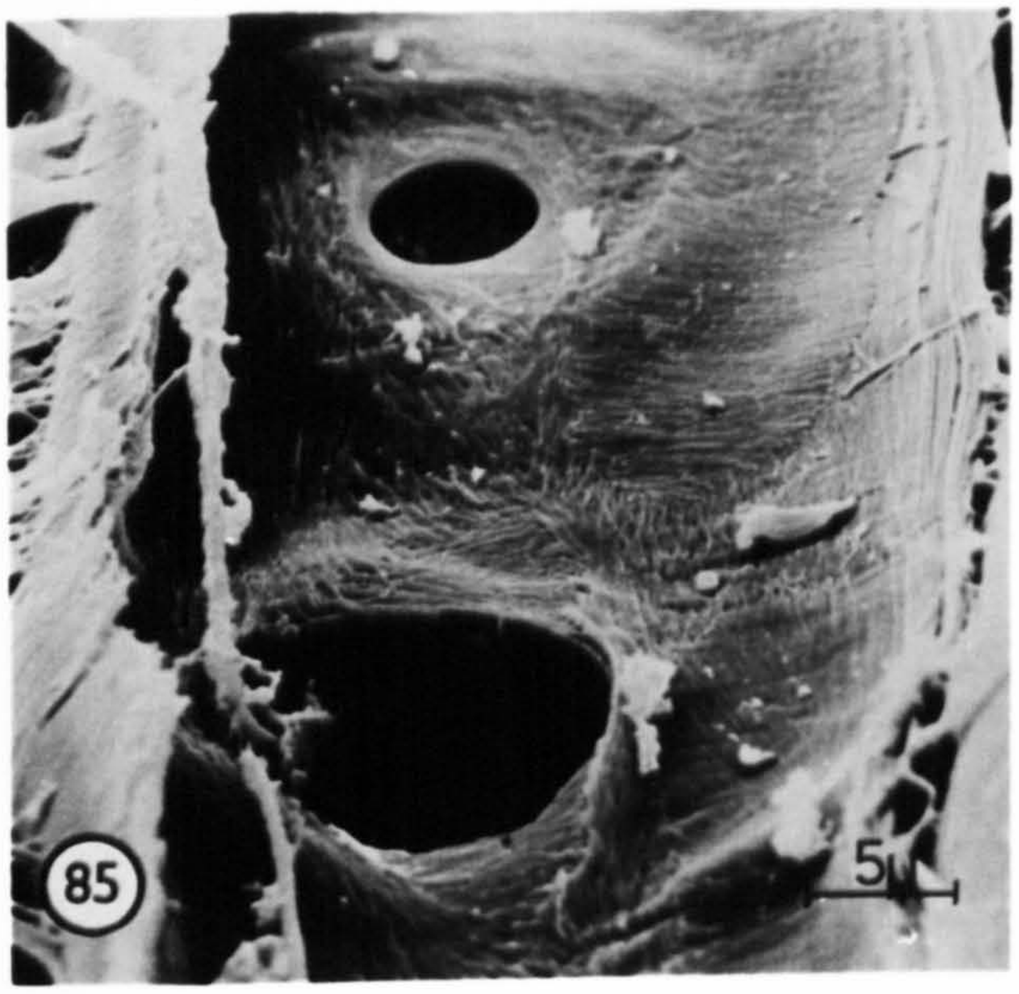
Final enlargement and heavy pit degrade are shown in figs. 85 (x 2290(1)) and 86 (x 2240(1)). Note the circular orientation of the microfibrils in the pit border being degraded by the overlying hypha.

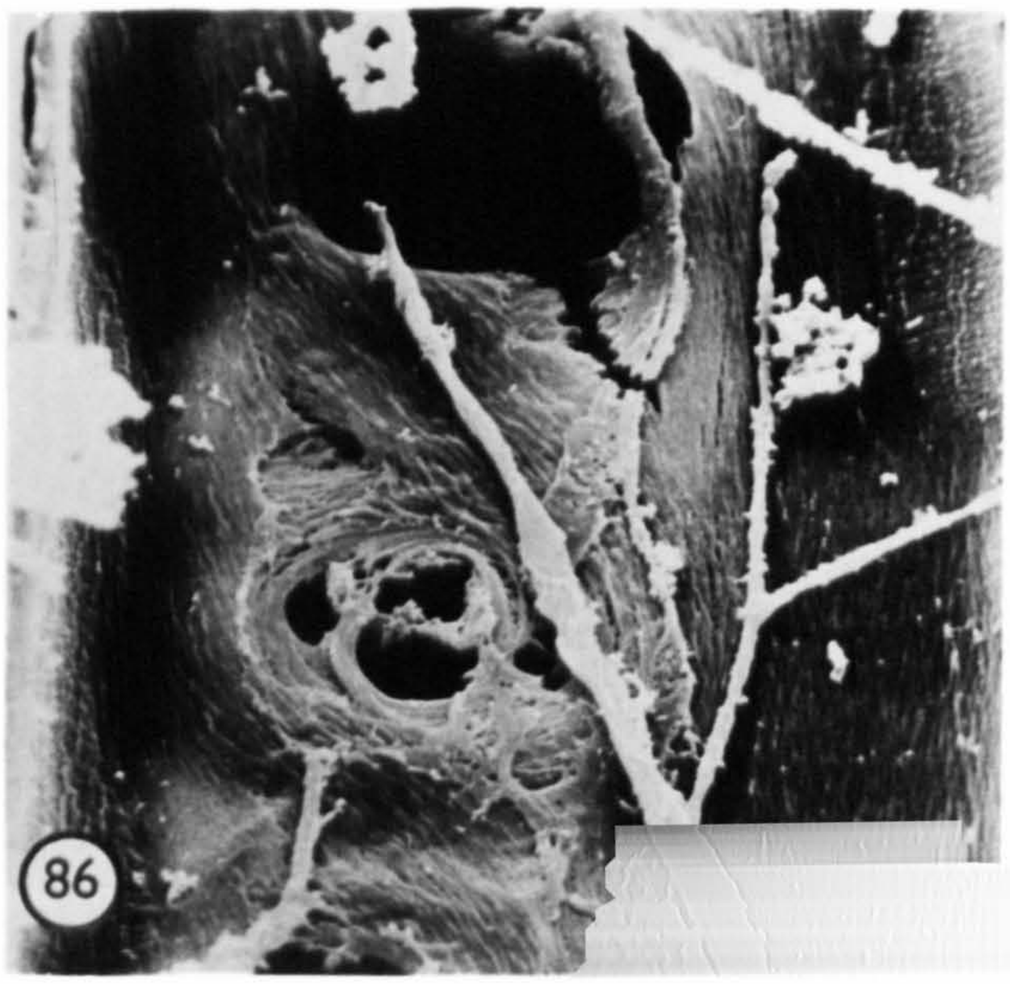

81
10μ


82


83
5μ


84
2·5μ


85
5μ


86

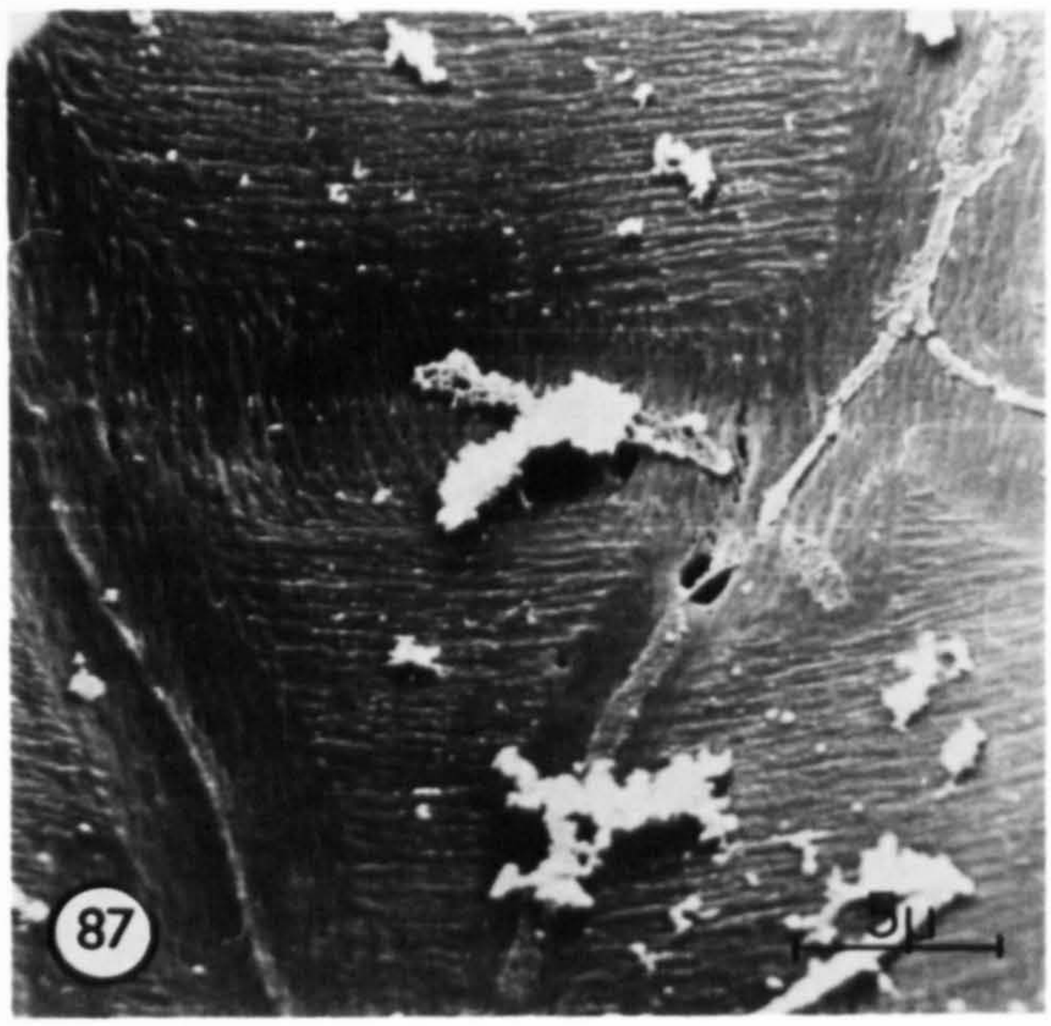
4.2.3.2 C. versicolor on Scots pine (Pinus sylvestris), 4 weeks

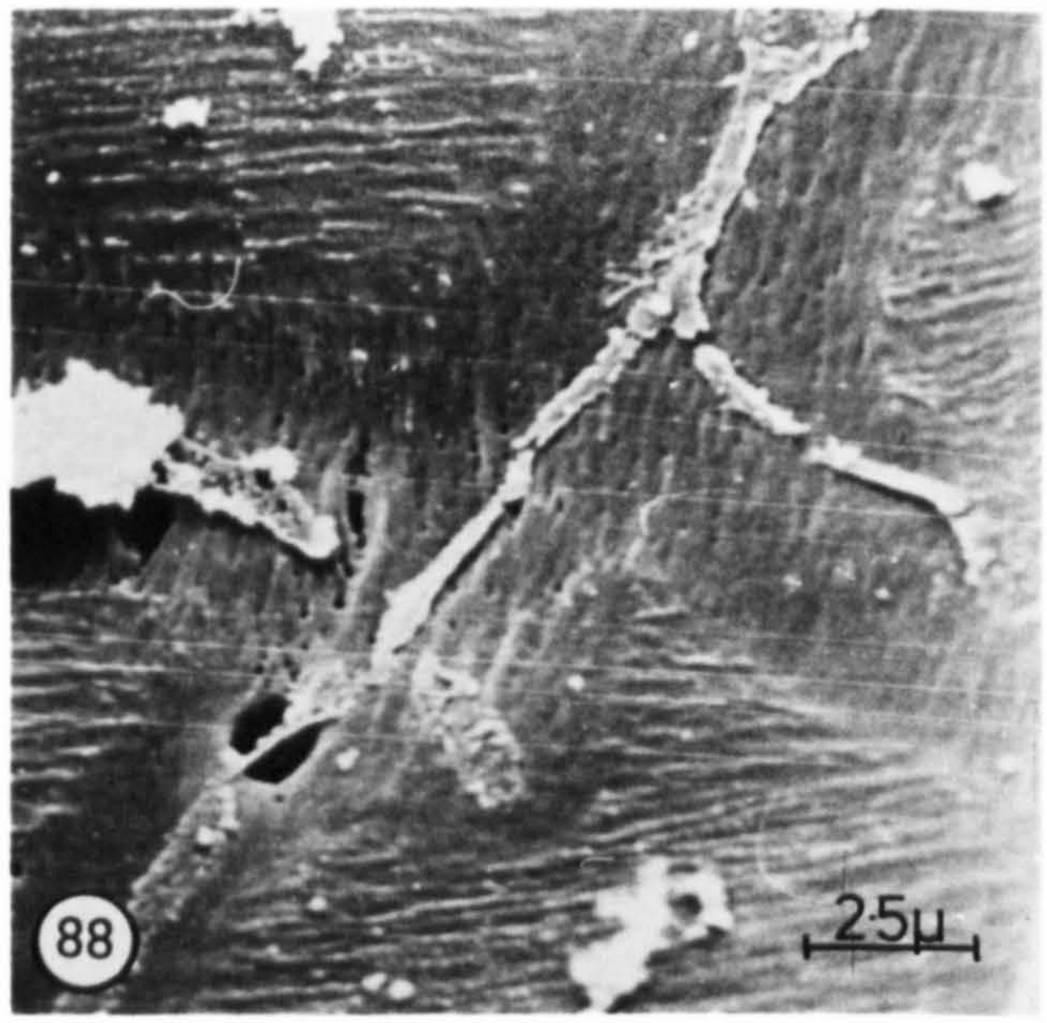
Figures 87 - 92 are examples of bore hole formation.

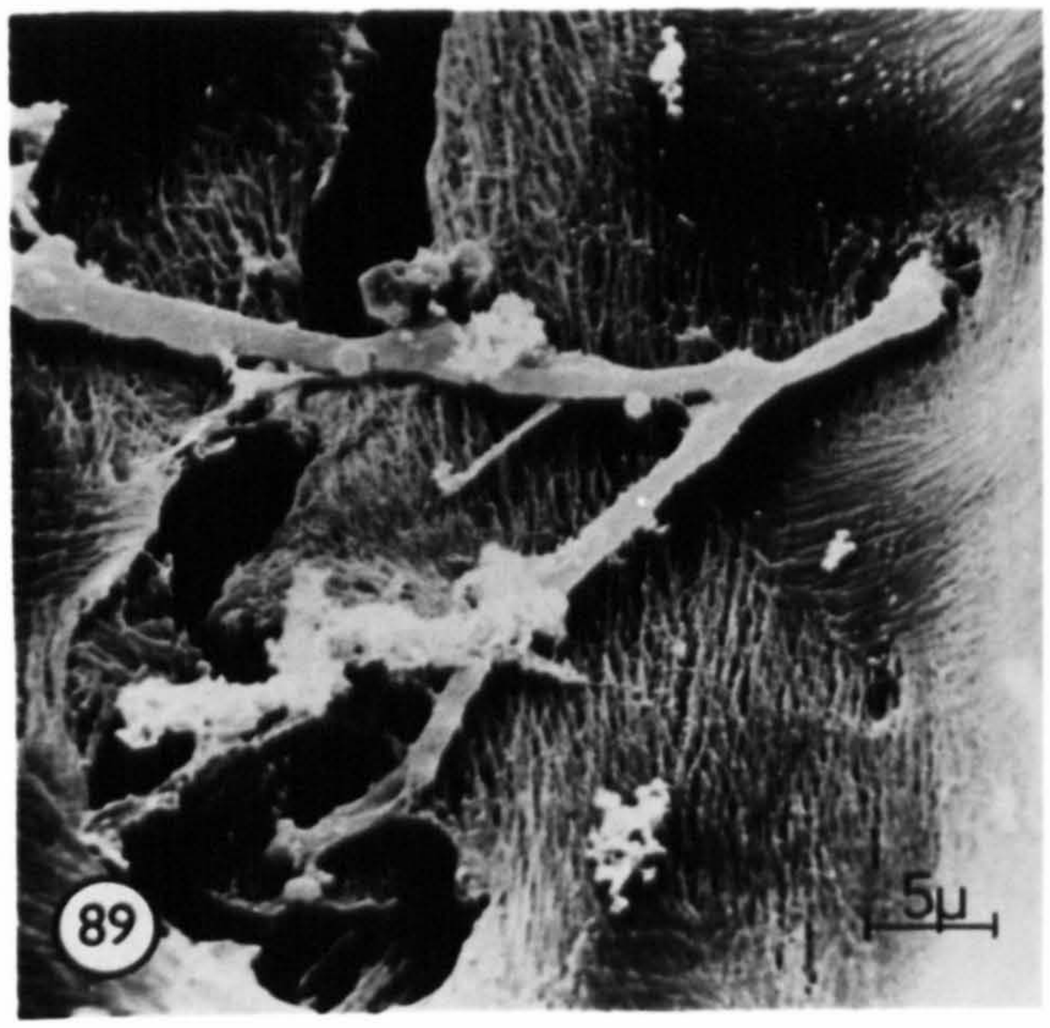
Figs. 87 (x 3220(1)) and 88 (x 5220(1)) show two bore holes with shallow channeling leading up to them. Some of the channels contain a residue and that on the left of fig. 89 bears a prominent central ridge.

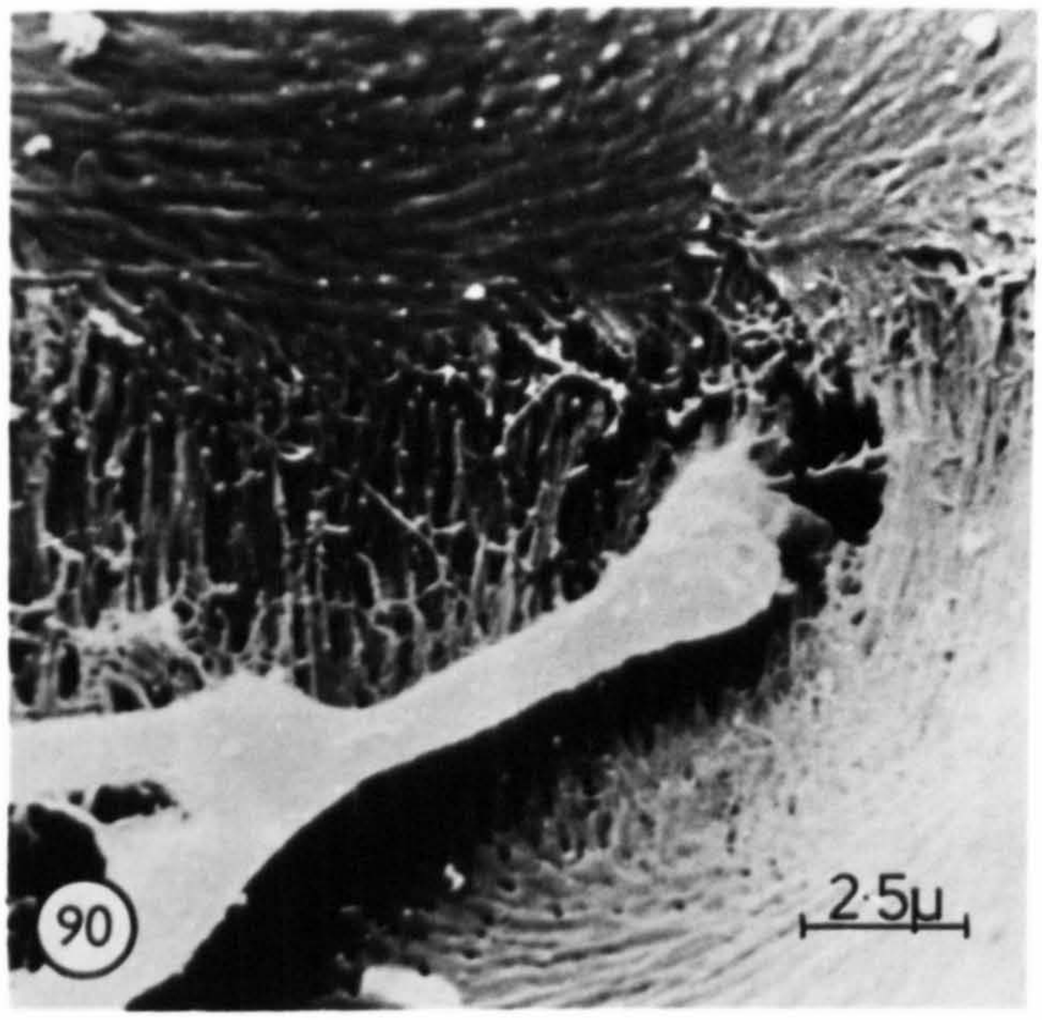
The detail of bore holes in figs. 89 (x 2080(1)) and 90 (x 5250(1)) reveals them to be more fibrillar in outline.

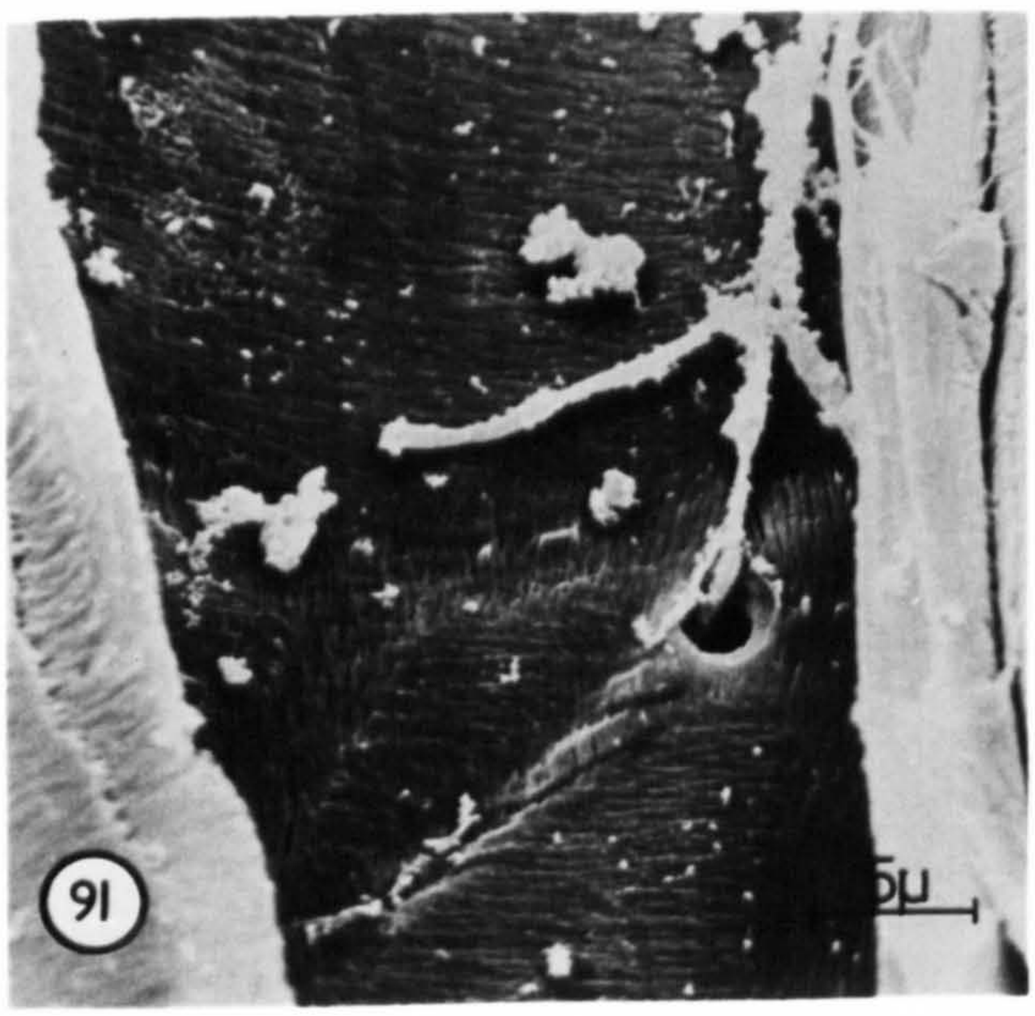
Figs. 91 (x 2510(1)) and 92 (x 4600(1)) reveal another smooth bore hole again with shallow channeling but also with the penetrating hypha which has been dislodged during preparation. The S_2 layer exhibits quite severe cracking with fine lateral bars traversing these cracks.

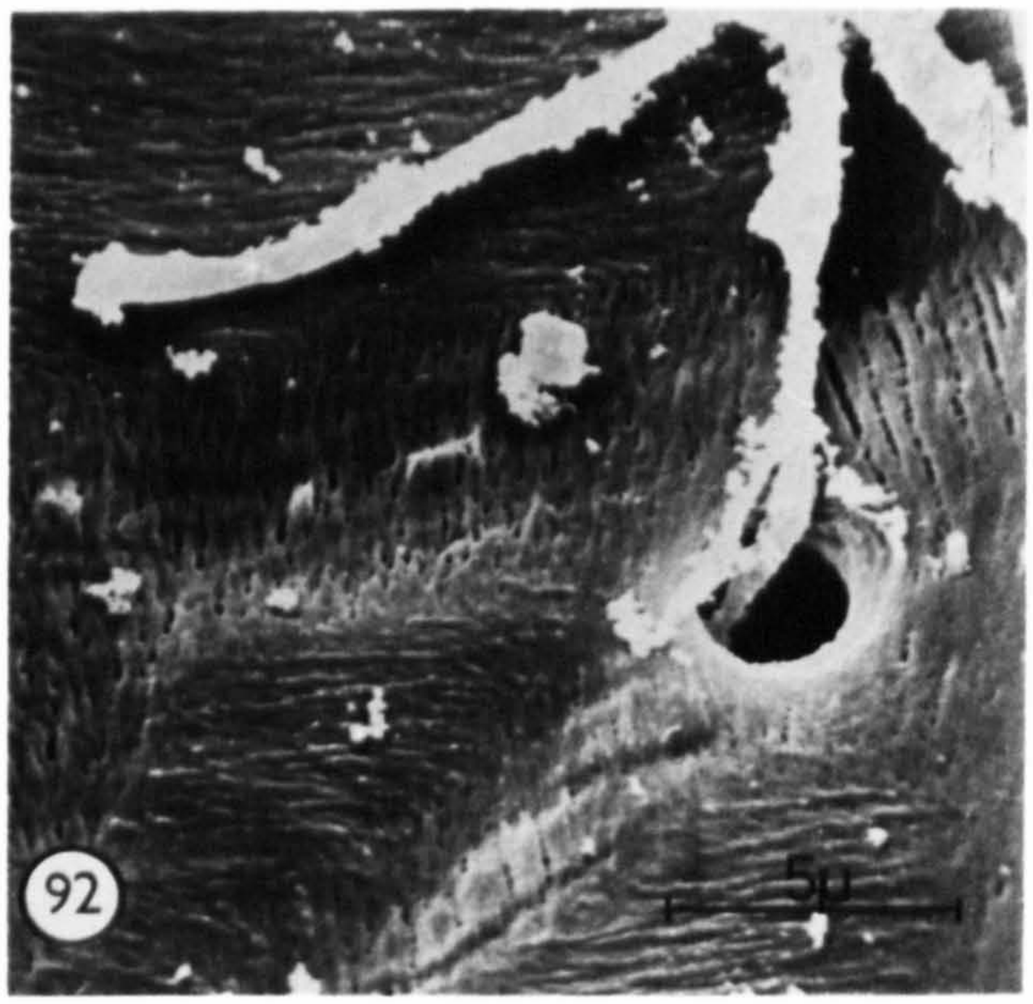

87
5μ


88
2·5μ


89
5μ


90
2·5μ


91
5μ


92
5μ

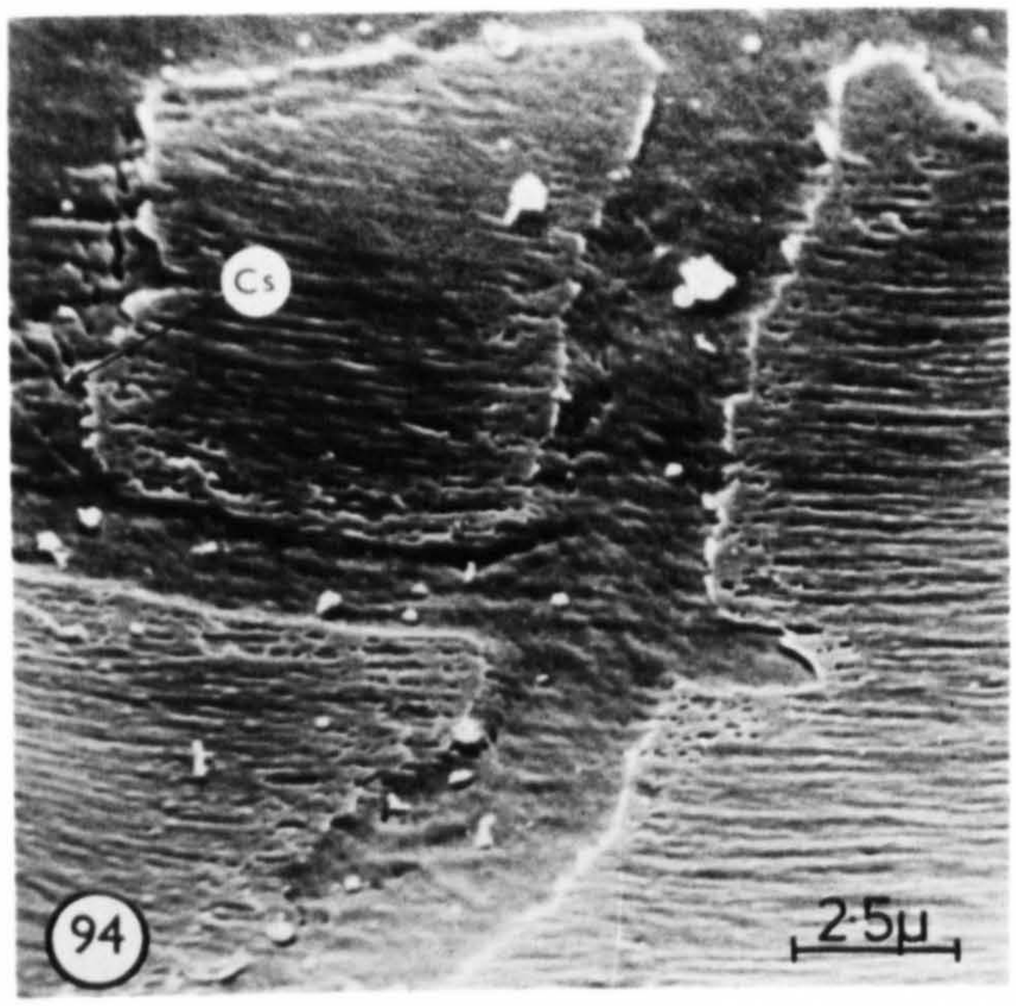
4.2.3.2 C. versicolor on Scots pine (Pinus sylvestris), 4 weeks

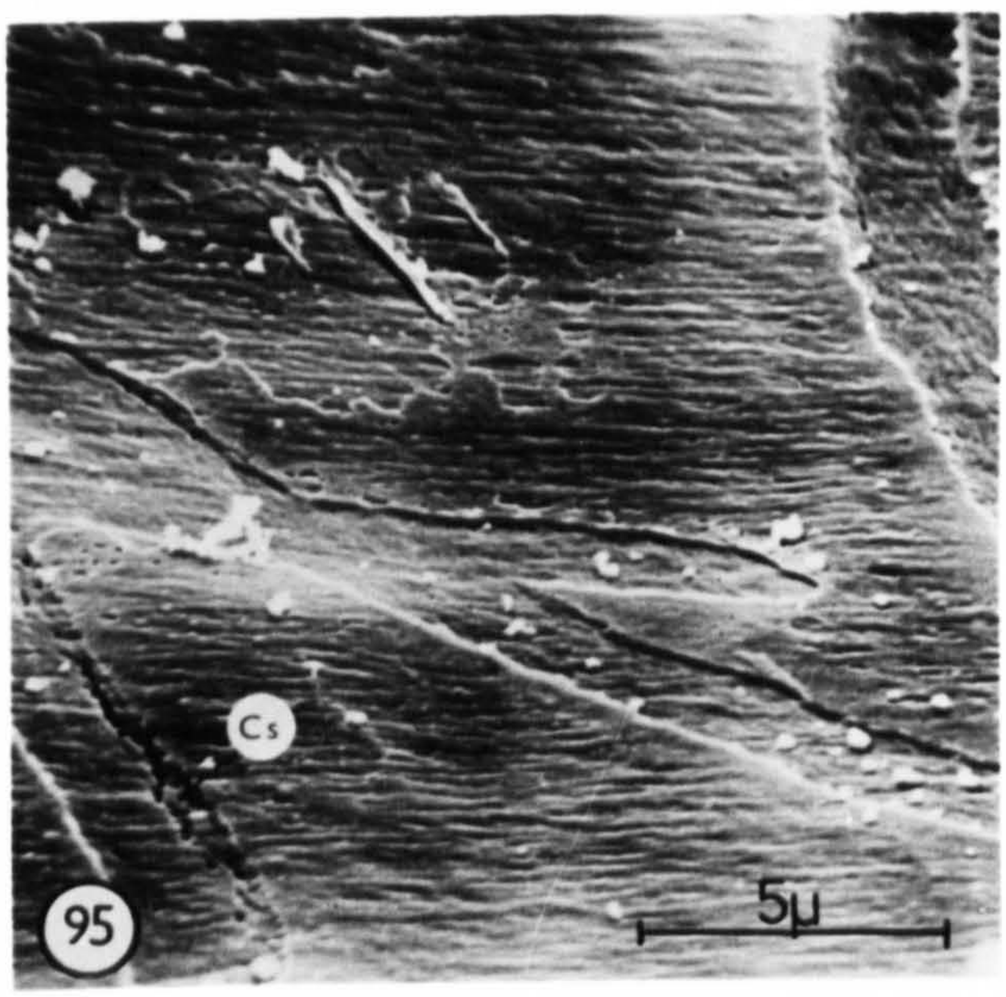
Figures 93 - 97 possibly indicate the development of a channel from the earliest signs, figs. 93 - 95, to the later more prominent type.

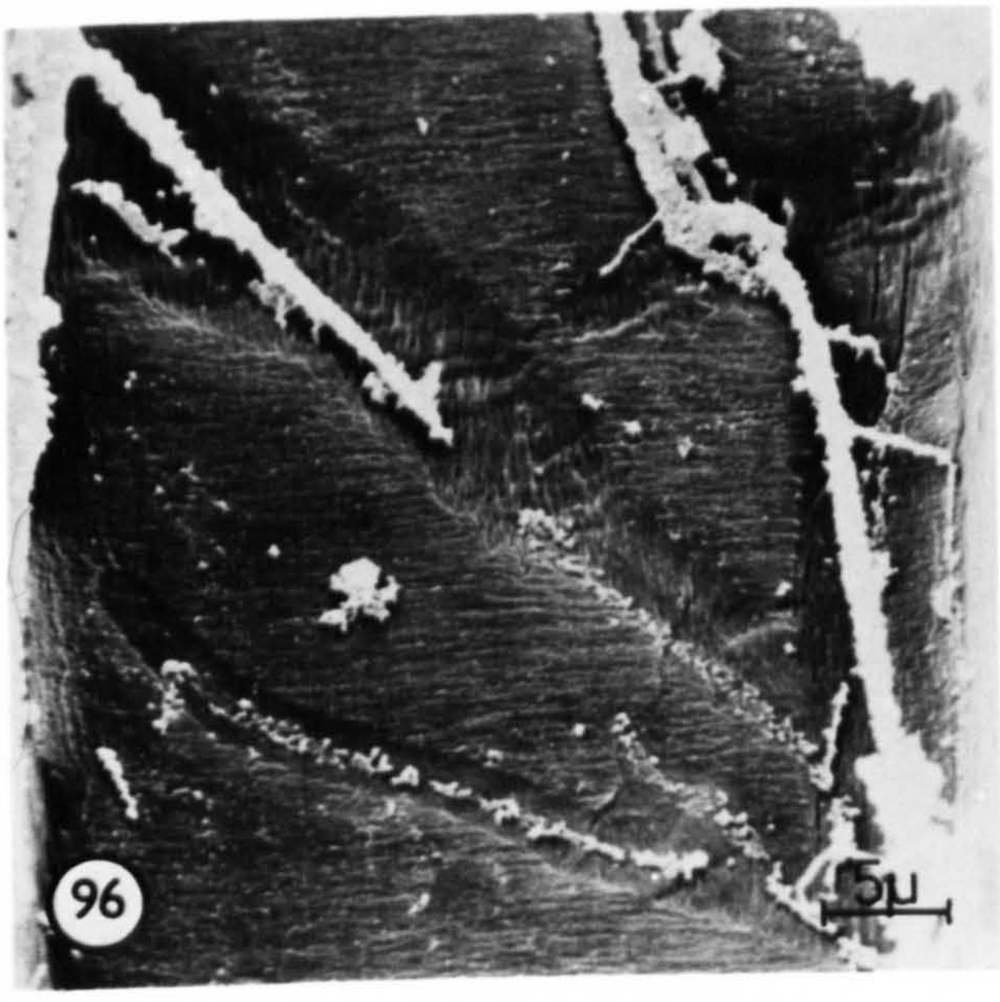
Figs. 93 (x 2150(2)), 94 (x 5240(1)) and 95 (x 4980(1)) reveal very shallow channels on the tracheid wall, the hyphae are absent, but the S_3 layering has been removed to reveal a smooth but frequently cracked layer (Cs), the cracks being along the expected S_2 orientation.

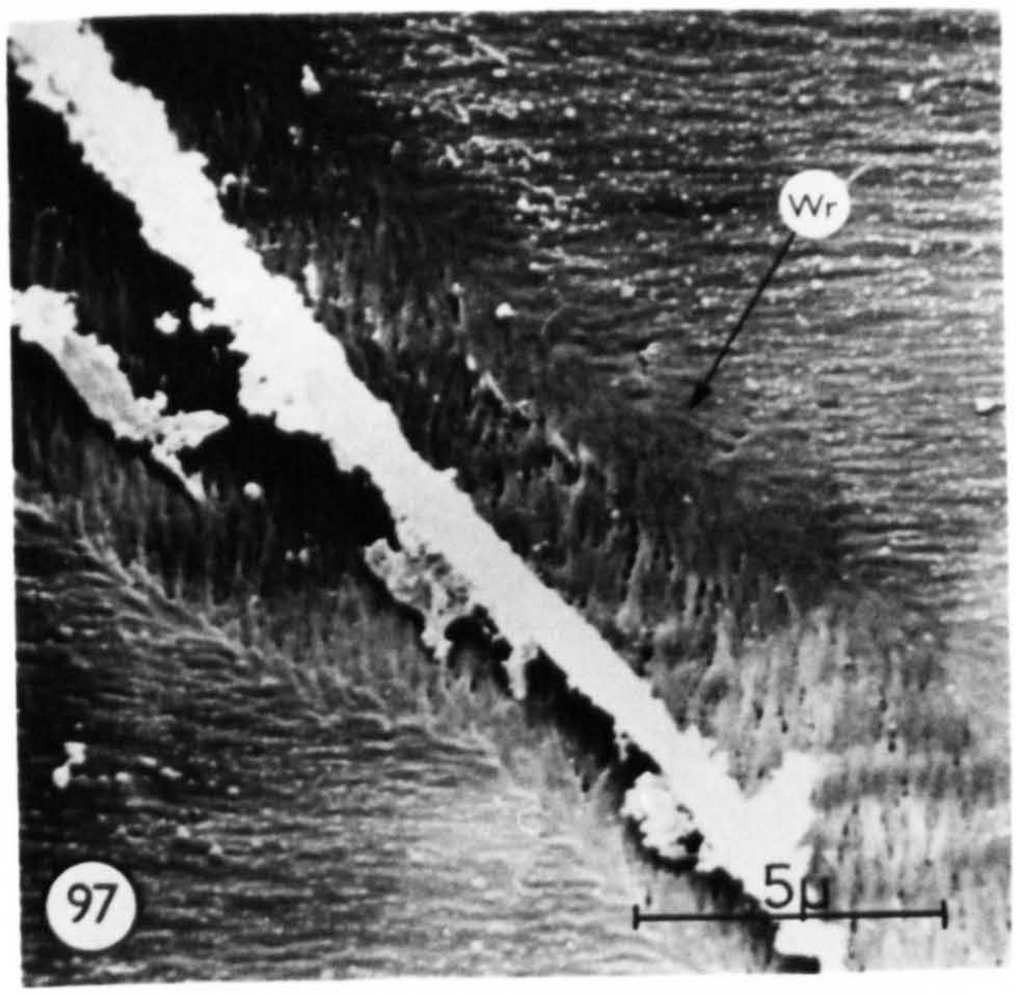
The progression into deeper channels, figs. 96 (x 2080(1)) and 97 (x 4970(1)), clearly demonstrates the S_2 microfibrillar angle. Note the investment of material on the hypha and its similarity to that observed previously. The removal of the warts (Wr) ahead of the S_3 dissolution can also be seen.


93
5μ


Cs
94
2·5μ


Cs
95
5μ


96
5μ

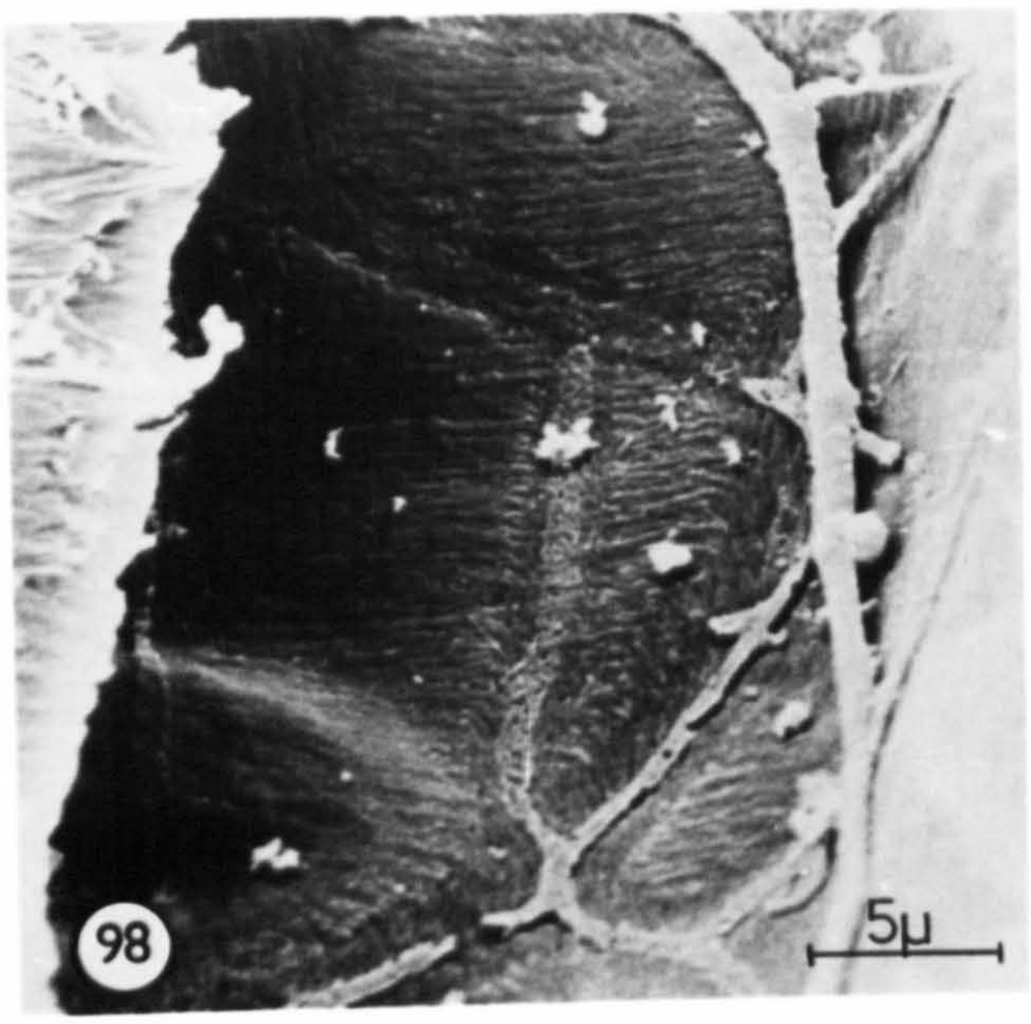

Wr
97
5μ

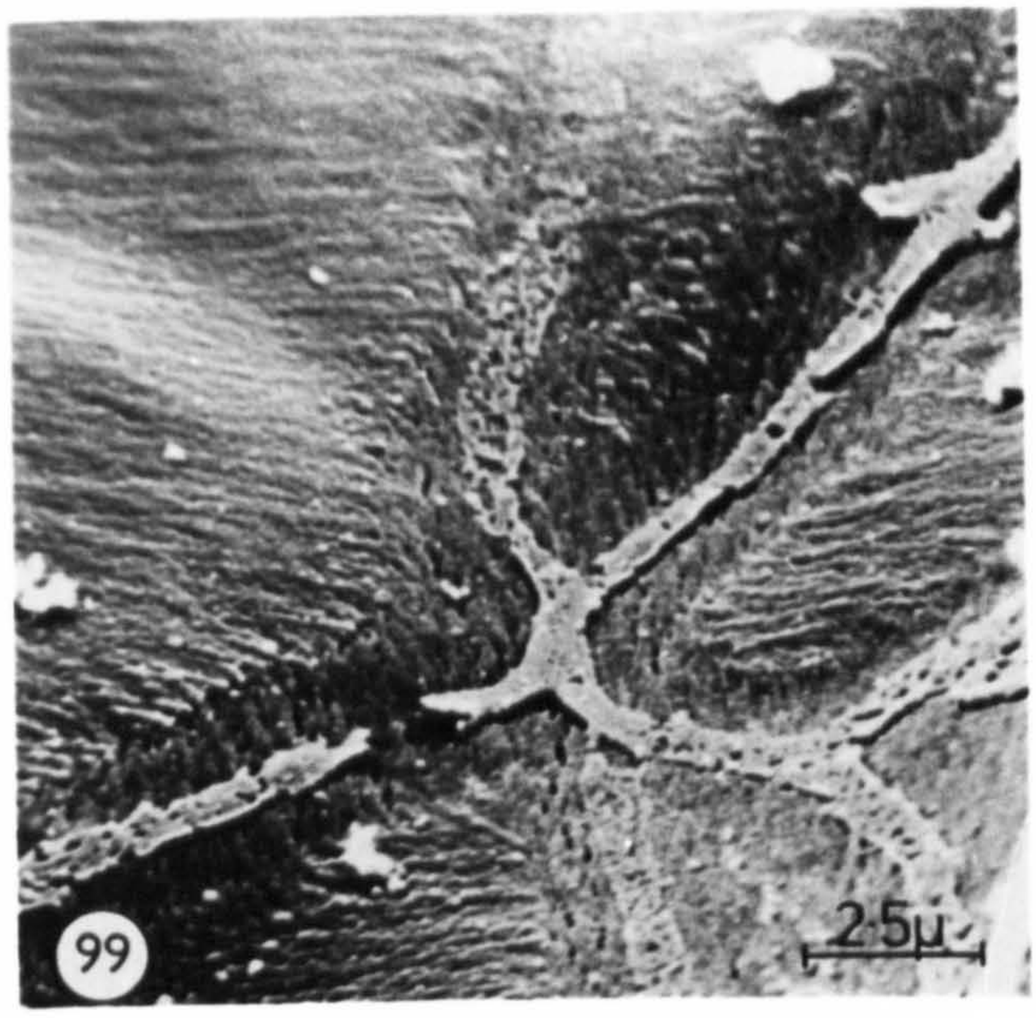
4.2.3.2 C. versicolor on Scots pine (Pinus sylvestris), 4 weeks

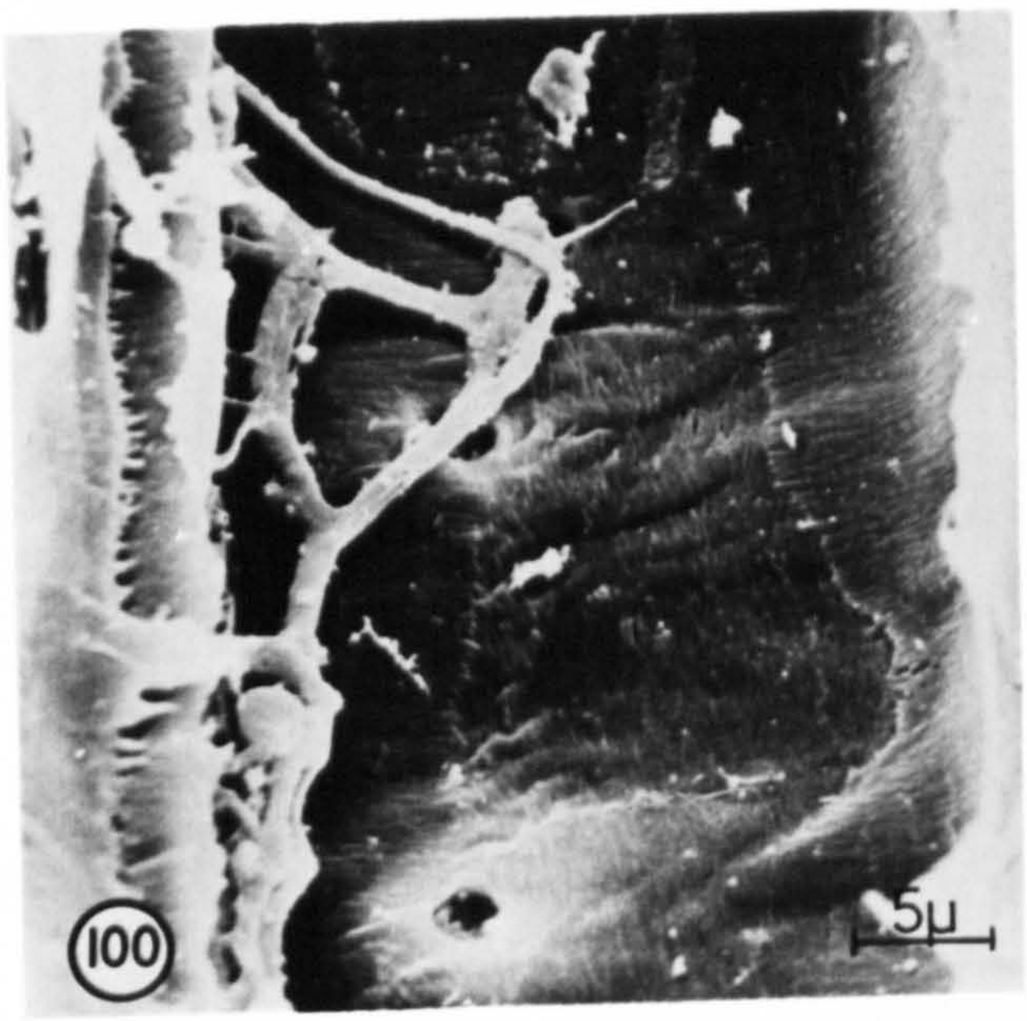
The channel residues previously noted are clearly evident in figs. 98 (x 2970(1)) and 99 (x 5400(1)). The typical channel features are shown though it is difficult to interpret this particular 'cross-roads' of hyphae.

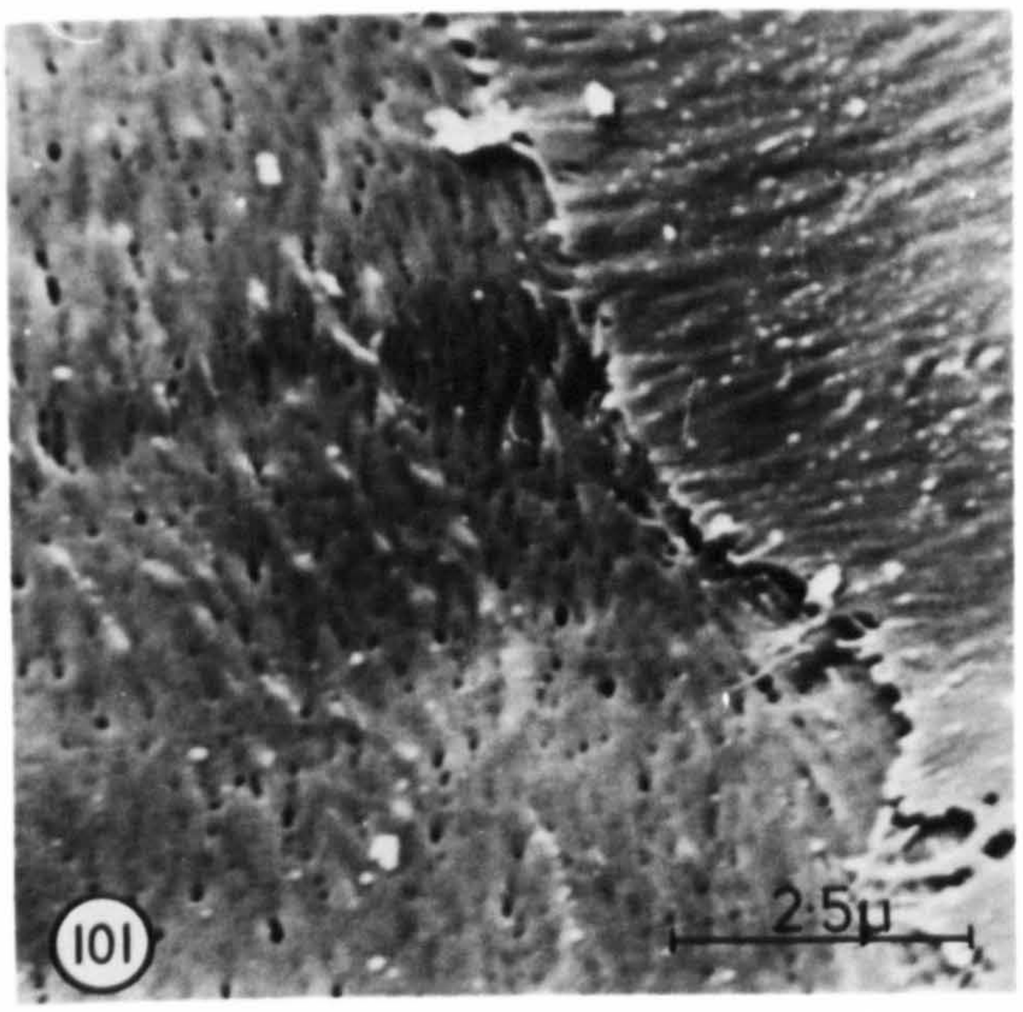
Fig. 100 (x 2200(1)) demonstrates the width some channels could attain, in this case the lysis has spread across the entire width of the tracheid. Fig. 101 (x 9430(1)) shows the margins of the channel to be very marked, almost wafer-like.

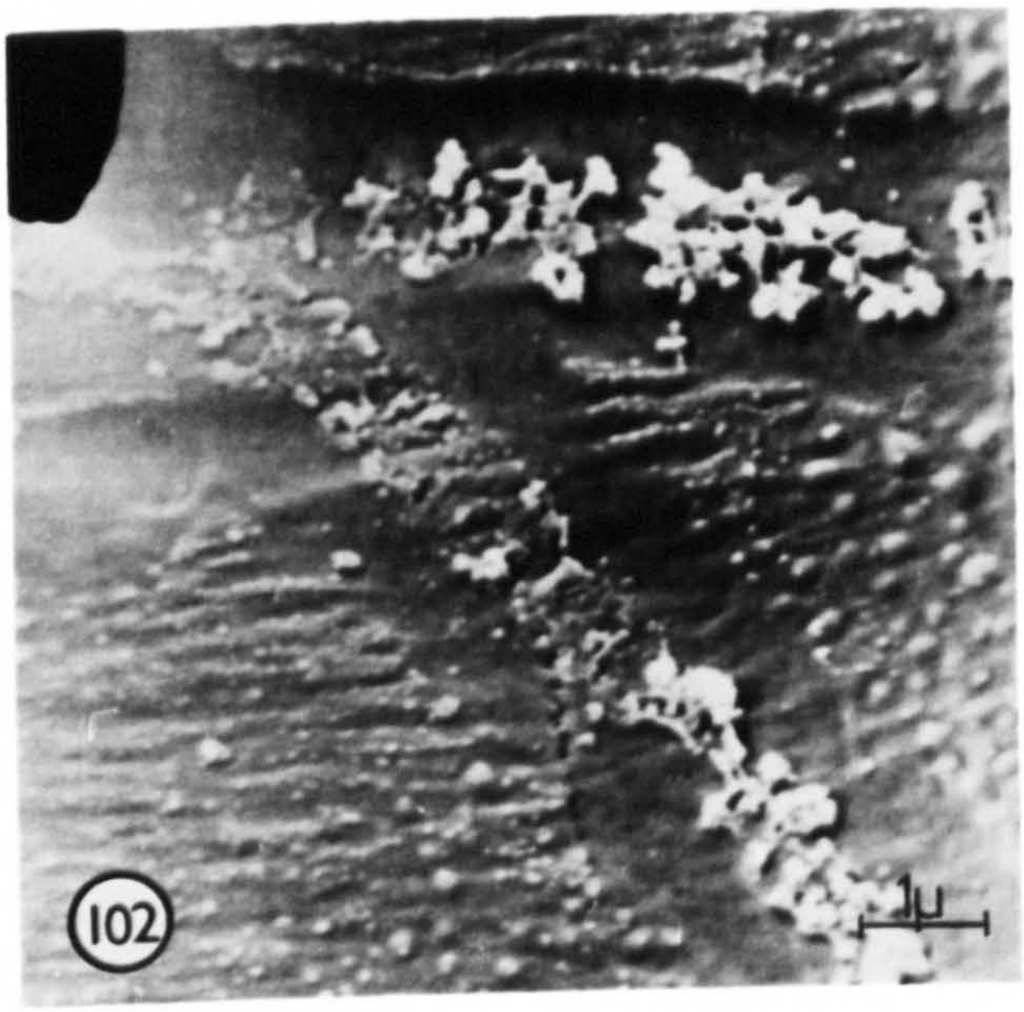
Figs. 102 (x 10410(1)) and 103 (x 10410(1)) reveal the presence of a smooth zone between the warty layer - S_3 and the familiar S_2. Both figures show the presence of residue; fig. 102 without and fig. 103 with the hypha present.

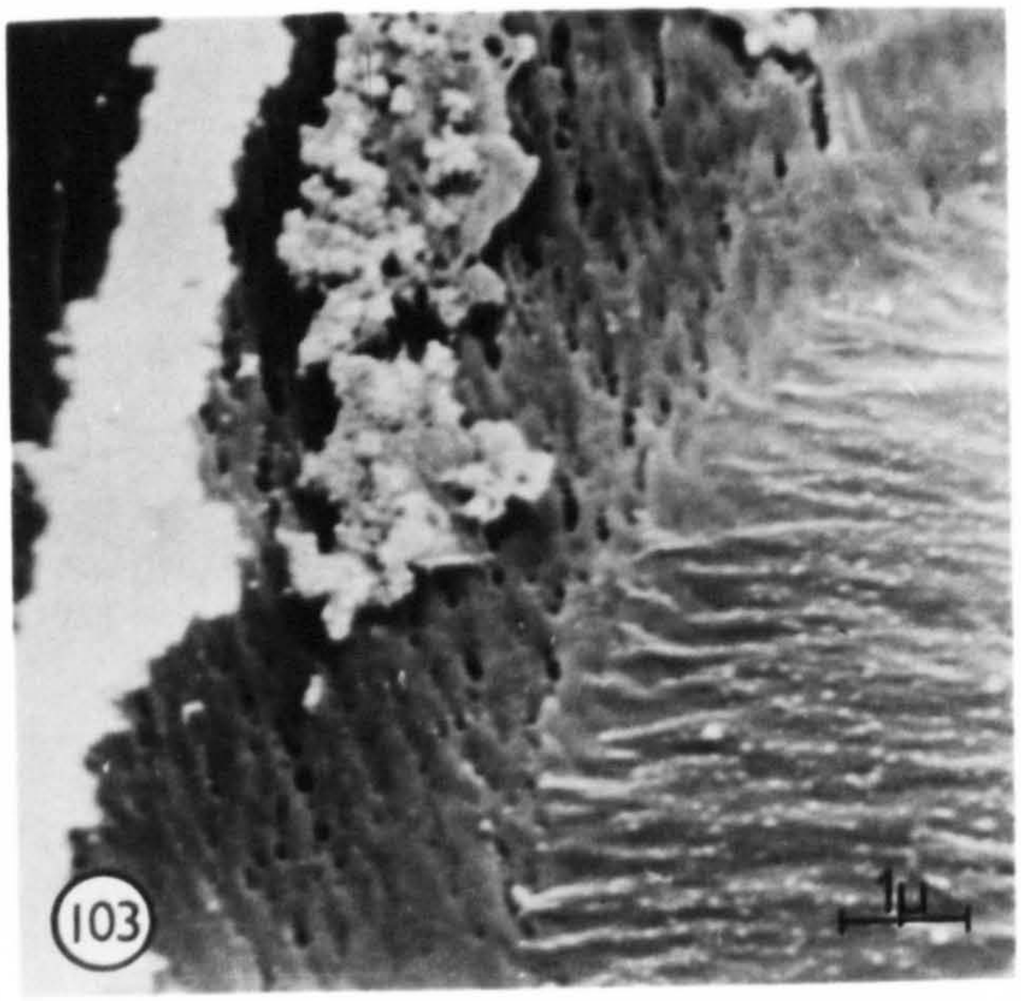

98
5μ


99
2·5μ


100
5μ


101
2·5μ


102
1μ


103
1μ

4.3 Mucilage

Throughout these S.E.M. observations it was apparent that residues and debris associated with the wood degrading hyphae could be more significant than was previously thought. An attempt was made both with S.E.M. and T.E.M. (Parts II and III) to elaborate on the significance of this material with regard to the degrade patterns observed with the three test fungi. High magnification studies were carried out on the hyphae and residues, where present, together with details of the lytic regions of the wood cell walls. It was suspected that this material might be a type of mucilage involved to some degree in the control of wall degrade. (See Part II).

Brown rot hyphae:- Coniophora puteana

Examination of brown rot decay in birch and Scots pine showed no signs of the presence of any form of mucilaginous residue on hyphae, figure 104, sinuous trails or areas of severe wall degrade, figures 105 to 107. Therefore either this fungus did not possess a significant mucilaginous layer or the preparation process did not preserve the layer. With the presence of residues in soft and white rot fungi the latter would seem unlikely.

It was noted however that the hyphae frequently appeared to have numerous pores in their walls, figures 105 and 106, which may or may not be preparation artefacts.

Soft rot hyphae:- Chaetomium globosum

As already mentioned in 4.1.3 close examination of the hyphae revealed the presence of structures found only on surface colonizing

hyphae. These structures were extremely variable in shape, possibly due to different degrees of preservation, with flat rings, spikes and vesicles being observed, figures 108 and 109. It was felt that the latter was more likely to be the true form of the extracellular investment.

However, material associated with the hyphae was also found in colonising and degrading fungi. Extensive surface debris giving a nodular appearance to cavity hyphae may also be a residue of mucilage, figure 110, as might the extensive 'woolly' investments observed on hyphae, especially in the vicinity of some form of cell wall lysis, for example bore holes, figures 43, 44 and 111.

Due to the poor results obtained for Scots pine degrade it was impossible to make comparisons of the extent to which mucilage is found on the same fungus in different woods.

White rot hyphae:- Coriolus versicolor

The presence of hyphal surface material was only extensively observed in the degrade of Scots pine by this fungus. On these hyphae extremely granular or sheet-like investments could be seen together with debris in lytic regions where hyphae had been removed during specimen preparation.

The possible involvement of this mucilaginous material in delimiting channelling can be seen in figure 112 where the edge of the channel is clearly defined together with the spread of mucilage over the hypha. The appearance of both sheet-like and granular debris on the hyphae of figure 113 could indicate that the two forms are different dehydrations of the same material.

Channels bearing a central line of debris similar to that on the hypha were frequently observed, figure 114, and the residual impressions of where the hyphae had been before removal during specimen preparation were also noted, figure 115 and also figure 102.

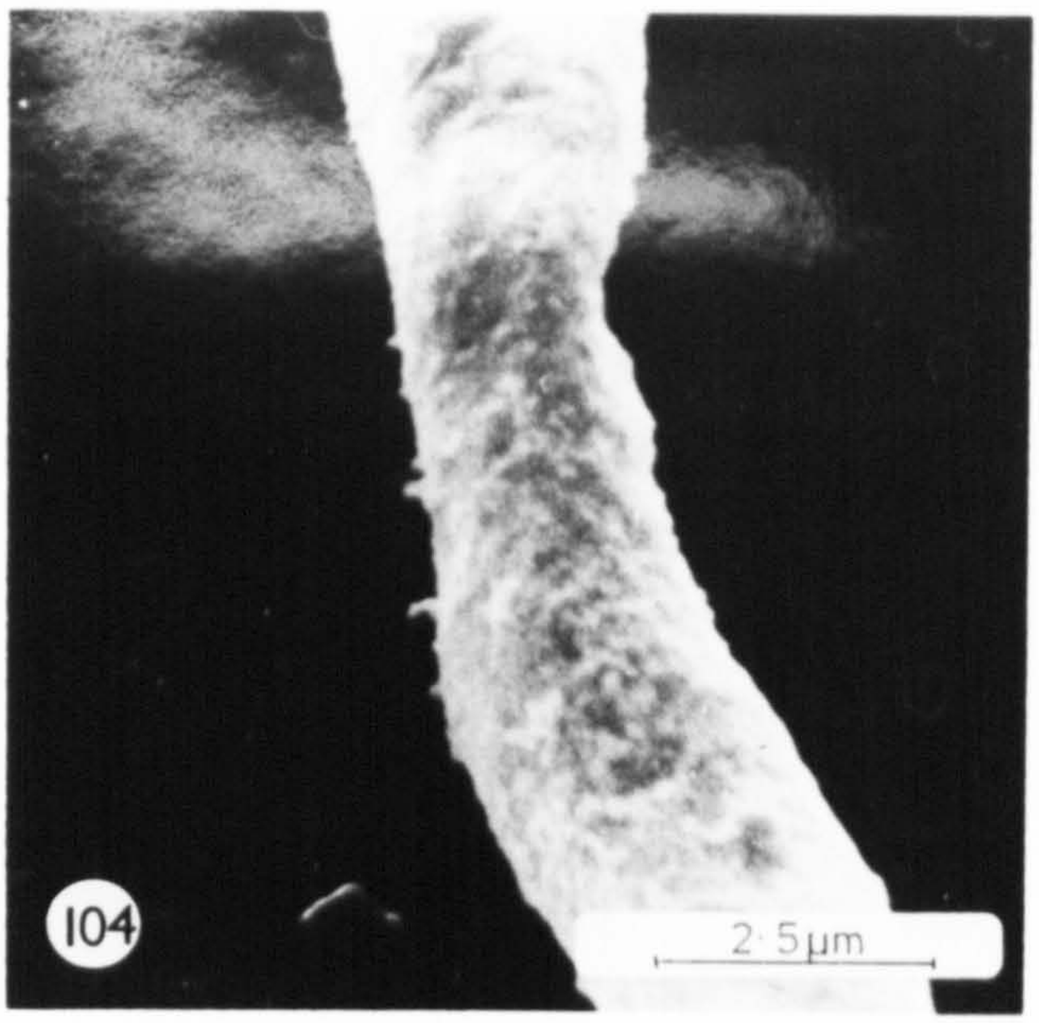
Coniophora puteana on birch (Betula sp.), figs. 104 - 107

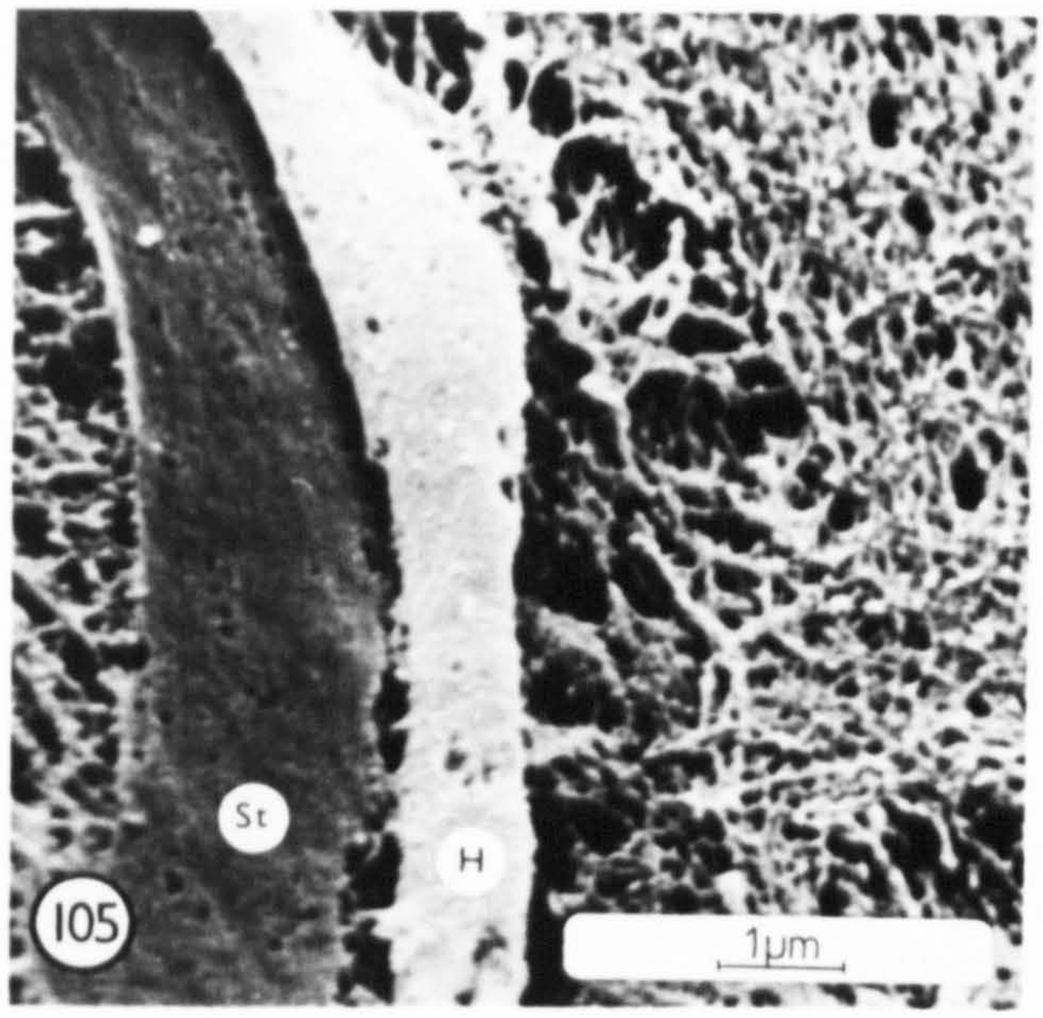
Fig. 104 (x 8700(1)) gives high magnification detail of a hypha. Although the surface does not appear perfectly smooth there is little evidence of any significant surface structuring or coating.

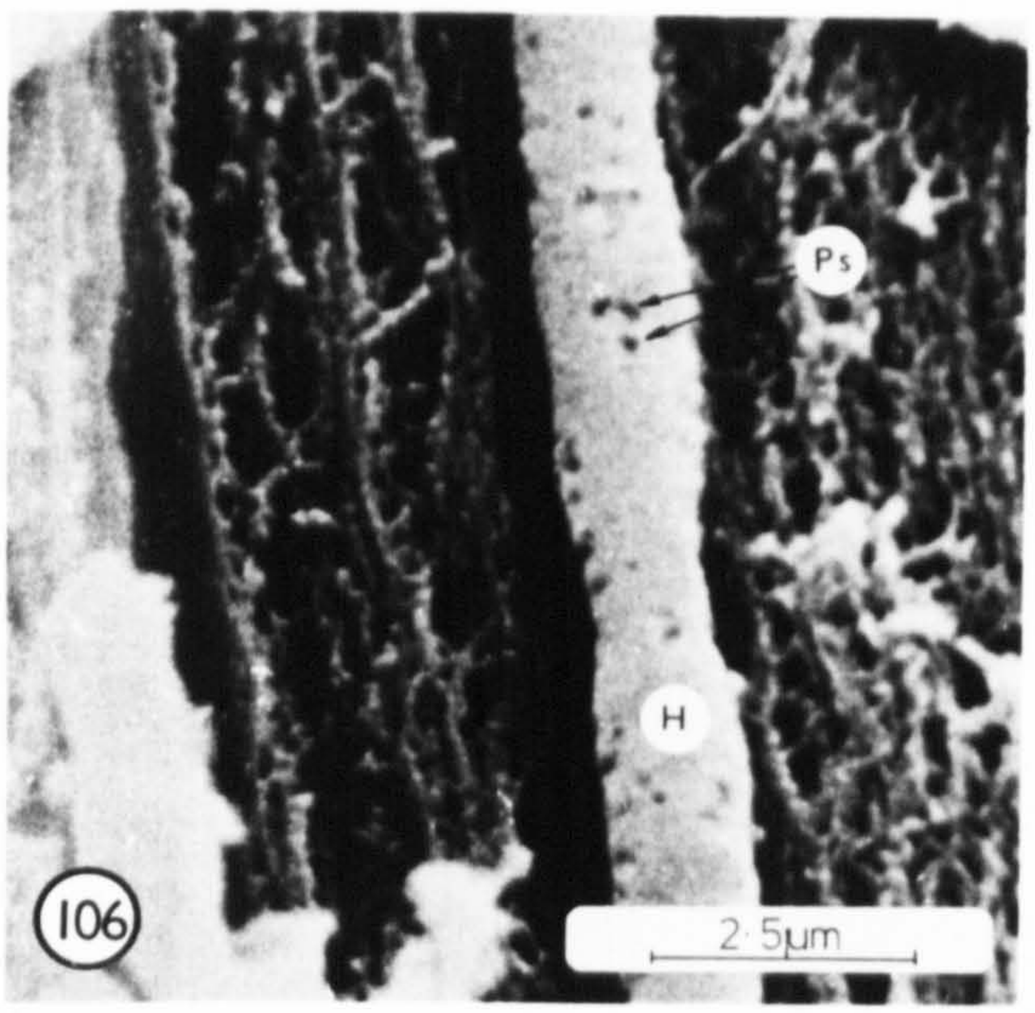
Even when hyphae actively involved in wall degrade were examined neither the hyphae(H) or the 'sinuous trails'(St) showed signs of surface mucilage or structure, figs. 105 (x 10130(1)), 106 (x 8500(1)) and 107 (x 8500(1)). However, features of the hyphae were the large variation in diameter (compare figs. 105, 106 and 107) together with the noticeable presence of pores (Ps) in the hyphal walls.

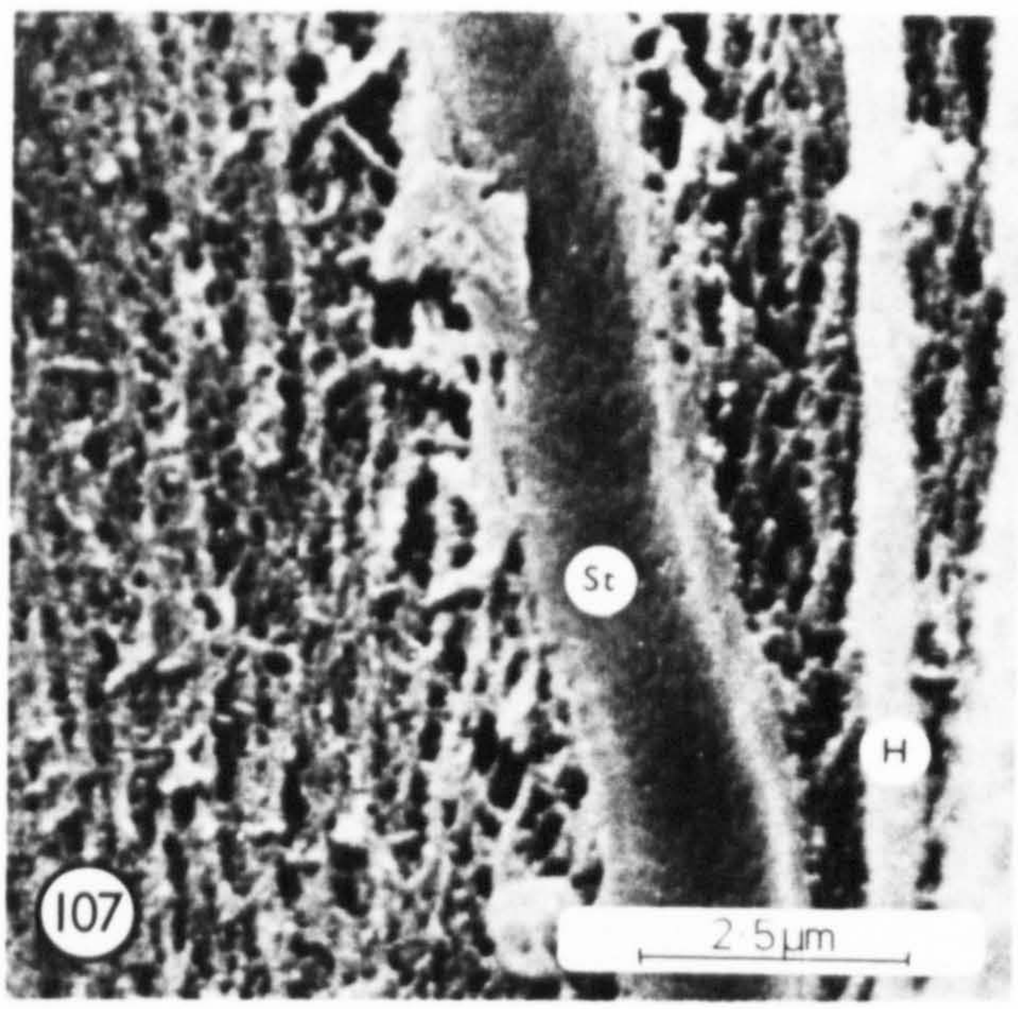
Chaetomium globosum on birch (Betula sp.), figs. 108 - 111

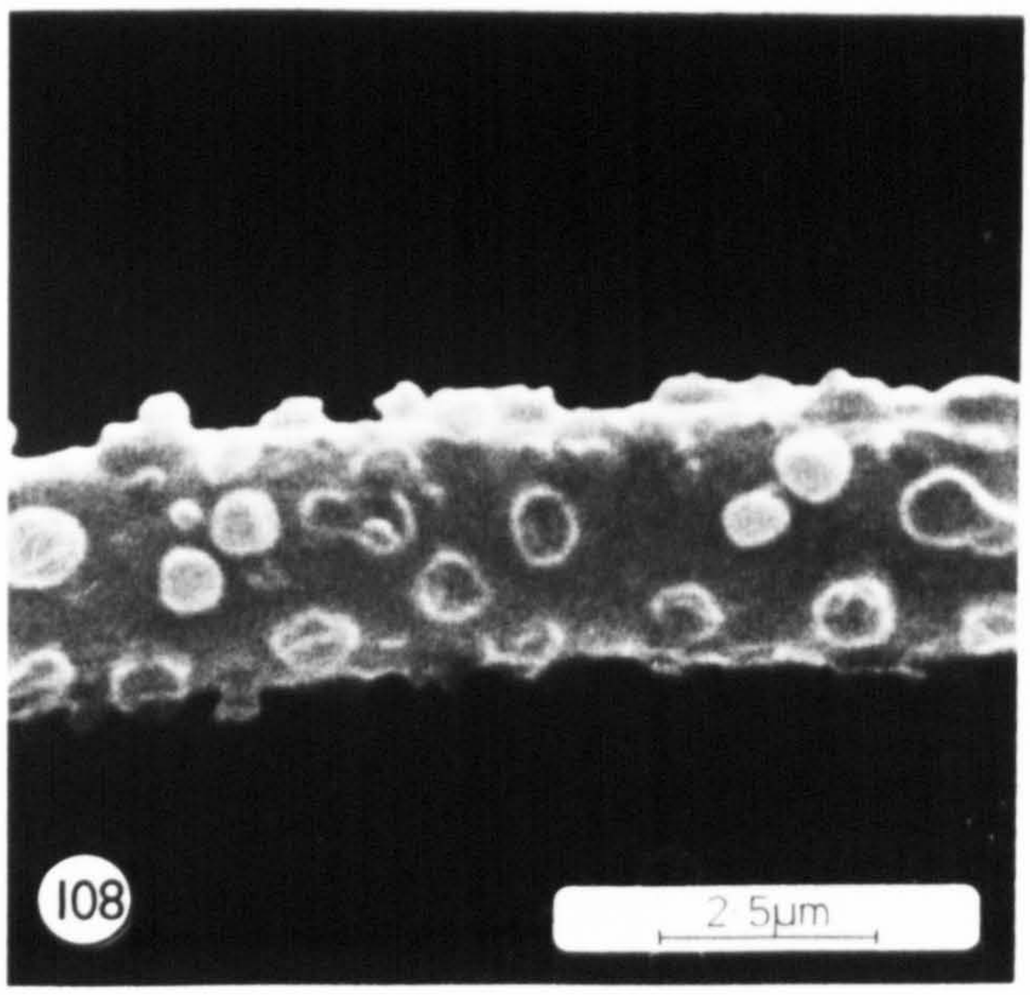
Details of surface colonising hyphae, figs. 108 (x 6880(1)) and 109 (x 4750(1)), reveals the presence of distinct vesicular and ring like surface structures. Possibly the collapse of a vesicle would result in the other forms of surface structure observed. Fig. 109 clearly shows the vesicles to be attached to the hypha.

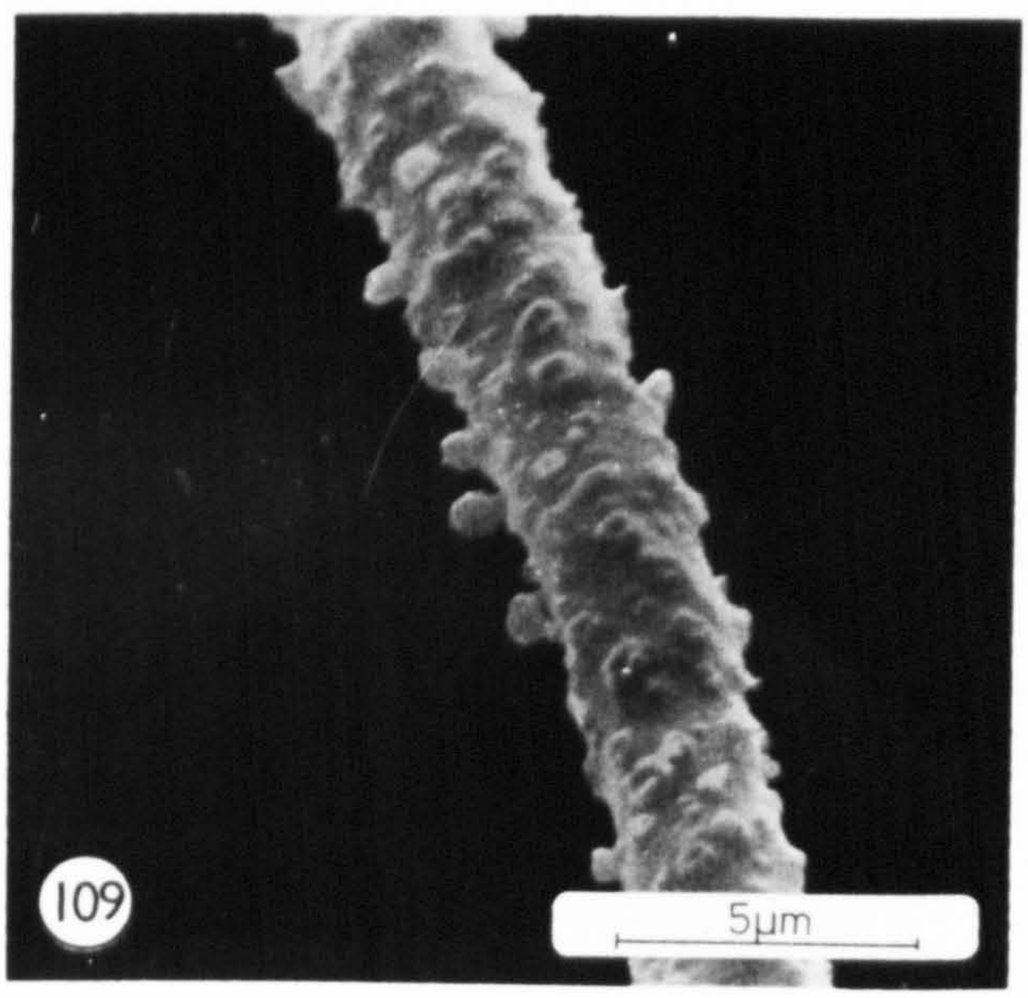

104
2·5µm


St
H
105
1µm


Ps
H
106
2·5µm


St
H
107
2·5µm


108
2·5µm


109
5µm

Chaetomium globosum on birch (Betula sp.) continued

The presence of debris on a cavity hypha is shown in fig. 110 (x 11000(1)). The finer 'proboscis hypha' (Ph) is devoid of this material as is the adjacent empty cavity.

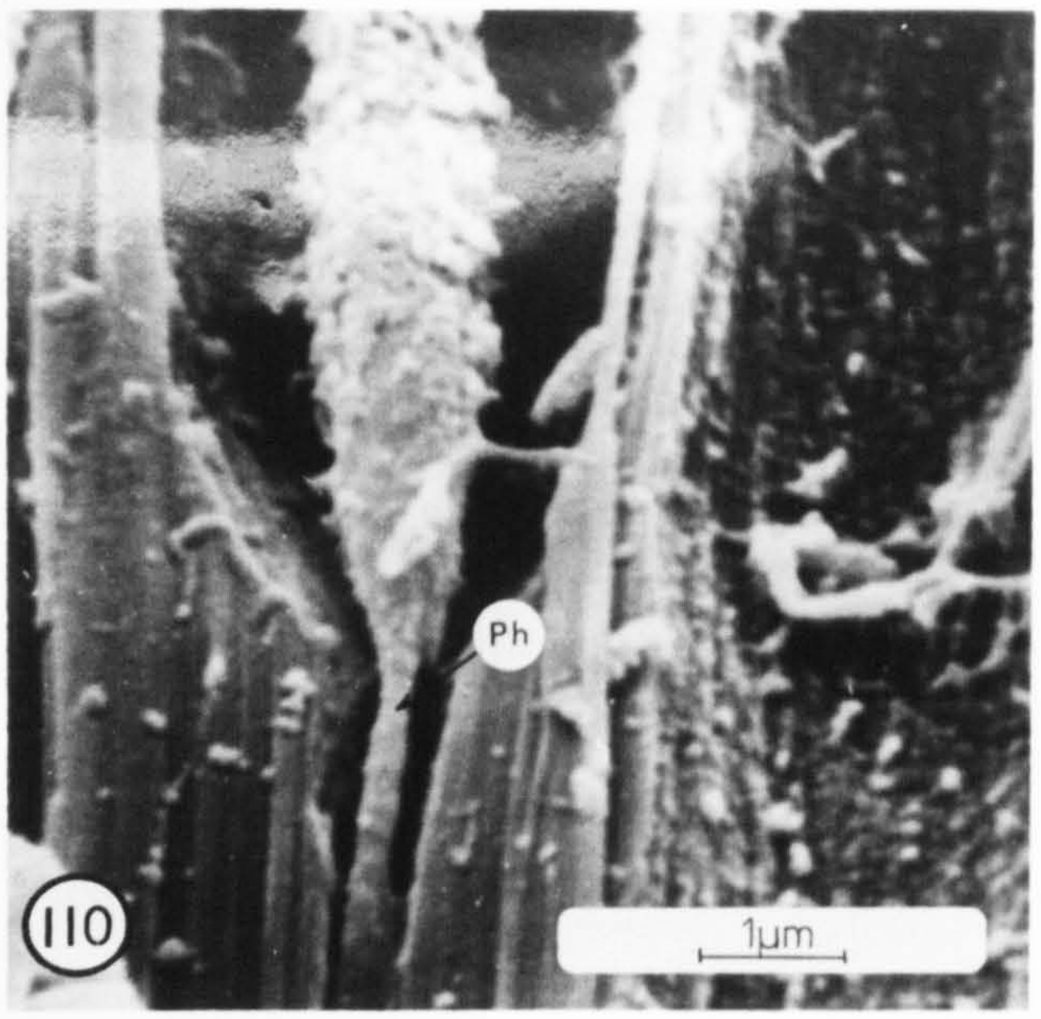
Fig. 111 (x 4490(1)) details the woolly investment of a hypha that has produced a bore hole in a fibre wall. See also fig. 45.

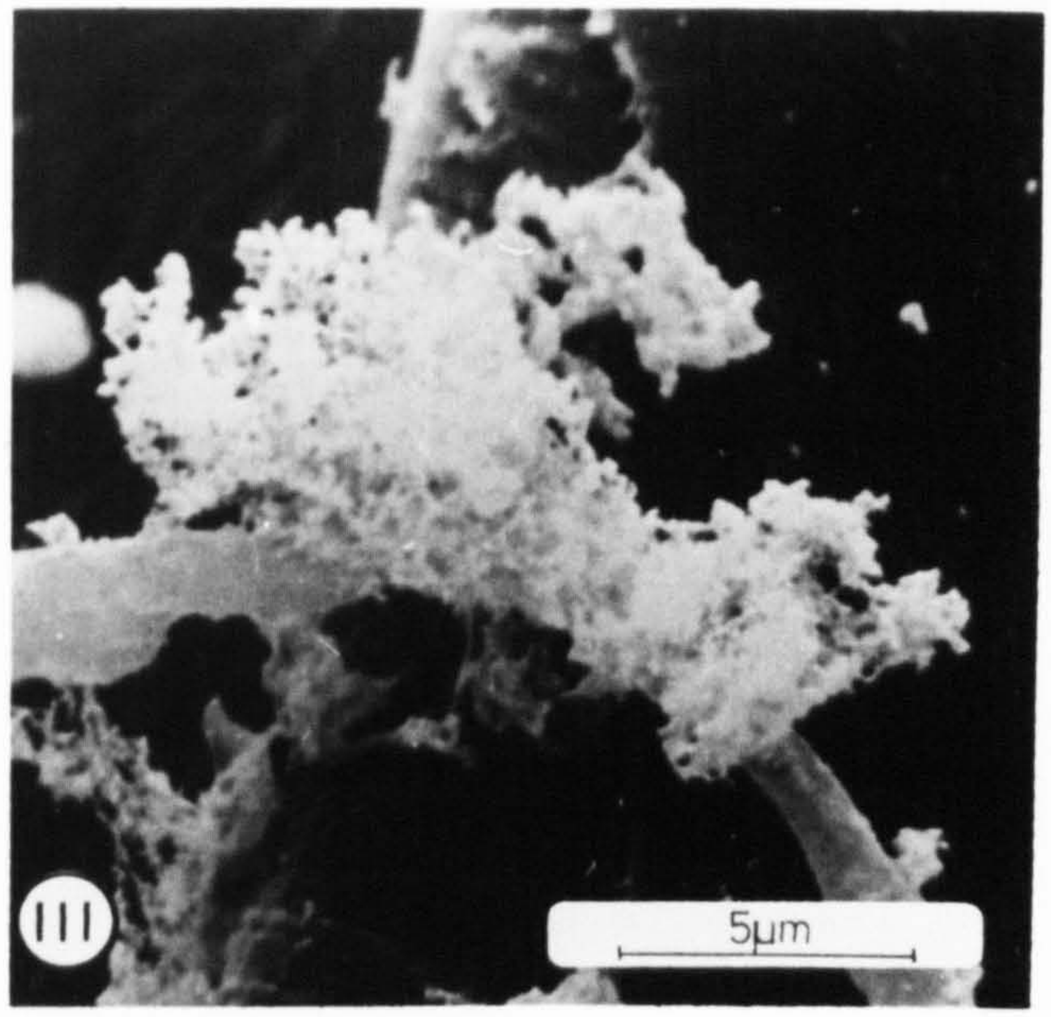
Coriolus versicolor on Scots pine (Pinus sylvestris), figs. 112-115

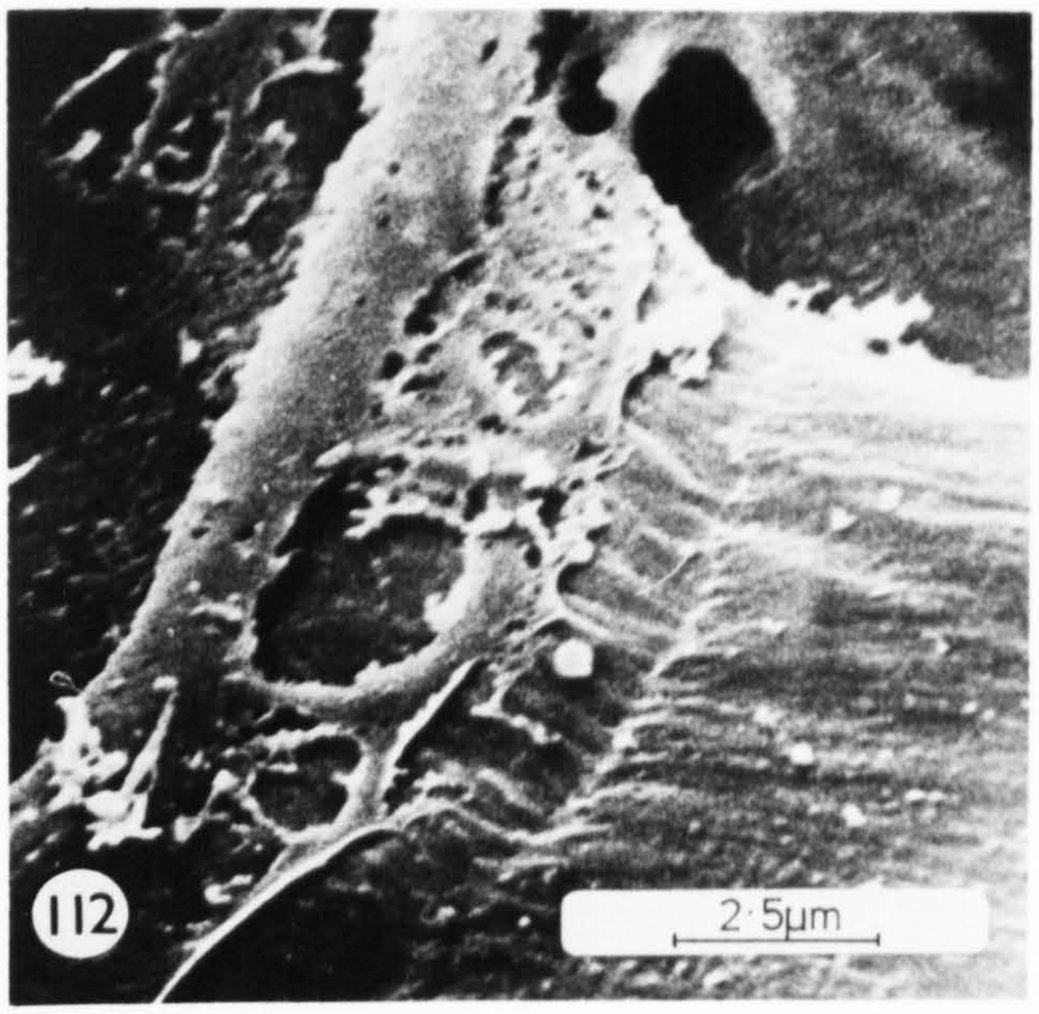
Fig. 112 (x 6190(1)) reveals the mucilaginous material coating the hypha crossing a pit border, see figs. 75 and 76. The lysis of the wall below the mucilage is clearly evident. The shrinkage of the mucilage upon drying has revealed the edge of the channel, which can be distinguished by the change in the microfibrillar details of the S_3.

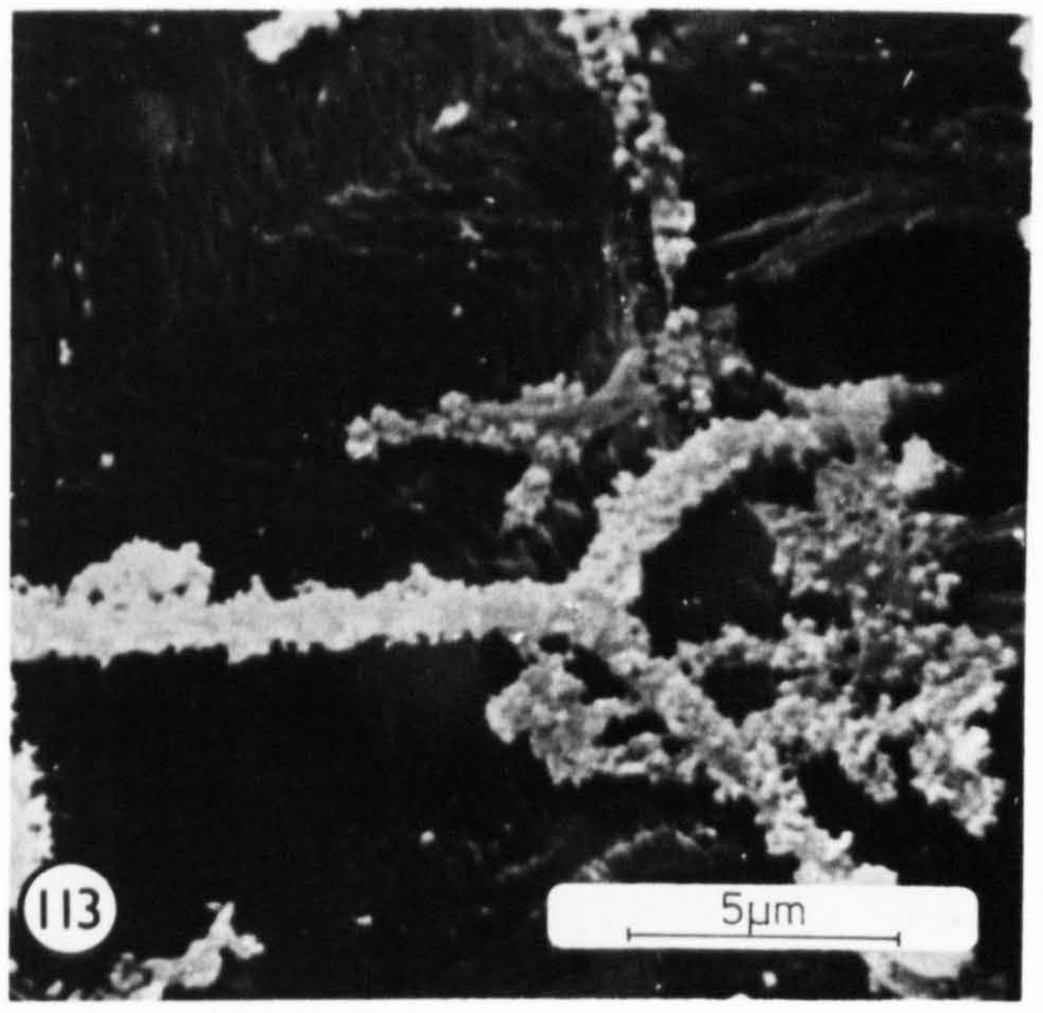
Fig. 113 (x 4270(1)) is a high magnification of fig. 82 demonstrating both sheet and granular forms of the mucilage associated with the hypha involved in bordered pit degrade. Several channels can be seen in the vicinity of the hypha which has suffered some degree of displacement.

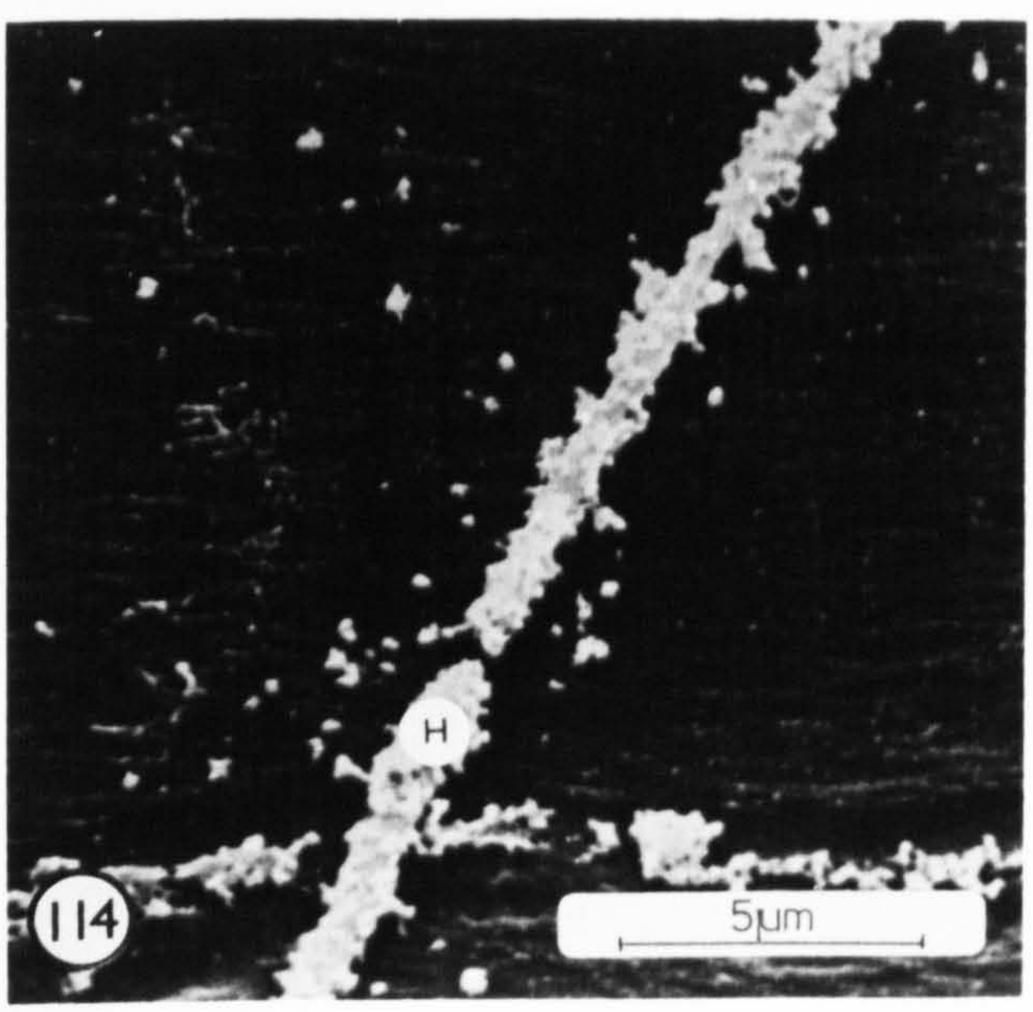
The displaced hypha of fig. 114 (x 4710(1)) crosses a shallow channel in the S_3 which bears a central line of debris similar to that on the hypha. Channels without hyphae but with a residue of debris indicating the previous presence of hyphae were frequently observed, as in fig. 115 (x 5040(1)).

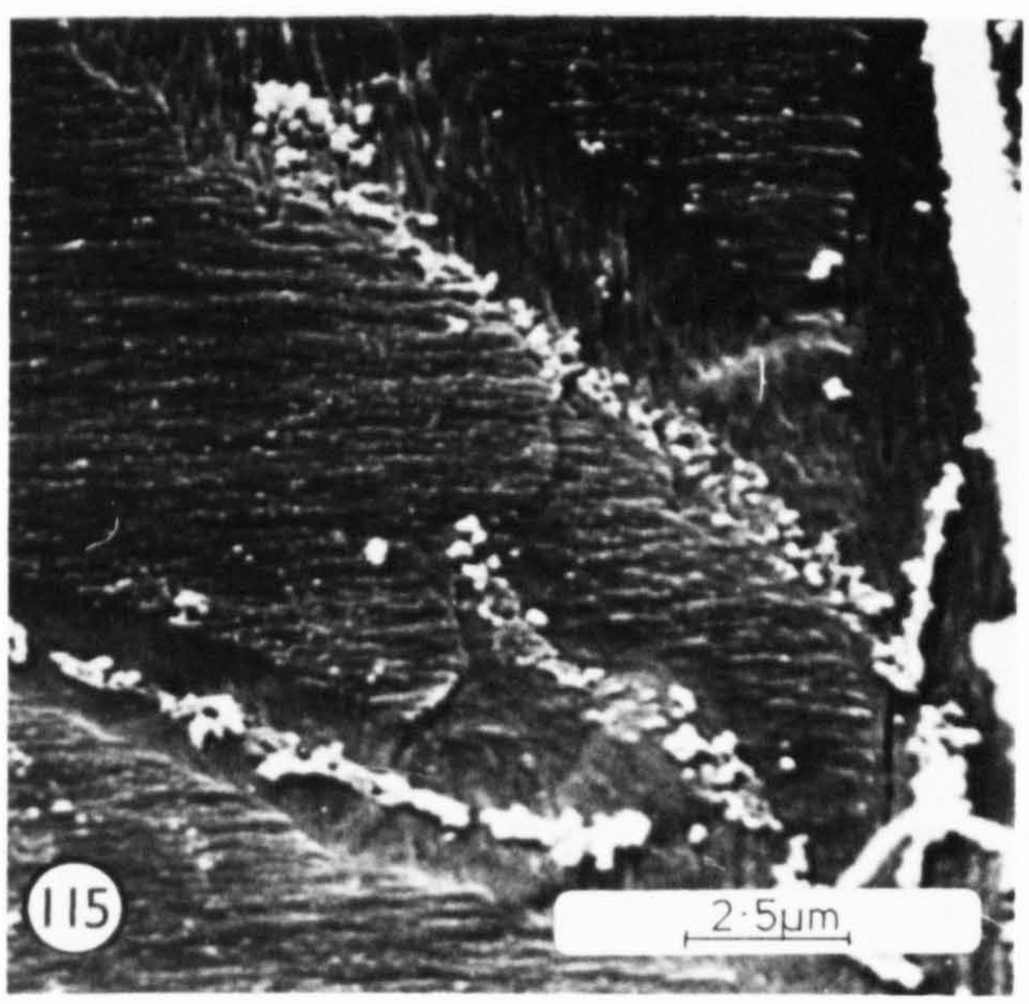

Ph
110
1µm


111
5µm


112
2·5µm


113
5µm


H
114
5µm


115
2·5µm

5. DISCUSSION

The present study examined wood decay mechanisms as observed using the S.E.M. and T.E.M.. Discussions of this part will be restricted to features seen only in the S.E.M. and these, together with observations made in the T.E.M. (part III),will be pooled with previous workers results to compile the decay mechanisms proposed in part IV. As such, only specific items of significance to the overall decay mechanisms will be discussed here in detail.

The results of the different methods employed in this section allow certain comments to be made on features of decayed wood preparation. Small refinements in culture mechanisms, such as block positioning on established, active, hyphal fronts, added to the accuracy of work based on time scales, especially when early decay features were being examined. A criticism of the culture method employed in this study might be the incubation of two different woods within the same plate. The natural preference of the fungus for a wood type produced markedly different degrees of wall degrade within a given time period. However, this yielded information on the comparative susceptibilities of the two test woods to the three fungal types. In general the results of this work have shown a significant preference for birch by the brown and soft rot fungi and equal attack of birch and pine by the white rot fungus.

Decay features observed were in agreement with previous results (Greaves and Levy, 1965; Wilcox, 1968; Bravery, 1972; George, 1974). This indicated that the natural development of wall lysis was not impeded to any great extent by the short axial dimension of the test blocks.

From the results of this S.E.M. study it is recommended that decayed wood specimens should be cut from the blocks rather than split. The tendency for the wood to sheer along the middle lamellae, especially of ray cells, during splitting produced extensive wall damage with large amounts of surface debris. This material, in conjunction with middle lamella views of the decay features, resulted in split specimens being difficult to interpret.

The majority of fungus - wall interactions begin on the lumen - wall interface and to view the mechanisms involved the cellular elements must be cut open. Cutting also produced cleaner, more accurate, views of lysis within the wall, for example, bore holes, cavities and wall penetrations. In examinations of the microfibrillar orientation of the wall layers a certain degree of wall tearing is essential. It has been the author's experience that the use of microtome knives or razor blades during specimen preparation does not eliminate wall tearing completely, thus allowing microfibrillar orientations to be determined.

The normal practise of air drying fungal decayed wood has been shown to produce severe distortion of the hyphae. This collapse, due to surface tension, was successfully overcome by the application of Critical Point drying resulting in hyphae appearing tubular, which compares favourably with direct observations on fresh material and with the results of freeze dried preparations (George, 1974). This appearance enables micromorphological decay features to be interpreted more accurately with regard to the position and shape of the causal hyphae. In spite of the possible adverse effects of chemical action by the dehydration solvents the application of C.P.D. should be regarded as standard practise in the S.E.M. of wood decay. Where access to freeze

drying facilities is possible then this method, with its minimal solvent extraction, would be preferred.

The gross colonisation patterns deduced from the material examined were in total agreement with those observed by Bravery (1971, 1972) and George (1974), with full use of vessels and rays as primary pathways followed by lateral spread into adjacent fibres and tracheids.

Brown rot

The degrade of birch by Coniophora puteana was rapid and extensive and although the vessels appeared to resist wall lysis (figs. 7 - 8) as noted previously by Meier (1955) and Bravery (1971, 1972), the adjacent fibres were severely attacked (figs. 9 - 24).

A notable feature was the resistance of the fibre cross-field pit membranes to the lytic agent(s) (figs. 9 - 11) even when the surrounding wall layers exhibited heavy lysis. The pit membranes represent the middle lamella between, and paired primary walls of, two adjacent cells. In birch, this layer contains a high percentage of pectic material (galactan, arabinan and pectic acid), a low cellulose content (1%) and is heavily lignified (Meier, 1964).

It has been established that brown rot fungi have the enzyme / lytic capability for digestion of cellulose and hemicelluloses with only a slight modification of lignin (Kirk, 1971, 1973). It is not surprising, therefore, that pit membrane dissolution was extremely difficult as they are constructed from carbohydrates that the fungus has only limited ability to degrade. However, penetration of the pits was observed to be the pathway for tangential spread, with fine penetration holes being created in the resistant membranes (figs. 12 and 13). The limited capacity for lignin attack, or modification, would

favour the easist route between cells. Extensive bore hole formation as reported by Proctor (1941), Cowling (1965) and Wilcox (1968) was not observed in this work and could have been due to the test block format or Coniochora puteana being unable to cause sufficient total wall lysis in birch required in complete wall penetrations.

The observation of 'sinuous trails' of undegraded wall material surrounded by extensive lysis has not been previously reported. Figs. 20 - 22 demonstrated that these regions were caused by the overlying hypha and this leads to interesting speculation on their formation.

Recent suggestions on brown rot decay mechanisms postulate the involvement of a highly reactive non-enzymic component as a pre-cellulolytic factor (see, Koenigs, 1975; Reese, 1977). The proposed H_2O_2-Fe^{++} agent presumably could also have a capability for chitin attack and, therefore, the fungus might secrete or bear a neutralising chemical to prevent autolysis. This chemical could impart resistance to the hemicellulosic material in the wall adjacent to the overlying hypha.

The concentration of the enzymes and lytic agents either side of the hypha resulted in localised heavy wall lysis (fig. 16). The more distant and extremely susceptible S_2 wall layers of low lignin content were severely degraded with the residues resulting in a very open matrix. This was particularly evident in broken sections of wall (figs. 9, 10, 17 and 24). The possibility that the trail represents a ridge comparable with the white rot degrade pattern (Bravery, 1971, 1972) is unlikely due to the high mobility of the lytic factor which would attack the wall beneath the hypha unless restrained by some mechanism.

Ultimate lysis of the 'trails' (figs. 18 and 19) could indicate

senescence of the hypha or a weakened neutralisation. Hyphae observed growing over totally degraded walls were probably secondary colonisers (figs. 14 and 15). The presence of pores in the hyphal walls (figs. 20 - 22, 105 and 106) were possibly artefacts of specimen preparation as they were not observed in the T.E.M. material (part III), though undoubtedly they would assist in enzyme release and product absorption.

Attack of Scots pine by Coniophora puteana was not as marked as that on birch. The general appearance of the hyphae indicated low activity (fig. 25). The most obvious lytic effect was the thinning, collapse and splitting of pit borders, previously noted by Bravery (1971, 1972). The orientation of the splits could not be attributed to the microfibrillar orientation of either the S_3 or S_2 and possibly reflected a combined effect of the two layers. Whether the splitting was caused by the stresses set up during the removal of water in specimen preparation or the enzymatic removal of wall material could not be determined.

Hyphae appressed to the cell wall produced very shallow lysis zones either side (figs. 26 - 28). The S_3 microfibrillar orientation was lost (indicating lysis) in these zones, to reveal the underlying steeply angled S_2 wall microfibrils. The warts, however, resisted degradation and could be clearly seen on top of the exposed S_2. The resistance of warts, and the remains of cell membranes, to the effects of brown rot fungi was shown by Liese and Schmid (1962) and Liese (1964). Where lysis had progressed further (figs. 29 and 30) the S_2 exhibited cracking due to the removal of wall material and became spongy in appearance, as noted by Bravery (1971, 1972).

The majority of penetrations between cells were via pits (as in

birch), in each case a very neat small hole had been created in the centre of the torus (figs. 29 and 31). Liese (1970) stated that sapwood bordered pits were easily degraded by brown rot fungi. The presence of cellulose in the thickened torus would result in preferential attack of this region of the pit membrane, with the pectic and lignified compound middle lamella producing the restricted aperture as seen in birch simple cross-field pit penetration.

The only observed bore hole, through the radial wall of an earlywood tracheid (fig. 32), was rather surprising as such walls are reported to be denser (Kisser and Lohwag, 1937) and more heavily lignified (Liese, 1970) than latewood and earlywood tangential walls.

Soft rot

In the attack of birch by Chaetomium globosum colonisation of all the blocks had taken place but there was little evidence of type 1 or type 2 (Corbett, 1965) erosion patterns. However, the few examples of cavities observed (figs. 33 - 40) have added new evidence for the presence and role of proboscis hyphae (Corbett, 1965) in cavity formation. Several cavities contained hyphae with extremely nodular investments and a number of these tapered at their ends into fine proboscis hyphae, with fig. 40 demonstrating the length that these fine structures could attain. A detailed analysis of how this particular cavity developed has been given in Crossley and Levy (1977)(see pages 300 - 303). The proboscis hyphae were smooth and about 0.2µm in diameter. Measurements on proboscis hyphal development previously carried out by Leightley and Eaton (1977) demonstrated that proboscis hyphae increase in diameter, from that given above, to full cavity hyphal dimensions.

The investment to the cavity hyphae was believed to be mucilage. The presence of mucilaginous sheaths on other wood destroying fungi (Schmid and Liese, 1965) and for Chaetomium globosum (Maret, 1972) supported this proposal. From the observations reported in this section it is possible to postulate that mucilage fills the space between hypha and edge of the cavity, which, during drying, has contracted severely producing a nodular appearance. This surface coating material was reported to be lignin residue by Findlay (1970) and Zainal (1975) but their observations on its presence around the hypha and on the lysed wall surface could also be explained by the dehydration of a mucilaginous sheath.

Mucilage was also present around hyphae involved in bore hole formation (figs. 43 - 45) though the variable appearance draws attention to the problems of interpretation in dehydrated and solvent extracted material.

The lack of significant wall degrade of Scots pine by Chaetomium globosum indicated that the culture mechanism and/or the moisture contents of the test blocks were not correct for active attack. The reluctance of soft rot organisms, especially Chaetomium globosum, to degrade softwoods under laboratory conditions has already been noted (Duncan, 1960; Scheffer, 1973) and the results of this S.E.M. study give strong support to this observation. The colonising fungus appeared to behave as a stainer, the capacity to do so was suggested by Corbett (1965), with thick pigmented hyphae colonising the tracheids (fig. 50) producing lateral branches near the ray tissues, where a certain degree of attack could be observed (figs. 48 - 49). Cavities or lumen erosion were not observed.

White rot

Colonisation of birch by Coriolus versicolor was extremely rapid via the vessels (fig. 51), with the ray tissue being heavily attacked even in the early stages of decay. Numerous bore holes were produced in all tissue types but more extensively in the rays, though in the examples of figs. 52 - 54 hyphae could only be seen within the vessels. The degradative effect, with the absence of hyphae, was a common feature of this particular wood - fungus combination and suggested that the colonisation was followed by autolysis as the hyphae grew through the block. The bore holes had frequently become enlarged or coalesced to produce large connections between cell elements, as found by Liese (1970). Attack of the cross-field pits between ray and vessel elements indicated a preferential lysis of the membranes although the secondary thickenings were eventually and totally degraded (figs. 55 - 56).

A useful side effect of the electron beam scanning the material was the generation of lighter zones (halos) around enlarged bore holes and pit apertures. These halos were created by specimen charging effects due to a change in the wall texture allowing electrons to penetrate and become trapped. This demonstrated that wall lysis was still in progress, or that one or more wall components had been removed some distance away from the bore hole margin by a preferential degrade system.

It was extremely difficult to determine whether bore hole formation was through the cell walls or via existing pitting (figs. 64 and 65). In birch attack there appeared to be no correlation between the bore hole pattern and the normal distribution of pits. Wilcox (1968)

indicates that the two are indistinguishable in the later stages of decay. As the final bore hole, even without enlargement, was greater in diameter than normal pitting (see fig. 54) only continuous monitoring of the decay sequence would enable this point to be clarified. Continuous monitoring (Lundstrom, 1970) and time lapse photography (Leightley and Eaton, 1977) of soft rot attack have been successfully achieved and the application of these techniques to white and brown rot would resolve the controversy between bore holes and pit enlargements in hardwoods (see Cowling, 1961; Greaves and Levy, 1965; Wilcox, 1968; Bravery, 1971, 1972 and Jutte and Zabel, 1974).

Fine strands of hyphae or mucilage observed in association with normal colonising hyphae (figs. 60, 66 and 67) require further investigation to determine their nature and function.

Erosion troughs, or channels, of the type observed by Bravery (1971, 1972) in the attack of birch and beech vessels by Coriolus versicolor were not observed in this material. However, a broad shallow form of erosion in two adjacent fibres (figs. 68 - 71) illustrated a number of points of interest. The predominantly steep microfibrillar orientations of the intact fibre wall was covered with amorphous material, presumed to be lignin and hemicelluloses. The fungal ecto-enzymes preferentially removed the amorphous material resulting in a fibrillar appearance to the erosion trough. Preferential degrade of the matrix by white rot was also noted by Wilcox with sweetgum fibres (1968) and Bravery in beech vessels (1971, 1972). The appearance of the channel margins varied with the relationship to the microfibrils, whose angle corresponded to that expected of the S_2. When parallel the result was a sharply defined edge but at right angles

deep indentations in the microfibrillar network were created. Higher magnifications showed the removal of encrusting material had resulted in the clarification of the microfibrils (fig. 70). The removal of the latter produced the erosion channel shapes observed. The effective range of the enzymes was limited to the zones immediately surrounding the hyphae, in contrast to brown rot where the effect was spread throughout the entire cell wall.

The only significant degrade of Scots pine was achieved with Coriolus versicolor. Extensive colonisation of all elements resulted in the formation of channels, bore holes and pit enlargement. The utilisation of bordered and cross-field pits as pathways into adjacent cells was frequently observed (figs. 72 - 74). Pit penetration has been reported to be the feature of early decay stages, with bore holes produced later (see Scheffer, 1936; Cowling, 1961; Schmid and Liese, 1964; Greaves and Levy, 1965; Wilcox, 1968).

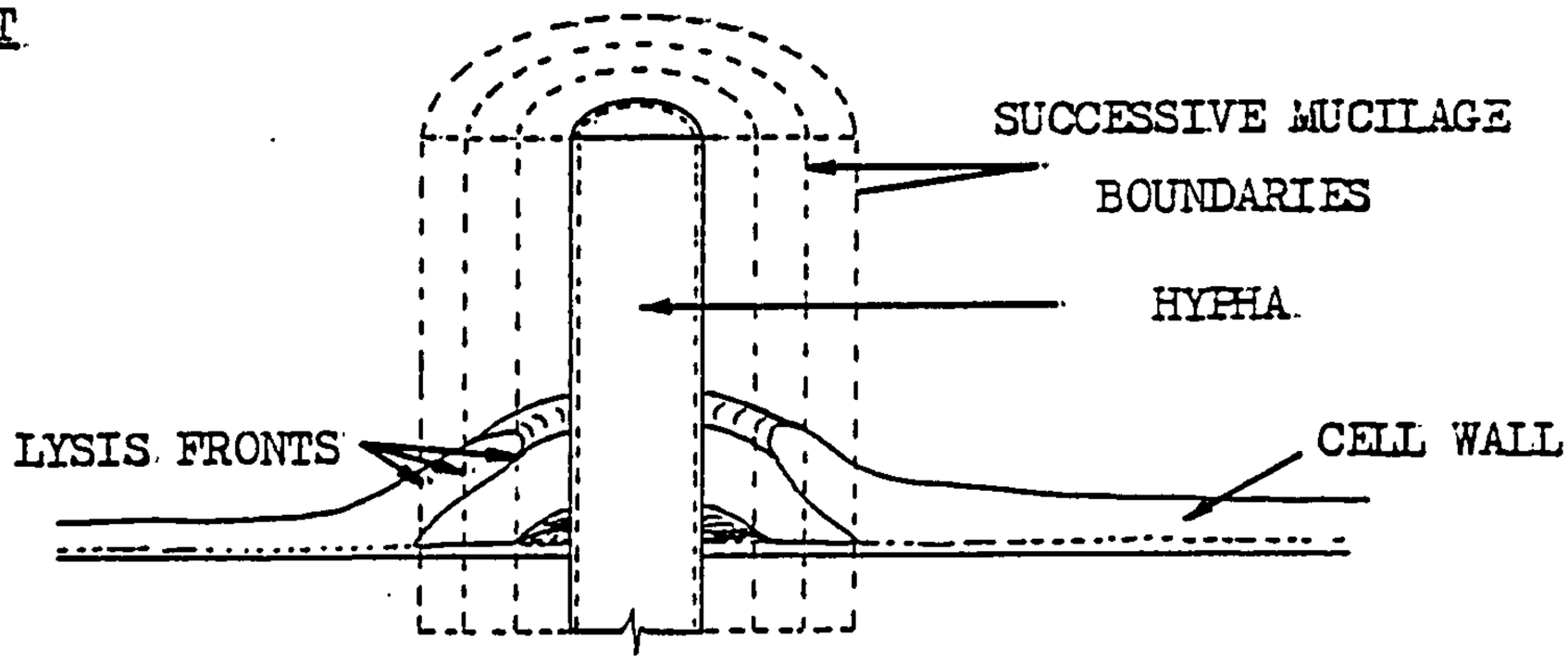
Wall lysis was localised around the causal hypha (Liese, 1970) and the ectoenzymes released removed the warts first (fig. 78), then the S_3, exposing the steeper orientation of the underlying S_2 (figs. 77 - 80, 96 - 101, 103). Frequently the hyphae bore a surface investment, which was believed to be the remains of a mucilaginous sheath (figs. 76 and 77), and this will be discussed in more detail later.

The variable microfibril orientation observed after the removal of the shallow S_3 helices could be explained by the interference in the wall structure by cross-field and bordered pits (figs. 77 and 78). The S_2 showed cracks and openings between the microfibrils due to the preferential removal of the amorphous material, as observed in birch attack. This preference for certain wall components, therefore is a

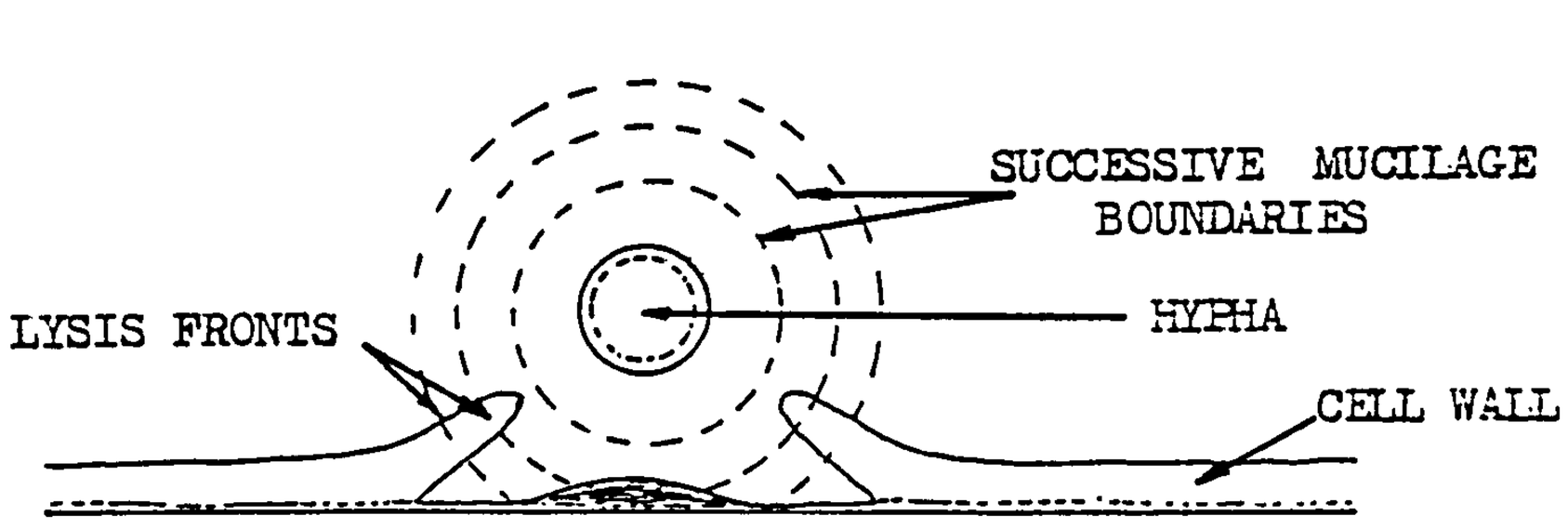
factor determined by the enzyme complement of the fungus, not the difference between woods in their structural and chemical compositions.

Bordered pit penetration was invariably accompanied by aperture enlargement, achieved by a controlled removal of the wall layers from the lip of the border creating a progressively larger pit aperture, finally extending to the diameter of the pit chamber (figs. 81 - 85). However, when pit borders were degraded by overlying hyphae the concentrically orientated border microfibrils were exposed (fig. 86). The presence of a mucilaginous sheath around the fungus would assist in the interpretation of the above feature of pit lysis. Controlled activity of the enzymes within, or attached to, a sheath would produce the observed effects.

HYPHA PENETRATING BORDERED PIT



HYPHA OVERLYING BORDERED PIT



Pit enlargement and bore hole formation varied in appearance from smooth, regular features (figs. 81, 87, 91) to extremely fibrillar degrade (figs. 83, 89). Further examination of the cell elements revealed the fibrillar degrade to be present within earlywood, especially the first formed, tracheids. The observed lytic effects would be produced by the preferential removal of matrix material from the thinly encrusted microfibrils. It would appear from these results that the earlywood tracheids have less encrusting material than the latewood elements, at least in the later formed wall layers.

Detailed examination of channel formation revealed that the first phase was the removal of the warts (figs. 78, 102, 103) with progressive stripping of the amorphous matrix material, clarifying the microfibrils of the S_3 (fig. 103) which were then rapidly removed to produce a general smoothing of the wall surface (fig. 102). Where the hypha had been pulled away a lytic impression (Bravery, 1971, 1972) was left behind (figs. 79, 81, 87, 96, 98, 102). Along the lysis centre line, residues of mucilage could be seen (figs. 81, 96, 98, 102) and in some examples (fig. 102) this region was undegraded. In the majority of specimens the presence of a central ridge was not observed. Progressive lysis of wall material exposed the S_2 and in later stages of decay other wall layers would become exposed.

Mucilage

Examination of the S.E.M. material for the presence of an external sheath resulted in a significant difference being shown between the brown rot and the soft and white rot fungi. The hyphae of Coniophora puteana appeared smooth and free of residues even when actively involved in wall degrade (figs. 104 - 107). However, soft and white rot

hyphae indicated a presence of surface material and residues. In soft rot these were more evident in cavity and decay features, with hyphae possessing nodular investments (figs. 108 - 111). In white rot attack, the involvement of surface material in channel formation and pit enlargement was noted (figs. 112 - 115).

However, these coatings and residues, regarded as being mucilage, could be metabolic products and undegraded wall material and the work of parts II and III in this thesis was aimed at characterising and demonstrating the presence of this material in micromorphological decay features of the rot types, using the transmission electron microscope.

This S.E.M. study showed up the extreme variability of wood itself. Many of the micromorphological decay variations could be explained by the chemistry and architecture of the cell walls. In birch the presence of an S_3 appeared to be variable and an examination of S.E.M. micrographs of birch walls revealed that the characteristic shallow helix of the S_3 was always present in the vessels. In fibres, however, the appearance of the lumen surface ranged from typical S_3 shallow helices with warts to steeply orientated microfibrils (indicating S_2 only). Whether this variation could be linked with seasonal growth patterns was not elucidated in this study. Meier (1955) suggested that the S_3 in birch fibres was either absent or the microfibrillar orientation paralleled that of the S_2, making it indistinguishable. The results of fibre lysis by brown rot indicated that some form of wall layer, internal to the S_2, was present. Possibly this was only a chemical layer showing initial resistance to brown rot but susceptible to white rot.

A warty layer is present in all cells of the tree, in the tracheids, fibres and vessels of softwood and hardwood species, throughout springwood, summerwood, sapwood, heartwwod, the stem, branches and the roots (Liese, 1965b). The visualization of such a layer is due to the presence of small particles trapped between the plasmalemma and tonoplast membranes. If such particles were absent then only the microfibrillar orientation of the underlying wall layer would be visible. The warty layer has been shown to be resistant to the effects of brown rot fungi but susceptible to the white rot and some soft rot fungi (see Liese, 1965b). A warty layer without particles might, therefore, explain the resistance of walls where apparently the S_3 and/or warty layer is absent.

Further work should be carried out on the finer details of birch and the other decay test woods, using S.E.M. and T.E.M. methods before accurate interpretations can be made of observed micromorphological decay features.

The present work has confirmed the findings of Findlay and Levy (1969), Findlay (1970), Bravery (1971) and Zainal (1975) that the S.E.M. is an extremely versatile instrument for the study of wood and its decay. The relatively simple preparation procedures, even with Critical Point Drying or freeze drying, enable results to be obtained quickly and effectively. The high depth of field, surface feature images produced by the instrument are very easy to interpret and, with the improved resolutions of the modern instruments, then biological materials can be satisfactorily examined up to magnifications of 20,000 times (above which the variable stability of the specimen becomes limiting). Although a different type of image is generated, the S.E.M. provides an important magnification link between light and transmission electron microscopes.

PART II

TRANSMISSION ELECTRON MICROSCOPY OF MUCILAGE

1. INTRODUCTION

The observations with the Scanning Electron Microscope, (S.E.M.) (Part I), suggested that some form of investment was present around the hyphae of the Soft rot and White rot fungi, but was not associated with hyphae of the Brown rot fungus. This material was thought to be mucilage and consideration was given to its possible role in the decay of wood. It seemed possible that its presence could be associated with the extracellular enzyme activity of the fungi and might be correlated with the characteristic lysis patterns observed for the three main types of wood decay.

To characterise the material and determine its exact location with respect to both fungus and decayed wood cell wall, the high magnifications possible with ultrathin sections examined in the Transmission Electron Microscope (T.E.M.) was required.

A literature search was made to determine the available information on the chemical, physical or visual structures and preparation of mucilages. Bacterial, algal and some fungal extracellular coatings have been examined to a limited extent and cytochemical analyses suggest that the sheathing material might be pectic acids and acid mucopolysaccharides for Anabaena sp. (Leak 1967) and, more specifically, glucans in the fungal types.

The fungal cell wall is 80 - 90% polysaccharides with most of the remainder consisting of protein and lipid. The polysaccharides are built from a variety of sugars resulting in the synthesis of cellulose, glycogen, glucan, chitin, mannan and galactan, (Bartnicki-Garcia 1968). Fungal cell wall research has shown a very strong correlation between chemical composition and major taxonomic groupings

based on morphological features. As such the taxonomy of the fungi can be divided into eight chemical orders with the most numerous category, harbouring all mycelial forms of the Ascomycetes, Basidiomycetes and Deuteromycetes, being the chitin - glucan wall type, (Bartnicki-Garcia 1968). Further division of this group is possible by the identification of minor monosaccharides within the wall; xylose (Basidiomycetes) and D-galactosamine (Ascomycetes).

The structural chemistry of chitin and its role in fungal walls is fairly well established but the second component, ambiguously termed glucan, covers a range of chemically separate wall components. The division of the water insoluble glucans is based on their solubility in alkali giving the soluble S-glucans and the insoluble R-glucans, (Wessels et al. 1972). The S-glucan from Schizophyllum commune (Wessels et al. 1972) was chemically identified as α 1,3 linked D-glucosyl units whereas the R-glucan contained both β 1,3 and β 1,6 linkages of D-glucosyl units. The Basidiomycetes contain both the 'S' and 'R' glucans in their wall layering with the Ascomycetes and Deuteromycetes having only 'R' glucans, possibly with an associated glycoprotein reticulum, (Hunsley and Burnett 1970).

Wessels et al. (1972) also identified a mucilage present on the outer surface of the wall of S. commune and this consisted of chains of 1,3 linked β D-glucosyl units to which single β D-glucosyl units were attached by 1,6 linkage to every fourth unit, on average, in the chain. The chemical structure of this mucilage resembled that of the viscous extracellular products of Sclerotium rolfsii and Claviceps spp. (Buck et al. 1967), Plectonia occidentalis

(Davis et al. 1965) and Pullullaria pullulans (Bouveng et al. 1963). It has therefore been established that certain fungi produce an extracellular mucilaginous coating distinct from the other wall components and that this material is a β 1,3, β 1,6 linked glucan with a fairly linear structural arrangement.

The presence of mucilage or slime on wood inhabiting fungi has been shown for Chaetomium globosum (Maret 1972), Polyporus versicolor (Liese and Schmid 1962), Aureobasidium pullulans, Ceratocystis pilifera, Scopularia phycomyces (Schmid and Liese 1965), Hypholoma fasciculare and Paecilomyces sp. (Schmid 1966).

A study of the hyphal wall components of Chaetomium globosum by Maret (1972) agreed with the presence of β 1,3 and β 1,6 linked glucans. His less detailed work on the capsule material indicated that glucans with β 1,3 linkages were present together with galacto-glucomannans and a protein fraction.

The visual appearance of the mucilage ranged from smooth and amorphous through granular to fibrillar and filamentous. Schmid (1966) attributed this variability to the physio-chemical consistency of the slime, the drying procedures employed during preparation of the replicas and the applied fixatives. Although the mucilage of wood inhabiting fungi had been prepared for electron microscopical examination the majority of the examples were of freeze etched and shadowed replicas. Examination using ultrathin sections after fixation with $KMnO_4$ - OsO_4 and glutaraldehyde - OsO_4 (Schmid 1966) have not produced very satisfactory representations of this extremely hydrated (90 - 95%) polysaccharide structure.

Work on other organisms, especially bacteria, has resulted in

a number of experimental procedures being adapted to try to detail extracellular mucilages and slimes.

In 1964 Luft used ruthenium red to stain acid mucopolysaccharides in animal tissues for examination by electron microscopy and this fixative - stain was later used by Pate and Ordal (1967) to demonstrate peripheral fibrils on the bacterium Chondrococcus columnaris. By modifying the procedures of Pate and Ordal (1967), Jones, Roth and Sanders (1969) were able to visualise the extracellular fibres in aquatic slime layers produced by bacteria. They also showed the requirement of ruthenium red in conjunction with OsO_4 to demonstrate the polysaccharide matrix. Neither fixative employed on its own revealed the mucilage layer.

The often drastic removal of water during dehydration with ethanol (Fink 1960) stimulated the development of new dehydration schedules using Epon 812, miscible with water, 40% by volume, (Craig et al. 1962) and a water soluble resin, Durcupan (Staubli 1963). These methods were aimed at preserving delicate cell structures and reducing lipid extraction due to solvent dehydration.

Springer and Roth (1973) applied the techniques of Luft (1961), Craig et al. (1962) and Staubli (1963) in a study of the bacteria Diplococcus pneumoniae and Klebsiella pneumoniae with the use of ruthenium red as the fixative stain. Their results indicated that the use of Epon 812 resulted in slightly better preservation of the polysaccharide capsules than with alcohol or Durcupan dehydrations, which were very similar to one another.

In view of the comments on alcohol dehydration and the results obtained by previous workers using this method on wood inhabiting

fungi, (admittedly without ruthenium red fixation), the techniques of Craig et al. (1962) and Staubli (1963) were applied to the slime layer thought to be surrounding the fungi in this study.

To enable a clearer evaluation of the techniques, the methods were applied to a known source of mucilage, being the investment of the blastospores produced by the Deuteromycete Rhinocladiella mansonii. As mentioned earlier, this fungus belongs to the same wall chemical group as the Basidiomycetes and Ascomycete used in this study but shows a closer relationship with the latter on the basis of wall architecture.

Satisfactory results would allow the application of the new methods to the test fungi in the wood decay situation.

2. MATERIALS AND METHODS

2.1 Culture growth and specimen selection

The culture organism selected as being a suitable test fungus was;

Rhinocladiella mansonii Nannf.

due to the prolific production of mucilage coated blastospores. Cultures were grown on 2% malt - 2% agar at 22°C and allowed to develop until the blastospore stage had been formed in the colony. This was recognisable as a ring of glistening mucilage on the hyphal network. Samples of the hyphal growth were picked out, using fine forceps and a mounted needle, from two areas.

(i) small spherical colony growths of "dry" hyphae

(ii) regions of the blastospore ring which were extremely mucilaginous.

About twenty examples of each type of hypha were selected and immediately immersed into the fixative solution contained in four glass stain blocks, ten of each example per dish.

2.2 Fixation

The fixative used was that described by Luft (1961) as being specific for acid mucopolysaccharides and employed ruthenium red in conjunction with glutaraldehyde and osmium tetroxide in a double fixation process.

1st fixation stage; used a 1:1:1 mixture of

Glutaraldehyde	- 3.6% aqueous solution
Sodium cacodylate buffer	- 0.6M, pH 7.2
Ruthenium red	- 1500ppm in distilled water

giving working strengths of;

Glutaraldehyde	1.2%
Sodium cacodylate	0.2M
Ruthenium red	500ppm

The specimens were left immersed in the first fixative stage for one hour at room temperature (R/T).

Between the first and the second fixation stages the specimens had to be thoroughly washed to remove all traces of unbound glutaraldehyde because osmium tetroxide was employed in the second stage and would react with any free glutaraldehyde. This was achieved with 0.2M sodium cacodylate buffer at R/T for ten minutes for each of three washings. The exchange of the fluids was carried out using a fine pasteur pipette taking great care not to disturb the specimens.

It should be noted here that the handling of fixatives, buffers and resins was carried out with caution because of their hazardous chemical natures utilising fume cupboards and closed dessicators, ($4^{o}C$ stages in the fridge), at all times. Sodium cacodylate buffer contains arsenic and is a grade 1 poison. Two winchesters were used for the disposal of the waste chemicals. One for the fixatives and buffers and one for the waste resins; when full these could then be disposed of correctly. Methanol was added to the fixative winchester to absorb the unbound osmium tetroxide rendering it harmless.

2nd fixation stage; used a 1:1:1 mixture of

Ruthenium red	- 1500ppm in distilled water
Sodium cacodylate	- 0.6M, pH 7.2
Osmium tetroxide	- 5% in distilled water

for a period of three hours at R/T in a fume cupboard, followed by three washes of 0.2M sodium cacodylate, detailed previously.

2.3 Dehydration

This followed two methods, the first by Staubli (1963) using the water soluble resin Durcupan and the second by Craig et al. (1962) using Epon 812 / buffer mixtures. The exact procedures given by the above authors were adjusted slightly because of the nature of the specimens but the underlying methods were the same. Of the two replicate dishes of specimens, one was taken through the Durcupan method, the other through the epon/buffer system.

The specimens were treated with increasing concentrations of the dehydrating media with all stages being at 4°C for Durcupan and at R/T for epon/buffer as outlined below.

Durcupan at 4°C

25% Durcupan / 75% 0.2M buffer for 45 mins.

50% Durcupan / 50% 0.2M buffer for 45 mins.

75% Durcupan / 25% 0.2M buffer for 45 mins.

100% Durcupan for 45 mins.

100% Durcupan for 90 mins.

Epon 812 at R/T

25% Epon 812 / 75% 0.2M buffer for 90 mins.

100% Epon 812 for 90 mins.

100% Epon 812 for 90 mins.

2.4 Infiltration

This stage continued the two methods of dehydration with the Durcupan treatment being infiltrated with Araldite and the Epon method with Epon 812.

The constituent proportions of the infiltrating and embedding resins were:-

Araldite mix I for infiltration only

Araldite AM resin	-	20gms
964B hardener	-	20gms

Araldite mix II for final infiltration and embedding

Araldite AM resin	-	30gms
964B hardener	-	30gms
964C accelerator	-	1.2gms

For Epon 812 one mix was used for both infiltration and embedding, after Zainal (1975)

Epon 812 mix for infiltration and embedding

Epon 812 resin	-	57.5gms
DDSA hardener	-	30.9gms
MNA hardener	-	28.5gms
BDMA accelerator	-	1.4gms

It should be noted that whereas Staubli (1963) gave components as volumetric measures these chemicals can only be satisfactorily and accurately dispensed by gravimetric methods and as such the measurements given were converted to grams on a 1:1 basis, (this is not strictly accurate as explained in part III).

Infiltration schedule for Durcupan/Araldite method

25% Araldite mix I / 75% Durcupan	at R/T for 90 mins.
50% Araldite mix I / 50% Durcupan	at R/T for 90 mins.
75% Araldite mix I / 25% Durcupan	at R/T for 90 mins.
100% Araldite mix I	at R/T overnight
100% Araldite mix II	at 50°C for 105 mins.
100% Araldite mix II	at 50°C for 105 mins.

Infiltration schedule for Epon method

Epon 812 full mix at R/T for 90 mins.

Epon 812 full mix at R/T for 90 mins.

Epon 812 full mix at R/T for 90 mins.

2.5 Embedding

Four flat polythene dishes, 40mm in diameter x 5mm deep, were used for the specimen embedding, two containing Araldite mix II and two Epon 812 full mix. Into the centre of each dish was placed a typed label coding the dehydration method and the hyphal form. The specimens were gently transferred from the stain blocks and arranged, equally spaced, within their respective embedding dishes ready for polymerization as below:-

Araldite mix II dishes at 50°C for 48 hrs.

Epon 812 dishes at 55°C for 24 hrs.

The stain blocks were wiped clean of old resin, using tissues (which were later polymerized in foil) and then thoroughly washed with hot soapy water.

2.6 Mounting, trimming and sectioning

These were carried out as detailed by Zainal (1975). Sections, 70 - 150nm, silver - gold (Peachey 1958), were cut on a Reichert OmU2 ultramicrotome using a diamond knife, with water as the collecting fluid and were picked up on 100 mesh copper/rhodium plated grids. Sections were double stained in uranyl acetate for 30 minutes at 60°C, and lead citrate (Reynolds 1963) for 15 minutes at R/T. Examinations were made on AEI EM6B and Philips 301 electron microscopes at an accelerating voltage of 60 KV. Micrographs were taken on Agfa F071p film, developed in Kodak D19 and fixed in Ilford Ilfofix.

3. RESULTS

An initial examination of a block of each preparation type revealed that the 'dry' hyphae of the colony mycelium bore no significant layer of extracellular material and therefore have not been included here. However, the blastospore material in both Durcupan and Epon preparations exhibited the presence of a matrix between the spores. Difficulties were experienced when sectioning the Epon dehydrated material and this was reflected in the section quality, figures 5 - 8, and possible reasons for this are discussed later.

The general appearance of the spores and the matrix was very similar in both preparations and this probably indicated comparable fixation of the specimens. Some of the spores were not properly infiltrated resulting in tearing of the contents, especially under the electron beam, see figure 1. At low magnification the two preparations looked very similar, compare figures 1 and 5. The matrix appeared to be comprised of short interconnecting filaments with occasional denser bodies evident, figure 2. There was a certain degree of flow in the matrix material resulting in pulling away from the spores, figures 1 and 6.

At higher magnifications, however, the quality of the two methods began to differ. Durcupan preparations continued to detail the short filaments and their obvious origin from the spore wall, figures 3 and 4. The Epon material, however, appeared extremely granular and although filaments could be interpreted from the matrix, figure 7, the details, figure 8, became progressively lost. Comparison between figures 4 and 8 demonstrated this point very clearly.

Blastospores of Rhinocladiella mansonii, Durcupan dehydration

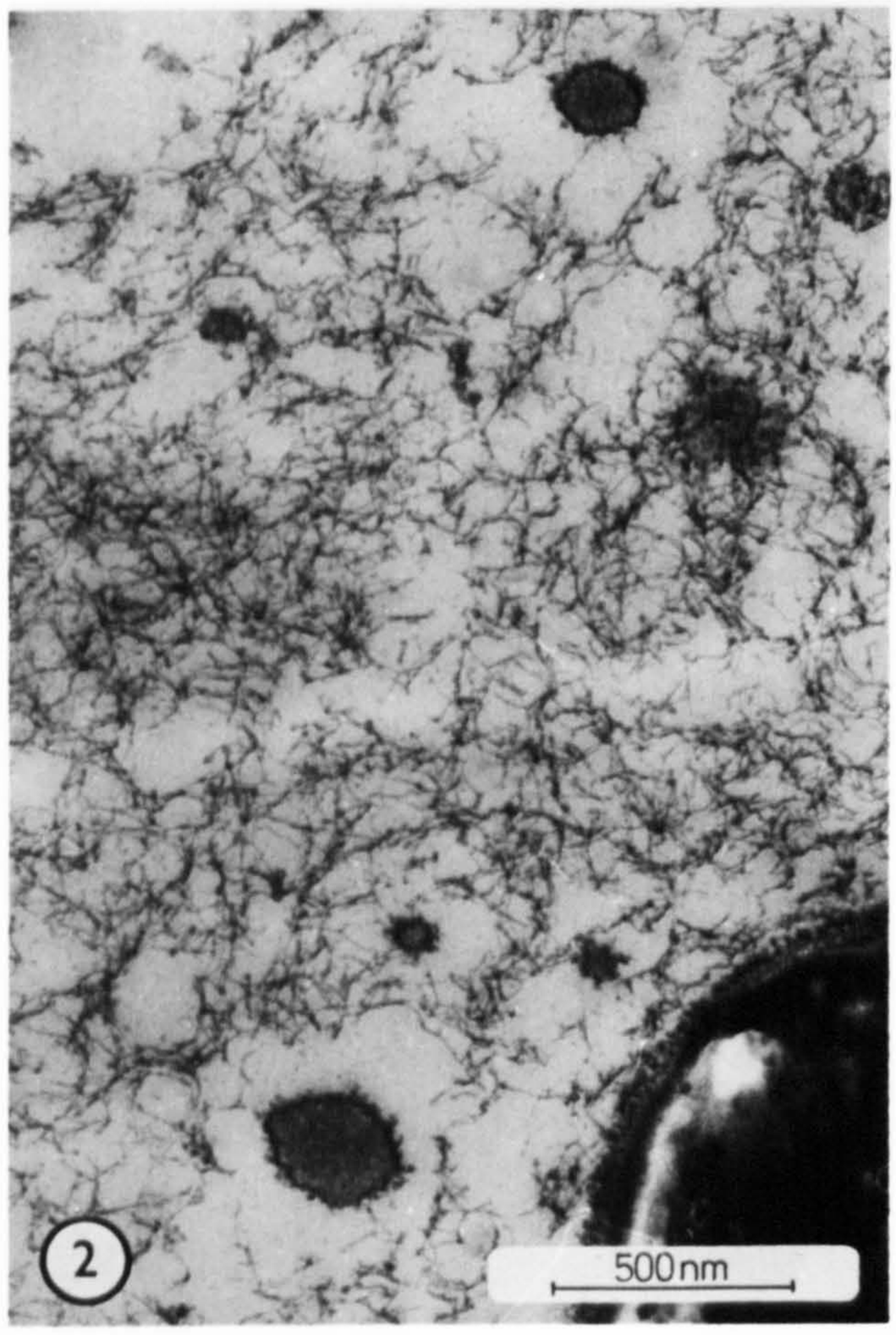
Fig. 1 (x 22150) is a low magnification to show the inter-relationship between the polysaccharide matrix and the blastospores (note these are sectioned in random planes). The pulling away of the matrix from the spore wall can be seen together with the denser bodies within the matrix.

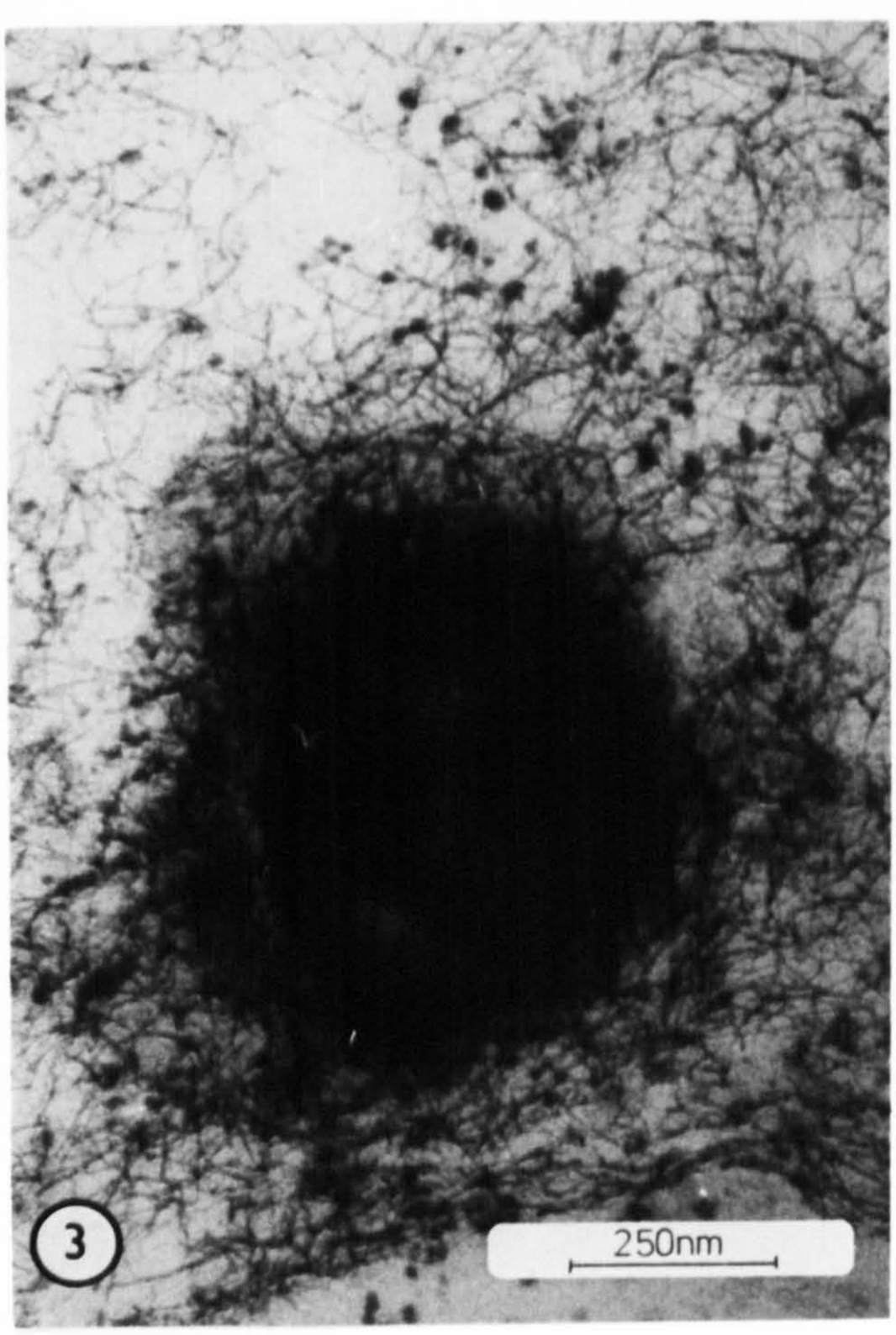
Fig. 2 (x 44300) shows higher magnification detail of the matrix and included denser bodies. Note that there appears to be collapse of the matrix structure around the denser bodies that have a darker margin. A spore in section can be seen lower right.

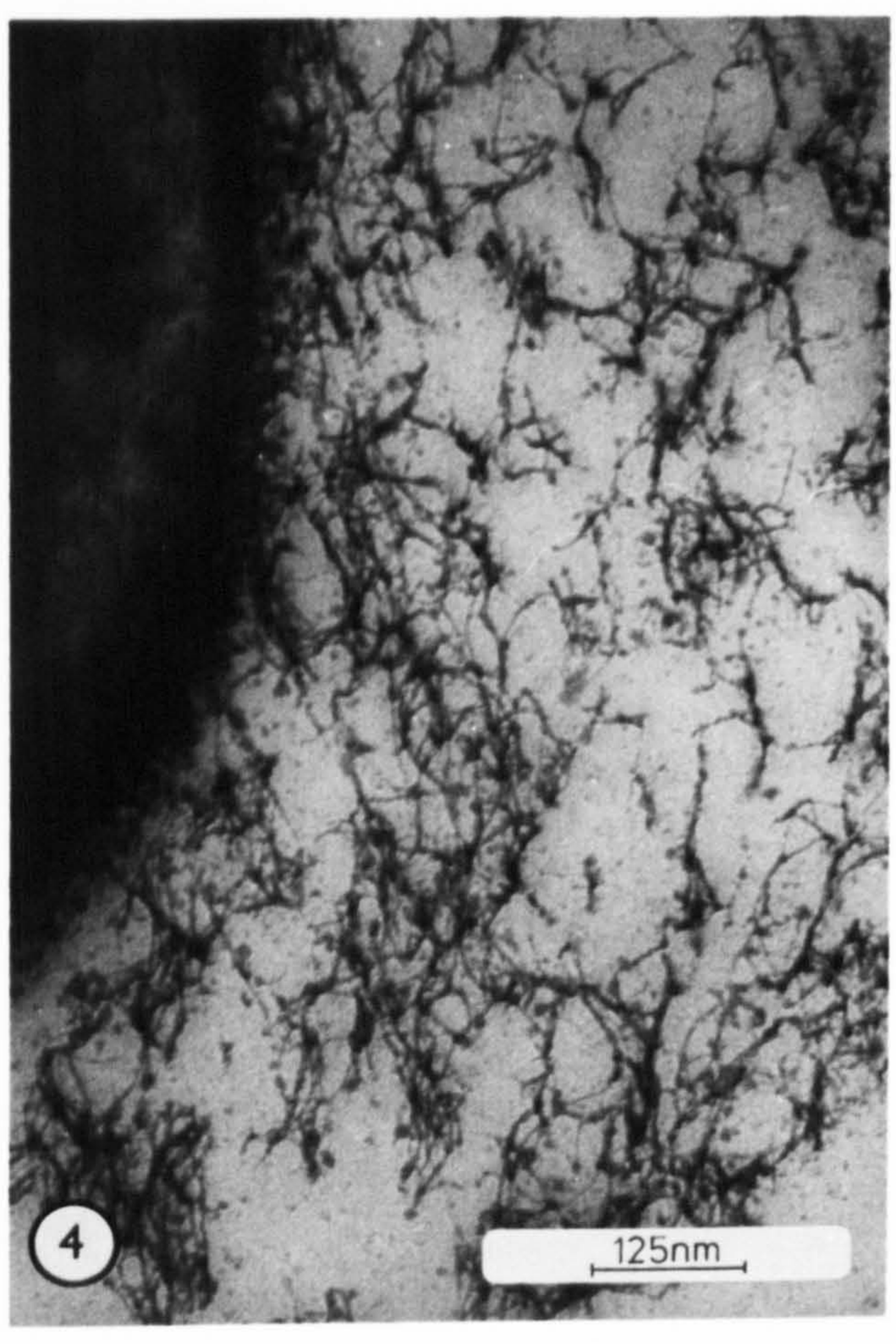
Fig. 3 (x 76450) is a section across the top of a spore showing the continuity between the spore wall and the matrix. The very small dark bodies are probably residues of stain as they can also be seen in the clear region at the bottom of the micrograph.

Fig. 4 (x 112750) is a high magnification of the matrix - spore wall connection. Membranes can be seen within the darker stained spore and the wall can be seen to become progressively looser in structure towards the outside producing the more open framework of the mucilaginous matrix.


1
500nm


2
500nm

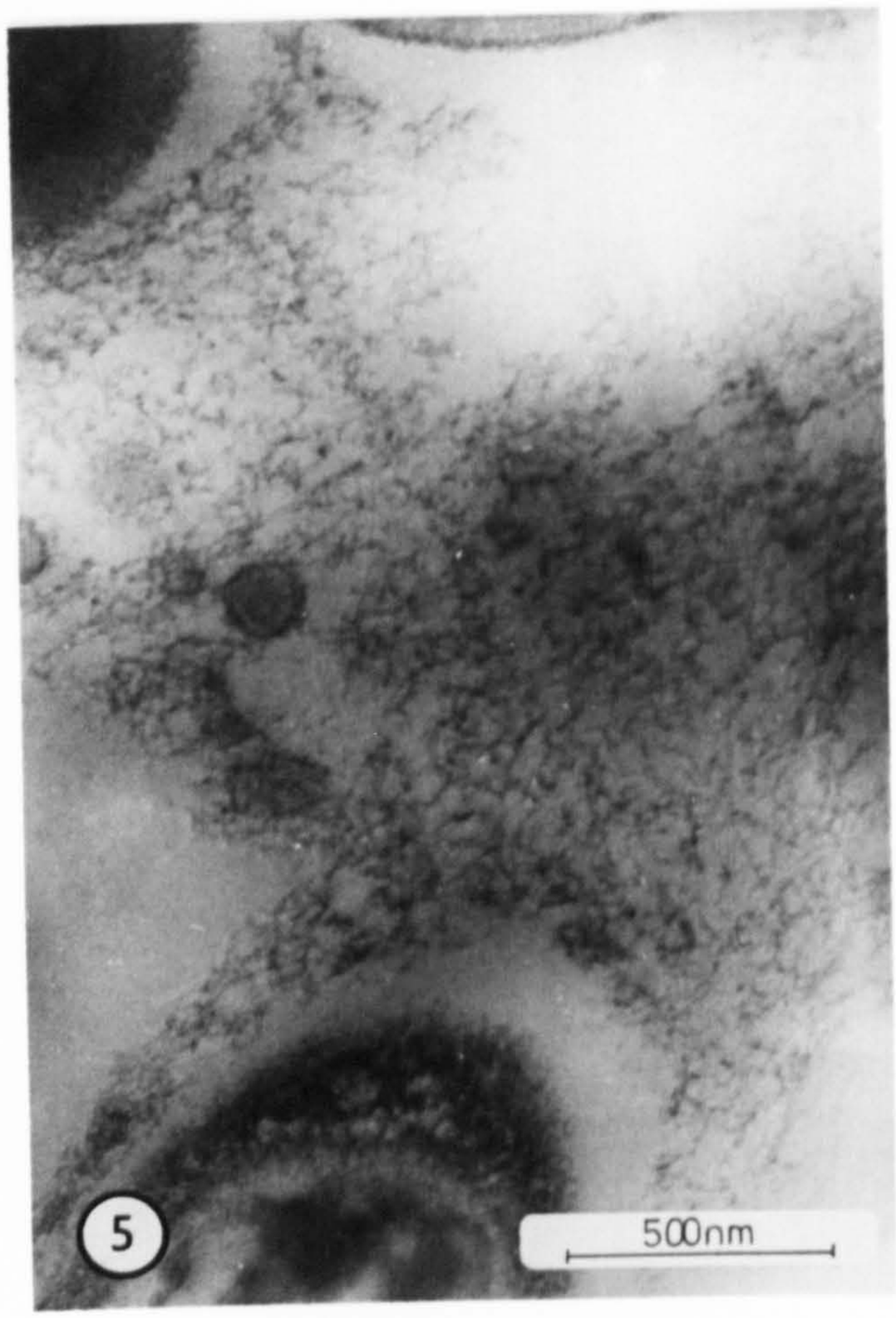

3
250nm


4
125nm

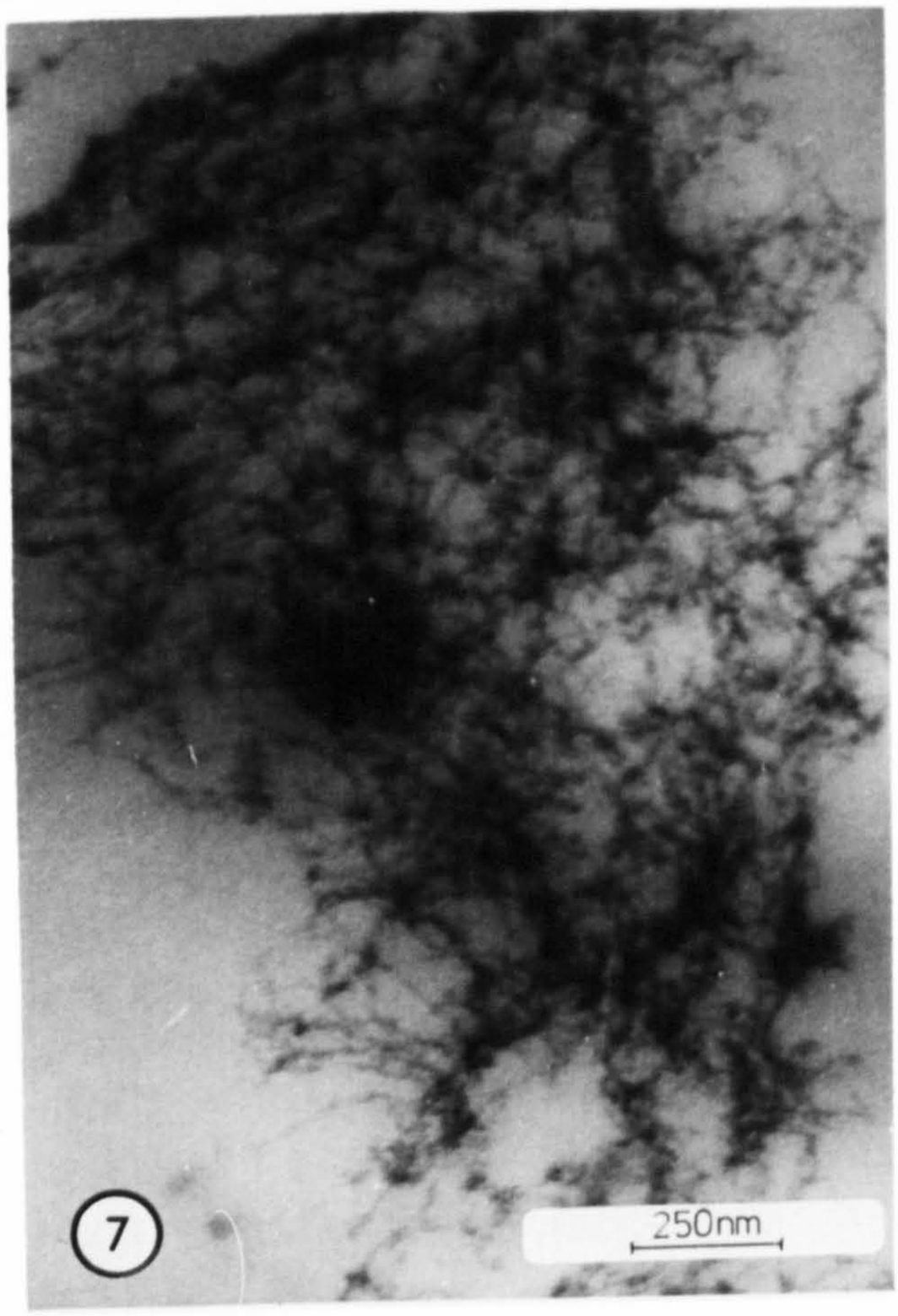
Blastospores of Rhinocladiella mansonii, Epon 812 dehydration

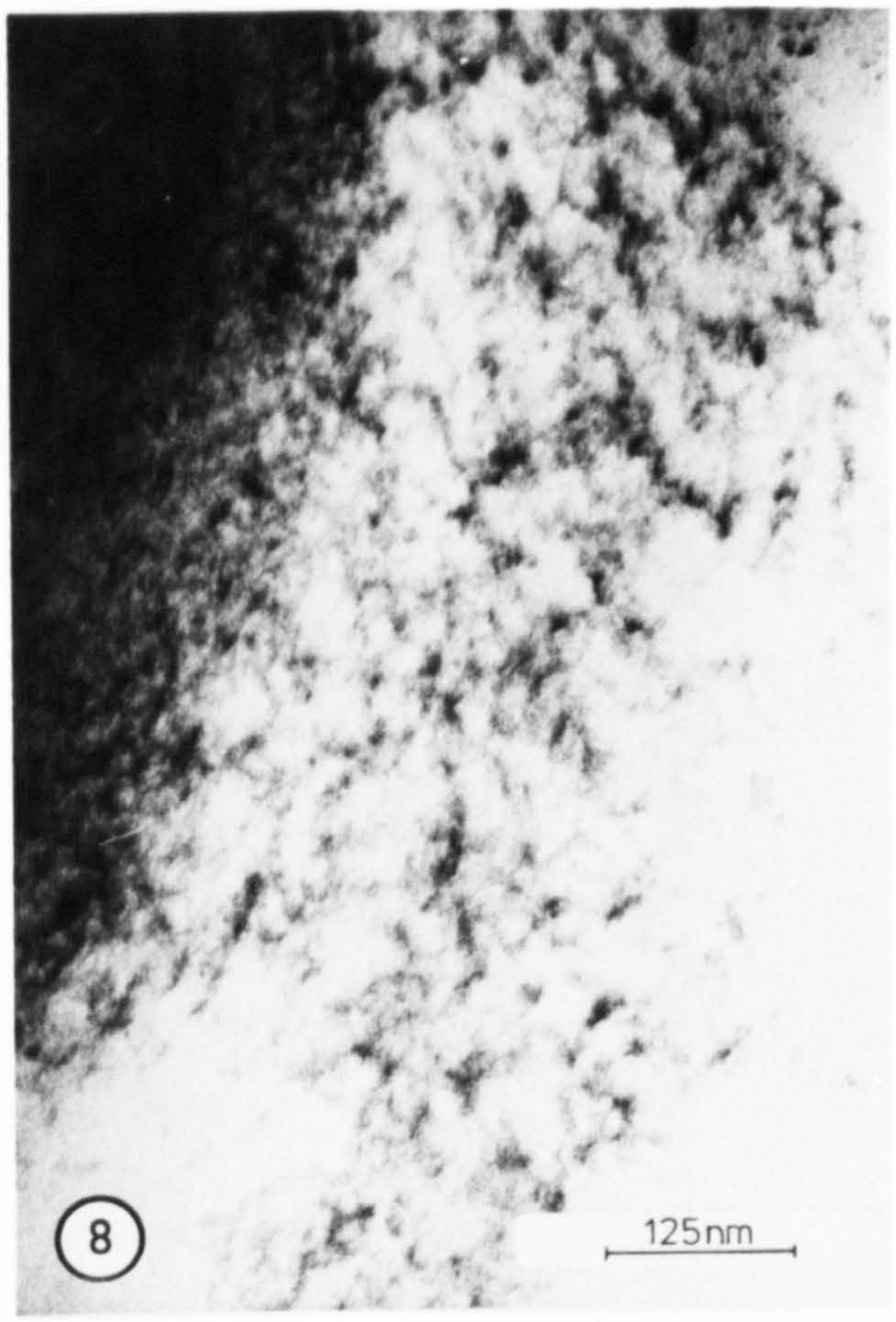
Fig. 5 (x 49600) is comparable with fig. 2 and shows spores, the less pronouced matrix material again containing denser bodies, together with the flow of the mucilage away from the spore walls.

Figs. 6 (x 58800), 7 (x 99500) and 8 (x 133750) demonstrate the matrix material at progressively higher magnifications. Although structure is present in the matrix the definition is poor. Fig. 8 shows the extremely grainy appearance of the wall - matrix details and in comparison with fig. 4 presents a poorer image of the mucilage.


5
500nm


6
250nm


7
250nm


8
125nm

4. DISCUSSION

The results have shown that both preparation methods were able to demonstrate the presence of a matrix between the blastospores of Rhinocladiella mansonii.

The specimen blocks produced using the Durcupan dehydration were very easy to section and resulted in good sections which revealed the finer details of the matrix even at very high magnifications. Some of the problems with incorrectly embedded spores could be overcome with longer infiltration periods.

The poorer results for the Epon 812 method could have been caused by incomplete dehydration of the specimens. This would have led to uneven polymerization resulting in the sectioning problems encountered. At higher magnifications the uneven sections exhibited an extremely grainy resin background and the matrix details were poorly defined.

The polysaccharide details, revealed by the ruthenium red - OsO_4 fixation, resulted in the matrix being an interconnecting reticulum of short densely stained filaments. Figures 3 and 4 have clearly shown that the matrix has a structural connection to the spore wall and possibly, therefore, the production of mucilage from individual spores results in their coatings coalescing as a single enveloping matrix to the spore mass. The presence of granular bodies within the matrix is unexplained but the variation in appearance could be due to the collapse of the surrounding network resulting in darker margins to some of the bodies.

Although there was very little similarity between the mucilage demonstrated for R. mansonii and that previously shown for other wood

inhabiting fungal slimes this could be explained by the fixation procedures and specimen dehydration, (Schmid 1966).

There was a strong similarity between the structure of this fungal mucilage, as revealed by Durcupan dehydration, and the structure of a slime produced by aquatic bacteria examined by Jones, Roth and Sanders (1969). The bacterial slime was dehydrated using ethanol and as such it would appear that the structures demonstrated by the slime and the R. mansonni mucilage were a result of the ruthenium red fixation procedure employed by both methods. However, although comparable results can be obtained by the cheaper, standard, ethanol dehydration procedures the possible excessive specimen shrinkage and lipid extraction by ethanol (Fink 1960) would favour the Durcupan dehydration for this type of preparation.

No cytochemical analyses were carried out on this mucilage to determine precisely its structure and chemistry but the demonstration of its presence in a known situation enables the preparation method to be applied to the examination of the three types of wood degrade.

PART III

TRANSMISSION ELECTRON MICROSCOPY OF WOOD DECAY

1. INTRODUCTION

There are a number of specimen preparation techniques available for the examination of materials in the Transmission Electron Microscope (T.E.M.). In the study of wood the following approaches have been documented;

(i) Replicas

(ii) Sections with the resin removed

(iii) Cryosectioning

(iv) Ultrathin sections.

These procedures were evaluated to select a suitable technique for this study.

1.1 Replicas (Cote et al (1964), Wardrop (1964), Harada (1965), Liese (1965b and c), Frey-Wyssling (1968), Preston (1974))

This method results in the production of a metal shadowed carbon replica of the specimen surface and was employed extensively in the earlier work on wood as the technology for reliable, precision ultramicrotomes had not then been developed. By pretreating the cell walls, to remove surface debris, microfibrillar details can be very clearly shown at high magnifications. The very nature of the preparation limits the application to surface features only and would, therefore, yield only limited information in a study of enzymic effects of fungi on wood cell walls. The application of the S.E.M. has virtually superceded all replica work except those of very high magnification studies.

1.2 Sections with the embedding resin removed (Wardrop (1964))

This interesting technique utilises relatively thick sections of wood elements. The chemical removal of the embedding medium and subsequent metal shadowing produces a three dimensional visualisation of the section. This enables examination of both internal and surface wall details to be made. However, the extra chemical treatment needed to achieve this effect must raise questions as to the reliability of the features observed.

1.3 Cryosectioning (Fengel and Stoll (1975), Stoll and Fengel (1977))

The application of this more recent preparation method to wood has been very limited even though the cutting of ultrathin sections without any chemical processing is extremely desirable. This restricted use reflects the speciality of this technique requiring great skill on behalf of the ultramicrotomist. To the authors' knowledge there have been no documented methods using this technique to examine decayed wood. Perhaps the tendency of fungal hyphae and loosened material to drop out of prepared sections has precluded its use in this work.

1.4 Ultrathin sections (Meier (1955), Liese (1965b and 1965c), Findlay (1970), Chou (1971), Zainal (1975))

Preparation of ultrathin sections of embedded wood, both sound and decayed, has been used successfully by a number of workers. This technique allows examination of cell wall details, variation in wall density and organisation due to fungal attack and the hyphal cytology, to be carried out in one section. Serial sections enable three dimensional constructions to be made of features examined. With the

introduction of diamond knives into ultramicrotomy the production of thin serial sections of hard dense material, such as wood, was made very much easier. The most important factor in applying this technique is the knowledge of the plane of section necessary for accurate interpretations to be made of the features present.

On the basis of the above, the technique of cutting ultrathin sections was selected as being the most applicable to this study and an analysis of the problems and desirable preparative features was required to determine how far current techniques achieve these aims.

1.5 Problems and requirements of preparative techniques

Some of the problem areas in preparing wood for ultramicrotomy have been outlined by Fengel (1967). The natural variation in structure and chemistry of a single wood cell element together with the density and thickness that the cell walls can achieve make wood one of the most difficult materials to prepare for ultramicrotomy. This variability is increased with a range of tissue types, for example, fibres, parenchyma, tracheids and vessels being found within different regions of the wood structure according to the species type. In this study two woods, birch (Betula sp.) and Scots pine (Pinus sylvestris) were examined after decay by each of three types of wood destroying fungus. These wood tissues, colonised by the relatively soft, more delicate fungal hyphae, define the condition of the specimen under examination and the preparative techniques, therefore, should be aimed at preserving this situation as accurately as possible.

The actual area of a specimen examined in the electron micro-

scope is limited by the maximum block face area, recommended for decayed wood as being approximately 0.2mm x 0.2mm. The specimen format should be such that the desired area to be examined can be orientated and trimmed so as to be presented in the correct plane to the knife of the ultramicrotome. For full interpretation of features examined, sections of the material in the three planes x, y, and z is extremely advantageous.

Determination of the specimen format should be based on a number of interrelating factors.

(i) The specimen should be thin in at least one dimension to allow rapid penetration of the fixation and preparative chemicals.

(ii) Specimens should be such that once satisfactorily embedded they contain enough material, with retrimming if necessary, to avoid excessive replication.

(iii) Ideally the format should be small enough to fit within the face area of a trimmed block.

(iv) The specimen should be capable of accurate orientation with regard to the plane of the ultramicrotome knife.

Other desirable features of a preparative technique include, that the specimen handling , which will produce artefacts, should be reduced to a minimum and that the embedded specimen, presented as a block, has the maximum support by a resin of equal hardness to the material.

The development of a preparation technique, therefore, was the result of numerous trials and evaluations, which are covered in the following section.

2. DEVELOPMENT AND ANALYSIS OF METHODS

2.1 Selection of specimen format

The format requiring an easily infiltrated specimen could be answered in one of three ways.

(i) Thin in one dimension resulting in a sheet-like specimen as employed by Fengel (1967).

(ii) Thin in two dimensions producing a thin stick-like specimen..

(iii) Thin in three dimensions resulting in small cuboidal specimens such as those used by Zainal (1975).

Evaluation of these three approaches must consider specimen orientation, ease of trimming and the relative information obtainable from a single specimen.. The embedding of sheet-like specimens was rejected due to the inefficient wastage of material and effort as a large proportion of the specimen is "cut out" during the trimming of the block.. Specimens that are small enough to fit within the block face have a double advantage in that a) the specimen would not require trimming away and therefore be wasted and b) all trimming operations would be through pure resin. It has been the authors' experience that in trimming through embedded wood "furring" of the wood cell walls frequently occurs, especially in longitudinal cuts. This was due to the microfibrils being pulled out of the resin by the blade in the walls where they are orientated "against the grain" and was always encountered to a varying degree in all but the perfect match between specimen and resin. These "furred" surfaces caused severe problems during sectioning. Both stick and cuboidal specimens could be cut to fit within the face area of the block but many more rep-

licates of the latter would have to be prepared to contain the same volume of material as a single stick specimen.

On the basis of the above criteria, the small stick-like specimen was selected as being the most desirable specimen format, with the ultrathin section plane being parallel to the small cross sectional face of the specimen. Therefore, to examine material in the three planes, transverse, tangential and radial, simply required the specimens to be cut in such a way that these planes are represented by the smallest faces of the specimen.

2.2 Specimen format - orientation and preparation

Specimen orientation could be approached in two ways;

(i) The specimens can be cut randomly, embedded randomly or roughly orientated in flat dishes then cut out and orientated by eye when positioning and glueing onto perspex dowel (Zainal (1975)). The reference point to which the specimen is aligned being the top of the dowel, representing the section plane at right angles to the dowel axis.

(ii) Alternatively the specimens could be cut very accurately in the desired orientation and then embedded such that they aligned up with a known reference, e.g. the block axis or the section plane at right angles to it.

To orientate specimens cut from flat embedding dishes requires the formation of a glue line between specimen and supporting dowel. This represents a line of weakness which during sectioning of the wood might allow the set up of vibrations resulting in section chatter. If this method is not used, then the alternative has its own set of

problems relating to the orientation of the specimen within the resin block. The first requirement being some method of cutting accurately orientated sticks of wood with cross-sectional dimensions of 150μm x 150μm and of a suitable length, (2 - 2.5mm is suggested). These sticks being such that transverse, tangential and radial sections can be cut on the ultramicrotome.

Using the method detailed in Part I sections 3.1 to 3.3.1, accurately orientated sections could be produced from decayed wood blocks. By cutting sections 150μm thick then one of the three specimen dimensions was achieved and from one decayed block both tangential and radial 'macro' sections could be cut. In theory these could then be further subdivided to produce microspecimens of the desired orientation, see fig. A. The practical problem was to find a device capable of making this further subdivision. In other words a piece of apparatus which having made one cut could be moved on a selected distance, in this case 150μm and the cut repeated. To cover the planes of the microspecimen, the cutting mechanism or the specimen should be able to turn through at least 90°.

By utilising the following pieces of equipment such a device was constructed:-

Stereo binocular microscope

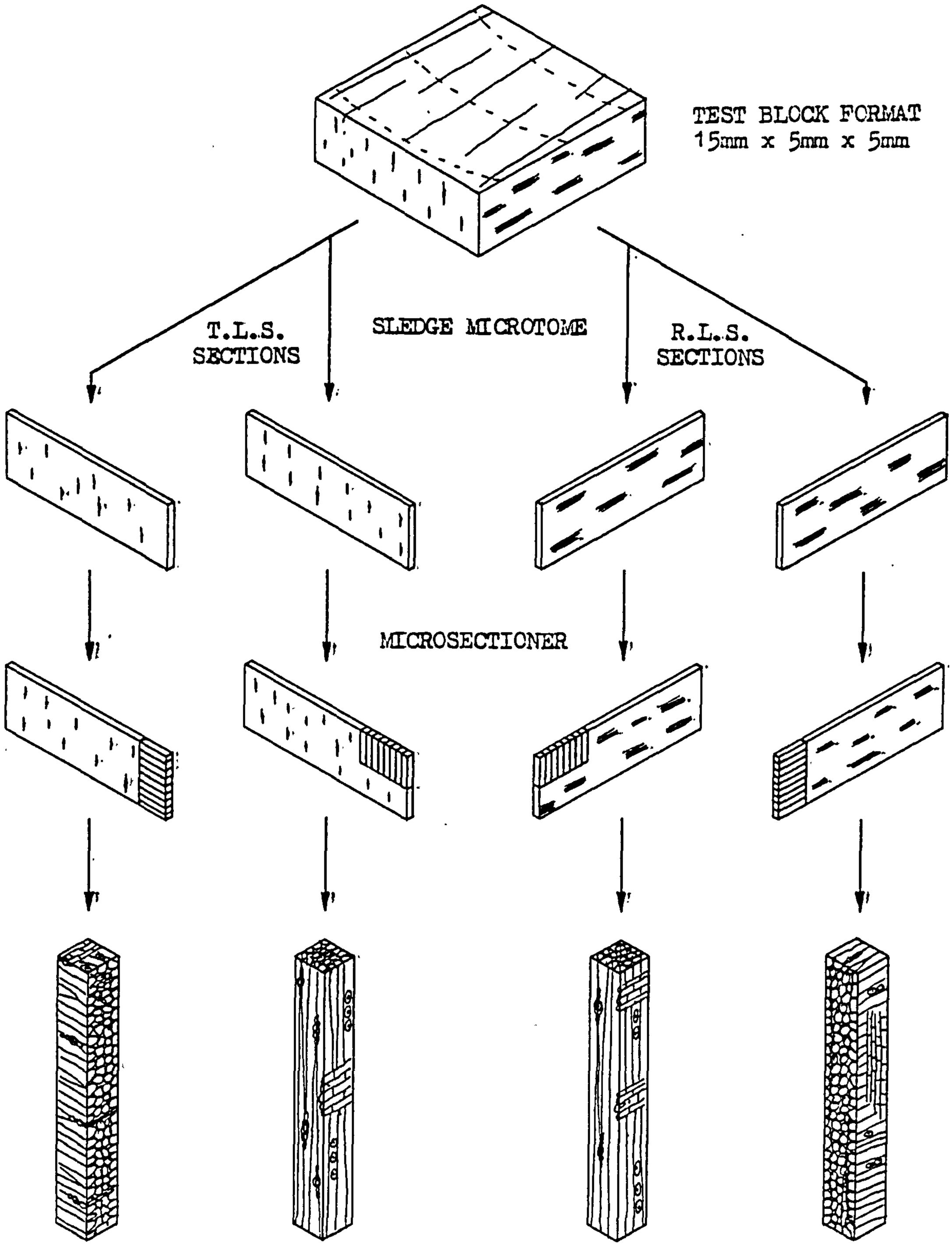
Micromanipulator

Drill chuck

the details being given in appendix A.

The prepared microspecimens now required some means of embedding in a fixed orientation with respect to the block. The avoidance of a glue line required the use of gelatin or polypropylene capsules (TAAB).

FIG. A


TEST BLOCK FORMAT
15mm x 5mm x 5mm
T.L.S.
SECTIONS
SLEDGE MICROTOME
R.L.S.
SECTIONS
MICROSECTIONER
MICROSPECIMEN
PRESENTING
RLS FACE FOR
ULTRAMICROTOMY
MICROSPECIMENS PRESENTING TS
FACES FOR ULTRAMICROTOMING
MICROSPECIMEN
PRESENTING
TLS FACE FOR
ULTRAMICROTOMY

The latter were prefered as the preshaped design reduced the amount of initial block trimming. Specimens embedded in this way are positioned at the tip of the capsule and the rest of the block acts as the holding gripped by the microtome chuck. The required orientation of the specimen would be such that the long dimension aligned with the block axis with the small cross-sectional face centred in the tip of the block face.

A simple method of securing the specimen in this orientation used a prepolymerised resin block drilled on a lathe, with a small specimen receiving hole. By determining the diagonal dimension of the stick a drill 250μm in diameter was selected, allowing enough clearance for specimen insertion but not too much so as to allow the specimen to deviate too far from the block axis. Small corrections in alignment could be made using the adjustments of the knife position provided on the microtome.

Initial trials with these blocks immediately illustrated a problem in that the blind hole was difficult to fill completely with resin resulting in air being trapped around the specimen. It appeared that two holes were required in the block, one of small diameter as the specimen support and the other larger diameter hole as a resin "feeder". See fig. B. This was quite easily achieved using the lathe which also meant that the two holes were on the same axis as the block. Resin added to the larger hole would dispel the air in the small support hole as it flowed down under gravity. Drilling the holes without the capsule being ruined simply required the drilling of the larger hole first and with the aid of a 4BA thread tap the block could be withdrawn to drill the small hole leaving the capsule free

FIG. B

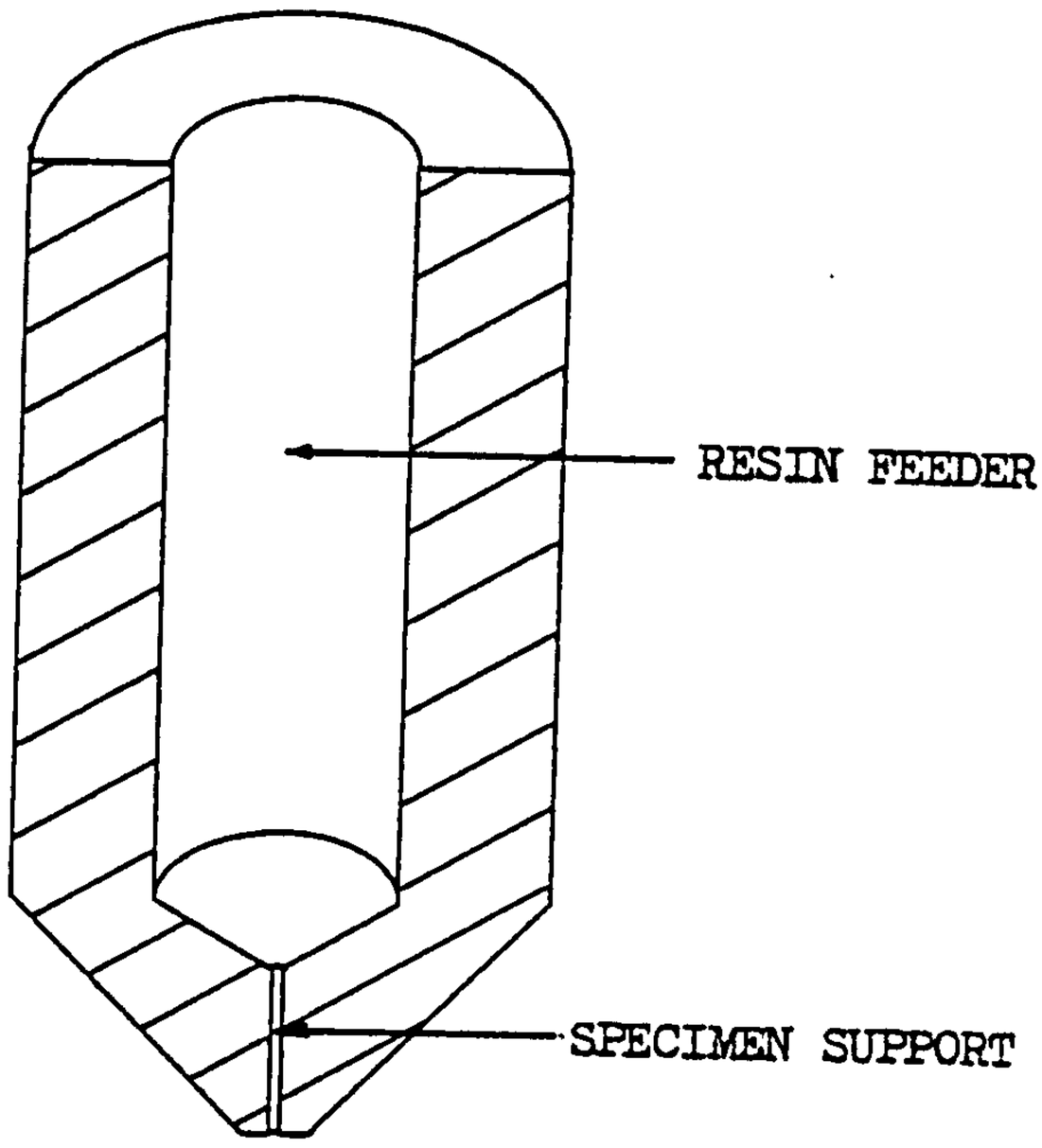
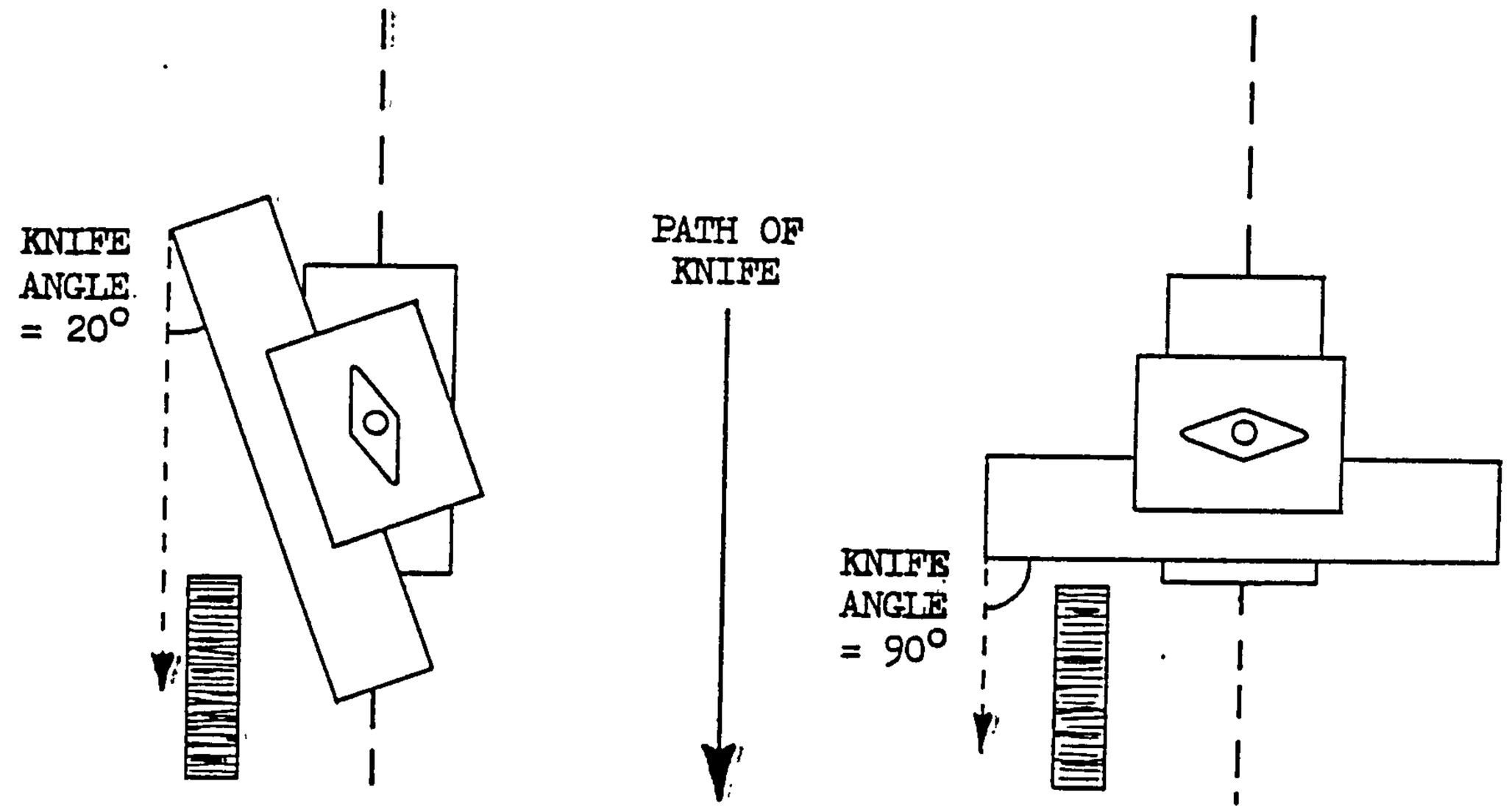

RESIN FEEDER
SPECIMEN SUPPORT

FIG. C


KNIFE ANGLE = 20°
PATH OF KNIFE
KNIFE ANGLE = 90°

to be used again.

This orientation ran into further problems with some of the microspecimens, 150μm x 150μm, not fitting within a hole 250μm in diameter. Closer examination of these specimens revealed that of the two sets of parallel sided faces one was perfect and the other was extremely variable. The poor faces were those produced during the cutting of the macrosection from the decayed block and the distance between the faces ranged from 3 - 8 cells. This gross irregularity caused the location problems encountered during specimen insertion. Analysis of this fault indicated that possibly the angle of attack, for the sledge microtome knife, was to blame. Routinely for cutting thin sections of wood the angle is usually set at about 20° to the line of the cells, fig. C. This produces satisfactory thin sections but when thick sections are cut the knife cleaves off the section rather than cutting it. The knife acting as a wedge results in a cleavage line following the lines of weakness in the wood, producing the variable surface topography. This irregularity was acceptable on the lower surface of the S.E.M. preparations.

By varying the knife angle it was found that progressively larger angles resulted in less disorted, more uniform thickness sections with an attack angle of 90° producing the best results, even though when sectioning the process looked and sounded worse. A simple measure of section distortion could be made by allowing the sections to dry, whereupon the 90° cut produced slightly curved but parallel sections and the 20° cut resulted in sections that were twisted.

Embedded material prepared as above revealed the presence of

swarf in the fresh resin regions of the section surrounding the specimen. This swarf was fine powdered resin produced during the drilling of the holes and the use of a compressed air jet (in a fume cupboard) removed the majority of this contaminant. The more resistant residues did not appear to adversely affect the sectioning of the blocks.

2.3 Resin selection

When considering the choice of resin the following criteria had to be followed.

a) Final hardness possible with the resin

b) Ease of infiltration

c) Resistance to beam damage

d) Resistance to distortion during polymerization.

Fengel (1967) has examined some of the features of epoxy resins used in the transmission electron microscopy of wood.

Araldite resins cover the hardness range required but have not been used to any great extent in the preparation of wood, so available techniques and methods were limited. Many of the resin components, for example, Resin A1502 have very high viscosities, 2100 - 3600 centipoise, such as to prohibit their use on the extremely dense wood cell wall.

Methacrylates suffer from high distortion during polymerization, sublimation in the electron beam with the subsequent microscope contamination and were not recommended (Zainal, 1975).

Spurr's resin (1969) was rejected on the grounds of component ERL 4206 (Resin) having too high a level of carcinogenicity for use in the quantities to be employed by the preparation block (appendix C).

Also there was little in the way of documented applications to wood research, although the extremely low viscosities of some of the components (ERL 4206 = 8 centipoise) would make infiltration very much easier.

Epon 812 (Shell:- see also page 159) was found to be an acceptable resin for this work. It had a high enough hardness range, was easily obtainable from a variety of suppliers, had a reasonably low viscosity (around 100 - 300 centipoise), especially when compared to Araldite, and had been well documented with regard to botanical applications. This resin was used extensively in this department and was recommended by my predecessor in this field (Zainal, 1975).

2.4 Resin matching

Up to this stage the methods have satisfied the requirements stipulated in the introduction for a specimen of decayed wood suitable for T.E.M.. A small easily infiltrated, suitable format, orientated specimen that could be embedded so that the transverse, tangential and radial planes could be cut.

However, although the physical location of a specimen in the block had been achieved the most important critererion for successful ultramicrotomy is that there should be a hardness match between the specimen and embedding resin. As already mentioned, the material is extremely variable resulting in severe problems in hardness matching. Therefore, a sound knowledge of the resin to be employed in specimen embedding is advisable. The chemistry of the constituents, method of polymerization and ways in which the resin hardness can be varied will aid the researcher in understanding the complexity of the embedding process, its possible effects on the specimen and how the resins

could be manipulated to suit the users requirements.

From the literature the majority of workers use four components in the preparation of Epon 812 epoxy embedding resins:-

Epon 812 resin Mol. wt. (260) 100-170 cps :- a complex of epoxies

M.N.A. hardener Mol. wt. (178) :- methyl nadic anhydride

D.D.S.A. hardener Mol. wt. (266) 300 cps :- dodecenylsuccinic anhydride

D.M.P.-30 accelerator Mol. wt. (265) :- tri(dimethylaminomethyl)phenol

A plasticiser component is also available (Fink, 1960) but rarely found to be required. An excellent reference on epoxy resins (Lee and Neville, 1967) has been used in conjunction with other data to compile a summary of the chemistry of the epoxy resin system used for the specimen embedding in this study and is given in appendix B.

2.5 Compounding of the resin.

Viscous liquids are difficult to measure accurately by volume and therefore the components should be mixed by weight.

As mentioned in appendix B, the chemistry of the polymerization process using the above components favours an anhydride/epoxide (A/E) ratio of about 1.0. However, Luft (1961) recommended that lowering this molar ratio to 0.7 improves the cutting properties of the cured resin. Ratios as low as 0.55 may be used but the cure might not be as complete. Throughout this work an A/E ratio of 0.7 was used.

Selection of the MNA/DDSA ratio controls the final hardness of the resin and is therefore very important in specimen matching. The higher the proportion of MNA the harder the final resin. Ratios between 3:1 and 1:3 are generally used.

The accelerator DMP-30 or BDMA (benzyldimethylamine) is generally added as 1 - 1½ % by weight of the total mix.

In the following formulations the component ratios are calculated on a molar basis. Consequently the MNA/DDSA molar ratios must not be confused with the MNA/DDSA volumetric ratios given by Luft (1961) in the mixing of his A and B components. This means that a 3:1 molar ratio is about equivalent to a 2:1 parts ratio for MNA/DDSA.

The information required for the calculation of the resin component weights is:-

(i) The equivalent weight of each component

MNA :- 178 = Mol. wt.

DDSA:- 266 = Mol. wt.

Epon:- this is variable between 140 and 160 (as covered in appendix B) but should always have been determined by the manufacturer and labelled on each batch of resin. In the calculation example a value of 154 was used.

(ii) The selected anhydride/epoxide molar ratio, in this work the recommended value (Luft, 1961) of 0.7 was used.

(iii) The MNA/DDSA molar ratio. Resins ranging from 5:1 to 1:3 were examined in this study but for the calculation example 4:1 (i.e 0.8:0.2) has been selected.

Calculations

(i) Calculate the molar ratios,

MNA	0.7 x 0.8 = 0.56
DDSA	0.7 x 0.2 = 0.14
Epon	1.0 x 1.0 = 1.00

(ii) Multiply molar ratios by the equivalent weights to obtain the weight ratios,

MNA	0.56 x 178 =	99.6 g
DDSA	0.14 x 266 =	37.2 g
Epon	1.00 x 154 =	154.0 g
Total weight	=	290.8 g

(iii) Calculate actual weights, say for a 100g total mixture,

$$\text{MNA} \quad \frac{99.6 \times 100}{290.8} = 34.25 \text{ g}$$

$$\text{DDSA} \quad \frac{37.3 \times 100}{290.8} = 12.79 \text{ g}$$

$$\text{Epon} \quad \frac{154 \times 100}{290.8} = 52.96 \text{ g}$$

1 - 1.5g of DMP-30, or BDMA, accelerator are required to complete the mix.

A short computer programme, given in appendix D, was written to produce tables of component weights in a 100g mix for A/E molar ratios 0.55 - 0.85, epoxide equivalents 140 - 160, and MNA/DDSA molar ratios 5:1 to 1:3. These enable quick reference and simple weighings of desired resin mixes for any given batch of resin supplied.

This calculation method allows accurate, reproducible mixing and variation of the resin components. By using the molar ratios, components are always mixed by weight and therefore more accurately. Conversion of volumetric recipes to gravimetric values requires the use of specific gravities of each component (Epon = 1.22, MNA = 1.20, and DDSA = 1.05, DMP-30 = 0.97). As can be seen the 1 to 1 conversion (II 2.4) should have been corrected for specific gravity.

Epoxide and aromatic amines are generally unpleasant chemicals and contact with them should be avoided. General precautions covering all toxic and corrosive chemicals should be observed, especially with DMP-30 which can cause severe contact dermatitis (Lee and Neville (1957)).

NOTE

Shell chemicals Corp. have ceased to manufacture Epon 812 but a German company is producing an equivalent component under licence. The new epon has a narrower epoxide equivalent range (140 - 155), slightly lower viscosity and produces a slightly harder block than the Shell version. The new resin is just as readily obtainable but at a higher price.

2.6 Ease of infiltration of the embedding medium

This is dependant on two factors already noted, the dimensions of the specimen and the normal viscosity of the resin mix. However, a point which does not appear to be appreciated by some workers is the relationship between the resin viscosity and temperature. Temperatures significantly lower than room temperature (R/T) increase the resin viscosity by a large factor, indicating a preference for higher temperature work allowing more rapid infiltration of the specimens by a lower viscosity resin. It must be stressed, however, that higher temperatures will promote more rapid cures of full and even partial mixes (due to contaminants, see appendix B). This relationship between viscosity, cure time and temperature can result in preparation schedules lasting many days because infiltration stages were carried out at low temperatures, increasing the viscosity, reducing the penetration rate and thus requiring longer preparation schedules.

An attempt was made to increase the penetration rate by operating at R/T, for all stages using the resin, to achieve satisfactory infiltration before polymerization commences due to the higher temperature. Brief tests on the pot life of full resin mixes at R/T led to the development of a satisfactory rapid penetration schedule for the material examined.

2.7 Specimen handling

Frequently in studies of the type being undertaken here a large number of specimen variables are considered during the preparation. For example,

2 wood types

3 fungal species

3 planes of section

2 or 3 incubation periods.

Of these only the wood types and section planes can be satisfactorily separated out from a mixture of the above, requiring the fungal types and incubation periods to be kept separate. If variations in the chemical processing are also employed, for example, fixation methods, dehydration methods and variation in resin hardness, then the number of variables is increased factorily.

Many published methods of detailed wood specimen preparation involve repeated handling of the specimens. Such handling, no matter how gentle, will produce some degree of specimen damage which may be difficult to recognise as artefact when examining decayed wood. These methods also introduce the problem of coping with the numbers of specimens requiring preparation. To enable comparisons to be made between different specimens they should be treated identically to

eliminate differences being attributed to their processing treatments. No matter how meticulously one tries to create identical conditions of temperature, chemicals and exposure times between two different preparation runs the results can be very different indeed. The requirement, therefore, was for a method or means by which an operator could not only prepare specimens with the minimum of handling but also cater for a large number of different specimens through several chemical variations during processing. The development of such a device is given in appendix C and this appartus was used extensively throughout the assessment of the different chemical treatments applied to the specimens and enabled large scale preparation of specimens under identical conditions.

2.8 Vacuum infiltration and embedding

Zainal (1975) strongly recommends the use of vacuum to aid the resin infiltration of the wood specimens. This vacuum application was applied to try to remove air trapped within the cells. These air pockets inhibit the normal diffusion exchange processes during the chemical processing and when polymerized cause problems during ultramicrotomy. However, the successful application of vacuum only occurs when the air pocket expands enough to reach the outside of the specimen and dissipates. If this is not achieved then the end result is just a larger air pocket within the wood.

The effect of vacuum on fungal cytology can only be detrimental with any gas vacuoles present expanding, resulting in cytoplasmic disruption. Vacuum applications can also cause the resin to 'boil' in the sense that air present in the resin after mixing expands and bubbles out. This resulted in problems of specimen displacement when

applied during resin stages using the specimen holder, (appendix C). Vacuum application during infiltration was, therefore, dropped but was occasionally used, when examining extremely parenchymatous material, during the first fixation stage. The principle being that removal of air with a low vacuum at this stage, is much easier due to the low viscosity liquids, and that reintroduction of air would only be through severe mishandling of the specimens.

3. MATERIALS AND METHODS

3.1 Woods

These were the same as for the S.E.M. work, see part I 2.1.

3.2 Fungi

These were the same as for the S.E.M. work, see part I 2.2.

3.3 Preparation of the decayed microspecimens

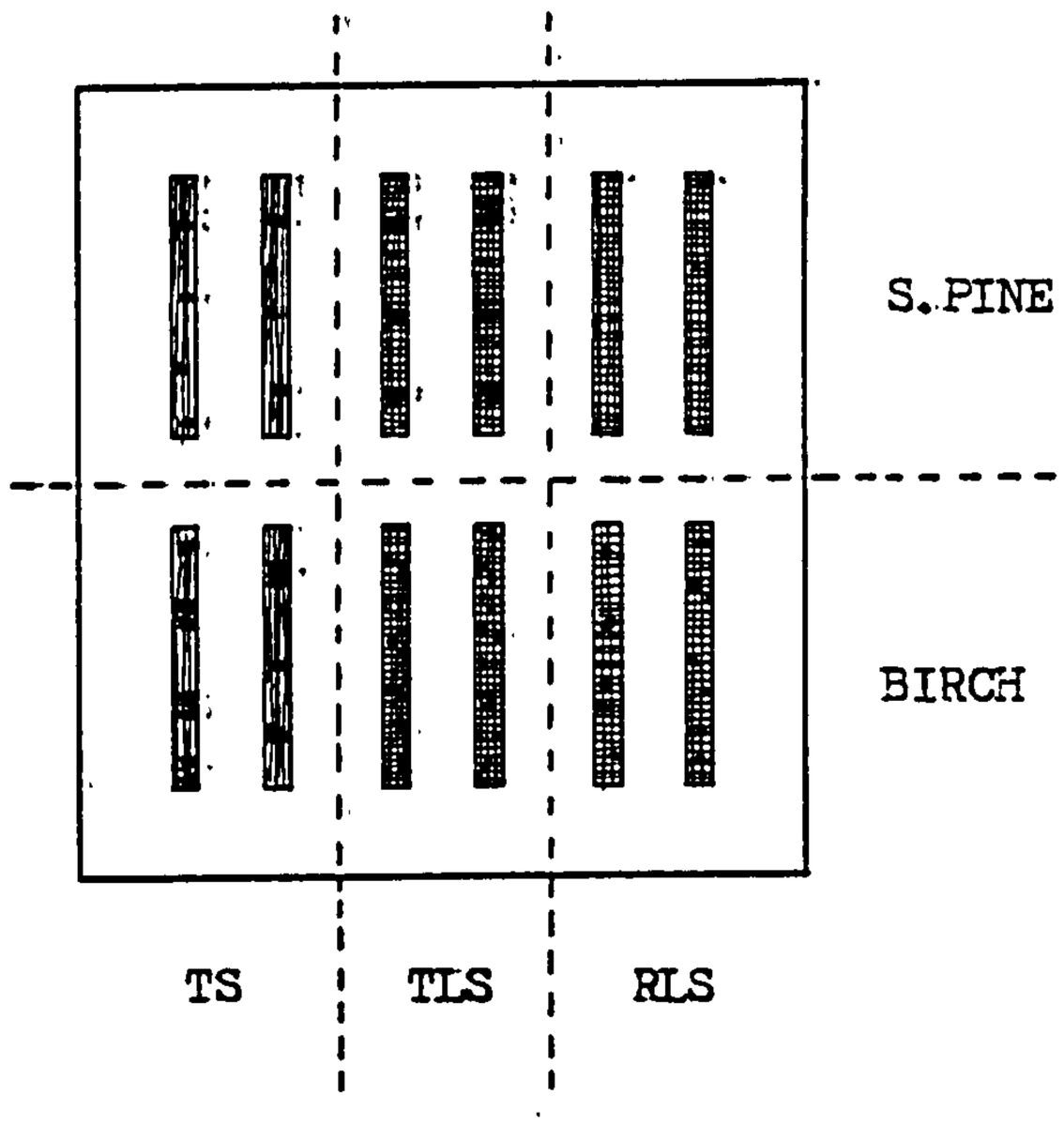
3.3.1 From blocks

After the experiences with the S.E.M. decay material, the original proposal to examine a number of incubation periods was dropped. It was felt that the decay features required could be selected out from two or three incubation periods at the most. The early preparation runs employed the principles set out in section 2.2, modifying the S.E.M. preparations of Part I 3.1 to 3.3.1. After four or six weeks incubation the decayed blocks were immersed into the first fixative solution (Part II 2.2). Then 150µm sections were cut using a sledge microtome, as in Part I 3.3.1, but using an attack angle of 90° (III 2.2). During sectioning, the later stages of microspecimen production, and searching for decayed regions, the material was kept flooded with fixative solution. The sections were examined under a high power dissecting microscope to determine the regions of decay and these were subdivided as described in 2.2. Using a light microscope the microspecimens were searched to select out the required specimens which were inserted into their allocated chambers within the specimen holder, containing the washing buffer (II 2.2). At least two replicates of each specimen variable (including chemical) were prepared and transfer of the material was achieved with fine forceps and a camel hair brush.

3.3.2 Improved methods

Improved methods were later employed to reduce the creation of artefacts during the preparation of the microspecimens from heavily decayed blocks and to reduce the incubation periods still further. It was also felt that exposure of the operator to fixative solutions during sectioning and microsectioning was undesirable and should be avoided if at all possible. The dry, roughly orientated blocks, 15mm x 15mm x 5mm were soaked overnight in distilled water. These were then sectioned and subdivided, as in section 2.2, to produce the required microspecimens which were arranged on squares of fine stainless steel mesh (to prevent the specimens waterlogging due to contact with the agar) as below in fig. D.

FIG. D



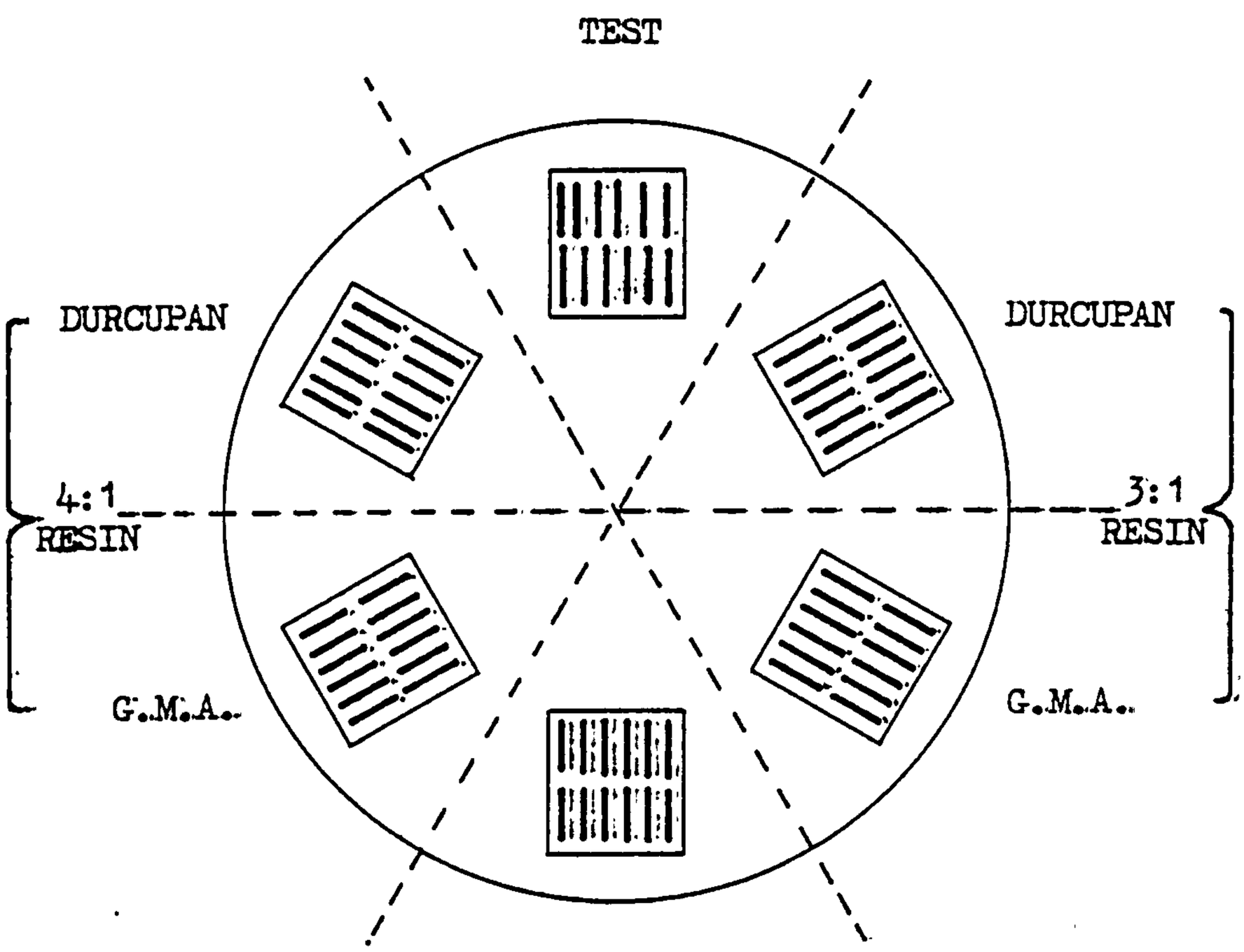
The mesh squares were then autoclaved in glass petri dishes, at 120°C for 20 minutes, before positioning on the cultures of test fungi. Two culture methods were employed for the microspecimen work. Initially, the culture plates were comprised of core innoculi, from 2% malt - 2% agar cultures, centred on plates of 2% malt - 2% agar. These were incubated at 22°C for two days to establish hyphal fronts onto which the meshes were placed. This method enabled comparisons to be made between the results from large decay blocks and small microspecimens.

Later the method was altered slightly to use core innoculi from 2% malt - 2% agar cultures centred on plates of Abrams (1948) mineral medium agar. Again the plates were incubated for two days and the meshes positioned as before. This procedure attempted to create growth conditions closer to those experienced in the natural environment. For both methods the number of meshes and plates used depended on the specimen variables being examined. This was frequently in the order of 50 to 100 which, with replicates, required large numbers of microspecimens.

Four meshes, each carrying two replicates of six specimen variables, were positioned on each plate allowing two chemical variables to be employed. Also positioned were two test meshes bearing six microspecimens, to allow periodic observations on the progress of decay without disturbing the actual specimens to be examined in the T.E.M., see fig. E. This procedure meant that only three culture plates were required to examine 72 specimen variables. By examining the test specimens, the material was incubated for the required period after which the microspecimens were removed, positioned and fixed

overnight within the specimen holder.

FIG. E



3.4 Resin mixing

During the incubation periods the resin mixes were made up. Using the required data (2.5) and the computed tables the weight of each component in 100 grams of resin mix was determined. From the number of processing steps, specimens, and receiving blocks, the total volume of resin required was calculated and converted to the nearest 50 grams (above the required value).

Using a top pan balance in a fume cupboard the Epon 812 and the two hardeners were weighed into a wide mouthed 500ml polypropylene bottle. With a glass rod these components were thoroughly mixed. With a disposable syringe the correct percentage of accelerator (DMP-30)

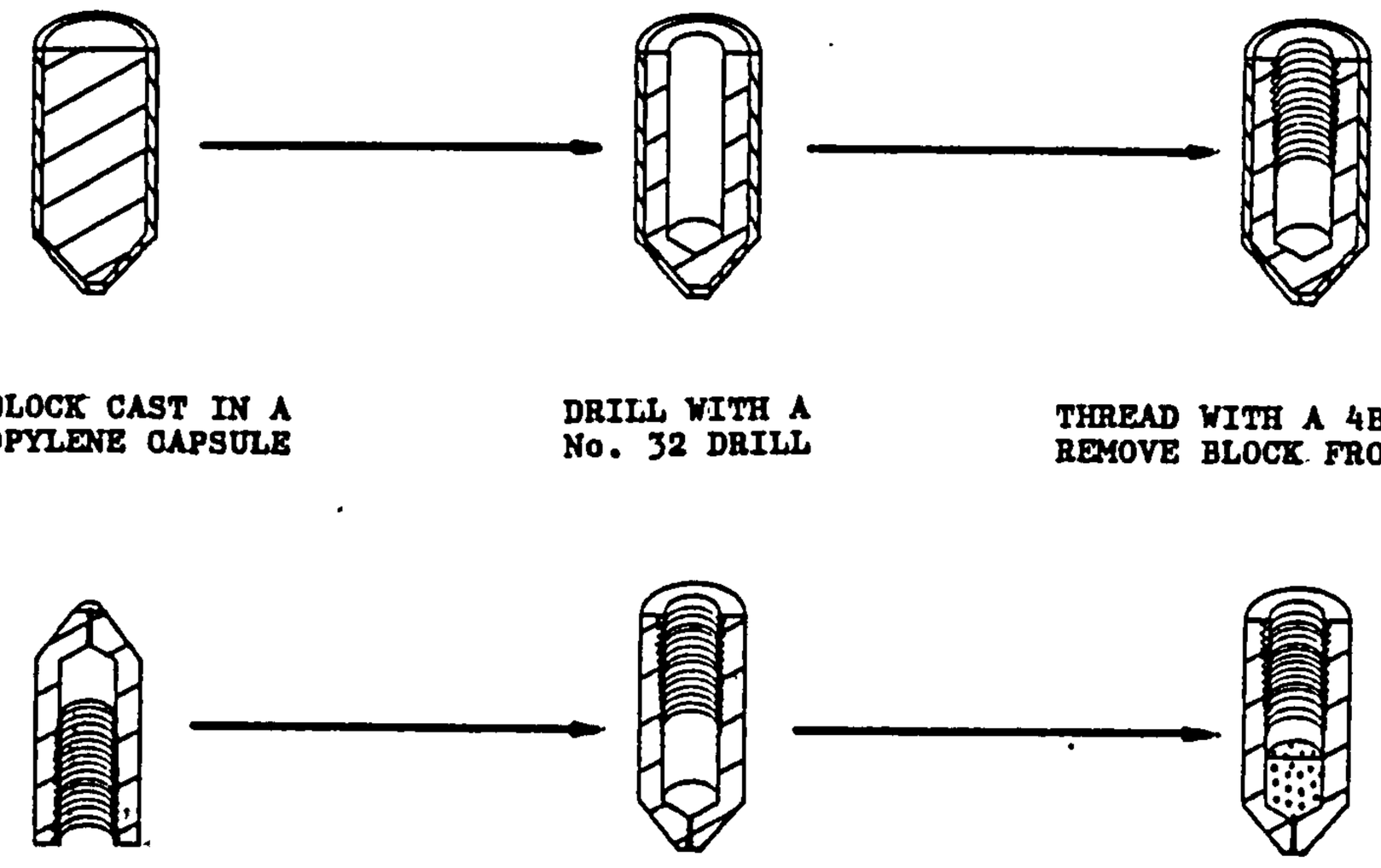
was slowly added drop by drop, with continuous mixing. The resin was again thoroughly stirred, capped, sealed in a plastic bag and placed in a deep freeze. When required the resin was allowed to attain R/T before unsealing the bag and bottle (to prevent absorption of water condensation by the resin).

3.5 Preparation of the orientation receiving blocks

Before the specimen processing, the receiving resin blocks were prepared. Enough polypropylene capsules, to cater for the number of microspecimens to be examined, were set up in a rack and divided up into the various resin mixes being used. Into each capsule a small typed label was inserted to identify the microspecimen. Using a disposable syringe a small drop of the resin was added to each capsule. This drop flowed down the capsule side to occupy the very small conical tip. Further resin was then added to fill the capsules. This procedure eliminated the problem of tiny air pockets being trapped in the conical tip. The capsules were then polymerised overnight at 60°C. Using a lathe, the large 'feeder' hole was drilled, a set distance into each block, with a No. 32 drill. With a 4BA 'tap' the blocks were pulled from the capsules which were set aside to be cut; fig. F summarises the block preparation. The fine orientation hole was then drilled in each block with a 0.25mm drill and the swarf removed with compressed air (see 2.2). The blocks were set up in the rack again, in an order corresponding to the arrangement of the microspecimens in the specimen holder, ready for filling.

Once the last microspecimen processing stage (see 3.8) was reached a few drops of matching resin was added to each block. This resin slowly filled the orientation hole (in about 10 minutes) and the block was ready for specimen insertion (see 3.10).

FIG. F Block preparation



3.6 Fixation

Essentially the double fixation process given for the mucilage preparation, II 2.2, was employed. However, the solution strengths and exposure times were varied to suit the material. The blocks or microspecimens were immersed in the first fixative solution (II 2.2) overnight at R/T, as detailed in 3.3.1 and 3.3.2 respectively, before three buffer washes (II 2.2), each being of 20 minutes duration at R/T. In the earlier preparations the second fixation stage (II 2.2) was applied for 3 hours at $4^{o}C$, as with the mucilage preparations, but with a 2% osmium tetroxide solution to reduce chemical extraction of the hyphal cytoplasm.

The recommendation by Zainal (1975) to use potassium permanganate ($KMnO_4$) stimulated its later incorporation into the second fixation

stage. Since $KMnO_4$ has a destructive effect on cell cytoplasm the fixation time was reduced to 20 minutes at 4°C in conjunction with the other second fixative solutions (II 2.2) as below:-

Ruthenium red	1500ppm	in distilled water
Sodium cacocylate buffer	0.6M	pH 7.2
Osmium tetroxide	2%	in distilled water
$KMnO_4$	2%	in distilled water

mixed on a 1:1:1:1 basis.

3.7 Dehydration

The results of part II demonstrated that Durcupan (Fluka) proved to be very suitable as a dehydration medium. However, due to the cost of this chemical, a second, cheaper, water soluble resin was also tried. This was the polar, 2-hydroxyethyl methacrylate, more commonly known as glycol methacrylate (G.M.A.). The commercial product is stabilised with 200ppm p- methoxyphenol (TAAB). This second resin was employed exactly as the Durcupan resin. As in part II 2.3, the specimens were subjected to increasing concentrations of the resin at 4°C, though the exchange periods were increased to:-

25% water soluble resin	/ 75% distilled water	for 1 hr
50% water soluble resin	/ 50% distilled water	for 1 hr
75% water soluble resin	/ 25% distilled water	for 1 hr
100% water soluble resin		overnight
100% water soluble resin		for 1 hr.

3.8 Infiltration

More rapid infiltration (see 2.6) was achieved at room temperature with a range of resin mixes (see 2.5) during the preparation runs. MNA/DDSA ratios between 5:1 and 1:3 were examined and the details of these variations are given in the specimen preparation table (Table 1) for

the figures given in the results.

The following schedule was used for specimen infiltration.

25% Epon full mix /	75% water soluble resin (Durcupan or GMA)	at R/T for 1 hr
50% Epon full mix /	50% water soluble resin	at R/T for 1 hr
75% Epon full mix /	25% water soluble resin	at R/T for 1 hr
100% Epon full mix		at R/T for 1 hr
100% Epon full mix		at R/T for 1 hr
100% Epon full mix		at R/T overnight
100% Epon full mix		at R/T for 1 hr
100% Epon full mix		at R/T for 1 hr.

After this short processing period the specimens were ready for insertion into the prepared receiving blocks.

3.9 Use of the specimen holder

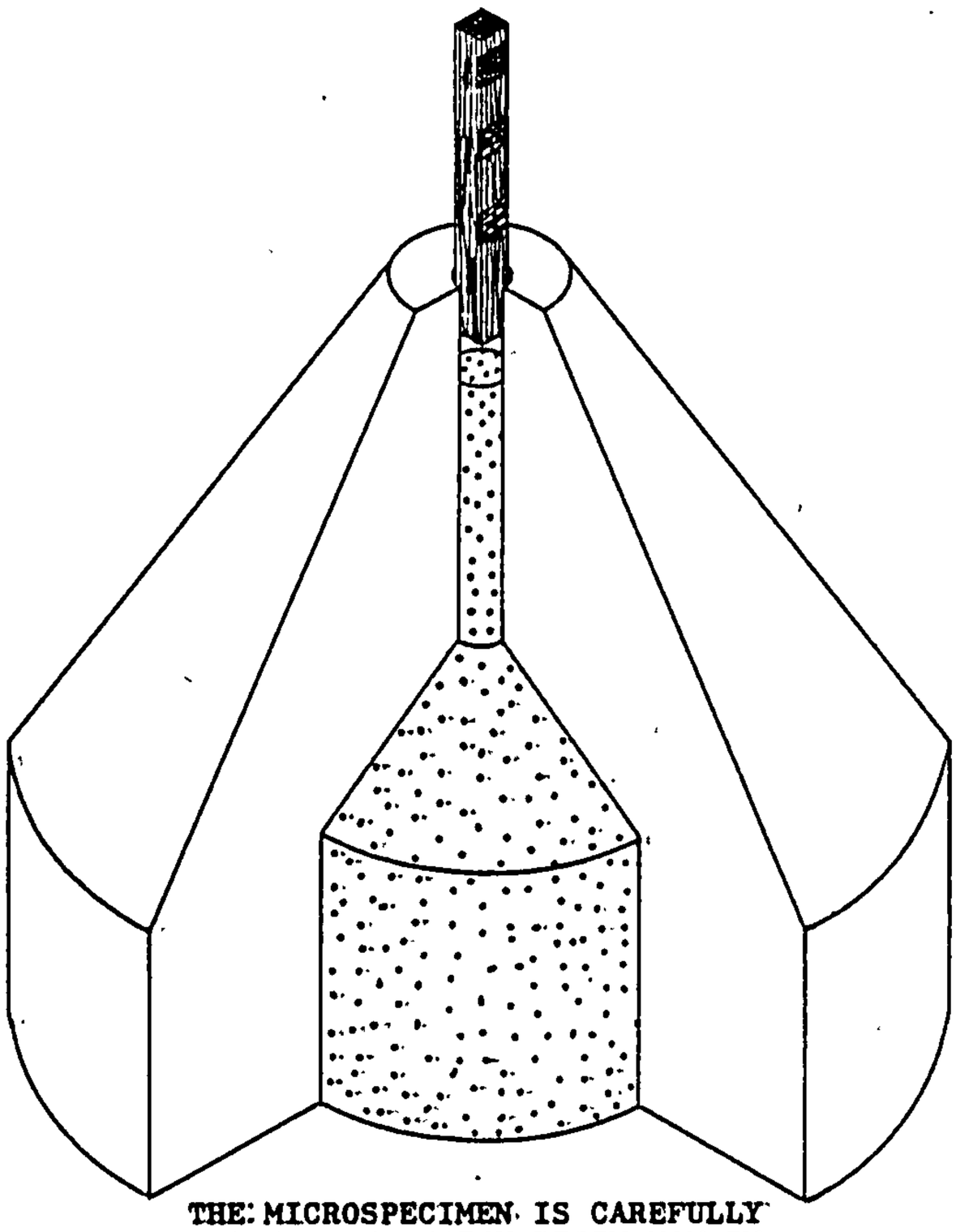
Virtually all the processing of the specimens was achieved with the specimen holder described in appendix C. Each trough fed 10 chambers with the same chemical treatment and 10mls of fluid was found to be adequate for filling all the chambers of one trough.

Using the vacuum probe (see appendix C) the old fluid was drawn off from each of the chambers and the new fluid added. This process being repeated at each step and for the other troughs in use. With the exception of the fixatives the chemical treatments were made up before a preparation run and, using 10ml disposable syringes, dispensed into the relevant troughs.

3.10 Microspecimen insertion

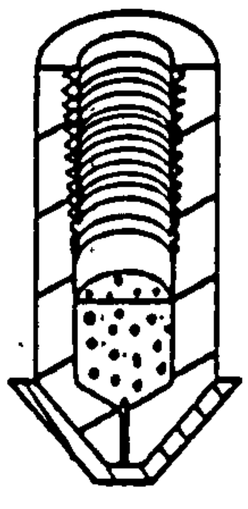
After the last infiltration stage was completed the specimen holder was dismantled and the middle, specimen support, section removed. The appropriate prepared receiving block (see 3.5) was set up in the drill chuck (fine orientation hole uppermost) of the apparatus described in appendix A, without the micromanipulator attachment. Using fine

forceps the microspecimen was quickly transferred and inserted into the hole aided by viewing the procedure through the binocular microscope, see fig. G.



THE MICROSPECIMEN IS CAREFULLY PLACED INTO FRESH RESIN NOW IN THE APEX OF THE PREPARED BLOCK

With the microspecimen positioned, the block was inverted and set back in the rack on the small cone of capsule, see fig. H.



Each block was carefully loaded in this way and the process completed by topping up the 'feeder' holes with more fresh resin. The set of capsules were then polymerised by placing the rack in an oven at 60°C for 48 hours. After cooling the cones were removed and set aside for re-use leaving the finished blocks ready for trimming.

3.11 Precautions and waste disposal

Wherever possible the processing stages using fixatives were carried out in a fume cupboard or a sealed vessel. Waste fixatives, buffers and resins were collected in the winchesters previously mentioned (II 2.2). When the vacuum probe was being used this was simply and effectively achieved by connecting the relevant winchester into the vacuum line as a waste trap. All operations involving the preparative chemicals were carried out wearing protective clothing and gloves in a well ventilated space. Contaminated syringes were collected in polythene bags and polymerised, where appropriate, before disposal. After a preparation run, the specimen holder was thoroughly scrubbed in acetone, followed by hot, soapy water and dried ready for the next preparation run. The small stainless steel grids and the meshes were cleaned with acetone in an ultrasonic cleaning tank. Contaminated acetone being added to the waste resin winchesters. Waste toxic chemicals can be disposed of via the Public Health Authority.

3.12 Trimming

The principles of trimming were covered in detail by Zainal (1975) and modifications and adaptations of those procedures are given here. Trimming was achieved using new, clean, single edged razor blades for

all stages up to the final cuts which were made with new, clean, double edged blades held in a pin vice, as these had superior cutting qualities. The slopes of the "truncated pyramidal" block shape being cut at an angle of about 30° to the plane of the block face. All the trimming was through pure resin and clean smooth sides were invariably produced. However, because hard resin mixes had been employed there was a tendency for chonchoidal fracturing of the resin to occur and warming the blocks to $60^{\circ}C$, immediately before trimming with the aid of a high intensity spot light enabled smooth, regular cuts to be made due to the slightly elevated temperatures reducing the resin hardness (McGee - Russell and de Bruijn, 1964).

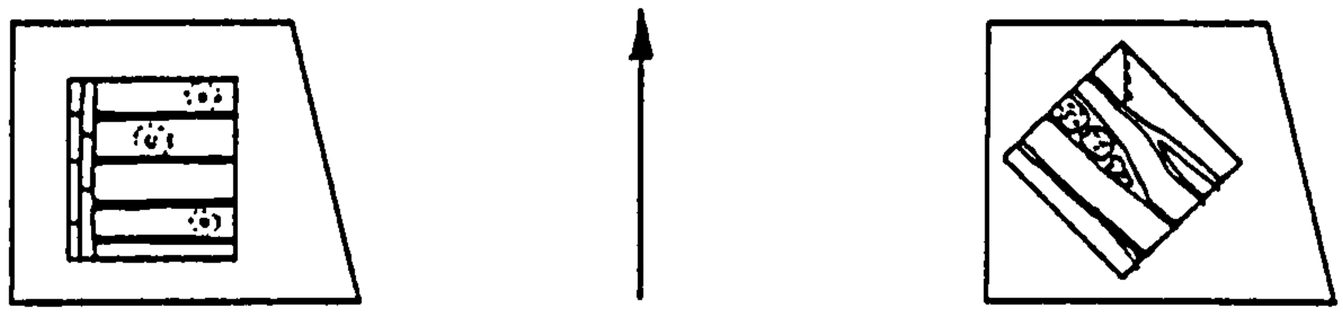
The trapezoidal block face (Zainal, 1975) was reduced to a part trapezium, recommended by Meek (1976), see fig. I,



and as such it was possible to determine which way up the sections were being examined. The slightly reduced block face area for the same specimen area was also advantageous in reducing the cutting forces.

Orientation of the specimen within the block face was initially the same as that of Zainal (1975). This method proved to be quite satisfactory for the transverse sections but with longitudinal sectioning distortion within the paired cell walls was frequently encountered. This distortion, as previously mentioned, results from the opposite microfibrillar angles of a wall pair resulting in "with" and "against"

the grain cutting. Two alternative specimen arrangements were therefore tried, see fig. J.



in which (B) was more successful than (A) in reducing wall distortion. The interuption of the cutting forces between wall and lumen resin caused section folding in (A).

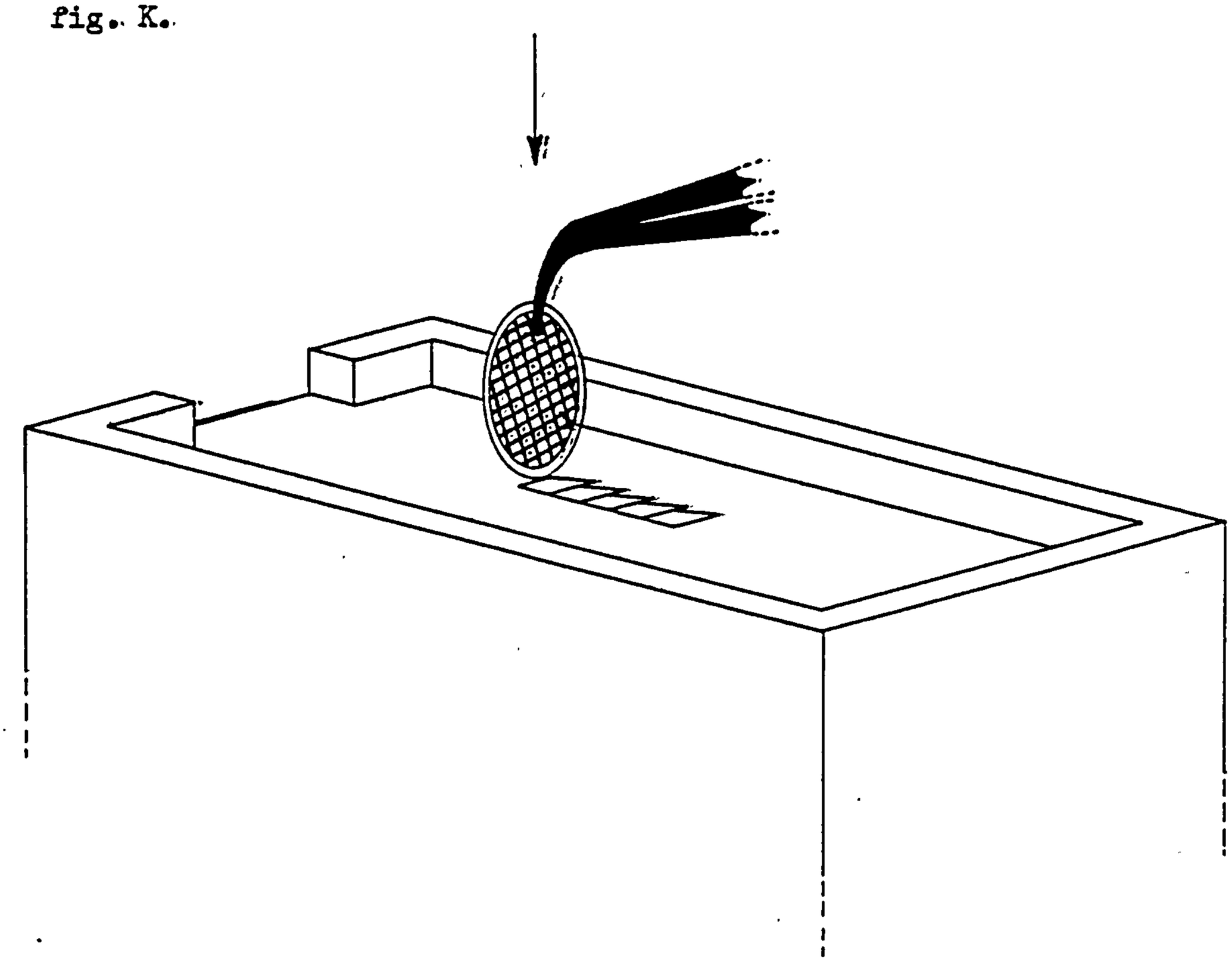
It must be stressed at this point that where specimen embedding was such that there was a perfect match between resin and material, then the cutting of ultrathin sections presented no problems. The variation in orientation given above attempted to produce satisfactory sections from slight mis-matches which are invariably the case in this type of work.

3.13 Sectioning

LKB ultratome, Riechert OmU2 and Huxley Mk II ultramicrotomes were available for sectioning but it was found that only the Huxley Mk II had low enough cutting speeds for this material. Sections 100 - 150 nm thick (silver - gold (Peachey, 1958)) were produced at a cutting speed of 0.2 mm/sec. Faster speeds increased section compression which in epon embedded specimens was very difficult to relieve and has been reported as being virtually permanent (Wachtel et al, 1966).

A diamond knife was used throughout the sectioning of decayed wood material with water as the trough fluid. Sections were collected on 100 or 200 mesh copper-rhodium plated (one side only) grids (TAAB)

by one of a number of methods. The simplest used the electrostatic forces between the sections and the grid, detailed by Zainal (1975). However, excessive folding in the section was frequently encountered by this method. Flatter sections were achieved by collecting the ribbon from below but, in practice, was often very difficult to achieve without damage to the grid or the sections in the very confined volume of the trough. A simple method which seemed to produce satisfactory results was to lower the grid, edge first, onto the ribbon of sections (sacrificing one section) using the surface tension forces to spread the sections onto the grid as it was pushed down into the water, see fig. K.



Initially, formvar coated grids (Drummond, 1950) were used but the strength of the epon sections enabled the supporting membrane to

be dispensed with when using 200 mesh grids thus eliminating a further source of section contamination.

Sections cut from specimen blocks produced by the methods previously described frequently exhibited a periodic distortion in regions of pure resin. For a detailed investigation of block and section distortions produced during ultramicrotomy see Helander (1969). This type of distortion can also be found in other workers' material and seems to be a feature predominant in sections of wood. In this work the distortion was extremely pronounced in the second embedding resin with a marked junction between this and the specimen or the first block resin. The alternating light - dark banding could not be focussed in the electron microscope and was either corrugations or thick - thin regions in the section. Using the eucentric goniometer stage of the Philips 301 microscope such sections were tilted to + and - 45° and this demonstrated that the periodicity became condensed, proving the distortion to be of the thick - thin type. An examination of a block face, that produced these sections, in the S.E.M. revealed the same distortion to be present in the surface topography of the block, with the specimen and first (block) resins cutting smoothly along a plane higher than the distorted second resin regions. Obviously there was a physical difference between the first and second resins even though chemically they were identical. It appeared that the second resin suffered more severe and permanent distortion, possibly during the compressive forces created by the knife (Helander, 1973a & b, 1974), and that this physical difference could well have been due to the thermal polymerization of a second resin within a solid first resin cylinder. Although these distortions did not interfere with the

production of serial sections , possible methods of overcoming this fault are being tested.

3.14 Staining

Double staining with uranyl acetate (Watson, 1958) and lead citrate (Reynolds, 1963) was applied to the early material following the timing details of part II 2.6 and the manipulative procedures of Zainal (1975). These stained sections illustrated very high contrast with fungal details being almost obscured by dense staining. Unstained sections proved to have enough contrast, inherited from the fixation procedures, to be examined without further treatment. In the majority of the material, therefore, unstained sections have been examined.

3.15 Electron microscopy

Grids were examined in AEI EM6, EM6B and Philips 301 transmission electron microscopes using an accelerating voltage of 60 KV and liquid nitrogen cooled specimen anticontaminators where available. Details of plates and their development were the same as in part II 2.6.

4. RESULTS

As already mentioned the results produced by the transmission electron microscopy are derived from a variety of trials and tests examining different preparation methods. Because of difficulties during sectioning, caused by miss-matching resins and specimens, a complete coverage of all decay types by one preparation method was not achieved.

The results presented here therefore are representative of all the material that could be sectioned in the time available. Many more blocks remain uncut and if examined should yield more information to add to our knowledge of the lysis patterns produced by the decay types studied..

Material selected from microspecimens and blocks had been incubated for 10 days and 4 weeks respectively and these periods have been indicated on each caption page together with the details of the fixation and dehydration chemicals used in the specimen preparation. The plane of the section is given in brackets after each figure magnification.

To assist in their interpretation, regions of micrographs shown at higher magnification have been marked out by four right-angles on the relevant lower magnification figures. A table (Table 1) summarising the details of the figure preparations has been included at the end of this results section.

The results are presented along the same lines as those for the S.E.M. material ;-

4.1 Brown rot decay, Coniophora puteana

4.1.1 on hardwood:- birch (Betula sp.)

4.1.2 on softwood:- Scots pine (Pinus sylvestris)

4.2 Soft rot decay, Chaetomium globosum

4.2.1 on hardwood:- birch (Betula sp.)

4.2.2 on softwood:- Scots pine (Pinus sylvestris)

4.3 White rot decay, Coriolus versicolor

4.3.1 on hardwood:- birch (Betula sp.)

4.3.2 on softwood:- Scots pine (Pinus sylvestris)

4.1.1 Coniophora puteana on birch (Betula sp.)

The inclusion of $KMnO_4$ in the fixation stages highlighted the cytoplasmic membrane detail of the fungi. Nuclei, mitochondria, endoplasmic reticulum and large deposits of glycogen could be identified within the hyphae, figs. 1 - 4. In all the hyphae examined there did not appear to be any form of mucilaginous sheath comparable with that shown for Rhinocladiella mansonii in part II.

Some aspects of wall architecture in vessel-vessel pitting were clearly demonstrated, figs. 5 and 6, together with the use of natural pathways by the fungus in penetrating cell walls, figs. 7 and 8, as already observed in the S.E.M. study. Interpretation of decay in the wood cell elements was complicated by the obvious presence of mechanical damage, illustrated by the physical fitting of broken pieces of wall, fig. 9.

Possible regions of wall lysis could be indicated by deeper staining due to increasing the permeability to fixatives, fig. 4 and 9. Fine hyphal strands, 0.5μm - 1μm in diameter, were observed in conjunction with normal hyphae in regions of possible wall lysis, figs. 9, 10 and 11. Decay features were limited because early time periods were used, since the older blocks were too fragile to withstand the preparative procedures.

More severe degrade of birch fibres was demonstrated in a number of fibre walls, figs. 12 and 13, which had been heavily attacked leaving a spongy - reticulate residue. The containment of the lytic effect by the middle lamella was very marked with decayed and sound walls adjacent to one another separated only by this layer, fig. 13.

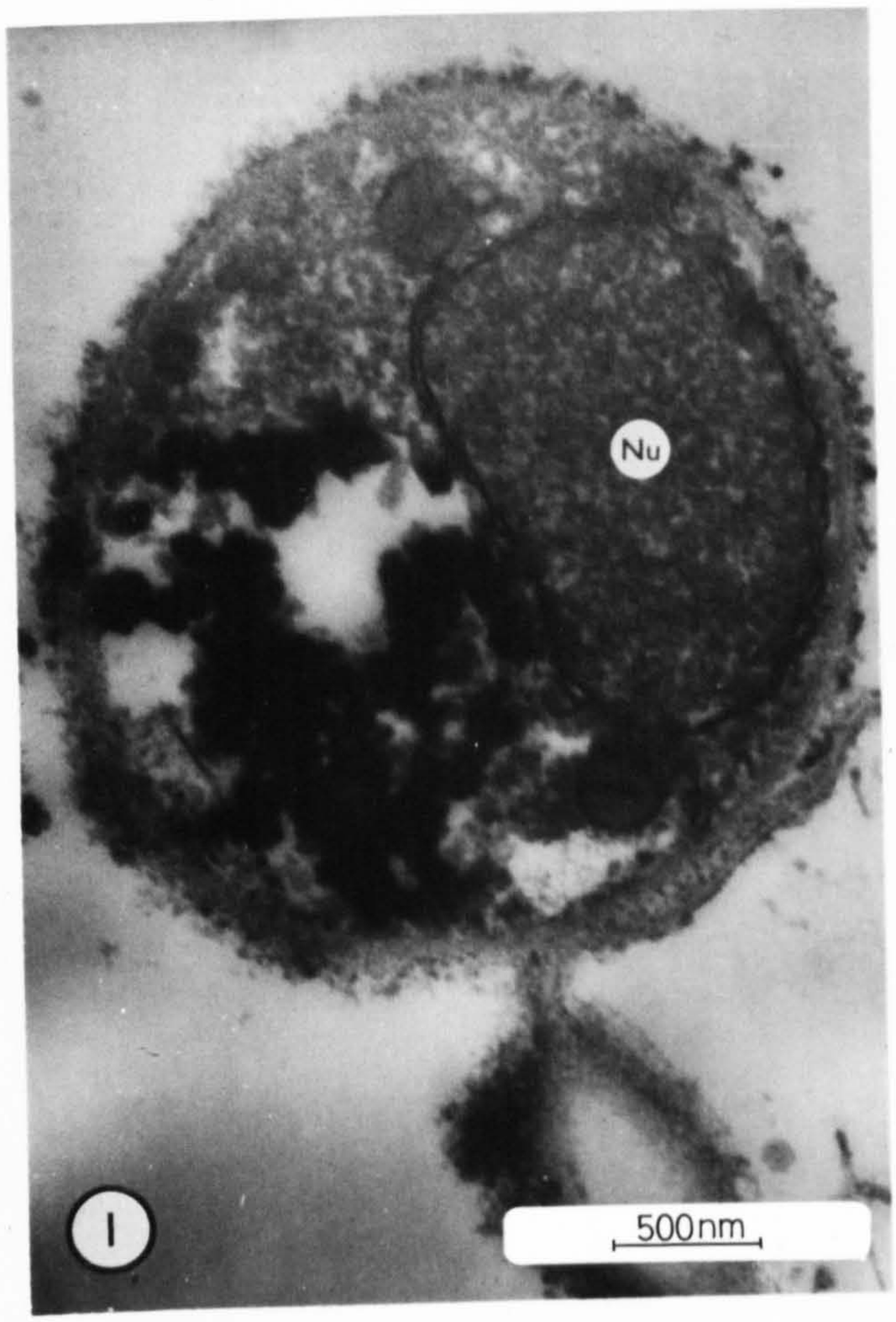
3.1.1 Coniophora puteana on birch (Betula sp.), 10 days

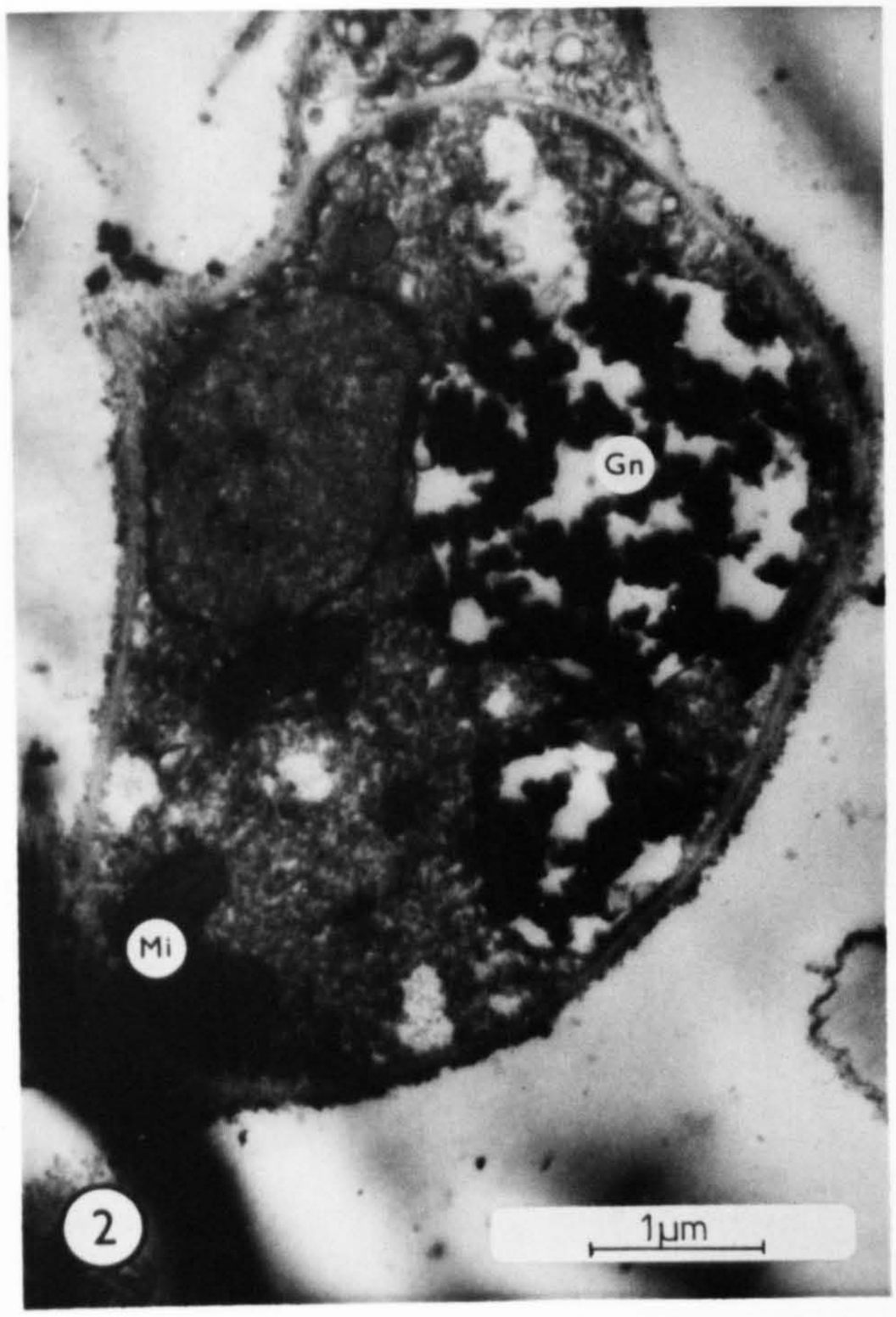
Figures 1 (x 27500 (TS)) and 2 (x 16000 (TS)) illustrate some of the features of the normal colonising hyphae. From the scale lines the variability in hyphal diameter is clearly evident. A number of the cell organelles have been well preserved by the fixatives employed, these include nuclei (Nu), mitochondria (Mi) and large deposits of glycogen (Gn) which have stained black due to the action of the $KMnO_4$ fixative. There was very little evidence of any mucilage structure of the type seen in part II.

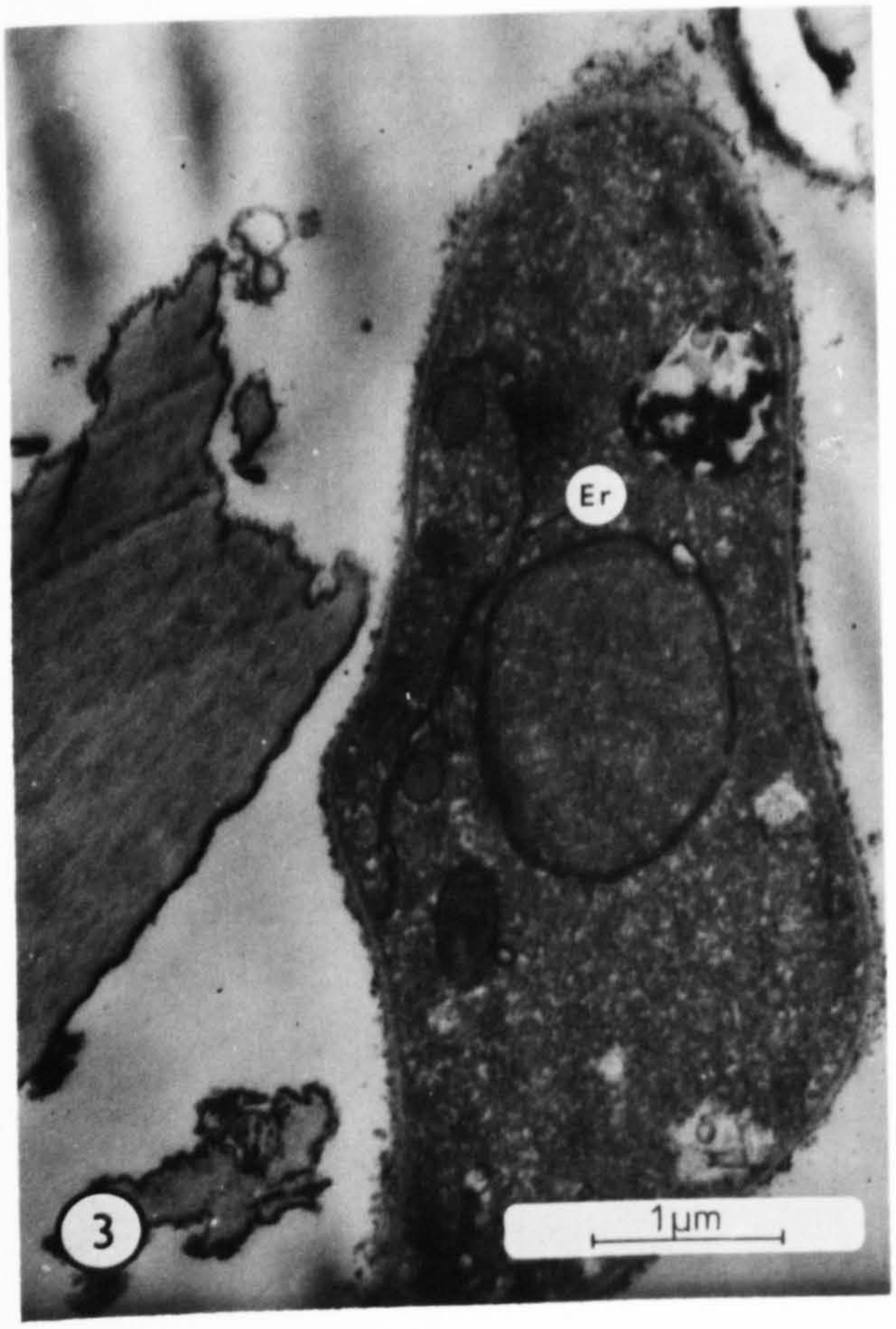
The hyphae observed close to the wood cell walls, figures 3 (x 18170 (TS)) and 4 (x 18460 (TS)), were apparently fairly similar in structure to the previous examples. There was still no evidence of mucilage even though the darker stained areas of the wall in figure 4 could suggest lytic action increasing the permeability of the wall to the fixatives.

Note that endoplasmic reticulum (Er) can clearly be seen together with a much lower glycogen content.

Figures 1-4:- Fixed with glutaraldehyde (G), ruthenium red (R), osmium tetroxide (O) and potassium permanganate (K) and dehydrated with Durcupan (Dur). Unstained sections.


Nu
500nm
1


Gn
Mi
1µm
2


Er
1µm
3


Ds
1µm
4

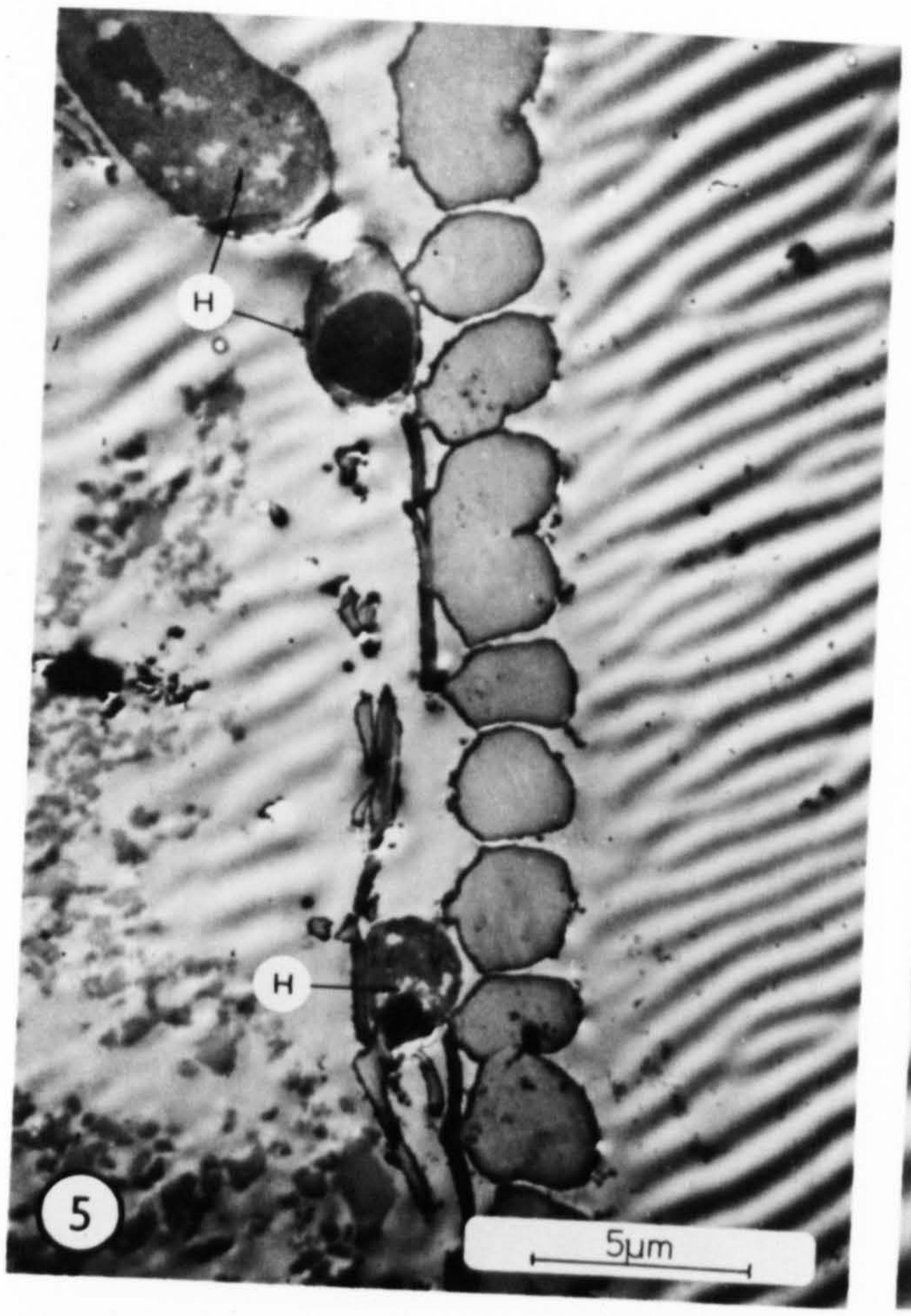
3.1.1 Coniophora puteana on birch (Betula sp.), 10 days

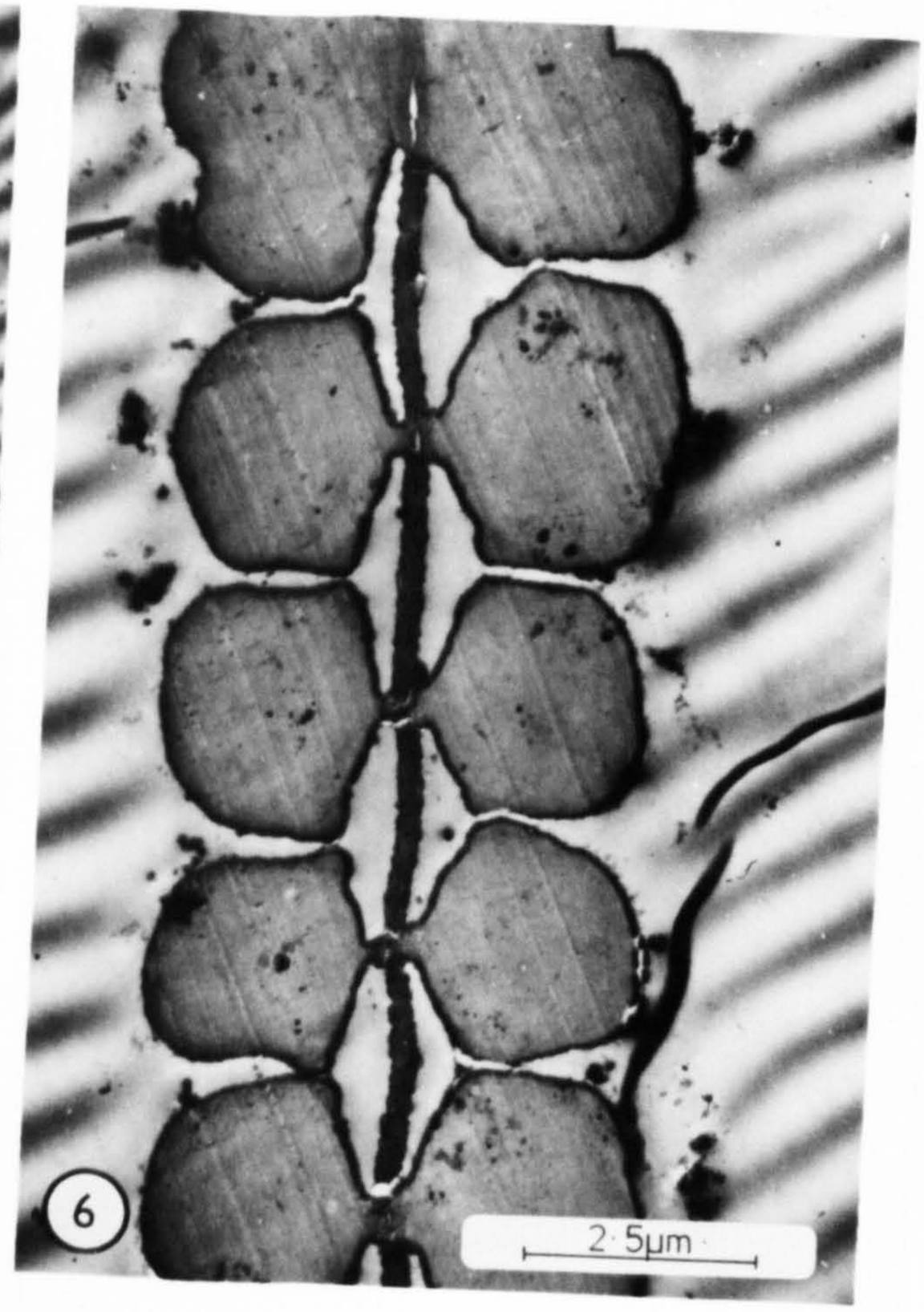
Figure 5 (x 4280 (TLS)) shows hyphae (H) in close association with a degraded, heavily pitted, vessel wall pair. The normal vessel - vessel wall connection can be seen in figure 6 (x 8670 (TLS)) where the darker middle lamella - primary wall complex is continuous across the pit membranes. The wide trumpet shaped pit chambers connect to the lumen through narrow slit-like apertures (c.f. S.E.M. fig. 1). The pear shaped secondary wall thickenings are entirely encased by the S_3, as far as the wall/space interfaces are concerned. Some of the observed degrade in figure 5 could have been mechanical due to damage incurred during specimen preparation.

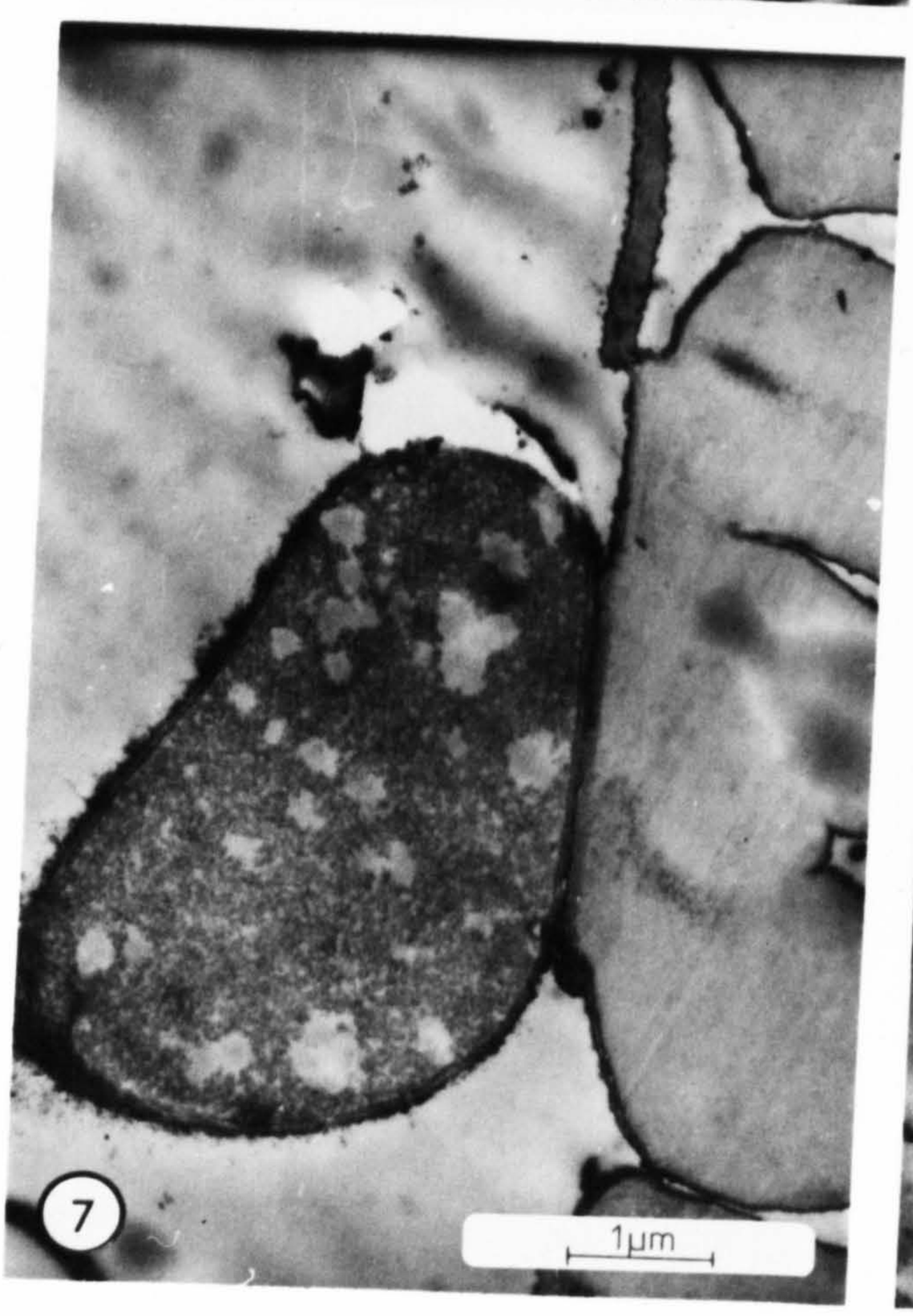
Figures 7 (x 13950 (TLS)) and 8 (x 17730 (TLS)) detail the presence of fungal hyphae on the well pitted regions of partly degraded vessel walls and the hypha in figure 8 can be seen penetrating the pit chamber and aperture of the adjacent cell wall. Note the general absence of mucilage.

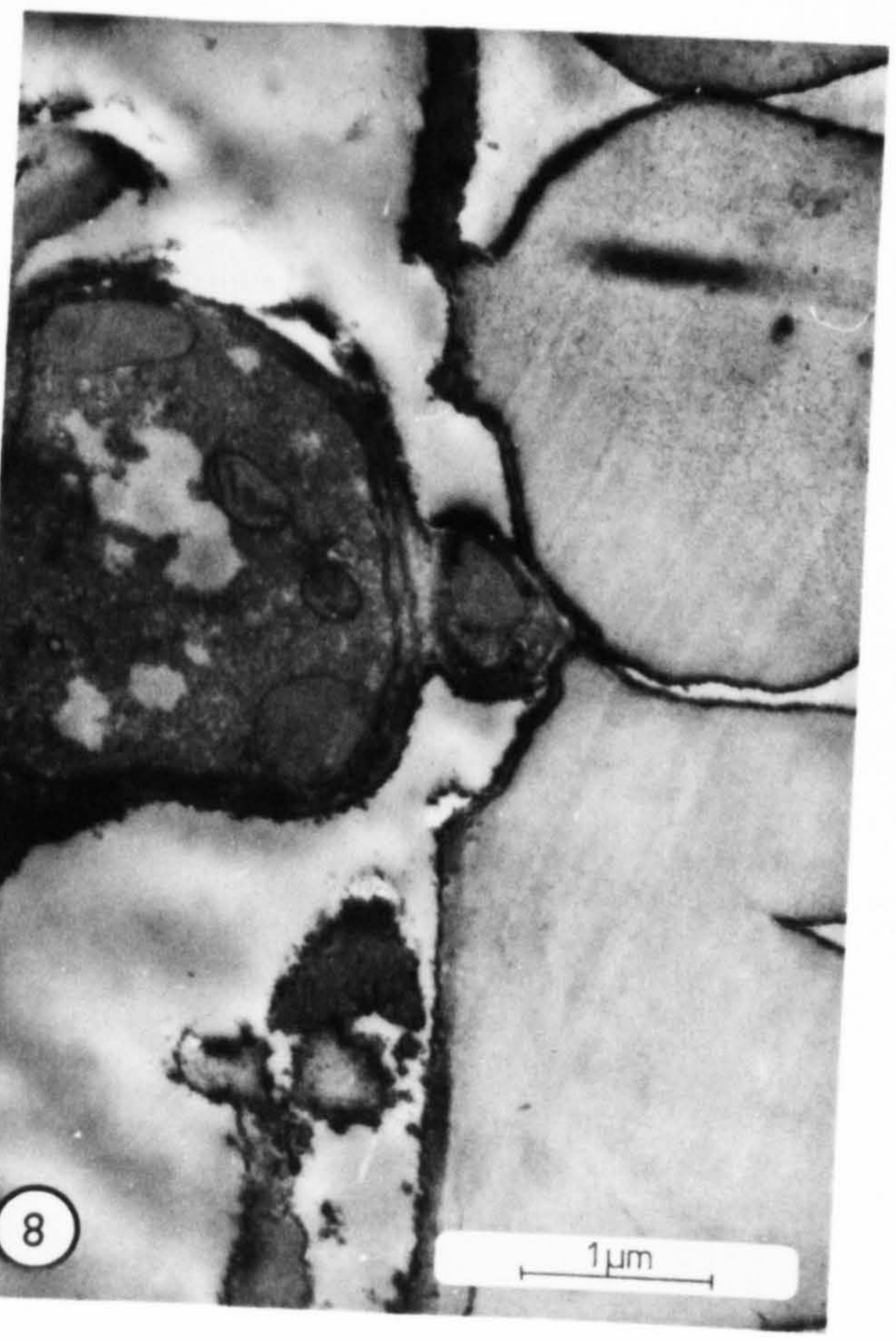
Figures 5-8:- Fixed with G, R, O and K and dehydrated with Durcupan.

Unstained sections.


H
O
H
5
5μm


6
2·5μm


7
1μm


8
1μm

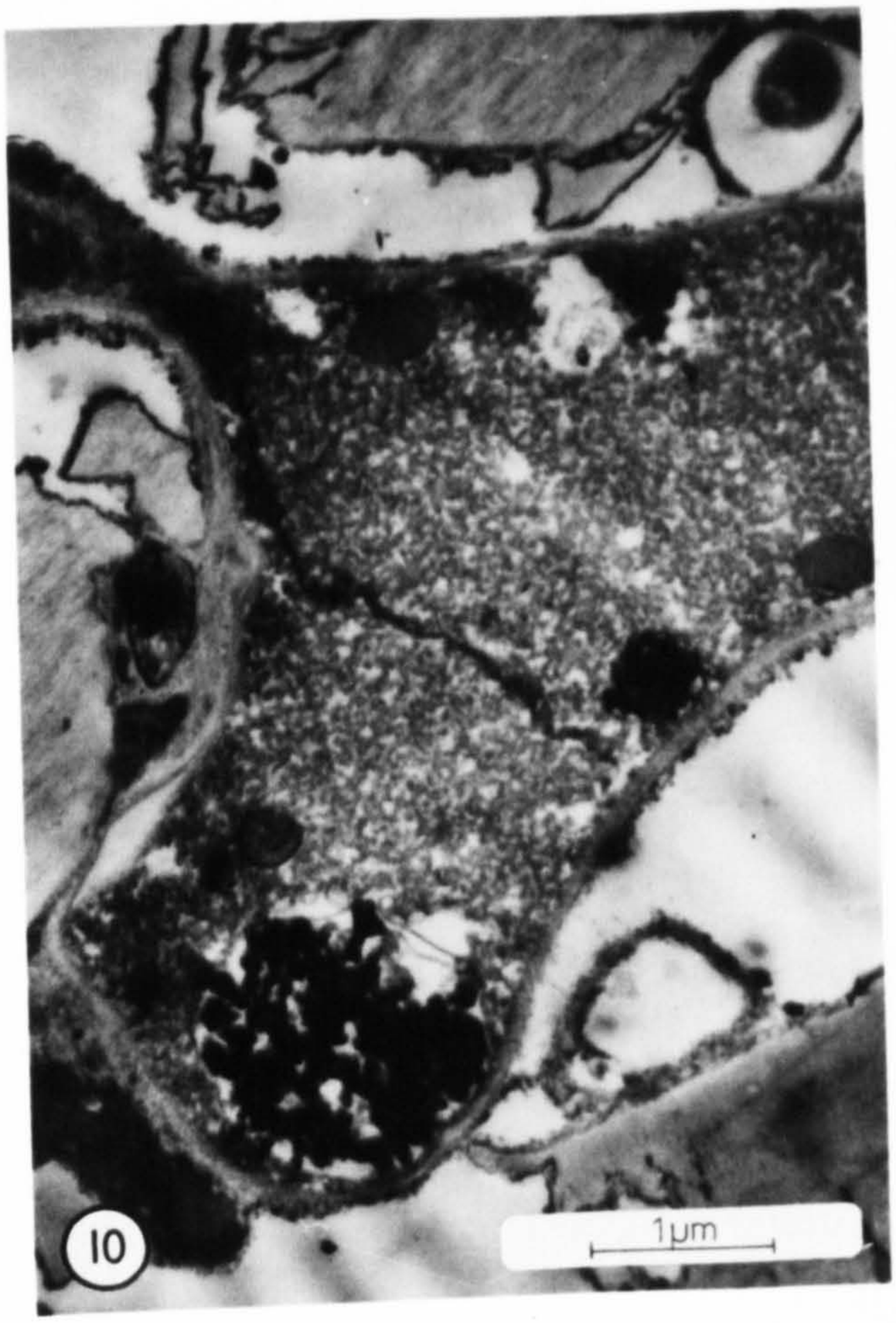
3.1.1 Coniophora puteana on birch (Betula sp.), 10 days

Figures 9 (x 9430 (TS)), 10 (x 17290 (TS)) and 11 (x 34250 (TS)) show one or two features on the attack of birch fibres. From the jig-saw fit of many of the wall fragments most of the wall damage had occurred during specimen preparation. However, within figure 9 several sections of normal hyphae, with detailed contents, can be seen. Also present were a number of very fine hyphae (Fh) in close association with areas of possible wall lysis (note the notching in the fibre walls). Most of these fine hyphae had suffered severe plasmolysis but organelles can clearly be seen in the fine hypha (Fh) detailed in figure 11.

The large accumulations of glycogen in some of the normal hyphae should be noted, a feature which appears to be very variable with no significant correlation to decay or other function in the material examined. Again note the general absence of mucilage.

Figures 9-11:- Fixed with G, R, O, K and dehydrated with Durcupan.
Unstained sections.


Fh
Fh
2·5µm
9


1µm
10


Fh
500nm
11

3.1.1 Coniophora puteana on birch (Betula sp.), 10 days

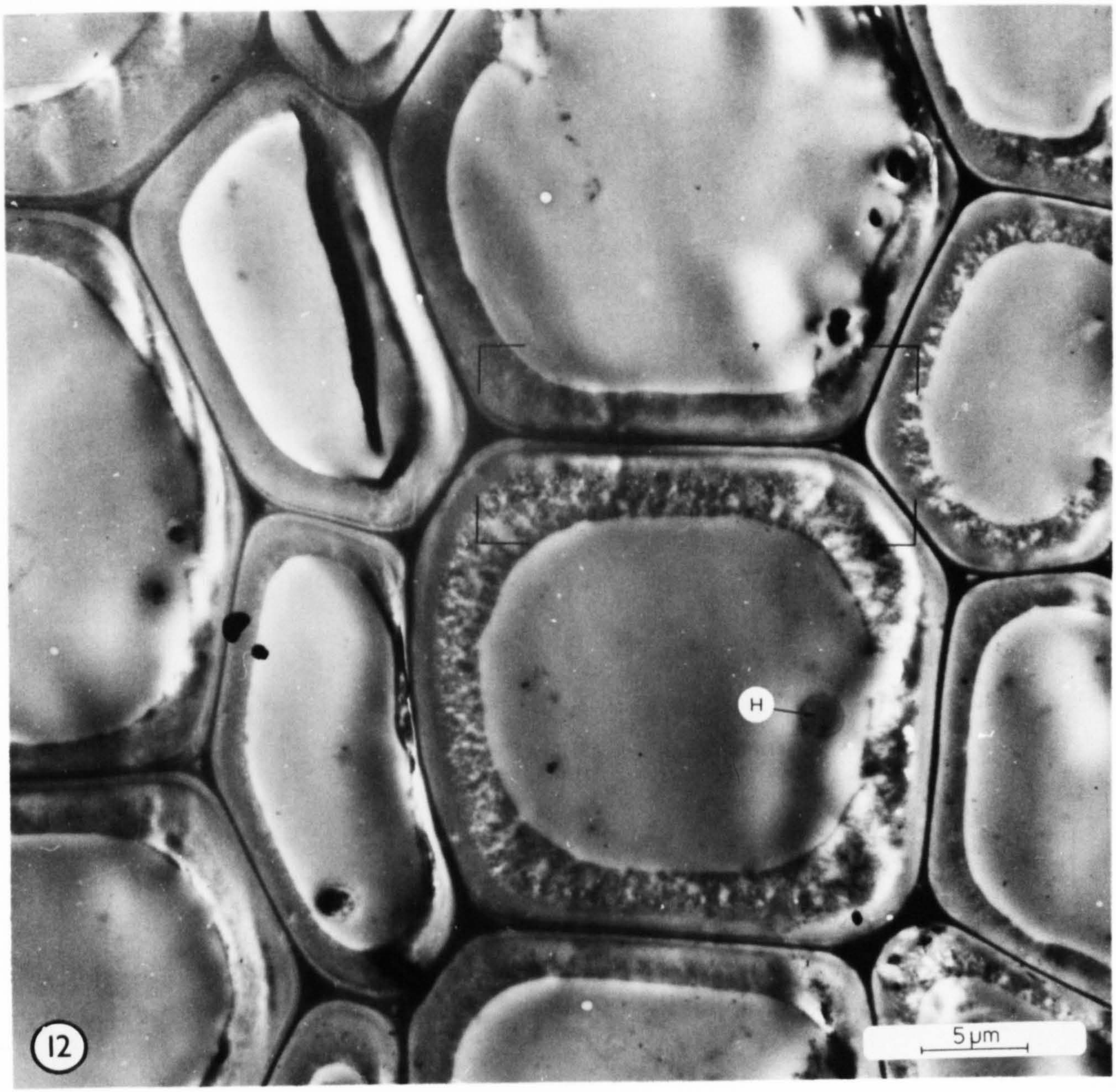
Figures 12 (x 3140 (TS)) and 13 (x 9720 (TS)) show very clearly extensive brown rot decay of birch fibres. The appearance of the wall lysis, resulting in a spongy residue, is in total agreement with other workers. The large central fibre has suffered severe degrade by the hypha (H) in the lumen and a comparison between a virtually sound wall and a degraded wall, figure 13, clearly demonstrates the change in structure of the wall.

The confinement of the lytic effect to individual cells is shown together with the apparent inability of the degrade to spread across the middle lamella. Although hyphae can be observed in apparently sound cells the walls indicate that lysis has not been initiated.

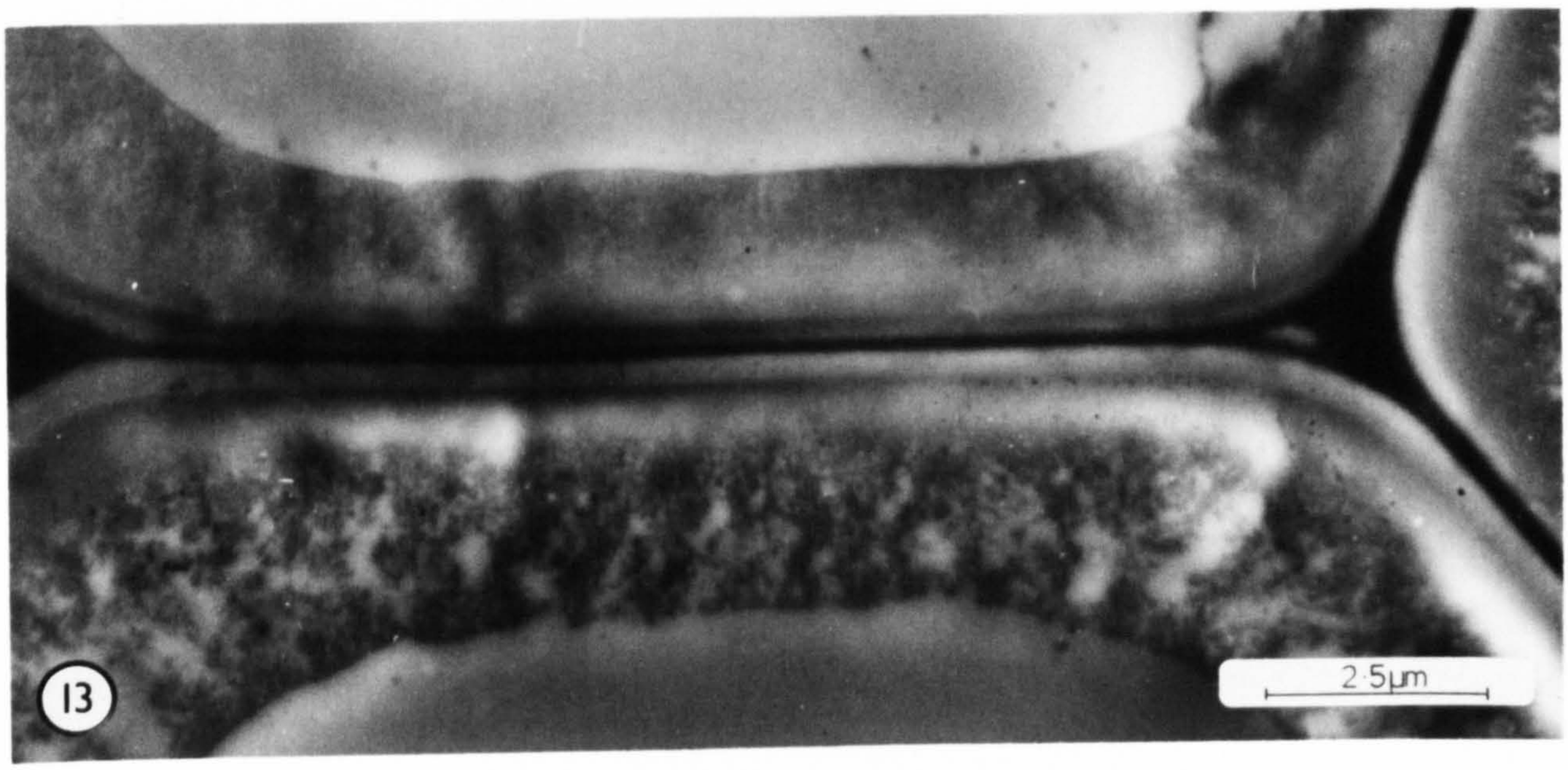
There was no evidence of mucilage being involved in wall lysis.

Figures 12 and 13:- Fixed with G, R, O and dehydrated with Durcupan.

Unstained sections.



12



13

4.1.2 Coniophora puteana on Scots pine (Pinus sylvestris)

The lack of membrane differentiation within the cytoplasm of these preparations could be attributed to the $KMnO_4$ component being absent from the second fixation stage. There was no evidence of an external mucilaginous sheath, as was also noted in the birch material, although debris, of unknown origin, was present on the hyphae and also on the cell walls, figs. 14 and 15. This debris was not a function of the wood formation as it could be seen coating resin drops on the S_3 of the tracheids, figs. 14 and 16.

Where wall lysis had occurred peculiar 'boot shaped' penetrations of the wall indicated a preference for S_1 wall material, with wall degrade ahead of the lysed regions shown by darker staining and cracking, fig. 17.

Sections of bordered pits between axial - ray tracheids, fig. 18 and axial - axial tracheids, fig. 19, revealed a difference in the appearance of the torus. Earlywood tori appeared to be thinner and more uniform in comparison with the thick lens-shaped profile of latewood tori between axial and ray tracheids. Hyphal passage through an earlywood bordered pit torus was achieved via a small, clean, penetration hole, leaving the remainder of the torus virtually undisturbed, figs. 20 - 21. This observation was in complete agreement with the scanning electron micrograph results of figs. 28 and 29.

3.1.2 Coniophora puteana on Scots pine (Pinus sylvestris), 4 weeks

Figures 14 (x 27530 (TS)), 15 (x 28140 (TS)) and 16 (x 14950 (TS)) detail some of the hyphal features observed. The contents apparently lack membrane details and this was attributed to the absence of $KMnO_4$ in the fixation. A certain degree of debris, of unknown origin, is visible around the hypha and on the cell walls.

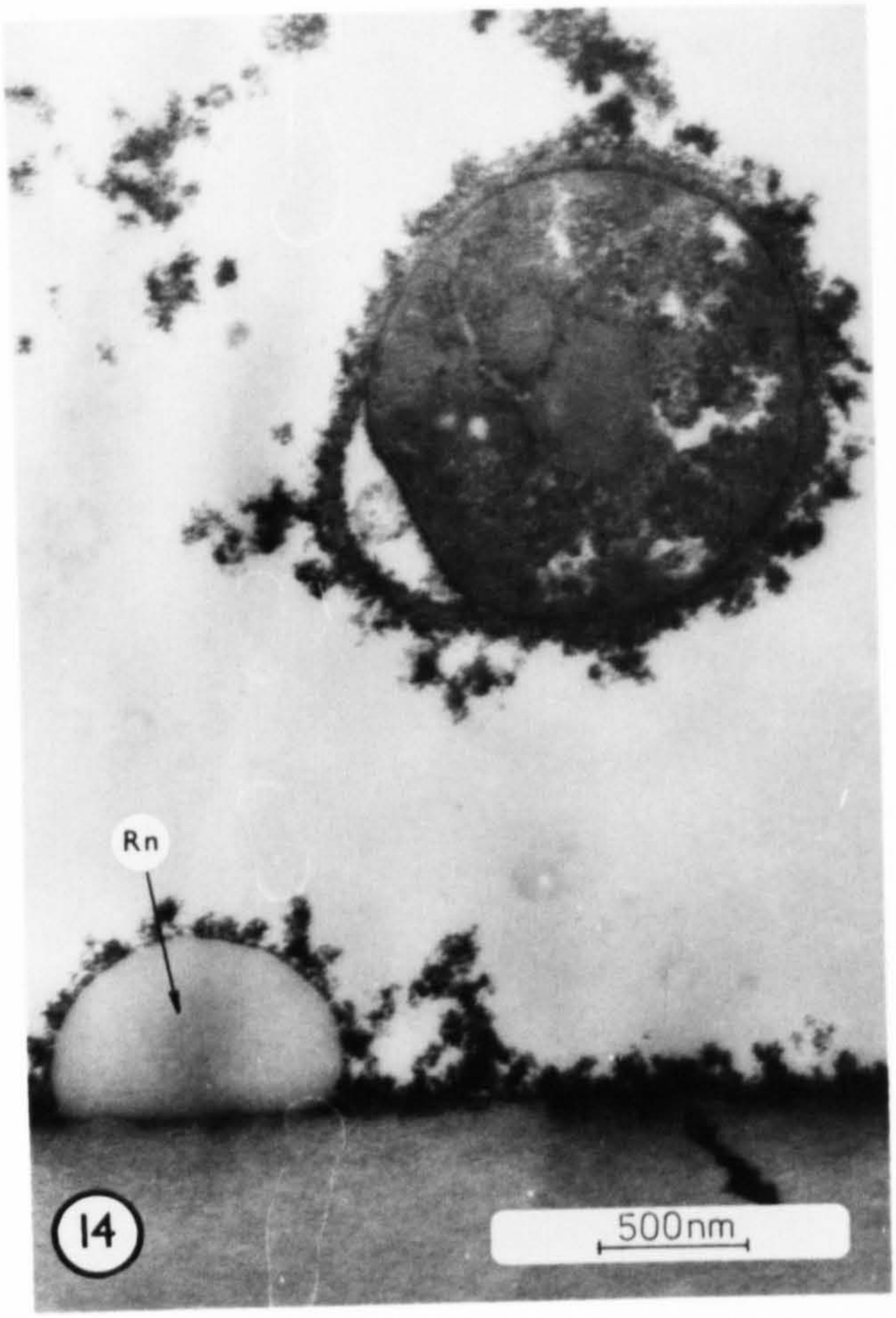
The extremely dense accumulation of vesicles in the hypha of figure 16 might be an artefact of fixation.

Smooth, hemispherical, deposits were frequently observed on the tracheid walls and these are probably resin (Rn) droplets originating from the wood.

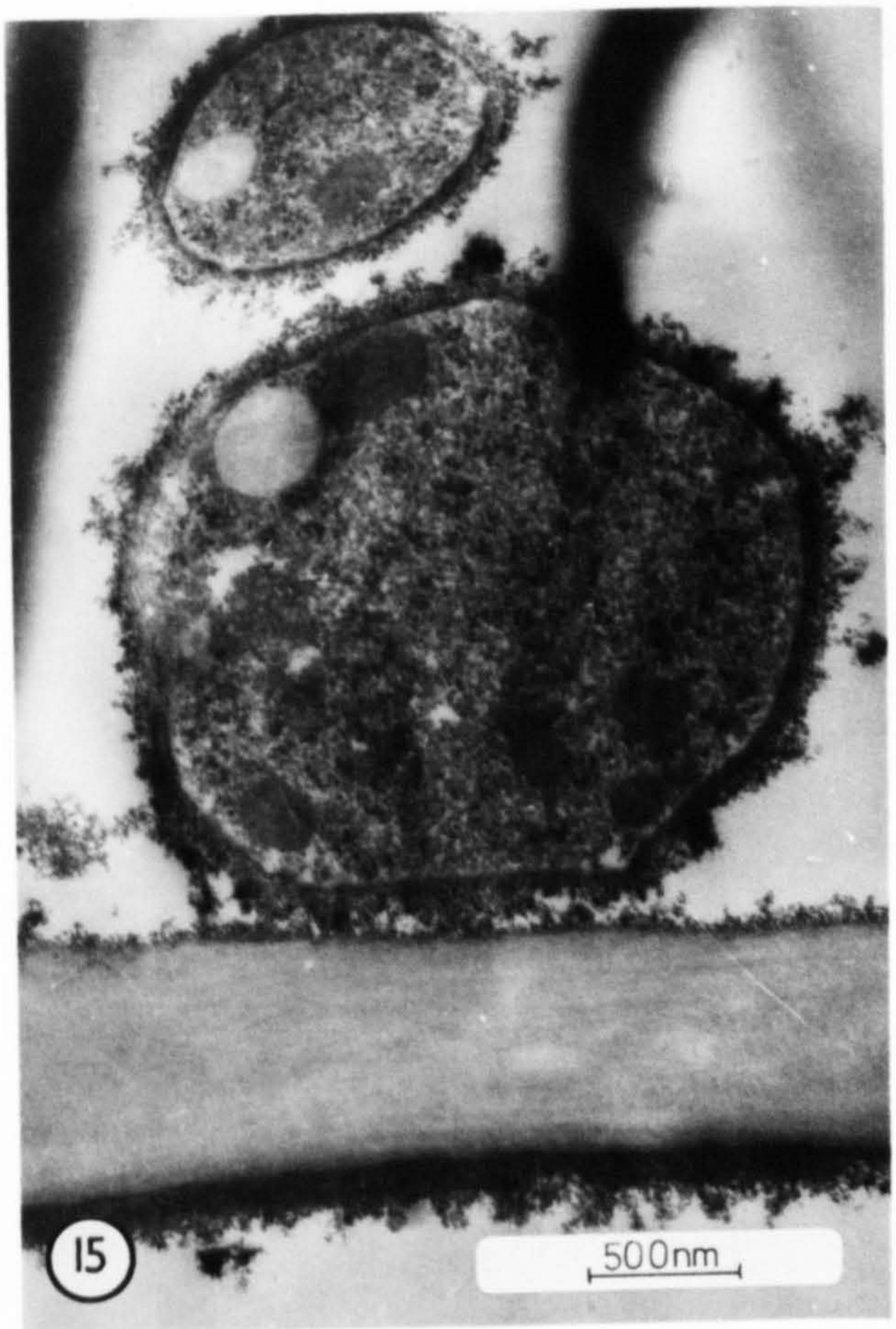
Figure 17 (x 11150 (TS)) shows the junction between three tracheids and illustrates a feature frequently observed but very difficult to interpret. The 'boot' shaped lysis regions, often without sign of any hyphae, always showed a right angled turn in the S_1 region of the wall where degrade ahead of the cleared wall was evident as cracked and deeper staining regions.

Figures 14-17:- Fixed with G, R, O and dehydrated with Durcupan.

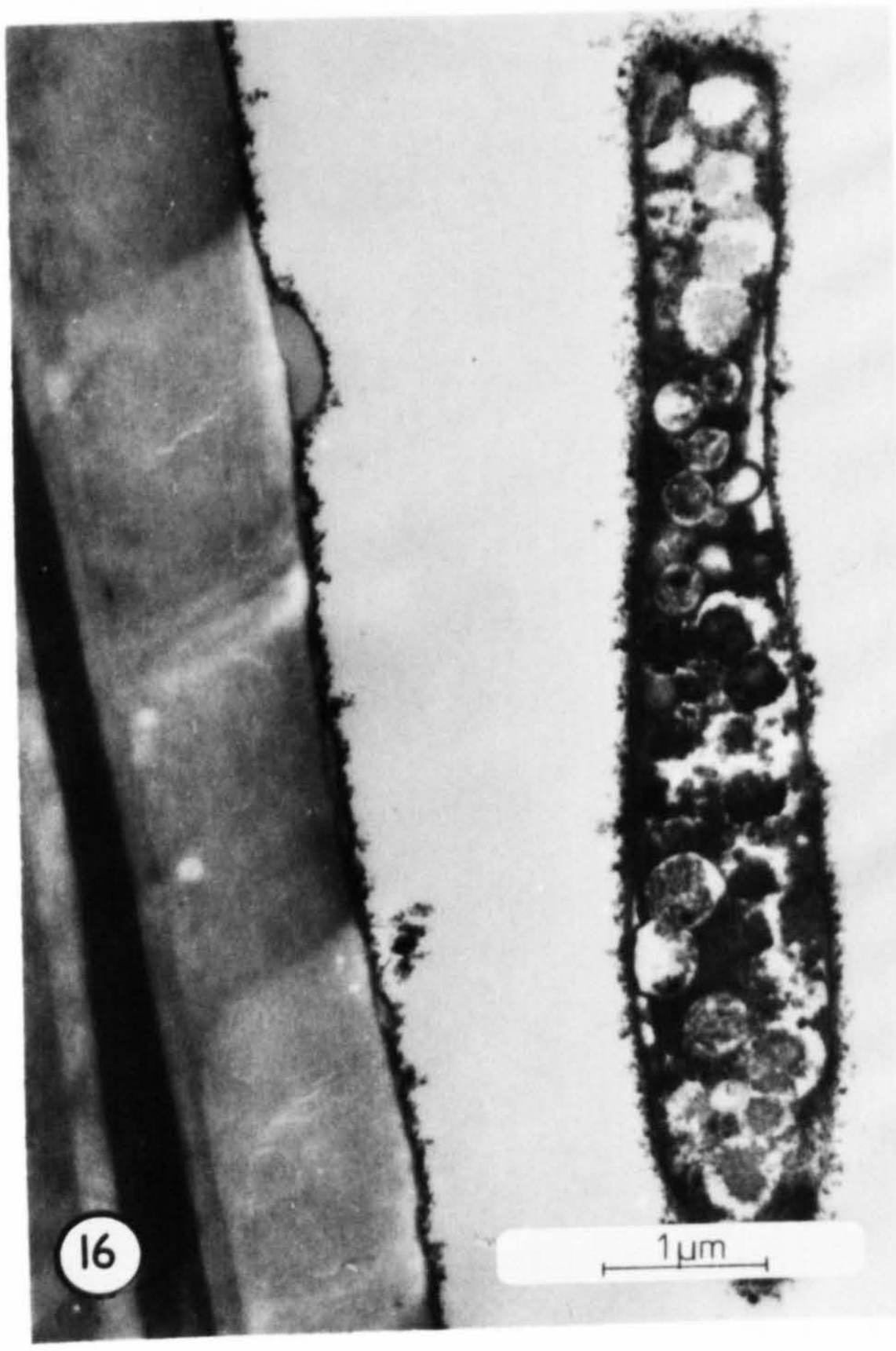
Unstained sections.



14



15



16



17

3.1.2 Coniophora puteana on Scots pine (Pinus sylvestris), 4 weeks

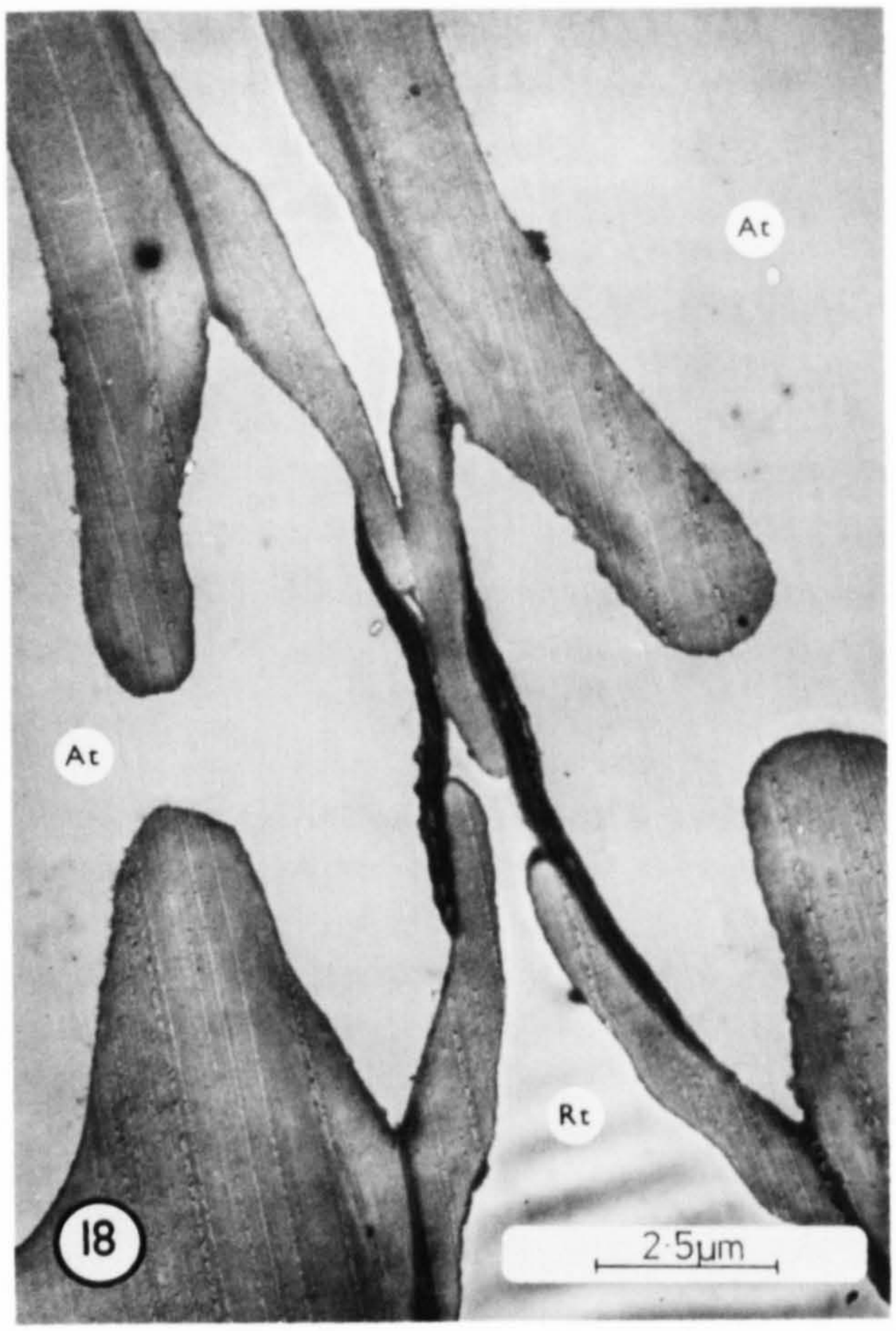
Figure 18 (x 6880 (TS)) has been included to illustrate bordered pit pairing between two latewood axial tracheids (At) and a common ray tracheid (Rt). The thinner, irregular (dentate), thickening of the ray tracheid is clearly evident together with thick tori bearing darker and lighter staining inclusions.

The normal earlywood axial tracheid bordered pit pair in figure 19 (x 6590 (TS)) differs from figure 18 in that the pit borders are equally thickened and the torus (delimited (Ts)) is thinner and more uniform. A small hypha (H) in section can also be seen.

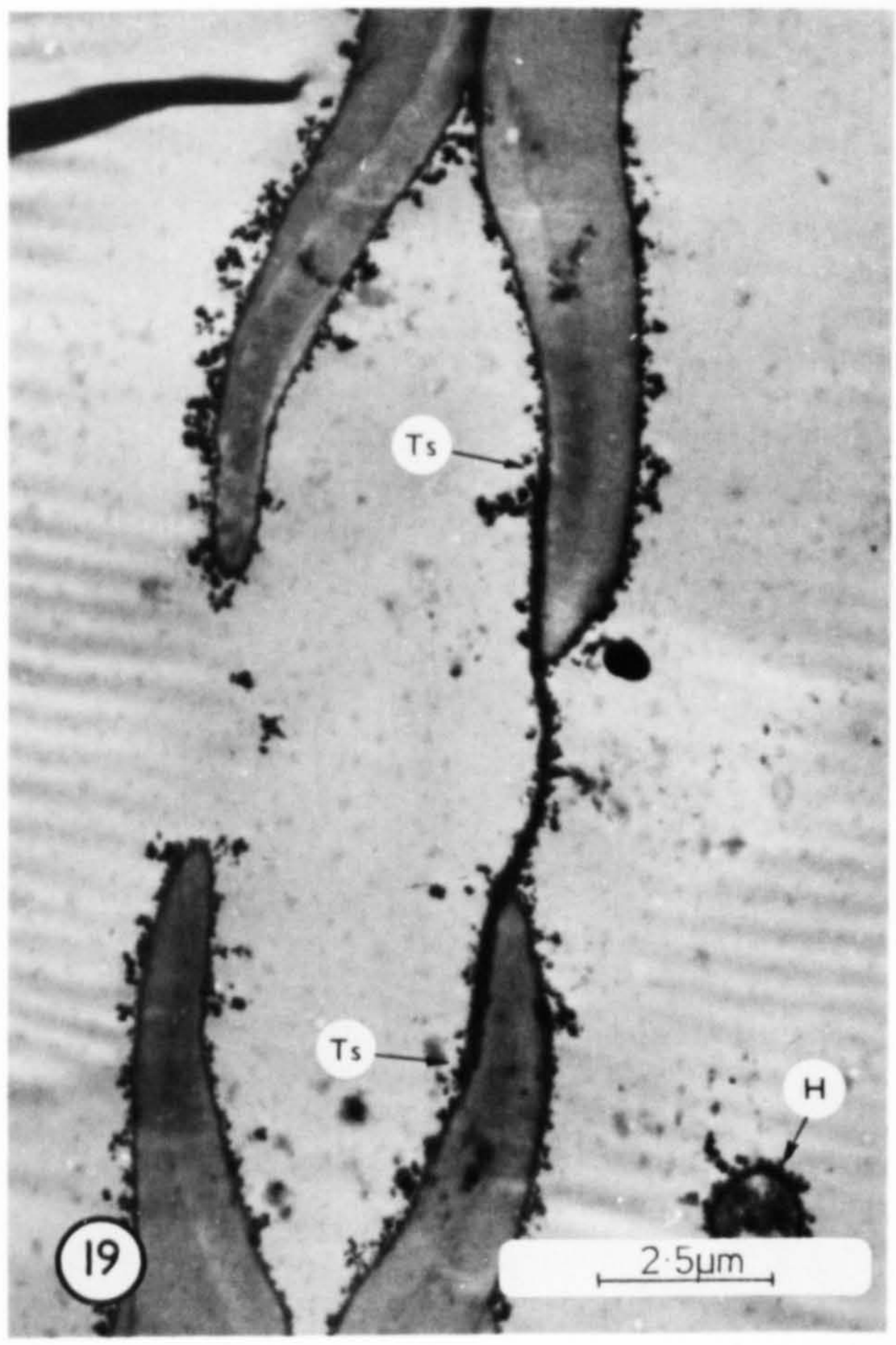
Penetration of a bordered pit pair, on the earlywood - latewood junction, by the fungus is demonstrated by the serial sections of figures 20 (x 6740 (TS)) and 21 (x 6740 (TS)). A neat hole has been made in the torus just large enough for the passage of the hypha and the remains of the torus can be seen on either side of the fungus.

Figure 18:- Fixed with G, R, O and dehydrated with glycol methacrylate (GMA).

Figures 19-21:- Fixed with G, R, O and dehydrated with Durcupan. All sections were unstained.



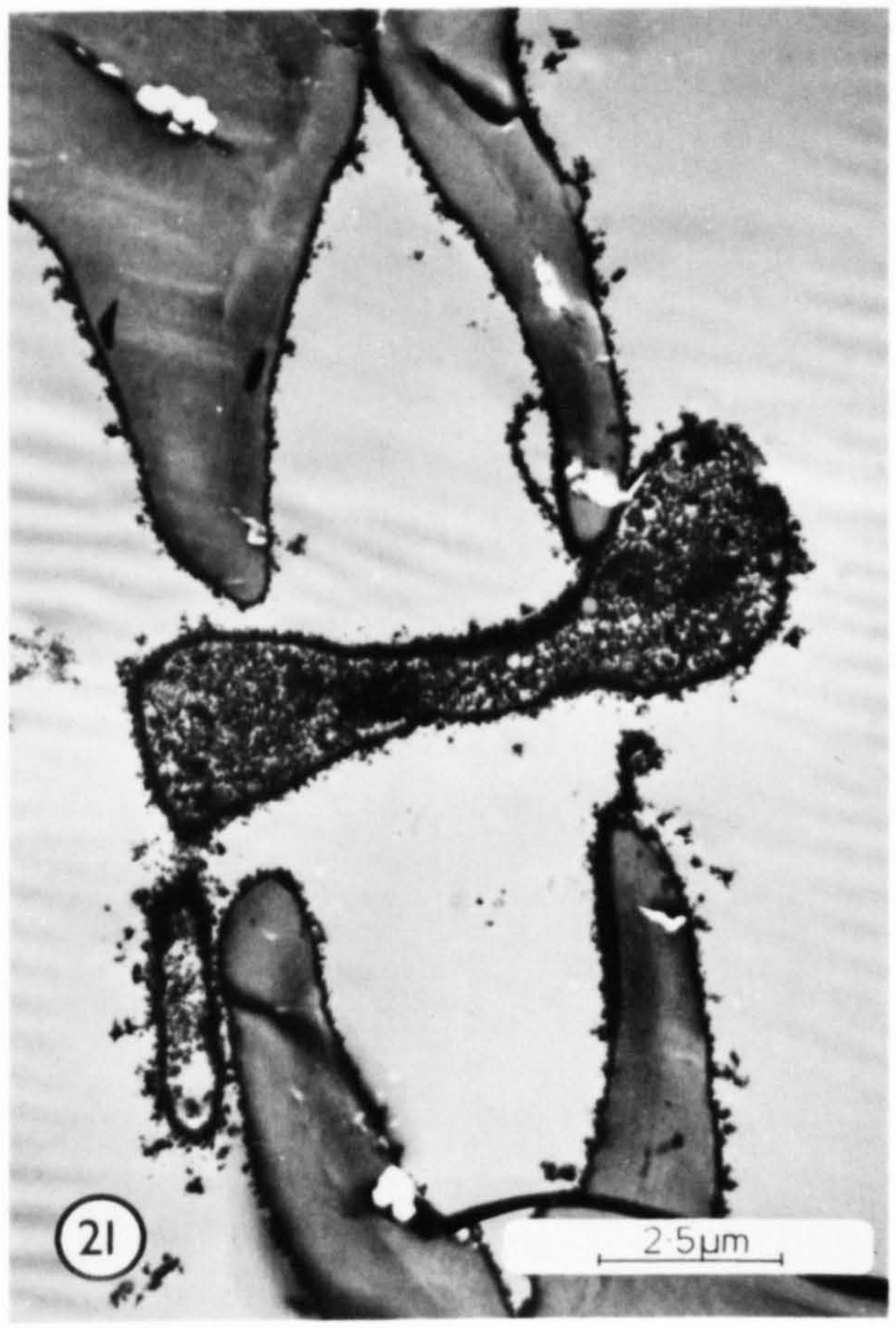
18



19



20



21

4.2.1 Chaetomium globosum on birch (Betula sp.)

Although cavities were not found in this material a number of interesting points of soft rot attack on birch were revealed. A common feature was the presence of notching in fibre walls (Corbett type 2, 1965) caused by hyphae closely appressed to the S_3, fig. 22. In many examples, these 'V' shaped notches were very precise and were frequently filled with a dense staining material continuous over the hyphal surface, figs. 23 and 24. The angle of the notching was similar to that expected for normal cavity points in S_2 degrade of birch fibres by Chaetomium globosum. Extremely large erosion zones were also encountered in older material, fig. 25. Some views of notching indicated that the S_3 was resistant to lysis in the early stages of attack, fig. 27, although in the later stages it was frequently absent.

The presence of mucilage in association with soft rot hyphae was observed for a number of hyphal-wall contact situations. Mucilage was evident in bore holes, fig. 29, penetration hyphae, fig. 31, surrounding hyphae in fibre lumina, fig. 32 and extensive fibre lysis, fig. 33.

A sequence of serial sections identified the formation of a 'T' branch by a hypha actively involved in wall erosion from the lumen, fig. 35. Penetration of, and growth along, the middle lamella region and S_1 wall layers was also observed in a number of specimen examples, fig. 36.

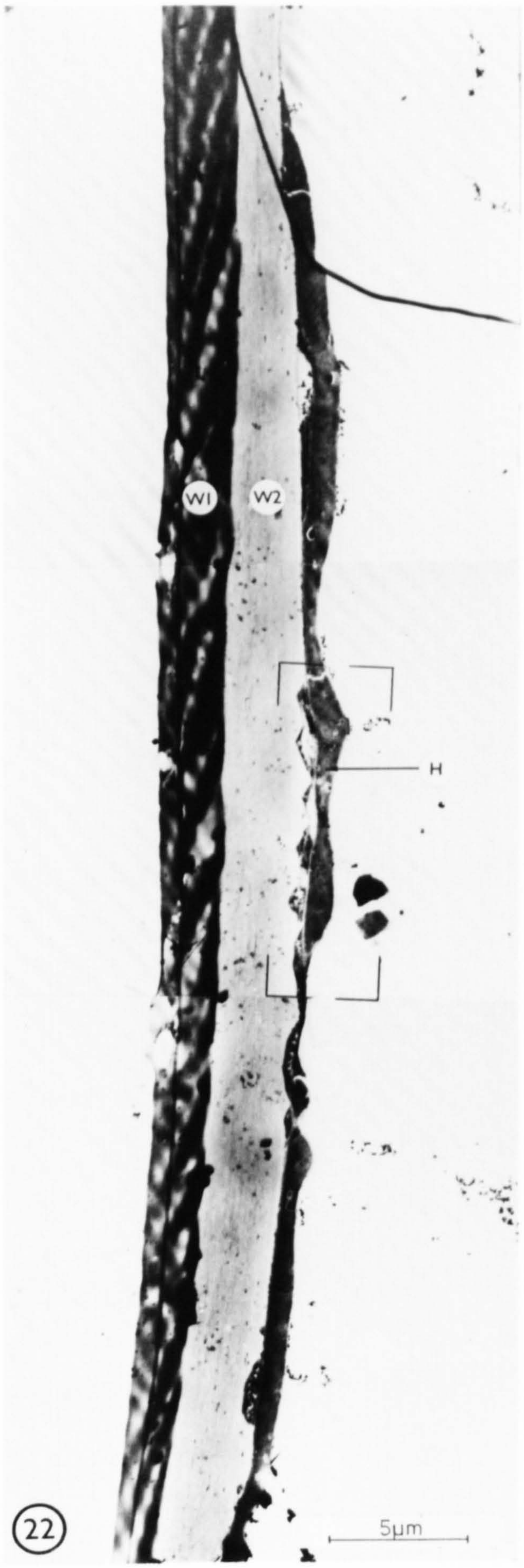
The progressive development of wall erosion and the lysis patterns created are shown by a series of micrographs indicating the roles of surface tension and mucilage in the formation of erosion channels, central hyphal ridges and, later, severe erosion troughs, figs. 37 - 40.

3.2.1 Chaetomium globosum on birch (Betula sp.), 10 days

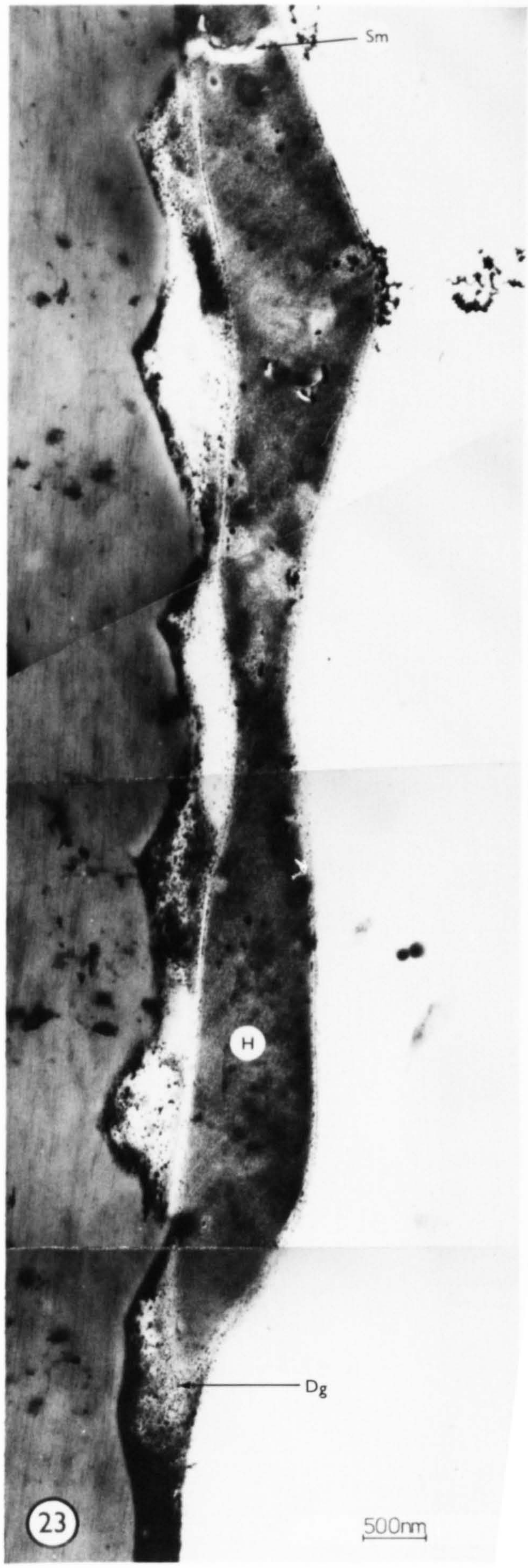
Figures 22 (x 4370 (TLS)) and 23 (x 20580 (TLS)) demonstrate the only significant decay pattern observed in the T.E.M. for the soft rot attack of birch. Figure 22 shows two fibre walls (W 1, W 2) (the details of W1 being obliterated by wrinkling) with a fungal hypha (H) closely appressed to the visible fibre wall. A number of 'V' shaped notches in the wall (Corbett type 2, 1965) can be seen and at higher magnification, figure 23, show remarkable precision in their formation. The angle of the 'V' follows very closely the expected angle for cavities formed in the S_2 of birch fibres by this fungus.

The notches are frequently filled with a dense, almost granular, material and it might be significant to note that the dark staining granules (Dg) present within the notches appear to be continuous over the hyphal wall. Note also that the septum (Sm) appears to straddle a ridge of sound fibre wall.

Figures 22 and 23:- Fixed with G, R, O and dehydrated with Durcupan. Stained with uranyl acetate (U.ac) and lead citrate (PbC).



22



23

3.2.1 Chaetomium globosum on birch (Betula sp.)

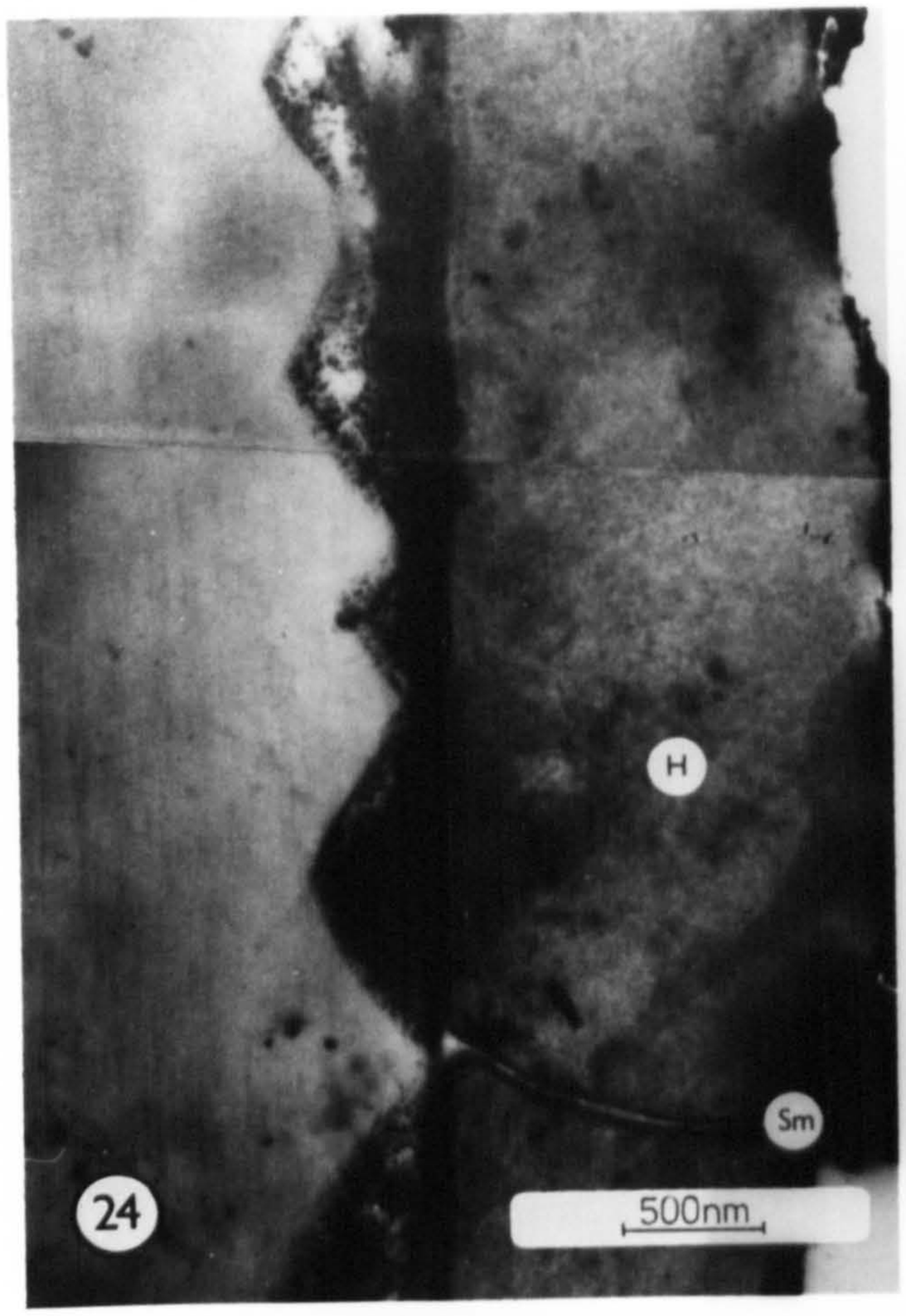
Figures 24 (x 26730 (TLS)) and 25 (x 26730 (TLS)) continue to illustrate the extremely geometrical patterning of the notches, all with the same angles but of varying depth. The dense material is present together with the septum (Sm) straddling a ridge. Organelles are faintly visible within the hyphae but the absence of $KMnO_4$ has resulted in little information on membrane-bound structures.

Figure 26 (x 20000 (TLS)) shows how precise and large some of the notches can be cut. The causal hypha lies along the line of the old S_3, a remnant of which is visible at the top of the micrograph. Extensive plasmolysis and cytoplasmic disorganisation of the hypha has occurred. It may be significant to note that figure 26 was from 4 week material compared to 10 day material for figures 24 and 25.

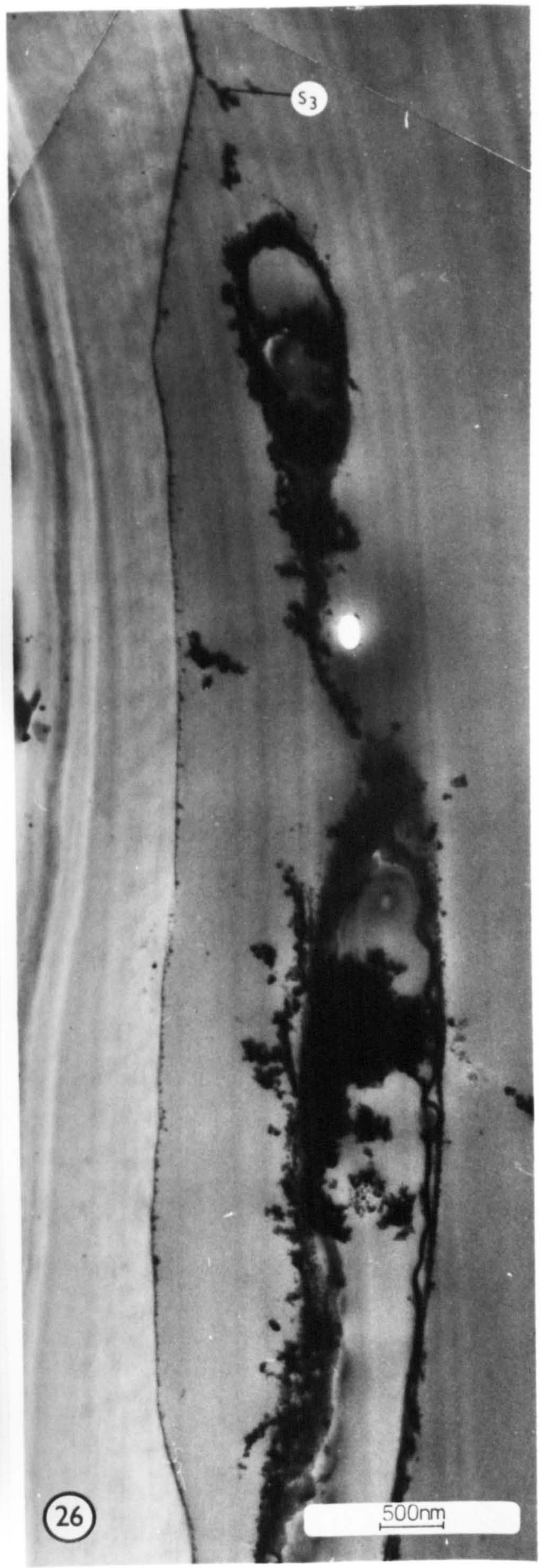
Figures 24-26:- Fixed with G, R, O and dehydrated with Durcupan.

Figures 24-25:- 10 day material stained with Uac and PbC.

Figure 26:- 4 week material, unstained.


H
Sm
24
500nm


25
500nm


S3
26
500nm

3.2.1 Chaetomium globosum on birch (Betula sp.)

The extremely plasmolysed hyphae (H) of figure 27 (x 32870 (TLS)) can be seen in conjunction with notches in the fibre wall as previously described. However, also present in this micrograph is an intact S_3 wall layer and indications of the possible presence of mucilage (Mu) in this lytic process.

Figure 28 (x 21230 (TLS)) shows the notches being eroded at the contact point between hypha and wall. As serial sections were not available of this particular view it is impossible to say whether this was a hyphal tip or whether the hypha bent out of the plane of section, the latter being more likely from the thickness of the hyphal wall.

The strange geometry of the bore hole in figure 29 (x 14820 (TLS)) is difficult to explain but has been included to demonstrate the presence of mucilage (Mu) in active wall lysis.

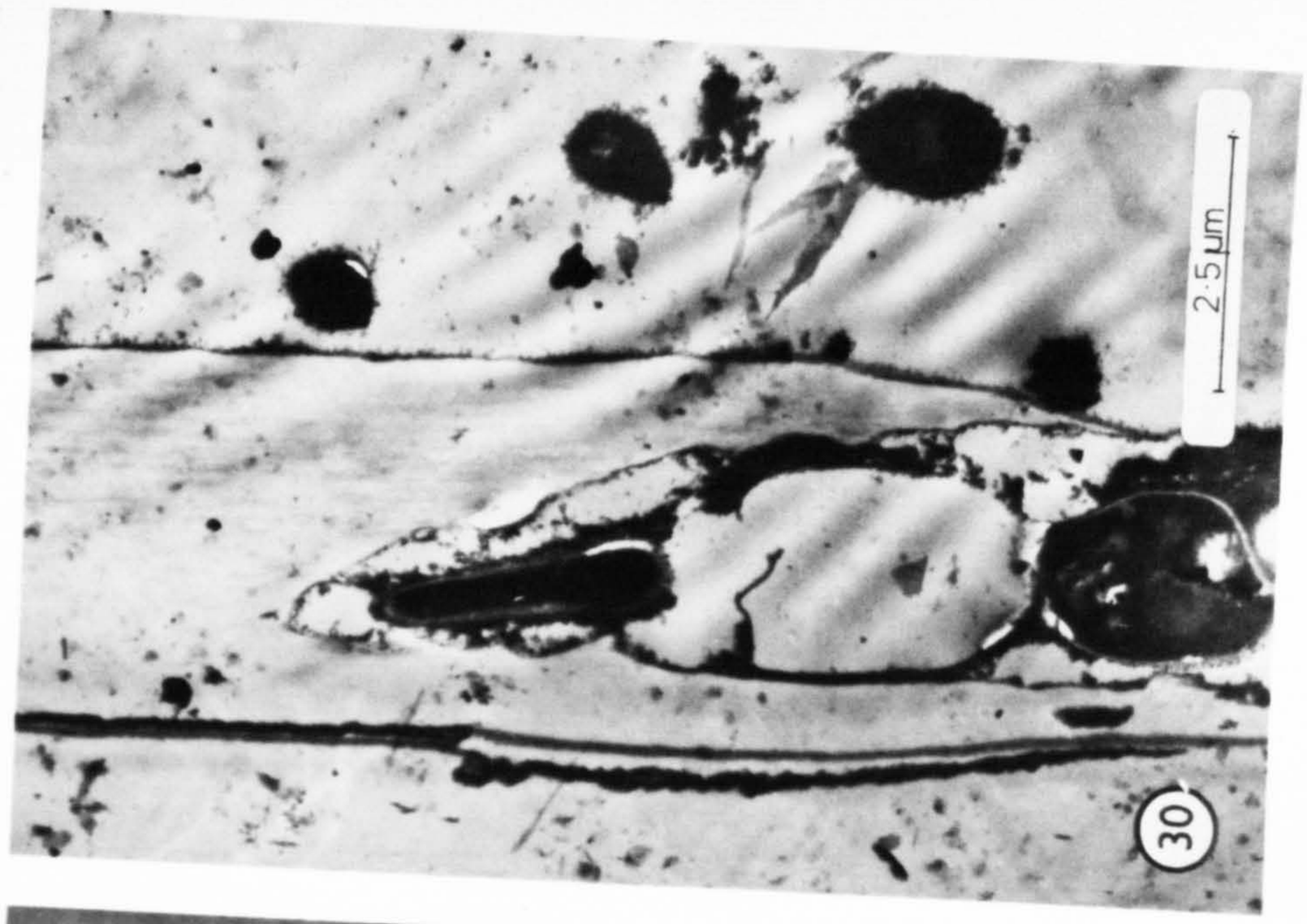
The hypha degrading the fibre S_2 in figure 30 (x 9620 (TLS)) and the surrounding hyphae bear significant investment material which could be mucilage. The hypha has penetrated the open cell wall via the cut fibre wall just out of the field of view.

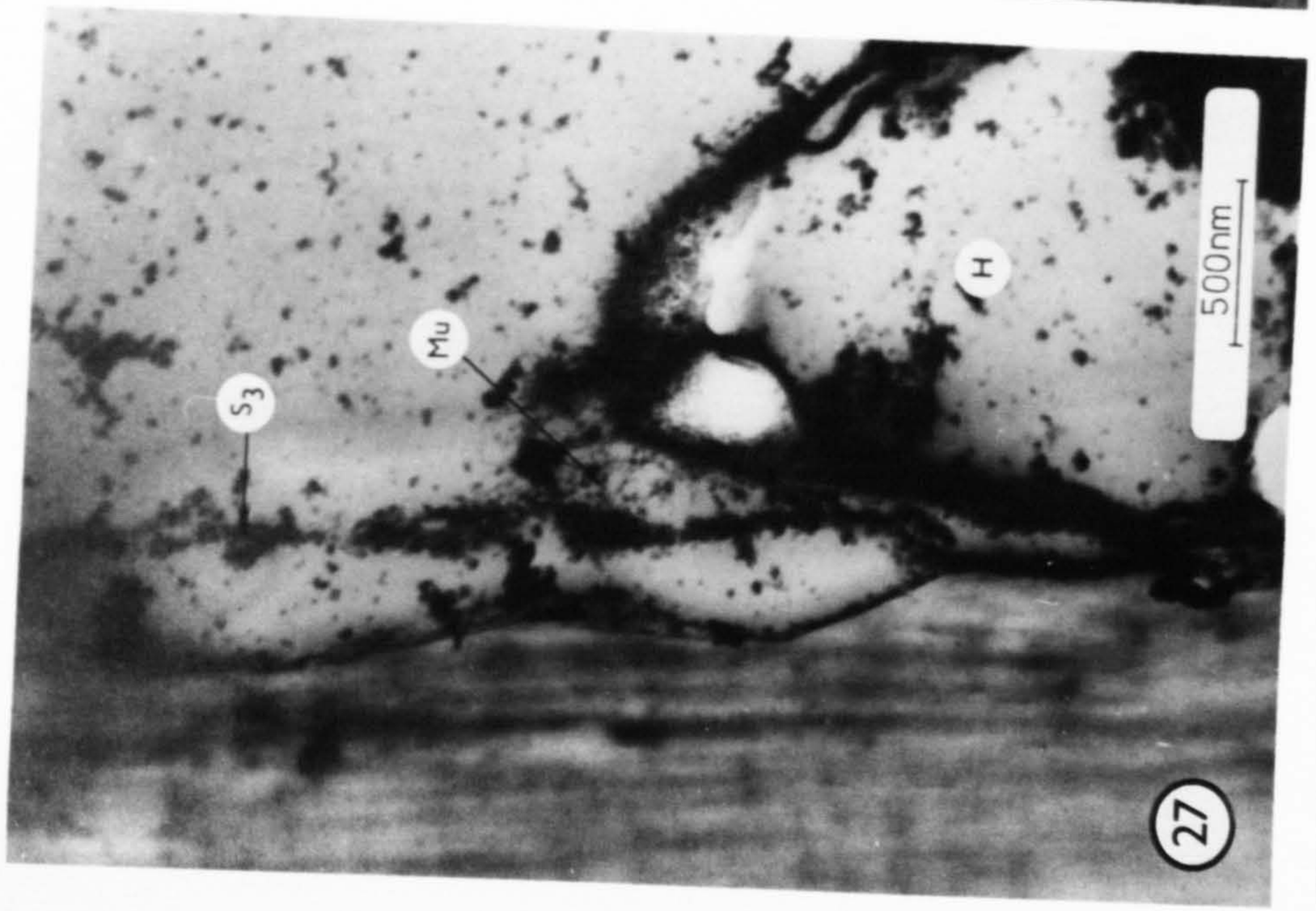
Figures 27-30:- Fixed with G, R, O and dehydrated with Durcupan.
All stained with Uac and PbC.

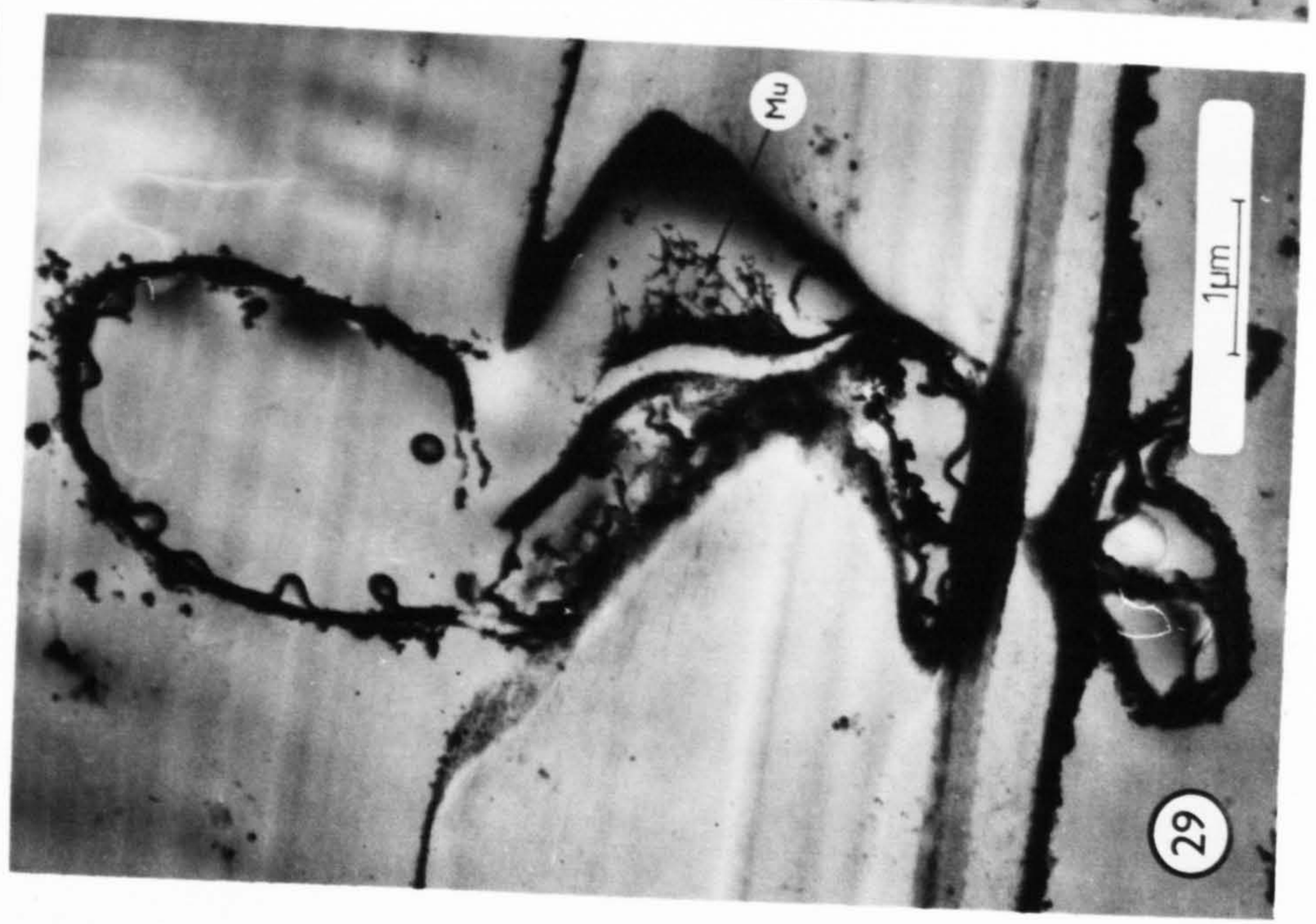
Figures 27 and 29:- 4 week material.

Figures 28 and 30:- 10 day material.


500nm
28


2·5 µm
30


S3
Mu
H
500nm
27


Mu
1µm
29

3.2.1 Chaetomium globosum on birch (Betula sp.)

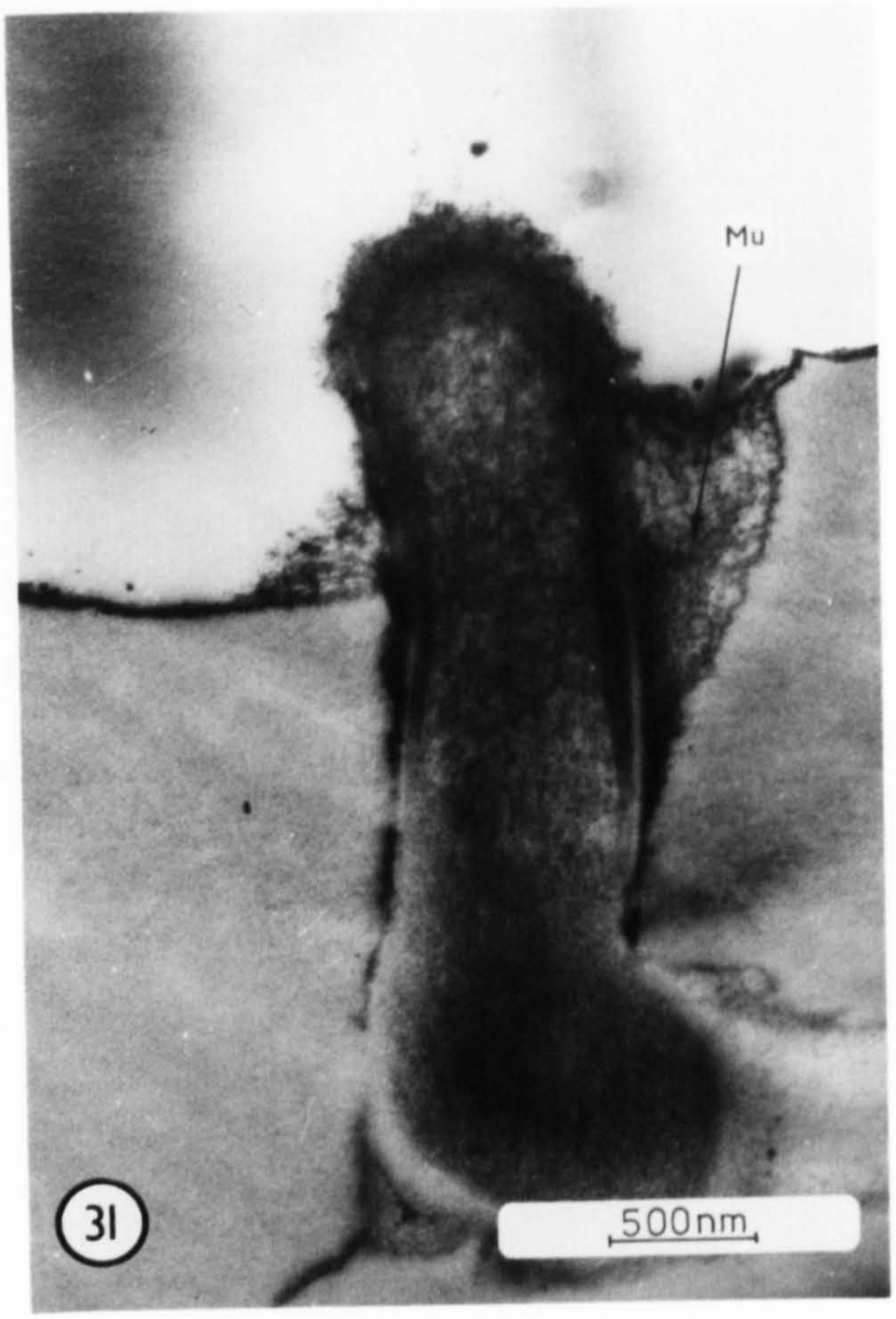
Figures 31 (x 28810 (TS)), 32 (x 8730 (TLS)) and 33 (x 13500 (TS)) show the presence of mucilage with hyphae involved in a variety of wall contacts. The fine penetrating hypha of figure 31 has created a funnel-shaped lysis of the wall which is filled with mucilaginous material (Mu). Figure 32 demonstrates abundant mucilage around a hypha present in a fibre lumen. The severe degradation of the fibre in figure 33 has been caused by the hyphae (H) with an extensive investment of mucilage (Mu).

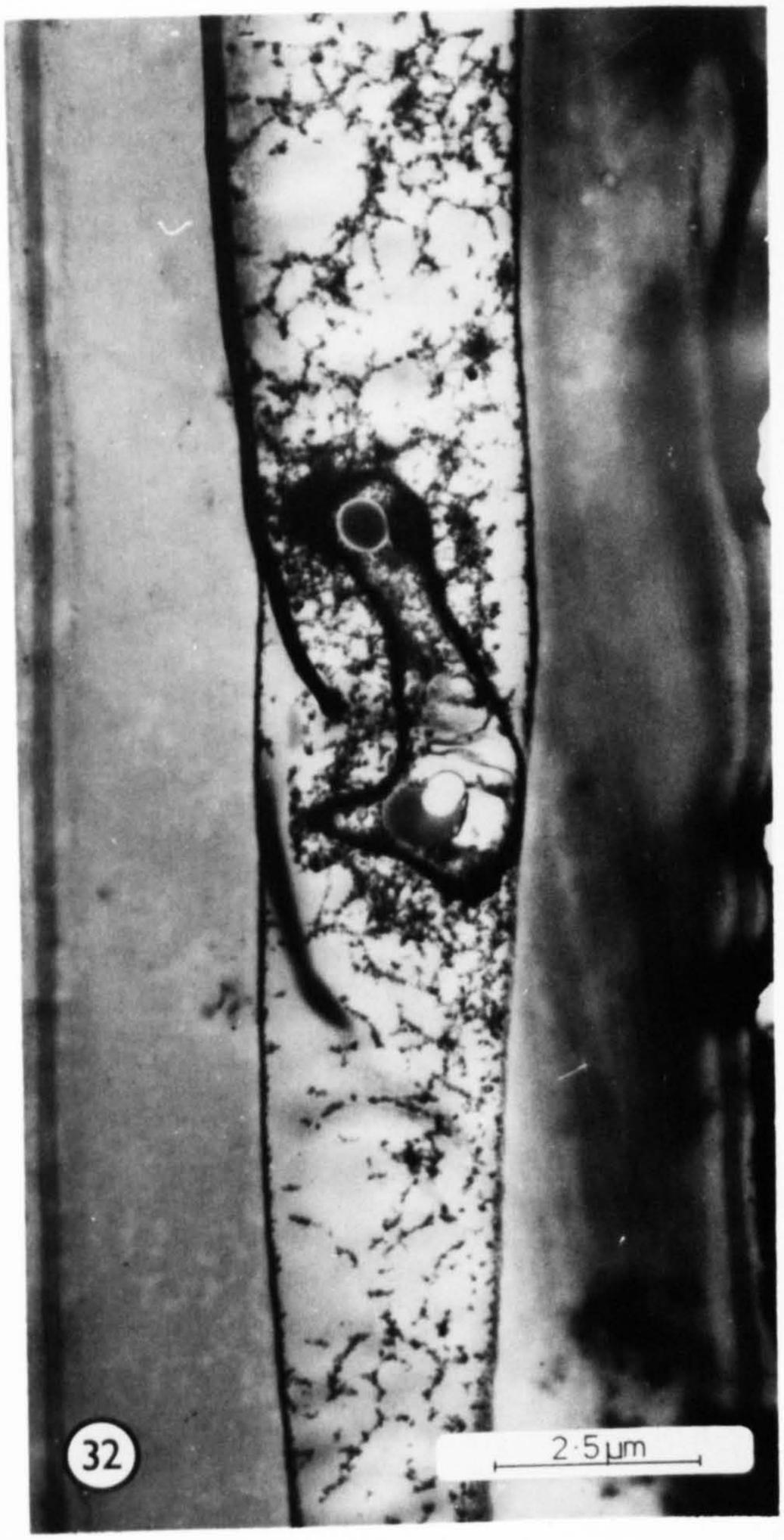
Figure 34 (x 20220 (TS)) shows a hypha engaged in lumen erosion of a fibre wall and has also produced a fine penetration hypha reaching deep into the S_2 of the wall. This possibly represents the first stage of 'T' branch formation.

Figures 31, 33, 34:- Fixed with G, R, O, K and dehydrated using Durcupan. 10 day material.

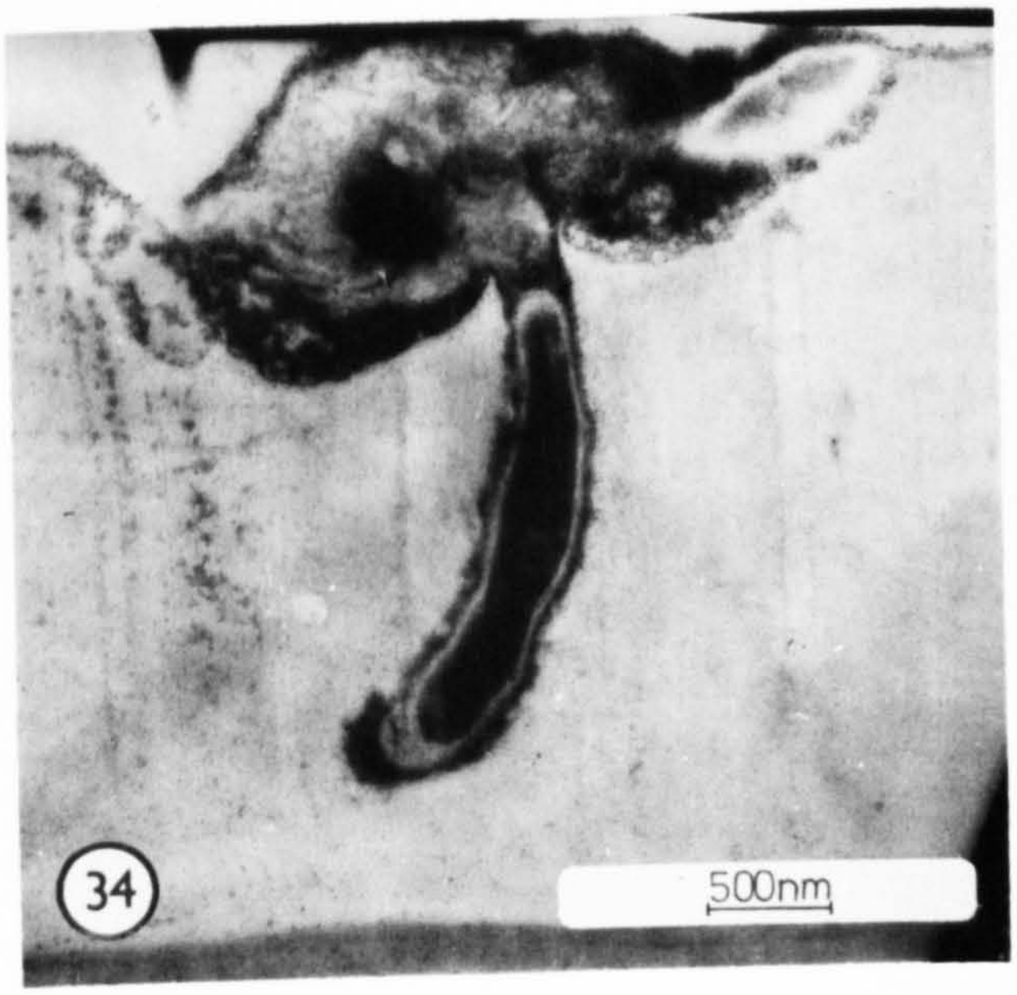
Figure 32:- Fixed with G, R, O and dehydrated using GMA. 4 week material.

All sections were unstained.


Mu
31
500nm


32
2·5µm


Mu
H
33
1µm


34
500nm

3.2.1 Chaetomium globosum on birch (Betula sp.), 10 days

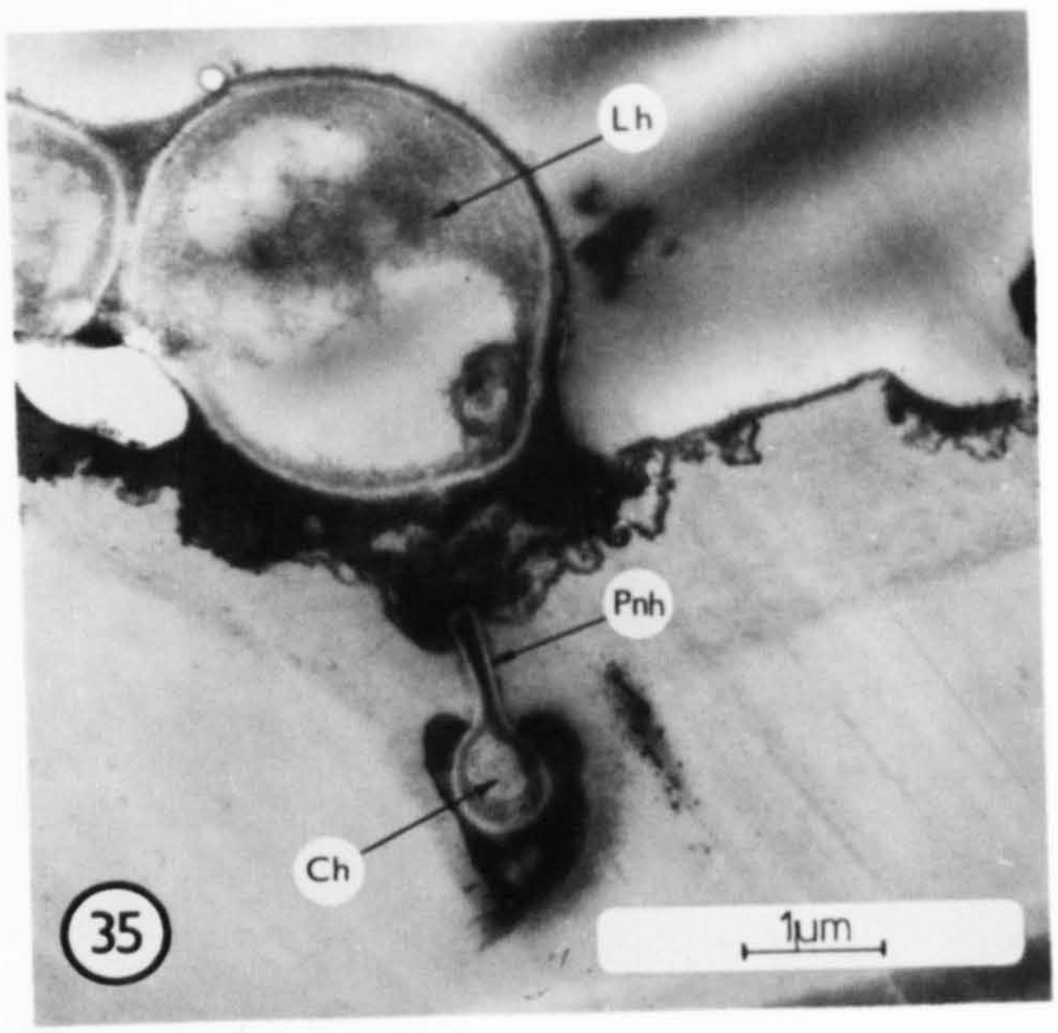
Figure 35 (x 11390 (TS)) shows a hypha (H) actively involved in wall erosion from the lumen of a birch fibre. The hypha has produced a penetration hypha (Pnh) that has 'T' branched into the active soft rot cavity hypha (Ch) growing at right angles to the plane of the micrograph.

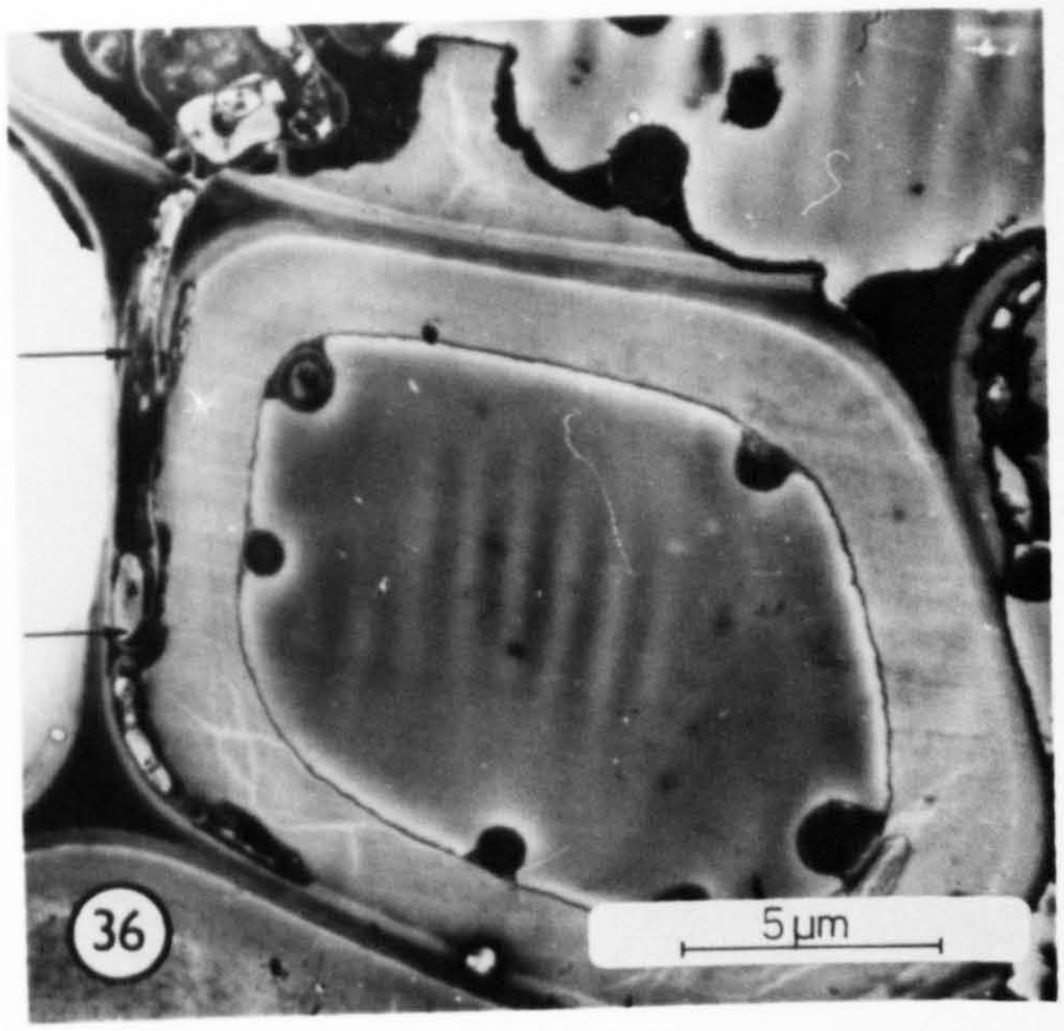
Figure 36 (x 3940 (TS)) illustrates extensive colonisation of a birch fibre together with invasion of the middle lamella - S_1 region by a hypha (arrowed) originating from surface colonisation.

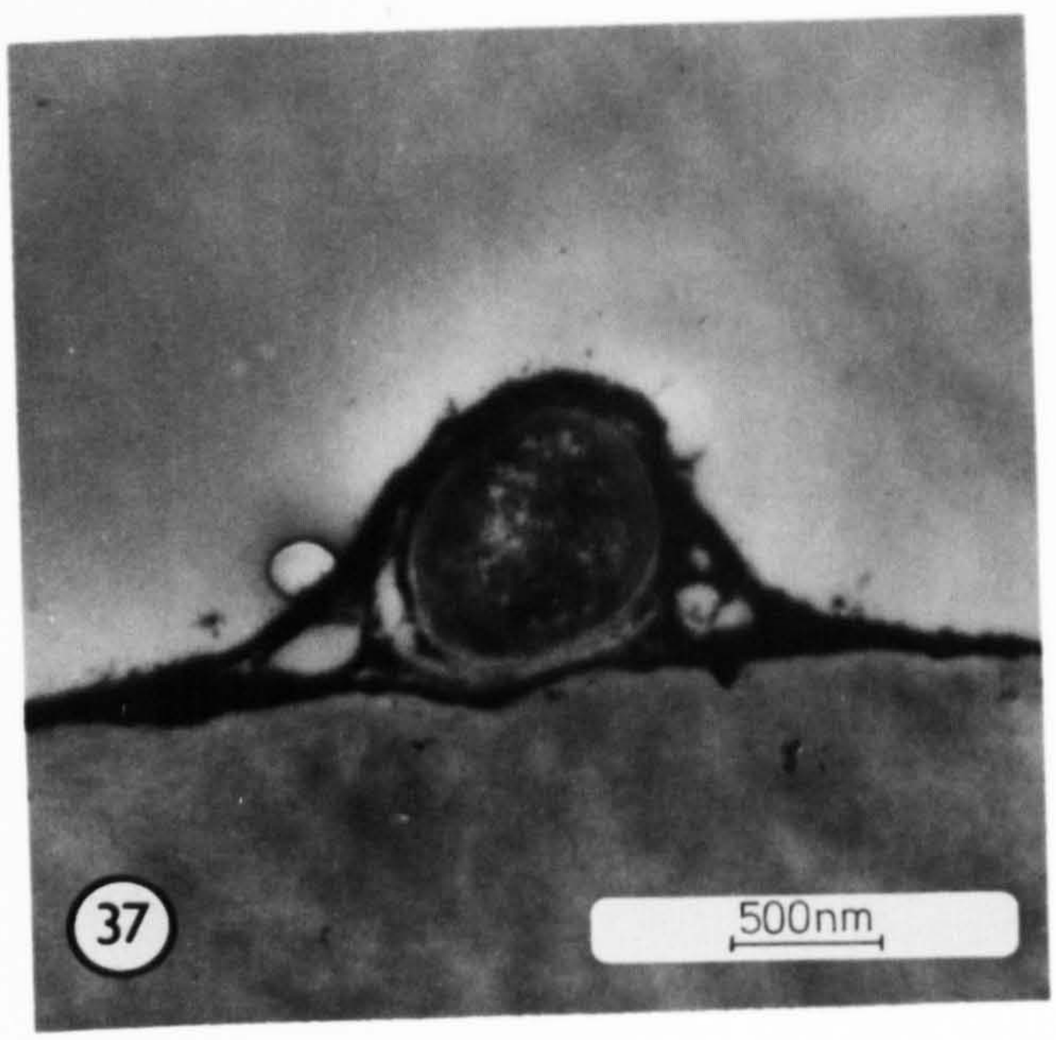
Figures 37 (x 24620 (TS)), 38 (x 21800 (TS)), 39 (x 23690 (TLS)) and 40 (x 8210 (TS)) demonstrate progressive wall erosion from the lumen. The initial hyphal - wall contact results in the investing mucilage accumulating by surface tension on either side of the hyphae where the lytic effect is therefore concentrated. Lysis produces shallow channels, figure 38, which vary in appearance according to the section plane, figure 39, either side of a central, hyphal supporting ridge. Progressively the channels enlarge, merge together under the hypha, producing deep lysis troughs, figure 40.

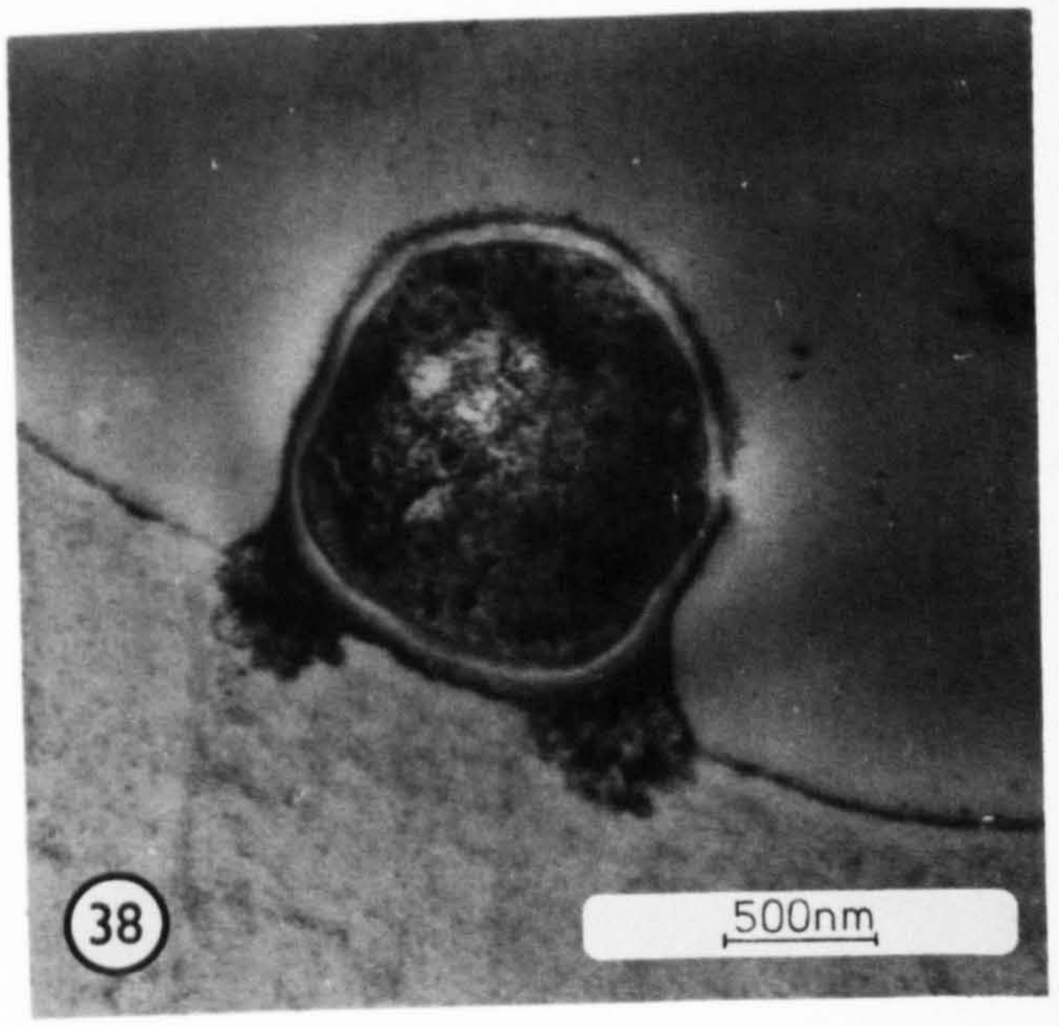
Figures 35, 36, 37, 38, 40:- Fixed with G, R, O, K and dehydrated using Durcupan.

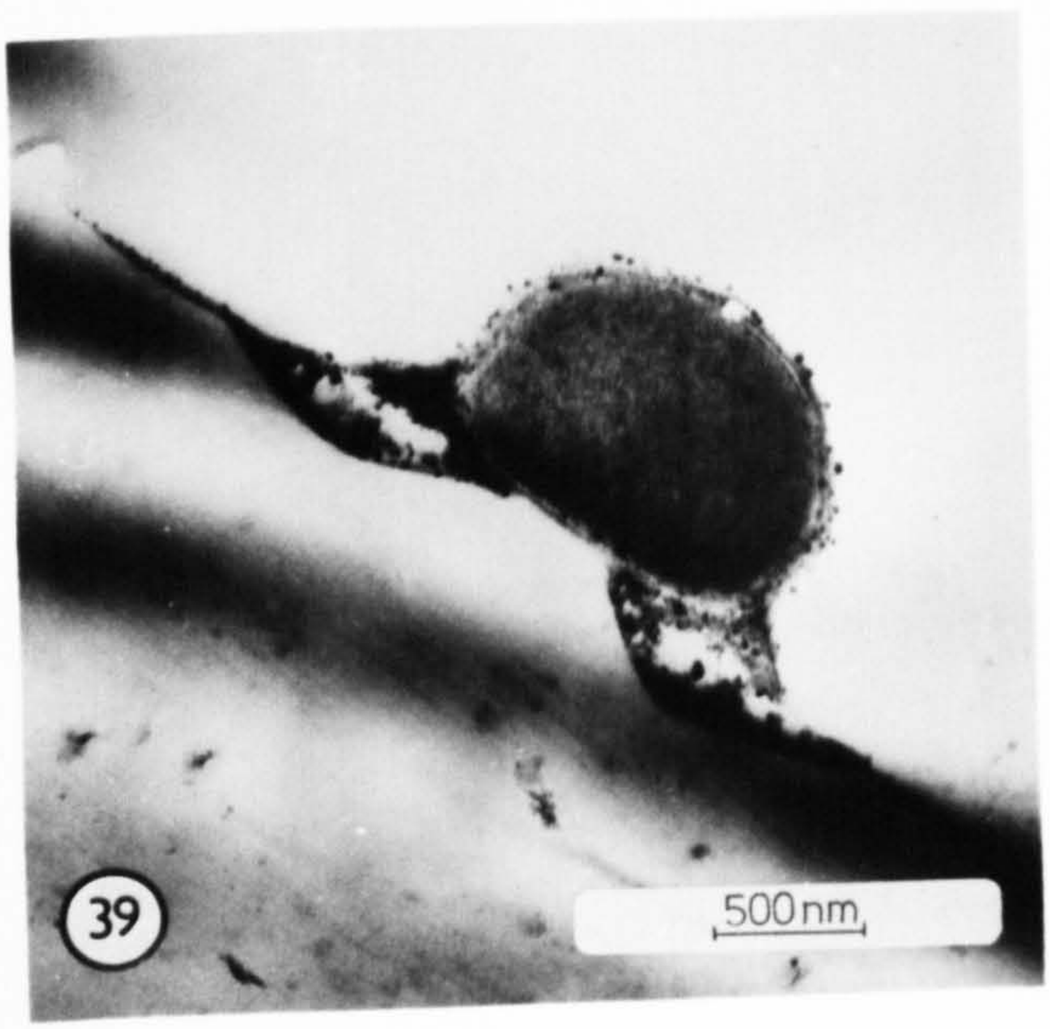
Figure 39:- Fixed with G, R, O and dehydrated using Durcupan. All sections were unstained.

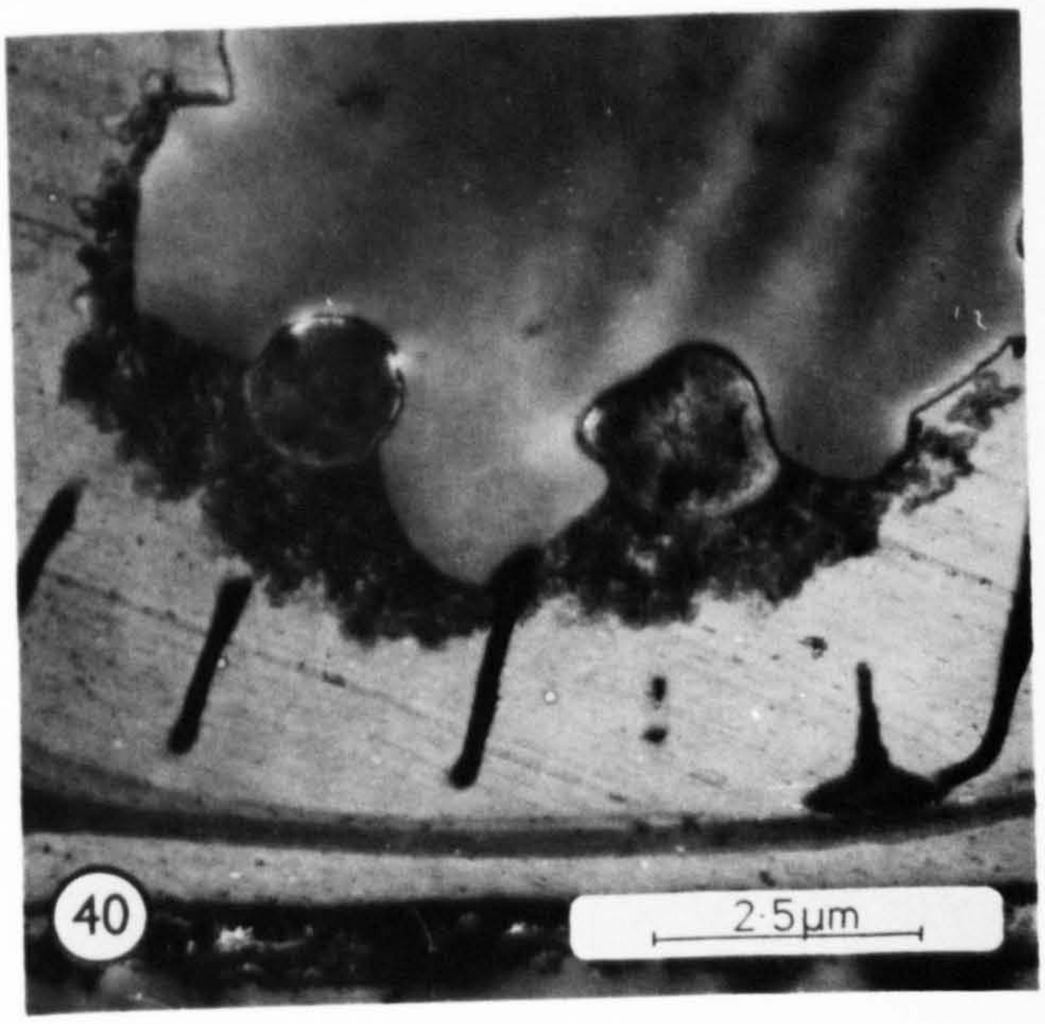

Lh
Pnh
Ch
35
1µm


36
5µm


37
500nm


38
500nm


39
500nm


40
2·5µm

4.2.2 *Chaetomium globosum* on Scots pine (*Pinus sylvestris*)

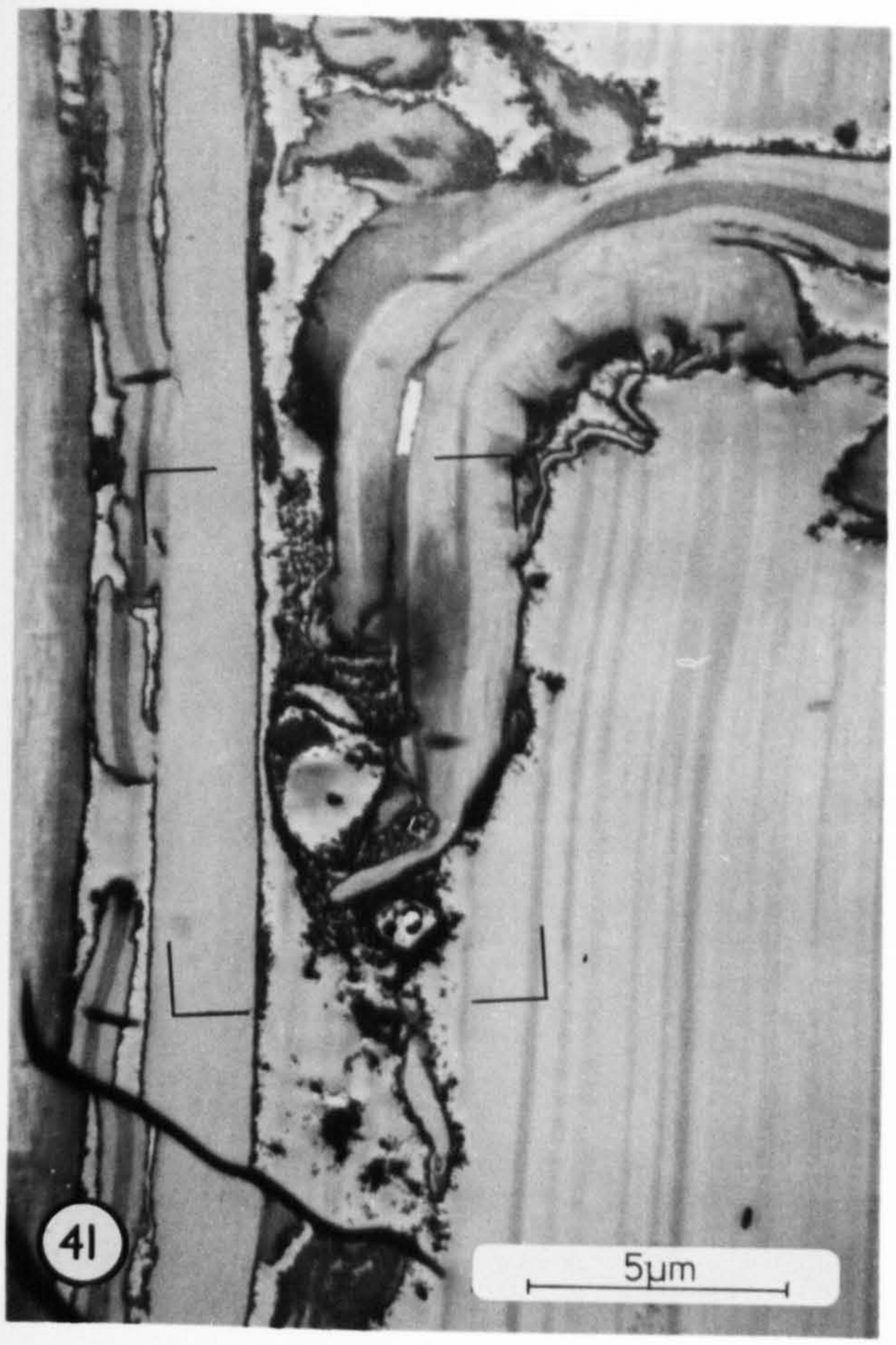
Only a limited number of blocks of this fungus - wood combination were sectioned in the time available and the appearance of the extensively degraded tracheids in the material examined could not be attributed to hyphal attack alone. Observations on the presence of hyphae within degraded regions in association with large amounts of mucilage were very common. Regions of wall lysis could possibly be indicated, as before, by the denser staining due to the lytic effect resulting in the wall being made more permeable to the fixatives. There was severe cytoplasmic distortion, with many of the hyphae showing no cellular contents at all, and over-fixation problems were the likely cause of these features.

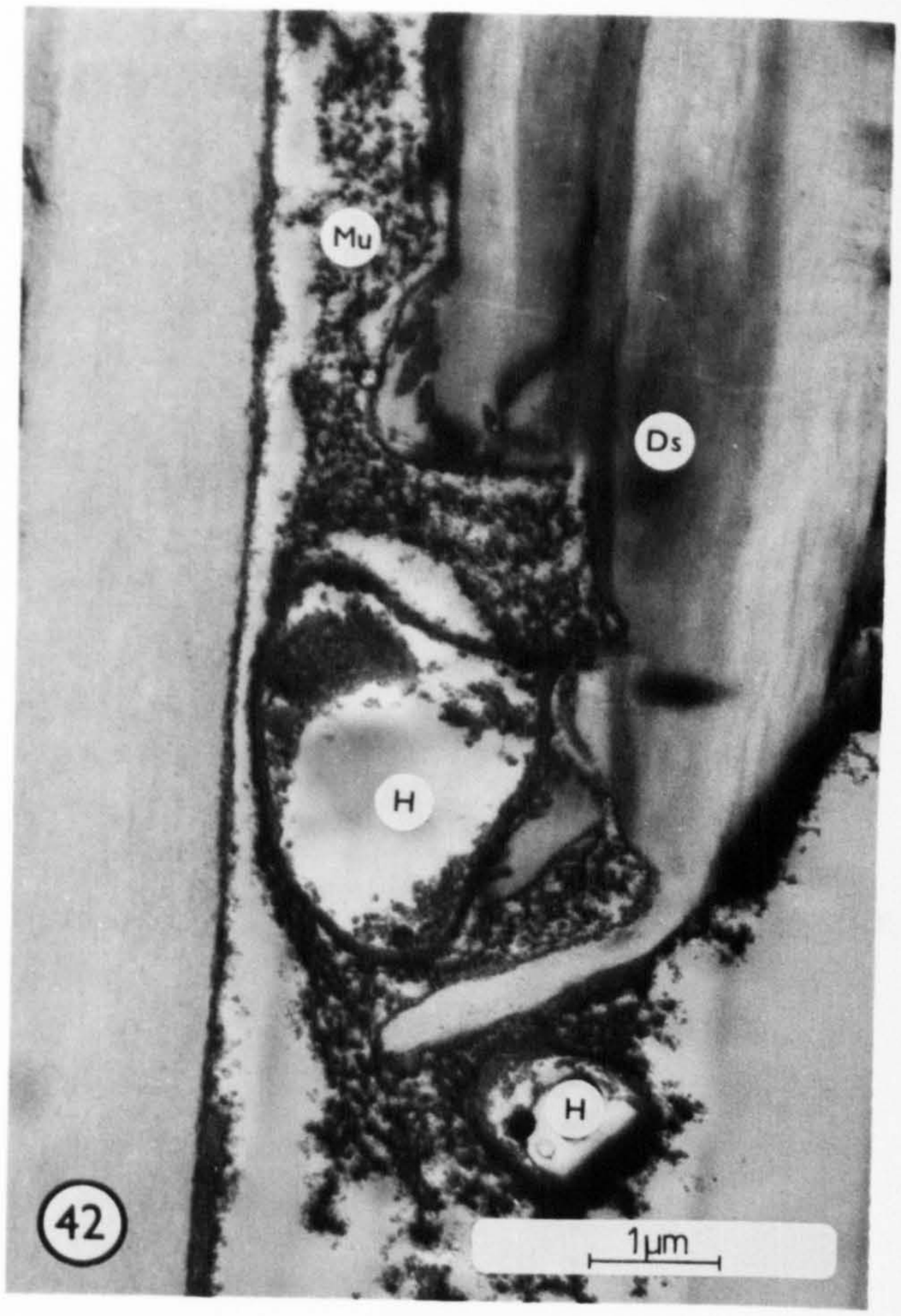
3.2.2 Chaetomium globosum on Scots pine (Pinus sylvestris), 4 weeks

Figures 41 (x 4740 (TLS)) and 43 (x 4905 (TLS)) with their enlargements, figures 42 (x 11540 (TLS)) and 44 (x 12590 (TLS)) respectively, illustrate heavily degraded tracheids. The walls have almost entirely been removed by the activities of the hyphae (H). There are significantly large amounts of mucilage (Mu) present in association with the lysis. The darker staining (Ds) of some wall regions is again possibly attributed to some lytic effect increasing the permeability of the wall to the denser fixatives. Note the possible preferential lysis of the S_1 wall layer as seen in figure 41.

Figures 41-44:- Fixed with G, R, O and dehydrated using GMA.

All sections were unstained.


41
5µm


Mu
Ds
H
H
42
1µm

43
5µm

H
Mu
Ds
H
44
1µm

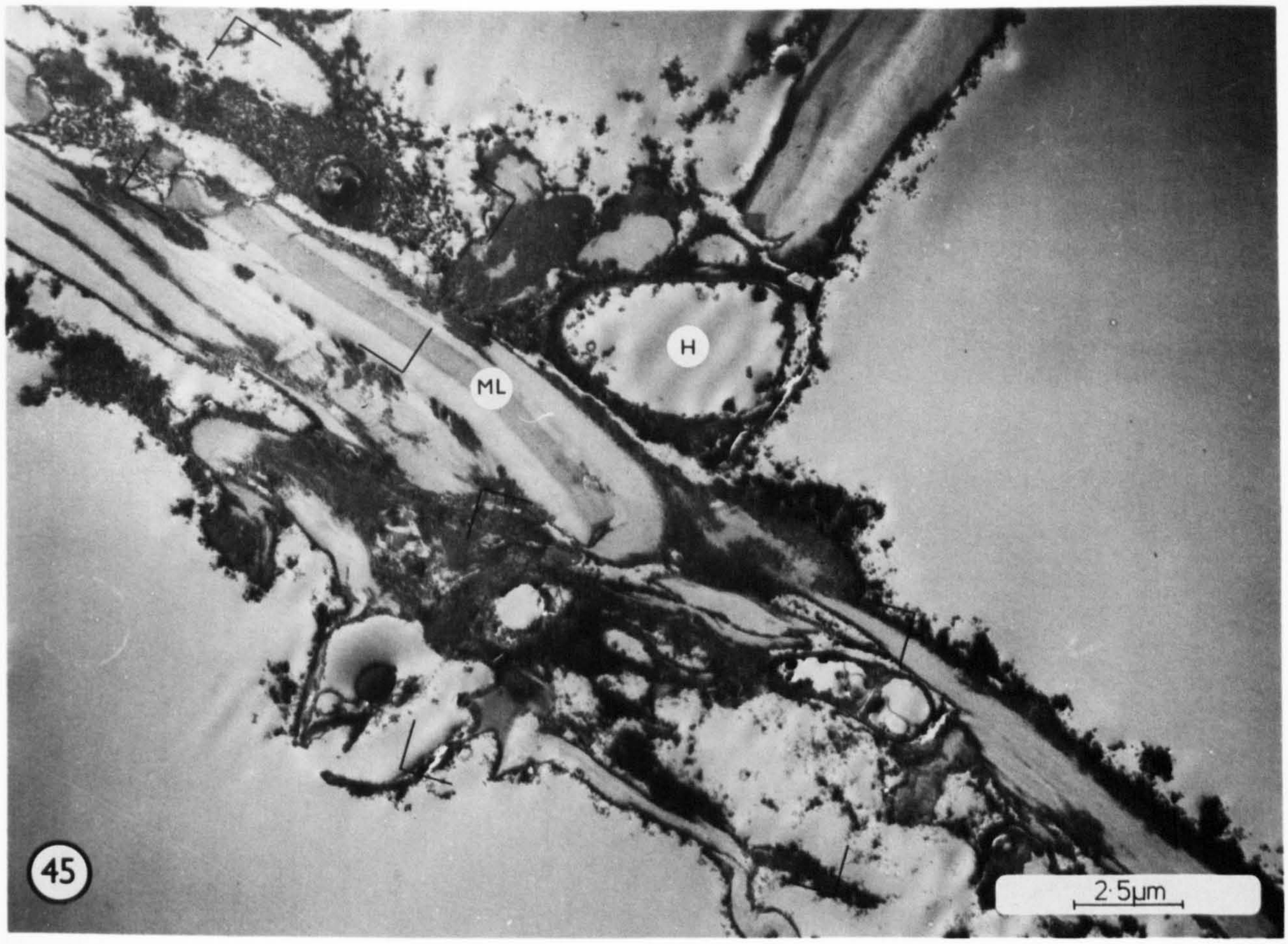
3.2.2 Chaetomium globosum in Scots pine (Pinus sylvestris), 4 weeks

As in the previous plate extensive wall degrade is evident, figure 45 (x 5570 (TLS)), with only fragments of wall remaining where the darker middle lamella (ML) regions can be identified.

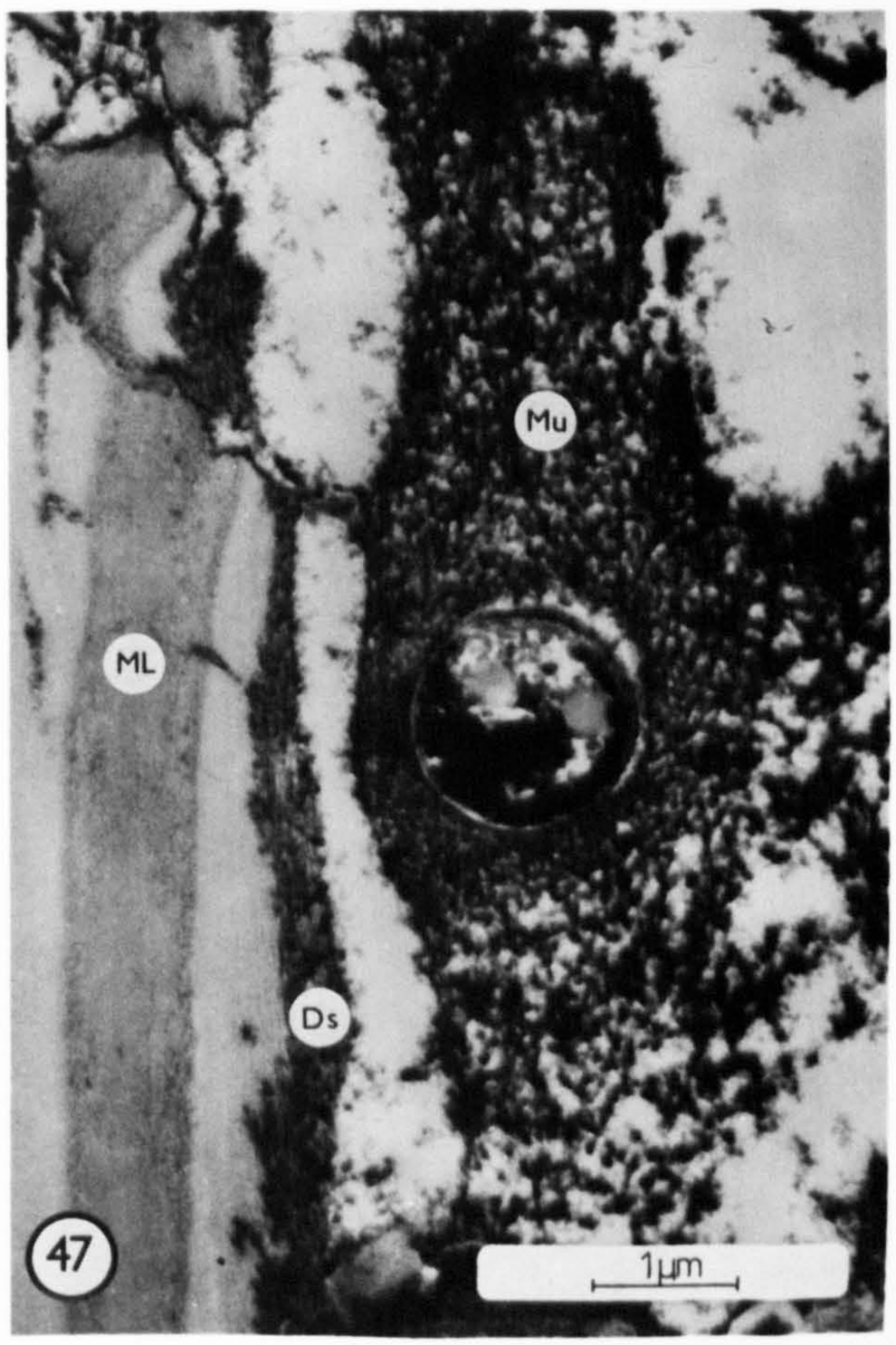
The higher magnifications in figures 46 (x 17030 (TLS)) and 47 (x 12590 (TLS)) show the presence of hyphae (H) surrounded by copious mucilage (Mu) and fragments of degraded wall. The hypha in figure 47 has an extensive investment of mucilage (Mu) and lysis of the wall is evident from the deeper staining (Ds) regions.

Figures 45-47:- Fixed with G, R, O and dehydrated using GMA.

All sections were unstained.


H
ML
45
2·5µm


H
Mu
H
H
46
1µm

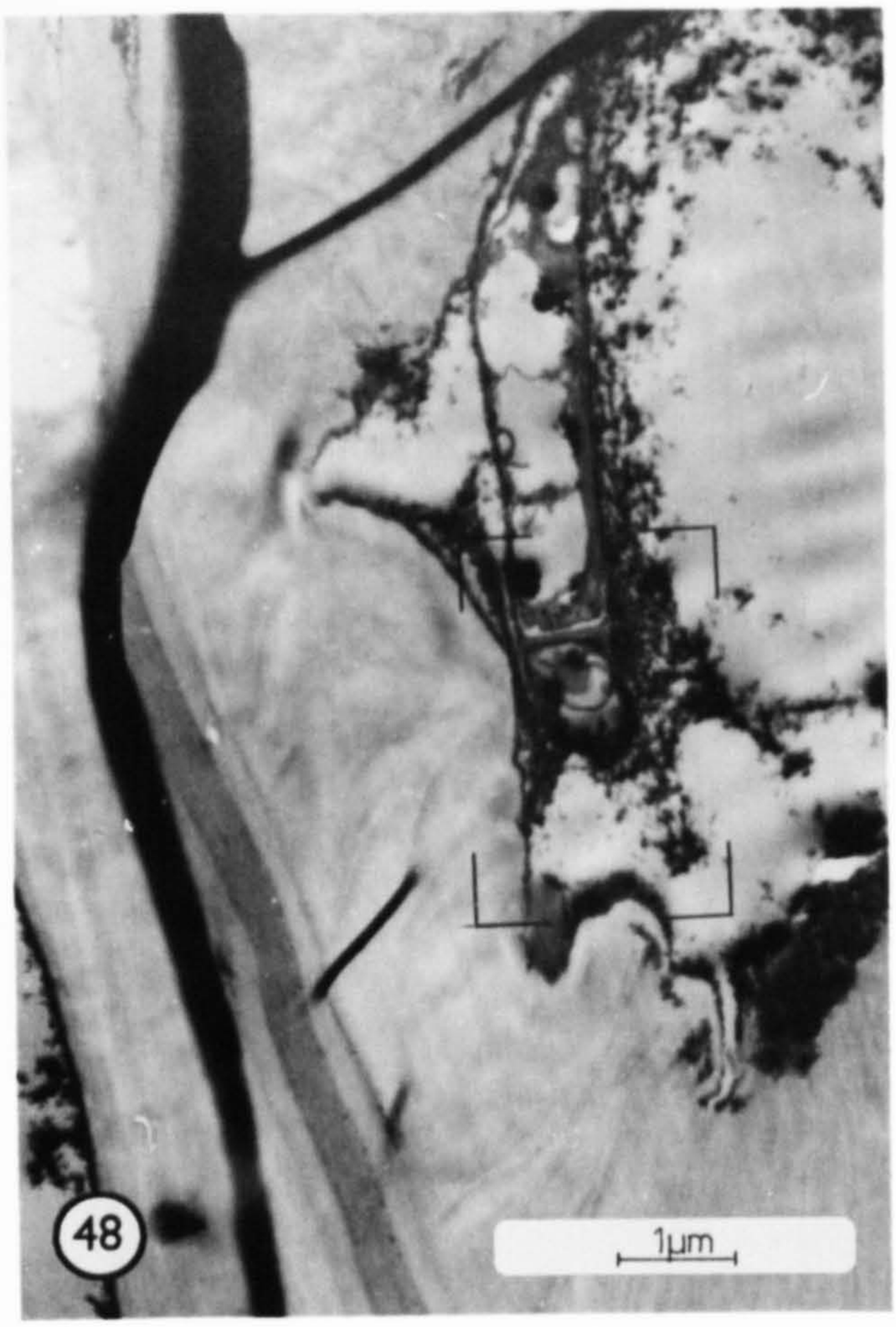

Mu
ML
Ds
47
1µm

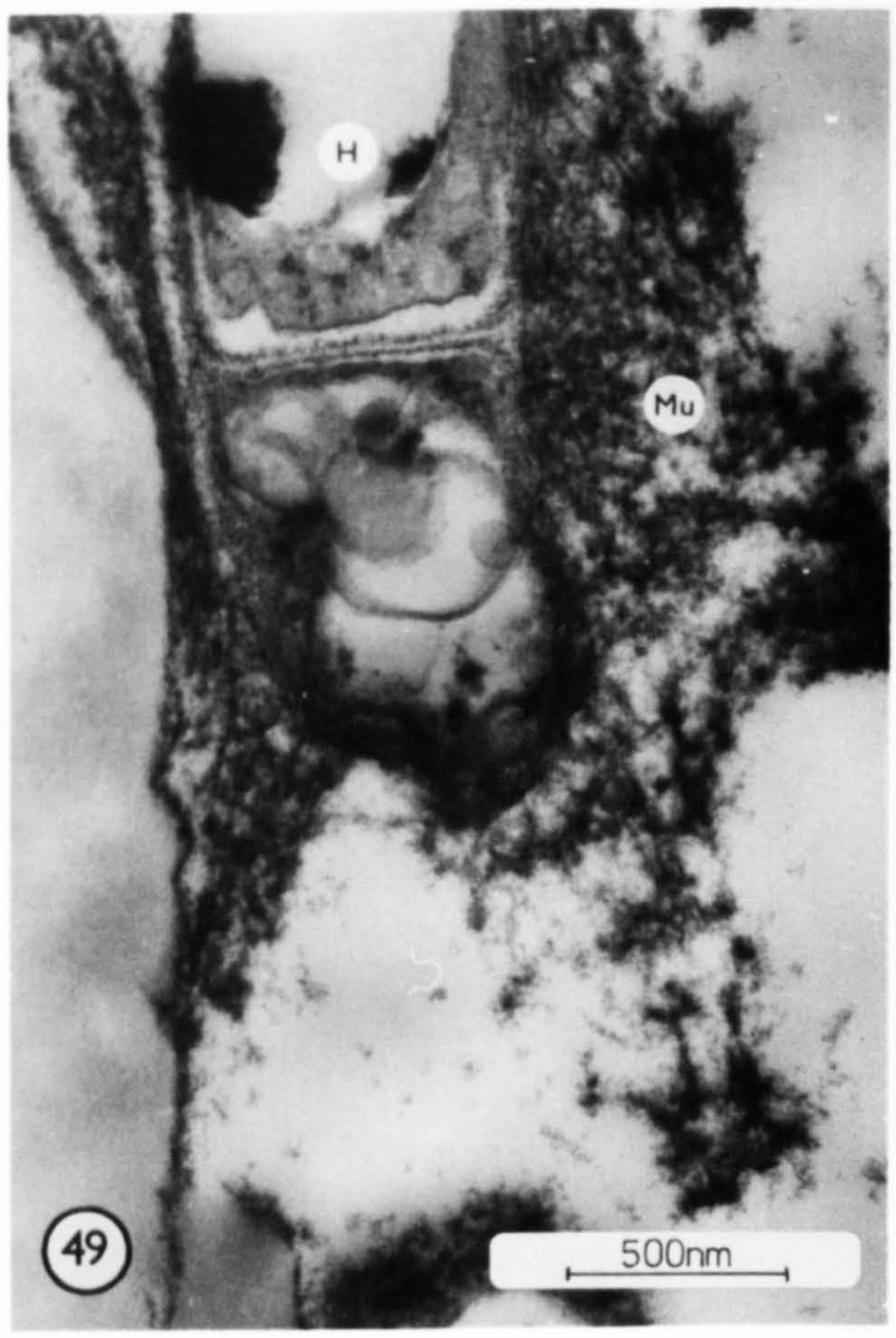
3.2.2 Chaetomium globosum on Scots pine (Pinus sylvestris), 4 weeks

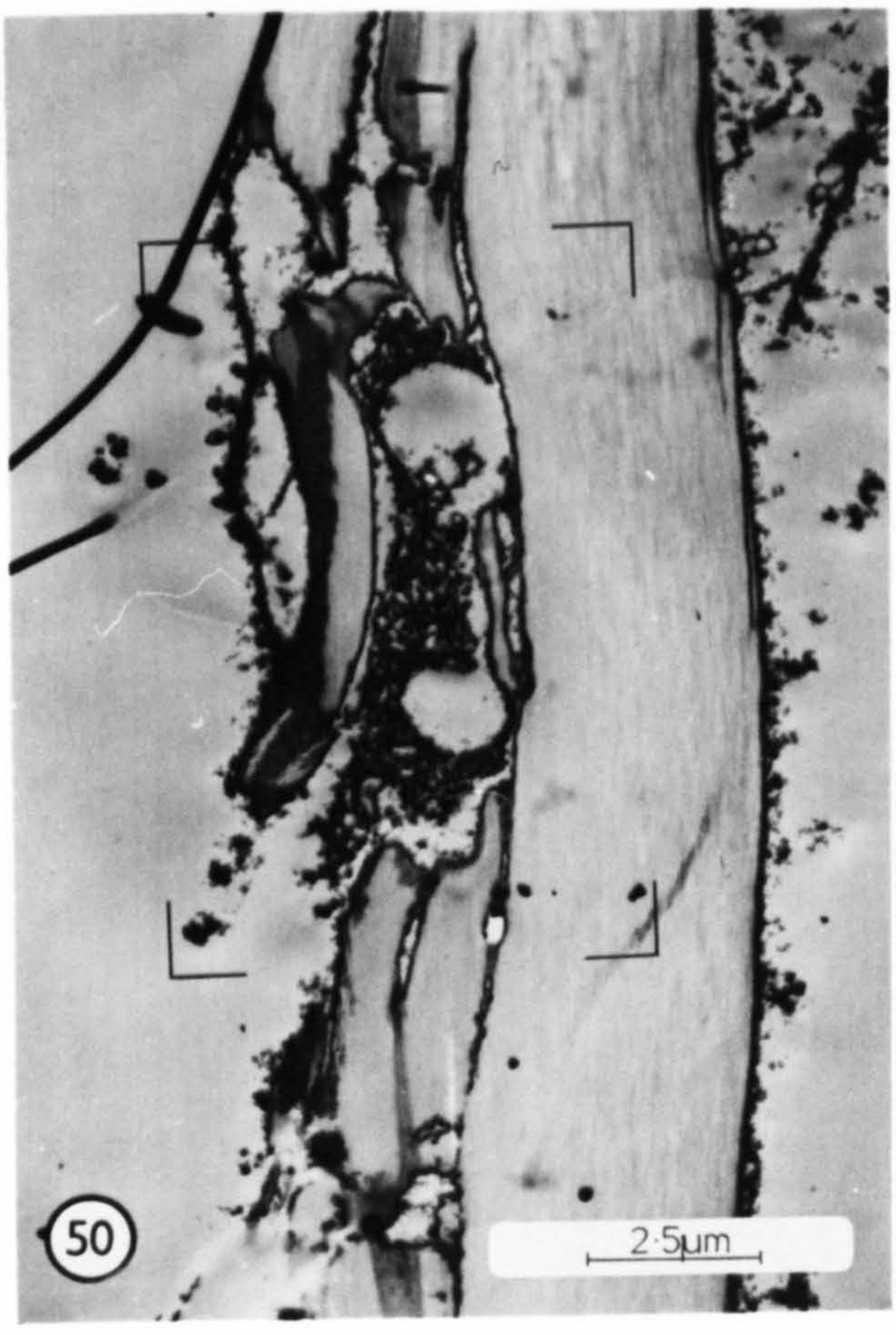
Figures 48 (x 10770 (TLS)) and 50 (x 6450 (TLS)) with their respective higher magnifications, figure 49 (x 39160 (TLS)) and 51 (x 9530 (TLS)) continue the illustration of the presence of mucilage around hyphae actively degrading tracheid walls. The hyphae (H) with their surrounding matrices of mucilage (Mu) together with darker stained (Ds) regions of lysed wall again are clearly shown. The cytoplasmic contents of the hyphae in these preparations were largely absent, probably as a result of fixation problems.

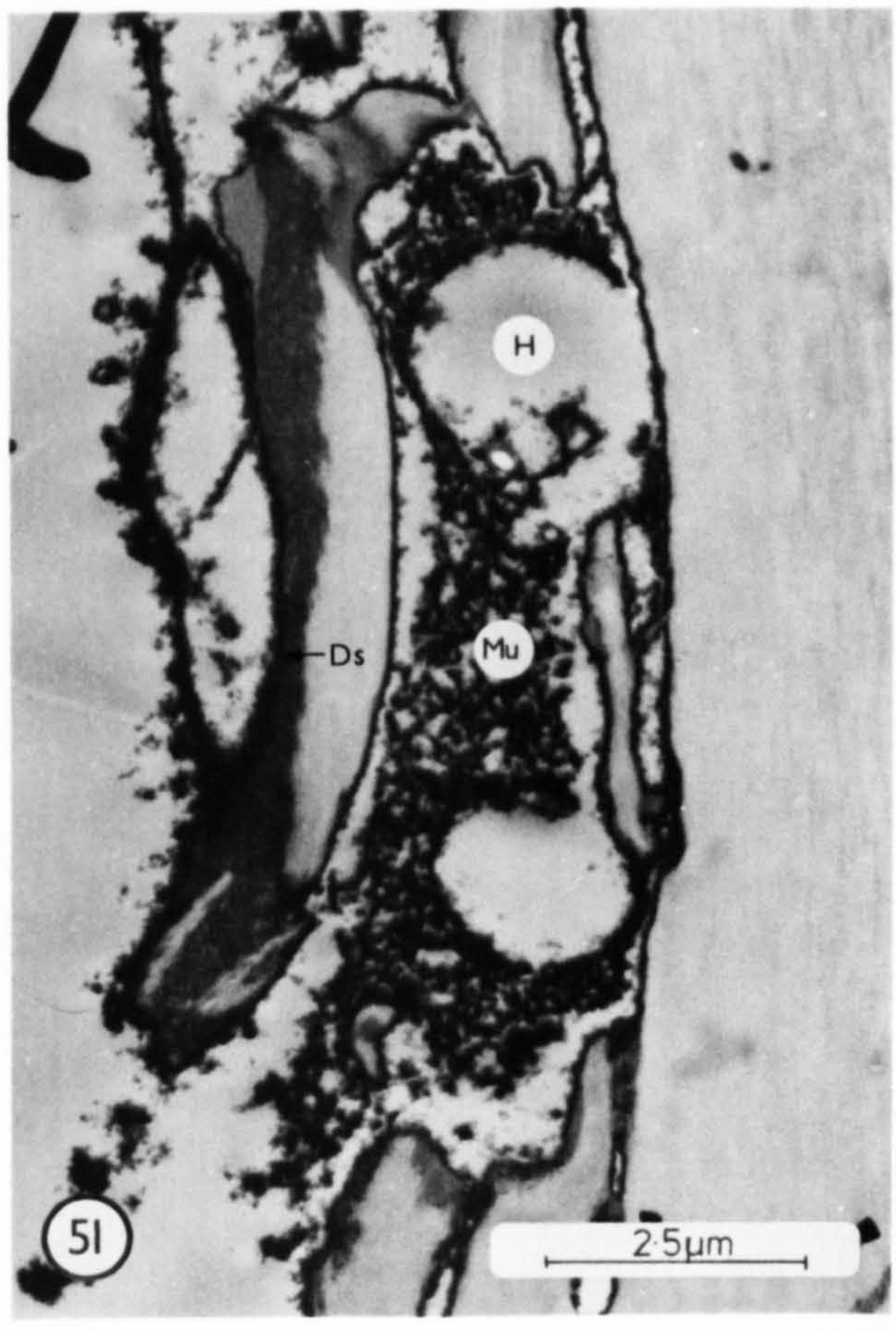
Figures 48-51:- Fixed with G, R, O and dehydrated using GMA.

All sections were unstained.


48
1µm


H
Mu
49
500nm


50
2·5µm


H
Ds
Mu
51
2·5µm

4.3.1 Coriolus versicolor on birch (Betula sp.)

The hyphal contents showed a reasonable level of preservation with cell organelles being discernible. The fungal walls were very much thicker than the previous two types and seemed to be comprised of a number of discrete lamellae, figs. 52 - 54. A characteristic feature of Basidiomycete hyphae is the presence of the dolipore septum and an example of this is given in figures 60 and 61. Immediately apparent was the investment of mucilage around the hyphae both in and out of contact with wood cell elements, figs. 55 and 56 and 52 - 54 respectively.

The degrade patterns were extremely variable with the formation of bore holes through fibre and ray walls, lysis troughs and regions of extensive wall degrade, fig. 57. A noticeable feature was the degrade of the S_2 wall layers, apparently through the S_3, fig. 58. The resistance of the S_3 to lysis appeared to vary but the presence of mucilage with the hyphae in most regions of wall lysis was very significant, figs. 59 - 63 and 68 - 70.

Wall degrade was extremely irregular but always confined to the vicinity of the hyphae. A number of serial section sequences, figs. 71 - 78, indicated the variable resistance, to lysis by the fungus, of several different wall layers. As already mentioned the S_3 sometimes showed resistance, as did the layers on the junction between the S_1 and compound middle lamella and in some ray tissues the compound middle lamella alone, figs. 57, 58 and 60.

3.3.1 Coriolus versicolor on birch (Betula sp.), 10 days

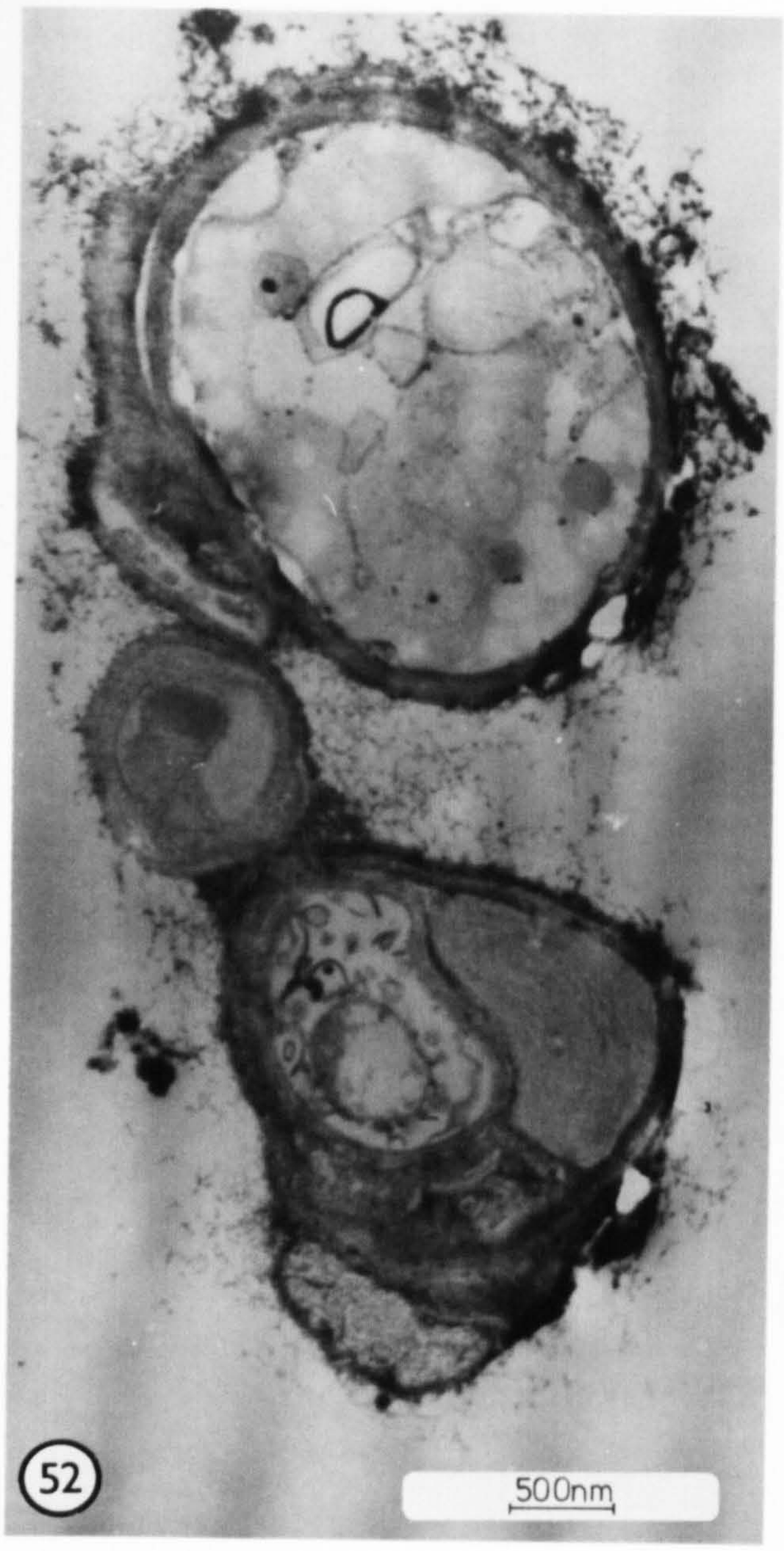
Figures 52 (x 21450 (TLS)) and 53 (x 11570 (TLS)) with its higher magnification, figure 54 (x 57720 (TLS)), demonstrate the appearance of surface colonising hyphae. The cytoplasmic contents have suffered some disruption and the hyphal walls are noticeably thicker in this and other white rot material examined than in the other two fungal types. The hyphae also bear extracellular coatings of mucilage detailed in figure 54.

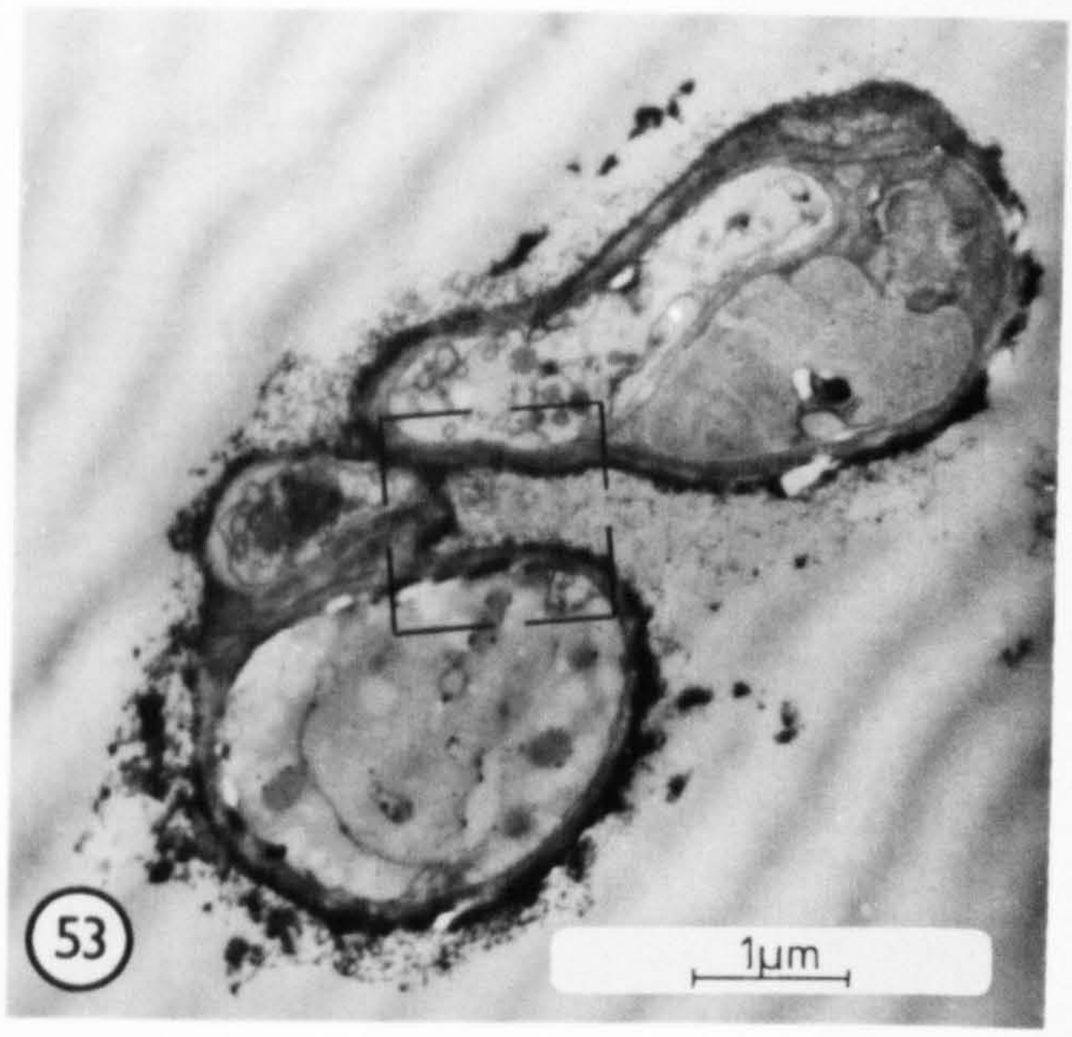
The continued presence of the mucilage is evident in figures 55 (x 35550 (TLS)) and 56 (x 15470 (TLS)) where the hyphae are in close association with fibre walls (W11).

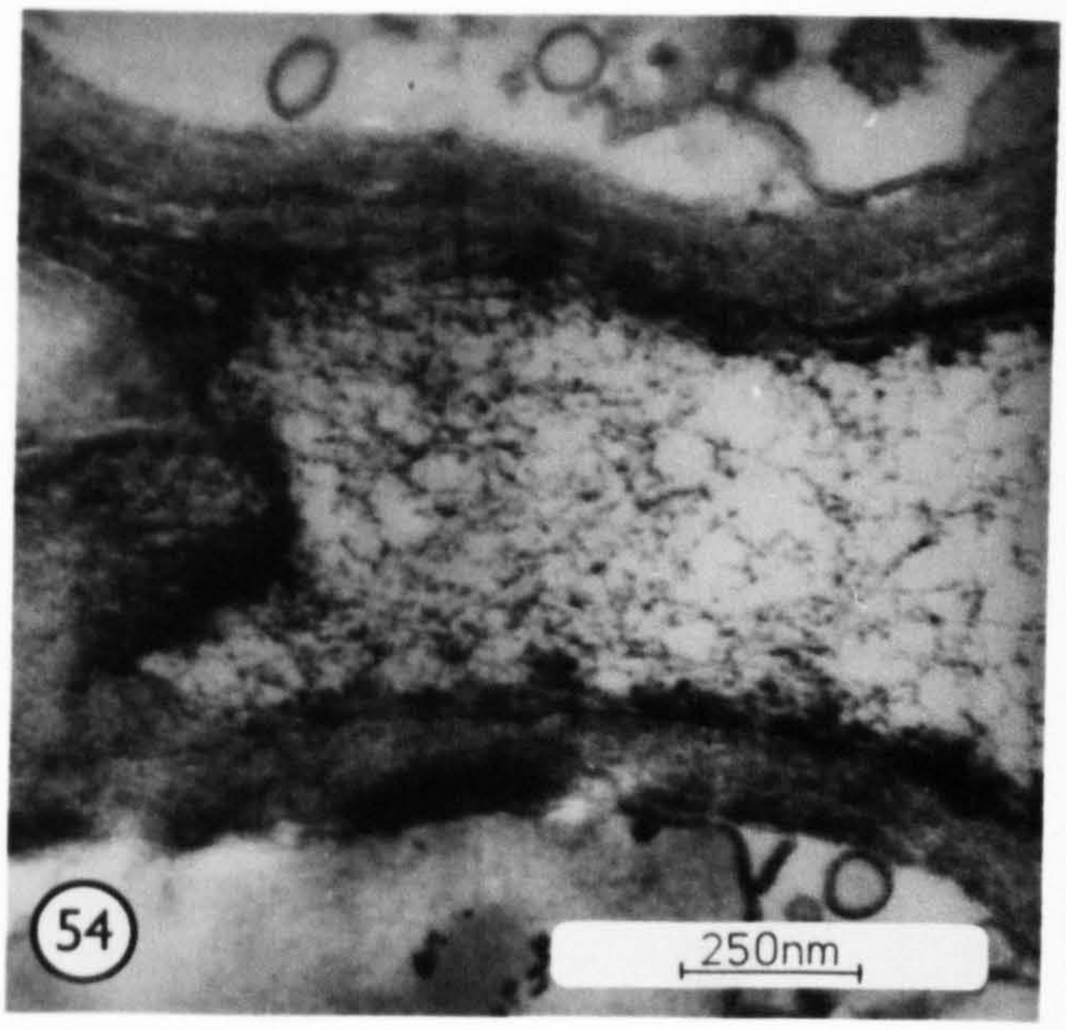
Figures 52-54:- Fixed with G, R, O, K and dehydrated using Durcupan.

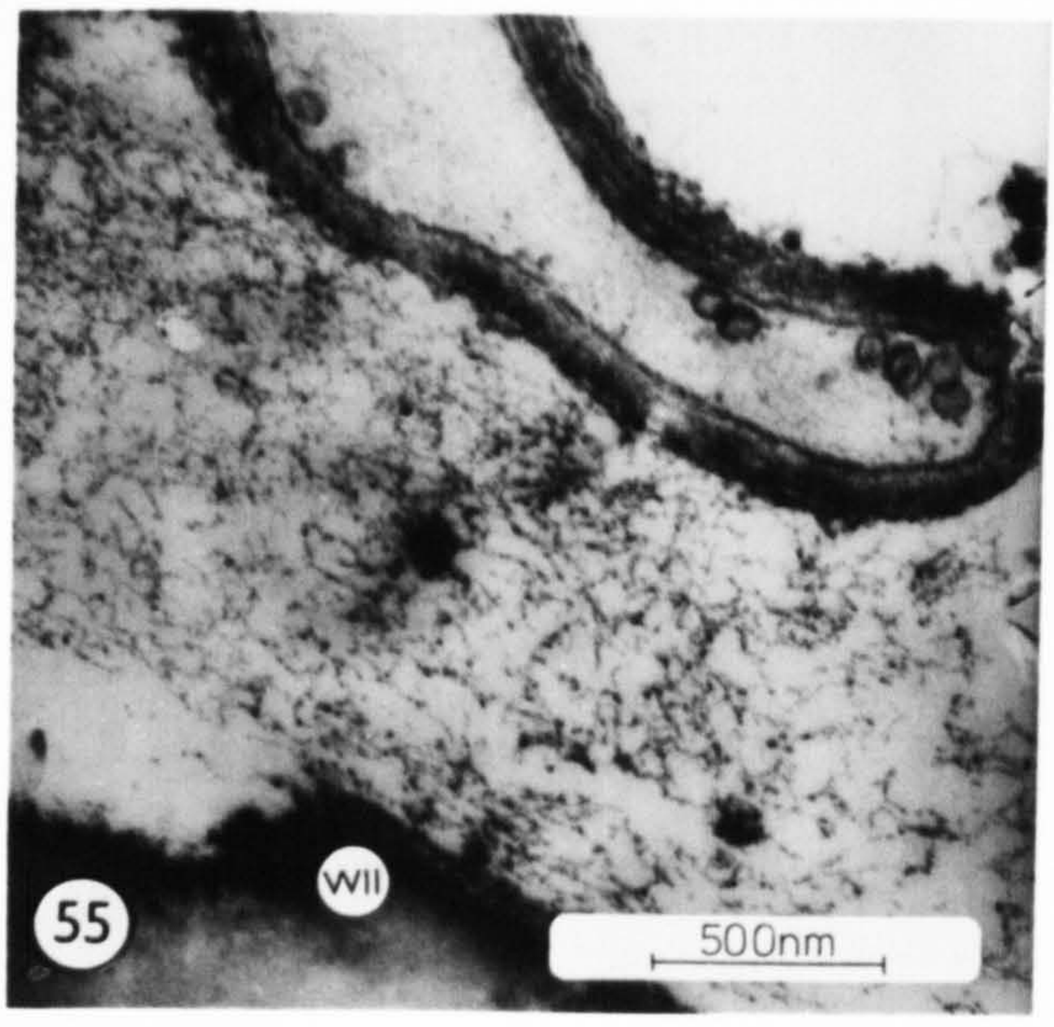
Figures 55-56:- Fixed with G, R, O and dehydrated using Durcupan.

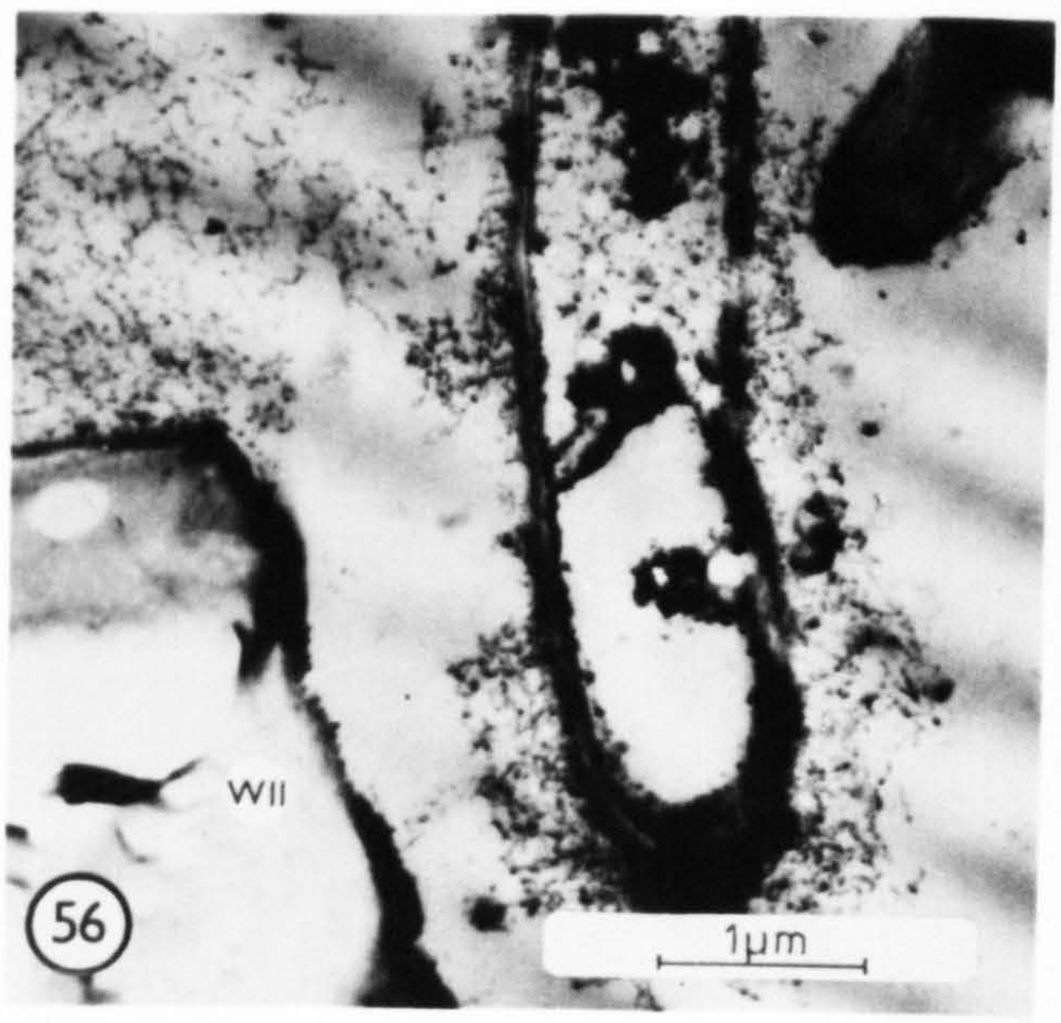
All sections were unstained.


52
500nm


53
1µm


54
250nm


55
WII
500nm


56
WII
1µm

3.3.1 Coriolus versicolor on birch (Betula sp.), 4 weeks

Figure 57 (x 2340 (TLS)) shows a group of birch fibres together with a ray that have been extensively colonised by the hyphae. A number of lysis types can be observed with total wall lysis (Twl), bore holes(Bh), extensive ray degrade (Rd) and trans S_3 wall erosion (TS_3) being present.

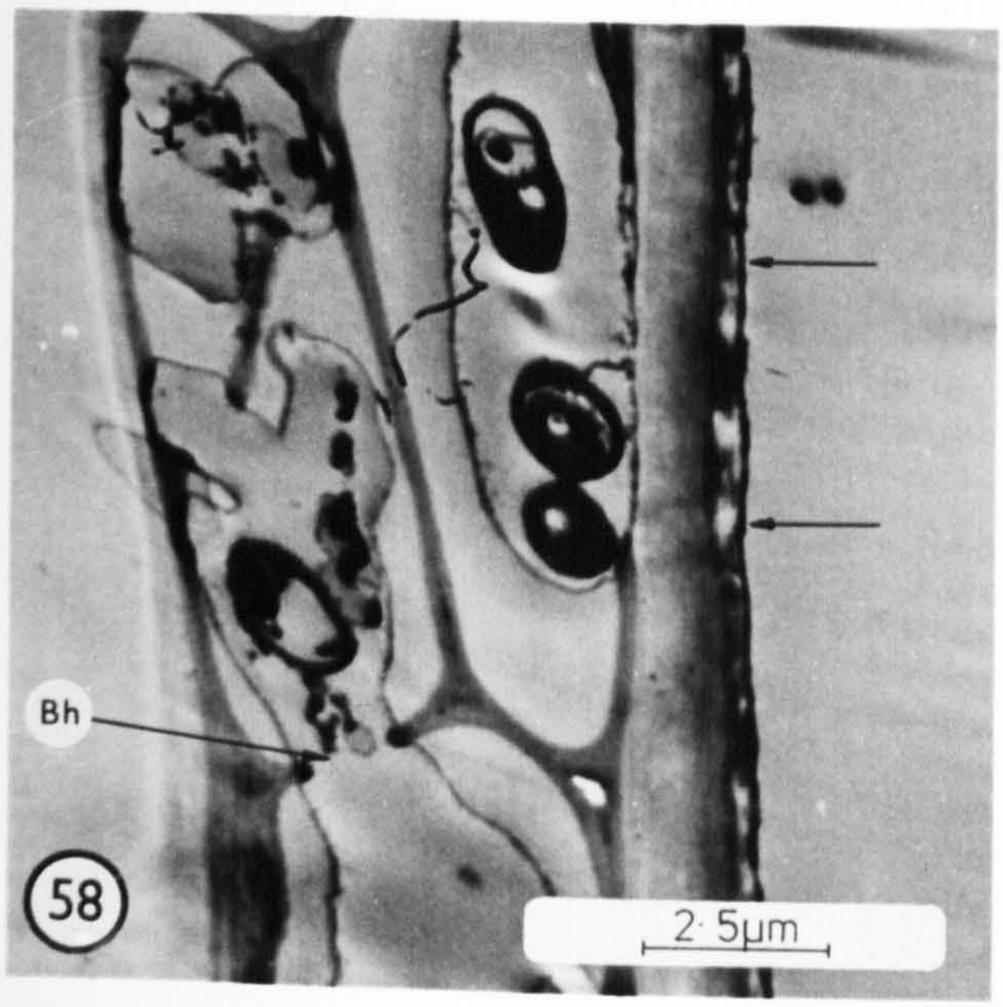
Details of the latter two are given in figures 58 (x 5990 (TLS)) and 59 (x 6710 (TLS)). In figure 58 the ray parenchyma contains several hypahe which have totally removed the S_2 wall in many regions together with a bore hole (Bh) through the ray cell walls. Also evident is erosion of the S_2 wall layers leaving the S_3 layer intact (arrowed).

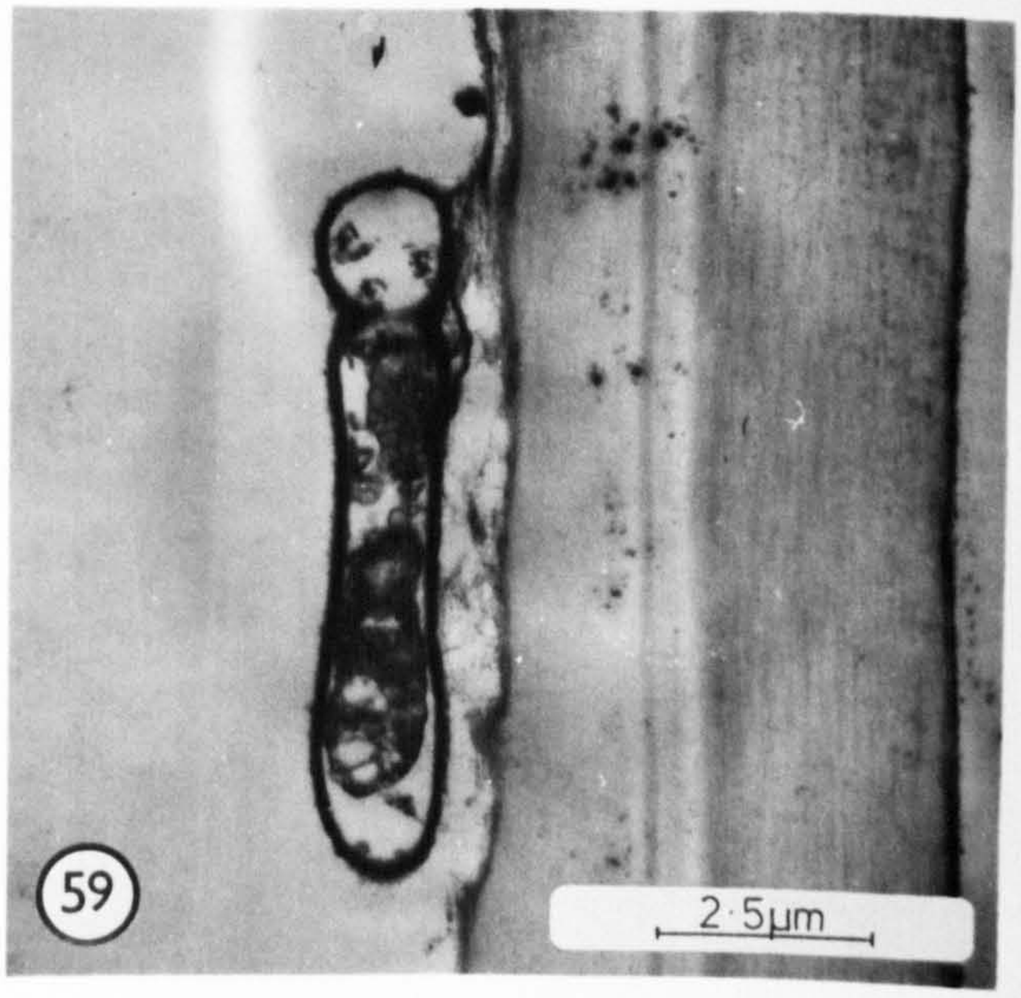
Figure 59 details the presence of a hypha in this type of wall erosion with the residual S_3 evident together with opening up and lysis of the S_2 wall layers around the hyphal - wall contact zone. There are possible indications of mucilage present between the hypha and the wall.

Figures 57-59:- Fixed with G, R, O and dehydrated using GMA.

All sections were unstained.


TS3
Rd
Twl
Bh
57
5μm


Bh
58
2·5μm


59
2·5μm

3.3.1 Coriolus versicolor on birch (Betula sp.), 4 weeks

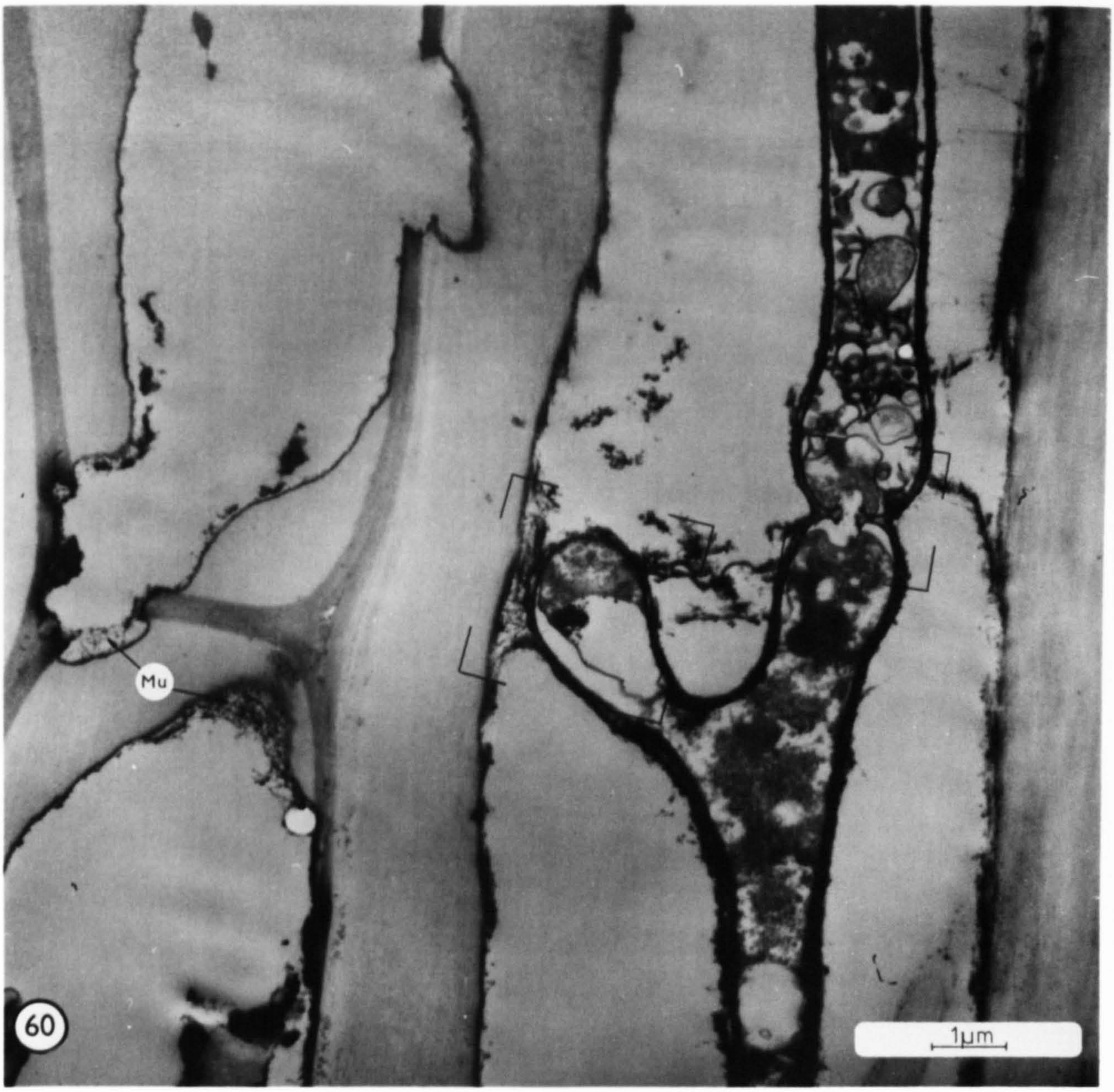
Figure 60 (x 11360 (TLS)) details some features of white rot degrade. The two ray parenchyma cells to the left have suffered extensive wall lysis with the majority of the S_2 being removed. Lysis into and across the middle lamella region has occurred leaving pockets of mucilage (Mu) and/or wall debris.

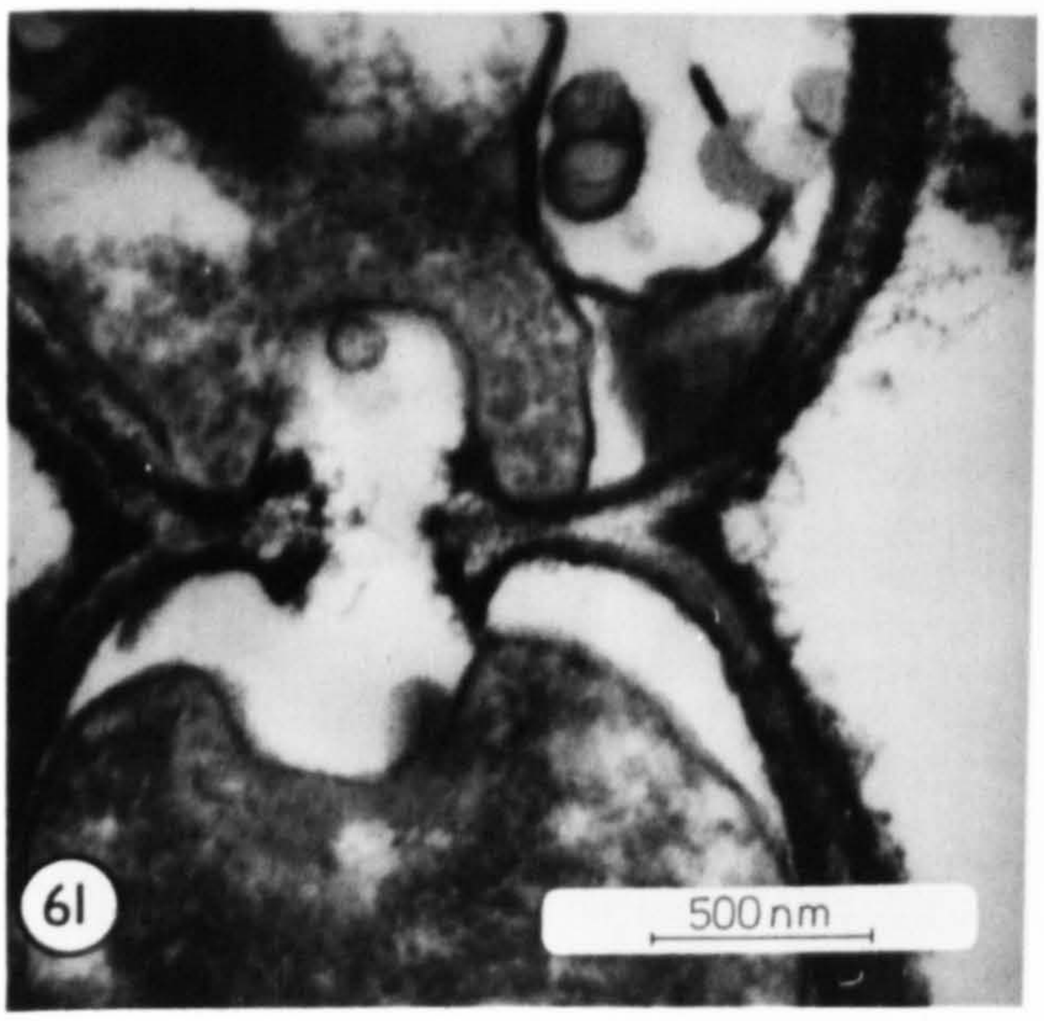
The hypha in the fibre lumen shows some degree of cytoplasmic disruption together with a clear section through a dolipore septum. This septum is shown at higher magnification in figure 61 (x 34730 (TLS)).

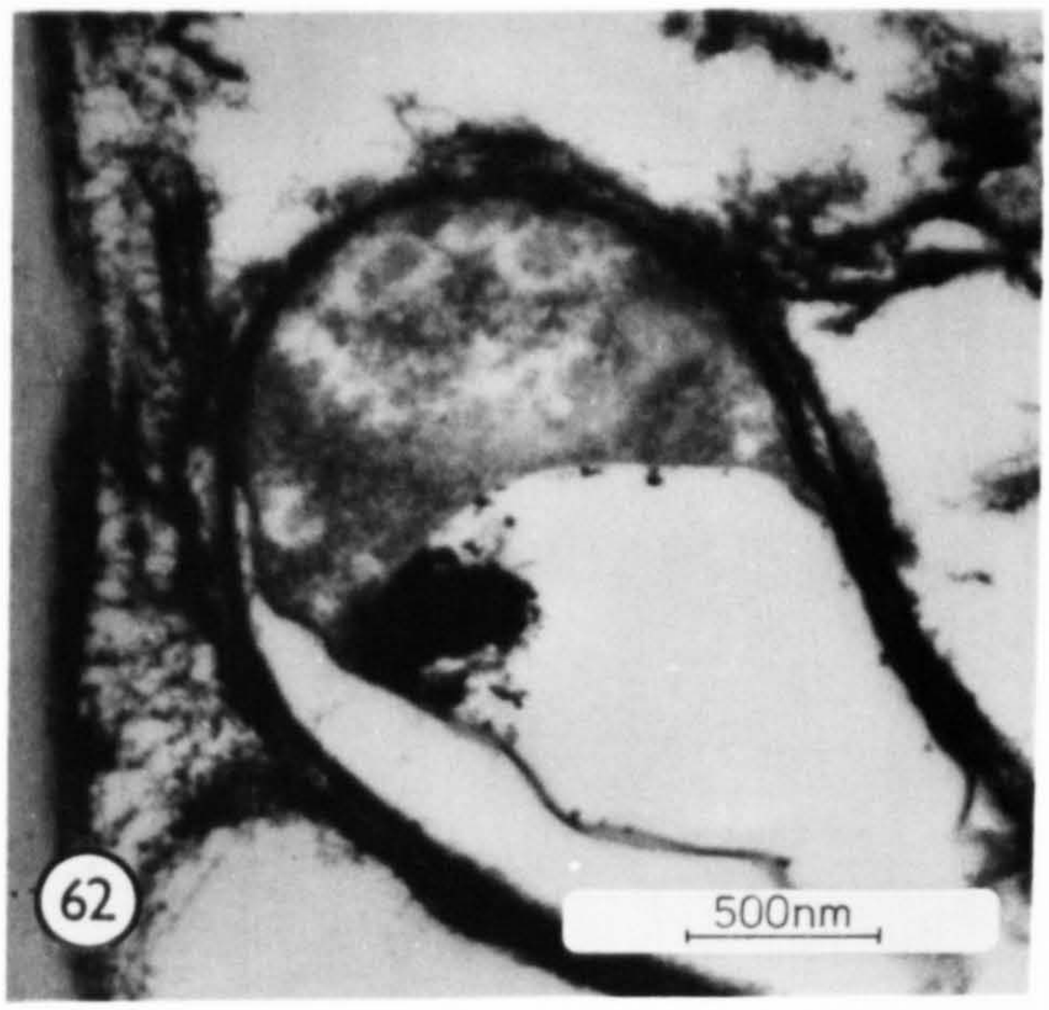
Fibre wall lysis is evident and mucilage can be seen between the hypha and the wall detailed in figure 62 (x 29380 (TLS)).

Figures 60-62:- Fixed with G, R, O and dehydrated using G/A.

All sections were unstained.


Mu
60
1µm


61
500 nm


62
500nm

3.3.1 Coriolus versicolor on birch (Betula sp.), 4 weeks

Figure 63 (x 11360 (TLS)) shows fungal hyphae present in two ray parenchyma cells. Lysis of the walls between the two hyphae is in progress and there is abundant mucilage in this region. The S_3 of the adjacent fibre wall can clearly be seen with erosion of the underlying S_2 layers.

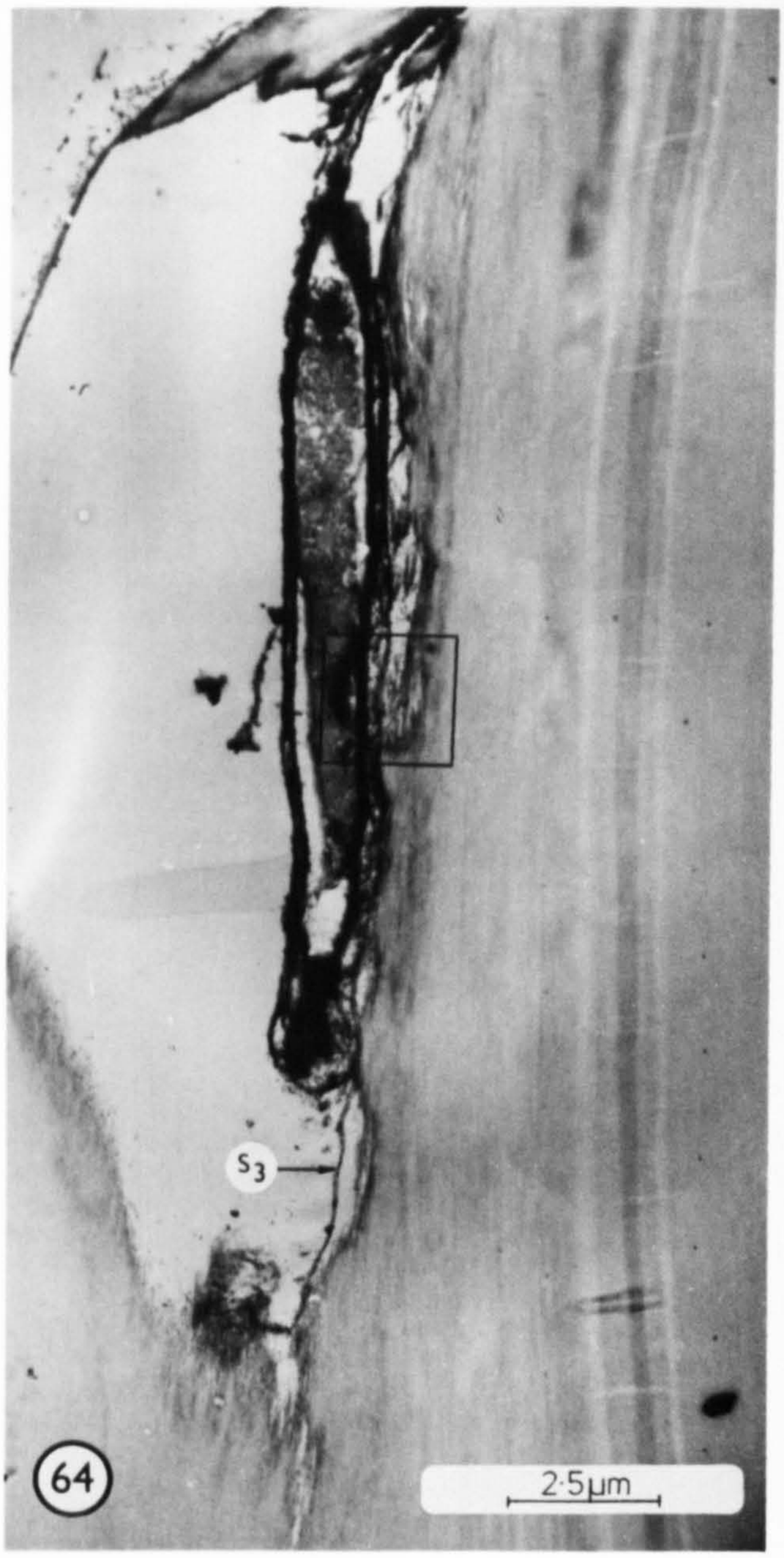
Figure 64 (x 6200 (TLS)) demonstrates trans S_3 wall erosion with extensive lysis of the S_2 microfibrils, yet the S_3 can be seen to be relatively intact. The higher magnification, figure 65 (x 51070 (TLS)) shows the close appression of the hyphal wall (Hw), the resistant S_3 and the lysed S_2 microfibrils.

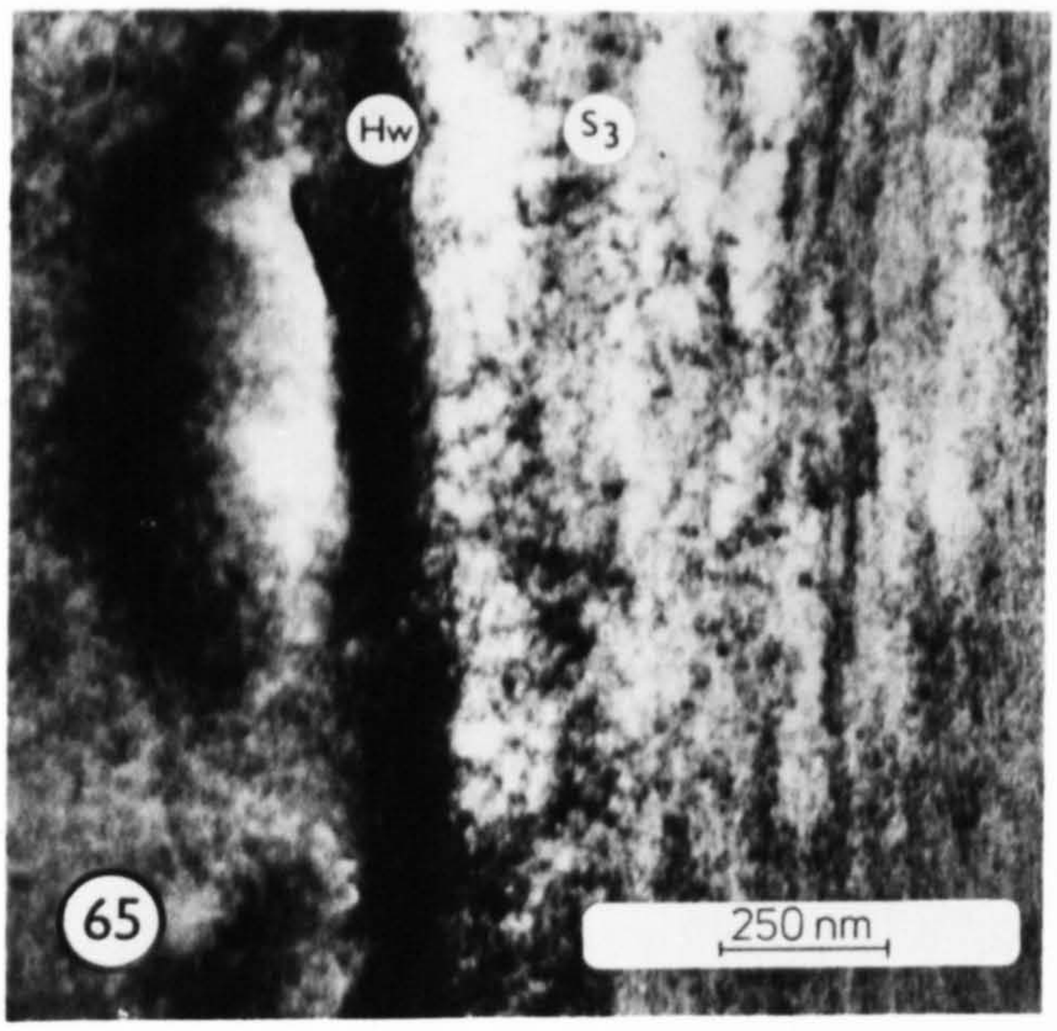
Lysis of the wall without the S_3 appearing resistant was also observed, figure 66 (x 14300 (TLS)), and interpretation of this anomally is difficult.

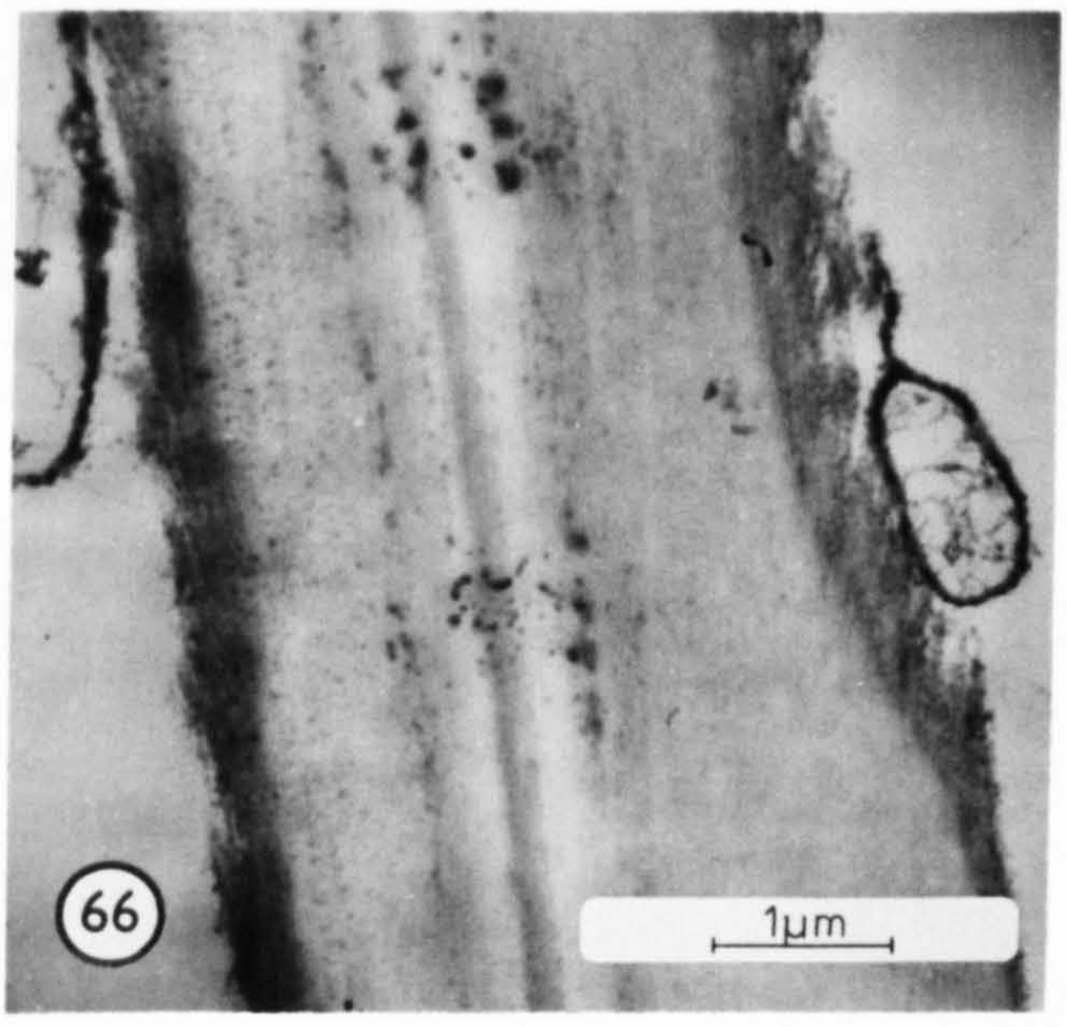
Figures 63-66:- Fixed with G, R, O and dehydrated using GMA.

All sections were unstained.


S3
63
1µm


S3
64
2·5µm


Hw
S3
65
250 nm


66
1µm

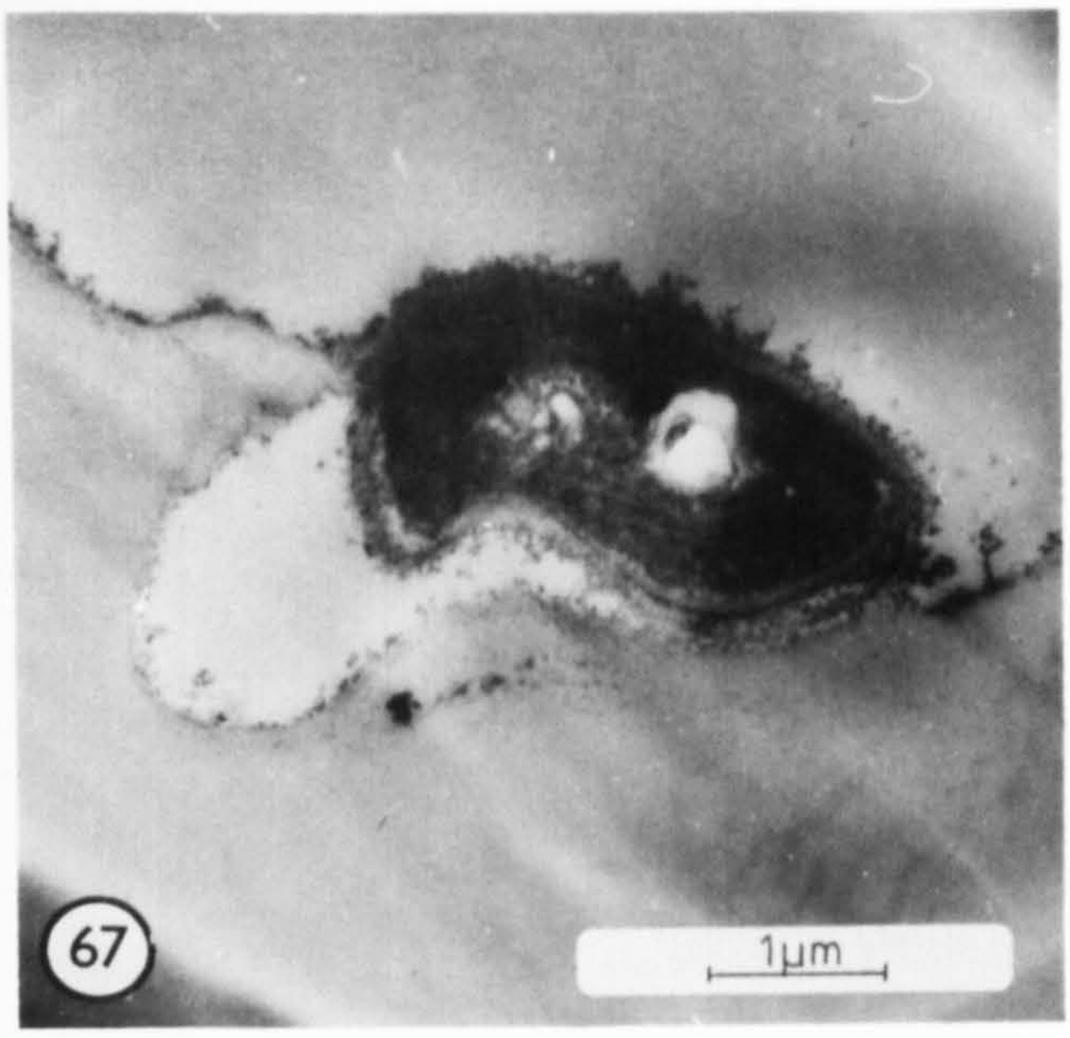
3.3.1 Coriolus versicolor on birch (Betula sp.), 4 weeks

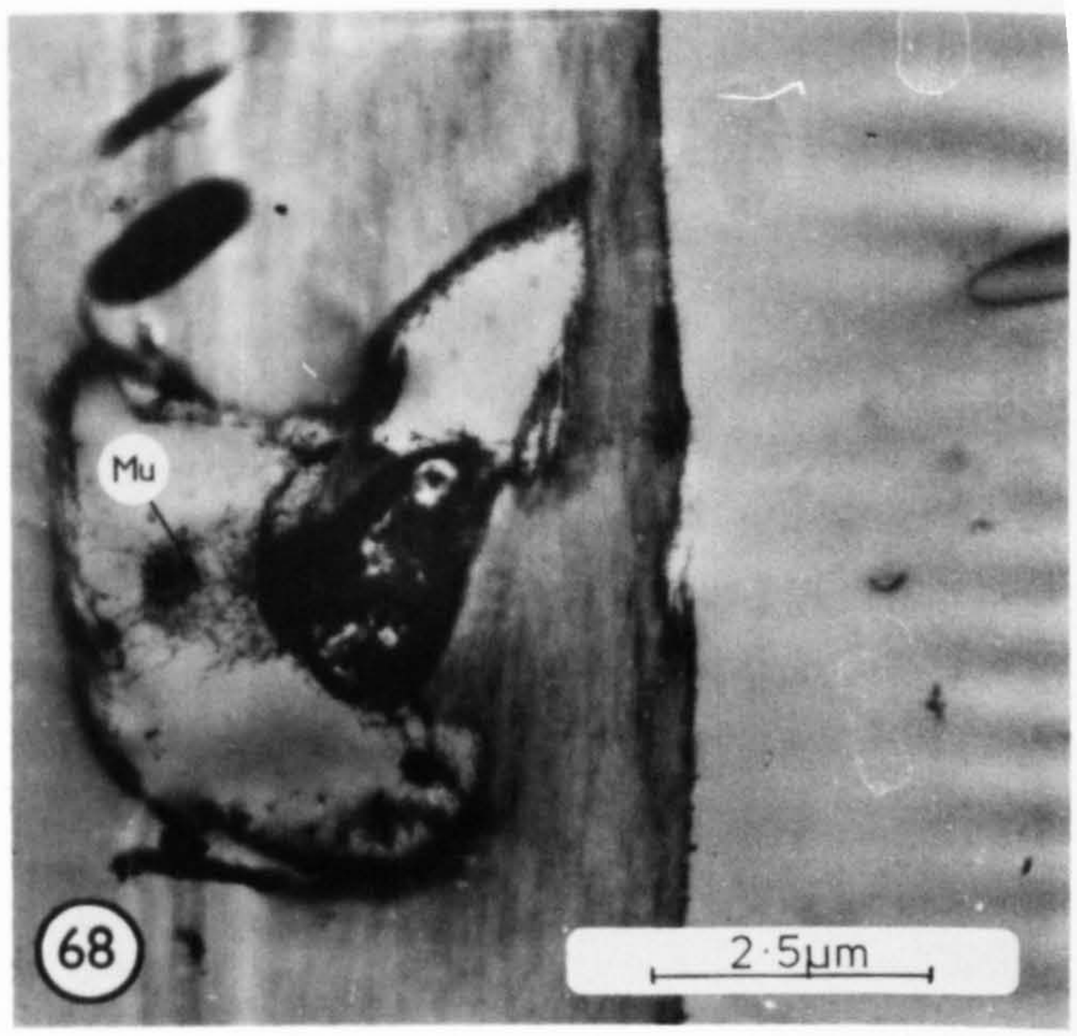
Figure 67 (x 13720 (TS)) shows a hypha closely associated with a fibre wall with a lysis region progressing into the S_2 layers, with the S_3 apparently showing no resistance.

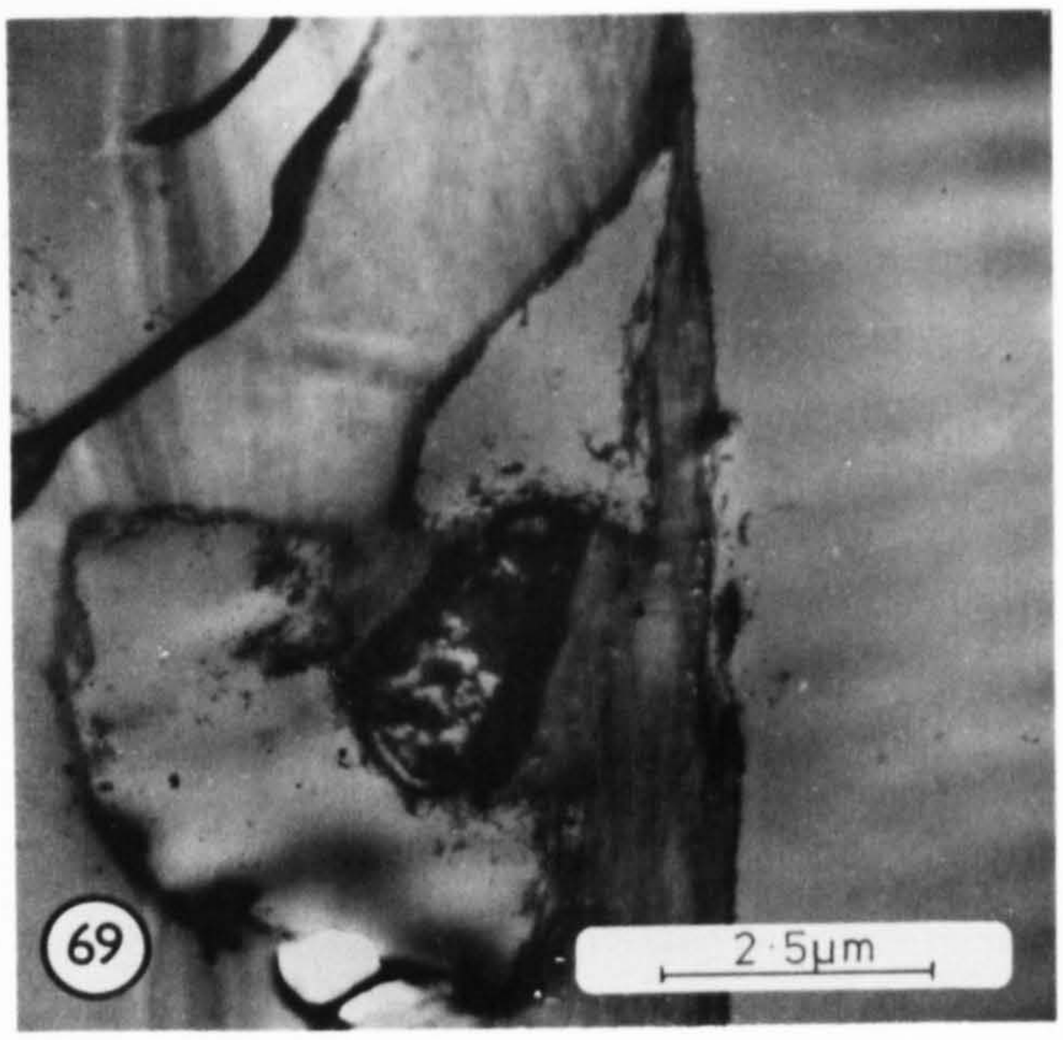
Figures 68 to 70 (x 8470 (TLS)) are serial sections of a hypha involved in bore hole formation. Mucilage (Mu) in the bore hole can be seen, especially in figure 68. The hypha appears to have been cut obliquely and even from serial sections the shape of the wall lysis is difficult to explain. Note the middle lamella (Ml) has been traversed without any significant difference in the erosion pattern.

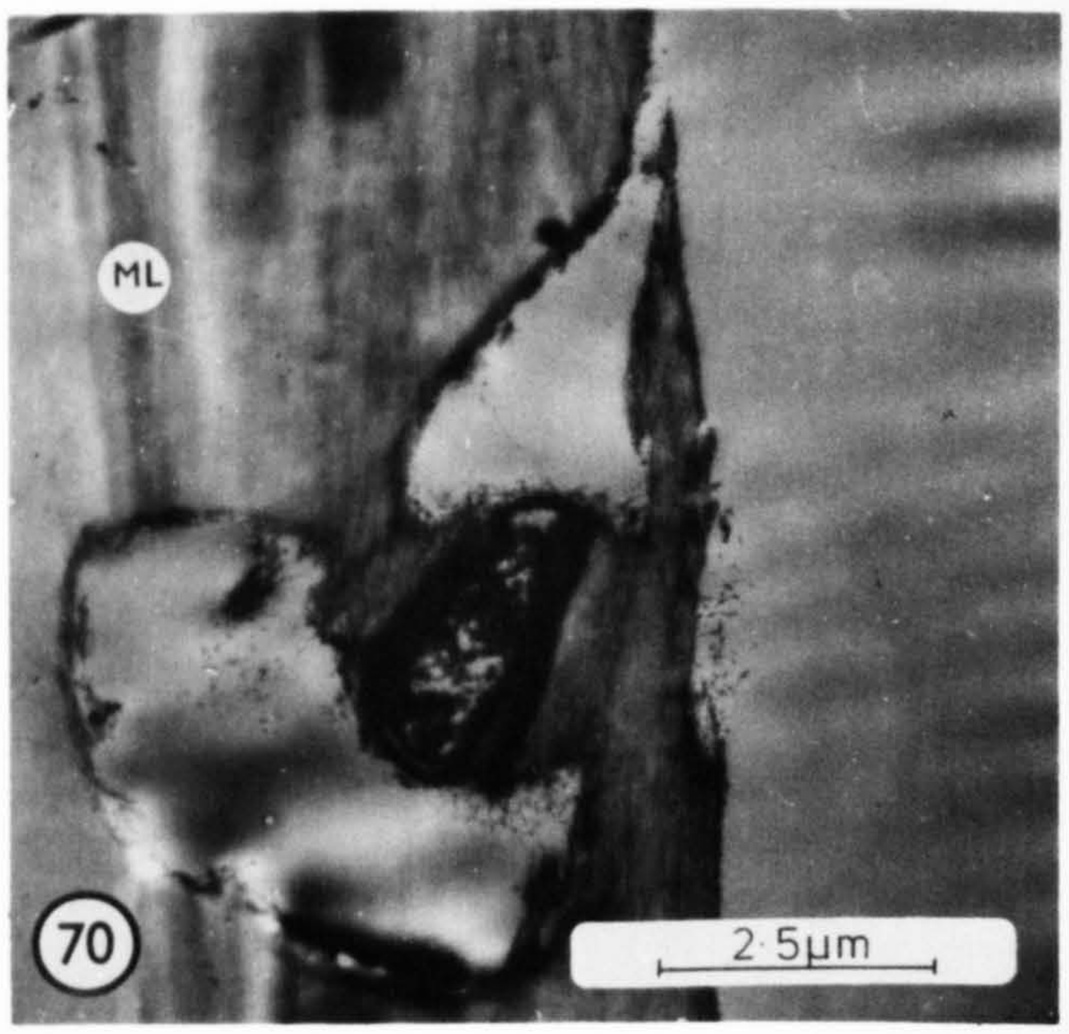
Figures 71 and 72 (x 7880 (TLS)) show a lateral branch of a lumen hypha degrading a fibre wall. From the profile of the erosion zone the junction between the compound middle lamella and the S_1 layer of the fibre appears more resistant.

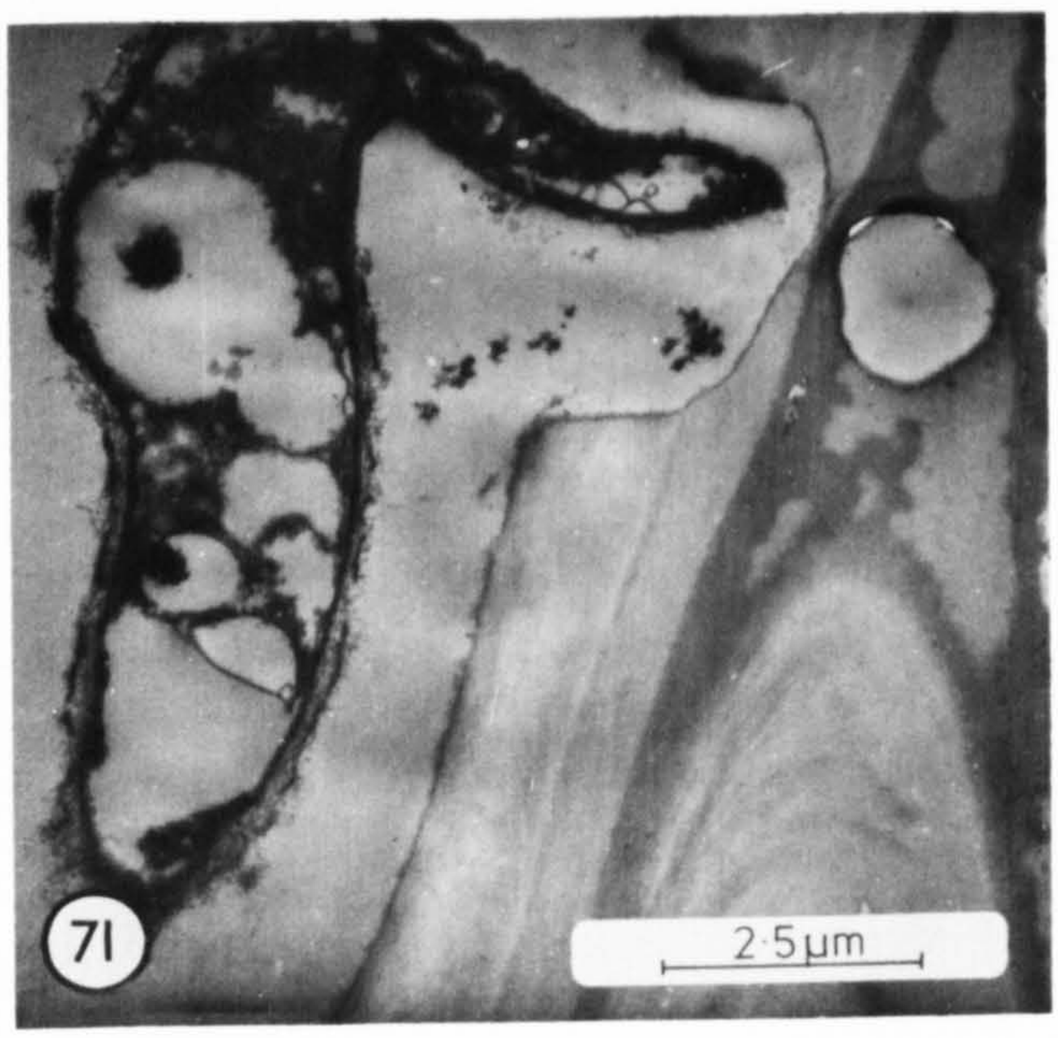
Figures 67-72:- Fixed with G, R, O and dehydrated using GMA.
All sections were unstained.

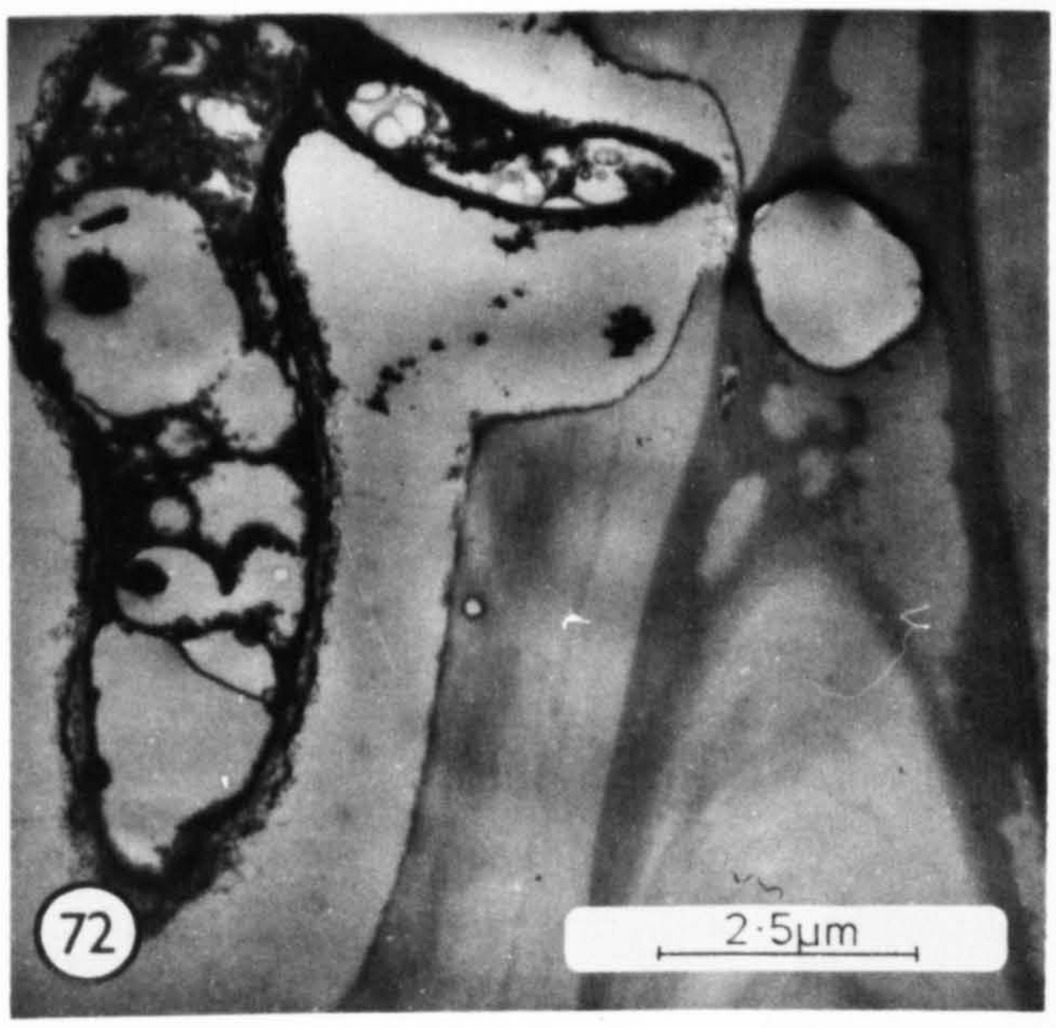

67
1µm


Mu
68
2·5µm


69
2·5µm


ML
70
2·5µm


71
2·5µm


72
2·5µm

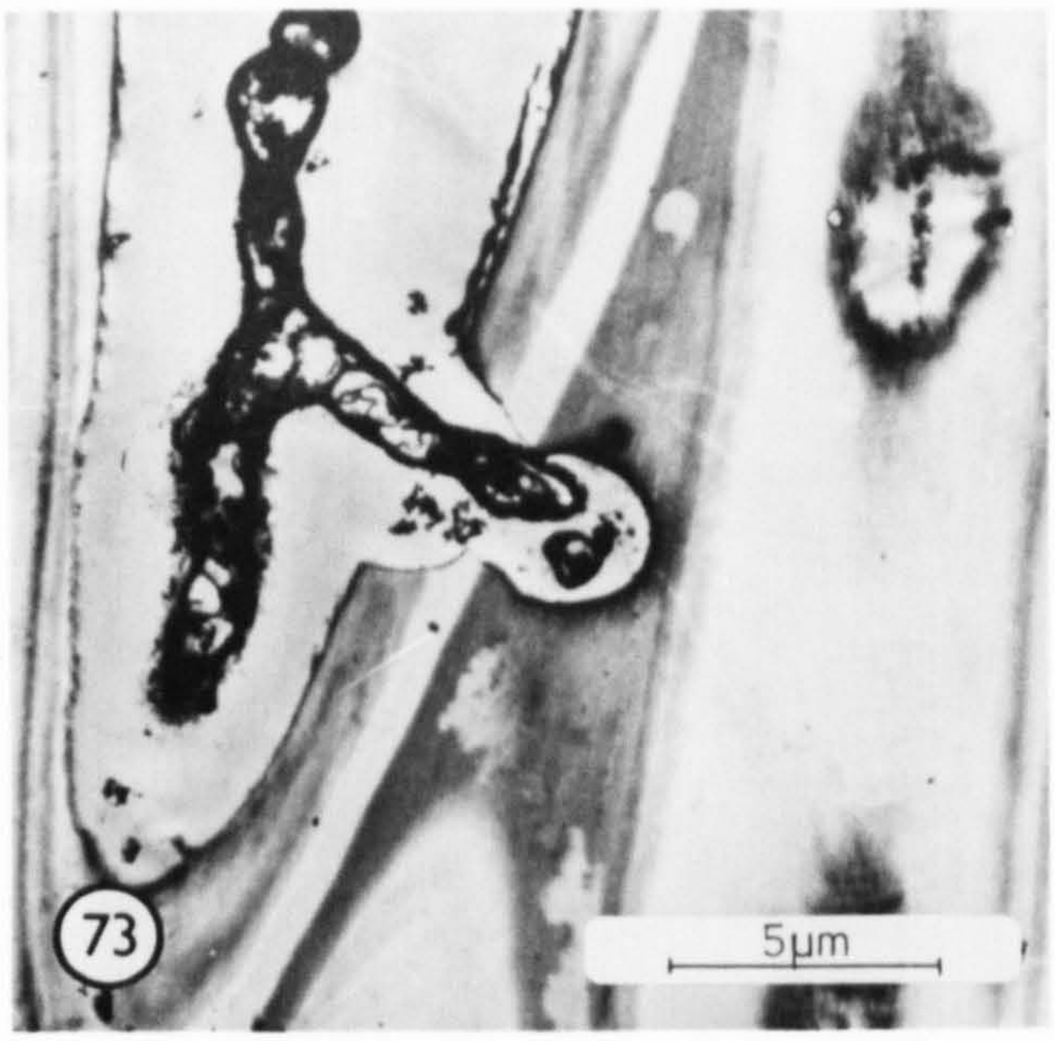
3.3.1 Coriolus versicolor on birch (Betula sp.), 4 weeks

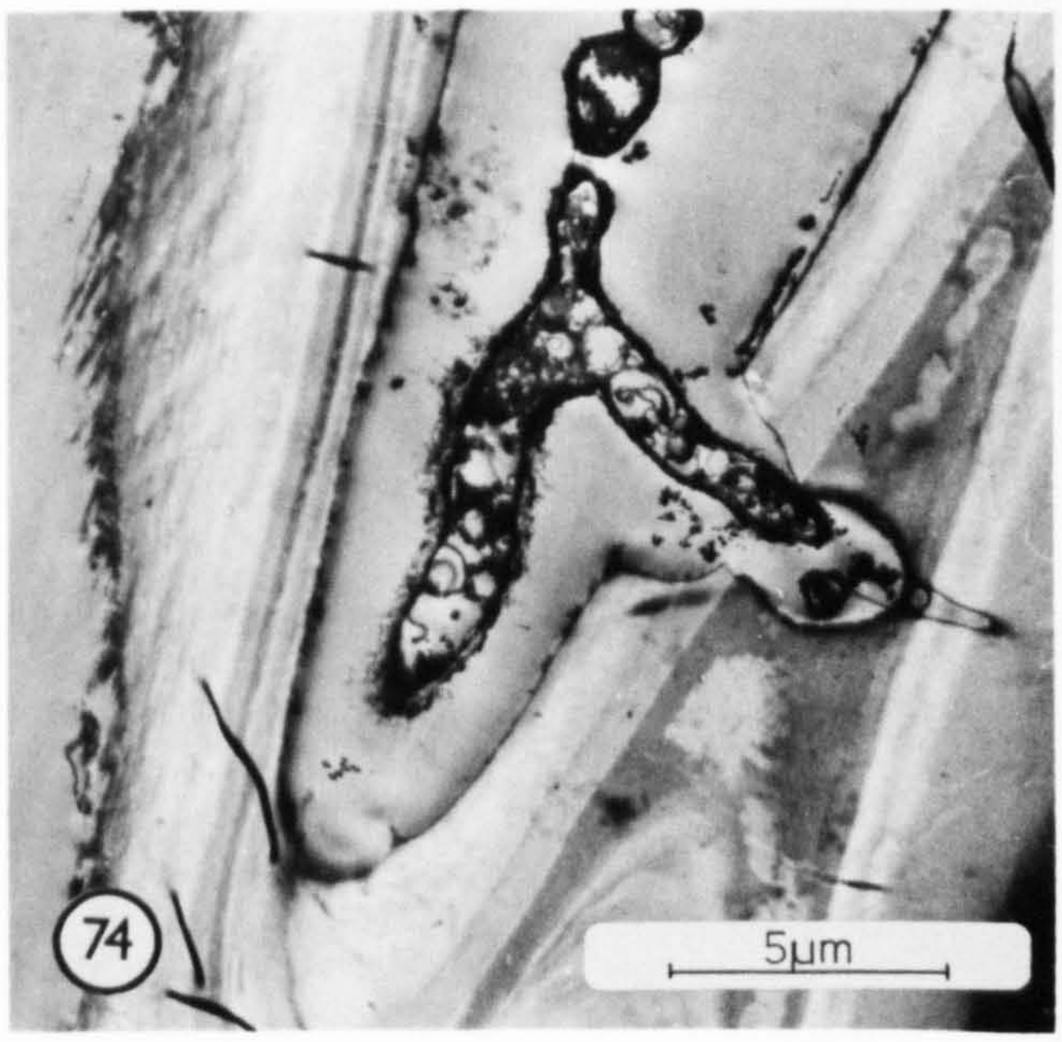
Figures 73 to 75 (x 4220 (TLS)) are lower magnification serial sections to figures 71 and 72. The continued resistance of the S_1 - middle lamella junction is still evident together with the intensive staining (Ds) of an adjacent fibre wall due to the lytic effect of a fungal hypha (H) present within the lumen, see figure 75.

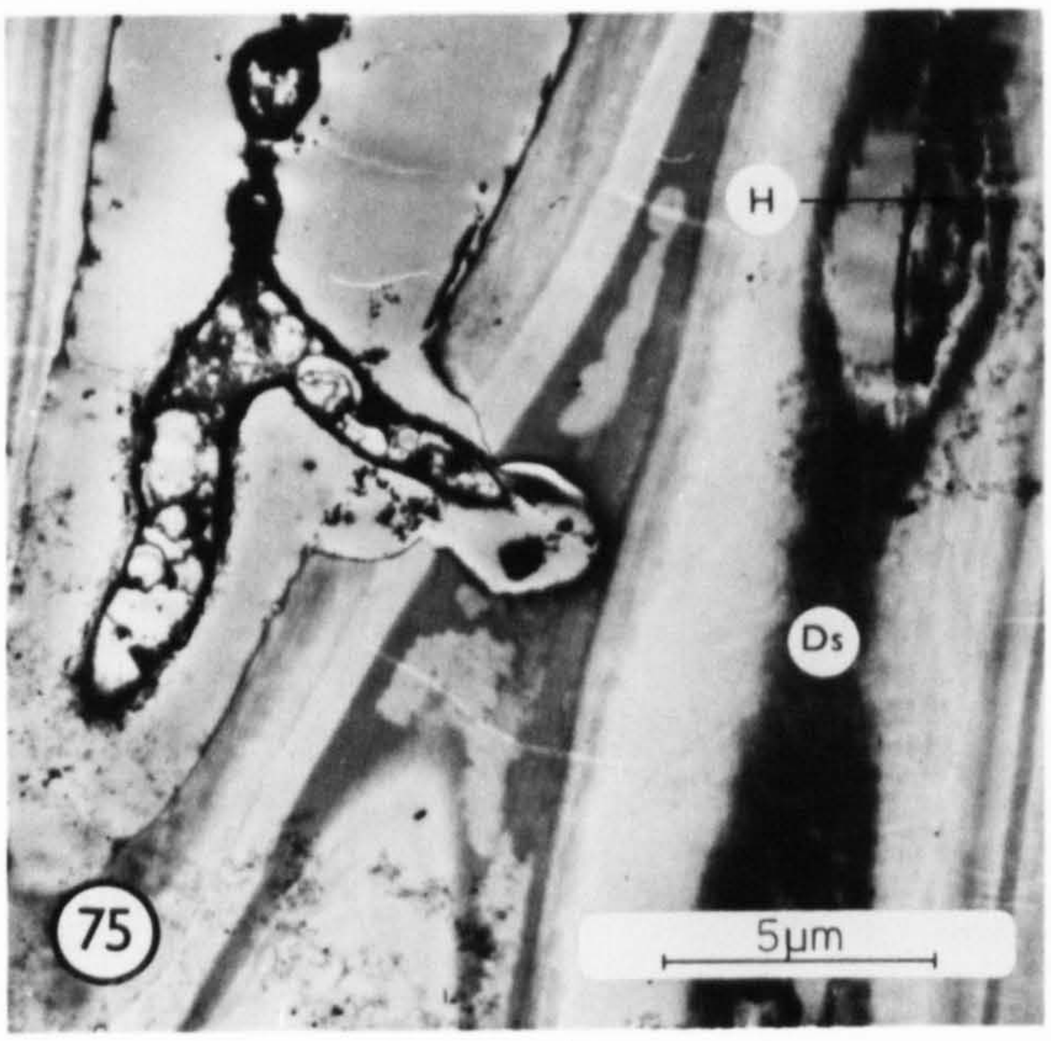
Figures 76 to 78 (x 3460 (TLS)) are serial sections of a bore hole through two fibre walls. Severe wall lysis around the hyphae has occurred with some indications of S_3 resistance (arrowed). Note that as in figures 71 to 75 the S_1 - middle lamella junction has shown resistance resulting in a double peak (Dp) to the eroded wall surface.

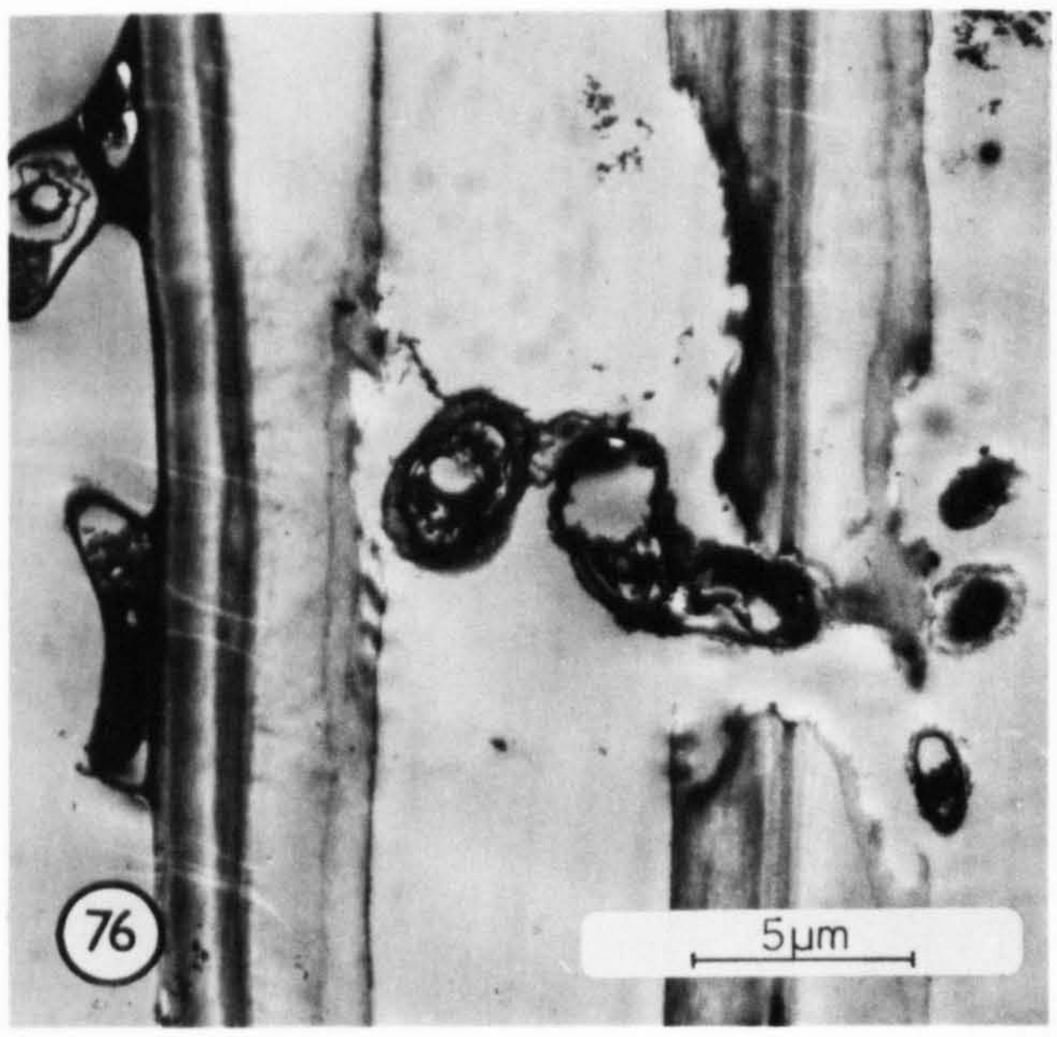
Figures 73-78:- Fixed with G, R, O and dehydrated using GMA.

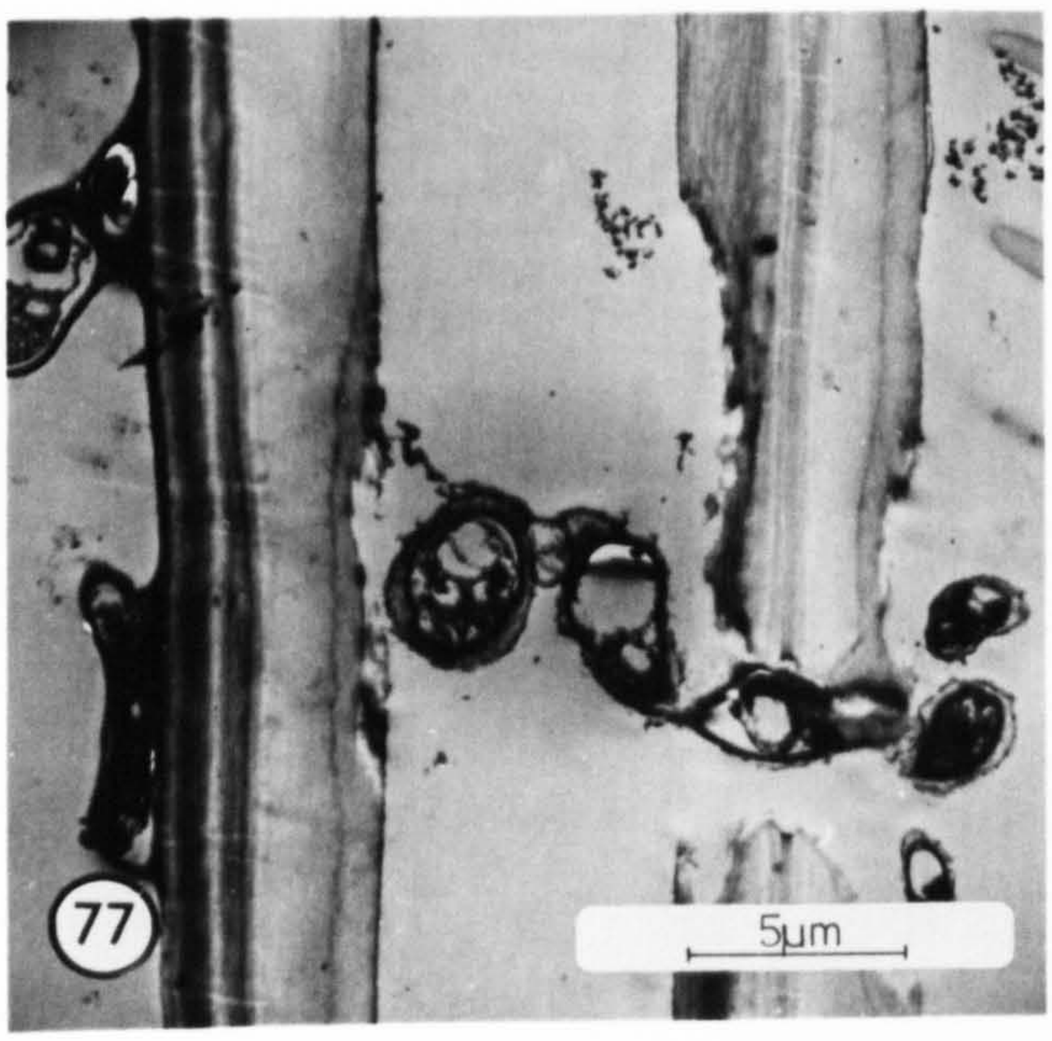
All sections were unstained.

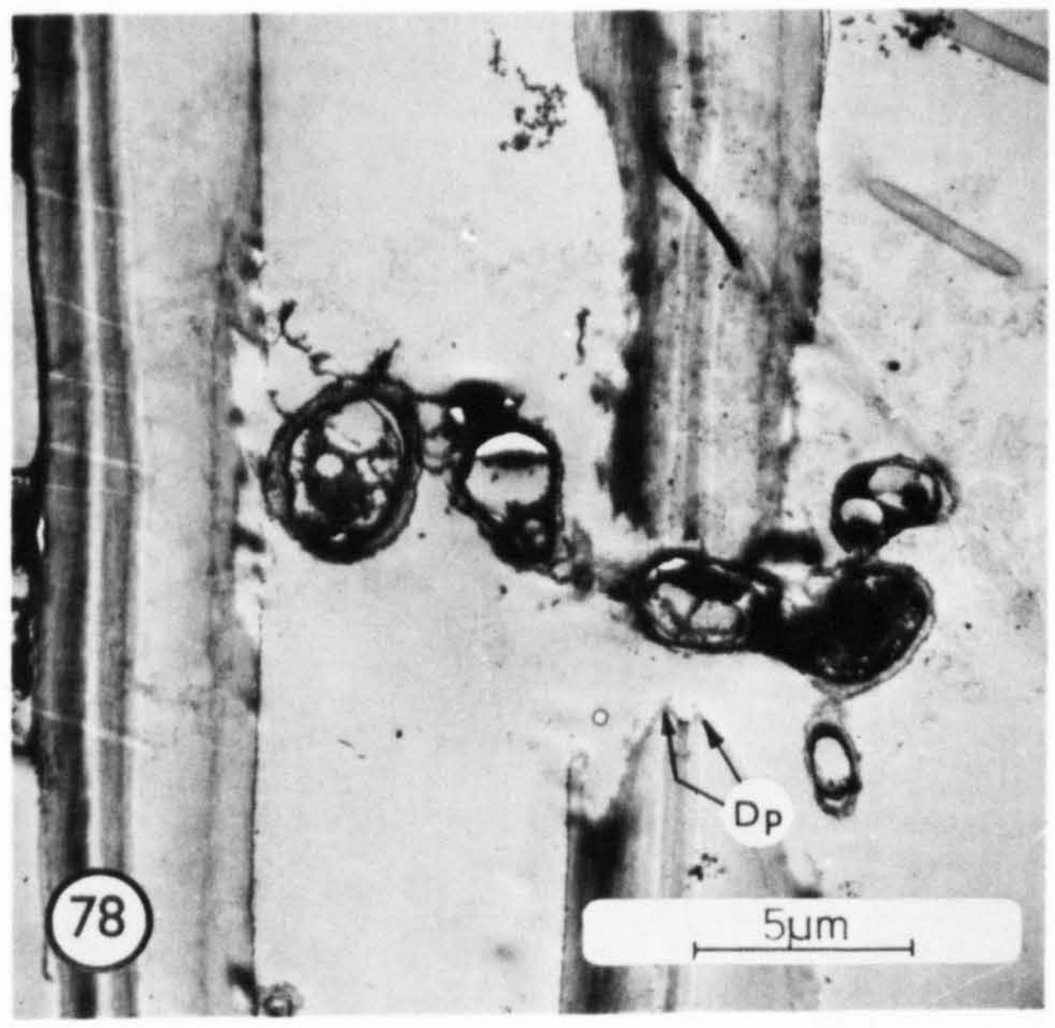

73
5µm


74
5µm


H
Ds
75
5µm


76
5µm


77
5µm


Dp
78
5µm

4.3.2 Coriolus versicolor on Scots pine (Pinus sylvestris)

The results for this wood - fungus combination were very poor. Very few of the blocks tried proved to be sectionable although some points of interest have emerged from the material that could be examined.

White rot penetration of a bordered pit torus was shown to be achieved by a distinct dissolution of the centre layers of the torus, figs. 79 and 80. The central middle lamella line and the outer S_3 regions appeared to show less degradation. Whether the penetration was achieved entirely by chemical means could not be determined from the available sections, though it may be significant that the torus has shown a slight deformation away from the hypha, indicating possible mechanical pressure.

Where lysis of the wall appeared to have occurred, high magnification detail showed the preferential attack of the matrix material exposing the microfibrillar structure, figs. 81 - 83. A limited investment of mucilage was also present in these areas.

3.3.2 Coriolus versicolor on Scots pine (Pinus sylvestris)

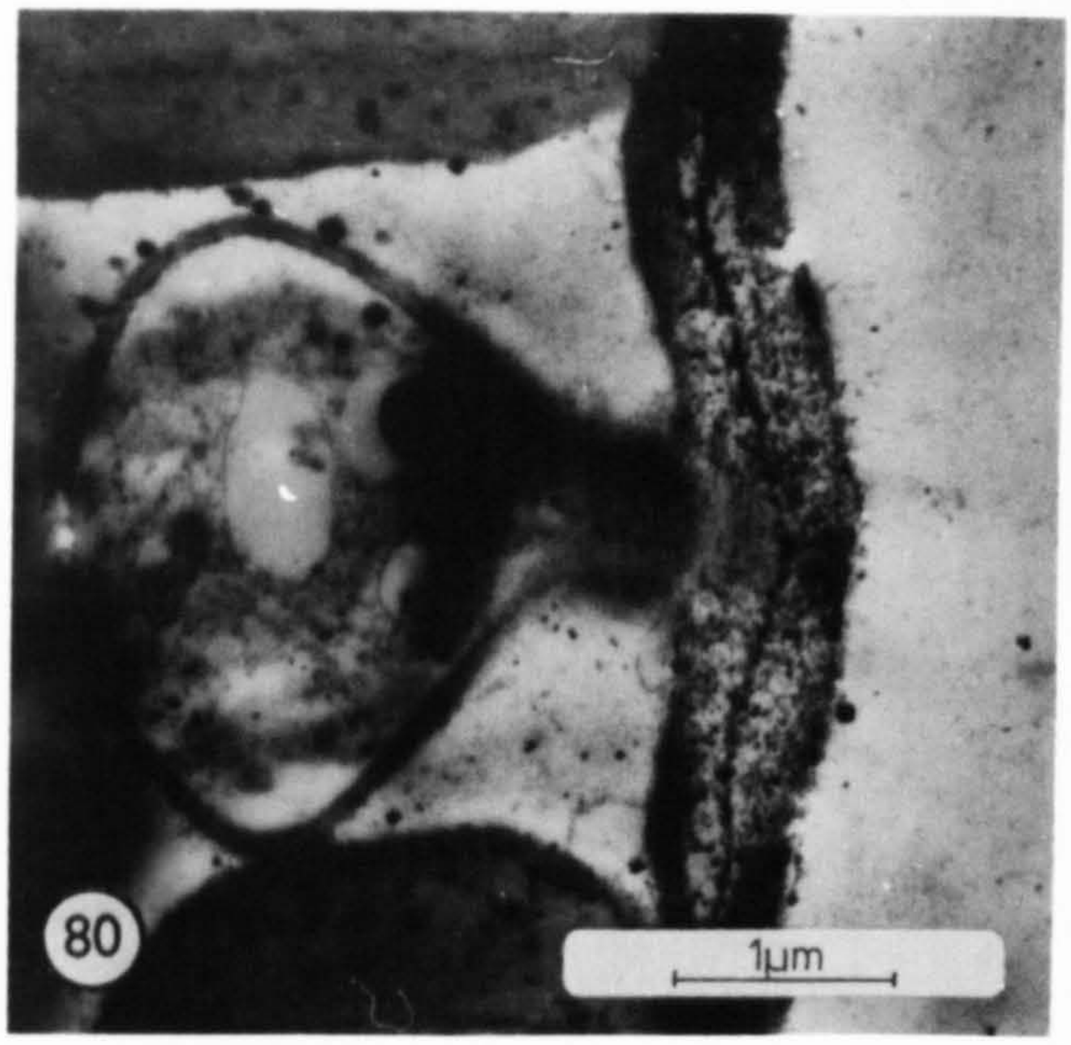
Figures 79 (x 8418 (TS)) and 80 (x 17290 (TS)) show the dissolution of a bordered pit torus. The bordered pit is on the junction between earlywood and latewood, (shown by the relative tracheid wall thicknesses). Unfortunately not enough serial sections were obtained to determine whether the hyphal restriction was real or due to the fungus bending out of the plane of section. Note also the curve in the torus indicating possible mechanical pressure. The high magnification details of figure 80 show a distinct centre line to the torus, this being a continuation of the middle lamella, together with a loosely organised central region to the torus where lysis has occurred.

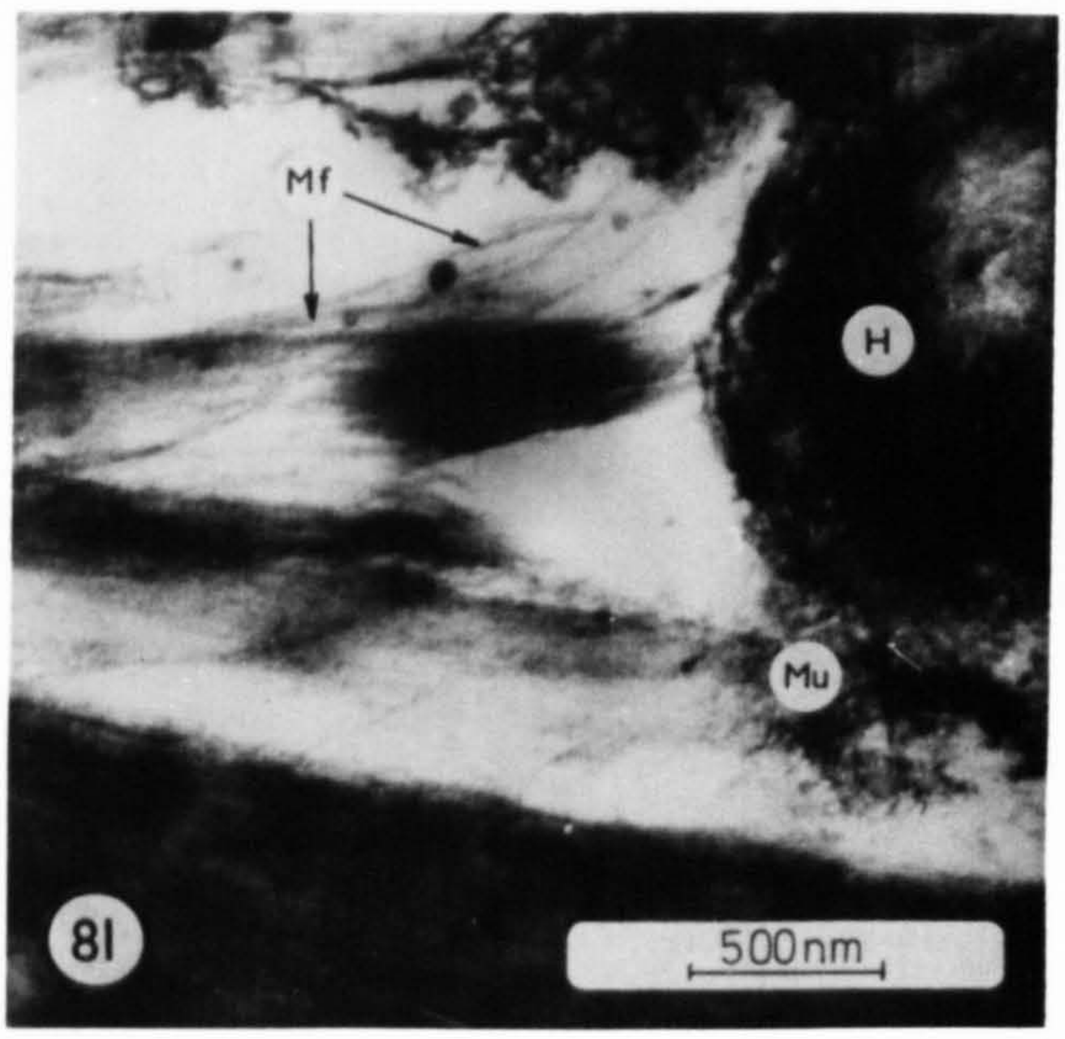
Figures 81 (x 30520 (TLS)), 82 (x 11940 (TLS)) and 83 (x 29730 (TLS)) illustrate some areas where limited wall lysis was occurring with the hyphae (H) opening up the microfibrillar structure in conjunction with the presence of mucilage (Mu). Microfibrils (Mf) can be seen in figure 81.

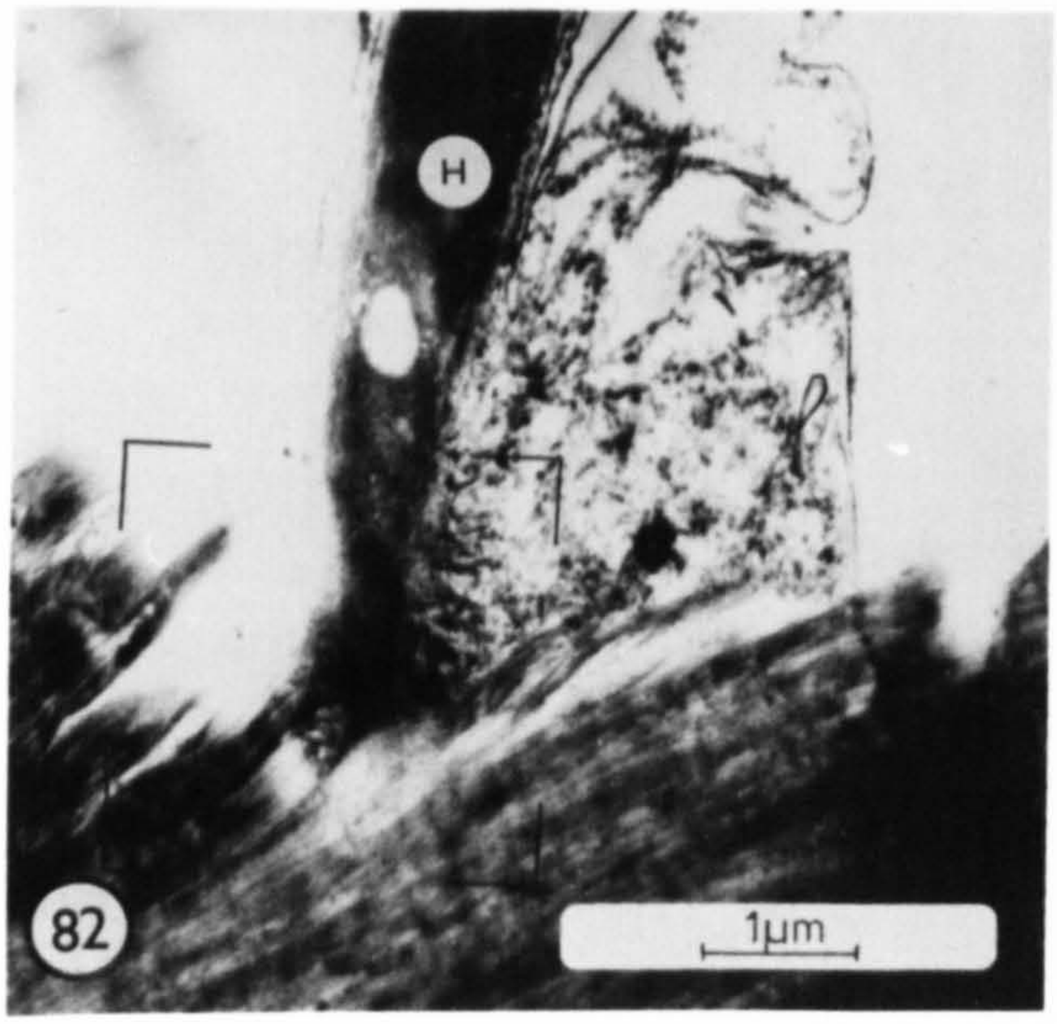
Figures 79 and 80:- Fixed with G, R, O, K and dehydrated using Durcupan. 10 day material.

Figures 81-83:- Fixed with G, R, O and dehydrated using Durcupan. 6 week material. All sections were unstained.


79
2·5µm


80
1µm


Mf
H
Mu
81
500nm


H
82
1µm

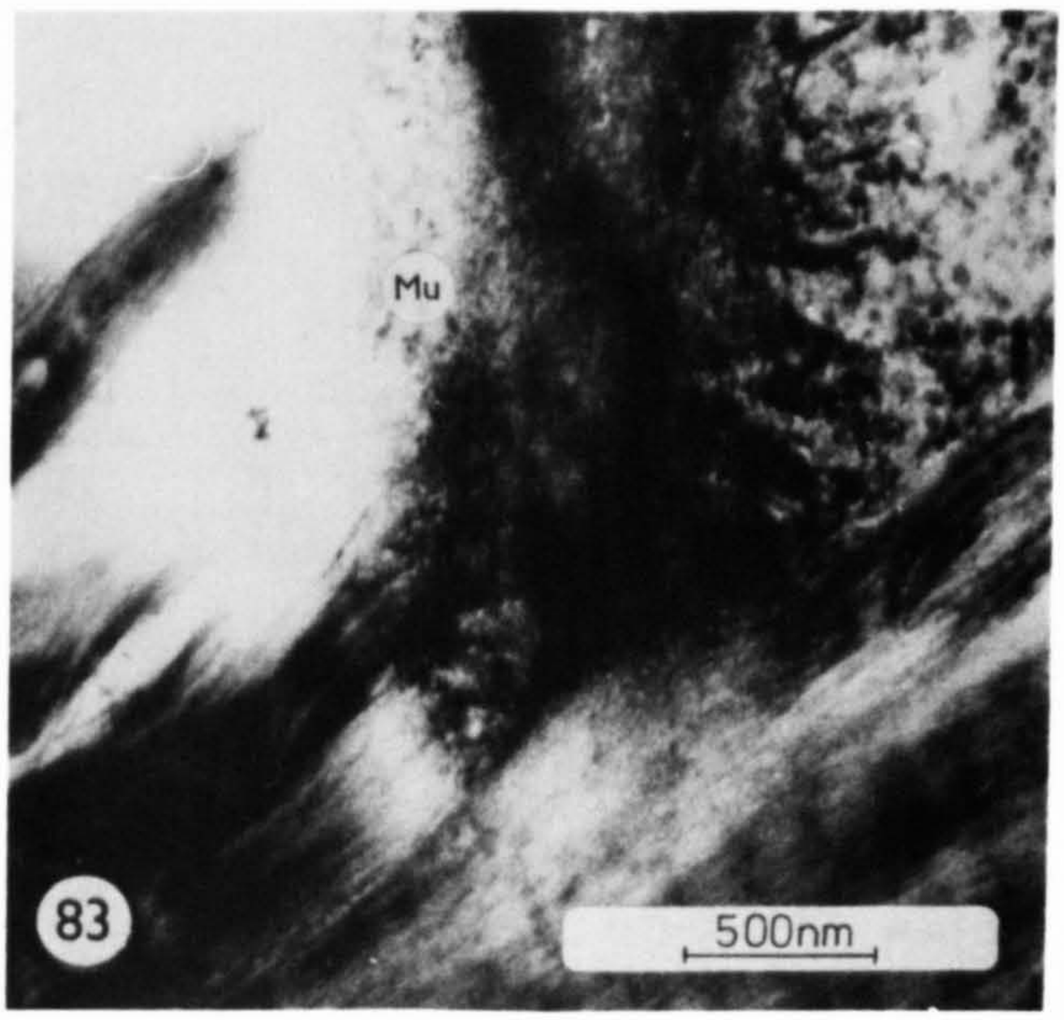

Mu
83
500nm

TABLE 1

FIGURES	FUNGUS	WOOD	INC.	DEHYDN.	FIXN.	PLANE	RESIN	MEDIUM	FORMAT	SPEC.NO.
1,2,3,4,9,10,11,	C.p.	Br	10d	Dur	GROK	TS	4:1	Abms	Mcspn.	5436/A
5,6,7,8,	C.p.	Br	10d	Dur	GROK	TLS	4:1	Abms	Mcspn.	5437/A
12,13,	C.p.	Br	10d	Dur	GRO	TS	2:1	Malt	Block	5261/A
14,15,16,17,19,20,21,	C.p.	Sp	4w	Dur	GRO	TS	3:1	Malt	Block	5321
18,	C.p.	Sp	4w	GMA	GRO	TS	3:1	Malt	Block	5462/C
22,23,24,25,28,30,39,	C.g.	Br	10d	Dur	GRO	TLS	4:1	Abms	Mcspn.	5498/C
26,27,29,	C.g.	Br	4w	Dur	GRO	TLS	3:1	Malt	Mcspn.	5324/B
31,34,37,	C.g.	Br	10d	Dur	GROK	TS	4:1	Malt	Mcspn.	5483/A
33,	C.g.	Br	4w	GMA	GRO	TLS	3:1	Malt	Block	5499/C
32,35,36,38,40,	C.g.	Br	10d	Dur	GROK	TS	4:1	Abms	Mcspn.	5467/A
41,42,43,44,45,46,47,48,49,50,51,	C.g.	Sp	4w	GMA	GRO	TLS	3:1	Malt	Block	5464/B
52,53,54,	C.v.	Br	10d	Dur	GROK	TLS	4:1	Malt	Mcspn.	5442/A
55,56,	C.v.	Br	10d	Dur	GRO	TLS	4:1	Malt	Mcspn.	5439/C
57,58,59,60,61,62,63,64,65,66,68, 69,70,71,72,73,74,75,76,77,78,	C.v.	Br	4w	GMA	GRO	TLS	3:1	Malt	Mcspn.	5466/B
67,	C.v.	Br	4w	GMA	GRO	TS	3:1	Malt	Block	5465/C
79,80,	C.v.	Sp	10d	Dur	GROK	TS	4:1	Malt	Mcspn.	5443/A
81,82,83,	C.v.	Sp	6w	Dur	GRO	TLS	4:1	Malt	Block	5331/B

5. DISCUSSION

Successful transmission electron microscopy using ultrathin sections primarily depends on the ability to produce satisfactory sections of known orientation. To achieve this there must be a good match between the hardness of the embedding resin and the specimen, with precise orientation of the latter during sectioning. The detailed methods given in this thesis have outlined the problems, requirements and some possible solutions to produce ultrathin serial sections of fungal decayed wood.

To avoid wasted effort and chemicals on unsectionable blocks, variations in fixation, dehydration and staining procedures should only be applied in conjunction with, or after, specimen - resin matching. The extreme variability of the specimens, due to incubation times, wood tissue and type of decay fungus, virtually precludes the development of a fixed preparation schedule. The results of this work have shown that with present methods it is not possible to predict the required resin hardness for a given wood - fungus - incubation time. Only broad guidelines can be suggested.

Brown rot attack of wood cell walls produces softer decay blocks of a susceptible wood species than white or soft rot for the same incubation period (this applies to the early time periods mainly). Depending on the fungal enzyme complement and the natural susceptibility of the woods, differences in decay rates can be extremely marked. In this work birch suffered heavier degrade by both brown and soft rot fungi than did the Scots pine, with equal attack of both by the white rot fungus.

According to the nature of the study being undertaken specimen

preparation should be approached in one of two ways:-

(i) Where a single fungus - wood combination is being examined then a number of incubation time specimens should be prepared in a range of resins (for example, three time periods embedded in each of three resin hardnesses). Using this method the chances of obtaining a resin / specimen match are greatly enhanced and can be further improved when decay regions are searched by incorporating a range of degrade and tissue types in the specimen replicates.

(ii) In comparative studies of a number of woods, fungi and preservative treatments the materials to be examined should be prepared and processed together so as to eliminate variations due to preparative procedures. If a range of resins is again employed then a match of the softest resin with the most severely brown rotted wood and the hardest with poorly white or soft rotted material may be achieved.

The development of a specimen holder, essential for the handling of large numbers of individual decayed wood specimens during processing, has enabled extensive comparative studies to be successfully carried out with the production of satisfactory blocks and sections, even when the number of specimen variables was increased, due to different chemical processes being employed in the preparation procedures. Without such a specimen holder studies comparing large numbers of specimen variables (biological and/or chemical) would have to be carried out by a number of preparation runs. This may lead to errors in the interpretation of observed differences if consideration is not given to the possible effects that separate preparations may have on the final result.

The above comments point to a recommendation to reduce the

number of specimen variables when preparing material for T.E.M. and should be borne in mind when setting up T.E.M. projects and studies, especially those of a comparitive nature.

A perfectly matched specimen block was sectionable with relative ease but slight mis-matching produced a number of problems during sectioning. Longitudinal sections were especially difficult to cut free from distortions and this was due to the microfibrils of the thick S_2 wall layer being cut "with and against" the grain, as found in the trimming stages (see 3.12). The slightest degree of microfibril "pulling", due to mis-matching, resulted in distorted sections with the microfibril fragments accumulating on the knife edge producing severe knife marks in the sections. This "grain" effect was more obvious in adjacent wall pairs where the helices of the thick S_2 wall layer run in opposite directions. Consequently one of the walls cut perfectly (with the microfibrils) and invariably the other showed signs of distortion (against the microfibrils). For a mild example of this effect see the right hand wall pair in figure 57. As a result of this microfibril influence on sectioning qualities, and contrary to what has been previously suggested, transverse sections were found to be the easiest to cut free from tearing and distortion, even in poorly matched material, the bulk of the microfibrils being cut laterally rather than oblique - longitudinally. However, transverse sections require much higher cutting forces and consequently dull the knife edge more rapidly, especially of glass knives. Therefore a compromise has to be achieved between the ease of preparing distortion free sections against the service period of the microtome knife. The variation in trimming and knife paths, given in section 3.12, attempted to utilise the above

findings to achieve longitudinal sections from mis-matched specimens and found that an axial attack angle of 45° was the most successful in these cases.

Further studies on wood decay using the T.E.M. should incorporate fixation procedures to preserve the extracellular mucilage as this appears to have an important role in the decay micromorphology of soft and white rot. The application of a range of fixatives resulted in improved cellular preservation and detailing of the wood cell wall. The ruthenium red demonstrated the mucilaginous matrix, though not as effectively as with Rhinocladiella mansonii (see part II) and this could have been due to infiltration problems, different processing procedures, or the lower osmium tetroxide level which may have reduced the enhancement of the ruthenium red staining (Luft, 1971). Although there was a certain degree of cytoplasmic preservation and detailing by the glutaraldehyde and osmium tetroxide many of the specimens exhibited signs of over fixation by osmium. The introduction of $KMnO_4$ fixation, in conjunction with the other fixatives, produced by far the best results for both wall and fungal details. The brief exposure of 20 minutes and thus reduced time for osmium resulted in clear definition of membrane structures and little or no loss of cytoplasm. It would appear, therefore, that the three hour exposure to osmium tetroxide in fixation stage 2, as recommended by Luft (1971), was too long for this type of tissue. The wall layers were clearly defined with a clarification of the microfibrils resulting from the reduction of the $KMnO_4$ to MnO_2 by the lignin (Crocker, 1921) producing greater contrast with the unstained microfibrils. The affinity of $KMnO_4$ for lignin has resulted in its widespread application as a

fixative, especially in fungal decay and chemically treated wood, and plant cell lignification studies, (see Wardrop, 1965; Hepler et al, 1970; Bland et al, 1971; Wilcox et al, 1974 and Sinner et al, 1976).

Attempts at increasing the specimen contrast of material that had been fixed without $KMnO_4$ by post staining the ultrathin sections with 2% $KMnO_4$ (adapted from Lawn, 1960) were unsuccessful as the resin reacted strongly with the stain. The resulting sections inherited electron opacity throughout the resin and specimen, were fragile and distorted. Reedy (1965) noted similar problems with permanganates and in a personal communication to him, J. H. Luft suggested that the interaction was due to the presence of an unprotected double bond in the MNA component remaining reactive in the cured resin.. Reedy (1965) showed conclusively that the MNA was the only component of Luft's (1961) resin system that reacted with the permanganates and that replacement of the MNA with other hardeners, such as HHPA (Fink, 1960) eliminated the interaction..

The question over the use of permanganate, therefore, can be separated into two approaches. The $KMnO_4$ can either be added during the fixation stage but only for short exposure times, to reduce cell damage, followed by normal embedding in resin mixes containing MNA, or the specimens can be embedded in non-MNA resin and the ultrathin sections then stained with Permanganate (after Lawn, 1960).

The results from GMA dehydrated material, see figures 32, 41 - 51, 60 - 63, compare favourably with those of the Durcupan dehydration preparations, see figures 33, 52 - 56. The basic stabilisation of the mucilage structure would appear to be dependant on the fixative, ruthenium red (see part II 4), with the gentle removal of water using

the water soluble resin assisting in the preservation of the gross structures. On a cost effective basis, therefore, GMA would be preferable over Durcupan. However, with improvements in cytoplasmic preservation the differences between the two may be revealed by their interaction with and preservation of the finer components of the fungal cell. Neither of the two water soluble resin dehydration agents appeared to have any adverse effects on the polymerisation and sectioning qualities of the final embedding resin, implying that if there was contamination then this was not detrimental to the end result.

There is no doubt that preservation of cytoplasmic details of fungi actively degrading wood can still be improved upon. This may be achieved by variations in fixatives and stains, solution strengths, exposure times, temperatures and buffers, or by the application of different preparation procedures. Recent work by Howard and Aist (1979) has introduced new interpretations of fungal cytology as a result of using freeze substitution preparation methods (see also Hayat, 1972 and Pease, 1973) and successful future application of these techniques to decayed wood may greatly assist the interpretation of decay micromorphology.

As with the S.E.M. discussion (see part I) only features relevant to the complete decay mechanisms (see part IV) will be covered in detail, for the fungal - wood combinations studied, in the following discussions.

Brown rot

Throughout the observations on Coniophora puteana attack on birch there was a significant absence of a mucilaginous layer (figs. 1 - 11) comparable with that observed on Rhinocladiella mansonii. This agreed completely with the S.E.M. results showing no extracellular investments for the brown rot fungus (see part I).

The presence of fine structures in conjunction with normal colonising hyphae was unexpected and cytoplasmic contents indicated that they were probably of hyphal origin (Figs. 9 - 11). These hyphae, between 0.5µm and 1.0µm in diameter, were observed in situations where active wall lysis was in progress and possibly perform some function of increasing the surface area of enzyme release and product absorption (George, 1974). They were too large to be regarded as the 'myco-fibrils' described for Chaetomium globosum by Liese (1964) and Liese and Schmid (1963) which were more likely to be the dehydrated residues of an extracellular coating.

The containment of the lytic effect only to the wall of the cell colonised by the hypha, as demonstrated by figures 12 and 13, could be explained by microchemistry of the wall. As mentioned earlier (I. 5) the compound middle lamella represents a chemical barrier, with the absence of cellulose and significant hemicelluloses in this region resulting in the hypha having little capacity to degrade its components. Only by concentrated enzymatic / chemical and possibly physical penetration via pits or bore holes can the hypha have any influence on the wall layers of an adjacent cell.

Wilcox et al (1974) demonstrated the spread of the lytic effect through the wall from a single lumen fungus, and it would appear from

the infrequent observations of partially degraded walls that the dissolution of the wall polysaccharides, once initiated, progresses very rapidly through the entire cell wall.

The presence of water within the wall would be essential as the medium for the lytic mobility and product return. The capacity of certain brown rot fungi, for example Serpula lacrymans, to degrade wood at moisture contents apparently below fibre saturation reflects their ability to transport water to the areas of wood under attack.

As noted in the S.E.M. study the decay of Scots pine by Coniophora puteana was very limited, but as in birch there was no significant mucilage (figures 14 - 16). However, features which appeared regularly in the T.E.M. work were the wall penetrations which had deviated near the S_1 region of the wall (fig. 17). The susceptibility of the S_1 - S_2 wall layers was indicated by lysis zones, splits and regions of denser staining, progressing laterally away from the bore hole. Sinner et al (1976), using enzymatic and ultrastructural studies, have shown that the cellulose fibrils of the $S_1 - S_2$ layer in birch and beech fibre holocellulose were heavily encrusted with hemicelluloses. Wilcox et al (1974), studying brown rot attack of untreated douglas fir treated with a pentachlorophenol wood preservative, also demonstrated the apparent susceptibility of the $S_1 - S_2$ region even in preservative treated material.

On the basis of this work and the results of previous studies it would seem that the $S_1 - S_2$ region of a number of wood species examined, both hardwoods and softwoods, would appear to be more susceptible to the effects of brown rot fungi than the other wall layers. The abundance of hemicelluloses, with the corresponding

reduction in lignin, could have a strong promoting influence on the decay of this region resulting in the observed dissolution of these wall layers.

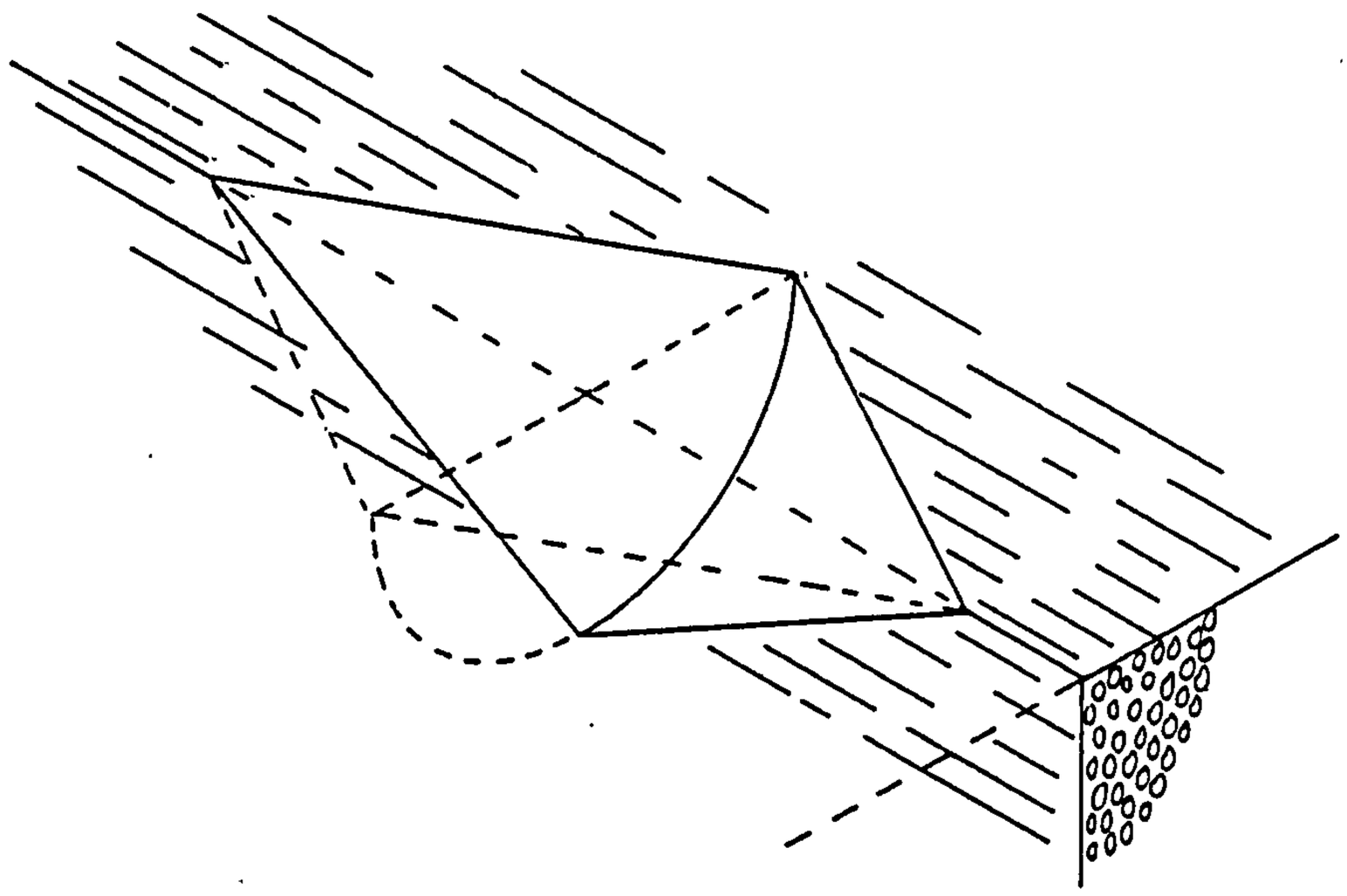
Bordered pits exhibited different membrane / torus structures depending on their location within the cell and within the annual ring. The observations were only made on a few isolated examples and, therefore, the comments on their structures should not be regarded as being the results of an extensive survey. In general though, of the earlywood tracheids examined the tori of both tangential and radial wall pits were thin and uniform (figs. 19 - 21). This contrasted with the thickened torus found in the bordered pit of the tangential wall pairs on the earlywood - latewood tracheid junction (see fig. 103). These observations were in general agreement with the results indicated by Koran (1974 and 1977). Although thin tori should present little resistance to fungal penetration the neat perforations noted in the S.E.M. work were also observed in T.E.M. sections and can only be attributed to the resistance of the thin compound middle lamella component of the membrane to the fungal degradative agents.

Soft rot

The predominance of type 2 decay (Corbett, 1965) for the soft rot (Chaetomium globosum) attack of birch confirmed the findings of Corbett (1965), Greaves and Levy (1965) and Levy and Stevens (1966). The geometry of the notching (figs. 22 - 28) indicates that the same enzyme system is in action as that used by the fungus in cavity formation. The material filling the notches is probably mucilage as the dark staining granules present in this material were continuous over the hyphal surface.

Figures 26 and 27 demonstrated that the innermost wall layer, the S_3 and/or warty layer, appears to show some degree of resitance to the enzymes though the underlying S_2 was susceptible, and once exposed, was rapidly degraded. This type of attack was referred to as "trans-S_3 erosion" by Zainal (1975). Localised concentrations of enzymes resulted in the production of a series of 'V' shaped lysis zones (Corbett, 1965). These progressively enlarged and fused to produce the large erosion troughs often observed in older material with the S_2 degraded as far as the S_1 wall layers, see figure 26.

The lateral concentration of the lysis by surface tension effects on the mucilage was clearly demonstrated in figures 37 - 40, and explains the development of a central ridge as observed in white rot attack of beech vessels (Bravery, 1971, 1972). Figures 38 and 39 indicated that the shape of the early erosion was in the form of half a double cone:-



a section parallel to the microfibrils producing a 'V' shaped notch and one at right angles producing an approximate curve (see also Corbett, 1963). The presence of significant amounts of mucilage in soft rot attack of birch (figures 31 - 33) supports the proposal that

it has a major function in the lysis patterns observed.

Only one set of sections demonstrated the formation of type 1 decay with the development of a cavity within the S_2 of a fibre wall by the 'T' branching of a lateral hypha derived from a lumen hypha, figure 35. Although the sections did not demonstrate the connection between the perforation hypha and the parent lumen hypha the dimensions were in keeping with typical 'T' branch hyphae previously observed (Corbett, 1963, 1965; Levy and Stevens, 1966). The ability of soft rot fungi, actively involved in lumen erosion, to produce a 'T' branch and subsequent cavity formation was previously demonstrated by Nilsson (1973) in a range of soft rot organisms and by Zainal (1975) with Phialophora fastigiata on birch.

Growth of hyphae through intercellular regions, along middle lamellae and into the S_1 wall regions, was difficult to explain. The possible natural susceptibility of the S_1 – S_2 junction, as previously noted, might be a reason for the latter effect, but the heavily lignified middle lamella and intercellular spaces would present severe problems to the enzyme systems characterised for normal soft rot hyphae. It may be significant that this type of attack was observed in specimens cultured on Abra ms medium (see table 1). The excess of available nitrogen might allow the fungus to produce more of the enzymes required for such penetrations without fear of wasting nitrogen, which under normal decay circumstances would be a limiting factor.

Because the results obtained were limited and difficult to interpret, there is little to discuss on the interaction between Chaetomium globosum and Scots pine. The presence of mucilage in decay situations was clearly shown although the lysis patterns appeared to be disorganised.

The possible susceptibility of the S_1 - S_2 wall layers was again demonstrated, but not conclusively, and so no attempts will be made to interpret the lysis patterns from the material examined.

White rot

Throughout the material examined for the degrade of birch by Coriolus versicolor the presence of mucilage on the hyphae was demonstrated. This was believed to play a role in the development of lysis regions in the cell walls.

Although all the wall components were completely degraded there was a slight preference for the matrix material (see also Bravery, 1971, 1972). This was evident as a removal of the material between the microfibrils (figures 64 and 65) together with regions of denser staining due to removal of wall components allowing deeper penetration of fixatives (figures 66, 73 and 75). Determination of the material removed was not possible in this study but with the application of cytochemical stains it could be possible to determine whether preferential lignin or hemicellulose attack has occurred.

In some examples, however, the wall lysis appeared to progress without the advanced removal of matrix material (figures 67, 71 - 75) and cytochemical and ultrastructural organisation variables probably account for this range of wall degrade observed. A number of wall layers appeared to exhibit variable resistance to degrade. The S_3 in some regions was still intact when the underlying S_2 microfibrils exhibited severe lysis (figures 59, 64 and 65). This trans-S_3 erosion, previously referred to in soft rot attack, type 2, appeared to be found mainly in fibres that were in direct contact with ray cells. The significance of this, if any, is not understood but perhaps during

development these fibres differentiated with slightly resistant inner wall layers. Nečessaný (1963) also found the S_3 microfibrils were resistant to white rot but did not specify whether this was a uniform feature or variable as in this work.

Resistance by the compound middle lamella was evident mainly in ray tissue. The attack of this layer being accompanied by denser staining and, when penetrated, by spurs of resistant material projecting into the lumen of the erosion hole (figures 58 and 60). The resistance of this layer had been well established by Meier (1955), Cowling (1961) and Wilcox (1968), with the cell corners being the last remnants of the tissue to be digested by the white rot enzymes.

Although resistance of the S_1 layers was proposed by Meier (1955) and attributed to a greater density, or different chemical composition, the present studies indicated that the wall layers on the boundary between the S_1 and compound middle lamella were resistant (figures 71 and 72). This was more apparent in tangential sections of the cell wall (figures 71 - 75) than in radial sections (figures 76 - 78). In the latter two, fine ridges could be distinguished and were presumed to form continuous restricting annuli within the bore hole.

Only two points of interest could be drawn from the results of Coriolus versicolor on Scots pine. Firstly, penetration of a bordered pit with a thickened torus (see also page 237) appeared to be via a combination of enzymatic and mechanical actions (figures 79 - 80). The matrix material of the torus was extensively degraded resulting in a sharply contrasting line of resistant middle lamella and dark granules representing the concentrically arranged microfibrils of the torus in section. The bulge in this weakened structure indicated

slight pressure from the hypha which may or may not have already passed through the torus. Secondly, preferential degrade of matrix material could be indicated in figures 81 - 83 where the separation of individual microfibrils could be seen together with the presence of mucilage, from the hyphal surface, which may be actively involved in the wall lysis.

In summary, therefore, the results of the T.E.M. of the three decay types have shown that the hyphae of the brown rot fungus Coniophora puteana bear little or no extracellular mucilage whereas both soft rot, Chaetomium globosum and white rot, Coriolus versicolor hyphae possess an external mucilaginous sheath which appears to be significant in the observed decay micromorphology.

The diffuse, rapid, degrade of the cell wall cellulose by brown rot hyphae may be assisted by fine hyphal strands and it was found that the S_1 region of the cell wall appeared to be more susceptible to attack. Growth from cell to cell was frequently via existing pitting with restricted dissolution of the resistant compound middle lamella, which also prevented spread of the wall lysis from degraded to undegraded cells.

Soft rot attack of birch was predominantly Corbett type 2 (Corbett, 1965) with precise 'V' shaped notches being cut into the susceptible S_2 through a more resistant S_3 and/or lumen surface layer. Mucilage appeared to provide a continuum between the hyphae and the various erosion surfaces, for example, bore holes, lumen erosion and early cavities. The development of erosion channels with a central ridge (normally associated with white rot attack) was probably a function of the surface tension effects on the mucilage, concentrating

the enzyme attack to the lateral vicinity of the hyphae. Extensive accumulations of mucilage were evident around the hyphae degrading Scots pine although the limited results, in themselves, were difficult to interpret.

Mucilage was also present on the hyphae of white rot, both in and out of cell wall contact situations. Wall erosion was variable with apparent trans-S_3 attack of the S_2, extensive bore holes in fibre walls and total lysis of ray cell walls being observed. Certain wall layers, notably the S_3, S_1 - S_2 junction and compound middle lamella exhibited partial resistance to lysis and the general impression of wall lysis illustrated a preferential removal of the matrix material.

There is no doubt that wood is one of the most difficult materials to prepare and section for examination in the transmission electron microscope. Whereas transmission electron microscopy techniques were initially poorly defined and gave unpredictable results, refinements in specimen preparation and a greater understanding of the technologies involved are gradually converting the subject into a precise, specialised science. Only the intricacies of ultramicrotomy can still be regarded as being subject to individuals and experience. The approaches made in this work have introduced detailed methods and techniques to the field of wood electron microscopy and hopefully make the user aware of the problems and possible solutions in this difficult subject.

Further studies of wood decay micromorphologies at high magnifications can only be achieved using the electron microscopes and simplifying their applications should be reported and encouraged.

PART IV

PROPOSED DECAY MECHANISMS AND CONCLUSIONS

1. PROPOSED DECAY MECHANISMS

The results obtained in this thesis indicate new features of wood decay micromorphology, especially the role of mucilage in the hyphal - cell wall interactions. Using this evidence and the general features of wood decay previously established (see introduction) the following mechanisms for brown, soft and white rot decay are proposed and discussed.

The classification of decay fungi reflects their ability to degrade the components of the wood cell wall together with the observed patterns of lysis. The distinction between hardwoods and softwoods can not only be based on the range of tissues and cell types present but also on the variations in chemical and microstructural composition determined at the ultrastructural level. The preferential attack of different wood tissues could be explained by their chemical variations combined with the enzyme limitations of the fungus and the anatomical characteristics of the cell types involved. The proposed decay mechanisms therefore apply to the constituents of the wood cell wall using their variations in attempts to explain the observed differences in micromorphology, where appropriate.

1.1 Brown rot

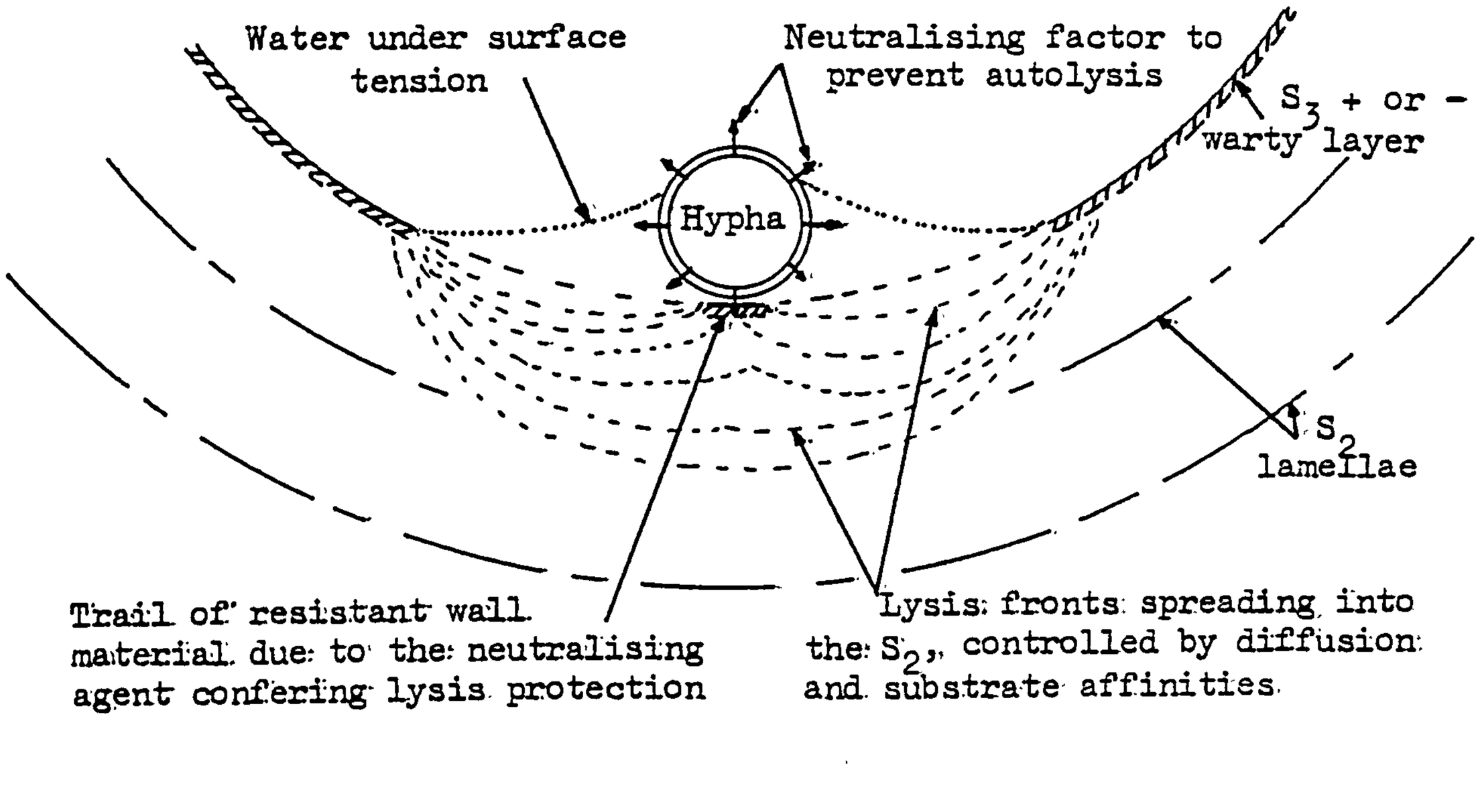
The brown rot fungi are capable of degrading cellulose and hemicelluloses with only a slight modification of lignin, which is therefore regarded as being virtually undegradable (Kirk, 1973). These fungi have the specialised capacity to attack the wood cell wall components at a relatively great distance from the hypha leaving undegraded lignin residues between the regions of enzyme attack and the fungal wall. To achieve this would require an extremely mobile, special component to open up the wall

structure allowing the hemicellulases and cellulases, which are larger than the natural pores within the cell wall, to act on their otherwise inaccessible substrates. Recent prcposals of an H_2O_2- Fe^{++} complex (Koenigs, 1975) being utilised by brown rot fungi would meet the requirements for small dimensions although the precise details of its mechanism in wall attack have not been clearly defined yet. Such a component probably would not have the specificity exhibited by enzyme cleavages and could, therefore, act upon the carbohydrate components of the fungal wall. It was proposed in part I that the fungus secretes, or bears on its surface, a component to neutralise this unspecific lytic agent so as to prevent autolysis.

It is clear from the literature that the individual wood cells are usually colonised by a single hypha. This grows along the lumen interface of the wall secreting the lytic precellulytic agents and the enzymes which accumulate either side of the developing hypha. The high concentration of the lytic agents results in all the available wall components being digested fully to produce lateral zones of maximum wall lysis around the fungus. The lignification of the S_3 and/or the resistance of the non-polysaccharide warty layer could explain the results (fig. 16, p.59) in limited lateral spread along this layer. This, combined with the highly cellulosic and thus less resistant underlying S_2, results in rapid radial and tangential spread of the lysis into the wall. The wall regions under attack presumably must be fully hydrated to allow free diffusion of the precellulytic factor and enzymes between substrate and hypha and to open up the interfibrillar spaces of the wall enabling the chemical and enzymatic reactions to take place. This water would also cause the concentration of the enzymes either side of the hypha, by surface tension

effects, during the early stages of wall attack. Diagrammatically these early stages can be represented as follows.

Fig A



The movement of the lytic agents to their substrates and the movement of the products back to the hypha will be impeded to a certain extent by the residual framework of lignin. To overcome this impedance high substrate affinities would assist in the former and the rapid absorption of products by the hypha, generating a strong gradient of utilisation, in the latter. The combined effect of the two could explain the extremely rapid removal of wall material observed during brown rot attack. It is difficult to visualise product absorption as being restricted to the hyphal tip unless its growth was extremely slow. The absorption probably takes place over a length of hypha, from the tip, where the chitinous wall is still developing. It is not difficult to conceive of a situation where the tip and first millimetre or so behind it absorb all the essential nutrients and the hyphae then subsequently go into physio-

logical decline and eventual autolysis (Jennings, 1976). Some of the absorbed products could then be used to promote tip growth and maintain the metabolism, with the remainder being directed to the growth of "non producing hyphal tips". Once lysis has been initiated the entire wall is rapidly and efficiently degraded leaving only the lignin skeleton which may collapse in the later stages of decay.

The susceptibility of different wall layers is dependant on the proportions of lignin, cellulose and hemicelluloses present and on the wall texture. The less lignin present the easier the layers can be degraded and the more obviously the lytic effect will be manifested. The absence of celluloses and hemicelluloses in the middle lamella region could effectively prevent the passage of the lytic agents through this layer resulting in the wall lysis being contained to the cell bearing the colonising hypha. The presence of more than one active hypha within a single cell would obviously result in competition for the available polysaccharides due to the mechanisms of their widespread action on the wall.

Penetrations of hyphae into individual cells must either be achieved by a combination of physical and chemical/enzymatic actions or by the secretion of special enzymes capable of limited lignin degradation. The utilisation of natural pitting would theoretically be more economical with either method as the proportion of "difficult" wall components would be less through the pit membrane than in an entire wall (which would be encountered in bore hole formation). Possibly this explains the apparent preference for this pathway in the material examined. In simple pit membranes the lignins and pectins of the middle lamella line would represent the only barrier to the colonising hypha and therefore may be penetrated mechanically, the accompanying polysaccharides being digestible

by the fungus. With bordered pits, the central cellulosic torus although thickened is still susceptible to brown rot attack as lignification of this region does not occur until heartwood formation (Liese, 1970). Again only the thin middle lamella represents a chemical barrier to penetration. Bore hole formation requires at least a limited degrade of lignin to penetrate the thicker compound middle lamella found in unpitted wall regions. The capacity of the fungus to produce a lignin degrading enzyme or agent may determine whether bore holes were observed as a frequent pathway between cells.

The nutrient benefit of lignin is extremely low (Bailey et al, 1968) therefore the ability of brown rot fungi to remove the energy rich polysaccharides without the problems of lignin digestion could be regarded as being more efficient than white or soft rot attack. The nature of the wood cell wall decay mechanisms of brown rot fungi results in successful colonisation and absorption of a suitable substrate being achieved simply by the ability of the hypha to spread from one cell to another.

1.2 Soft rot

The mechanisms of soft rot attack on the wood cell wall are more difficult to explain than brown or white rot. The soft rot enzymes are closer in action to those of brown rot than white rot, with attack of cellulose, hemicelluloses and a certain degree of lignin degradation (Kirk, 1973). However, the micromorphological decay features resemble those of white rot, in that lysis zones are always demonstrated as surface erosions, that is without wood cell wall material between the hypha and the regions of enzyme action.

Soft rot action is complex with at least three recognised decay features; wall penetrations (fine bore holes), lumen erosion (Corbett

type 2, 1965) and cavity formation (Corbett type 1, 1965). The factors that determine which feature is developed after hypha - wall contact will include the natural enzyme complement of the hypha, the microchemistry and structure of the wall and the physiological condition of the fungus.

Many soft rot fungi can produce all three types of wall lysis within a given wood species (Nilsson, 1973) although preferences for lumen erosion in hardwoods have been shown (Corbett, 1963; Nilsson, 1973). It would appear, therefore, that providing the fungus has the necessary enzymes, the development of the various lysis patterns is a result of the correct external stimuli and the growth requirements of the fungus.

The development of wall penetrations possibly indicates a requirement to colonise and explore the nutrient surroundings and may therefore reflect the culture conditions employed in the study or test. Particularly aggressive lumen erosion was observed in birch specimens cultured on Abrams medium and this could have been due to the abundance of nitrogen allowing the fungus to direct its attack on the polysaccharide of the cell wall which would also be the only carbon source present. Where nitrogen is scarce then perhaps the fungus has to search, by wall penetration, for nitrogen rich areas in the tissues. It can then produce sufficient enzymes for active wall degradation. Wall penetrations may, therefore, be expected in a search system with erosions and cavities developing secondarily depending on other limiting factors.

The type of wall lysis, type 1 or 2, appears to be determined by the nature of the wall itself. Where the S_3 or lumen interface wall layers are chemically and/or structurally unsuitable for the fungal enzyme systems then direct lumen erosion would be precluded. The fungus would have either to produce a bore hole into an adjacent, perhaps more

favourable cell, or penetrate and 'T' branch in a more favourable wall layer.

The incapacity for extensive lignin degradation probably determines whether lumen erosion or cavities are developed. Heavily lignified S_3 wall layers may restrict the development of type 2 erosion restricting the fungus to cavity formation in the less resistant S_2. Beech vessels demonstrate this feature particularly well (Bravery, 1971) with extensive development of cavities being observed yet no evidence for lumen erosion. During white rot attack, however, deep channels are developed pointing to the presence of a thick lignified S_3 (see white rot mechanisms). Where an S_3 is poorly developed or absent, for example in many hardwood fibres, the soft rot lumen erosion would be expected and is in fact predominantly observed (Corbett, 1965). Bravery (1971, 1972) indicated the importance of the S_3 in the development of micromorphological decay features and the present study substantiates his findings.

The following hypotheses are proposed as the detailed micro-mechanisms by which soft rot hyphae colonise and degrade wood. They have been derived from previous results and theories (see introduction) in conjunction with the new evidence for the presence of mucilage and ideas on the enzyme systems involved.

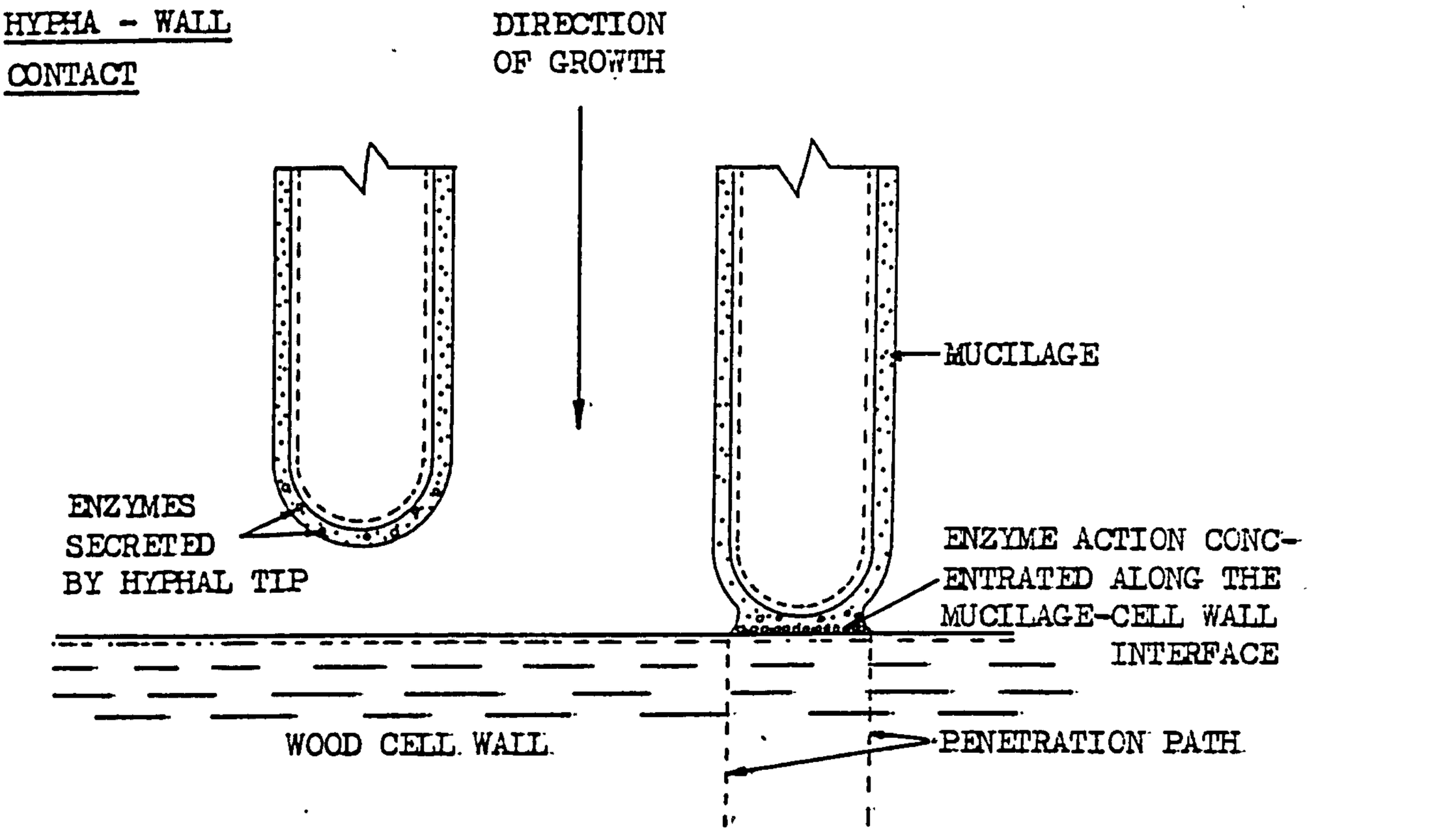
Soft rot cavities, in general, are initiated by a fine lateral branch of the lumen colonising hypha penetrating the cell wall from the lumen, (although wall penetration via pit chambers and canals have also been observed (Levi, 1965; Levi and Preston, 1965)). The most important factor in the attack of the microfibrils in all of the lysis forms, with one major exception discussed later, appears to be by the enzymes approaching the microfibrils laterally and not end-on. The localisation of the

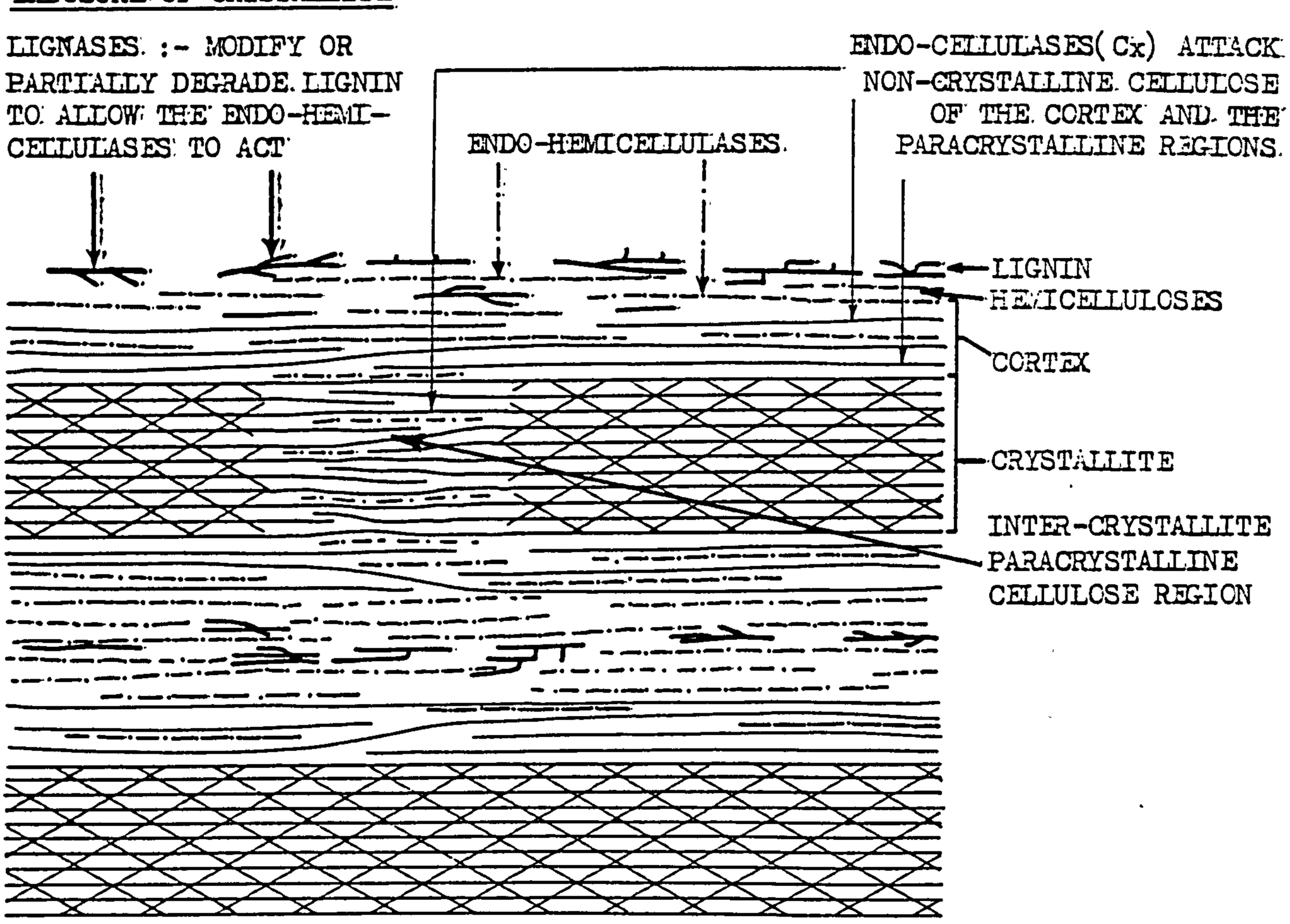
enzymes around the hypha and maintenance in a suitable fluid medium would be achieved by the mucilaginous envelope.

Growth of a hyphal tip towards a cell wall should result in the initial contact being made by the enzyme-bearing mucilage. The enzymes that constitute the precellulytic factors (Bailey et al, 1968) begin to clear or modify the obstructing lignin, remove the hemicelluloses by endo-hemicellulase action and to expose the cellulose of the microfibril. The lateral limit of this attack would be determined by the presence of mucilage and its extent. The non-crystalline cellulose chains of the microfibril cortex and paracrystalline regions between crystallites would be attacked by endo-cellulases (Cx) which act randomly on the cellulose to produce short chain oligomers. The non-reducing ends of the chains exposed in this way allow further attack by the exo-cellulases to produce the glucose trimers, dimers, and monomers that are absorbed by the fungus (Reese, 1977). The Cx endo-cellulases and the exo-cellulases can only act on cellulose chains that are partially or totally liberated from the microfibril (Reese, 1977) and further cellulose degrade is, therefore, presumed to be restricted by the highly ordered crystallites of the microfibril core. These crystalline cellulose chains are attacked by a special endo-glucanase (the C_1 factor according to Reese, 1977) which cuts the exposed surface chains and disrupts the associated hydrogen bonding allowing rapid degrade of the liberated chain by the Cx factors and exo-cellulases (Reese, 1977). Without the presumed Cx and exo-cellulase clearance of the chains released by the action of the C_1 factor progression through the crystallite would be severely restricted.

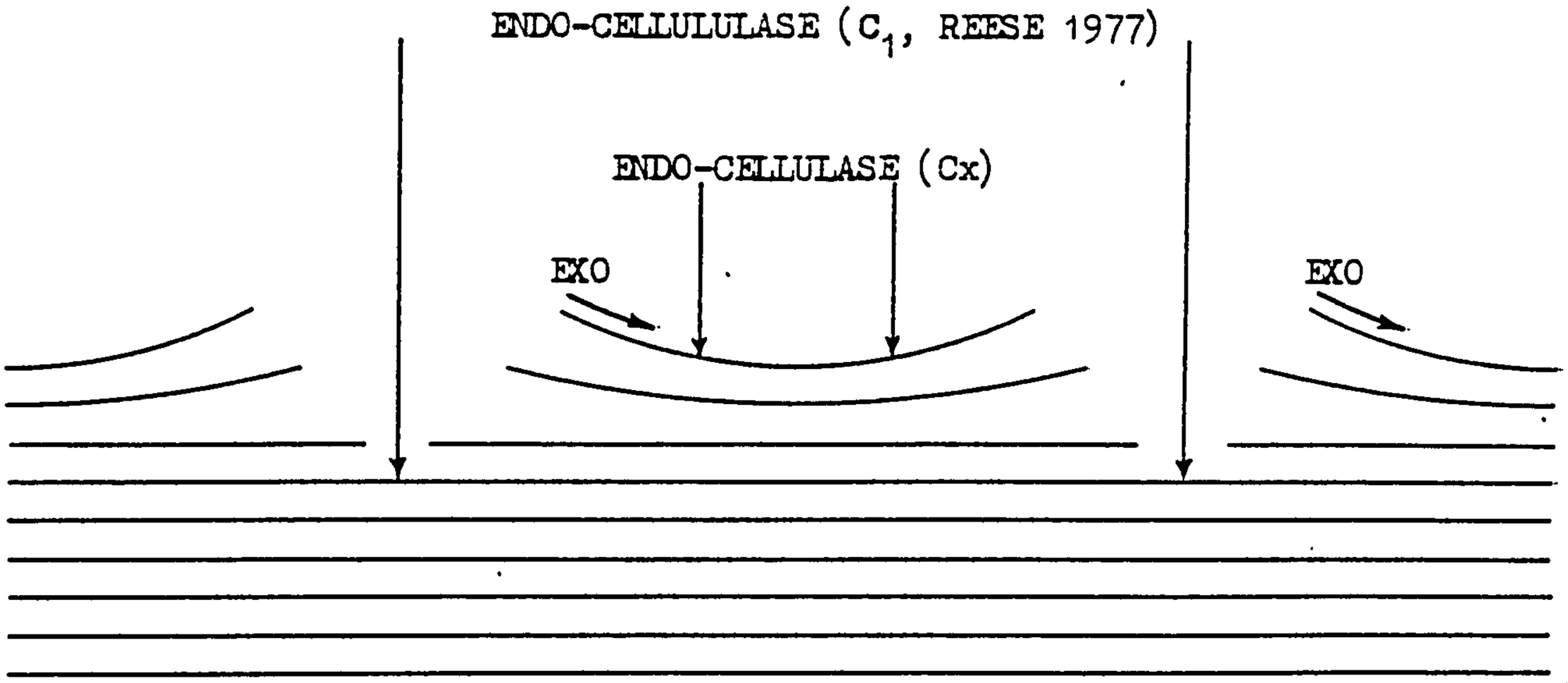
Therefore, as each cellulose chain is removed then the underlying chains are sequentially exposed to the enzymes until the crystallite has

been completely degraded. Diagrammatically these processes would be:-





CRYSTALLITE DEGRADATION

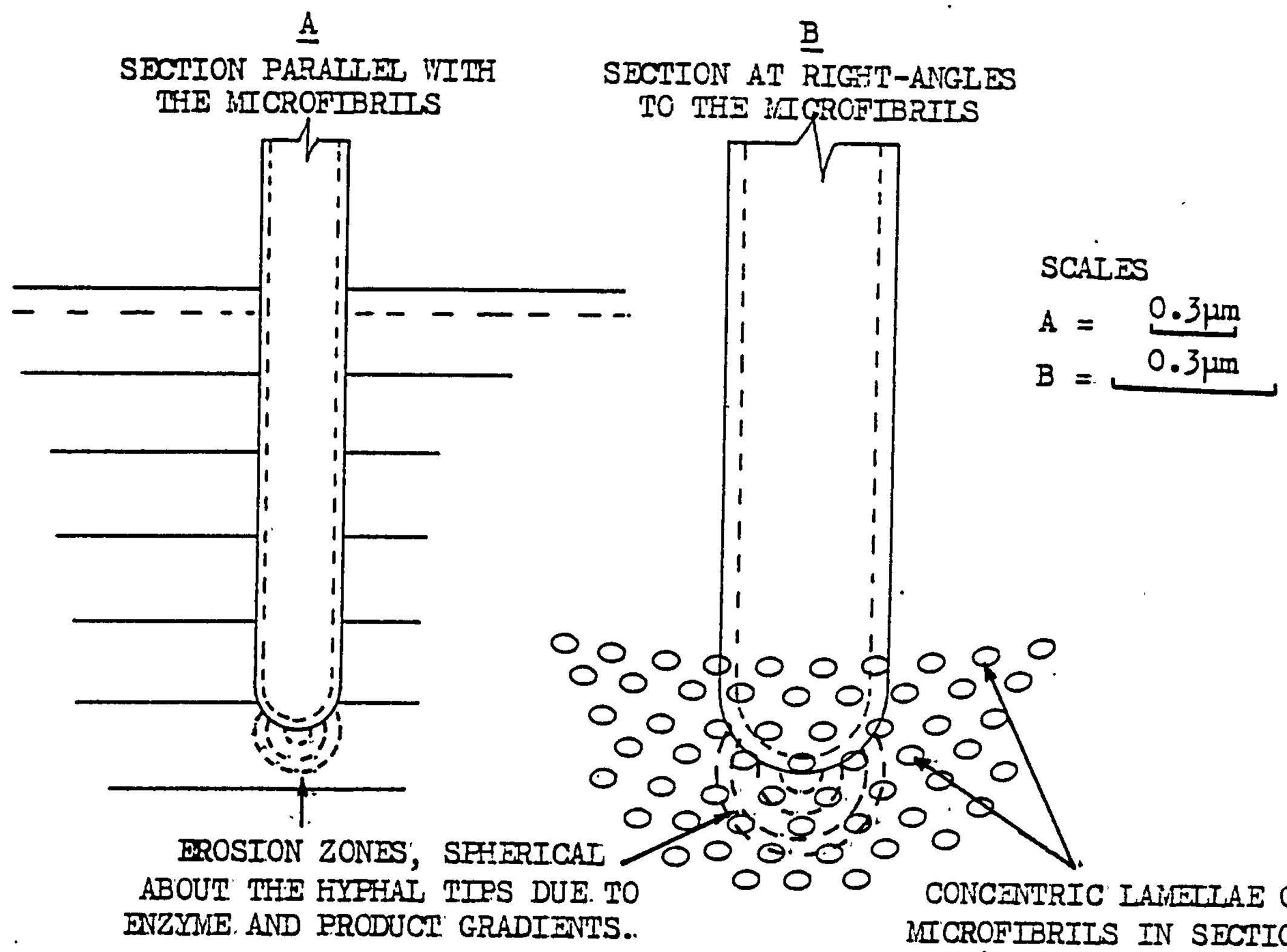


Further lignin clearing and endo-hemicellulase action would then be required to expose the next microfibril.

Once a number of wall layers have been penetrated in this way the lateral spread would be restricted by the cut ends of the previous microfibrils, with penetration of the matrix material between them being impeded by the inaccessible hemicelluloses. Depending on the chemistry of the wood cell wall and the physiological condition of the hypha this type of penetration may continue right through the wall pair. Alternatively, the hyphal tip may detect from the products of its enzyme action that the S_2 region of the wall had a favourably low lignin content and this may stimulate the cavity development sequences of 'T' branching and proboscis hyphal growth.

The formation of a 'T' branch could be iniated by switching off the endo-hemicellulases and replacing them by a special lysis system. This system would have to be capable of attacking the matrix material "end-on" to render the cellulose accessible to the cellulase enzymes. Cellulases have been shown to be in the order of 25 - 80 Å (average 60 Å) in diameter, if spherical, and 15 x 80 Å - 40 x 250 Å (average 35 x 200 Å), if ellipsoidal in shape (Cowling and Brown, 1969; Cowling, 1975). These dimensions would not permit access into the majority of the transient capillaries of the wood cell wall (Cowling and Brown, 1969) which, on average, are only about 10 Å in diameter. The special lysis system should, therefore, consist of small mobile components, possibly exo-hemicellulases, which may or may not be assisted by a non enzymatic factor (see also Keilich et al, 1970) similar to that proposed for brown rot degrade (Koenigs, 1975).

This switch between enzyme systems would curtail any further radial lysis into the S_1 wall layers and would initiate lysis between the microfibrils either side of the hyphal tip along planes parallel with the microfibrillar orientation. As the encrusting materials are removed then the cellulases can act on the exposed microfibrils as previously described. Apical control presumably divides at the same time as the enzyme switch-over and the two new tips develop at 180° to one another, along the microfibrils. Without the release of endo-hemicellulases during this growth phase the enzymatic effect ahead of the hyphal tip would be effectively limited to the diameter of the first formed erosion parallel to the microfibrils. The resultant narrow cavity would be occupied by the fine extending hypha, termed a "proboscis hypha" by Corbett (1965). The 'T' branch development may be more easily demonstrated by diagrams.



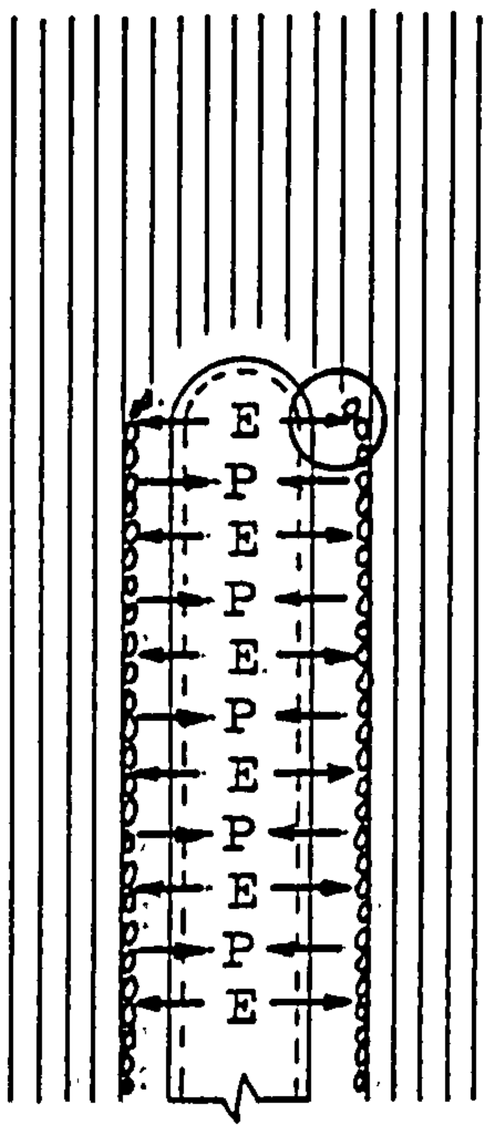
By continued growth the fine proboscis hyphae increase in length.. Proboscis hyphal development has been shown to be phased (Leightley and Eaton, 1977; Hale, pers.. comm.) with discrete pauses in their extension.. The proboscis hyphal length before a growth pause is variable and appears to be determined in particular by the wood species, fungal species and the moisture content of the wood cell wall (Liese, 1970). The growth phase could be terminated simply by switching off the special exo-hemicellulases thus preventing further longitudinal spread of the effect of this special lysis system.

A feature of fungal development that is not clearly understood is the factors that may control wall formation. In soft rot examples the bore hole hyphae and penetration hyphae develop mature walls as they grow into the wood cell wall. During the growth of a proboscis hypha,

however, mature hyphal walls would not be expected as, in later stages, these proboscis hyphae have to expand. Their surface areas have been shown to increase up to fifteen times that of the original hypha (Leightley and Eaton, 1977). Possibly the control for the type of wall laid down around the hypha may be linked to the special exo-hemicellulase release system of proboscis hyphal growth as it is only during this phase that the immature walls would be produced.

Once the special exo-hemicellulases are switched off the release of endo-hemicellulases and the other digestive enzymes over the entire surface area of the immature hyphal wall would be iniated. This changeover would represent the first stage in the development of a cavity. The inability of the precellulytic factors to attack the matrix material between the microfibrils ahead of the hyphal tip would restrict their action to the exposed lateral surfaces of the adjacent surrounding microfibrils. Removal of the lignin, hemicelluloses and non-crystalline cellulose would proceed radially outward from the hypha. The enzyme dimensions and the requirement for close fits for hydrolysis of the polysaccharide chains may result in the cut ends of the hemicelluloses and paracrystalline cellulose exerting a restrictive influence on the proximity of the terminal hydrolysis point of the underlying chain. This effect would generate an angled cleavage of the matrix material towards the crystalline core of the microfibrils.

Once exposed the crystallites would be subject to attack by the C_1 enzymes in conjunction with the Cx and exo-cellulases, as previously described, and would also be expected to demonstrate enzyme interference by the previously cut chains. Diagrammatically these early stages would be represented in two dimensions as follows:-



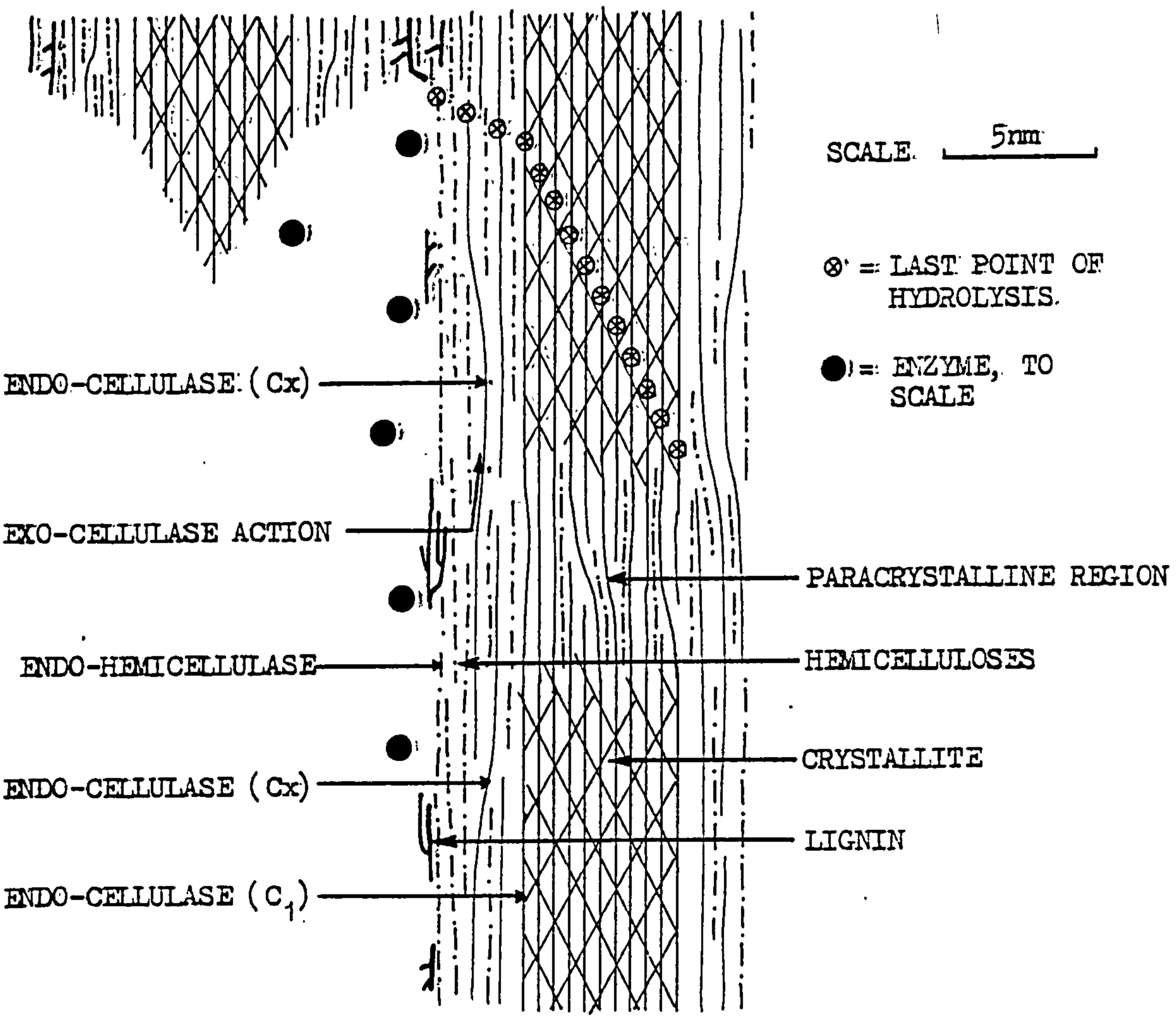
○ = SHOWN AT HIGHER MAG. BELOW

∞∞ = LYSIS

E → = ENZYME RELEASE

P ← = PRODUCTS ABSORBED

ENZYMES RELEASED OVER THE ENTIRE SURFACE AREA OF THE PROBOSCIS HYPHA. ATTACK OF THE MICROFIBRILS AHEAD OF THE HYPHAL TIP IS RESTRICTED BECAUSE THE SPECIAL LYSIS FACTORS REQUIRED ARE NOT RELEASED. THE PRODUCTS OF THE LATERAL LYSIS WOULD BE RAPIDLY ABSORBED BY THE HYPHA.



A typical glucanase, if spherical, would be 60 Å in diameter (Cowling and Brown, 1969) and would therefore span 12 glucose units of a cellulose chain. Values of between 4 and 10 units have been suggested as the substrate recognition sites required by a range of glucanases examined (see Reese, 1975). Assuming that the bond being hydrolysed was in the middle of the recognition site then the displacement of the terminal hydrolysis point of one cellulose chain from the previous cut end would vary between 2 and 5 glucose units.

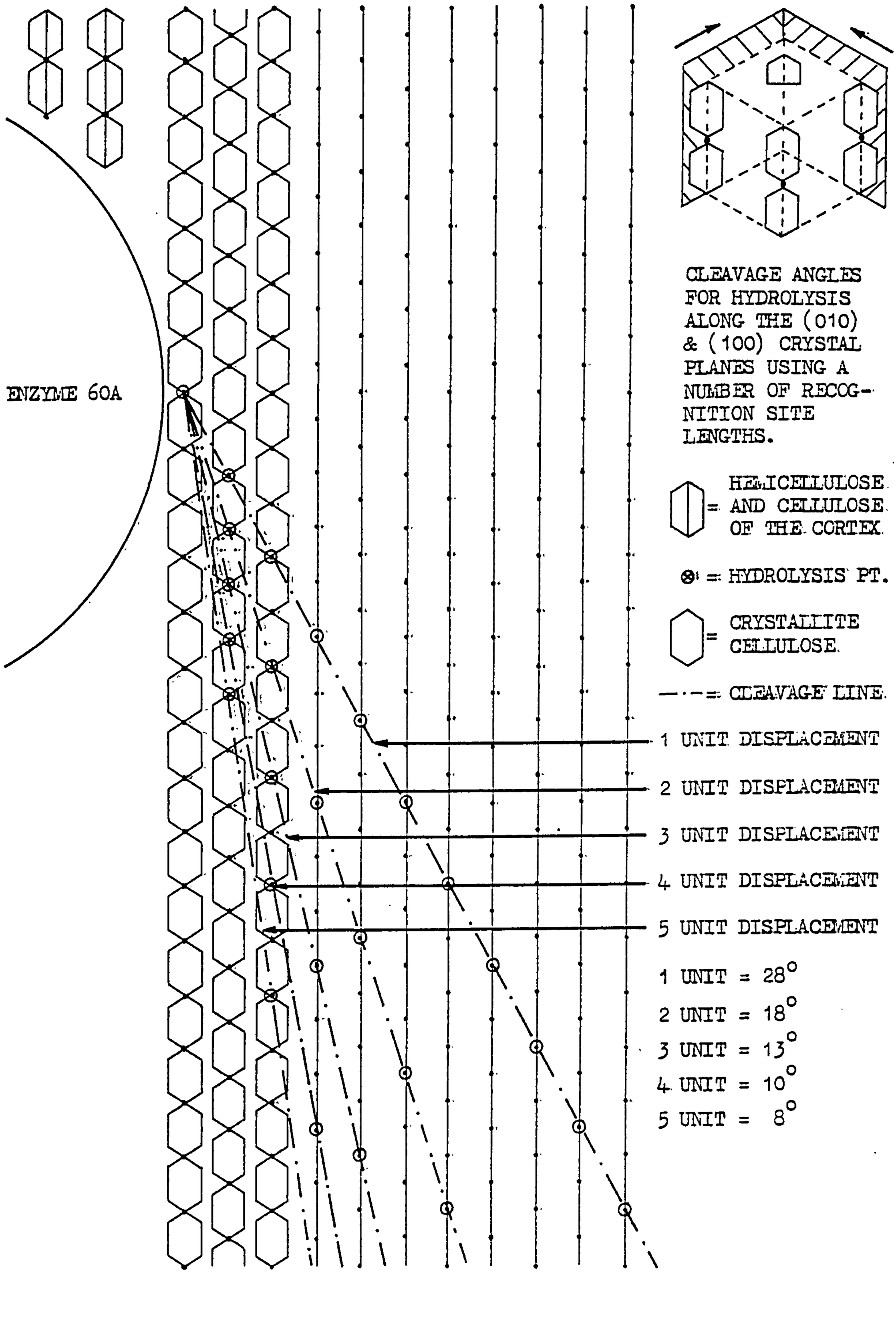
Using the unit cell dimensions of the cellulose crystallite a series of cleavage angles can be drawn across the chains for hydrolysis parallel to the (010) and (100) crystal planes, see fig. B. These angles would increase if the hydrolysis proceeded along the diagonal dimension of the unit cell. The approximate cleavage angles, with respect to the cellulose chain axis, for the various site lengths would therefore range between,

28 – 37°	for 2	recognition glucose units
18 – 24°	for 4	recognition glucose units
13 – 17°	for 6	recognition glucose units
10 – 14°	for 8	recognition glucose units
8 – 11°	for 10	recognition glucose units

with the lower angles being favoured for enzyme substrate fits in this particular model. Smaller or specially shaped enzymes and asymmetrical recognition/catalysis sites would allow the higher cleavage angles to be formed in the crystallite. The precise binding site requirements and position of the catalysis points for the cellulases have still to be determined. On the basis of enzyme shape and length of recognition site the cleavage plane for the cellulose crystallite could be calculated.

Once the crystallite had been severed a new region of paracrystalline

Fig B


ENZYME 60A
CLEAVAGE ANGLES FOR HYDROLYSIS ALONG THE (010) & (100) CRYSTAL PLANES USING A NUMBER OF RECOG-NITION SITE LENGTHS.
= HEMICELLULOSE AND CELLULOSE OF THE CORTEX.
= HYDROLYSIS PT.
= CRYSTALLITE CELLULOSE.
= CLEAVAGE LINE.
1 UNIT DISPLACEMENT
2 UNIT DISPLACEMENT
3 UNIT DISPLACEMENT
4 UNIT DISPLACEMENT
5 UNIT DISPLACEMENT
1 UNIT = 28°
2 UNIT = 18°
3 UNIT = 13°
4 UNIT = 10°
5 UNIT = 8°

cellulose, hemicelluloses and lignin would be sequentially exposed. However, the total length of this region would be reduced because of the angled crystallite cleavage. Binding site requirements and catalysis points have been proposed for a number of hemicellulases (see Dekker and Thomas, 1976) justifying the postulated angled cleavage of the inter-microfibrillar matrix material and the microfibril cortex regions. Continued successive attack of microfibrils and matrix material in this way would result in a conical taper being generated at the cavity apex.

Frey-Wyssling (1938) suggested that cleavage of the cellulose was via specific bonds within the crystallite giving rise to the 23° cavity angle observed for softwoods and this was supported and extended by Wardrop and Jutte (1968) utilising other crystal planes to explain the higher cavity angles predominantly observed in hardwoods.

It is proposed here that the observed cavity angles in the soft rot of wood cell walls result from the superimposed effect of the crystallite and the cellulose - hemicellulose - lignin cleavage angles. A means of explaining the difference between observed softwood (20 - 25°) and hard-wood (30 - 35°) cavity angles (Liese, 1970), is therefore required. Firstly some features of cell wall architecture should be established.

Cell wall microfibrils tend to be oval or rounded rectangles in cross section due to surface tension effects during their synthesis, and are arranged in the concentric wall lamellae with their shorter dimensions parallel with the radii of the cell (Preston, 1974). The progressive development of a soft rot cavity within the S_2 wall layers would therefore result in the asymmetrical microfibrils being cut along a variety of planes. During examination by light microscopy the cells are usually viewed in a radial direction, when measuring cavity angles, resulting in

the microfibrils presenting their broadest dimensions. In the majority of transmission electron micrographs of soft rot cavities, the section plane of the cell is radial presenting a tangential view of the microfibrils which would therefore exhibit the narrower dimensions. This distinction is very important when constructing models of microfibril cleavage angles to explain observed cavity angles. As the majority of cavity angle measurements have been derived from light microscopical observations the models presented here utilise the broader microfibril dimensions in the development of wall/cavity angle interrelationships.

By using Preston's (1974) model of the microfibril and matrix organisation within the plant cell wall, and retaining his assumptions in creating the model, approximate centre to centre microfibrillar distances and expected thickness of the matrix layer can be calculated for various cellulose percentage contents for the wood cell wall.

Data on chemical analyses of the cell wall layers (Meier, 1961) shows that the S_2 of birch contains 40 - 50% cellulose whereas that of Scots pine has 50 - 60% cellulose. The calculated centre to centre distances (a) and matrix layer thickness (b) would be approximately:-

birch	(a) = 130 Å	(b) = 15 Å
Scots pine	(a) = 120 Å	(b) = 10 Å

Using this information models of the wall microfibrils through which the observed cavity angles develop can be drawn. On the assumption that the crystallite cleavage angle would probably be the same for Scots pine and birch then their matrix cleavage angles would have to be different to accommodate the overall cavity angles of 23° and 33° respectively. The hemicellulose complements in conjunction with the slight variation in the crystallite spacing would probably contribute to this

difference. Fig. C demonstrates that with the assumptions made in the proposed model a cellulose cleavage angle of 18°, reflecting a four unit recognition site (with two unit displacement) in conjunction with 28° and 66° matrix cleavage angles for Scots pine and birch respectively combine to produce the characteristic angles observed. More accurately the progressive decline of the cellulose and increase in hemicelluloses away from the crystallites towards the mid line between the microfibrils would probably result in a slightly sigmoid cleavage between microfibrils.

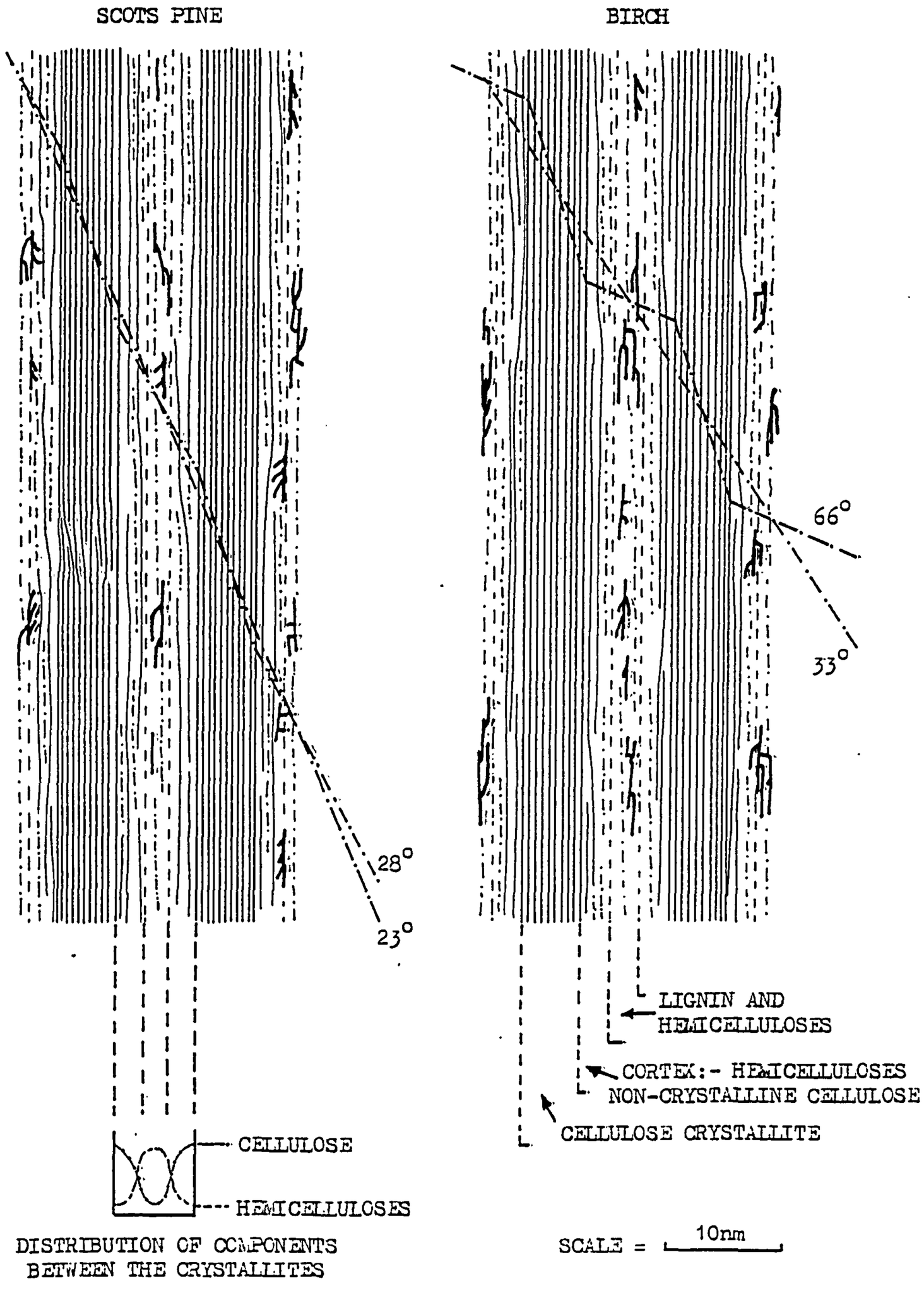
The observations of Bailey and Vestal (1937) that the cavity angle increased with higher moisture contents could also be explained by the model. Hydration and swelling of the non-crystalline wall materials would increase the microfibrillar separation and thus cause an effective increase in the overall cavity angle.

The principles involved in this explanation of cavity angles result in variations in wood moisture content, intermicrofibrillar separation, crystallite dimensions and cleavage angle, and matrix cleavage angles having an influence on the overall cavity angle expressed. It must be emphasised that, because of the large number of unknown factors, this proposed model can only be regarded as hypothetical until precise details on the enzymes and wall structure have been determined.

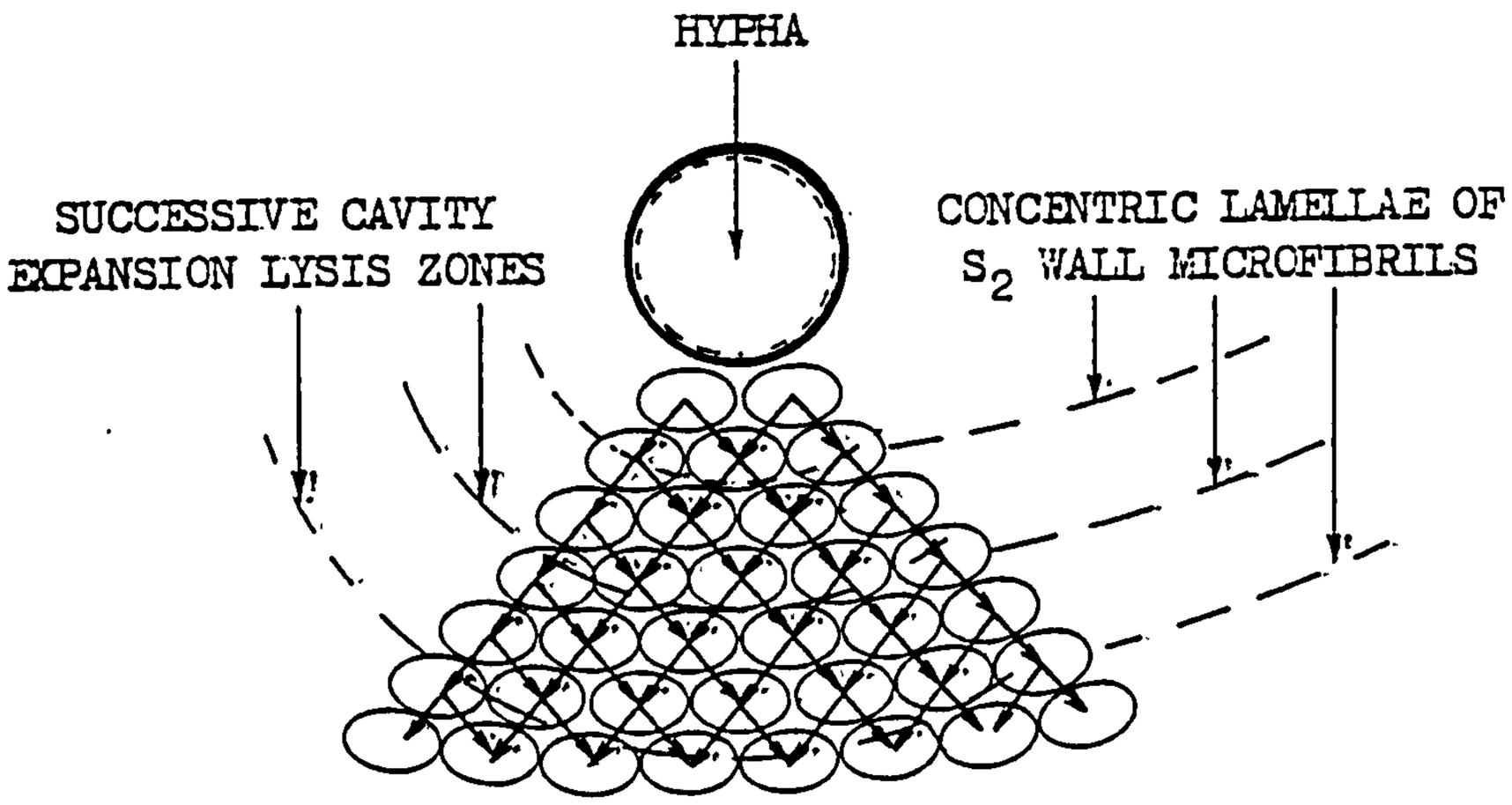
The changes in the angle between crystallite and matrix would have to be at the microfibril and sub-microfibril levels and would therefore be very difficult to detect with current methods, as previously noted by Findlay (1970) with reference to the stepped cavity cones resulting from the differential diffusion rates linked with the paracrystalline regions as proposed by Levi and Preston (1965).

These explanations cover cavity development in two planes and

Fig. C


SCOTS PINE
BIRCH
28°
23°
66°
33°
CELLULOSE
HEMICELLULOSES
LIGNIN AND
HEMICELLULOSES
CORTEX:- HEMICELLULOSES
NON-CRYSTALLINE CELLULOSE
CELLULOSE CRYSTALLITE
DISTRIBUTION OF COMPONENTS
BETWEEN THE CRYSTALLITES
SCALE = 10nm

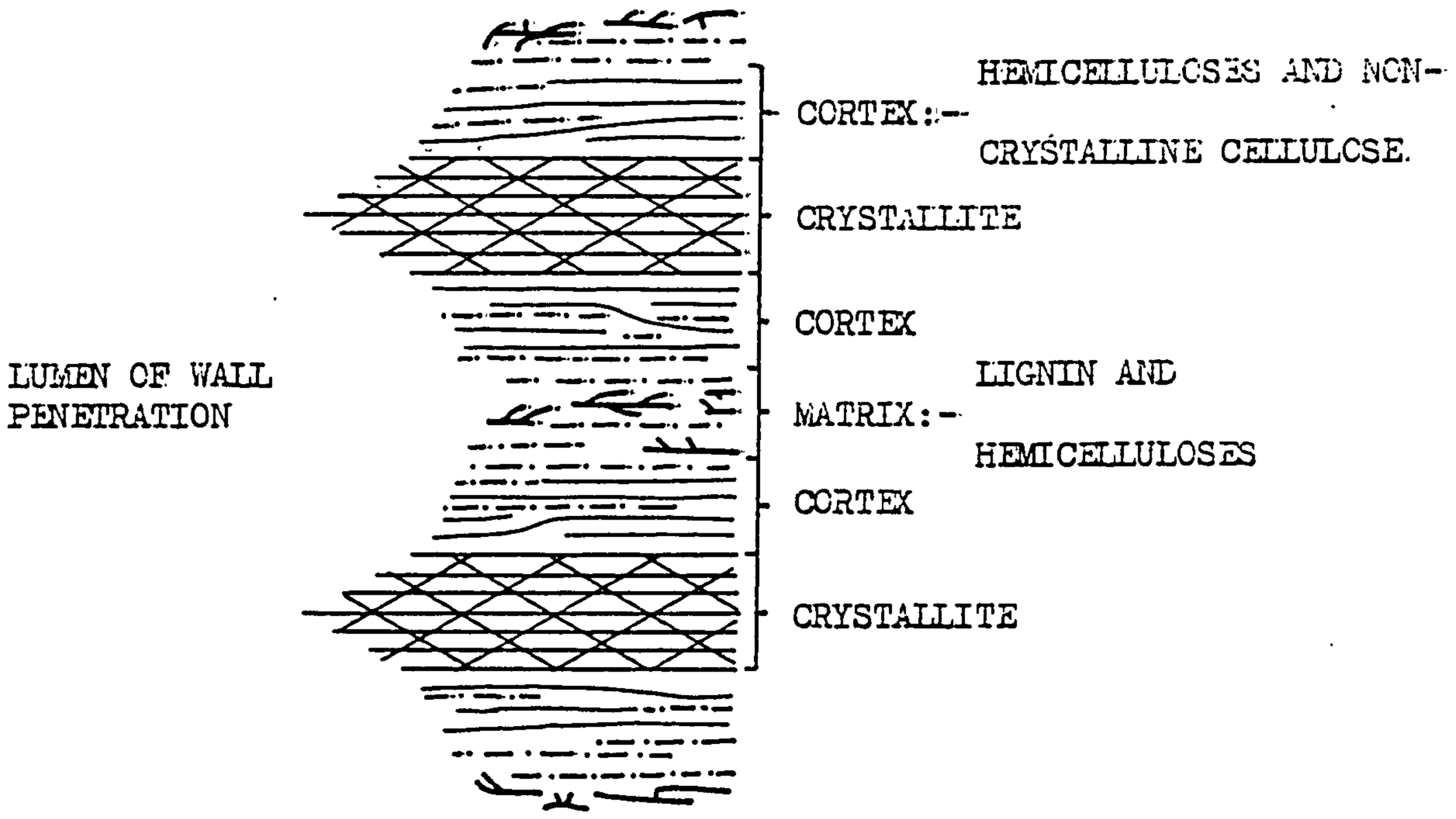
conversion to three dimensional cavity shapes could simply be achieved by regarding the two dimensional model as a radius of the concentrically expanding cavity. The increasing surface area of the developing cavity means that an individual cellulose chain probably influences the hydrolysis of two underlying chains. In the simplest form this could be represented in transverse section of the microfibrils as:-



This mechanism can be used to explain the conical cavity point at the hyphal tip but requires further definition to account for the other cone surface at the opposite end of the cavity. Levi and Preston (1965) suggested that the presence of septa in hyphae at the majority of cavity constrictions would restrict the release of the lateral enzymes at these points. Visual observations by Findlay (1970) and Zainal (1975) have substantiated the presence of septa, though Nilsson (1973) disputes this point indicating that septa are found in hyphae within the cavity. It may be that the phased growth with a switching system between exo- and endo-hemicellulases is also coupled in some way with the stimulus to develop the necessary precursors of septum formation. This would explain the

presence of a septum at a point of cavity constriction. It is possible that the septa observed in hyphae within a cavity arise at later stages during senescence of the hypha. Whether the septa or some other mechanism is involved, the restricted release of enzymes at this point will result in the development of a cavity slope in the opposite direction but simultaneously with that of the hyphal tip.

As the same enzymes are involved in both cavity and bore hole formation the different patterns of attack observed need further explanation. During wall penetration the endo-hemicellulases are able to attack the entire encompassing sheath of matrix and cellulose cortex chains, as a result of which the cleavage planes across the crystallite would result in the formation of a tapered point, see below.

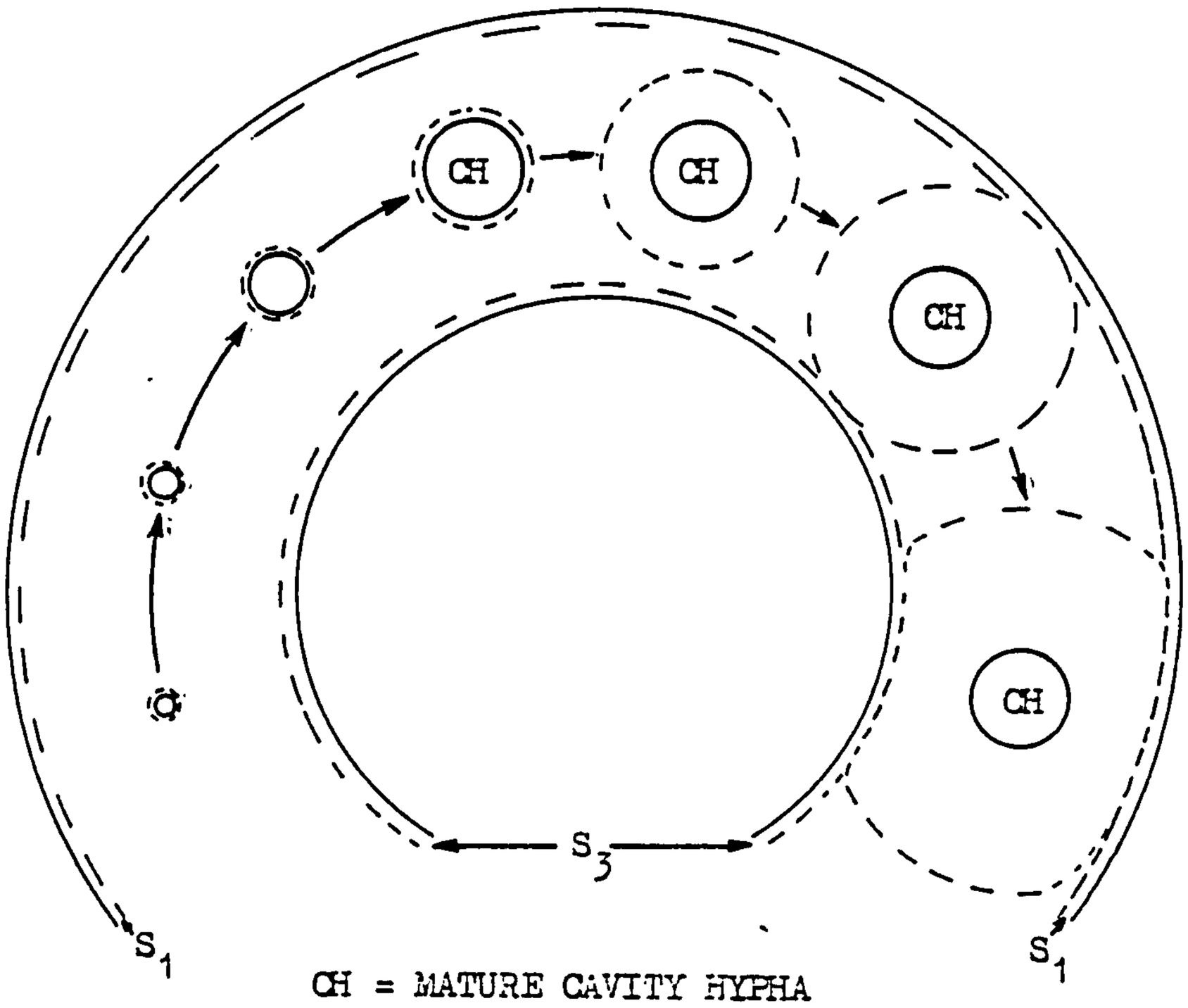


In the developing cavity, however, the progressive attack of the various microfibril components and interspersed matrix material occurs simultaneously around the interface between wall and cavity. Each

successive displacement is therefore transmitted to the underlying chain whether it is cellulose or hemicellulose. Only the presumed change in cleavage plane would differentiate the two polysaccharides.

The loose texture of the proboscis hyphal wall, necessary to accommodate its surface expansion into a mature cavity hypha, would allow the products of wall breakdown to be readily absorbed and presumably utilised in the production of new hyphal wall, maintenance of the cytoplasmic metabolism and to produce a reserve of energy which the rest of the hypha, outside the wood cell wall, could utilise for further growth.

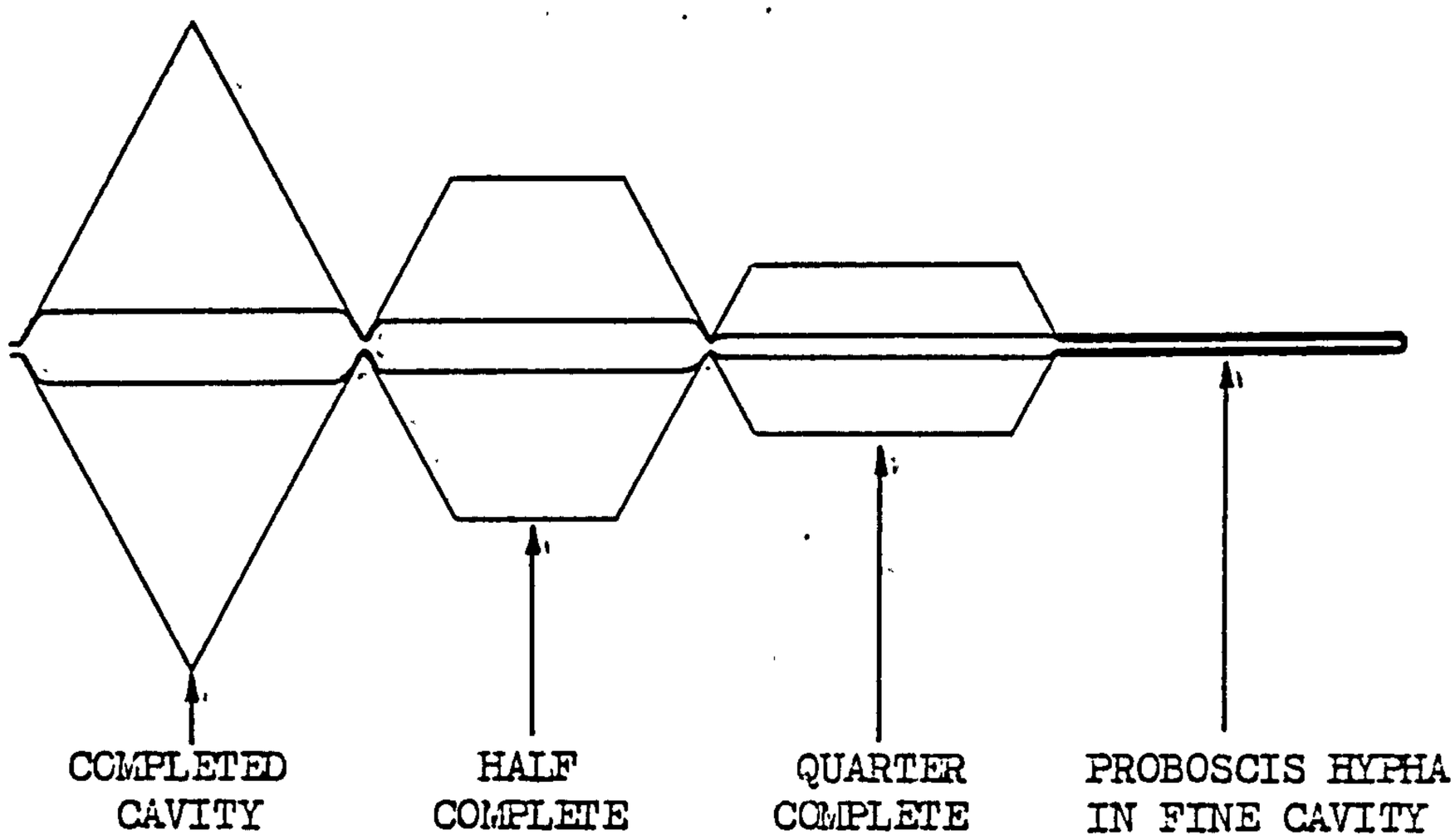
Cavity expansion continues with the concentric removal of microfibrils and if allowed to go to completion would result in diamond shaped cavities, when viewed laterally, with a three dimensional structure of two cones joined base to base. However, the S_3 and compound middle lamella produce physical and chemical constraints on cavity expansion and, as such, the result in the progressive development of a cavity may be shown as below (when viewed in transverse section).



CH = MATURE CAVITY HYPHA

Initially the expansion of the hypha matches that of the cavity until the hypha reaches mature dimensions after which the cavity continues to expand either coalescing with adjacent cavities or terminating due to some controlling factor (this is discussed later). The interface between the cavity and the S_3 or compound middle lamella would be parabolic on the conical slopes though this is rarely observed as it only reflects a change in the plane of erosion.

The variety of cavity shapes could reflect a time sequence in cavity development as shown below.



The results of work by Leightley and Eaton (1977) indicate that the cavity hypha is still developing some two or three cavities behind the proboscis hyphal apex. If the hypha is capable of absorbing wall products during its lateral expansion but not after maturity then the rate of hyphal maturation would determine how far cavities go to completion. However, another important factor is the cavity length. Longer cavities

tend to be found in woods with higher moisture contents (Liese and Ammer, 1964). This possibly may be due to easier penetration along the microfibrils by the developing proboscis hypha. Longer cavities also tend to be characteristic of certain fungal species, for example, Chaetomium globosum on birch, which may reflect the hypha possessing a more active exo-hemicellulase system. If a hypha can degrade microfibrils at a uniform rate then not only will the rate of lateral expansion slow down as the number of concentric microfibrils increases but also a longer cavity would present more wall material for digestion. Thus from longer cavities enough wall material may be obtained for hyphal maturity before cavity completion. The mature hyphal wall might restrict further product absorption and therefore create product inhibition of its enzymes, or the fungus may reabsorb the enzymes for recycling in the newer cavity developments.

Lumen erosion attack of the walls, with the same angle of microfibril cleavage as that indicated by the cavity cone, demonstrates that the same enzyme systems are in action. The predominance of this erosion in cells with a poorly developed S_3 indicates that this layer normally represents a barrier to lumen erosion. Penetration of the thinner S_3 wall layers is achieved by concentrated enzymic activity either side of the hypha with a high requirement for lignase and hemicellulase action, but once breached the less lignified S_2 is rapidly attacked undercutting the S_3 which remains intact as noted in some of the material examined. This may account for the observations of trans-S_3 erosion by soft rots. (See Zainal, 1975). Each 'V' shaped notch (Corbett, 1965) was in fact half a double cone so that in longitudinal section a 'V' was observed but in transverse section more of a semi-circular profile was exhibited. Further attack of the S_3

results in these erosion zones fusing to produce large regions of total wall lysis. The range of lumen erosion profiles reflects the length of the S_3 that has been digested to expose the S_2.

Using these hypotheses a soft rot fungus would simply represent a stainer with the added capacity to produce the special lysis system required during proboscis hyphal growth. Although the mechanisms can explain cavity shapes and constrictions the reasons for the phased growth sequences instead of continuous development within the S_2 have yet to be determined.

1.3 White rot

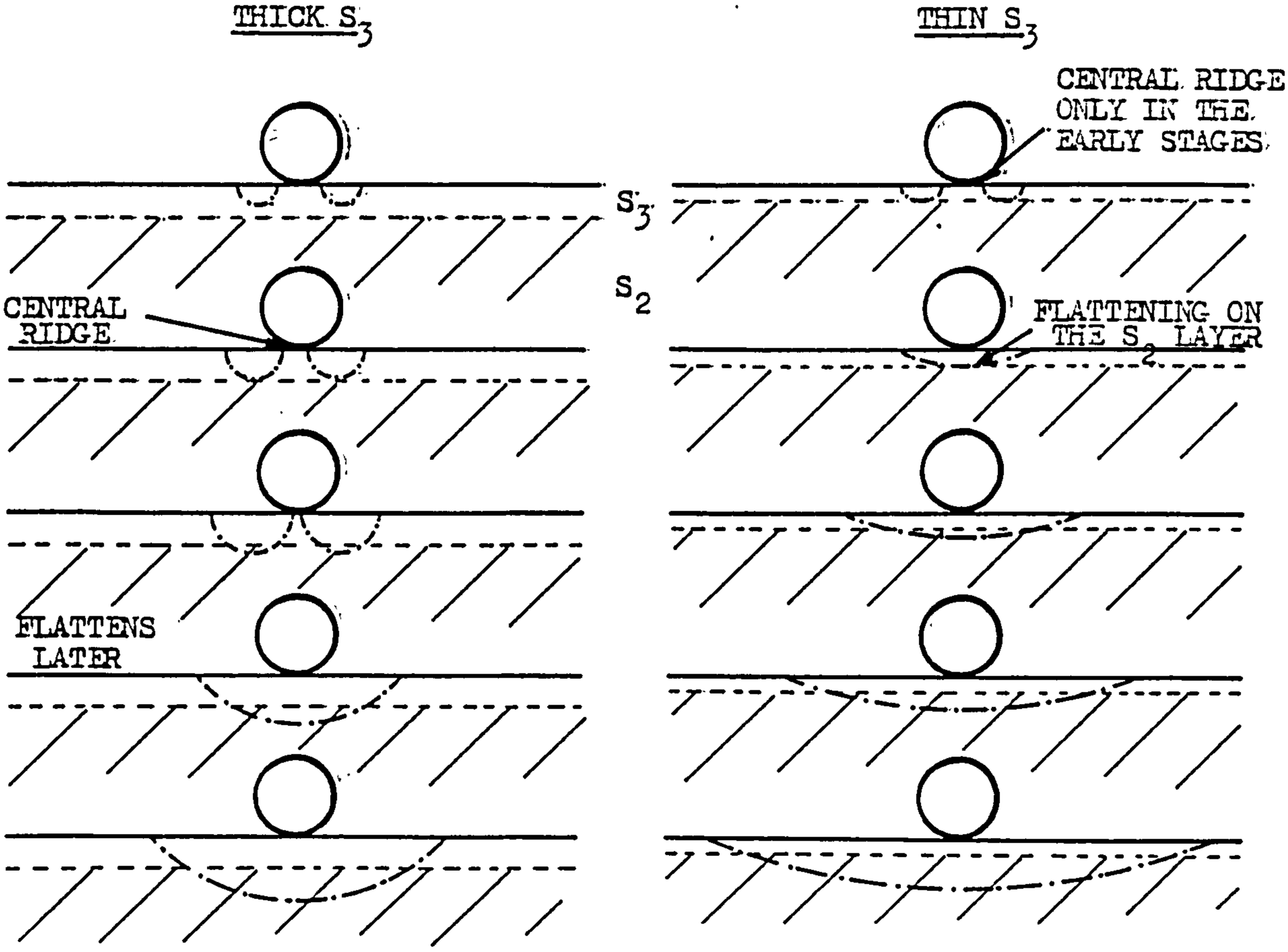
The degrade of wood cell walls by white rot fungi results in the production of erosion troughs (channels) or bore holes which frequently enlarge. White rot fungi are capable of attacking all the cell wall components although Coriolus versicolor appears to preferentially degrade the amorphous matrix material (see also Bravery, 1971, 1972). Warts are easily degraded and with the removal of the matrix material ahead of the cellulose cores, then the cellulase systems control the observed micro-morphology of channels and bore holes.

In the development of channels the natural susceptibility of the wall layers to the enzymes released by the fungal hypha determines the shape of the erosion. Initially the enzyme effect is concentrated either side of the hypha by surface tension action on the surrounding mucilaginous sheath, into which the enzymes are released. If the surface S_3 layer microfibrils are heavily encrusted with matrix material then deep lysis troughs will be formed with the rapid removal of lignin and hemicelluloses being accompanied by the celluloses. However, on reaching the less encrusted S_2 microfibrils the observed radial lysis would be

slowed by the limiting effect of the cellulases and tangential spread into the S_3 would be effectively increased. If the S_3 layer is thin or non existent then lysis radially would be much slower and consequently tangential spread would be wider resulting in broad and shallow erosion troughs. The rapid removal of matrix encrusting materials would result in the microfibrils with thin investments becoming more pronounced and fibrillar. Therefore two points of significance may be deduced from the white rot erosion channel.

1. The more matrix material in the S_3 would probably result in greater radial lysis.
2. The more cellulose material would probably produce a greater tangential spread and more fibrillar appearance.

Diagrammatically channel formation in the two types of wall could be:-



A THICK S_3 RESULTS IN A DEEPER, NARROWER, EROSION CHANNEL

A THIN S_3 RESULTS IN A SHALLOWER, BROADER, EROSION CHANNEL

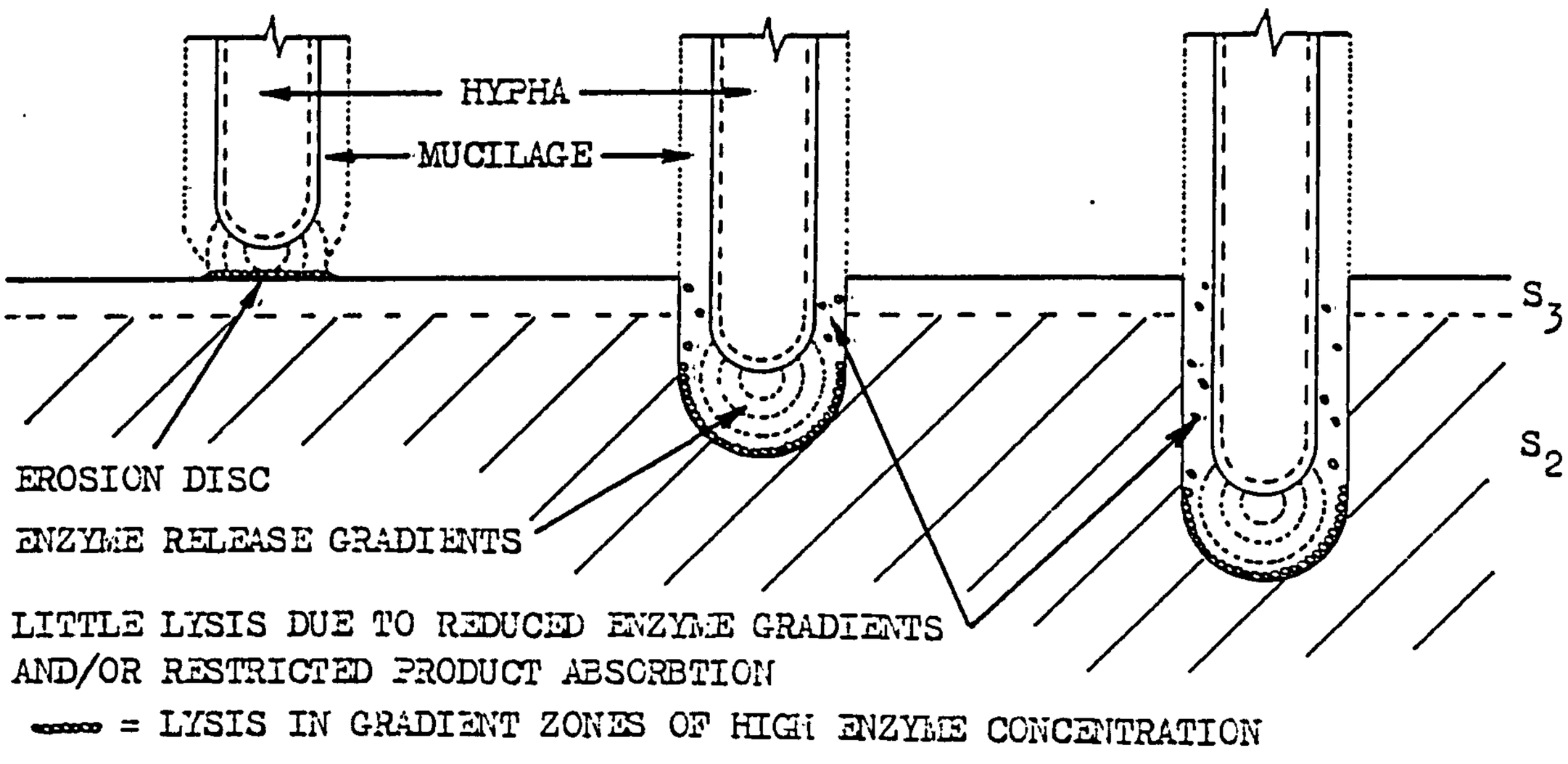
The tangential or lateral spread of theerosion channels would be controlled by the extent of the mucilaginous matrix again performing the role of medium for enzymes and products as suggested in the soft rot section.

In the production of bore holes, either the cellulase activity increases or the matrix enzymes decreases to produce the neat penetrations frequently observed. Again the approaching enzyme-bearing mucilage of the hyphal tip causes the development of a disc of erosion whose lateral limit would be determined by the mucilage. The ability to attack microfibrils and matrix material 'end on' may be restricted by enzyme access and/or hyphal tip gradients.. The enzymes are released into the mucilage at the hyphal tip thus setting up a gradient of enzyme concentration centred on the hyphal apex.. If breakdown product absorption was also restricted to the tip region then activity of enzymes at a great distance from the product sink would decline due to catabolite repression.. The development of a bore hole would,, therefore,, be controlled,,

a) by the mucilage delimiting the initial erosion disc

b) by the cut ends of the previous microfibrils

c) by diffusion gradients of enzyme and products from and to the hyphal tip..



Where certain wall layers are particularly resistant to lysis then the bore hole exhibits restricted degrade giving rise to annular ridges projecting into the bore hole being developed. The ability of white rot fungi to produce enzymes capable of degrading all the components of the wood cell wall, by lateral attack, results in no requirement for the specialised enzymes or non-enzymic factors required by the other rot types when enzyme capacity is restricted.

It is, therefore, postulated that the soft rot fungi possess a specialised enzyme system that allows them to attack the hemicelluloses of the wall during an end-on approach to the microfibrils and that this might be an exo-hemicellulase and/or non-enzymatic system that is only utilised in the developmental growth of proboscis hyphae within the wall. The other lysis patterns, bore hole formation and cavity development, being achieved by enzymes that can only approach the wall components in a lateral direction. This lateral approach would also appear to be the case for white rot attack with surface features also being delimited by the enveloping hyphal mucilage and characterised by the enzymes and substrate susceptibility. Bore hole formation being achieved by restricted enzyme release and action at the hyphal tip. The decay mechanisms indicate that there is a possible correlation between the areas of the hypha where enzymes are released and the regions of the hyphal wall which are still in the process of development. Though the products of extracellular enzymic activity are probably taken up over a larger surface area of the hypha. Mucilage does not appear to be significant in brown rot attack where enzyme-substrate access is currently thought to be assisted by a small non-enzymatic factor.

2. CONCLUSIONS

2.1 Conclusions from observations

1. When viewed in the transmission electron microscope and using a specific stain, the mucilaginous coating of Rhinocladiella mansonii blastospores is observed to be a fine, reticulate, network of short, randomly orientated strands of electron dense material.

2. Similar extracellular coatings of mucilage are present on the hyphae of Chaetomium globosum and Coriolus versicolor but absent from those of Coniophora puteana.

3. Wood cell wall lysis by soft and white rot hyphae, as exemplified by Chaetomium globosum and Coriolus versicolor, is confined to the regions in close proximity to the causal hyphae.

4. There is a strong correlation between the development of restricted lysis features and the presence of an extracellular investment of mucilage on the hyphae.

5. Mucilage appears to determine the spread of ectoenzymes with active lysis occurring along the interface between the wood cell wall and the mucilage.

6. The colonisation of individual wood elements by single hyphae of Coniophora puteana avoids competition for the available polysaccharides, due to the widespread, diffuse, action of their ectoenzymes.

7. The S_1 cell wall layers of birch fibres and Scots pine tracheids are more susceptible to the degradative agents of Coniophora puteana and Chaetomium globosum than those of Coriolus versicolor. This may reflect a lower lignin and higher cellulose and/or hemicellulose content in this region.

8. Surface tension effects on an enzyme bearing, extracellular, mucilaginous layer concentrates the early lytic activity to the immediate lateral vicinity either side of the hyphae during the development of lysis channels in wood cell walls by Chaetomium globosum and Coriolus versicolor.

9. This concentration enables the enzymes of Chaetomium globosum to penetrate the otherwise resistant S_3 and then undercut in the more susceptible S_2 leading to the apparent trans-S_3 lumen erosion.

10. The variation in channel micromorphology produced by Coriolus versicolor may be related to the proportion of matrix material present, with deep, narrower channels developing in heavily encrusted wall layers and shallow, broad types in the more cellulosic regions.

2.2 Conclusions from techniques

1. The scanning electron microscope combined with the simple and inexpensive technique of Critical Point Drying enables observations to be made of structurally undamaged, delicate, three-dimensional structures, especially fungal hyphae. However, the possible chemical effects, on the final specimen surface, as a result of the solvents used must not be overlooked.

2. Extracellular fungal mucilages can be demonstrated in transmission electron microscopy by specific staining with ruthenium red fixative and their structural preservation assisted by dehydration with a water soluble resin series.

3. Durcupan and Glycol methacrylate (G.M.A.) water soluble resins are equally acceptable dehydration agents at this level of study, although G.M.A. is perhaps more cost effective.

4. Substantial definition of fungal cytoplasm, extracellular material and wood cell wall microfibrils in the same specimen can be achieved by the combined application of established fixatives:-

   (i) Glutaraldehyde - general low contrast stabilisation

   (ii) Osmium tetroxide - enhances contrast in fungal cytoplasm

   (iii) Ruthenium red - specific staining of acid mucopolysaccharides

   (iv) $KMnO_4$ - increased contrast in lignin and cytoplasmic membranes.

ACKNOWLEDGEMENTS

I would like to thank my supervisor Dr. J.F. Levy for initiating this study and for his encouragement and discussions throughout the work and Professor R.D. Preston for reading and evaluating the proposed decay mechanisms.

I am indebted to the members of the technical staff of the Department, in particular Mr. R. Baker, for their assistance in obtaining chemicals and equipment and to Mr. R. Vickery, who built the specimen preparation holder despite my continual modifications.

Special thanks go to the staff of the Life Sciences Electron Microscope Unit, Miss. M. Martin for her tuition of ultramicrotomy and photographic processing and especially to Mr. N.L. Costa for his continuous support and detailed instruction in electron microscopy, without which this study would not have been completed.

I would also like to thank my colleagues within the Timber Technology Section, for their constructive criticism and discussions of ideas, especially Mr. E.F. Baines who also assisted in the development of the computer program.

The studies were financially supported by the Science Research Council to whom I express my gratitude.

Finally, I would like to reserve my deepest and most heartfelt thanks for my wife, Yvonne, who not only typed this thesis but also gave every encouragement and assistance during the course of the work and in the preparation, discussion and proof-reading of the resulting manuscript.

APPENDIX A

Microspecimen preparation device

A drill chuck was taken and four holes at 90° to one another were drilled in the jaw collar, providing the specimen movement required. This was then mounted into a ball race set in a plate to allow 360° rotation. This whole unit was then coupled up to the stereo binocular microscope so that viewing through the eyepieces focused on the centre of the chuck. The bolt holes securing the microscope to the chuck assembly were slotted so as to allow movement of the microscope with respect to the chuck, in one plane, enabling a large specimen to be covered by the viewing system. The built-in swing of the microscope head also aided in the latter aspect. The securing of a spring-loaded but lockable locating rod to the micro-scope base, such that the rod aligned with the holes drilled in the chuck collar, resulted in rotation of the chuck being variable between 90°, 120°, or free rotating depending on which set of holes were utilised or not as the case demanded. (This 120° range was due to the holes being drilled on the same plane as the existing chuck key holes provide in the chuck as supplied).

This device was capable of performing the basis of the rotational movement required. A small 'T' profile table was made out of perspex and the centre 20mm circle of the table recessed to accept a disc of P.T.F.E. which was bonded to the table using Evo-stick. (No doubt some other less expensive plastic would have sufficed but a sample of P.T.F.E. was available. To one side of centre (about 1cm) a threaded hole was cut and a bar of stainless steel prepared as the

clamping mechanism. On the same radius a slight step (150μm) was machined so that the clamping bar was parallel to the section it clamped. This table could then be secured in the drill chuck.

The second major adaptation was of the micromanipulator. This had scaled movement in two horizontal directions and was bolted so that the range of movement of the operating arm covered the specimen support table. On the operating arm was a drilled block in which normally a fine tungsten needle would be clamped. A razor blade holder was devised that would securely hold and expose sufficient of the blade to act as a cutter. By polishing the holder the blade was shown up as a sharp dark line when veiwed from above. Thus the plane of the blade could be established and all that was needed was some means of observing the plane of the wood elements and cross correlating the two. This was achieved by inserting a simple eyepiece graticule (which had two crossed lines at right angles to one another), into one of the stereo binocular eyepiece lenses. By using this sections could be located and one of the lines aligned with the tracheid plane by twisting the eyepiece. The blade holder, secured on the operating arm, would then be brought into the field of view and with the vertical focussing control only the plane of the blade could be determined. The clamp securing the blade holder was released and the holder rotated until the plane of the blade aligned with that of the eyepiece line. In this way the planes of the blade and the the wood elements could be precisely paralled. Cuts into the macrosection made this way would produce long sticks in the longtitudinal direction and hence a TS face presented for the ultra-microtome. To produce RLS or TLS final faces simply required aligning

the blade with the cross-wire at right angles to that of the tracheids, or by using the chuck rotation, to rotate the table through 90° to achieve the same end result.

With this blade holder and alignment device, cuts could be made in the macrosection at whatever plane desired and by utilising the vernier scale of the micromanipulator horizontal controls the interval between cuts could be selected. To make a cut simply required racking down of the operator arm whereupon the end of the blade would cut into the specimen. The P.T.F.E. base being hard enough to support the specimen satisfactorily and yet soft enough to prevent damage to the blade edge.

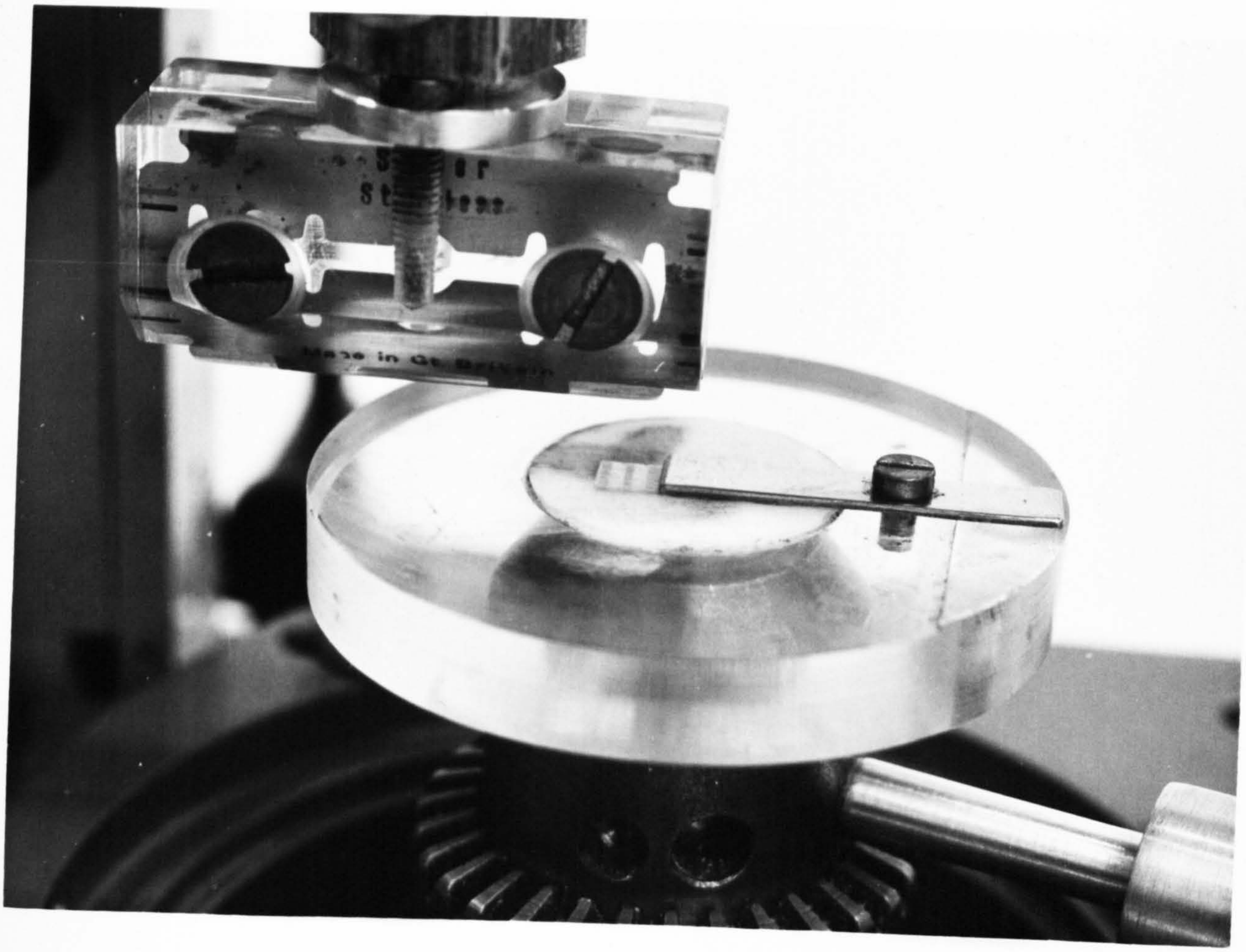
An interval of 150µm between succesive cuts, however, was only two divisions of the vernier scale and in practice proved to be very difficult to achieve repeatedly. This required further modification to the micromanipulator with a rod being secured horizontally into the base of the unit. Onto this could be clamped a dial test indicator which accurately recorded movement down to 10µm. This when coupled to the operating arm, and the fitting of a larger knob, proved to be a more satisfactory means of controlling the cutting interval.

Thus by using this adaptation of the three standard pieces of equipment a satisfactory piece of apparatus was constructed for accurately and repeatedly producing orientated microspecimens of wood 150µm x 150µm by approximately 2.0mm. Figures A and B show the general set up of the apparatus together with details of the cutting block and section clamped to the table.

FIG. A



FIG. B

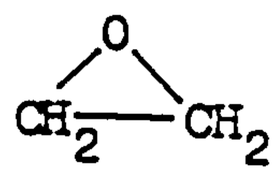


APPENDIX B

The Chemistry of the Epoxy Resin System used in this TEM study

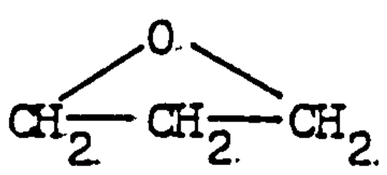
The term epoxy broadly refers to a chemical group consisting of an oxygen atom bonded with two carbon atoms which themselves are already united in some way and such that a ring format is expressed.

The simplest epoxy is a three membered ring to which the term 1,2 epoxy is applied. i.e. ethylene oxide :-

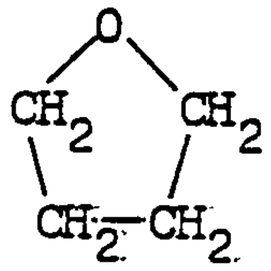


Four and five membered rings are termed 1,3 and 1,4 epoxies respectively and the simplest examples are :-

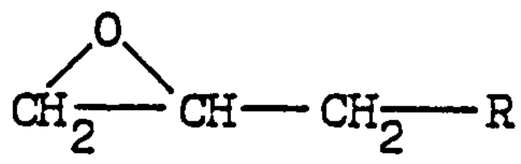
trimethylene oxide



tetra hydrofuran

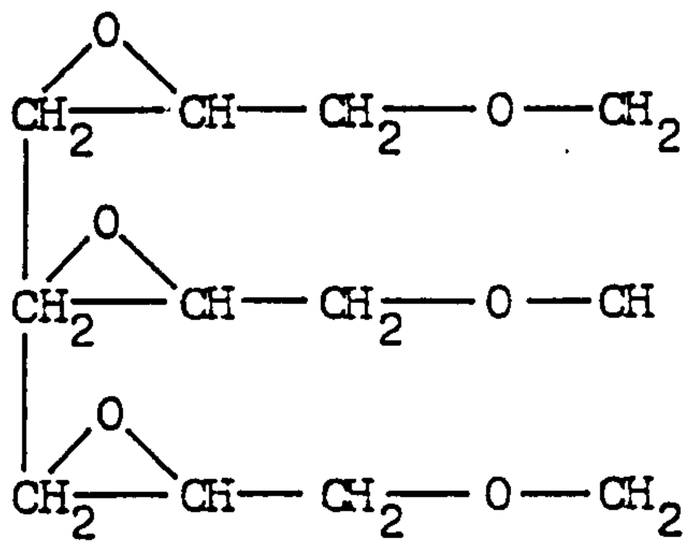


The majority of the commercial epoxy resins are based on the three membered ring, the glycidyl group.



A large number of epoxy resins are available as commercial products and the one used in this work - Epon 812 - is a member of the aliphatic group of epoxies and has a chemical formula and structure of :-

triglycidyl ether of glycerol (1,2,3, tris(2,3-epoxy propoxy) propane)



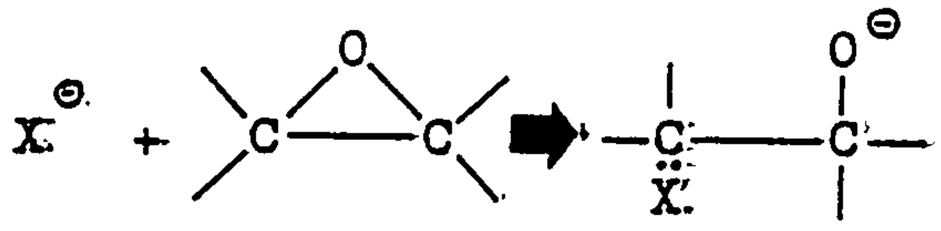
The epoxy groups are separated from one another by six other units and the complete molecule would have a compact tetrahedral structure. The epoxide equivalent of the resin is defined as the weight of resin in grams which contains one gram equivalent of available epoxy. From the chemical structure of Epon 812 one would assume this to be about 87gms as there is almost the same weight of epoxy as there is backbone in the molecule. However, the commercial preparations of Epon 812 range in epoxy equivalent between 140 and 160. This discrepancy is caused by the presence of impurities within the resin preparations, mainly chlorine, due to the synthesis route of the aliphatic based epoxy being via epichlorohydrin. This chlorine can activate the epoxy groups enabling etherification (homopolymerization) to occur thus reducing the number of free epoxy groups and increasing the overall molecular weight, as it is now strictly a polymer.

Thus in any batch of resin produced the number of free epoxy groups has to be determined by the chemical titration of an indicator, for example a halide, and to monitor its absorption into the epoxy groups. In this way the number of grams of resin containing one gram of free epoxy groups can be calculated.

The most valuable property of epoxy resins is their ability to transform readily from the liquid state into tough, hard, thermoset solids, a conversion which normally occurs without the evolution of byproducts. However, epoxy resins are incapable of achieving this conversion themselves as they are unable to open up the epoxy ring without external chemical action. The conversion is normally accomplished by the addition of a chemically active compound known as a curing agent (hardener, activator or catalyst). Some of these agents

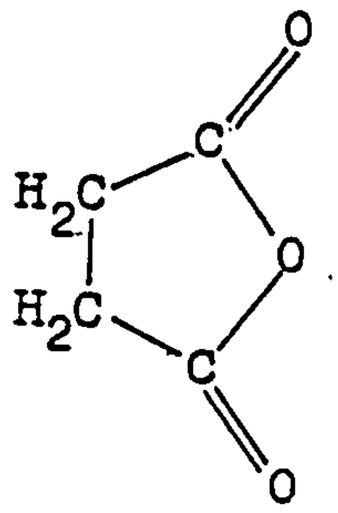
promote curing by catalysis, others participate directly in the reaction and are chemically bound into the resin structure. Depending on the particular agent, curing may be accomplished at room temperature with heat produced by exothermic reaction or may require the application of external heat.

The cured structure may be a homopolmer composed essentially of epoxy resin molecules linked together through the reactive sites of the curing agent, or a mixture of both types. In this system the epoxy group reacts to produce an activated anion species capable of further reaction :-

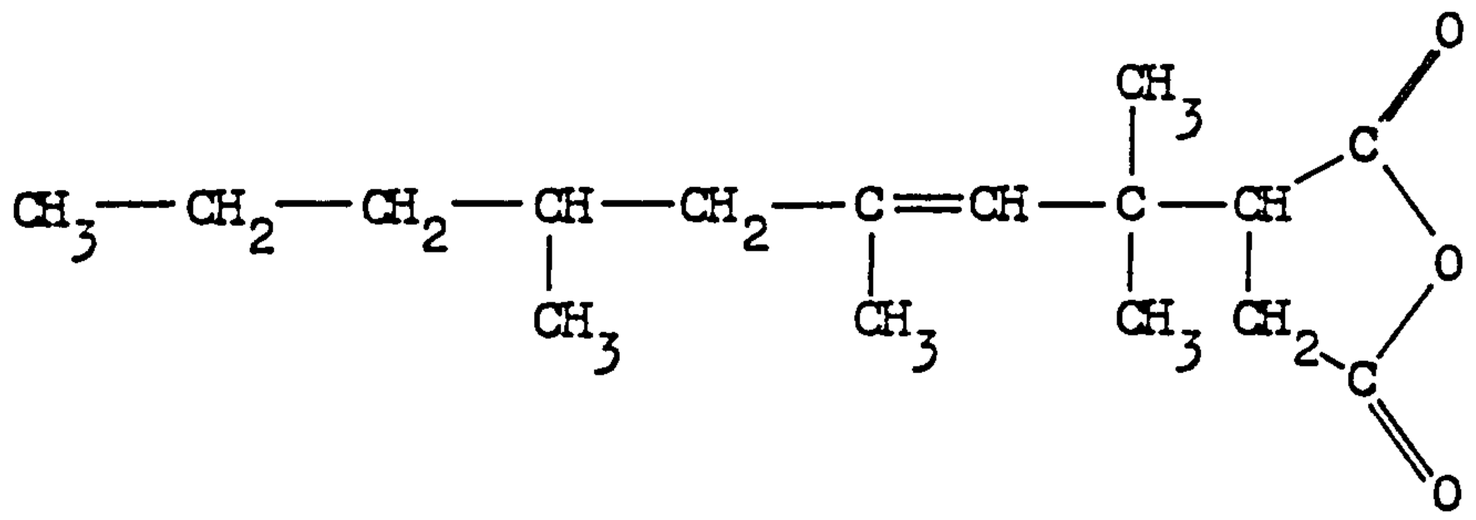


The curing agents used in the resin system employed in this study were both hardeners, DDSA and MNA. Both are alicyclic anhydrides but belong to different sub-groups, because of their structures. Simple alicyclic anhydrides are those where the only ring is the cyclic anhydride group and DDSA is such a chemical whereas MNA belongs to the multi-ring alicyclic anhydrides where the anhydride is attached to another cyclic structure. This classification is clearly illustrated by the different structures of these two hardeners.

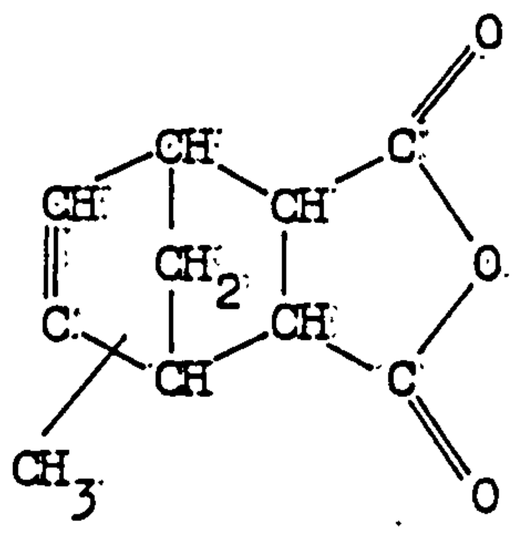
The simplest single ring alicyclic anhydride is succinic anhydride :-



DDSA is a substituted form of this anhydride with a structure of :-



and is a light yellow liquid with a low viscosity (300 centipoise) and a molecular weight of 266. It is used in resin compilation because its long aliphatic chain reduces the brittleness of the cured system. MNA, however, has a far more compact structure and lends itself to harder, more brittle resin cures. MNA is normally a solid but is made into a light yellow liquid, M.P. below 12°C, by the addition of about 0.1% phosphoric acid, has a molecular weight of 178 and structure of :-



MNA cured systems are also found to have good resistance to electron irradiation, (Luft, 1961).

The usefulness of employing these two hardeners as the curing agents for the epoxy resin is that varying their proportions alters the resulting physical properties of the cured resin. A resin system cured with pure MNA would be much harder and more brittle than one cured with DDSA alone. Such variability is very desirable in E.M. work as a match in the physical properties of the

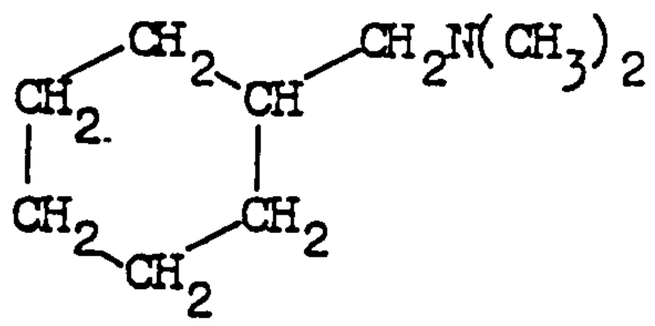
specimen and the embedding medium is all important for successful ultramicrotomy.

However, to simply just add these two hardeners in the proportions desired will only result in a very slow cure. This is because, as in the epoxy resin, the anhydride ring is unreactive until opened and the anhydride itself is incapable of doing this. The fact that a cure is obtained, but only very slowly, is a reflection of the prescence of impurities within the resin and the anhydrides.

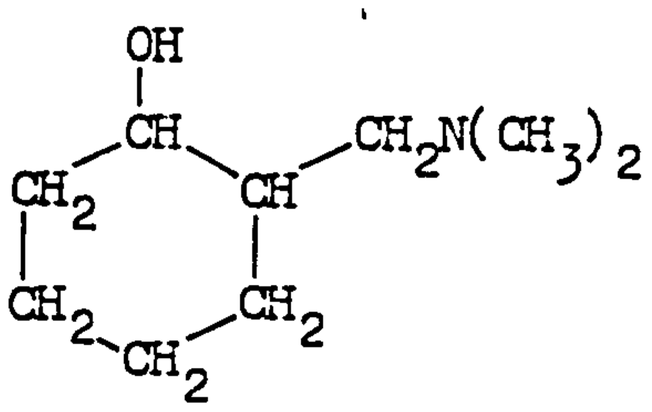
To effect a cure of the resin system, an active chemical has to be added which will open up the epoxy and anhydride rings allowing them to interact and thus polymerise into the cured structure. The required chemical is called an accelerator and a number are available. The one chosen in this system was DMP-30, (Luft 1961), but other literature cites the use of BDMA, (Fink 1969, Zainal 1975) and DMP-10 as alternative accelerators.

All three accelerators, however, belong to the same chemical group of aromatic-ring-containing aliphatic tertiary amines and have the following structures :-

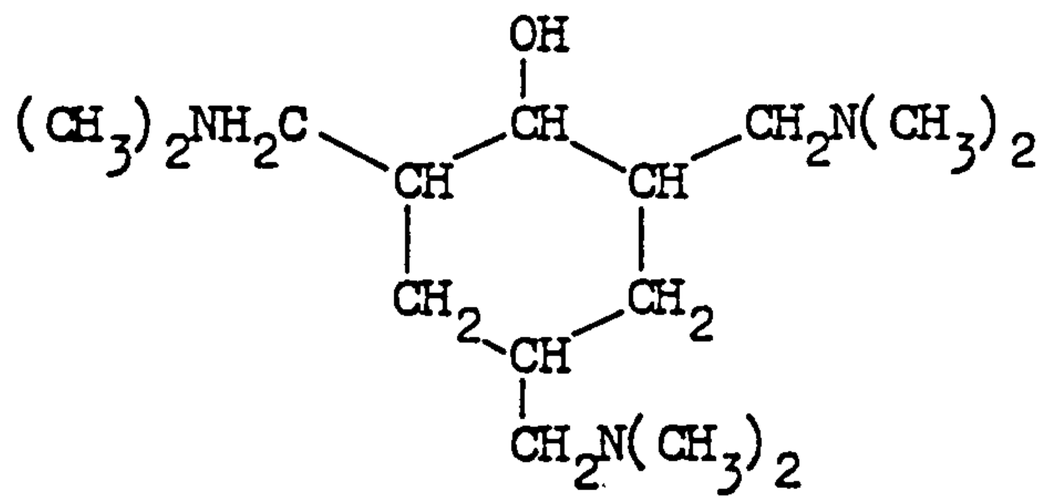
Benzyldimethylamine (B.D.M.A.)



2 (Dimethylaminomethyl) phenol (D.M.P.-30)



2,4,6 - Tris (dimethylaminomethyl) phenol (D.M.P.-30)



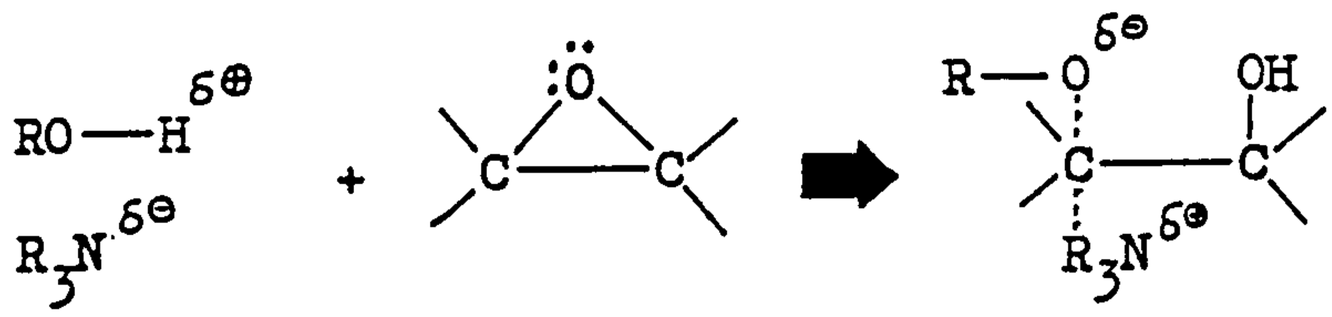
This group of amines are more widely used in epoxy technology than any other. They are frequently employed as accelerators for dicarboxylic acid and anhydride cures and their activity results from the unshared pair of electrons on the nitrogen. The structure of the tertiary amine determines how available or reactive the unshared electron pair will be. This form of activation is of the Lewis base type. As has already been mentioned the curing rate of epoxide and anhydride alone is extremely slow, yet with the introduction of very small quantities of accelerator total cures can be effected in under 8 hours.

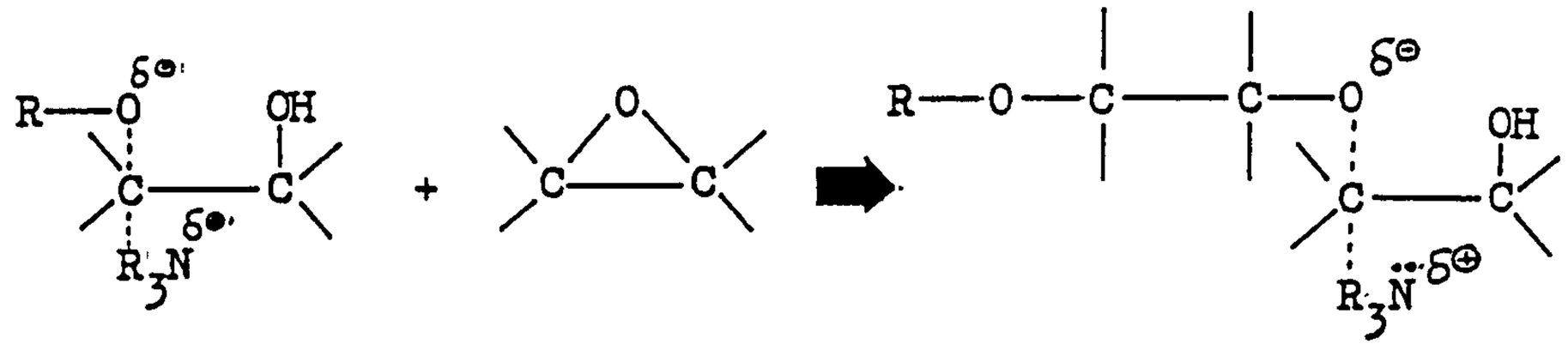
The chemistry of the action of a Lewis base should be examined a little closer to understand exactly how a cure is promoted. The reaction proceeds by an ionic mechanism which is sensitive to both temperature and the prescence of active hydrogen impurities. A Lewis base is capable of opening an epoxy and an anhydride ring and both examples are explained.

<u>Lewis base opening of an epoxy ring</u>

The tertiary amine approaches one of the carbon atoms of the epoxy group. The reaction then requires the presence of a hydroxyl group or the equivalent which provides hydrogen bonding for the epoxy oxygen and attaches itself to produce an alkoxide ion complex which

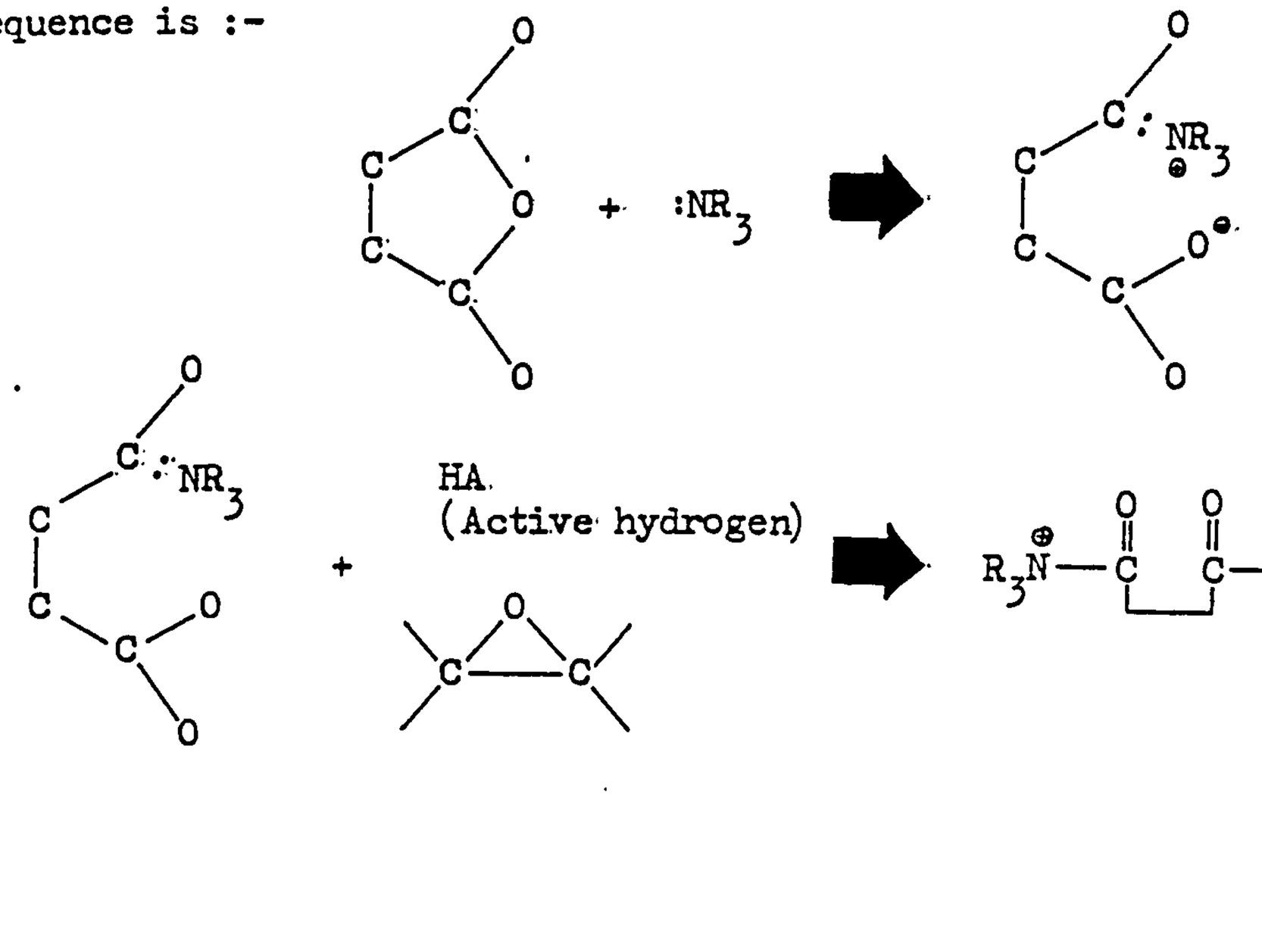
is an active species capable of opening and linking to an adjacent epoxide ring or an anhydride ring.





Lewis base opening of an anhydride ring

The reaction between a Lewis base and an anhydride is preferential over that between a Lewis base and an epoxy ring and results in the generation of a carboxyl ion. This carboxyl ion then reacts with an epoxy and another ion (alkoxide) is generated which may then open a second anhydride ring. There is evidence to suggest that an active hydrogen is required in the carboxyl ion – epoxy step as amine/phenol catalysts were more efficient than amine or phenol catalysts alone, (Lee and Neville 1967). This would also explain the greater efficiency of DMP-30 and DMP-10 over the non-phenolic BDMA. The ring opening sequence is :-



From these Lewis base reactions and the activity of the various alkoxide ion reactions being given as:-

Anhydride > Carboxyl > Phenol > Epoxy - Alcohol

then catalytic curing of Epon 812 with DDSA and MNA would be such that the Lewis base preferentially catalyses the production of carboxyl ions from the anhydrides which would then cross-link with epoxide rings to produce active ion complexes capable of reacting with anhydrides or epoxides. Thus the complex polymer structure would be built up by a series of cross-linkage reactions between activated ion complexes of anhydrides and epoxides to produce the final cured polymer. Some Lewis base epoxide activations will occur but these complexes will also be incorporated into the gross cross-linked structure.

The epoxy anions will react in the order given above such that once all the anhydride - carboxyl sites have been used up the phenolic groups of the accelerator molecules themselves will be used in a much faster reaction thus incorpporating the accelerator into the polymer structure and the final and most rapid reactions of the mopping up of alcohol - epoxy complexes produced by preceding reactions completes the curing of the resin.

When a tertiary amine catalyst is present in an anhdride curing of Epon 812 then esterification is favoured and thus the anhydride/epoxide ratio (A/E) of nearly 1.0 is favoured. However, Luft (1961) recommends that a lowering of this ratio to 0.7 improves the cutting qualities of the cured resin and so the latter ratio was employed throughout this work, though ratios as low as 0.55 have been documented.

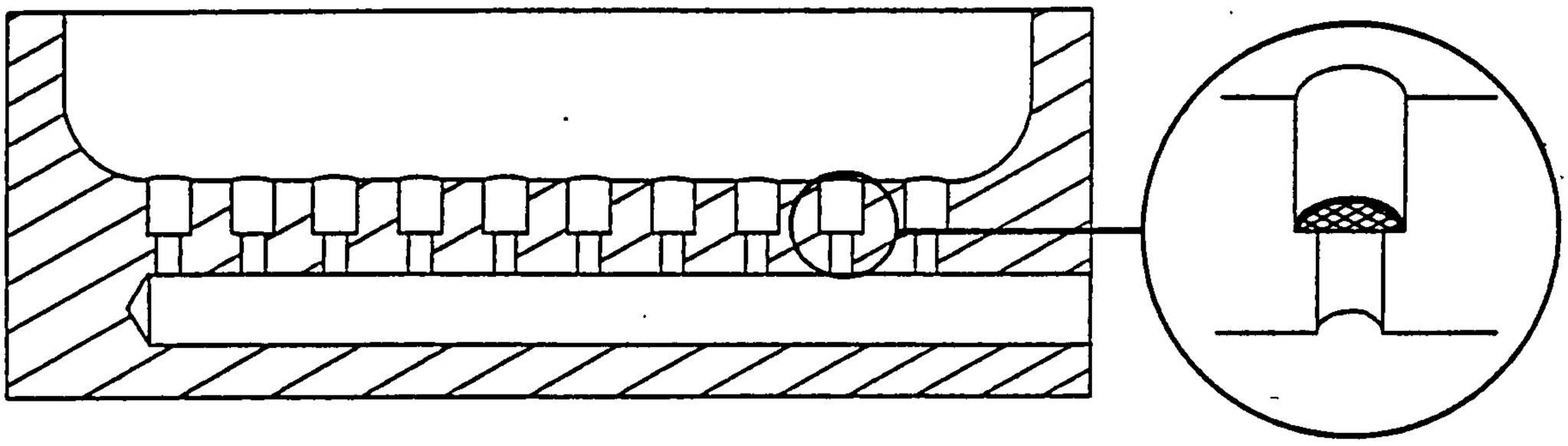
APPENDIX C

Specimen preparation holder

The development of this apparatus extrapolated from the specimen holder and container system described in paper 1 (see page 296). The aim being to support the specimens on very fine E.M. grids and to exchange the various chemicals used in the preparation steps by vacuum withdrawal. In this way the specimens are only physically handled during loading and unloading of the specimen holder.

The initial design was a brass block with shouldered holes on which 3.01mm 100 mesh T.E.M. copper grids could be positioned (Fig. 1). These holes connected through to the same void which could be evacuated when required. By making the upper access to the holes trough shaped then to apply the new chemical of the preparation simply required the filling of the trough.

FIGURE 1



This method soon illustrated a major problem which confronts any work with vacuum or pressure systems in that release of either will always occur by the easiest route. In other words, by applying the withdrawal vacuum to all the specimen chambers simultaneously using the common manifold resulted in the situation of the holes being evacuated together until one of the holes was totally evacuated (the rate of evacuation of the chambers being extremely variable depending on how the specimens obstructed the flow of the solution during withdrawal). Once clear, this hole was then the major pathway for the release of the vacuum with the result that the other chambers ceased draining. Thus to evacuate a number of chambers by a common manifold was impractical as only the rapid draining chambers would be subjected to the correct sequence and total exchange of the preparative solutions.

There only seemed to be two solutions to this problem.

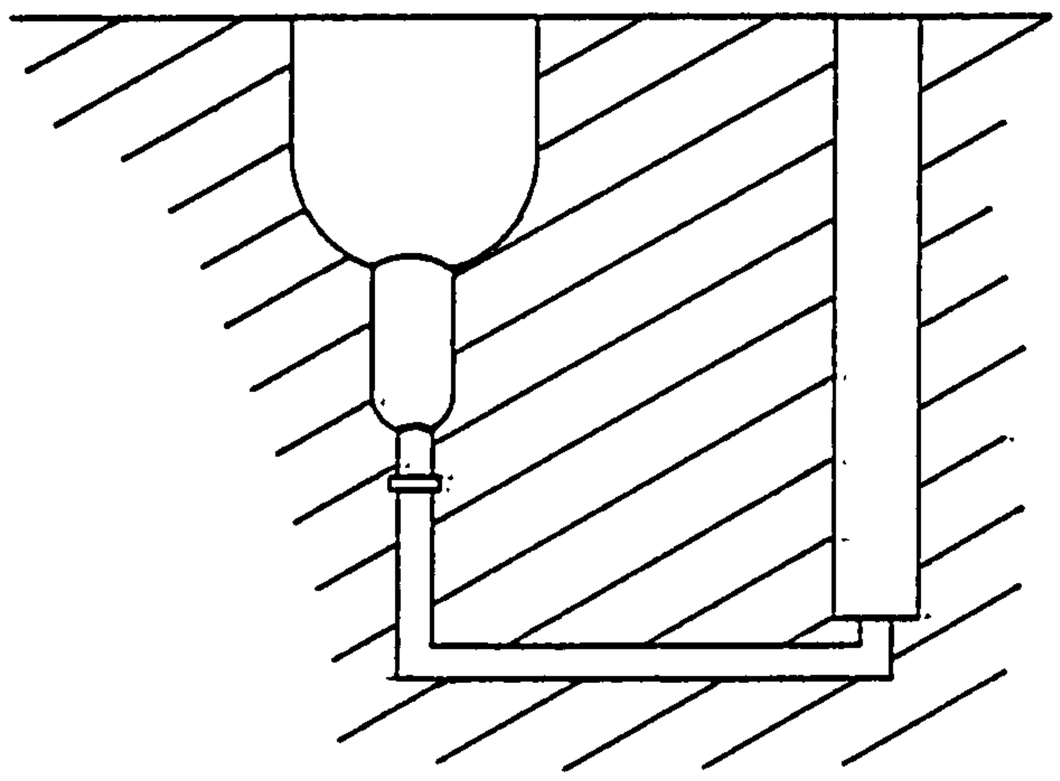
a) Vacuum withdrawal of the chambers in line.

b) Vacuum withdrawal of the chambers individually.

In line withdrawal would require the specimen chambers to be connected end to end with air-tight sealing between. Although considered, this idea was rejected because of the tremendous drag created by such an arrangement, especially when trying to withdraw viscous epoxy resin. The latter solution was chosen as the only feasible was around the problem that the technical resources could cope with and, as such, a specimen holder was designed so that a large number of specimens could be handled on the grid mechanism and yet still be convenient to use with regard to fluid exchange. Comprehensive drawings of the holder are included in the back pocket of this thesis and the features

are briefly described here.

The specimens were housed within a cylindrical specimen chamber at the base of which lay an E.M. support grid. Ten chambers were connected in line by a single feeder trough into which exchange fluids could conveniently be poured. From the withdrawal side of each support a small bore hole was cut through a 'U' bend for ease of access, with this hole being increased in diameter to accept the vacuum withdrawal probe, see fig. B.

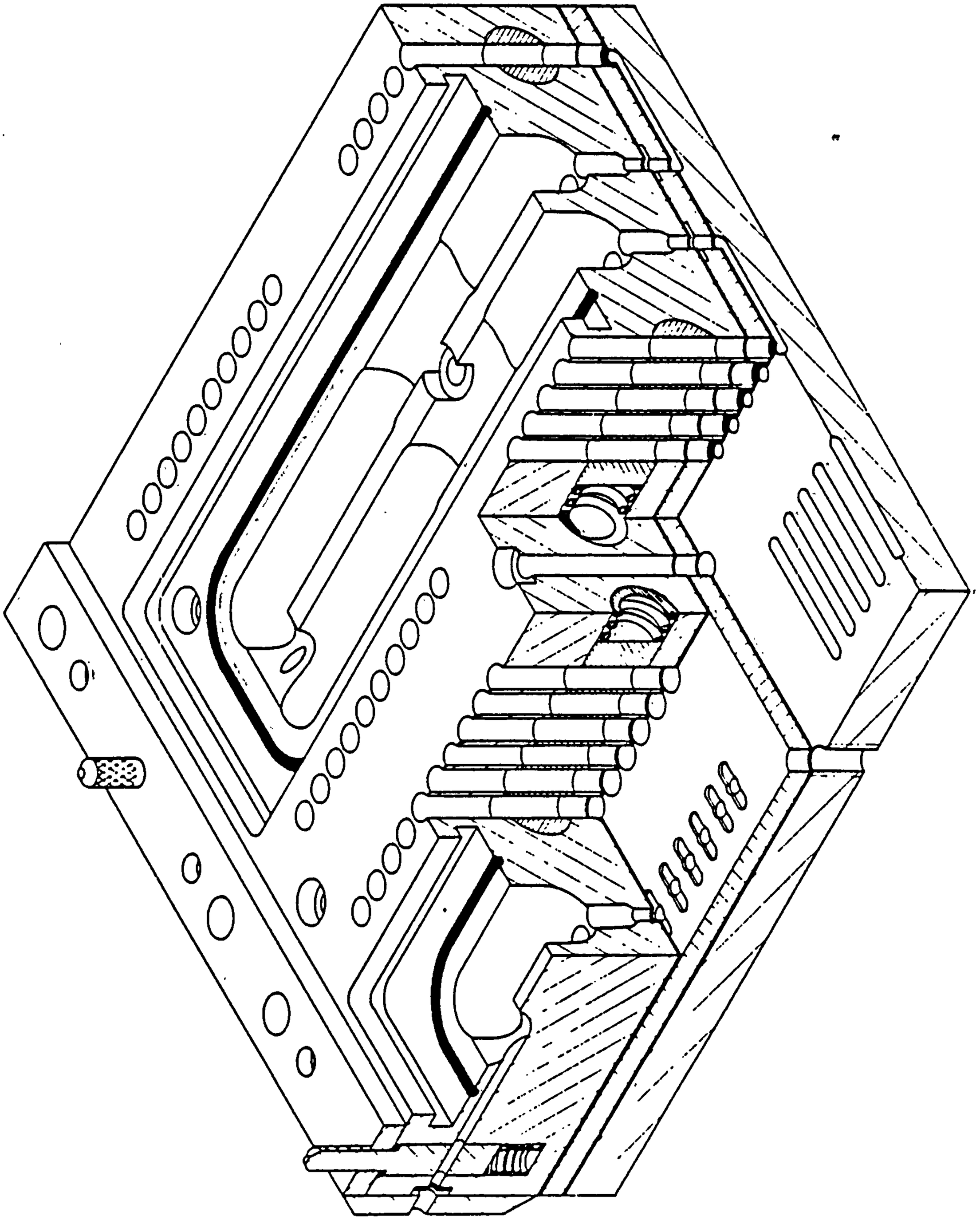


Thus each specimen chamber had its own exit port to the outside of the holder, into which could be inserted a vacuum probe to withdraw the old fluid surrounding the specimen. Having the probe nozzle at a lower height than the grid support prevented back flow of old fluid into the specimen area.

With ten of these chambers being fed by one feeder trough meant that the chemical treatment of all ten chambers would be the same. However, as already mentioned, frequently several chemical variations are required so the design format was extended to comprise of eight such troughs and, therefore, 80 specimen chambers. If each specimen chamber contained 2 specimens then a holder of this type could easily accomodate 160 specimens in any single preparation and, what was more

important, if required the number of specimen variables could be as high as 80. This holder had the necessary potential for coping with extremely variable specimens, as in this type of work, and to process all the material at the same time.

ISOMETRIC CUT-AWAY DRAWING OF THE T.E.M. SPECIMEN HOLDER



APPENDIX D

Program to produce tables of resin components in 100 gram mixes for various epoxide equivalents of epon 812 with a range of A/E and MNA/DDSA ratios.

```
      PROGRAM ALAN C (INPUT,OUTPUT,TAPE5=INPUT,TAPE6=OUTPUT)
      DIMENSION EQUIV(21),A(21),B(21),C(21),MNAR(21),MDDSAR(21)
      WTMNA = 178.
      WTDDSA = 266.
      DO 1 I=1,21
      RI=I
    1 EQUIV(I)=RI+139.
      READ(5,2) NI,NR, (MNAR(L),L=1,NR), (MDDSAR(L),L=1,NR)
    2 FORMAT( 2(I2,1X),30(I1,1X))
      DO 6 J=1,NI
      RJ=J
      RJ1=RJ/100.
      ANEPR=0.54+RJ1
      WRITE(6,3)ANEPR,(EQUIV(I),I=1,21)
    3 FORMAT(1H1/////1X,28HANHYDRIDE - EPOXIDE RATIO = F4.2,15X,
     159H ACCELERATOR, DMP-30  1-1.5 PERCENT BY WEIGHT = 1-1.5 GMS.////
     21X,4HMNA/50X,34HEPOXIDE EQUIVALENT OF THE EPON 812 /1X,4HDDSA/
     31X,5HRATIO,5X,21(1X,F4.0,1X))
      DO 6 L=1,NR
      MNA=MNAR(L)
      MDDSA=MDDSAR(L)
      EMNA=MNA
      DDSA=MDDSA
      EPEQ=EQUIV(1)
      IF(DDSA.LT.1.0)DDSA=1.0E-10
      X=ANEPR/(EMNA+DDSA)
      T=X*WTMNA*EMNA
      U=X*WTDDSA*DDSA
      DO 4 I=1,21
      A(I)=T/(T+U+EPEQ)*100.
      B(I)=U/(T+U+EPEQ)*100.
      C(I)=EPEQ/(T+U+EPEQ)*100.
    4 EPEQ=EPEQ+1.0
      WRITE(6,5)(A(I),I=1,21),MNA,MDDSA,(B(I),I=1,21),(C(I),I=1,21)
    5 FORMAT(//6X,3HMNA,2X,21(1X,F4.1,1X)/1X,I1,1H-,I1,2X,4HDDSA,1X,
     121(1X,F4.1,1X)/6X,4HEPON,1X,21(1X,F4.1,1X))
    6 CONTINUE
      STOP
      END
```

© *Journal of Microscopy, Vol.* 108, *Pt* 3, *December* 1976, *pp.* 349–352.
Revised paper accepted 15 *September* 1976.

Short Technical Note

A versatile multi-specimen holder for processing and critical point drying of materials for examination in the scanning electron microscope (SEM)

by A. CROSSLEY, *Timber Technology Section; Department of Botany, Imperial College of Science and Technology, London, S.W.7*

SUMMARY

A specimen holder has been designed specifically for use in the Polaron E.3000 critical point drier (CPD) and is capable of drying up to twenty different specimens within a size range of 4·5 mm to 30 μm by utilization of a variable grid system. The principle, however, could be employed in designs for most other critical point dryers.

A large number of designs have been produced for handling small specimens during preparation and CPD procedures prior to observation in the scanning electron microscope (SEM). In a great number of cases these have been specific to one particular organism or preparation method. Marchant (1973) suggested culturing organisms on Millipore filters which could then be used in conjunction with a plain filter as a sieve mechanism to contain the specimens, the complete unit being housed in a BEEM embedding capsule. Scott *et al.* (1973) produced another design, again utilizing the BEEM capsule together with 100 grade copper mesh as the specimen retaining section. Both these designs were flexible in that different grade filters and meshes could be employed.

The disadvantage of using BEEM capsules was noted by Taylor (1975) in that the chemical plasticizers present in the capsule material could leak out in the presence of substitution solvents. To overcome this he produced an all metal design for a container employing a similar type of grid system as in this multispecimen holder. His design was for a single chamber specimen holder with a maximum specimen thickness of 1 mm and was such that the complete chamber could be placed directly into the SEM.

The need for a multispecimen holder arose when large numbers of specimens, each specific in its preparation required critical point drying without tedious repetition of critical point drying runs.

It was necessary to consider the inflexible features of the design. These were, the external dimensions of the container, which had to fit within the existing aluminium specimen-holder of the Polaron E.3000 CPD, and the dimensions of the transmission electron microscope (TEM) grids used as the specimen retainers. Transmission electron microscope grids are available in two sizes, 3·01 mm and 2·3 mm, with a large

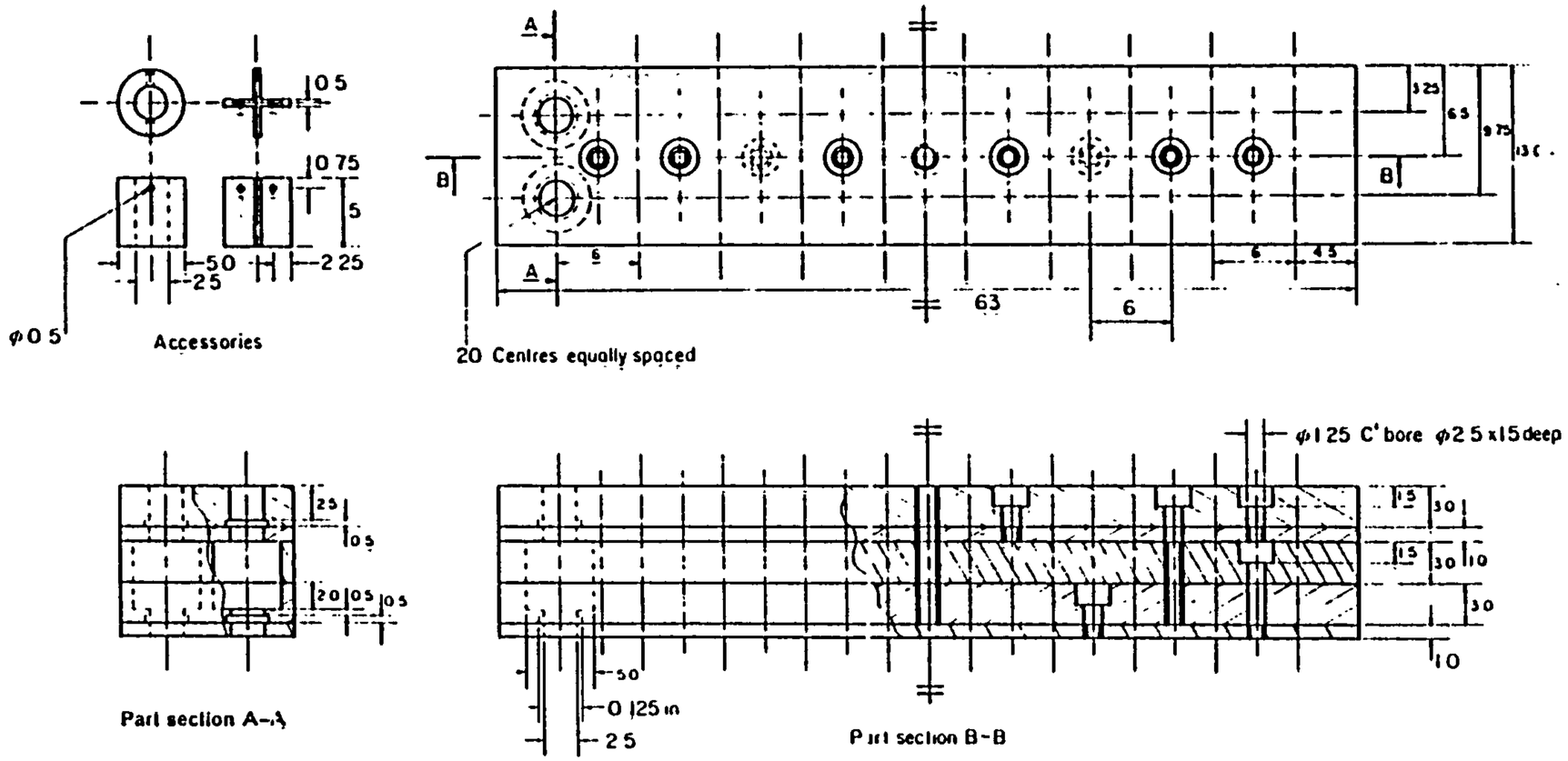


Fig. 1. Third angle projection views of the assembled specimen holder and accessories. Constructed from machine quality brass with all dimensions in mm unless otherwise stated.

range in patterns and materials to choose from to suit most types of specimen preparation. From these fixed dimensions a design was drawn up which allowed specimens of up to 4·5 mm across to be prepared and yet still gave the large number of individual chambers required.

The construction of the holder can be seen, from the drawing (Fig. 1) and the photographs (Fig. 2) to be comprised of large dimension chambers with a TEM grid housed at each end to contain the specimens and yet still allow the free flow of dehydrating and substitution agents. The complex arrangement of screws was necessary to facilitate the assembly and use of a container which has a separate lid section that can be dismantled to allow different grids to be inserted depending on the dimensions of the material under preparation. The specimens are supported on the lower grid system which can also be varied and for the ease of removal of larger specimens the chamber section divides leaving the specimens readily accessible in the lower half.

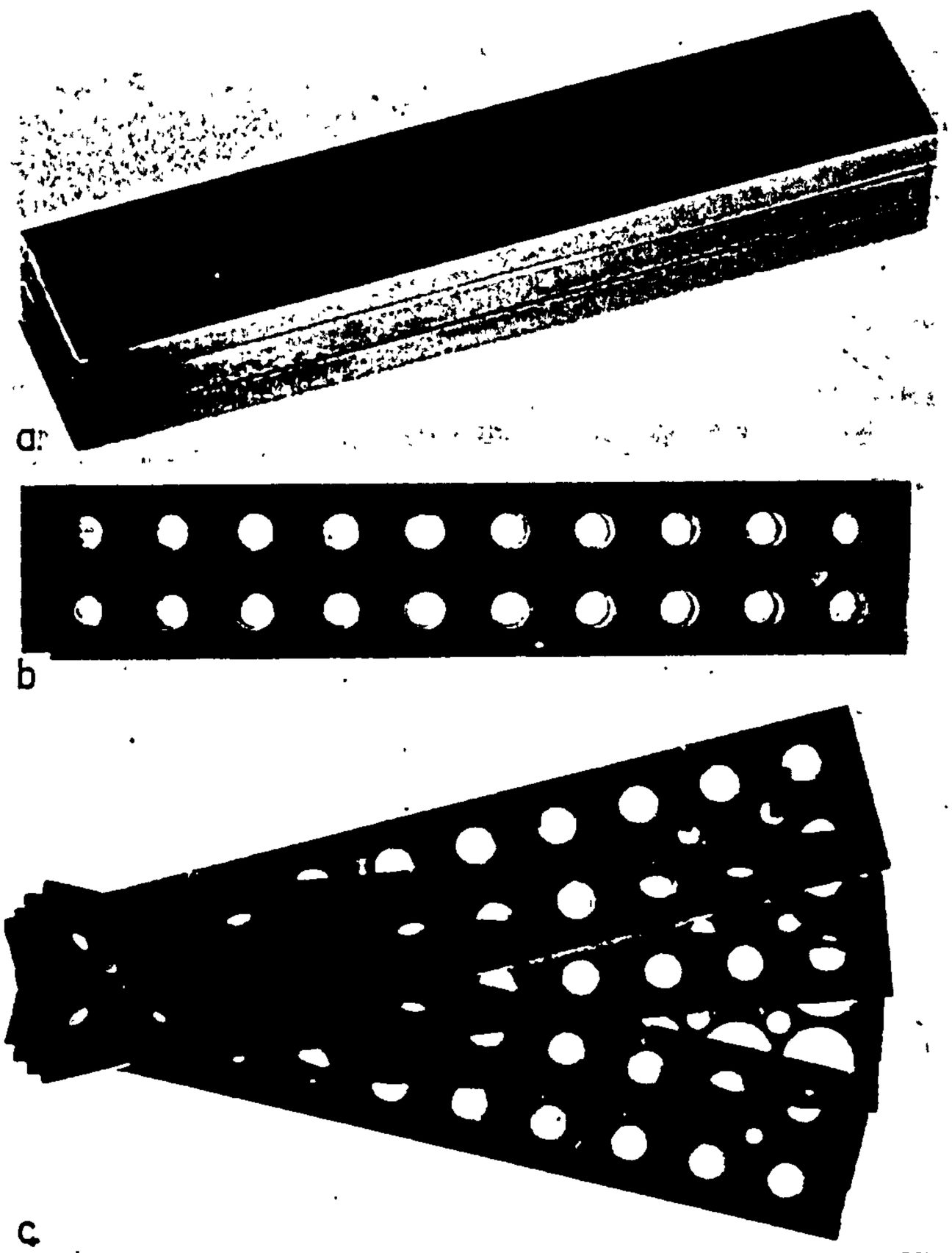


Fig. 2. Views of the specimen holder to illustrate the assembled appearance, the permeability of the chambers allowed by the use of grids and the separated components showing maximum use of the available metal volume in the chamber construction.

Where the specimens are very small, the chamber section can be completely removed by carefully removing all screws and then screwing a stud down the centre thread and extracting the chamber section leaving all the specimens supported on their grids on the base plate. These can easily be transferred directly onto the SEM stub and secured either by double-sided sellotape or careful application of an adhesive such as Durafix. It has even been found that discs punched out of Visking tubing can be used in place of the TEM grids to provide a finer sieve mechanism. It was noted, however, that the tubing was hardened by substitution solvents but this still did not seem to impair the results as satisfactory preparations of *Penicillium expansum* sporangiophores and pollen of *Dactylis glomeratus* have been achieved (Medi-Cine, 1976).

The container has been made out of high quality brass because of its good machining properties necessary when such fine work has to be carried out. The metric design utilizes standard milling cutters with the inclusion of the $\frac{1}{8}$th cutter to produce satisfactory grid housings allowing free movement to ensure that they always settle on the base plate.

The versatility of the design can be further increased with the production of two accessory structures (see Fig. 1). The first, simply produced by cutting brass tubing, is for the preparation of small numbers of specimens per chamber, and ensures that the specimens are deposited onto the grid. The holes drilled through the tube wall allow easy removal with fine forceps. The second structure simply partitions the large chambers increasing the capacity to eighty specimens where such a large specific separation is required.

The production of artifacts resulting from specimen handling is reduced considerably with this specimen holder. Once the specimens have been loaded, all the processing stages can be carried out on all the material at once and the specimens are ready for mounting prior to observation.

References

Marchant, H.J. (1973) Processing small delicate biological specimens for Scanning E.M. *J. Microsc.* 97, 369.

Medi-Cine (1976) A film called Allergic rhinitis (not on general release). Sponsored by Fisons Produced by Medi-Cine.

Scott, J.R., Thurston, E.L. & McKee, T.R. (1973) A fine sieve processing container for use in C.P.D. *J. Microsc.* 99, 359.

Taylor, J. (1975) A container handling small specimens during preparation and examination in the Scanning Electron Microscope (S.E.M.). *J. Microsc.* 105, 335.

PROBOSCIS HYPHAE IN SOFT ROT CAVITY FORMATION

by A. CROSSLEY* and J. F. LEVY*.

Summary

Fungal 'Proboscis hyphae' have rarely been observed with the Scanning Electron Microscope (S.E.M.) and for this reason some micrographs of the feature are illustrated and described. The example being from the soft rot attack (Savory, 1954) by *Chaetomium globosum* L. on birch. Because of the clarity and completeness of the cavity and its associated features this provides conclusive support for Corbett's (1963) proposed theory of soft rot cavity formation.

The first observation and naming of proboscis hyphae was made by Corbett (1963) and illustrated by Levy and Stevens (1966), using the light microscope. Observational studies by a number of workers (Lundström, 1970; Casagrande and Ouellette, 1971) have only been achieved with the use of the light microscope and until this year no S.E.M. recordings of the feature had been published. Presumably this was due to the extreme difficulty in obtaining a specimen such that the cavity and enclosed hypha were revealed and yet remained undamaged. A recent paper by Leightley and Eaton (1977) included three micrographs illustrating proboscis hyphae in soft rot cavity formation by the marine Ascomycete *Halosphaeria mediosetigera* in Scots pine. The paper included an examination of the mechanics and sequential progress of soft rot degrade in the marine environment.

This paper examines the soft rot cavity formed by the terrestrial Ascomycete *Chaetomium globosum* on a test hardwood, birch, *Betula sp.* Orientated blocks of birch, 1 cm^3, were inoculated with the fungus and incubated for 3, 4, 6 and 8 weeks at 22°C. After their relevant incubation periods the blocks were fixed by vacuum impregnation with a 2·5 per cent aqueous solution of glutaraldehyde and dehydrated using the Critical Point Drying process. Small pieces of the surface and internal regions of the blocks were cut using new, clean razor blades and positioned on S.E.M. stubs with the adhesive Durafix. The stub and specimens were then coated with 475 Å of gold in a Polaron Sputter Coater.

Plate I shows a complete soft rot cavity formed in the external uncut surface of a 6 week incubated block of birch. The line drawing, Fig. 1, picks out the extent of the cavity, and its features, which is orientated parallel to the microfibrils of the exposed wall layer. This microfibrillar orientation can be clearly seen, especially in the lower area of Plate I and indicated that the specimen surface had suffered damage during the preparation of the 1 cm. cube. This has resulted in the S_2 layer of the cell wall being revealed as the surface feature. (the definitions of the wall layers are those of Kerr and Bailey (1934) and Bailey and Kerr (1935)). Emphasis must be made here that since it was the external surface of the block that was examined, any removal of cell wall layers must have occurred before the inoculation of the fungus: as this was an external surface of the block. This is important in the later interpretation of the sequence of cavity formation, in this example.

There was no evidence for the formation of the cavity being derived from surface hyphae so our interpretation of the sequence of events giving rise to the cavity is as follows:

Somewhere below the surface of the wood specimen probably in the lumen of the adjacent cell, lay the parent hypha. This produced a fine lateral hypha which penetrated the S_3, S_2 and S_1 layers of the secondary wall and crossed the primary wall/middle lamella complex then through the S_1 and into the S_2 wall layer of the damaged surface cell. see Fig. 1 (Section II). Once in this layer a 'T' branch was formed. (Corbett, 1963; Corbett and Levy, 1963) with the two hyphal tips growing away from each other along the line of the microfibrils and thus at right-angles to the axis of the lateral hypha region. The probable site of this branching has been indicated, see Fig. 1. The growth axis was just below the surface of the specimen and the inclination of this to the surface of the block is indicated by the centres of the proboscis hyphae in sections I and III of Fig. 1. These two line, 0·25 µm diameter hyphae were the proboscis hyphae and they continued to grow through the S_2 wall layers. Behind the proboscis region the hypha enlarged in diameter in conjunction with an increase in width of the surrounding cavity until the cavity hypha reached a maximum diameter of approximately 1 µm. However cavity formation continued to the point where it was three times the diameter of the enclosed hypha at the time of fixation. It was this cavity growth that produced such a clear picture of the process of proboscis hyphal involvement in the formation of cavities. As the cavity continued to grow beyond the diameter of the hypha then the remaining layers of the S_2 overlying it were removed, so exposing the whole system. The cavity has thus retained the true structure even when a surface feature and this possibly indicates that the enzyme systems involved are somehow co-ordinated and contained so as to produce a controlled degrade of the wall layers.

This could possibly be explained by envisaging the enzyme systems being contained within a mucilaginous matrix exuded by the cavity hypha, such a theory having already been proposed by Schmid and Liese (1965). The matrix would then delimit cavity formation and retain the cavity shape when the surface layers were broken through. Support for this could be taken from the condition of the hyphal surface which, on close examination, shows a heavy investment of dried material on the

*Timber Technology Section, Botany Department, Imperial College of Science & Technology, London SW7.



Plate I.

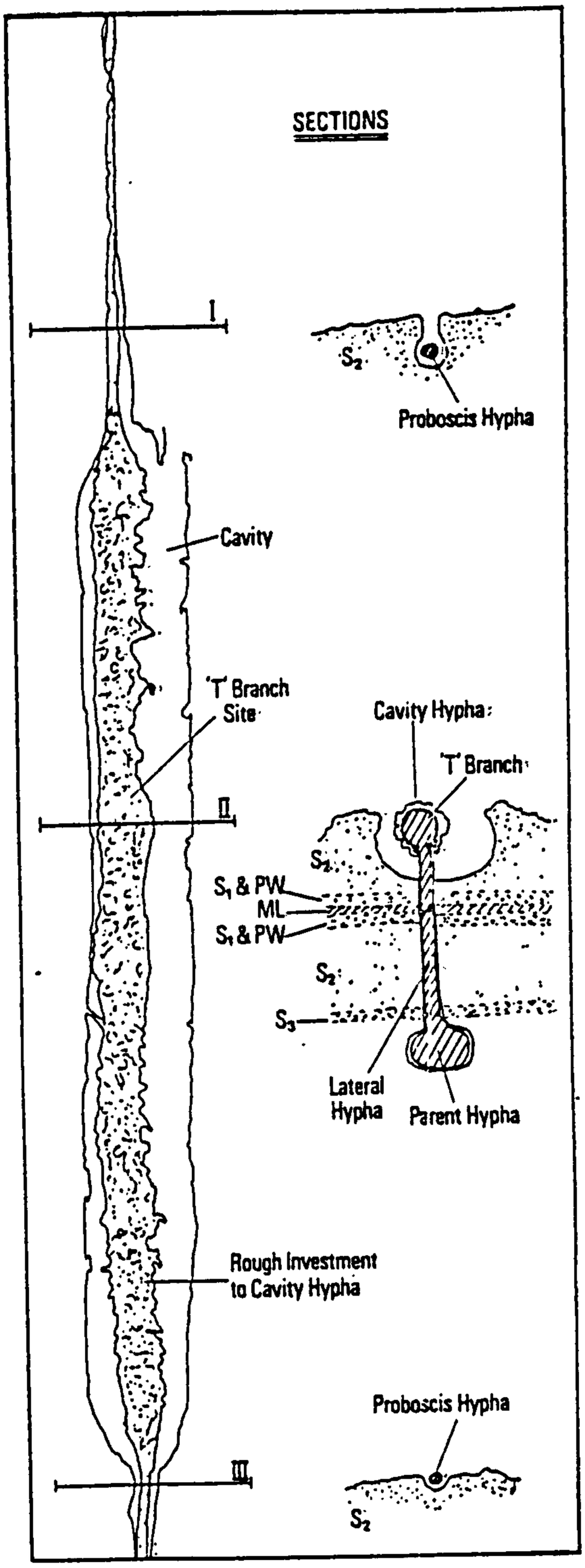

SECTIONS
I
II
III
S_2
Proboscis Hypha
Cavity
'T' Branch Site
Cavity Hypha
'T' Branch
S_2
S_1 & PW
ML
S_1 & PW
S_2
S_3
Lateral Hypha
Parent Hypha
Rough Investment to Cavity Hypha
Proboscis Hypha
S_2

Fig. 1.

cavity hypha, though the proboscis hyphae appear to be very smooth and therefore possibly lack or bear very little of this mucilaginous material. See Plates 1, 2 and 3.

Further work, especially Transmission Electron Microscopy, has to be carried out to try and answer some of the questions about the exact structure and function of proboscis hyphae. Such work, in part, is now in progress by the authors.

Acknowledgements

The study was carried out with the financial support of the Science Research Council and with the help of the Departmental Electron Microscopy Unit of the Division of Life Sciences, Imperial College. The authors wish to express particular thanks to the Unit's supervisor, Mr Norman Costa.

REFERENCES

Bailey, I. W. and Kerr, T. (1935). *J. Arnold. Arbor.* 18, 185-196.

Casagrande, F. and Ouellette, G. B. (1971). A technique to study the development in wood of soft rot fungi and its application to Ceratocystis ulmi. *Can. J. Bot.* 49 (1), 155-159.

Corbett, N. H. (1963). Anatomical, ecological and physiological studies on microfungi associated with decaying wood. *Ph.D. Thesis.* University of London.

Corbett, N. H. and Levy, J. F. (1963). Penetration of tracheid walls of Pinus sylvestris L. (Scots Pine) by Chaetomium globosum. *Nature* 198, 1322-1323.

Kerr, T. and Bailey, I. W. (1934). *J. Arnold. Arbor.* 15, 327.

Leightley, L. E. and Eaton, R. A. (1977). Mechanisms of decay of timber by aquatic micro-organisms. *B.W.P.A. Ann. Conv. 1977* (9).

Levy, J. F. and Stevens, M. G. (1966). The Initiation of attack by Soft Rot fungi in wood. *J. Inst. W. Sci.* 16, 49-55.

Lundström, H. (1970). Cavity formation in Soft Rot. A method for continuous microscopic direct study. *Holzforschung.* 24 (4), 132-133.

Savory, J. G. (1954) Breakdown of timber by Ascomycetes and fungi imperfecti. *Ann. Appl. Biol.* 41, 336-347.

Schmid, R. and Liese, W. (1965). Electronenmikroskopische Beobachtungen an Hyphen von Holzpilzen. *Proc. Symp. Wood and Organisms Berlin 1965. Mat. u. Org., Heft 1,* 251-261.



Plate 2.

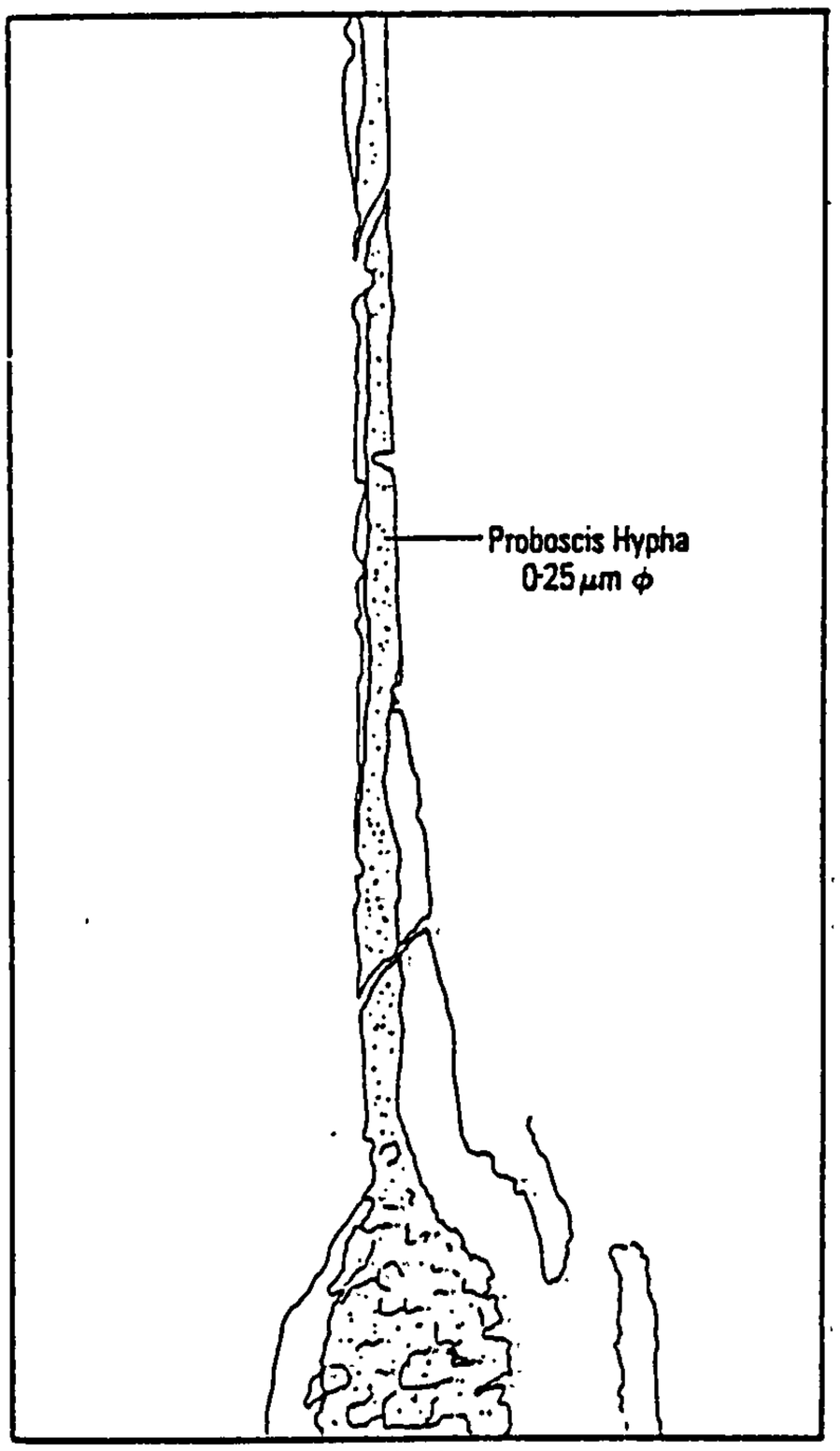


Fig. 2.



Plate 3.

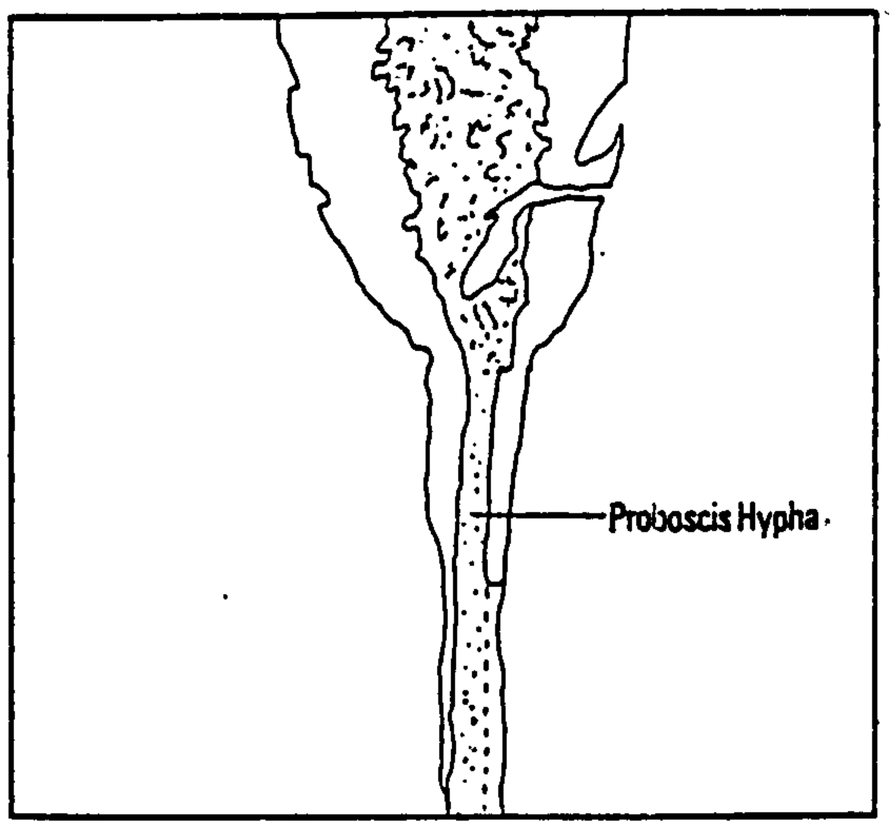


Fig. 3.

REFERENCES

ABRAMS, E. (1948).
Microbiological deterioration of organic materials; its prevention and methods of test. Nat. Bureau of Standards Misc. Publ. No. 188 U.S. Dept. of Commerce, Washington.

ANDERSON, T.F. (1951).
Techniques for the preservation of three-dimensional structure in preparing specimens for the electron microscope. Trans. N.Y. Acad. Sci., 13, pp. 130-134.

BAILEY, I.W. (1954).
Contributions to Plant Anatomy. Chronica Botanica, 15 (1) 262 p.

BAILEY, I.W. and VESTAL, M.R. (1937).
The significance of certain wood-destroying fungi in the study of the enzymatic hydrolysis of cellulose. J. Arnold Arbor., 18, pp. 196-205.

BAILEY, P., LIESE, W. and ROSCH, R. (1968).
Some aspects of cellulose degradation in lignified cell walls, pp. 546-557. In; Biodeterioration of Materials (ed. A.H. Walters and J.J. Elphick), London, Elsevier.

BANKS, W.B. (1971).
Structure of the bordered pit membrane in certain softwoods as seen by scanning electron microscopy. J. Inst. Wood Sci., 5, (4), pp. 12-15.

BARTNICKI-GARCIA, S. (1968).
Cell wall chemistry, morphogenesis and taxonomy of fungi. A. Rev. Microbiol., 22, pp. 87-108.

BLAND, D.E., FOSTER, R.C. and LOGAN, A.F. (1971).
The mechanism of permanganate and osmium tetroxide fixation and the distribution of lignin in the cell wall of Pinus radiata. Holzforschung, 25, pp. 137-143.

BOUVENG, H.O., KIESSLING, H., LINDBERG, B. and McKAY, J. (1963).
Polysaccharides elaborated by Pullularia pullulans. III polysaccharides synthesised from xylose solutions. Acta chem. scand., 17, pp. 1351- .

BOYDE, A. and WOOD, C. (1969).
Preparation of animal tissues for surface scanning electron microscopy. J. Microsc., 90 (3), pp. 221-249.

BRAVERY, A.F. (1971).
The application of scanning electron microscopy in the study of timber decay. J. Inst. Wood Sci., 5 (6), pp. 13-19.

BRAVERY, A.F. (1972).
The effects of certain wood preservatives and their distribution on some fungi causing timber decay. Ph.D. Thesis, University of London, Imperial College.

BRITISH STANDARD 838 (1961).
Methods for test for toxicity of wood preservatives to fungi. B.S. 838.

BUCK, K.W., CHEN, A.W. and DICKERSON, A.G. (1967).
Formation and structure of extracellular glucans produced by Claviceps species. J. gen. Microbiol., 51, pp. 337-352.

CARTWRIGHT, K.St.G. and FINDLAY, W.P.K. (1943).
Timber decay. Biol. Rev., 18, pp. 145-158.

CARTWRIGHT, K.St.G. and FINDLAY, W.P.K. (1958).
Decay of timber and its prevention. H.M.S.O., London, 2nd Edn.

CHOU, C.K. (1971).
Degradation of wood by fungi as affected by preservatives. Ph.D. Thesis, University of Leeds.

COHEN, A.L., MARLOW, D.P. and GARNER, G.E. (1968).
A rapid critical point method using fluorocarbons ("Freons") as intermeadiate and transitional fluids. J. Microscopie, 7, pp 331- .

CORBETT, N.H. (1963).
Anatomical, ecological and physiological studies on microfungi associated with decaying wood. Ph.D. Thesis, University of London, Imperial College.

CORBETT, N.H. (1965).
Micromorphological studies on the degradation of lignified cell walls by Ascomycetes and Fungi Imperfecti. J. Inst. Wood Sci. 14, pp. 18-29.

CORBETT, N.H. and LEVY J.F. (1963).
Penetration of tracheid walls of Pinus sylvestris L. (Scots pine) by Chaetomium globosum Kunz. Nature, 198 (4887), pp. 1322-1323.

CÔTÉ, W.A., KORAN, Z. and DAY, A.C. (1964).
Replica techniques for electron microscopy. Tappi, 47, pp. 477-484.

COURTOIS, H. (1963).
Mikromorphologische Befallsymptome beim Holzabbau durch Moderfäulepilze. Holzforsch. Holzverwert., 15 (5), pp. 88-101.

COURTOIS, H. (1965).
Mikromorphologische Veranderungen verholzer Zellwande durch Basidiomyceten (Braunfauleereger). Mat. u. Org., Bh. 1, pp. 41-53.

COWLING, E.B. (1961).
Comparative biochemistry of the decay of sweetgum sapwood by white-rot and brown-rot fungi. U.S. Dept. Agri. Tech. Bull. No. 1258, 79pp.

COWLING, E.B. (1965).
Microorganisms and microbial enzyme systems as selective tools in wood anatomy, pp. 341-368. In; Cellular ultrastructure of woody plants (ed. W.A. Côté), Syracuse University Press.

COWLING, E.B. (1975).
Physical and chemical constraints in the hydrolysis of cellulose and lignocellulosic materials, pp. 163-181. In; Cellulose as a chemical and energy resource (ed. C.R. Wilke), Biotech. and Bioeng. Symp. No. 5, New York, John Wiley & Sons.

COWLING, E.B. and BROWN, W. (1969).
Structural features of cellulosic materials in relation to enzymatic hydrolysis, pp. 152-187. In; Cellulases and their applications (ed. R.F. Gould), Adv. Chem. Ser., No. 95.

CRAIG, E.L., FRAJOLA, W.J. and GREIDER, M.H. (1962).
An embedding technique for electron microscopy using Epon 812. J. Cell Biol., 12, pp. 190-194.

CROCKER, E.C. (1921).
An experimental study of the significance of "Lignin" colour reactions. J. ind. Engng. Chem., 13, pp. 625-627.

CROSSLEY, A. (1976).
A versatile multi-specimen holder for processing and Critical Point drying materials for examination in the Scanning Electron Microscopy (S.E.M.). J. Microsc., 108 (3), pp. 349-352.

CROSSLEY, A. and LEVY, J.F. (1977).
Proboscis hyphae in soft rot cavity formation. J. Inst. Wood Sci., 7 (2), issue 38, pp. 30-33.

DAVIS, E.N., RHODES, R.A. and SHULKE, H.R. (1965).
Fermentative production of extracellular glucans by fleshy fungi. Appl. Microbiol., 13, pp. 267- .

DEKKER, R.F.H. and RICHARDS, G.N. (1976).
Hemicellulases; Their occurence, purification, properties and mode of action. Advan. Carbohyd. Chem. Biochem., 32, 277-352.

DUNCAN, C.G. (1960).
Wood-attacking capacities and physiology of soft rot fungi. U.S. For. Prod. Lab. Report, No. 2173, 28 pages.

DRUMMOND, D.G. (1950).
The practice of electron microscopy. J. Roy. microsc. Soc., 70, pp. 1-141.

FENGEL, D. (1967).
Ultramicrotomy, its application in wood research. Wood Sci. Technol., 1, pp 191-204.

FENGEL, D. and STOLL, M. (1975).
Gefrier-Ultramikrotomie als Methode der modernen Holzforschung. Instrument u. Forschung, 4/75, pp. 1-14.

FINDLAY, G.W.D. (1970).
Microscopic studies on soft rot in wood. Ph.D. Thesis, University of London, Imperial College.

FINDLAY, G.W.D. and LEVY, J.F. (1969).
Scanning electron microscopy as an aid to the study of wood anatomy and decay. J. Inst. Wood Sci., 23, pp.57-63.

FINK, H. (1960).
Epoxy resins in electron microscopy. J. biophys. biochem. Cytol., 7, pp. 27-30.

FREY-WYSSLING, A. (1938).
Submikroskopische Struktur und Mazerationbilder nativer Cellulosefasern. Der Papierfabrikant, 36, pp. 212-217.

FREY-WYSSLING, A. (1968).
The ultrastructure of wood. Wood Sci. Tech., 2, pp.73-83.

FULLER, D.B. (1970).
Studies on the cellulolytic enzymes of some wood destroying fungi. Ph.D. Thesis, University of London, Imperial College.

GEORGE, C.J. (1974).
Fungal enzymic degradation of timber with particular reference to the hemicelluloses. Ph.D. Thesis, University of London, Imperial College.

GREAVES, H. (1973).
Comparative morphology of selected sapwood species using the scanning electron microscope. Holzforschung, Bd. 27, H. 3, pp. 80-88.

GREAVES, H. and LEVY, J.F. (1965).
Comparative degradation of the sapwood of Scots pine, beech and birch by Lenzites trabea, Polystictus versicolor and Chaetomium globosum and Bacillus polymyxa. J. Inst. Wood Sci., 15, pp. 55-63.

HARADA, H. (1965).
Ultrastructure and organisation of Gymnosperm cell walls, pp.215-233 and ultrastructure of Angiosperm vessels and ray parenchyma pp. 235-249. In; Cellular ultrastructure of woody plants (ed. W.A. Côté), Syracuse University Press.

HARTIG, R. (1878).
Die Zersetzerscheinungen des Holzes der Nadelholzbäume und der Eiche. Berlin, 151 pages.

HAYAT, M.A. (1972).
Principles and techniques of electron microscopy. Biological applications, volume 2 (ed. M.A. Hayat), Van Nostrand Rheinhold Company.

HELANDER, H.F. (1969).
Surface topography of ultramicrotome sections. J. Ultrastruct. Res., 29, pp. 373-382.

HELANDER, H.F. (1973a).
Surface topography of ultramicrotome knives. J. Ultrastruct. Res., 42, p. 394.

HELANDER, H.F. (1973b).
Cutting force measurements in ultramicrotomy. J. Ultrastruct. Res., 44, p. 431.

HELANDER, H.F. (1974).
Some observations on knife properties and sectiong mechanics during ultramicrotomy of plastic embedding media. J. Microsc., 101 (1), pp. 81-93.

HEPLER, P.K., FOSKET, D.E. and NEWCOMB, E.H. (1970).
Lignification during secondary wall formation in Coleus: An electron microscopic study. Amer. J. Bot., 57 (1), pp. 85-96.

HOWARD, R.J. and AIST, J.R. (1979).
Hyphal tip cell ultrastucture of the fungus Fusarium: Improved preservation by Freeze-Substitution. J. Ultrastruct. Res., 66 (3), pp. 224-234.

HUNSLEY, D. and BURNETT, J.H. (1970).
The ultrastructural architecture of the walls of some hyphal fungi. J. gen. Microbiol., 62, pp. 203-218.

JONES, E.B.G. (1963).
Observations on the fungal succession on wood test blocks submerged in the sea. J. Inst. Wood Sci., 11, pp. 14-23.

JONES, H.C., ROTH, I.L. and SANDERS, W.M. (1969).
Electron microscopic study of a slime layer. J. Bact., 99 (1), pp. 316-325.

JURÁŠEK, L. (1958).
The influence of wood temperature and moisture content on the formation of tyloses in beech wood. Dřev. Výsk., 3, pp. 5-13.

JURÁŠEK, L. (1964).
Změny v mikroskopiké struktuře při rozkladu dřeva dřevokaznými houbami. Dřev. Výsk., 3, pp. 127-144. U.S. For. Prod. Lab. translation No. 549.

JUTTE, S. (1973).
Some examples of the interrelation between wood structure and the mode of attack of micro-organisms and cellulase preparations. Acta bot. neerl., 19, (6), pp. 906-917.

JUTTE, S. and LEVY, J.F. (1971a).
Scanning reflection electron microscopy in studies of wood structure and its degradation. I.A.W.A. Bull. No. 1, pp. 3-13.

JUTTE, S. and LEVY, J.F. (1971b).
The structure and degradation of bordered pits in gymnosperm tracheids as revealed by the scanning reflection electron microscope. Acta bot. neerl., 20 (5), pp. 453-466.

JUTTE, S. and SACHS, I.B. (1976).
S.E.M. observations of brown-rot fungus Poria placenta in normal and compression wood of Picea abies. Scanning electron microscopy 1976 (part VII), Chicago, April 1976.

JUTTE, S. and WARDROP, A.B. (1970).
Morphological factors relating to the degradation of wood fibres by cellulase preparations. Acta bot. neerl., 19 (6), pp. 906-917.

JUTTE, S. and ZABEL, R.A. (1974).
Initial wood decay stages as revealed by scanning electron microscopy. Scanning electron microscopy 1974 (part II), Chicago, April 1974.

KEILICH, G., BAILEY, P. and LIESE, W. (1970).
Enzymatic degradation of cellulose and fungal decay of wood. Wood Sci. Technol., 4, pp. 273-283.

KENNEDY, R.W. (1958).
Strength retention in wood decayed to small weight losses. For. Prod. J., 8, pp. 308-314.

KIRK, T.K. (1971).
Effects of microorganisms on lignin. Ann. Rev. Phytopathol. 9, pp. 185-210.

KIRK, T.K. (1973).
The chemistry and biochemistry of decay, pp. 149-181. In; Wood deterioration and its prevention by preservative treatments, Vol. 1 (ed. D.D. Nicholas), Syracuse University Press.

KISSER, I. and LOHWOG, K. (1937).
Histochemische Untersuchungen an verholzten Zellwanden. Mikrochemie 23 (1), pp. 51-60. U.S. For. Prod. Lab. Translation No.549.

KOENIGS, J.W. (1975).
Hydrogen peroxide and iron: A microbial cellulolytic system? pp. 151-159. In; Cellulose as a chemical and energy resource (ed. C.R. Wilke), Biotech. and Bioeng. Symp. No. 5, New York, John Wiley & Sons.

KORAN, Z. (1974).
Intertracheid pitting in the radial walls of black spruce tracheids. Wood Sci., 7 (2), pp. 111-115.

KORAN, Z. (1977).
Tangential pitting in black spruce tracheids. Wood Sci. Technol., 11, pp. 115-123.

LANGE, P.W. (1954).
The distribution of the components in the plant cell wall. Svensk Papperstidning, 57, pp. 563-567.

LAWN, A.M. (1960).
The use of potassium permanganate as an electron dense stain for sections of tissue embedded in epoxy resin. J. Biophys. Biochem. Cytol., 7, pp. 197-198.

LEAK, L.V. (1967).
Fine structure of the mucilaginous sheath of Anabaena sp. J. Ultrastruct. Res., 21, pp. 61-74.

LEE, H. and NEVILLE, K. (1957).
Epoxy resins: Their application and technology, New York, McGraw Hill.

LEE, H. and NEVILLE, K. (1967).
Handbook of epoxy resins, New York, McGraw Hill.

LEIGHTLEY, L.E. and EATON, R.A. (1977).
Mechanisms of decay of timber by aquatic micro-organisms. Record 1977 Ann. Conv. British Wood Preserving Assocn., Cambridge.

LEVI, M.P. (1965).
Decay patterns produced by Chaetomium globosum in beechwood fibres. Mat. u. Org., Bh. 1, pp. 119-126.

LEVI, M.P. and PRESTON, R.D. (1965).
A chemical and microscopic examination of the action of the soft-rot fungus Chaetomium globosum on beechwood (Fagus sylvatica). Holzforschung, Bd. 19, H. 6, pp. 183-190.

LEVY, J.F. (1965).
The soft rot fungi; their mode of action and significance in the degradation of wood, pp. 323-357. In; Advances in Botanical Research (ed. R.D. Preston), volume 2, London, Academic Press.

LEVY, J.F. (1967).
Decay and degrade of wood by soft rot fungi and other organisms. Pest Technol., 9 (6), pp. 28-34.

LEVY, J.F. (1969).
The spectrum of interaction between fungi and wood. Record 1969 Ann. Conv. British Wood Preserving Assocsn., Cambridge.

LEVY, J.F. (1974).
Fungi in wood. Scanning electron microscopy (Part II). Proceedings of the 7th Annual Scanning Electron Microscopy Symposium, Chicago, Illinois 60616, U.S.A.

LEVY, J.F. and STEVENS, M.G. (1966).
The initiation of attack by soft rot fungi in wood. J. Inst. Wood Sci., 3, pp. 49-55.

LEWIS, P.F. (1976).
The possible significance of the hemicelluloses in wood decay. Mat. u. Org., Bh. 3, pp. 113-119.

LEWIS, P.F. (1977).
Hemicellulase activity of fungi in wood decay. Ph.D. Thesis, University of London, Imperial College.

LIESE, W. (1963a).
Tertiary wall and warty layer in wood cells. J. Polym. Sci. Pt. C, 2, pp. 213-229.

LIESE, W. (1963b).
Neue Befunde uber den Abbau des Holzes durch Pilze. HolzZentralblatt, 89, pp. 505-507.

LIESE, W. (1964).
Über den Abbau verholzter Zellwände durch Moderfäulepilze. Holz als Roh-und Werkstoff, 22, pp. 289-295. C.S.I.R.O. translation No. 7294.

LIESE, W. (1965a).
Mikromorphologische Veränderungen beim Holzabbau durch Pilze. Mat. u. Org., Bh. 1, pp. 13-26.

LIESE, W. (1965b).
The warty layer, pp. 251-269. In; Cellular ultrastructure of woody plants (ed. W.A. Cote), Syracuse University Press.

LIESE, W. (1965c).
The fine structure of bordered pits in softwoods, pp. 271-290. In; Cellular ultrastructure of woody plants (ed. W.A. Cote), Syracuse University Press.

LIESE, W. (1970).
Ultrastructural aspects of woody tissue disintegration. Ann. Rev. Phytopathol., 8, pp. 231-258.

LIESE, W. and AMMER, U. (1964).
Über den Befall von Buchenholz durch Moderfäulepilze in Abhängigkeit von der Holzfeuchtigkeit. Holzforschung, 18, pp. 97-102.

LIESE, W. and HARTMANN-FAHNENBROCK, M. (1953).
Elektronenmikroscopische Untersuchungen an verblautem Kiefernholz. Holzforschung, 7, pp. 97-102.

LIESE, W. and SCHMID, R. (1962).
Elektronmikroskopische Untersuchungen über den Abbau des Holzes durch Pilze. Angew. Bot., 36, pp. 291-298.

LIESE, W. and SCHMID, R. (1963).
Fibrilläre Strukturen an den Hyphen holzzerstörender Pilze. Naturwissenschaften, 50, p. 102.

LIESE, W. and SCHMID, R. (1966).
Untersuchungen über den Zellwandabbau von Nadelholz durch Trametes pini. Holz als Roh-und Werkstoff, 24, pp. 454-460. C.S.I.R.O. translation No. 8800.

LUFT, J.H. (1961).
Improvements in epoxy resin embedding methods. J. biophys. biochem. Cytol., 9, pp. 409-414.

LUFT, J.H. (1964).
Electron microscopy of cell extraneous coats as revealed by ruthenium red staining. J. Cell Biol., 23, pp. 54A-55A.

LUFT, J.H. (1971).
Ruthenium red and violet I; Chemistry, purification, methods of use for electron microscopy and mechanism of action. Anat. Rec., 171, pp. 347-368.

LUNDSTROM, H. (1970)
Cavity formation in soft rot - A method for microscopic direct study. Holzforschung, 24 (4), pp. 132-133.

MARET, R. (1972).
Chimie et morphologie submicroscopique des parois cellulaires de l'Ascomycete Chaetomium globosum. Arch. Mikrobiol., 81, pp. 68-90.

MEEK, G.A. (1976).
Practical electron microscopy for biologists, 2nd edition, London, John Wiley & Sons.

MEIER, H. (1955).
Decomposition of the cell wall by wood-destroying fungi and the submicroscopic structure of tracheids of spruce and wood fibres of birch. Translated from, Holz als Roh-und Werkstoff, 13 (9), pp. 323-338. Dept. For. Canada translation No. 92.

MEIER, H. (1961).
The distribution of polysaccharides in wood fibres. J. Polymer Science, 51, pp. 11-18.

MEIER, H. (1964).
General chemistry of cell walls and distribution of the chemical constituents across the walls, pp. 137-151. In; The formation of wood in forest trees (ed. M.H. Zimmermann), New York, Academic Press.

MEYLAN, B. and BUTTERFIELD, B. (1972).
"Three dimensional structure of wood". A scanning electron microscopy study. 80 pages, London, Chapman and Hall.

McGEE-RUSSELL, S.M. and deBRUIJN, W.C. (1964).
Experiments on embedding media for electron microscopy. Quart. J. micr. Sci., 105 (2), pp. 231-244.

NEČESANÝ, V. (1963).
Veränderung der Zellwandstruktur bei Tannenholz (Abies alba Mill.) durch Pilzeinwirkung. Holzforschung, 17, pp. 57-60.

NILSSON, T. (1973).
Studies on wood degradation and cellulolytic activity of microfungi. Stud. for. suec., No. 104, 40 pages.

NILSSON, T. (1974a).
Comparative study on the cellulolytic activity of white-rot and brown-rot fungi. Mat. u. Org., 9 (3), pp. 173-198.

NILSSON, T. (1974b).
The formation of soft rot cavities in various cellulose fibres by Humicola alopallonella Meyers & Moore. Stud. for. suec., No. 112, 30 pages.

NILSSON, T. (1974c).
Microscopic studies on the degradation of cellophane and various cellulosic fibres by wood-attacking microfungi. Stud. for. suec., No. 117, 32 pages.

NILSSON, T. (1974d).
The degradation of cellulose and the production of cellulase, xylanase, mannanase and amylase by wood-attacking microfungi. Stud. for. suec., No. 114, 61 pages.

PATE, J.L. and ORDAL, E.J. (1967).
The fine structure of Chondrococcus columnaris. III, the surface layers of Chondrococcus columnaris. J. Cell Biol., 25, pp. 37-50.

PEACHY, L.D. (1958).
Thin sections. I, a study of section thickness and physical distortion produced during microtomy. J. biophys. biochem. Cytol., 4 (3), pp. 233-242.

PEASE, D.C. (1973).
Substitution techniques, pp. 35-66. In; Advanced techniques in biological electron microscopy (ed. J.K. Koehler), Berlin, Heidelburg, Springer-Verlag.

PECHMANN, H.von., AUFSESS, H., LIESE, W. and AMMER, U. (1967).
Untersuchungen über die Rotstreifigkeit des Fichtenholzes. Beih. Forst. Centralblatt, 27, 112 pages.

PRESTON, R.D. (1974).
The physical biology of plant cell walls, 491 pages. London, Chapman and Hall.

PRESTON, R.D. (1979).
The shape of soft-rot cavities - A hypothesis. Wood Sci. Technol., 13, pp. 155-163.

PROCTOR, P. (1941).
Penetration of the walls of wood cells by the hyphae of wood destroying fungi. Yale Univ. Sch. For. Bull., No. 47, 31 pages.

RAMSAY (1880).
Unreferenced; see Anderson, T.F. (1966). Electron microscopy of microorganisms, pp. 319-387. In; Physical techniques in biological research, volume III, part A - Cells and tissues, 2nd ed. (ed. A.W. Pollister), New York, Academic Press.

REEDY, M.K. (1965).
Incompatability of Methyl Nadic Anhydride with Permanganates. J. Cell Biol., 26, pp. 309-311.

REESE, E.T. (1977).
Enzymic degradation of polymeric carbohydrates, pp. 311-367. In; The structure, biosynthesis and degradation of wood (ed. F.A. Loewus and V.C. Runeckles). Recent Adv. Phytochem., 11, New York, Plenum Press.

REYNOLDS, E.S. (1963).
The use of lead citrate at high pH as an electron opaque stain in electron microscopy. J. Cell Biol., 17, pp. 208-212.

ROLOEFSEN, P.A. (1956).
Eine mögliche Erklärung der typischen Korrosionfiguren der Holzfaren bei Moderfäule. Holz als Roh-und Werkstoff, 14 (6), pp. 208-210. C.S.I.R.O. translation No. 5132.

SACHS, I.B., WARD, J.C. and KINNEY, R.E. (1974).
Scanning electron microscopy of bacterial wetwood and normal heartwood in poplar trees. Proceedings of the 7th Annual Scanning Electron Microscopy Symposium, Chicago, Illinios 60616, U.S.A.

SAVORY, J.G. (1954).
Breakdown of timber by Ascomycetes and fungi imperfecti. Ann. Appl. Biol., 41, pp. 336-347.

SAVORY, J.G. and PINION, L.C. (1958).
Chemical aspects of decay of beechwood by Chaetomium globosum. Holzforschung, 12, pp. 99-103.

SCHACHT, H. (1850).
Über eigenturnliche bisher noch nicht beobachtete Erscheingungen in der Verdickungsschichten gewissen Holzzellen. Botanische Zeitung, 8 (34), pp.697-702 and 713-719.

SCHACHT, H. (1863).
Über die Veranderungen durch Pilze in abgestorbenen Planzenzellen. Jahrbucher fur Wissenschaftliche Botanik, 3, pp.442-483.

SCHEFFER, T.C. (1936).
Progressive effects of Polporus versicolor on the physical and chemical properties of redgum sapwood. U. S. Dept. Agr. Tech. Bull., No. 527.

SCHEFFER, T.C. (1973).
Microbiological degradation and the causal organisms, pp. 31-106 In; Wood deterioration and its prevention by preservative treatments, volume I (ed. D.D. Nicholas), Syracuse University Press.

SCHULZE, B. and THEDEN, G. (1938).
Polarisationsmikroskopische Untersuchungen über den Abbau des Werkstoffes Holz durch holzzerstörende Pilze. Holz als Roh-und Werkstoff, 1, pp. 548-554.

SCHMID, R. (1966).
Studies on extracellular structures of fungal hyphae. VIth international congress for electron microscopy, 1966, 2, pp. 785-786.

SCHMID, R. and LIESE, W. (1964).
Über die mikromorphologischen Veränderungen der Zellwandstrukturen von Buchen- und Fichtenholz beim Abbau durch Polporus versicolor (L.) Fr., Arch. Mikrobiol., 47, pp. 260-276. C.S.I.R.O. translation No. 7130.

SCHMID, R. and LIESE, W. (1965).
Zur Aussenstruktur der Hyphen von Blauepilzen. Phytopathol. Z., 54, pp. 275-284.

SCURFIELD, G. and SILVA, S.R. (1970).
The vestured pits of Eucalyptus regnans F. Muell. a study using scanning electron microscopy. J. Linn. Soc. Botany, 63, pp. 313-320.

SEIFERT, K. (1966).
Die chemische Veränderung der Bucherholz-Zellwand durch Moderfäule (Chaetomium globosum Kunze). Holz als Roh-und Werkstoff, 24, pp. 102-113.

SINNER, M., PARAMESWARAN, N., YAMAZAKI, N., LIESE, W. & DIETRICHS, H. (1976).
Specific enzymatic degradation of polysaccharides in delignified wood cell walls, pp. 993-1024. In; Proceedings of the 8th cellulose conference, part III general papers (ed. T.E. Timell), J. Applied Polmer Science, applied polymer symposia, No. 28.

SPRINGER, E.L. and ROTH, I.L. (1973).
The ultrastructure of the capsules of Diplococcus pneumoniae and Klebsiella pneumoniae stained with ruthenium red. J. gen. Microbiol., 74, pp. 21-31.

SPURR, A.R. (1969).
A low-viscosity epoxy resin embedding medium for electron microscopy. J. Ultrastruct. Res., 26, pp. 31-43.

STAUBLI, W. (1963).
A new embedding technique for electron microscopy, combining a water-soluble epoxy resin (Durcupan) with water-insoluble Araldite. J. Cell Biol., 16, pp. 197-199.

STOLL, M. and FENGEL, D. (1977).
Studies on hollocellulose and alpha cellulose from spruce wood using Cryo-ultramicrotomy, part I, structural changes in fibre walls during delignification and alkali extraction. Wood Sci. Technol., 11, pp. 265-274.

UNLIGIL, H.H. and CHAFE, S.C. (1974).
Penetration hyphae of soft rot fungi in the wood of white spruce, Picea glauca (Moench) voss. Wood Sci. Technol., 8 (1), pp. 27-32.

WACHTEL, A.W., GETTNER, M.E. and ORNSTEIN, L. (1966).
Microtomy, pp. 173-250. In; Physical techniques in biological research, volume III, part A, Cells and tissues (ed. A.W. Pollister), New York, Academic Press.

WAGENFUHR, R. and ZIMMER, F. (1968).
The surface of wood under the electron microscope. Holztechnologie, 9 (3), pp. 151-152.

WARDROP, A.B. (1964).
The structure and formation of the cell wall in xylem, pp. 87-134. In; The formation of wood in forest trees (ed. M.H. Zimmermann), New York, Academic Press.

WARDROP, A.B. (1965).
Cellular differentiation in xylem, pp. 61-97. In; Cellular ultrastructure of woody plants (ed. W.A. Cote), Syracuse University Press.

WARDROP, A.B. and DADSWELL, H.E. (1957).
Variations in cell wall organisation of tracheids and fibres. Holzforschung, 11 (2), pp. 33-46.

WARDROP, A.B. and JUTTE, S.M. (1968).
The enzymatic degradation of cellulose from Valonia ventricosa. Wood Sci. Technol., 2, pp. 105-114.

WATSON, M.L. (1958).
Staining of tissue sections for electron microscopy with heavy metals. J. biophys. biochem. Cytol., 4 (4), pp. 475-479.

WESSELS, J.C.H., KREGER, D.R., MARCHANT, R., REGENSBURG, B.A. and DE VRIES, O.M.H. (1972).
Chemical and morphological characterization of the hyphal wall surface of the Basidiomycete Schizophyllum commune. Biochim. biophys. Acta, 273, pp. 346-358.

WILCOX, W.W. (1968).
Changes in wood structure through progressive stages of decay. U. S. For. Serv. Res. Paper FPL-70, 45 pages.

WILCOX, W.W. (1970).
Anatomical changes in wood cell walls attacked by fungi and bacteria. Bot. Rev., 36 (1), pp. 1-28.

WILCOX, W.W. (1973).
Degradation in relation to wood structure, pp. 107-148. In; Wood deterioration and its prevention by preservative treatments, volume I (ed. D.D. Nicholas), Syracuse University Press.

WILCOX, W.W., PARALESWARAN, N. and LIESE, W. (1974).
Ultrastructure of brown rot in wood treated with pentachlorophenol. Holzforschung, Bd 28, H 6, pp. 211-217.

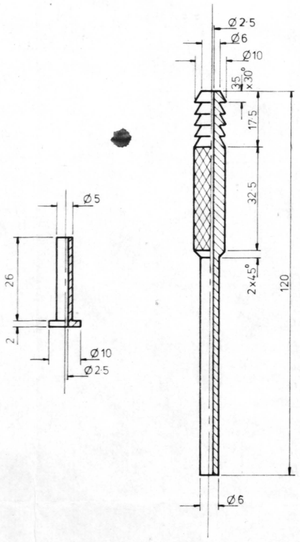
WILHELMSEN, G. (1965).
Mikromorfologiske og biokjemiske forandringer i trevirke ved enzymatisk nedbrytning. Norsk Skogind., 19, pp. 187-193. Dept. For. Canada translation No.195.

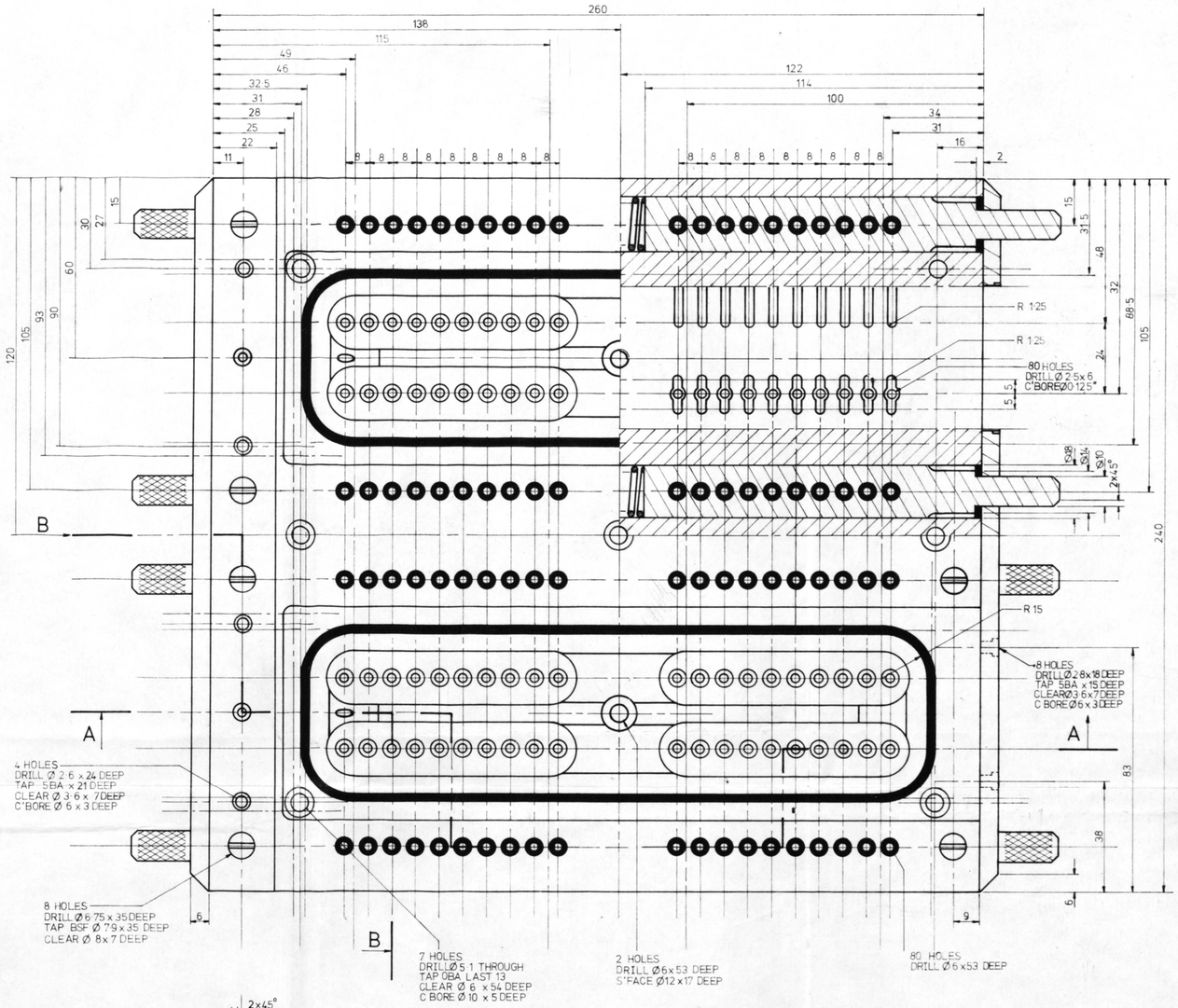
ZAINAL, A.S. (1975).
Micro-morphological studies of soft rot fungi in wood. Ph.D. Thesis, University of London, Imperial College.

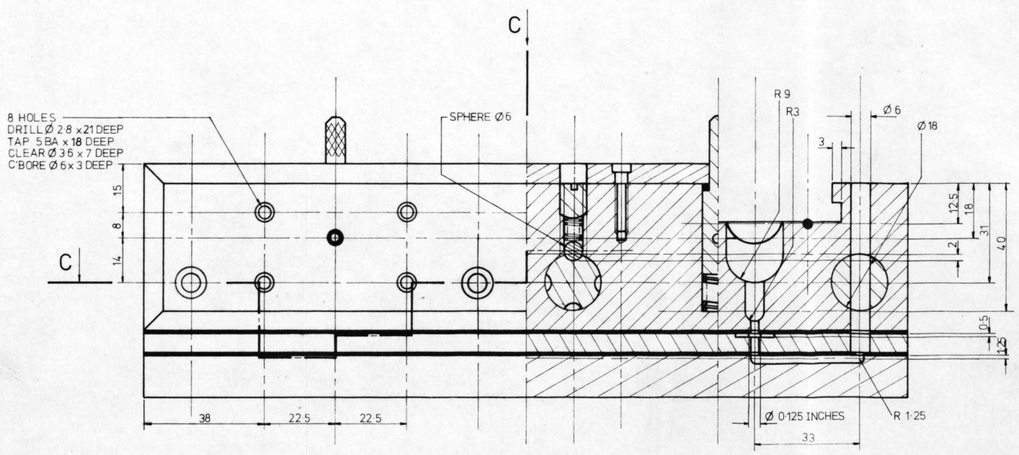
ZAINAL, A.S. (1976a).
The soft rot fungi : the effect of lignin. Mat. u. Org., Bh 3, pp. 121-127.

ZAINAL, A.S. (1976b).
The effect of a change in the cell wall constituents on decay of Scots pine by a soft rot fungus. Mat. u. Org., Bh 11 (4), pp. 295-301.

ZAINAL, A.S. (1978).
A new explanation for soft rot cavity formation in the S_2 layer of wood cell walls. Wood Sci. Technol., 12, pp. 105-110.

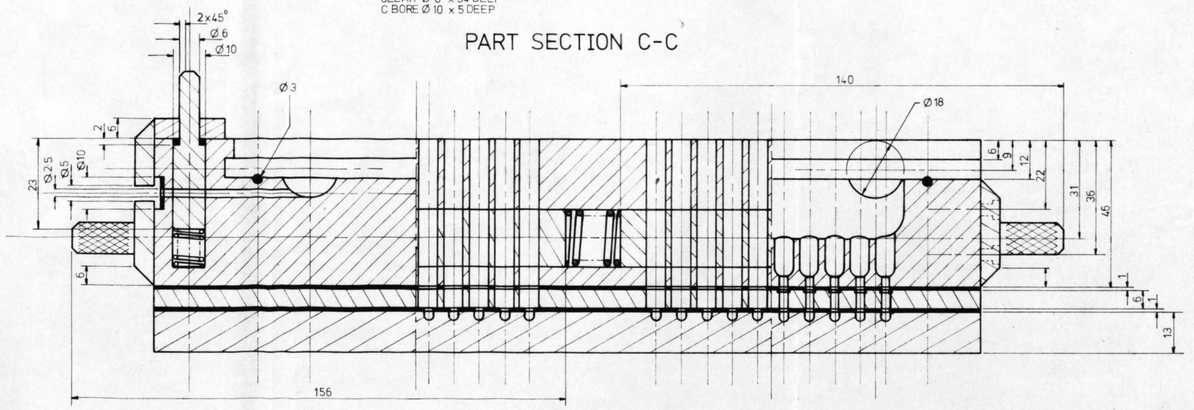






SECTION B-B

PART SECTION C-C



SECTION A-A

IMPERIAL COLLEGE OF SCIENCE AND TECHNOLOGY	DURAL H 15	DR'G. No. 1	1:1
T.E.M. SPECIMEN PREPARATION BLOCK	JULY 1976	THIRD ANGLE PROJECTION	A. CROSSLEY
	ALL DIMENSIONS IN MM UNLESS STATED OTHERWISE		